The anti-tumoral effects of a low protein diet and of the IRE1α signaling

Adriana Martinez Turtos

UNIVERSITÉ CÔTE D'AZUR

ÉCOLE DOCTORALE
SCIENCES DE LA VIE ET DE LA SANTÉ

THÈSE DE DOCTORAT

Les effets anti-tumoraux d'un régime pauvre en protéines et de la signalisation IRE1α

The anti-tumoral effects of a low protein diet and of the IRE1α signaling

Adriana MARTINEZ TURTOS

Centre Méditerranéen de Médecine Moléculaire (C3M)
Équipe 3 : Métabolisme, Cancer et Réponses Immunes

Présentée en vue de l'obtention du grade de docteur en Sciences de la Vie et de la Santé, spécialité Interactions Moléculaires et Cellulaires **d'**Université Côte d'Azur

Dirigée par : Dr. Jean-Ehrland RICCI
Soutenue le : 20 mai 2022

Devant le jury, composé de :
Dr. Frédéric BOST, Président du Jury, C3M, Université Côte d'Azur
Dr. Massimiliano MAZZONE, Rapporteur, VIB-KU Leuven Center for Cancer Biology
Dr. Serge MANIÉ, Rapporteur, CNRS 5286, Cancer Research Center of Lyon
Dr. Jean-Ehrland RICCI, Directeur de thèse, C3M, Université Côte d'Azur

Inserm U1065

METACAN Metabolism Immunity Cancer

MARIE CURIE ACTIONS

FRM FONDATION RECHERCHE MÉDICALE

Les effets anti-tumoraux d'un régime pauvre en protéines et de la signalisation IRE1α

Jury:

Président du Jury

Dr. Frédéric BOST
Directeur de recherche, INSERM U1065, C3M, Université Côte d'Azur

Rapporteurs

Dr. Massimiliano MAZZONE
Directeur de recherche, VIB-KU Leuven Center for Cancer Biology

Dr. Serge MANIÉ
Directeur de recherche, CNRS 5286, Cancer Research Center of Lyon

Directeur de thèse

Dr. Jean-Ehrland RICCI
Directeur de recherche, INSERM U1065, C3M, Université Côte d'Azur

Titre

Les effets anti-tumoraux d'un régime pauvre en protéines et de la signalisation IRE1α

Résumé

Les interventions nutritionnelles sont étudiées dans le contexte des maladies non transmissibles telles que le cancer. Les régimes alimentaires tels que la restriction calorique, le jeûne, les régimes cétogènes et restreints en protéines ont montré leur capacité à limiter la progression tumorale. Ainsi, récemment nous avons décrit l'effet protecteur d'un régime isocalorique partiellement réduit en protéines dans plusieurs modèles de souris cancéreuses. Nous avons ainsi établi que ces régimes appauvris en protéine limitaient la croissance tumorale via l'induction d'une immunosurveillance anticancéreuse dépendante de l'activation de la protéine IRE1α.

Inositol-requiring enzyme 1α (IRE1α) est le senseur du stress du ER (réticulum endoplasmique) le plus conservé au cours de l'évolution. Il est induit en réponse à un stress dit UPR (Unfolded Protein Response). L'UPR est activé par l'accumulation de protéines mal repliées dans le RE, les perturbations lipidiques de la membrane du RE, l'hypoxie et la privation de nutriments. IRE1α active des cibles en aval via son activité endoribonucléase notamment. Ainsi, IRE1α, via son activité endoribonucléase, conduit principalement à l'épissage de XBP1 et la dégradation concomitante de certains ARNs par un processus connu sous le nom de Regulated IRE1-Dependent Decay (RIDD). Alors que l'épissage XBP1 permet de préserver l'homéostasie cellulaire, l'induction massive de RIDD conduit à l'apoptose en réponse à un stress chronique du RE.

La signalisation IRE1α a été décrite comme jouant un rôle dual dans les cancers. Alors que l'axe IRE1α-XBP1 promeut la progression tumorale dans plusieurs tumeurs solides et liquides, la branche IRE1α-RIDD a été suggérée comme suppresseur de tumeur dans le glioblastome. Étant donné que nos découvertes précédentes ont montré que IRE1α est impliqué dans les effets protecteurs d'un régime pauvre en protéines contre les tumeurs, nous avons étudié l'effet de l'expression exogène de IRE1α dans des cellules tumorales implantées chez des souris immunocompétentes.

Nous avons constaté qu'une activation complète de l'activité ARNase d'IRE1α limitait la croissance tumorale de modèles de cancers colorectaux et pulmonaires. Les tumeurs présentaient une activité plus élevée IRE1α ce qui se traduisait par une activation des voies IRE1α-XBP1 et IRE1α-RIDD, une immunosurveillance anticancéreuse plus élevée et des cellules tumorales en apoptose. En conclusion, nos résultats indiquent qu'une activation complète de l'activité RNAse d'IRE1α peut jouer un rôle suppresseur de tumeur.

Mots clés
Cancer, régime alimentaire, stress du ER stress, réponse immunitaire anti-cancer, IRE1α, apoptose

Title

The anti-tumoral effects of a low protein diet and of the IRE1α signaling

Summary

Nutritional interventions are investigated in the context of non-communicable diseases such as cancer. Dietary regimens such as caloric restriction, fasting, ketogenic and protein-restricted diets have shown benefits to control tumor progression. Indeed, we have previously reported the protective effect of an isocaloric diet partially reduced in protein in several cancer mouse models. Beyond a stronger anticancer immunosurveillance dependent on cytotoxic T cells, the low protein diet limited tumor growth in an IRE1α-dependent manner.

Inositol-requiring enzyme 1α (IRE1α) is the most evolutionally conserved ER (endoplasmic reticulum) stress sensor induced as part of the Unfolded Protein Response (UPR). The UPR is activated by accumulation of misfolded proteins in the ER, lipidic disturbances in the ER membrane, hypoxia and nutrient deprivation. IRE1α activates downstream targets via its endoribonuclease activity resulting in XBP1 splicing as well as degradation of RNAs by a process known as the Regulated IRE1-Dependent Decay (RIDD). While XBP1 splicing recovers cellular homeostasis, massive RIDD induction leads to apoptosis under chronic ER stress.

The IRE1α signaling has been described to play dual roles in most hallmarks of cancer. While the IRE1α-XBP1 axis in tumor cells supports tumor progression in several solid and liquid oncogenic malignancies, the IRE1α-RIDD branch has been suggested as tumor-suppressive in glioblastoma. Since our previous findings showed that IRE1α is implicated in the tumor-protective effects of a low protein diet, we investigated the effect of the exogenous expression of IRE1α in tumor cells implanted in immunocompetent mice.

We found that overexpression of IRE1α and self-induction of its full RNAse activity was detrimental for subcutaneous tumor growth of colorectal and Lewis lung carcinomas. Tumors with higher IRE1α activity were characterized by active IRE1α-XBP1 and IRE1α-RIDD branches, a higher anticancer immunosurveillance and tumor cells undergoing apoptosis. The enhanced anti-cancer immune response elicits upon IRE1α overexpression was mainly dependent on T cell-mediated-cytotoxicity. In conclusion, our findings support the notion that IRE1α with a full RNAse activity can have tumor-suppressive roles.

Keywords
Cancer, diet, ER stress, anti-cancer immune response, IRE1α, apoptosis

To Leonor Turtos Carbonell and Arturo Martinez Pulido
To Maria Eduviges Figueroa Diepa and Otto Martinez Huet

Acknowledgements

This PhD thesis is the outcome of the combined effort of multiple parts.

I gratefully thank my PhD thesis director, Dr. Jean-Ehrland Ricci for giving me the opportunity of making research and graduating of PhD. I thank Dr. Jean-Ehrland Ricci for the challenge of making science with full responsibility.

I thank my colleagues from team 3, the former and the current ones. With special mention, I specially thank Dr. Els Verhoeyen for guiding my professional growth in the lab and for unconditionally teaching me how science should be addressed as long as scientists are smart, creative and happy to make it. I really thank Dr. Els Verhoeyen for showing me how much of yourself can be implicated in science while enjoying every part of it.

I thank Dr. Rachel Paul-Bellon for her help in long and hard days of experiments. I thank Dr. Sandrine Marchetti and Dr. Johanna Chiche for being there for any question and bring valuable ideas. I thank Dr. Eyal Gottlieb for teaching me metabolomics and science while spending the most amazing time in his lab. I really thank all the collaborators of this research project including the lab team of Dr. Eyal Gottlieb with special mention to Ifat Abramovich and Bella Agranovich. I also thank our collaborators Dr. Nao Yamakawa and Dr. Mohamed Abdel-Mohsen.

I thank Dr. Jozef P. Bossowski for teaching the basis. I thank Dr. Rana Mhaidly for all her help in long working days and her unconditional technical and emotional support without any questions. I thank Dr. Manuel Grima Reyes for the most productive and smart scientific discussions and for his unconditional support at any level, at any time. I thank Dr. Hussein Issaoui for helping during the last period of thesis. I thank MSc. Adrien Krug for his emotional and technical support during the last days.

I finally thank all the members of the Thesis jury for contributing to the end of this PhD research work and for the invested time and effort. I really thank, Dr. Frederic Bost for following this PhD project from the very beginning and for bringing valuable ideas. I really thank Dr. Massimiliano Mazzone and Dr. Serge Manié for accepting to be part of the PhD thesis jury and for their constructive and intelligent criticisms about our research work.

I thank all the staff of the C3M Animal Facility, with special mention to Veronique Corcelle and Alexandre Ipekdjian for their help, patience, kindness and understanding.

I thank my parents, sister, my whole family and friends for supporting and guiding my professional growth and being proud and happy of my career.

Thank you all for making it possible.

TABLE OF CONTENTS

Abbreviations

ADCC	antibody-dependent cell-mediated cytotoxicity
Akt	protein kinase B
AMPK	AMP-activated protein kinase
APCs	antigen-presenting cells
ATF4	activating transcription factor 4
ATF6	activating transcription factor 6
BMDM	bone marrow-derived macrophage
CAF	cancer-associated fibroblast
CCL2	C-C chemokine ligand 2
CCR2	CCL2 receptor
CHOP	C/EBP homologous protein
COP-II	coat protein-II
CR	caloric restriction
CRC	colorectal carcinoma
CSF-1	colony-stimulating factor
CTLA4	cytotoxic T lymphocyte-associated antigen 4
CTLs	cytotoxic T lymphocytes
DAMPs	damage-associated molecular patterns
DC	dendritic cell
EAAs	essential amino acids
ER	endoplasmic reticulum
ERAD	ER-protein associated degradation machinery
FMD	fasting mimicking diet
GA	Golgi apparatus
GDH	glutamate dehydrogenase
GEM	genetically engineered mouse
GM-CSF	monocyte colony-stimulating factor
GLS	glutaminase
HAS	hyaluronan synthase
HCC	hepatocellular carcinoma
HFD	high fat diet
HIF-1α	hypoxia-inducible transcription factor-1
HNC	head and head cancer patients
ICB	immune checkpoint blockade
ICD	immunogenic cell death
IDO	indoleamine 2,3-dioxygenase
IFN	interferon
IGF-1	insulin-like growth factor-1
IRE1	inositol-requiring enzyme 1
KD	ketogenic diet
KIRs	killer cell immunoglobulin-like receptors
LAG3	lymphocyte activation gene 3 protein
LPS	lipopolysaccharide
MAM	mitochondria-associated membrane
MAPK	mitogen-activated protein kinase
MDSC	myeloid-derived suppressor cell
MHC-I	major histocompatibility complex class I
MHC-II	major histocompatibility complex class II
mTOR	mammalian target of rapamycin
MUFA	monounsaturated fatty acid
NCR	natural cytotoxic receptor
NEAA	non-essential amino acid
NF-κB	nuclear factor kappa-light-chain-enhancer of activated B cells

NK cells	Natural killer cells
NOS	nitric oxide synthase
NSCLC	non-small cell lung cancer
ORF	open reading frame
OxPhos	oxidative phosphorylation
PAMPs	pathogen-associated molecular patterns
PD-L1	programmed cell death ligand 1
PD1	programmed cell death protein 1
PDAC	pancreatic ductal adenocarcinoma
PDX	patient-derived xenografts
PERK	protein kinase RNA- (PKR-) like ER kinase
PI3K	phosphatidylinositol-3-kinase
PPP	pentose phosphate pathway
PTEN	phosphatase and tensin homolog
PUFA	polyunsaturated fatty acid
Rb	retinoblastoma
RIDD	IRE1-dependent decay of RNAs
ROS	reactive oxygen species
RTK	receptor tyrosine kinase
SAMPs	self-associated molecular patterns
SCD	stearoyl-CoA desaturase1
TAAs	tumor-associated antigens
TAM	tumor-associated macrophage
TCA	tricarboxylic acid cycle
TCR	T cell receptor
TDO2	tryptophan-2
TGFβ	transforming growth factor β
TIM3	T cell immunoglobulin mucin receptor 3
TME	tumor microenvironment
TNBC	triple negative breast cancer
TNF	tumor necrosis factor
TRAF2	TNF-receptor associated factor-2
TRAIL	TNF-related apoptosis-inducing ligand
Treg cells	regulatory T cells
UDP-GlcNAc	uridine diphosphate N-acetylglucosamine
UPR	unfolded protein response
VEGF	vascular endothelial growth factor

List of figures

List of tables

INTRODUCTION

Cancer is a complex pathological condition characterized by highly proliferating and abnormal cells that become malignant upon acquisition of certain properties (Hanahan, 2022). Malignant transformation relies on the intrinsic cell capacity to deliberately growth independent of extrinsic signals. In addition, oncogenic transformed cells alter the surrounding heathy stromal tissue to make it tumor-friendly and integral part of the established tumor mass. Oncogenic diseases are really heterogenous depending on inherited and acquired mutations, the cell type undergoing neoplastic outgrowth, the tissue, the organ, and therefore, the nature of the tumor microenvironment (TME). Therefore, cancer hallmarks have been defined to cluster complex and common tumoral processes irrespective of the type of cancer for better understanding of this multistep disorder (Hanahan and Weinberg, 2011), (Hanahan, 2022).

Hallmarks of cancer

The pathological evolution of neoplastic cellular masses broadly includes tumorigenesis, tumor expansion and metastatic dissemination (Hanahan and Weinberg, 2011). In 2000, six hallmarks of cancer were described such as sustained proliferative signaling, evasion of growth suppressors, resistance to cell death, replicative immortality, facilitation of angiogenesis and acquisition of abilities for invasion and metastasis. In 2011, two new tumor properties were recognized as hallmarks of cancer including aberrant energy metabolism and the capability to avoid tumor cell clearance by the immune system (**Figure 1**). Emerging cancer properties that endow neoplastic tissues to acquire oncogenic potential have also been described such genomic instability and mutations as well as tumor-promoting inflammation (Hanahan and Weinberg, 2011), (Hanahan, 2022). More recently, aberrant protein glycosylation in tumor cells has been reported to contribute to most of the oncogenic hallmarks (Pinho and Reis, 2015). Interestingly, the gut microflora and likely the intra-tumoral microbiome have been also added to the list of cancer enabling characteristics (Hanahan, 2022).

Establishment of malignant neoplastic lesions relies on the capacity to halt apoptotic signaling pathways that are induced along the transit of a primary tissue mass from premalignant to transformed and immortalized (Hanahan and Weinberg, 2011) (**Figure 1**). Tumor suppressors such as retinoblastoma (Rb) and p53 are in charge of enabling cell cycle progression when cellular resources and conditions are enough and favorable for cell replication and division. Therefore, loss of these genes as well as alterations in members of their signaling endow cells with the capacity to proliferate and survive irrespective of extracellular availability of nutrients, oxygen and growth factors as well as intrinsic genetic damage. Through

mechanisms that avoid replicative senescence such as upregulation of telomerase, transformed cells become immortalized warranting malignancy (Hanahan and Weinberg, 2011).

Altered bioenergetic metabolism based on high consumption of glucose for production of lactic acid by aerobic glycolysis in tumor cells was first described by Otto Warburg along the second decade of 1900 (Koppenol et al., 2011) (**Figure 1**). The Warburg effect opened the understanding of how uncontrolled cellular proliferation is supported by a less energetically efficient but more rapid metabolic pathway. Up to date, the Warburg effect is known to support not only bioenergetics in tumor cells but biosynthesis for rapid cell proliferation since glucose is catabolized via glycolysis to render intermediates for synthesis of nucleotides, amino acids and lipids. Despite the original postulate of Warburg, not all tumor cells rely exclusively on glucose for oncogenic growth during their multistep evolution from malignant establishment of the primary tumor mass to its metastatic spread. Beyond the Warburg effect, critical roles of certain amino acids such as glutamine is an intense area of research (Koppenol et al., 2011), (Hanahan and Weinberg, 2011).

Cancer risk factors

Cancer as a non-transmissible disease was estimated by the World Health Organization in 2015 to be the first or the second cause of death in individuals below 70 years old in a vast number of countries including most of America, Europe, Asia and Oceania (Bray et al., 2018). The International Agency for Research on Cancer (IARC) reported in 2020 making use of databases of 185 countries and 36 types of cancers that breast, lung and colorectal cancers are the three top most newly diagnosed oncogenic diseases ranking in the top five cancers with the highest leading cause of death in both genders (Sung et al., 2021) (**Figure 1**).

The high prevalence of certain types of cancer reflects mainly the exposition to avoidable risk factors and in minor proportion a genetic inherited predisposition (Bray et al., 2018) (**Figure 1**). Individuals with genomes susceptible to cancer development are carriers of heterozygotic mutations in oncogenes or tumor suppressors. Loss of this heterozygosis in some cells by a second acquired mutation triggers persistent cell growth. As compared to the minor contribution of heritable oncogenic mutations, acquired somatic mutations due environmental and physiological factors increase the probability of tumorigenesis with aging. In Western countries, smoking, overweight mainly abdominal, poor physical activity, alcohol abuse, reproductive lifestyle and dietary habits are commonly described as modifiable factors that increase incidence of several types of cancers and their early onset. Other risk factors include radiation, pollution and viral infections (Hanahan and Weinberg, 2011), (Bray et al., 2018).

Colorectal carcinoma (CRC) is a good example of oncogenic diseases whose frequency rapidly increases in migrating populations (Keum and Giovannucci, 2019). Individuals coming from geographical areas with low CRC incidence have shown an increased CRC risk when migrate to countries with westernized dietary habits and high CRC rates. Western dietary patterns are characterized by high consumption of red and processed meat, low intake of fibers as well as consumption of refined sugars (Keum and Giovannucci, 2019).

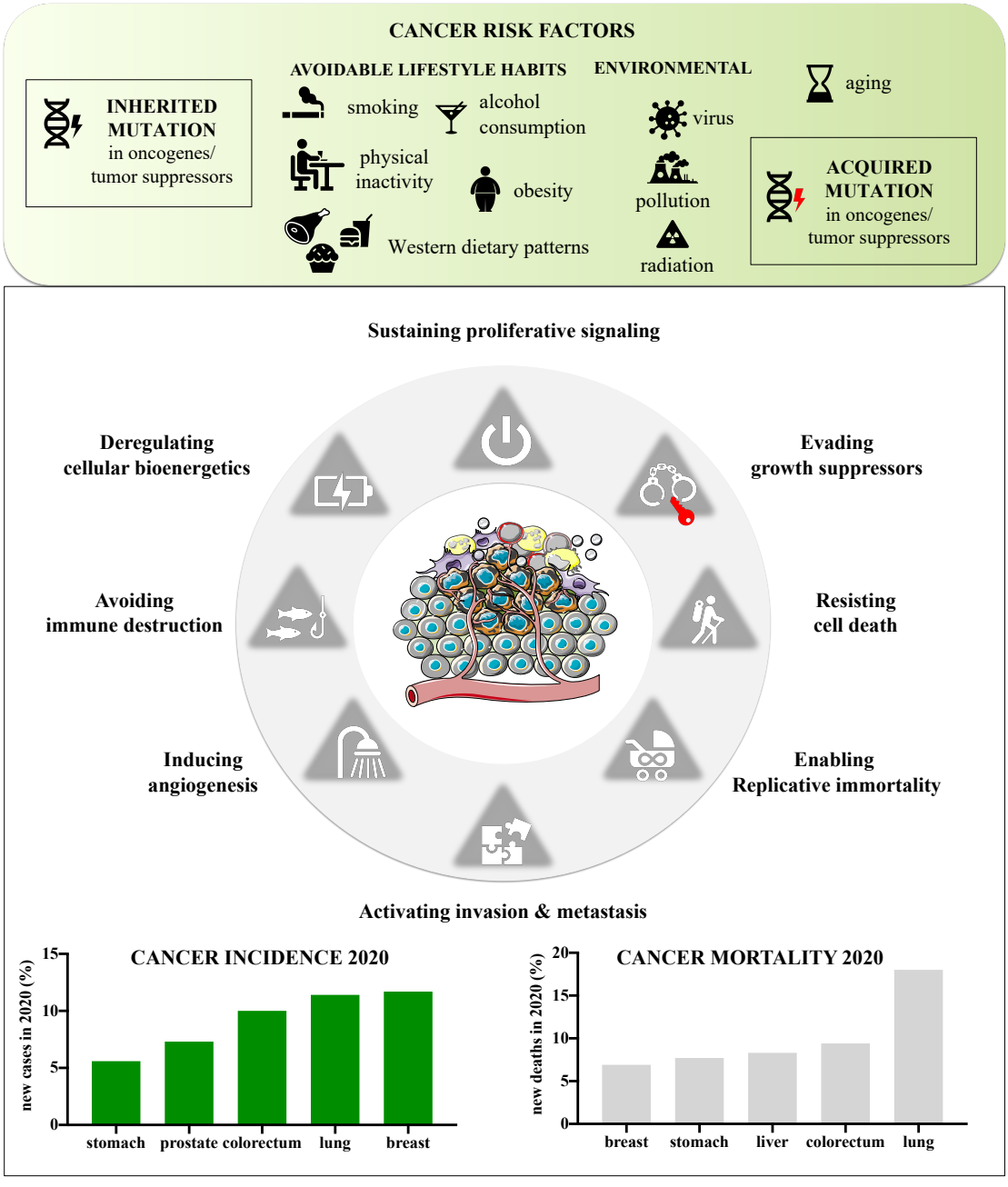

Figure 1. Cancer risk factors, hallmarks and global incidence and mortality in 2020

Global incidence and mortality are according to estimates from GLOBOCAN 2020 produced by the International Agency for Research on Cancer (IARC) in 2020. 19.3 million new diagnosed cancer cases and near 10 million of new cancer death were reported in 2020 based on worldwide data of 36 types of cancer from 185 countries including both sexes and all groups of age with no distinction of cancer stages (Sung et al., 2021).

Due to the high association between dietary patterns as environmental and modifiable risk factors and carcinogenesis, human nutrition is nowadays and from two or three decades ago an intense research area in the field of non-communicable diseases (Mozaffarian et al., 2018). Studies of human nutrition as a modern science date from almost a century ago (Mozaffarian et al., 2018) even though since the ancient Greeks and Romans, the benefits of a controlled food intake in terms of quantity were described for healthiness and longevity (Tajan and Vousden, 2020). Therefore, the following chapters are a compendium of scientific research illustrating the links among cancer, nutrition and the anti-cancer immune response. At the molecular level, cellular sensor pathways responsive to the nutritional status are detailed in the context of oncogenic disorders.

I. Diet, metabolism and cancer

Modern scientific studies in nutrition and their impact on human health started from individual nutrient characterization (Mozaffarian et al., 2018). Indeed, the first identified vitamin, thiamine was isolated in 1926 and around 1950, all vitamins were characterized and associated with multiple deficiency diseases. Between 1950 and 1990, total calories and macronutrients (fat, carbohydrate, and protein) were recognized as nutritional parameters implicated in general wellbeing status and associated with cardiovascular and metabolic diseases. From 1990, more sophisticated epidemiological studies brought the notion that nutritional regimens beyond consumption of single nutrients are associated with non-communicable diseases. This scientific new vision of the modern nutrition opened the door to research focused on the physiological effects of specific dietary regimens (Mozaffarian et al., 2018).

The first description of the Mediterranean dietary regimen was made by a nutritionist in 1945 who noted a high number of elderly and low prevalence of metabolic-related disorders in the Mediterranean population as compared to that from the United States consuming an Anglo-Saxon diet (Soldati et al., 2018). Indeed, consumption of the Mediterranean diet has been negatively associated with risks of cancer development and related mortality (Soldati et al., 2018). Based on the association between nutritional regimens and diseases, malnutrition is currently considered as a physiological condition driven by a poor nutritional quality and a risk factor for cardiovascular and metabolic disorders including cancer (Mozaffarian et al., 2018).

Studies on human nutrition are extremely controversial due to the lack of standardized healthy diets and restrictive dietary regimens in terms of macronutrient and micronutrient composition, macronutrient caloric input, nutrient sources and temporal feeding patterns (Lévesque et al., 2019). In parallel, the lack of guidelines to report physiological parameters

complicates the comparison among nutritional regimens and the interpretation of their impact on specific human pathologies. Despite these limitations, half of all cancer patients modify their diets as an attempt to prolong survival (Tajan and Vousden, 2020). Therefore, current scientific efforts in the cancer research field are focused on unraveling the metabolic pathways and molecular mechanisms elicited by protective custom dietary regimens in pre-clinical cancer models to benefit from them in clinical therapeutic settings (Lévesque et al., 2019), (Tajan and Vousden, 2020), (Kanarek et al., 2020).

This chapter intends to illustrate the wide spectrum of dietary interventions resulting in positive anti-cancer outcomes in a repertory of pre-clinical and clinical studies. Major oncometabolic and nutrient-sensing pathways will be also described as the molecular basis underlying cancer cell response to nutritional conditions.

I.1 Dietary interventions as anti-cancer therapies

The rational of nutritional interventions to attack cancer progression is a dual paradigm explained by the intrinsic metabolic requirements of malignant tissues and a sub-optimal anti-tumoral immunosurveillance due to malignant and amplifying immunosuppressive signals as well as nutrient competition within the tumor mass (Tajan and Vousden, 2020). Tumor cells are nutrient devouring and highly consumers not only of glucose but amino acids such as glutamine and serine as well as lipids to support their anabolic metabolism. This notion in parallel with more recent specific metabolic vulnerabilities of tumors are the bases of cancer research focused on anti-cancer dietary interventions including caloric restriction (reduction in calories), ketogenic (high fat and low carbohydrate content) and protein-restricted diets as well as fasting nutritional regimens alone or in combination with standard chemotherapies (Lévesque et al., 2019), (Tajan and Vousden, 2020) (**Figure 2**).

Anti-cancer interventions have also shown to boost the anti-cancer immune response (Buono and Longo, 2018), (Rubio-Patiño et al., 2018b), (Orillion et al., 2018) (Vernieri et al., 2022). As part of the anti-cancer immunosurveillance, cytotoxic T lymphocytes (CTLs) are major drivers of potent adaptive anti-cancer responses (Raskov et al., 2021). T cell priming and activation is a process dependent on antigen-presenting cells (APCs) loaded with tumor-associated antigens (TAAs) and releasing activating cytokines. Therefore, effective anti-cancer immune responses driven by CTLs also rely on the crosstalk between APCs and $CD4^+$ helper T cells (Borst et al., 2018). Homeostatic and pathological regulatory mechanisms decreasing the intensity of the immune response are also potentiated in cancer leading to immunosuppressive phenotypes in the TME and tumor progression (van der Leun et al., 2020), (Pathria et al., 2019), (Pawelec et al., 2019). In addition, cytotoxic NK cells as part of the innate immunity display an anti-cancer potential (Guillerey et al., 2016).

I.1.1 Caloric restriction and low carbohydrate diets

Caloric restriction (CR) diets with not more than 30% calorie reduction were one of first regimens to be investigated in the cancer field due to their positive impact on metabolic disorders such as obesity, diabetes mellitus and cardiovascular diseases (O'Flanagan et al., 2017). CR has also been reported to reduce cancer incidence in rodents (Lv et al., 2014) and non-human primates (Mattison et al., 2017). Some of mechanisms elicited by CR diets include reduction of glycemia, insulin levels and systemic attenuation of the signaling cascades induced by insulin-like growth factor (IGF-1) (Kanarek et al., 2020) (**Figure 2**). IGF-1 activates molecular pathways such as MAPK and PI3K-Akt-mTOR involved in cell proliferation as well as accelerated glycolytic and anabolic metabolism. Indeed, a catabolic metabolism by fatty acid oxidation and induction of apoptosis depending on activation of AMPK pathway have been reported under CR regimens (O'Flanagan et al., 2017), (Kanarek et al., 2020).

CR has also been involved in autophagy induction, cellular process with dual roles in cancer progression (Tajan and Vousden, 2020). CR has shown to reduce the expression of transcription factors involved in synthesis of inflammatory factors in cancer cells (O'Flanagan et al., 2017). Despite the impact that CR might have in these signaling cascades, some malignant cells can display resistance to this dietary intervention due to aberrant mutations in tumor suppressors such as p53 and phosphatase and tensin homolog (PTEN) as well as in oncogenes such as c-Myc, IGF-1 receptor and downstream effectors (Buono and Longo, 2018). CR restriction based on reduction of dietary carbohydrate content is not only beneficial by reducing glucose but fructose (Kanarek et al., 2020). Apart from glucose feeding devouring tumor cells, fructose has been shown to induce glycolysis in gastrointestinal tumor cells, lipogenesis and to enhance tumor growth. Indeed, consumption of fructose has been reported to induce the appearance of colorectal carcinoma in genetically modified mice. On the contrary, rather than deprivation, supplementation of mannose has shown to limit tumor growth in mouse xenografts. This is explained by mannose interfering with glucose metabolism due to the usage of the same enzymes while not generating cellular energy (Kanarek et al., 2020).

The anti-tumor effects of CR regimens do not count as anti-cancer therapies unless combined with standard chemotherapeutic treatments (O'Flanagan et al., 2017), (Lévesque et al., 2019) (refer to **Table 1** for clinical trials of dietary interventions in cancer). Indeed, caloric restriction in a 25% as well as CR mimetics such as 2-deoxyglucose sensitized lymphoma-bearing mice to a pro-apoptotic treatment (Meynet et al., 2013). However, even under chemotherapy, persistent CR diets might be detrimental rather than beneficial in cancer patients who have lost body weight and undergo cachexia, sarcopenia and immunodeficiency

following chemotherapy. As an alternative to sustained CR, intermittent CR regimens based on short-term fasting periods have been studied resulting in better outcomes in mouse models of solid cancers when combined with chemotherapeutics (O'Flanagan et al., 2017), (Kanarek et al., 2020).

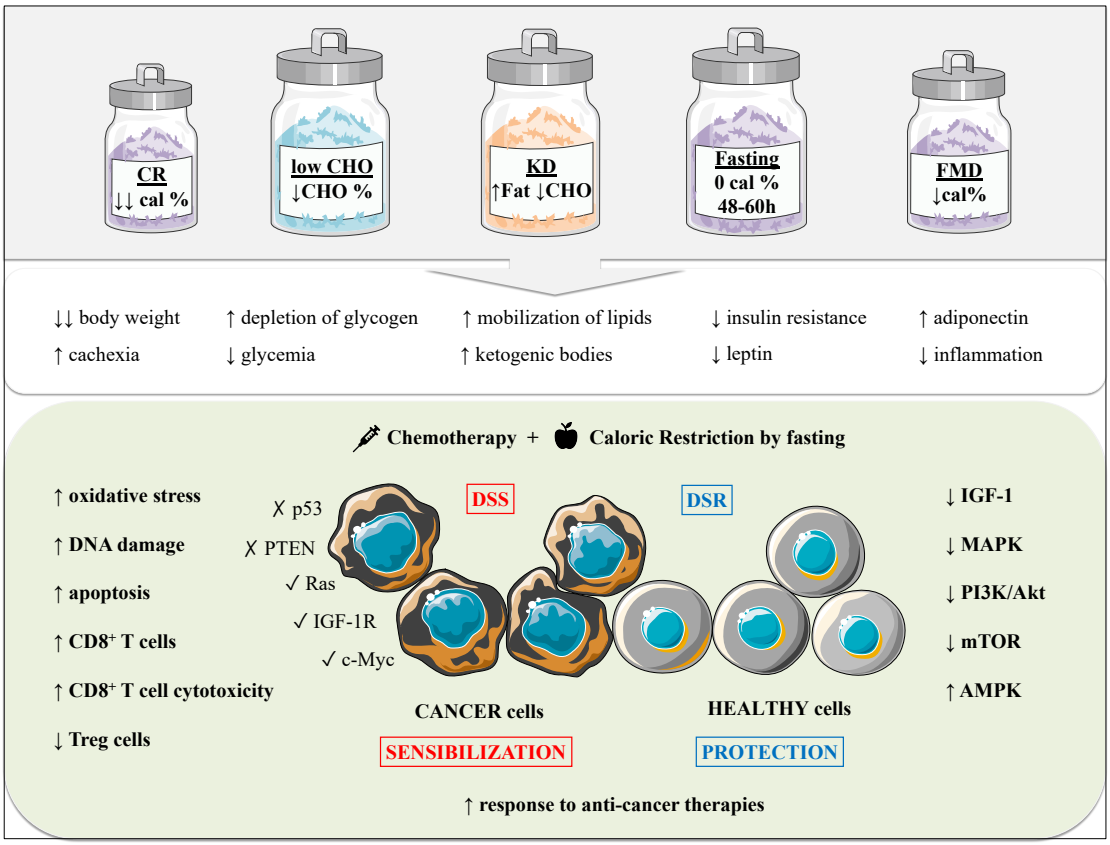

Figure 2. Effects of nutritional caloric restriction, ketogenic diets and fasting regimens

Physiological and metabolic effects of nutritional interventions. Sensibilization of tumor cells and resistance of healthy cells to chemotherapy under nutritional caloric restriction by fasting. CR, caloric restriction; low CHO, low carbohydrate diet; KD, ketogenic diet; FMD, fasting mimicking diet; DSS, differential stress sensibilization; DSR, differential stress resistance; PTEN, phosphatase and tensin homolog; Treg cells, regulatory T cells; IGF-1; insulin-like growth factor; MAPK, mitogen-activated protein kinase; PI3K, phosphatidylinositol-3-kinase; Akt, protein kinase B; mTOR, mammalian target of rapamycin; AMPK, AMP-activated protein kinase.

Alternatives to persistent and intermittent CR diets include the use of CR mimetics which are pharmacological compounds targeting some of the pathways modulated by CR diets (Lee et al., 2021). Rapamycin, the known inhibitor of mTOR, a common signaling pathway hyperactivated in tumors has shown anti-cancer outcomes in mouse models of solid cancers. Likewise, the anti-diabetic metformin has shown to limit tumor growth in several solid and liquid cancers as well as in combination with anti-cancer therapies in clinical trials. Resveratrol, a fruit polyphenol and sirtuin activator showed anti-tumoral effects in several cancer mouse models but the opposite in combination with a chemotherapeutic for breast

cancer. Hydroxycitrate, a weight-loss compound has shown anti-tumoral effects in combination with some chemotherapeutics (O'Flanagan et al., 2017).

Alternatives to caloric restriction by reduction in the content of dietary macronutrients without changes in total calories, isocaloric diets, have proved to have anti-cancer effects in combination with pro-apoptotic treatments (Rubio-Patiño et al., 2016) (**Figure 2**). An isocaloric nutritional regimen reduced 25% in carbohydrates has shown to promote apoptosis by decreasing the expression of the anti-apoptotic factor Mcl-1 in Eμ-Myc lymphoma-bearing mice. The low carbohydrate diet (low CHO) diet activated the AMPK pathway resulting in inhibition of mTOR, attenuation of protein translation and lower expression levels of Mcl-1 in malignant lymph nodes. Mice bearing lymphoma tumors showed prolonged survival when treated with a pro-apoptotic chemotherapeutic under low CHO diet. Therefore, the low CHO diet sensitized lymphoma-bearing mice to chemotherapeutics by targeting tumor intrinsic anti-apoptotic mechanisms involved in anti-cancer therapy resistance (Rubio-Patiño et al., 2016). Other alternatives to caloric restriction diets include isocaloric ketogenic diets that are low in carbohydrates but high in fat content that might be safer to implement in advanced cancer patients with impaired physical conditions (Kanarek et al., 2020).

I.1.2 Ketogenic diets

Ketogenic diets (KDs) are other regimens mimicking some of the physiological and systemic effects of CR regimens. This dietary intervention is based on extremely low carbohydrate, low protein and high fat content to potentiate the synthesis of ketogenic bodies (acetoacetate, acetone and D-β-hydroxybutyrate) by hepatic fatty acid β-oxidation (Weber et al., 2020) (**Figure 2**). The use of KG diets as an anti-cancer intervention was stimulated by the hypothesis based on the Warburg effect that tumors relying on a glycolytic metabolism might be more inflexible to generate energy from alternative carbon sources such as lipids and ketogenic bodies (Weber et al., 2020), (Tajan and Vousden, 2020). Nowadays, it is recognized that some tumor cells can metabolize ketone bodies. The anti-cancer impact of KDs can indeed be associated with the general improvement of life quality since ketogenic bodies are metabolic and signaling modulators of inflammation and oxidative stress (Puchalska and Crawford, 2017).

KDs have shown to limit tumor growth in mouse models of solid cancers and to synergize with anti-cancer therapies. In addition, cachexia preventive effects have been reported in cancer patients under chemotherapy (O'Flanagan et al., 2017), (Weber et al., 2020) (**Table 1**). Despite the positive impact of a KD (1% carbohydrate, 18% protein and 81% kcal fat) limiting tumor growth and lowering glycemia (Shukla et al., 2014), another ketogenic recipe (9% protein and 91% kcal fat) also diminished glycemia without changes in tumor

progression and survival of tumor-bearing animals (De Feyter et al., 2016). Versions of ketogenic regimens with very low or null carbohydrate content and different percentage of fat and protein might count for the different outcomes in mouse models of cancer. Aside from the anti-cancer benefits of diets limited in carbohydrates and enriched in fat, some studies have pointed out that the nature of these macronutrients such as low glycemic load carbohydrates and unsaturated fatty acids might have more impact on human health rather than their proportion (Ludwig et al., 2018).

A realistic review of 29 animals studies in which KDs were implemented in already tumor-bearing mice showed that 72% of the studies reported limited tumor growth and increased animal survival (Klement, 2017). In clinical trials, 42% of 24 human studies reported anti-tumoral effects (Lévesque et al., 2019) (**Table 1**). Different dietary ketogenic formulas, variability in the dietary compliance among patients, few numbers of participants in the studies and diet implementation at late disease stages might explain the lower number of clinical trials reporting clear anti-cancer benefits of KDs (Kanarek et al., 2020), (Weber et al., 2020). Apart from reduced glycemia, a decreased glycolytic flux with concomitant lower levels of lactate and markers of the pentose phosphate pathway have been detected in tumors. Other physiological benefits were gain of body weight in cachexic cancer patients and healthier parameters of body composition in patients under radiotherapy (Klement, 2017). Indeed, stage IV non-small cell lung cancer patients under KD in combination with short-term fasting and breast cancer patients under KD as complementary treatment to chemotherapy have displayed longer overall survival (Klement, 2020).

Table 1. Clinical trials of dietary regimens as monotherapy or in combination with anti-cancer therapies

Examples include recruiting, ongoing and completed clinical studies. Taken and adapted from (Lévesque et al., 2019)

Dietary intervention	**Cancer type**	**Anti-cancer intervention (Number of clinical trial)**
Fasting different versions	breast cancer/ advanced solid tumors	platinum chemotherapy (NCT00936364) docetaxel, doxorubicin, cyclophosphamide (NCT01175837 and NCT01304251) paclitaxel, trastuzumab, pertuzumab (NCT02379585)
Fasting- mimicking diets different versions	breast/ prostate/ ovarian/ melanoma/ non-small cell lung/ advanced lung adenocarcinoma/ gynecological	Chemotherapy (NCT01954836, NCT02710721 and NCT03162289) Neoadjuvant chemotherapy (NCT02126449) Standard therapies (NCT03340935)

Dietary intervention	Cancer type	Anti-cancer intervention (Number of clinical trial)
		Surgery (NCT03454282) Chemo-, hormono-, targeted or immunotherapies (NCT03595540) Carboplatin, pemetrexed and pembrolizumab (NCT03700437) Metformin (NCT03709147)
Ketogenic diets different versions	high-grade glial/ brain/ malignant glioma/ recurrent/refractory/end-stage glioblastoma/ glioblastoma multiforme/ head and neck/ breast/ breast ER^+/ stage IV breast/ non-small cell lung/ lung ovarian and endometrial/ pancreatic/ prostate primary central nervous system lymphoma/ metastatic cancers	None (NCT01092247, NCT01716468, NCT01865162, NCT02092753, NCT02286167, NCT03160599, NCT03171506, NCT03194516,) Chemoradiation (NCT01419483, NCT01419587, NCT01975766, NCT02046187, and NCT02516501) Surgery (NCT02744079 and NCT03285152) Surgery followed by chemo- and radiotherapy (NCT01535911) Radiation and temozolomide (NCT02302235) Paclitaxel (NCT03535701)
Very low-carbohydrate diet for 28 days	advanced cancer	None (NCT00444054)
Carbohydrate-restricted diet	non-squamous non-small cell lung	metformin with platinum-based chemotherapy (NCT02019979)
Low- or medium-glycemic diet for 12 weeks	colon	None (NCT02129218)
Carbohydrate restricted diet (6 months)	prostate	None (NCT03679260)
Very low-carbohydrate and high-fat diet	colorectal adenocarcinoma	None (NCT03221920)
Protein-restricted diet	prostate	None (NCT01692587)
Low protein diet from a week before to 10 days after treatment	metastatic castrate-resistant prostate	Sipuleucel-T (NCT03329742)
Vegetarian vs vegan diets	any type	prescribed therapy

Dietary intervention	Cancer type	Anti-cancer intervention (Number of clinical trial)
(6 months)		(NCT02437474)

Importantly, although most of tumors are fed by glucose, few of them can benefits from lipids for expansion (Kanarek et al., 2020). In these rare cases, carbohydrates as energetic sources would be more beneficial than ketogenic bodies as anti-cancer interventions. Therefore, the metabolic preferences of the type of tumor should be considered prior to recommend and implement dietary regimens to cancer patients (Kanarek et al., 2020).

I.1.3 Fasting

Fasting is nowadays a very common dietary approach in the research field due to the positive benefits seen in health indicators of individuals suffering of obesity, diabetes, cardiovascular diseases, neurodegenerative diseases as well as oncogenic pathologies (Lee et al., 2021). There is a wide spectrum of fasting nutritional regimens ranging from intermittent to periodic fasting. The former alternates periods from 16 to 48 h of none or low food intake with standard food consumption on regular basis whereas the latter refers to fasting or fasting-mimicking diets (FMDs) applied from 2 to 21 days or more (Mattson et al., 2017). FMDs based on plant-derived nutrients, restricted in total calories over the time, with similar percentage of carbohydrates and fats are designed to mimic the physiological and metabolic effects of fasting while decreasing the adverse effects associated with no food intake for long-term. Another eating program has been called time-restricted feeding where food consumption is scheduled at a specific time during the day for a limited period of hours (Buono and Longo, 2018). A phase I clinical trial in cancer patients receiving standard anti-cancer treatment has shown that a cyclic FMD (5 days consuming the FMD and from 16 to 23 days of refeeding) potentiates the systemic and intra-tumoral immune response based on reduction of circulating myeloid-derived suppressor cells and higher intra-tumoral infiltration of cytotoxic T cells (Vernieri et al., 2022).

All versions of fasting regimens result in a normal low glycemia, use of the glycogen stores, fatty acid catabolism, generation of ketogenic bodies and decreased plasma levels of leptin, a hormone controlling the appetite and increased plasma levels of adiponectin, a hormone with glycolytic and lipolytic effects (Mattson et al., 2017), (Lee et al., 2021) (**Figure 2**). These metabolic effects are shared between KDs and fasting regimens although there are distinctive processes potentiated by the particularities of each dietary regimen and their modalities. Usage of ketogenic bodies as energetic fuel is an adaptive mechanism to fasting developed by

animals along evolution that might be advantageous and provide resistance to challenging health conditions such as cancer (Mattson et al., 2017).

The different responses of healthy and malignant cells to short-term fasting have been shown to mediate a better physiological outcome upon chemotherapy (O'Flanagan et al., 2017). These physiological phenomena have been defined as differential stress resistance (DSR) and differential stress sensibilization (DSS) (**Figure 2**). Fasting impacting negatively on the mitogenic signaling driven by IGF-1 attenuates proliferation and metabolism of heathy cells. Therefore, healthy cells are more protected and resistant to the cytotoxic effects of chemotherapeutics targeting highly proliferating cells. On the contrary, tumor cells which elicit compensatory mechanisms driving cell growth and anabolic metabolism upon reduced IGF-1 signaling are sensitized to chemotherapy (Buono and Longo, 2018), (Tajan and Vousden, 2020).

Mice bearing subcutaneous breast cancer allografts have shown limited tumor growth after 2 cycles of fasting (48-60 h) (Lee et al., 2012). This effect was maximized under fasting and chemotherapy as an example of DSS. Likewise, allografts of melanoma and glioma as well as xenografts of human triple negative breast cancer and ovarian cancer showed limited tumor growth when fasting was combined with chemotherapy. As an example of DSR, fasting allowed multiple treatments with doxorubicin in tumor-bearing mice that in the absence of fasting showed early lethality. Mouse models of different solid cancers showed prolonged animal survival and less metastasis under the combination of fasting and chemotherapy. Mechanistically, starvation of *in vitro* tumor cells resulted in DNA damage and ROS generation, effects potentiated upon chemotherapy (Lee et al., 2012).

As chemotherapy is associated with adverse side effects but are the standard treatment for many types of cancer, fasting regimens are intensively studied to improve responses to chemotherapy by making malignant cells more vulnerable while conferring protection to healthy tissues (Tajan and Vousden, 2020). Indeed, FMDs low in calories, low in proteins, high in complex carbohydrates and high in fats have been beneficial in reducing physiological side effects when applied to patients prior and after chemotherapy in several clinical trials (de Groot et al., 2020), (Lévesque et al., 2019) (Table 1). Beyond the DSR and DSS phenomena, positive impact of fasting dietary regimens on the anti-tumoral immune response has been also reported to potentiate the effects of chemotherapy in cancer mouse models by enhancing recruitment of more cytotoxic $CD8^+$ T lymphocytes into the TME (Buono and Longo, 2018).

I.1.4 Protein-restricted diets

Low consumption of animal protein has been associated with low risks of all-cause and cancer mortalities at middle age while a negative correlation has been found with aging

(Levine et al., 2014) (**Figure 3**). This finding is based on a study with approximately 6000 adults with a mean age of 65 years reporting that high protein consumption in the group of 50-65 years old associated with high risk of cancer-related mortality even after controlling for the percentage of calories derived from carbohydrates and fat. Interestingly, higher consumption of protein specifically from animal sources was significantly associated with higher risk of cancer-related mortality. Furthermore, the association between protein intake and cancer mortality was the inverse in the older population (> 66 years old) indicating that protein consumption irrespective of the source is in indeed beneficial in elderly individuals probably due to different nutritional requirements of this age group. Mechanistically, levels of IGF-1 were positively associated with protein consumption in both age groups and were found to mediate the association between protein intake and risks of cancer-related mortality (Levine et al., 2014).

In pre-clinical studies, anti-cancer preventive effects of a low protein diet were reported in subcutaneous melanoma and breast tumor-bearing mice primed for a week with low (4-7 %) and high (18 %) protein isocaloric diets prior to tumor cell transplantation (Levine et al., 2014) (**Figure 3**). Mice under low protein diet showed limited tumor growth which negatively associated with blood levels of IGF-1. Indeed, melanoma-bearing mice deficient in IGF-1 signaling also displayed limited tumor growth (Levine et al., 2014).

Subcutaneous xenografts of prostate and breast cancer displayed limited growth when mice were fed a 7% protein-containing diet as compared to an isocaloric 21%-containing protein control diet irrespective of diet priming, body weight loss and alterations in glycemia (Fontana et al., 2013) (**Figure 3**). This finding suggests that low protein diets are not only preventive when consumed prior to tumor development but also displayed anti-tumoral effects when consumed during tumor progression. Lower blood levels of IGF-1 and the prostate cancer biomarker PSA as well as attenuation of the mTOR signaling were detected in tumor-bearing mice under low protein diet. Consistently, a synergic anti-tumoral effect was observed under low protein diet in combination with mTOR inhibition. Interestingly, priming mice with 20% protein diets limited tumor growth when proteins were derived from plants while 10% protein diets limited prostate cancer growth irrespective of the source. Therefore, anti-cancer preventive effects of low proteins diets can be achieved either by reducing the content of animal protein or consuming vegetal proteins with no restriction (Fontana et al., 2013).

Up to date, there are several clinical trials applying protein-restricted diets in prostate cancer patients (Lévesque et al., 2019) (**Table 1**). The clinical trial completed with patients no receiving anti-cancer therapies has reported metabolic benefits such as improvement of insulin and leptin sensibility (NCT01692587). A clinical trial applying dietary protein

restriction prior and after dendritic cell-based vaccination in metastatic castrate-resistant prostate cancer (NCT03329742) and a study of vegetarian versus vegan diet (NCT02437474) have been completed but results related to cancer progression, respond to anti-cancer therapies and tumor remission are not publicly available (Lévesque et al., 2019). Despite the lack of conclusive results, this dietary intervention seems to be promising in the clinic, at least for prostate cancer patients (**Table 1**).

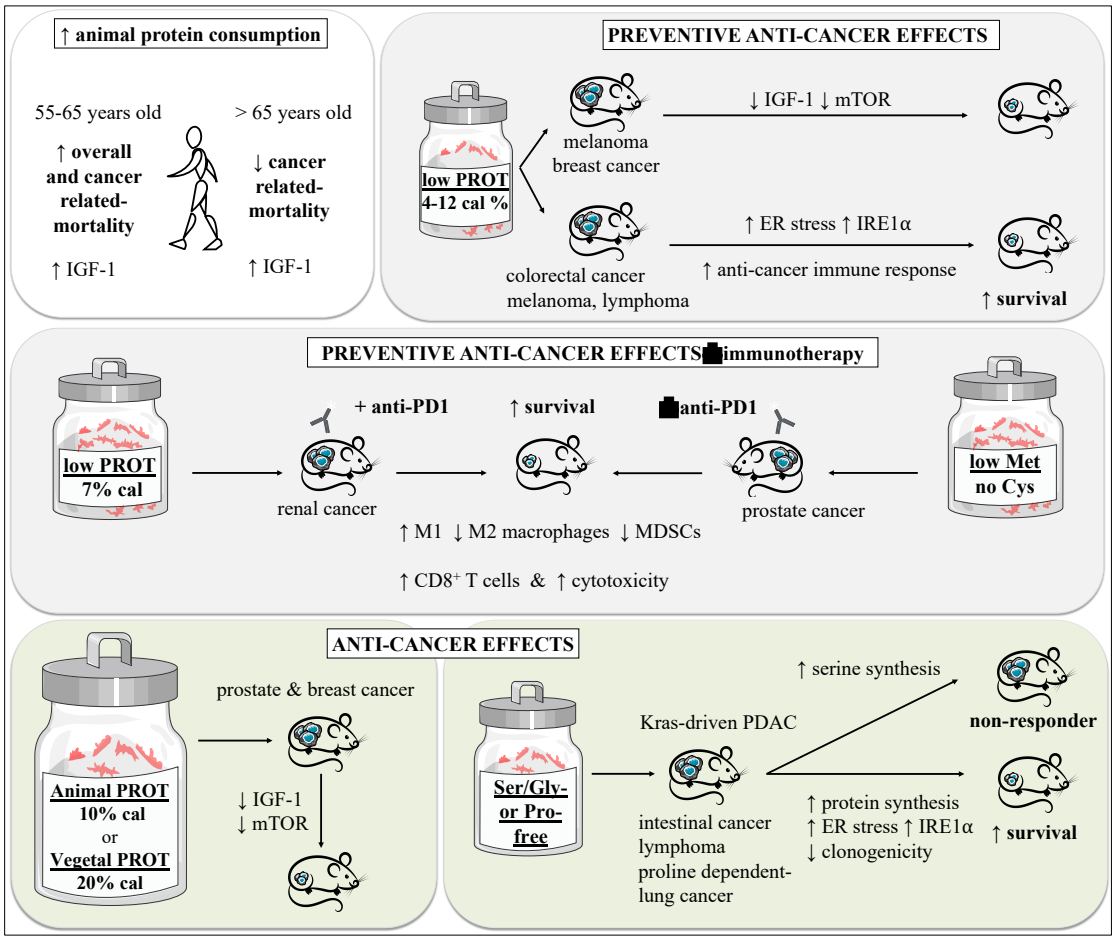

Figure 3. Anti-cancer effects of protein- and amino acid-restricted diets

Epidemiological human studies and pre-clinical studies in cancer mouse models show the benefits of consuming animal protein-restricted diets, vegetal protein-containing diets and amino acid-restricted diets. In pre-clinical studies, protein- and amino acid-restricted diets display preventive as well as anti-cancer effects by reduction of IGF-1 levels and mTOR activation, induction of ER stress and enhancement of the anti-cancer immune response. Low PROT, low protein diet, ER, endoplasmic reticulum; IRE1α, inositol-requiring protein 1α; IGF, insulin-like growth factor; mTOR, mammalian target of rapamycin; Met, methionine; Cys; cysteine; Ser, serine; Gly, glycine; Pro, proline; MDSCs, myeloid-derived suppressor cells.

No impact of reduction in dietary proteins on cancer progression in subcutaneous glioma-bearing mice fed a 4% protein diet ten days after tumor cell transplantation has been reported (Brandhorst et al., 2013). Although controversial results, low proteins diets with anti-tumoral

effects report an underlying attenuation of the IGF-1 signaling as CR, KDs and fasting. Therefore, mitigation of the signaling cascades triggered by this hormone such as the mTOR pathway is a common feature of dietary regimens as anti-cancer interventions. However, novel molecular pathways independent of mTOR activation have been found to mediate the protective anti-tumoral effects of low protein diets (Rubio-Patiño et al., 2018b).

A protein-restricted diet containing 12% of protein has been reported to extend survival of lymphoma-bearing mice and to limit tumor growth of subcutaneous melanoma and colorectal carcinoma mouse models (Rubio-Patiño et al., 2018b) (**Figure 3**). Among different low protein diets, only nutritional regimens with partial protein reduction of 12.5% and 25% displayed anti-tumoral effects in mice primed with the diet prior to tumor cell transplantation. Interestingly, neither modulation of the GCN2 (general control nonderepressible 2), the Akt/mTOR pathway nor autophagy induction were seen as underlying mechanisms of the protein-restricted diet. Rather, specific activation of a member of the endoplasmic reticulum (ER) stress response was found activated in colorectal carcinoma tumors under low protein diet. Indeed, the low protein diet showed an anti-tumoral protection dependent on activation of the ER stress sensor IRE1α in tumor cells (Rubio-Patiño et al., 2018b).

The vulnerability of tumors under low protein regimens are beyond the intrinsic molecular mechanisms of malignant cells (Tajan and Vousden, 2020). The enhancement of the anti-cancer immune response counts as one of the systemic physiological effects of protein-restricted diets. Indeed, the above-mentioned study reported a stronger anti-cancer immunosurveillance under low protein diet (Rubio-Patiño et al., 2018b) (**Figure 3**). The anti-tumoral effects of this protein-restricted diet depended on cytotoxic T lymphocytes that were highly recruited to the TME and displayed higher effect functions (Rubio-Patiño et al., 2018b). Another study has reported the synergism between a 7% protein diet and immune checkpoint inhibition based on PD-1 blockade. The low protein diet was shown to impair tumor growth and extend survival of orthotopic renal tumor-bearing mice under immunotherapy (Orillion et al., 2018).

Amino acid-restricted diets, rather than partial or full protein dietary restriction are also alternatives under investigation due to the high risk of cachexia (Tajan and Vousden, 2020) and sarcopenia in cancer patients (Buono and Longo, 2018).

I.1.5 Amino acid-restricted diets

Dietary protein-restricted regimens including nutritional formulas lacking methionine or methionine and cysteine have been reported to synergize with immunotherapies in pre-clinical studies (Orillion et al., 2018) (**Figure 3**). Reducing the content of methionine or methionine and cysteine in cell culture media polarized bone marrow-derived macrophages (BMDMs)

toward an anti-tumoral phenotype. Macrophages with anti-tumoral phenotypes (canonically considered as M1-like phenotypes) display immunostimulatory and anti-cancer properties including the expression of IL-12, inducible nitric oxide synthase (iNOS) and tumor necrosis factor α (TNFα) (Pathria et al., 2019) (refer to section III.1.4). An 80 % methionine-restricted diet lacking cysteine limited tumor growth in mice bearing prostate cancer depending on the presence of macrophages. Indeed, tumor slowdown under methionine-restricted diet was as effective as immunotherapy blocking the surface expression of the T cell immune checkpoint PD1 with an antagonist antibody (refer to section III.3.1). The combination of the diet and PD1 blockade enhanced the anti-cancer immunosurveillance by potentiating the recruitment of M1 macrophages and cytotoxic T cells while decreasing the infiltration of pro-tumoral M2 macrophages and myeloid-derived suppressor cells (Orillion et al., 2018).

Nutritional formulas deprived in serine and glycine (SG) also displayed anti-tumoral effects in genetically engineered mouse (GEM) models of Apc-driven intestinal cancer and Eμ-Myc driven-lymphoma (Maddocks et al., 2017) (**Figure 3**). Consumption of the SG-deprived diet by mice bearing neoplastic tumors increased survival of the two GEM models and limited tumor growth in the intestinal cancer model. The SG-deprived diet also limited tumor growth in mice with established subcutaneous human colorectal tumors and induced necrosis in subcutaneous Eμ-Myc tumors. Interestingly, the SG-free diet synergized with increased levels of reactive oxygen species (ROS) induced by genetic modification for extension of survival of lymphoma-bearing mice. Therefore, SG-free diets may be suitable in combination with chemotherapeutics and radiotherapy controlling tumor growth by induction of ROS in pre-clinical studies (Maddocks et al., 2017).

The anti-tumoral effects of dietary deprivation of non-essential amino acids such as serine and glycine may depend on the oncogenic signaling and the origin of the tissue (Maddocks et al., 2017). Indeed, a SG-free diet did not extend the survival of two GEM models of pancreatic ductal adenocarcinoma (PDAC) (**Figure 3**). Kras activation in the Kras-driven PDAC GEM model induced the expression of several enzymes of the serine biosynthesis pathway explaining the resistance of PDAC-bearing mice to SG nutritional starvation (Maddocks et al., 2017).

The anti-cancer effects of amino acid-deprived dietary formulas depend on the ability of tumor cells to compensate for the lack of that specific nutrient (Sahu et al., 2016). For instance, a proline-deprived diet has shown to limit tumor growth of subcutaneous lung cancer xenografts (**Figure 3**). This effect was only observed when tumor cells where highly dependent on *in vitro* exogenous supplementation of the non-essential amino acid proline for acquisition of tumor-initiating potential. Indeed, the tumor-suppressive potency of the proline-free diet was seen in mice with stablished tumors. The dependency on proline uptake

was a consequence of a defective proline synthesis pathway by c-Myc-mediated transcriptional downregulation of several enzymes contributing to proline synthesis in lung tumor cells. Mechanistically, depletion of proline led to uncontrolled protein synthesis in a mTOR-independent manner, unresolved ER stress mediated by IRE1α activation in exogenous proline dependent cells (Sahu et al., 2016).

The distinctive amino acid requirements of oncogenic malignances determine the impact of dietary protein restriction as anti-cancer interventions (Tajan and Vousden, 2020). Although cancers show different circulating amino acid profiles, glutamine, tryptophan and citrulline are commonly reduced in several solid cancers (Pavlova and Thompson, 2016). High requirement of these amino acids could be exploited to design amino acid-deprived diets that successfully control tumor progression (Pavlova and Thompson, 2016). In addition, the gut microbiota tightly involved in most physiological processes and the immune response is profoundly modulated by the wide repertory of nutritional regimens mentioned along this chapter. The interaction between the microbiome and nutrients under specific dietary regimens also count for the effects of nutritional formulas as anti-cancer interventions (Yin et al., 2018), (Tajan and Vousden, 2020).

I.2 Oncometabolism

Altered metabolism as a hallmark of cancer is exploited by neoplastic tissues to acquire an advantageous plasticity to support tumor cell development and expansion (Faubert et al., 2020). Opportunistic profit from the extracellular matrix at the expense of nutrient competition and stromal cell reprograming, nutrient channeling towards metabolic pathways supporting oncogenesis and quick adaptation to challenging metabolic conditions are involved in all the stages of tumor evolution. The main metabolic alterations associated with tumorigenesis include uncontrolled uptake of glucose and amino acids such as glutamine, anabolic metabolism and production of NAPDH using glycolytic and TCA cycle anaplerotic substrates, differential acetyl-CoA-mediated epigenetic modifications and environmental metabolic modifications (Pavlova and Thompson, 2016), (Faubert et al., 2020). State-of-the-art studies in the field of cancer metabolism benefits from metabolomics as the gold standard approach for identification and quantitation of the cancer metabolome (Jang et al., 2018), (Faubert and DeBerardinis, 2017). Whereas steady-state metabolomics informs about alterations in metabolite levels, stable isotope tracing of labeled nutrients helps to infer aberrant metabolic pathways deployed by malignant tissues (Antoniewicz, 2018), (TeSlaa et al., 2021), (Fernández-García et al., 2020), (Hui et al., 2020).

I.2.1 Catabolism of glucose

The most consumed exogenous nutrients by highly proliferating cells are glucose and glutamine which are catabolized to support cellular bioenergetics and biosynthesis (Pavlova and Thompson, 2016). Glucose, for instance, is metabolized through glycolysis which is an oxidative sequence of ten cytoplasmic reactions yielding either pyruvate that can be further channeling into the tricarboxylic acid (TCA) cycle for oxidative phosphorylation (OxPhos) or lactate (**Figure 4**). Production of lactate as in anaerobic fermentation but in the presence of oxygen occurs in rapidly proliferating cells by aerobic glycolysis (Pavlova and Thompson, 2016), (Lane et al., 2020).

The glycolytic pathway is characterized by reduction of NAD+ to NADH and inefficient but quick generation of energy (2 ATP molecules per mole of glucose) (Pavlova and Thompson, 2016) (**Figure 4**). Highly proliferating cells deployed aerobic glycolysis for rapid ATP production and recovering of oxidized NAD+ molecules when producing lactate to maintain the glycolytic flux. A higher ratio NAD+/NADH and lower accumulation of ATP in the cytoplasm when glycolysis is uncoupled to the TCA cycle and OxPhos positively feedback to continue glucose catabolism through aerobic glycolysis. Aerobic glycolysis is also deployed by rapid proliferating cells to support biosynthesis and increase cell biomass. Indeed, the ratio of NAD+/NADH determines the oxidative cellular power to support nucleotide and amino acid synthesis (Pavlova and Thompson, 2016), (Lane et al., 2020). Glycolytic intermediates are also channeled into the pentose phosphate pathway (PPP) for generation of ribose rings needed for *de novo* nucleotide biosynthesis. Glycolytic intermediates are also substrates for synthesis of amino acids such as serine and glycine and for fatty acid synthesis via acetyl-CoA (O'Neill et al., 2016), (Lane et al., 2020).

Full oxidation of glucose through the TCA cycle coupled to OxPhos as compared to aerobic glycolysis is a more efficient pathway for energy production (30 ATP/glucose). The TCA cycle is a series of ten mitochondrial reactions starting from acetyl-CoA condensation with oxaloacetate to render citrate and finishing in generation of 4 carbon-oxaloacetate to reinitiate the cycle. Acetyl-CoA can be supplied either by glycolysis via pyruvate or by fatty acid catabolism. The TCA cycle yields reducing equivalents such as NADH and FADH2 that generate the electrochemical gradient used for the electron transport chain for generation of ATP across the mitochondrial membrane (**Figure 4**). In addition, TCA cycle intermediates serve as carbon sources for amino acid and fatty acid synthesis, metabolic processes depending on growth factors or oncogenic signaling (O'Neill et al., 2016), (Lane et al., 2020).

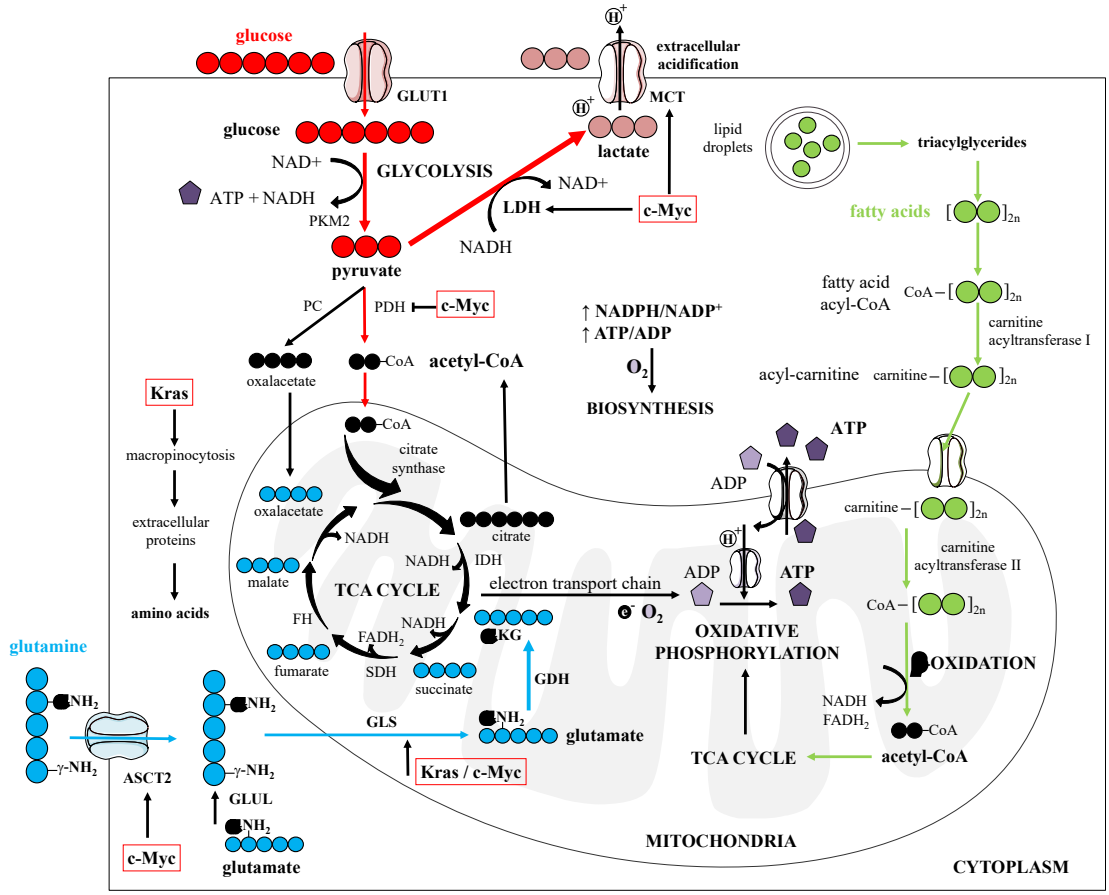

Figure 4. Catabolic metabolism and oncogenic regulation

Glucose, glutamine and fatty acid catabolism as energetic sources. The Warburg effect is represented with thicker red arrows. Intermediate metabolites derived from glucose, glutamine and fatty acids catabolism are represented with the corresponding colour of the precursor. Metabolites represented in black can be generated from more than an energetic source. GLUT1, glucose transporter 1; PKM2, pyruvate kinase muscle isozyme 2; PDH, pyruvate dehydrogenase; PC, pyruvate carboxylase; IDH, isocitrate dehydrogenase; SDH, succinate dehydrogenase; FH, fumarate hydratase; ASCT2, neutral amino acid exchanger; GLS, glutaminase; GDH, glutamate dehydrogenase.

I.2.2 Catabolism of glutamine

Replenishment of the TCA cycle is also mediated by glutamine at the level of α-ketoglutarate, an anaplerotic TCA cycle substrate (O'Neill et al., 2016) (**Figure 4**). Glutamine is enzymatically deamidated in the mitochondria losing its γ-nitrogen to render glutamate by the action of glutaminase (GLS). Glutamate is in turn deaminated losing its α-nitrogen by glutamate dehydrogenase (GDH) contributing to the mitochondrial of pool of α-ketoglutarate that fuels the TCA cycle. When glutamate is deaminated by aminotransferases, α-ketoglutarate and other non-essential amino acids (NEAAs) are generated such as aspartate, alanine and serine (Zhang et al., 2017), (Lukey et al., 2017), (Kurmi and Haigis, 2020).

I.2.3 Catabolism of fatty acids

Aside from glucose and glutamine as a bioenergetic fuels, fatty acids also count as energetic sources (O'Neill et al., 2016) (**Figure 4**). Catabolism of fatty acids by β-oxidation takes place in mitochondria and renders acetyl-CoA and reducing equivalents such as NADH and FADH2 for the largest production of ATP (Lane et al., 2020). Activation of fatty acids with acetyl-CoA is the first step occurring in the cytoplasm prior to transfer into the mitochondria by a process mediated by carnitine conjugation to the acyl-CoA-fatty acids containing chains of more than six carbons (O'Neill et al., 2016).

I.2.4 The Warburg effect

Cell origin, intrinsic oncogenic and mitogenic pathways dictate the tumor appetite for glucose, glutamine and other nutrients (Pavlova and Thompson, 2016), (Faubert et al., 2020). For instance, glucose uptake and the first reactions of glycolysis are highly upregulated by oncogenic PI3K/Akt/mTOR as well as Ras-driven signaling in cancer cells (**Figure 4**). Noteworthy, aerobic glycolysis decoupled from OxPhos is neither a consequence of defective mitochondrial respiration nor an exclusive feature of malignant tissues. Healthy cells highly proliferating during some differentiation stages or highly active such as effector T lymphocytes also deploy temporal and reversible aerobic glycolysis. On the other hand, cancer cells exhibiting a stem cell-like phenotype which are tightly associated with anti-cancer therapy resistance rely more in ATP production via OxPhos (Pavlova and Thompson, 2016). Indeed, increased mitochondrial respiration and biogenesis was found critical for metastasis of breast cancer cells but not for growth of the primary tumor (Vander Heiden and DeBerardinis, 2017). Lactate as a metabolic byproduct of cancer cells in hypoxic regions can be a carbon source for tumors cells in normoxic areas for anabolic metabolism (Dey et al., 2021).

Production and secretion of lactate while inhibiting generation of acetyl-CoA are processes enhanced by c-Myc and other oncogenic drivers (Faubert et al., 2020) (**Figure 4**). Lactate secretion and accumulation in the local microenvironment acidify the extracellular milieu and impact in stromal cells. High content of lactate has been associated with an immunosuppressive TMEs characterized by impaired anti-cancer functions of T lymphocytes. Furthermore, lactate impacts on endothelial cells and fibroblasts promoting angiogenesis and extracellular matrix remodeling (Pavlova and Thompson, 2016).

I.2.5 Glutamine oncocatabolism and nutrient scavenging in cancer

After Otto Warburg's observation about aerobic glucose metabolism with concomitant production of lactate by malignant tissues, Harry Eagle reported an elevated requirement of

the NEAA glutamine among the 20 dietary amino acids in some mammalian cell lines (Lukey et al., 2017). This is consistent with the highest enrichment of glutamine over the other amino acids in the circulation (Zhang et al., 2017). Indeed, ASCT2, the main transporter of glutamine into the cell is upregulated by c-Myc in some cancer cells (**Figure 4**). The high demand of glutamine explains the limited tumor growth in mice bearing myeloma xenografts and cMyc driven-tumors upon pharmacological inhibition of GLS. GLS expression is indeed altered in tumors and heterozygotic loss of GLS has been shown to delay hepatocarcinogenesis in mice. However, upon glutamine scarcity, tumor cells might need to *de novo* synthesize glutamine while fueling the TCA cycle with glucose through oxalacetate generated by pyruvate carboxylase as seen in mouse models of orthotopic glioma xenografts and Kras-driven lung cancer. Indeed, glutamine synthetase (GLUL), the enzyme catalyzing glutamine biosynthesis is highly upregulated by c-Myc in a Kras-driven pancreatic cancer mouse model and its inhibition limited tumor growth (Zhang et al., 2017), (Lukey et al., 2017), (Kurmi and Haigis, 2020).

Scavenging of proteins via engulfment of extracellular proteins by macropinocytosis, engulfment of cells and autophagy have been suggested as adaptive and opportunistic means of amino acid replenishment (Zhang et al., 2017), (Kurmi and Haigis, 2020) (**Figure 4**). Indeed, a xenograft of Kras-driven pancreatic cancer showed limited tumor growth upon treatment with a macropinocytosis inhibitor. This suggests that the engulfment of extracellular proteins could be an alternative route of nutrient absorption that upon degradation would yield not only glutamine but other NEAAs and essential amino acids (EAAs) enriching the pool of free amino acids (Zhang et al., 2017). Indeed, c-Myc-induced liver tumors have shown a metabolic plasticity upon GLS inhibition by compensatory mechanisms dependent on amidotransferases to sustain glutamine metabolism (Méndez-Lucas et al., 2020). Likewise, glycolysis was hyperactivated upon GLS deficiency to sustain the TCA cycle. In addition, blocking *de novo* synthesis of serine and fatty acids was overcome by tumor cells via exogenous uptake of nutrients (Méndez-Lucas et al., 2020).

I.2.6 Pentose phosphate pathway and nucleotide biosynthesis

Glucose-derived carbons are the building blocks for feeding the pentose phosphate pathway (PPP) and lipogenesis as well as the hexosamine biosynthetic pathway (HBP) (Pavlova and Thompson, 2016), (Kaushik and DeBerardinis, 2018) (**Figure 5**). The PPP is a cytosolic metabolic route starting from the glycolytic intermediate glucose-6-phosphate and following an oxidative phase that renders NADPH, a reducing cofactor needed for fatty acid synthesis. The second PPP phase is a sequence of non-oxidative reactions producing pentose sugars for nucleotide synthesis. *De novo* nucleotide synthesis also depends on specific amino acids such

as glycine as a carbon source for *de novo* synthesis of purines as well as glutamine and aspartate for formation of the nitrogenous ring of pyrimidine and purine bases (O'Neill et al., 2016), (Pavlova and Thompson, 2016).

I.2.7 De novo lipogenesis

Lipid biosynthesis is an mTOR-regulated pathway fed by intermediate metabolites of glycolysis, the TCA cycle and the PPP (Pavlova and Thompson, 2016). Mitochondrial citrate generated from α-ketoglutarate by reductive carboxylation can be exported into the cytosol to generate acetyl-CoA as the building blocks of straight-chain fatty acids and cholesterol which are synthesized via NADPH-dependent reactions (**Figure 5**). Palmitic acid is used as a precursor of straight- and long-chain fatty acids as well as unsaturated or branched-chain fatty acids. Branched-chain fatty acids also require branched-chain amino acids. Esterification between fatty acids and glycerol-3-phosphate renders a diverse plethora of triglycerides and phospholipids which are energy stores and constituents of biological membranes (O'Neill et al., 2016), (Pavlova and Thompson, 2016).

I.2.8 Synthesis of amino acids

Glutamine is a central NEAA that drives biosynthesis of amino acids as a carbon and nitrogen donor (Pavlova and Thompson, 2016) (**Figure 5**). Amino-transfer reactions of the α-nitrogen of the glutamine remaining in glutamate depend on how much cells rely on GLS activity. A high glutamate: α-ketoglutarate ratio determined by a high GLS activity dictates the transfer of the amine α-nitrogen of the glutamate into α-ketoacids by aminotransferases. Consequently, amino acids such as aspartate, alanine and serine are synthesized. Aspartate can further generate arginine and asparagine, the latter after amidation of aspartate with the amide γ-nitrogen of glutamine. Interestingly, glutamine might be also implicated in uptake of six EAAs and the NEAA tyrosine by efflux of intracellular glutamine through the neutral amino acid antiporter LAT1. Glutamine-derived glutamate is indispensable for biosynthesis of another NEAA such as proline (Pavlova and Thompson, 2016), (Lukey et al., 2017), (Kurmi and Haigis, 2020).

I.2.9 Anabolic oncometabolism

Nucleotide synthesis under oxygen availability seems to be the most limiting anabolic pathway for tumor growth (Vander Heiden and DeBerardinis, 2017). Malignant cells rely on *de novo* nucleotide synthesis and their capacity to promote angiogenesis since exogenous assimilation of nucleotides as compared to uptake of other nutrients is not a favored process. In addition, oxygen levels are also low as compared to the levels of circulating glucose. This

explains why several glycolytic and TCA cycle intermediates as well as amino acids contribute to nucleotide biosynthesis, therefore, to DNA replication and proliferative potential. Indeed, aerobic glycolysis with lactate production partial contributes to a high NAD+/NADH ratio required for nucleotide synthesis in tumor cells (Vander Heiden and DeBerardinis, 2017). Nucleotide biosynthesis is also upregulated by oncogenic signals (**Figure 5**). Expression of c-Myc, loss of the tumor suppressor retinoblastoma (Rb) and mutations in p53 associate with increased expression of several enzymes of this biosynthetic pathway. One of these enzymes is a direct c-Myc target and is also post-translationally regulated by the MAPK and mTOR pathways (Zhang et al., 2017). Indeed, c-Myc expressions regulate the uptake of glutamine and its contribution to nucleotides biosynthesis to sustain the high nitrogen demands of malignant cells (Pavlova and Thompson, 2016). In addition, essential enzymes of the PPP have been found upregulated by oncogenic signaling such as Ras-driven pathways (Pavlova and Thompson, 2016), (Lukey et al., 2017), (Kurmi and Haigis, 2020), (Faubert et al., 2020).

Several enzymes participating in biosynthesis of fatty-acyl chains have been reported upregulated in several tumor cells by c-Myc (Pavlova and Thompson, 2016) (**Figure 5**). Inhibition of these enzymes have anti-cancer effects. When *de novo* fatty acid biosynthesis is compromised in cancer cells, uptake of fatty acids from the extracellular milieu and induction of lipid release from stromal cells to feed tumor cells have been suggested as adaptive mechanisms. In addition, upon cytosolic acetyl-CoA deficit, acetate has been reported to be taken from the TME and incorporated into lipogenic biosynthetic pathways in brain malignancies (Pavlova and Thompson, 2016).

De novo synthesis of some amino acids to increase cellular biomass is a common metabolic feature of tumors (Zhang et al., 2017) (**Figure 5**). Indeed, mutations in PI3K in colon cancer drive upregulation of alanine aminotransferase. Upregulation of alanine and aspartate aminotransferases has also been seen in liver cancer. Upregulation of phosphoserine aminotransferase supports tumor growth and chemotherapy resistance in colorectal cancer. Proline biosynthesis is indeed upregulated by c-Myc. Accumulation of proline might enhance collagen synthesis and extracellular matrix deposition favoring cancer cell invasion (Pavlova and Thompson, 2016), (Faubert et al., 2020). Epigenetic repression of arginine synthesis is common in solid oncogenic malignancies promoting arginine uptake from the extracellular fluid. This may count as a tumor strategy to accumulate aspartate for nucleotide biosynthesis and destinate exogenous arginine to polyamide synthesis which induces tumor proliferation (Pavlova and Thompson, 2016), (Garcia-Bermudez et al., 2020). Indeed, depletion of this NEAA is studied in the clinics for treatment of several solid and liquid cancers. Likewise, depletion of asparagine with L-asparaginase is under investigation for treatment of

hematological tumors that depend on exogenous assimilation of this NEAA (Zhang et al., 2017), (Vander Heiden and DeBerardinis, 2017).

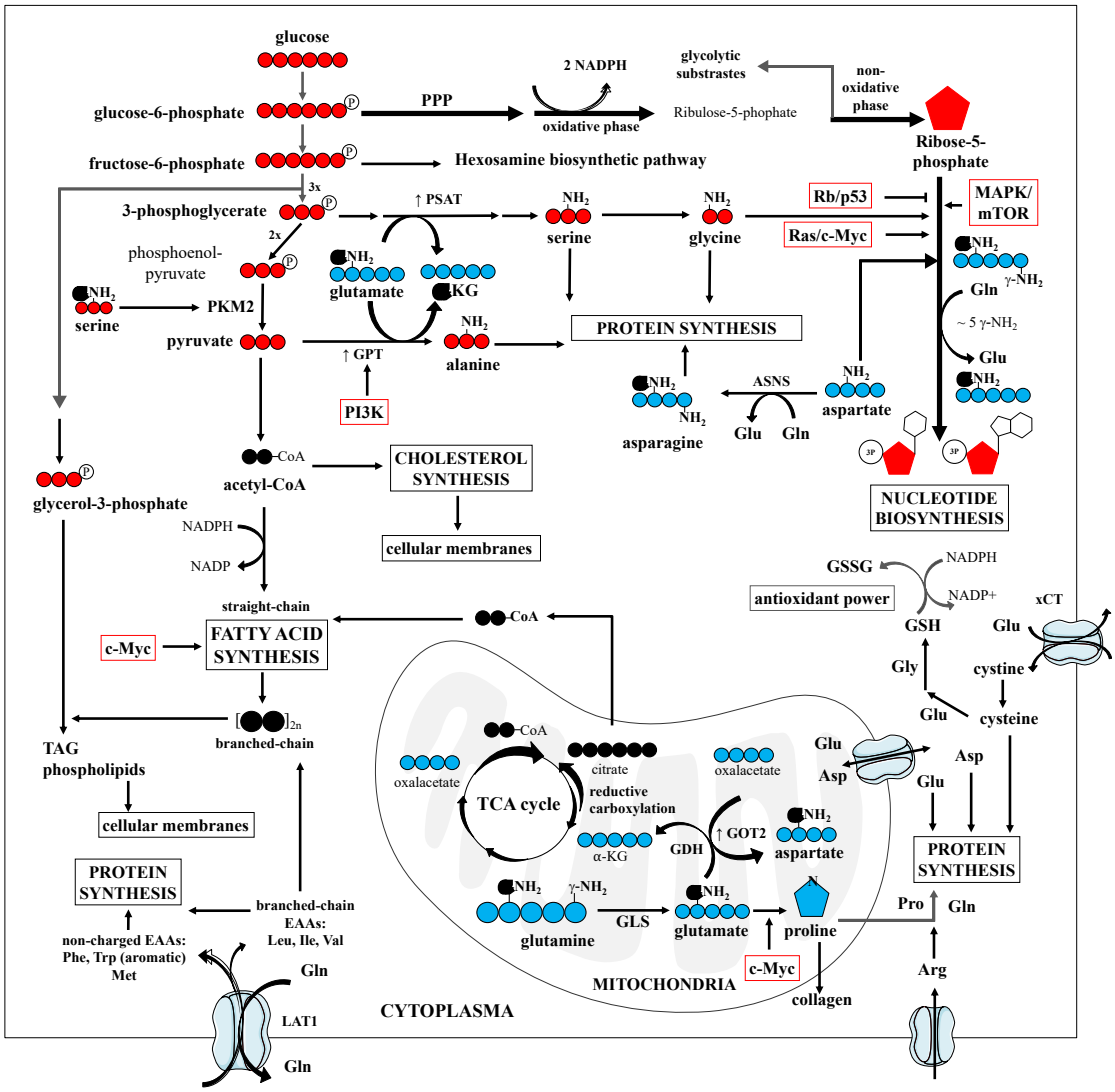

Figure 5. Anabolic metabolism and oncogenic regulation

Synthesis of pentose phosphates and hexosamines from glucose along its catabolism via glycolysis. Synthesis of serine, glycine, alanine from glucose-derived carbons and glutamate-derived amine nitrogen. Synthesis of nucleotides from glucose derived-pentose phosphates and glutamine- and aspartate-derived carbons and nitrogens. Synthesis of TCA cycle intermediates and amino acids from glutamine. Synthesis of proteins from glucose-derived amino acids, glutamine-derived amino acids and exogenous uptake of essential amino acids. Synthesis of cholesterol from acetyl-CoA and fatty acids from acetyl-CoA and branched-chain amino acids. Synthesis of TAG and phospholipids from glycolytic intermediates. Synthesis of glutathione from cysteine, glutamine and glycine. PPP, pentose phosphate pathway; PSAT, phosphoserine aminotransferase; GPT, glutamate pyruvate transaminase; TAG, triacylglycerides; EAA, essential amino acids; LAT1, amino acid transporter; GLS, glutaminase; GDH, glutamate dehydrogenase; GOT2, aspartate aminotransferase; Gln, glutamine; Glu, glutamate; Asp, aspartate; Pro, proline; Gly, glycine; GSH, reduced glutathione; GSSG, oxidized glutathione; , xCT, cystine-glutamate antiporter; ASNS, asparagine synthetase.

Serine is the third metabolite most consumed by cancer cells *in vitro* after glucose and glutamine (Lukey et al., 2017). Indeed, the gene encoding the first enzyme of the serine synthesis pathway was found to be critical for tumorigenesis in a breast cancer xenograft. Indeed, mitogenic signals have been reported to regulate the accumulation of glycolytic intermediates by inhibiting a cancer cell-expressed isoform of pyruvate kinase. Cancer cells benefit from biosynthesis of serine and other metabolites from glycolytic intermediates at expenses of a reduced glycolytic flux (Pavlova and Thompson, 2016), (Faubert et al., 2020),

The tripeptide glutathione and a master cellular antioxidant is also *de novo* synthesized from glutamate, cysteine and glycine to control the redox homeostasis (Lukey et al., 2017) (**Figure 5**). Strengthening of the cellular antioxidant mechanisms is an intrinsic strategy of neoplastic masses to support tumorigenesis, oncogenic evolution, metastasis and resistance to anti-cancer therapies. Indeed, human acute myeloid leukemia and metastatic liver cancer showed upregulation of the enzymes implicated in glutathione biosynthesis (Zhang et al., 2017). In addition, glutamine-derived α-ketoglutarate can function as a cosubstrate of histone demethylases and DNA demethylases driving epigenetic modifications that when suppressed associate with tumorigenesis and anti-cancer therapy resistance (Zhang et al., 2017), (Vander Heiden and DeBerardinis, 2017). Cytosolic acetyl-CoA also modulates epigenetics via acetylation of histones. Oncogenic signaling driven by Ras and Akt activation are implicated in the increase of global histone acetylation in glioblastoma and prostate cancer (Pavlova and Thompson, 2016).

A recent *in vitro* study has reported that despite the major consumption of glucose and glutamine followed by serine, lower uptake of other amino acids from the cell culture medium counts for the majority of the cellular carbon mass in highly proliferating mammalian cells (Hosios et al., 2016). Using lung cancer cells which rely on aerobic glycolysis, glucose and glutamine were shown to minimally contribute to the carbon biomass mainly governed by proteins. In contrast, 15 exogenous amino acids excluding glutamine were the major contributors to the carbon biomass to support proliferation at expenses of glucose and glutamine bioenergetic contributions. In general, glucose and glutamine as carbon sources to increase biomass is secondary to their catabolic fate which are essential to support cell proliferation in *in vitro* cancer cells (Hosios et al., 2016).

I.2.10 The hexosamine biosynthetic pathway

The hexosamine biosynthetic pathway (HBP) is a series of four cytoplasmic reactions starting from the glycolytic intermediate fructose-6-phosphate (Lam et al., 2021) (**Figure 6**). This minor pathway uses from 2 to 3% of the total intracellular glucose for *de novo* biosynthesis of the nucleotide sugar uridine diphosphate N-acetylglucosamine (UDP-GlcNAc) (Marshall et

al., 1991). The free pool of UDP-GlcNAc serves to glycosylate proteins in processes occurring in membranous cellular compartments as well as in the cytoplasm (Lam et al., 2021).

The HBP flux reflects nutrient availability and metabolic dynamics since its sequential reactions require ATP, glucose-derived carbons, the amide nitrogen of the glutamine, acetyl-CoA and nucleotides (Akella et al., 2019), (Lam et al., 2021). The HBP might be considered as a metabolic route favored as part of the oncoanabolism. Indeed, oncogenic Kras has promoted tumor cell growth by inducting the HBP. This pathway also exhibits nutrient-sensing properties since UDP-GlcNAc is involved in regulation of metabolic enzymes. Cytosolic levels of UDP-GlcNAc are dictated by the flux rate of its *de novo* synthesis via the HBP flux and its consumption rate. O-GlcNAcylation cycling by O-GlcNAc transferase (OGT) and O-GlcNAcase (OGA) is critical for controlling the free pool of UDP-GlcNAc. Indeed, OGT and OGA are considered the master regulators of the UDP-GlcNAc levels due to the high affinity of OGT for this substrate as compared to other glycosyltransferases (Hanover et al., 2018), (Biwi et al., 2018), (Akella et al., 2019), (Lam et al., 2021).

Incorporation of glycans to asparagine residues of proteins, known as N-glycosylation occurs co-translationally when peptides translated by ribosomes are simultaneously translocated into the endoplasmic reticulum (ER) for proper folding (Rudd et al., 2001) (**Figure 6**). Apart from the specific advantages that glycan branches confer to proteins such as solubility, stability and protection from proteolytic cleavage, N-glycosylation of proteins serves to signal whether a newly synthesized protein is properly folded and is suitable for trafficking to the Golgi apparatus (GA). If the nascent glycopeptide is misfolded, the protein is targeted by the ERAD machinery to be degraded in the proteasome (Ryan and Cobb, 2012).

The rate-limiting step during synthesis of the oligosaccharide precursor prior to glycosylation of nascent peptides is the incorporation of GlcNAc (Lam et al., 2021). GlcNAc as well as N-acetyl-galactosamine (GalNAc) can also be covalently attached to serine or threonine residues of glycoproteins in a post-translational modification known as O-glycosylation starting in the ER and continuing in the GA (Ryan and Cobb, 2012), (Rudd et al., 2001) (**Figure 6**). N- or O-glycosylation is more characteristic of secreted or surface proteins, fact that highlights the importance of glycans in ligand binding and interaction with extracellular entities. In contrast, O-GlcNAcylation occurring in the cytoplasm by OGT is a feature of post-translationally modified intracellular proteins and plays a regulatory role as protein phosphorylation (Munkley and Elliott, 2016) (**Figure 6**).

N-glycosylated proteins exhibit three major structures 1) high mannose 2) hybrid including terminal GlcNAc linked to downstream mannose residues and 3) complex with bi-, tri- and

tetra-antennary branches composed of galactose, fucose and terminal sialic acid (Ryan and Cobb, 2012) (**Figure 6**). Mammalian N-glycoproteins display complex glycan structures. O-glycosylated structures include 1) mucin-like motifs which are glycan branches elongated from O-GalNAc attached to a peptide and 2) Lewis antigens which are glycan motifs elongated from GlcNAc (Pinho and Reis, 2015). Stabilization of proteins at the plasma membrane is a common property conferred by O- and N-glycan modification. Indeed, N-glycosylation sites are enriched in surface growth factor receptors such as EGFR, IGF-1R, FGFR and PDGFR (Pinho and Reis, 2015).

Anomalies in glycosylated proteins are involved in autoimmunity, cardiometabolic diseases including diabetes and cardiovascular disorders (Štambuk et al., 2021). In addition, glycosylation has gained special attention in cancer beyond the already known functions of proteoglycans which are components of the extracellular matrix and glycosphingolipids constituents of biological membranes (Pinho and Reis, 2015). Indeed, all hallmarks of cancer are modulated by glycosylation (Munkley and Elliott, 2016). Cellular localization of specific glycosyltransferases and glycosidases, their expression and activity dictate the sequential incorporation of saccharidic units on proteins determining the glycan tree structure and composition (Munkley and Elliott, 2016). In general, most aberrant glycoconjugates show alterations in sialylation, fucosylation, O-glycan shortening and N-/O-glycan branching (Pinho and Reis, 2015).

I.2.1 N-glycosylation in cancer

Cancer cells display complex N-glycoproteins containing repeated N-acetyllactosamine units (galactose and GlcNAc) and terminal sialic acid (Pinho and Reis, 2015) (**Figure 6**). The enzyme GnT-V (mannoside acetyl-glucosaminyltransferase 5) mediates a β1-6 branching between mannose and GlcNAc allowing further elongation of the glycan tree in contrast to GnT-III mediating a β1-4 linkage. GnT-V is regulated by the Ras/MARK pathway and its upregulation has been found to drive breast cancer expansion and metastasis. In addition, GnT-V-mediated glycosylation has been implicated in stemness-like features and tumor growth of colon cancer. In contrast, GnT-III competing with GnT-V and blocking branch lengthening has shown to reduce the metastatic outgrowth of melanoma cells. For instance, E-cadherin glycosylation mediated by GnT-V opposite to the action of GnT-III in cancer cells leads to impaired cell-to-cell contacts while potentiating tumor cell migration and metastasis (Pinho and Reis, 2015).

Polysialylation of adhesion molecules on tumor cells is another aberrant modification that correlates with tumor aggressiveness and impaired prognosis in solid tumors (Munkley and Elliott, 2016), (Büll et al., 2014). Indeed, expression of the sialyltransferase ST6Gal-I is not

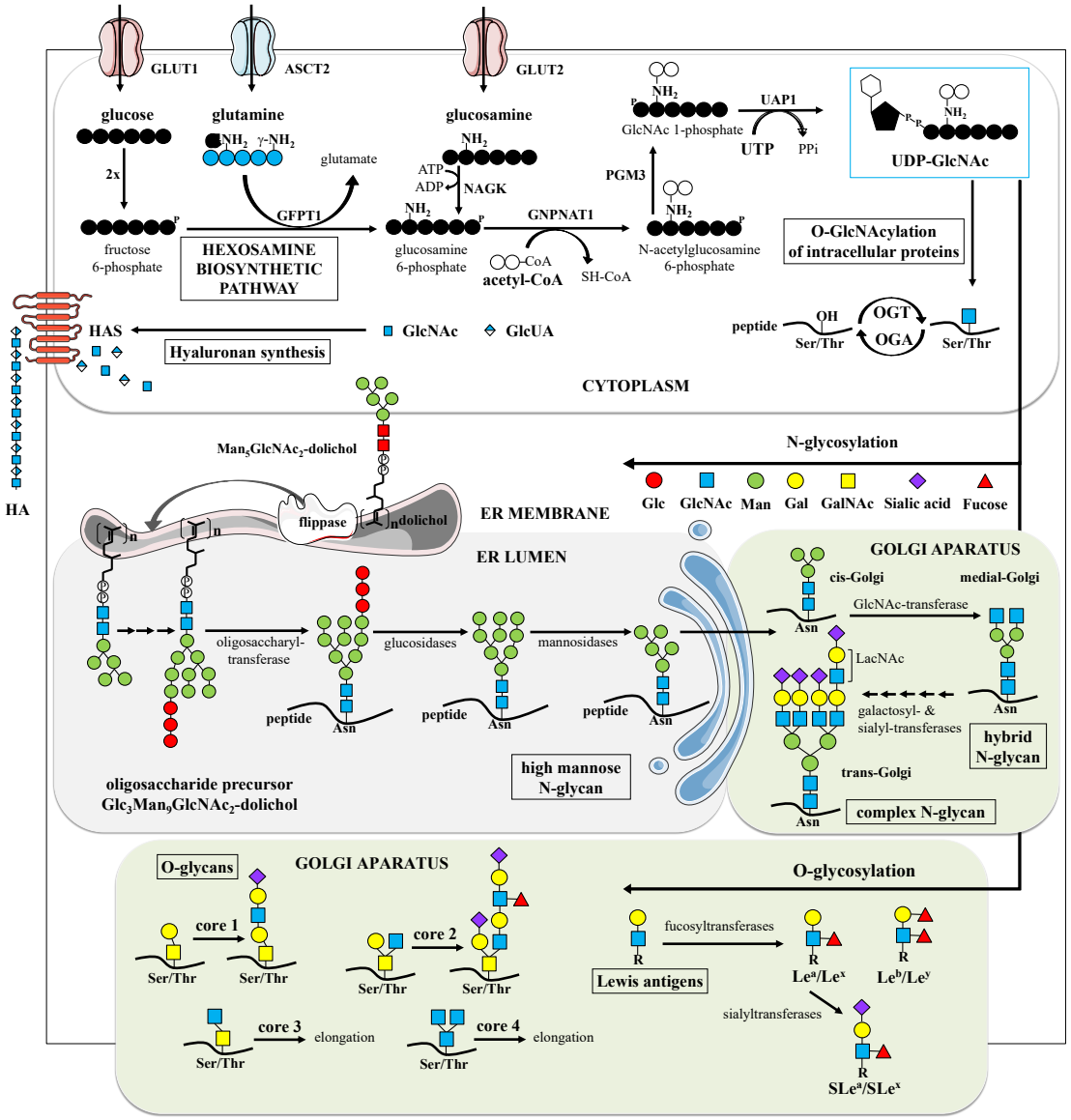

Figure 6. The hexosamine biosynthetic pathway, O-GlcNAcylation, N-glycosylation, O-glycosylation and HA synthesis

De novo synthesis of UDP-GlcNAc by the HBP in the cytoplasm. Usage of UDP-GlcNAc in the cytoplasm for O-GlcNAcylation of intracellular proteins by OGT and OGA cycling and for synthesis of HA at the plasma membrane. Usage of UDP-GlcNAc for N-glycosylation and O-glycosylation of surface and secreted proteins along the protein secretory pathway. Common N-glycan and O-glycan structures on proteins destinated to the plasma membrane and to the extracellular matrix. GLUT1/2, glucose transporter 1/2; ASCT2, neutral amino acid exchanger; GFPT1, glutamine-fructose-6-phosphate transaminase 1; NAGK, N-acetylglucosamine kinase; GNPNAT1, glucosamine-phosphate N-acetyltransferase 1; PGM3, phosphoglucomutase 3; UAP1, UDP-N-acetylglucosamine pyrophosphorylase 1; UDP-GlcNAc, uridine diphosphate N-acetylglucosamine; OGT, O-GlcNAc transferase; OGA, O-GlcNAcase; Ser/Thr, serine/threonine; GlcUA, glucuronic acid; HA, hyaluronic acid; HAS, hyaluronan synthase; ER, endoplasmic reticulum; Ans, asparagine; LacNAc, N-acetyllactosamine; Le, Lewis antigens; SLe, sialylated Lewis antigens; Glc, glucose; Man, mannose; Gal, galactose; GalNAc, N-acetylgalactosamine.

only altered in colon, stomach and ovarian tumors, but it is also a poor prognostic marker of colon malignancies. Expression of IGF-I is attenuated upon silencing of ST6GalNAc-I leading to impairment of the metastatic abilities of gastric tumor cells. Furthermore, sialylated glycoconjugates are sensed by Siglecs receptors expressed on immune cells. Aberrant sialylation of tumor antigens is associated with immunosuppression and tumor immune evasion (Munkley and Elliott, 2016). Binding of a fucose unit to the GlcNAc residue of glycoproteins is another modification characteristic of hepatocellular carcinoma as well as lung and breast cancers (Pinho and Reis, 2015).

I.2.2 O-glycosylation in cancer

Mucin-like motifs are part of the Tn and T antigens expressed on cancer cells (Pinho and Reis, 2015) (**Figure 6**). These antigens and their sialylated versions can be generated as truncated forms of O-glycans in cancer cells. Sialylated Tn antigen functions as a tumor-associated epitope highly expressed on several solid cancers including colorectal tumors and associated with enhanced tumor expansion, migration, invasion and impaired clinical outcome (Pinho and Reis, 2015).

Sialylated versions of the Lewis antigens, glycan motifs which are part of the blood group system have been found highly expressed in tumors and negatively associate with cancer patient survival (Pinho and Reis, 2015). Several terminal fucosyltransferases critical for synthesis of Lewis antigens are also deregulated in several cancer types, including colorectal cancer. Indeed, surface expression of tumor-associated sialylated Lewis antigens has been associated with upregulation of some sialyltransferase and fucosyltransferases in gastric and pancreatic tumor cells. Generation of neoantigens in tumor cells by aberrant O-glycosylation can be used for detection of soluble glycoproteins. For instance, serum biomarkers of colorectal, pancreatic and gastric carcinomas include sialylated versions of the Lewis antigens. In colorectal carcinoma, sialylated Lewis antigen A is a circulatory biomarker (Pinho and Reis, 2015), (Munkley and Elliott, 2016), (Moffett et al., 2021).

I.2.3 O-GlcNAcylation in cancer

OGT and OGA have been reported to mediate transcriptional, epigenetic and metabolic regulation (Yang and Qian, 2017). For instance, OGT and OGA cycling controls the transcription cycle by activating O-GlcNAcylation of RNA polymerase II for the formation of the pre-initiation complex. Competition of O-GlcNAcylation and phosphorylation at common sites regulates the activity of RNA pol II for binding to transcription start sites as well as transcription initiation and elongation (Yang and Qian, 2017).

Hyper O-GlcNAcylation is a feature of many oncogenic malignancies mediated by overexpression of OGT (Pinho and Reis, 2015). O-GlcNAcylation has been detected in several key proteins of oncogenic signaling such as cyclin D1, c-Myc and p53 (Munkley and Elliott, 2016). OGT stabilizes cyclin D1 which controls the progression of cell cycle from G1 to the synthesis S phase. OGT was shown to bind and O-GlcNAcylate cyclin D1 in the nucleus of human breast and colorectal cancer cells promoting its stabilization. O-GlcNAcylation of cyclin D1 increased its half-life by decreasing its ubiquitination and proteasomal degradation. The protection conferred by O-GlcNAcylation against proteasomal degradation of the oncogene cyclin D1 has been also described for other cell cycle controllers such as p53, β-catenin and FOXM1. This highlights the implication of O-GlcNAcylation in the cell cycle deregulation occurring in tumor cells (Masclef et al., 2019).

Components of the PI3K/Akt and NF-κB pathways, matrix metalloproteases, E-cadherin and VEGF-A are also O-GlcNAcylated (Pinho and Reis, 2015). Resistance to apoptosis induced by death receptors such as Fas and TNFR1 is another process regulated by glycosylation downstream of ligand binding (Munkley and Elliott, 2016). Likewise, several enzymes involved in epigenetic modifications and repairing of DNA breaks occurring in cancer cells have been reported to be regulated by O-GlcNAcylation (Hanover et al., 2018), (Pinho and Reis, 2015). Glycolytic and mitochondrial enzymes as well as components of the electron transport chain are O-GlcNAcylated. (Munkley and Elliott, 2016), (Hanover et al., 2018). Hypoxia inducible factor-1 (HIF-1) has been shown to be regulated by O-GlcNAcylation, modification associated with the increase of the glucose transport GLUT1 mediated by the HIF-1 upon hypoxia (Hanover et al., 2018).

Beyond the UDP-GlcNAc synthesis depending on the nutritional status of the cell, O-GlcNAcylation regulates the activity of major metabolic pathways (Yang and Qian, 2017). To do so, OGT has three isoforms including a nucleocytoplasmic and short OGT isoforms localized in the cytoplasm and nucleus and a mitochondrial isoform. OGA presents a nucleocytoplasmic isoform that beyond the O-GlcNAc hydrolase domain contains a histone acetyltransferase (HAT)-like domain. The OGA short isoform localizes in the ER and lipid droplets and lacks the HAT domain. Indeed, OGA acetylates pyruvate kinase M2 (PKM2) via its HAT domain and mediates the interaction between OGT and PKM2 upon glucose availability. This leads to O-GlcNAcylation of PKM2 and the enhancement of aerobic glycolysis. During fasting, OGT has been described to O-GlcNAcylate PPARγ co-activator 1α (PGC1α) promoting gluconeogenesis. Apart from the coupling of the UPR and the HBP by XBP1s transcriptional control of several HBP enzymes and the induction of protein O-GlcNAcylation, O-GlcNAcylation has been described to directly control protein homeostasis

by co-translational O-GlcNAcylation of nascent proteins. This has been suggested to stabilize the nascent proteins by avoiding premature degradation mediated by ubiquitination. Likewise, OGT has been shown to inhibit the activity of the proteosome (Yang and Qian, 2017).

I.2.4 Glycosaminoglycans in cancer

The glycocalyx of cells and the extracellular matrix are enriched in glycosphingolipids, proteoglycans and glycosaminoglycans (Pinho and Reis, 2015), (Reily et al., 2019). Glycosphingolipids are glycosylated structures attached to a hydroxyl group of ceramides which are highly abundant glycolipids in the cellular membranes of humans and contribute to membrane dynamics and signaling. Proteoglycans are proteins modified with classical N- and O-linked types of glycans and the distinctive O-linked extended repeats of disaccharide residues containing GlcNAc or GalNAc in combination with glucuronic acid (GlcUA) or galactose. These long sugar chains are known as glycosaminoglycans. Proteoglycans including heparan sulfate, keratan sulfate and chondroitin sulfate are part of the cell glycocalyx that mediates the interaction of cells with the surrounding and signaling. Other glycosaminoglycan mainly produced as a sugar free chain is hyaluronic acid (HA) (Reily et al., 2019) (**Figure 6**).

Production of HA has been described to contribute to most hallmarks of cancer (Caon et al., 2020). HA is a polymer of repeated disaccharide units of GlcNAc and GlcUA (**Figure 6**). Synthesis of HA from UDP-sugars present in the cytoplasm is mediated by the hyaluronan synthase (HAS) family. Whereas in healthy conditions HA is a polymer with a high molecular weight (HMW HA), under pathophysiological states HA displays lower molecular weight (LMW HA). LMW HA is associated with angiogenesis, inflammation, tumor cell proliferation by activating mitogenic pathways, EMT induction, metastasis and chemotherapy resistance. Within the TME, activated $CD8^+$ T cells expressing CD44 and its interaction with HA has been suggested to mediate intra-tumoral infiltration. On the contrary, HA surrounding tumor cells has been reported to act as a barrier limiting the interaction with immune cells (Caon et al., 2020).

Higher accumulation of HA in the TME in parallel with collagen deposition, hypoxia, vascular alterations and metastatic potential have been reported in tumors of patients and mouse models of pancreatic cancer (Li et al., 2018). Aberrant production of HA by tumor cells has been reported in colorectal, breast, gastric, hepatic, lung and pancreatic cancer and associates with tumor aggressiveness and impaired prognosis. Beyond tumor-promoting roles, lower levels of HA and CD44 have also been described to associate with impaired survival and prognosis of oral carcinoma and melanoma. Therefore, HA production in tumors plays dual roles in regulating tumor progression (Caon et al., 2020).

I.3 Cellular nutrient-sensing molecular pathways

Cell proliferation is coupled to the nutrient-sensing molecular signaling for induction of an anabolic metabolism depending on the available carbon, nitrogen and energy sources as well as extrinsic stimulation by growth factors (Robles-Flores et al., 2021). This connection is mediated by the crosstalk between the mitogen-activated protein kinase (MAPK) pathway involved in cell growth and mitogenic division in response to growth factors and the mTOR pathway that induces anabolic reactions in nutrient-rich conditions. Strikingly, malignant cells increase biomass and cell growth at expenses of anabolism and persistent activation of mTOR even when nutrient supply is limited (Robles-Flores et al., 2021). Indeed, the MAPK pathway starting by activation of Ras is a major molecular signaling deployed by neoplastic cells to acquire oncogenic malignancy and uncouple cell growth and environmental signals (Drosten and Barbacid, 2020).

I.3.1 The MAPK pathway

Nearly 100% of pancreatic ductal adenocarcinoma bears mutation in the isoform KRas whereas around a 50% and 30 % of colorectal cancer and lung adenocarcinoma present mutated version of KRas, respectively (Drosten and Barbacid, 2020). Other isoforms of Ras (HRas and NRas) as well as Braf and Raf, downstream components of the MAPK pathway are found mutated in a minor percentage in most human oncogenic malignancies. Activating mutations in growth factor receptor tyrosine kinases also count for constitute activation of the MAPK pathway. Therefore, several clinical trials with inhibitors targeting the MAPK pathway are ongoing (Drosten and Barbacid, 2020).

The MAPK pathway is hierarchically composed of three levels of serine/threonine kinases (Fang and Richardson, 2005) (**Figure 7**). The MAPK-ERK pathway is triggered upon binding of growth factors to cognate receptors tyrosine kinase (RTK) on the plasma membrane. Ras is recruited to the cytoplasmatic domains of the receptor and becomes active upon binding to GTP. Activation of the oncogene Ras results in recruitment and phosphorylation of the first layer of MAPK proteins (MAPK3), Raf1, Braf or Araf. Phosphorylated MAPK1 proteins activate the second level of MAPK proteins (MAPK2), MEK1/2. MAPK2 phosphorylates and activates the transcription factors ERK1/2 that determine the cellular outcome by transcriptional regulation in the cell nucleus (Fang and Richardson, 2005), (Roberts and Der, 2007), (Terrell and Morrison, 2019). Activation of transcription factors such as c-Myc, c-Fos and Elk1 ultimately mediate the cellular response to growth factors to drive cell survival, proliferation and differentiation (Drosten and Barbacid, 2020). In colorectal cancer for instance, cell proliferation is mainly mediated by the MAPK-ERK pathway and has been

implicated in angiogenesis, tumor niche remodeling, invasion and metastasis (Fang and Richardson, 2005), (Roberts and Der, 2007).

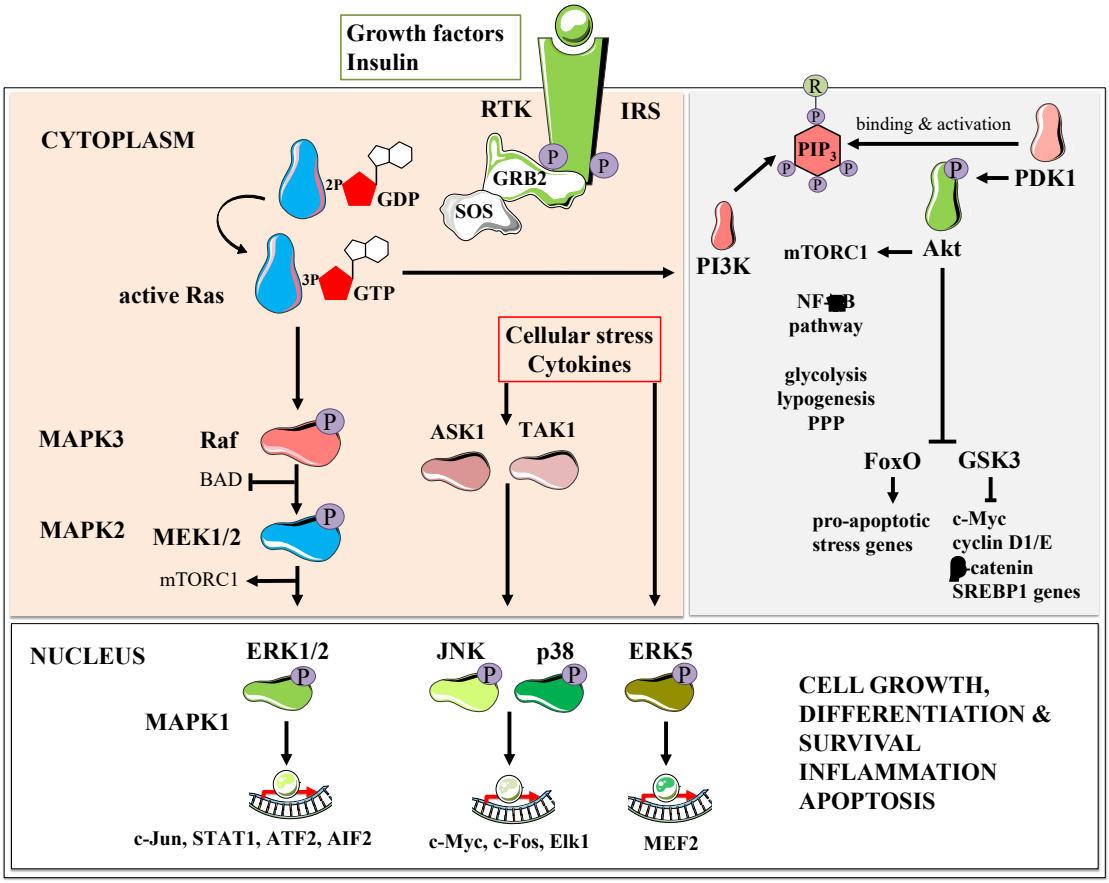

Figure 7. The MAPK and PI3K pathways, cellular outcomes

The three MAPK pathways and the activation triggers are depicted. Activation of transcription factors in the nucleus leads to different cellular outcomes depending on the stimulus and the downstream activated transcription factors. Activation of PI3K pathway by growth factors and insulin leads to activation of mTORC1 and transcriptional regulation mediated by Akt promoting cell proliferation, survival and anabolic metabolism. RTK, receptor tyrosine kinase; IRS, insulin receptor substrate 1; GRB2 and SOS, adaptor proteins; MAPK, mitogen activated protein kinase; MEK, mitogen activated protein kinase-ERK kinase; ERK, extracellular signal regulated kinase; STAT, signal transducer and activator of transcription; ASK1, apoptosis signal-regulating kinase 1; TAK1, transforming growth factor β-activated kinase 1; JNK, c-Jun N-terminal kinases; mTORC1, mTOR complex 1; BAD, Bcl2 associated agonist of cell death; PI3K, phosphatidylinositol-3-kinase; PIP3, phosphatidylinositol (3,4,5)-triphosphate; PDK1, phosphoinositide-dependent kinase 1; Akt, protein kinase B; GSK3, glycogen synthase kinase-3.

The other MAPK pathways, namely c-Jun N-terminal kinases (JNK1/2/3) and stress-activated protein kinases, p38 kinases (α/β/γ/δ) and ERK5 are activated by growth factors as well as stress signals whereas JNK and p38 are specifically activated by cytokines (Fang and Richardson, 2005) (**Figure 7**). Activation of these downstream kinases induces transcription factors such as c-Jun and STAT1 as well as post-translational modifications of cytoplasmic

proteins resulting in cell proliferation, differentiation, secretion of inflammatory factors as well as apoptosis (Fang and Richardson, 2005), (Roberts and Der, 2007).

Tumorigenic functions of Ras are also associated with activation of the catalytic subunit of the phosphatidylinositol-3-kinase (PI3K) (Shaw and Cantley, 2006). Activation of PI3K occurs at the levels of Raf1 along the MARK ERK pathway by binding of the catalytic subunit of PI3K to Ras-GTP. Apart from Ras-mediated activation of PI3K, mutations of the p110α catalytic and p85α regulatory subunits of PI3K as well as other elements of this pathway have been reported in around 30% of all human oncogenic malignancies (Fang and Richardson, 2005), (Roberts and Der, 2007).

I.3.2 The PI3K pathway

Activating mutations in the catalytic subunit of PI3K drive oncogenic cell transformation in colorectal, gastric and breast cancers (Shaw and Cantley, 2006). However, the most common mutation responsible for activation of the PI3K signaling in human cancers occurs in phosphatase and tensin homolog (PTEN). PTEN is a phosphatase catalyzing the inverse reaction of PI3K, thus blocking this molecular pathway. The PI3K pathway starts by activation of this kinase upon binding of insulin to the insulin receptor substrate 1 (IRS1), a RTK. Subsequently, synthesis of phosphatidylinositol (3,4,5)-triphosphate (PIP3) drives recruitment of the serine/threonine protein kinase B (Akt) to the plasma membrane. Akt is activated upon phosphorylation by phosphoinositide-dependent kinase 1 (PDK1) (Shaw and Cantley, 2006), (Sengupta et al., 2010), (Robles-Flores et al., 2021) (**Figure 7**).

PI3K pathway is involved in cell survival, growth, cell differentiation and metabolism (Robles-Flores et al., 2021) (**Figure 7**). For instance, Akt mediates the inhibition of glycogen synthase kinase-3 (GSK-3) by phosphorylation. GSK negatively impacts on cell cycle by phosphorylation of c-Myc and cyclins as well as on cell survival and differentiation by post-translational modification of c-Jun, β-catenin, mesenchymal markers and sterol-regulatory element-binding transcription factor 1 (SREBP1). Therefore, upon Akt-mediated inhibition of GSK-3, those processes are stimulated. In addition, Akt is implicated in DNA repair, inactivation of the pro-apoptotic factor BAD, activation of the NF-κB pathway and inactivation of the transcription factor FoxO. Activation of FoxO by cellular stress leads to induction of pro-apoptotic factors and genes responsive to stress. In addition, the roles of Akt in metabolism encompass the direct activating phosphorylation of enzymes of the glycolytic pathway and fatty acid biosynthesis beyond its functions as a major activator of the mTOR signaling (Shaw and Cantley, 2006). Moreover, PI3K signaling increases the PPP flux in transgenic mice developing PTEN-deficient breast tumors (Mossmann et al., 2018).

I.3.3 The mTOR pathway

mTOR, the mammalian target of rapamycin mTOR is a metabolic manager of anabolic and catabolic processes that monitors the cellular provisions of energy, nutrients and oxygen to achieve the optimal coupling among intracellular biosynthesis, bioenergetics and extrinsic signaling (Sengupta et al., 2010), (Robles-Flores et al., 2021) (**Figure 8**). mTOR is the catalytic serine/threonine kinase factor driving formation of two different complexes, mTORC1 and mTORC2 which are rapamycin-sensitive and insensitive, respectively (Mossmann et al., 2018).

mTOR belongs to the family of PI3-related kinases. mTORC1 includes four additional components such as Raptor, mLST8, PRAS40 and Deptor (Sengupta et al., 2010), (Mossmann et al., 2018) (**Figure 8**). Raptor, a regulatory element controls complex assembly, its cellular localization as well as amino acid sensing properties and recruitment of substrates. PRAS40 and Deptor are regulatory elements that suppress mTOR kinase activity. This complex regulates mRNA translation through phosphorylation of S6 kinases (S6Ks) and the translation initiation factor 4E-binding proteins (4EBPs). Unphosphorylated 4EBPs bind to the initiation factor eIF4E interrupting the formation of the cap-binding complex and inhibiting cap-dependent translation. mTORC1-mediated activation of S6Ks leads phosphorylation of different substrates, thus contributing to the protein translational process (Sengupta et al., 2010), (Mossmann et al., 2018).

mTORC1 activation requires recruitment and anchor to the lysosomal membranes (Sengupta et al., 2010) (**Figure 8**). One of the activating stimuli is the presence of intracellular amino acids such as leucine, arginine and glutamine while the lack of extracellular leucine and arginine causes a strong suppression of mTOR activity (Sengupta et al., 2010), (Mossmann et al., 2018).

mTORC1 transcriptionally regulate enzymes participating in glycolysis, amino acid, sterol and lipid metabolism as well as in the pentose phosphate pathway and nucleotide biosynthesis (Robles-Flores et al., 2021) (**Figure 8**). mTORCs1 via S6K1 activates the transcription factor sterol regulatory element binding proteins (SREBP)-1 that upregulated the expression of fatty acid transporters and enzymes of the lipogenesis pathway and the oxidative phase of the PPP under insulin and fatty acid stimulation or low levels of sterols. In that way, mTORC1 upregulates biosynthesis of lipids as part of mechanisms induced by Akt. mTORC1-mediated lipogenesis supports cellular biomass and modulates the composition of biological membranes. In addition, mTORC1 activation positively impacts on mitochondrial biogenesis through activation of PGC1α and oxidative bioenergetics (Sengupta et al., 2010), (Mossmann et al., 2018).

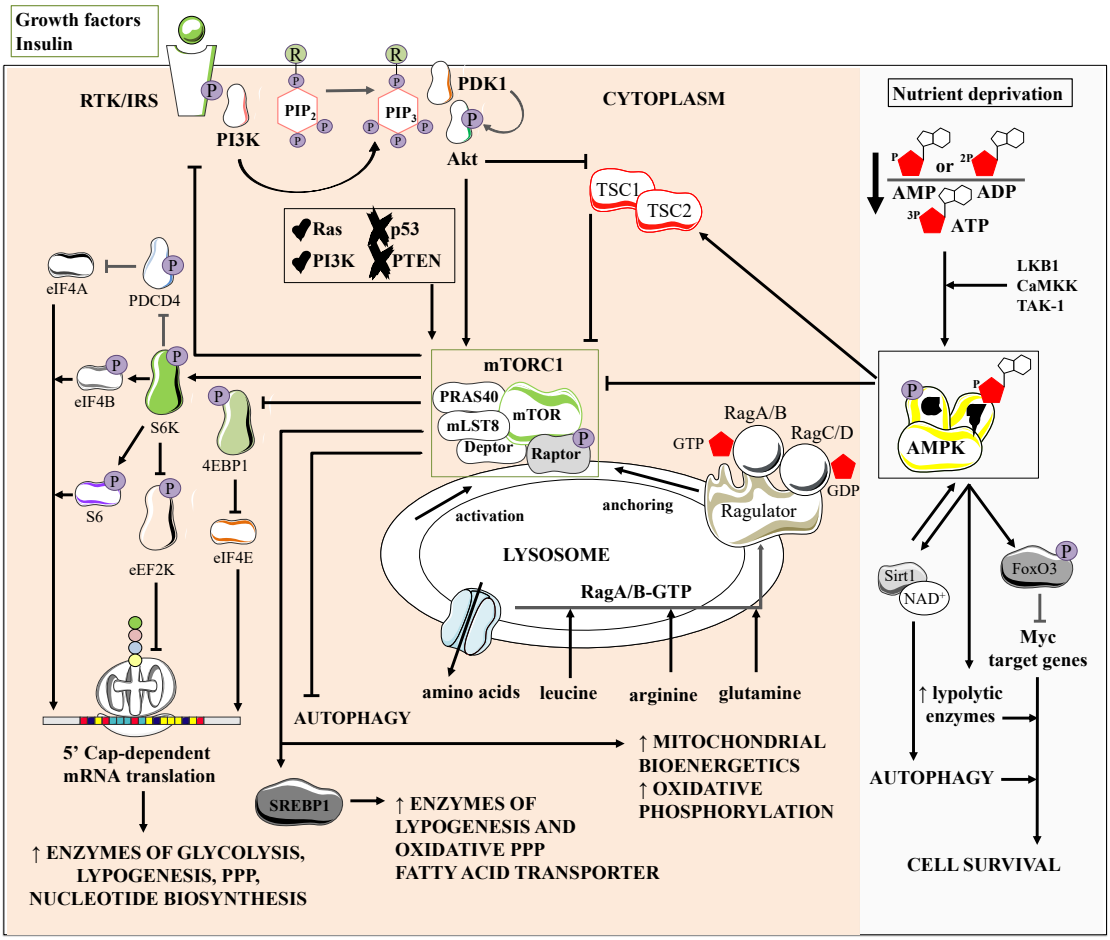

Figure 8. The mTOR and AMPK pathways, cellular outcomes

The mTOR pathway is activated upon growth factor and insulin stimuli as part of the PI3K/Akt pathway and enhanced by mutations in oncogenes and tumor suppressors in cancer cells. mTORC1 activation in the lysosome drives transcriptional, translational and post-translational regulations to induce the energetic and anabolic metabolism and inhibit autophagy. The AMPK pathway is activated upon nutrient deprivation decreasing the AMP/ADP to ATP ratio. AMPK activation induces autophagy and promotes cell survival by inhibition of mTORC1 and induction of a catabolic metabolism. RTK, receptor tyrosine kinase; IRS, insulin receptor substrate 1; PI3K, phosphatidylinositol-3-kinase; PIP2, phosphatidylinositol (4,5)-triphosphate; PIP3, phosphatidylinositol (3,4,5)-triphosphate; PDK1, phosphoinositide-dependent kinase 1; Akt, protein kinase B; mTORC1, mTOR complex 1; S6K, S6 kinase; eIF4A/B/E, eucaryotic initiation factor 4A/4B/4E; PDCD4, programmed cell death protein 4; eEF2K, eucaryotic elongation factor 2 kinase; 4EBP1, translation initiation factor 4E-binding protein 1; SREBP1, sterol-regulatory element-binding transcription factor 1; TSC1/2, tuberous sclerosis complex; AMPK, AMP-activated protein kinase; LKB1, liver kinase B1; CaMKK, calcium/calmodulin kinase kinase; TAK-1, TGF-β-activated kinase 1; Sirt1, sirtuin 1; PPP, pentose phosphate pathway.

mTORC1/2 is activated by growth factors such as insulin and IGF-1 through induction of the PI3K/Akt pathway and the MARK-ERK signaling (Robles-Flores et al., 2021) (**Figure 8**). Akt and ERK1/2 indirectly activate mTORC1 by inhibitory phosphorylation of the TSC2. Akt also activates mTORC1 via stimulatory phosphorylation of Raptor and inhibitory

phosphorylation of PRAS40. Under nutrient and growth factor-enriched conditions, mTORC1 inhibits autophagy while under starvation, mTOR inhibition leads to concomitant induction of autophagy. Restoration of the cytoplasmic pool of amino acids by transporters mediating their efflux from lysosomes after autophagic degradation of proteins positively impact on mTORC1 activity while autophagy is inhibited (Kroemer et al., 2010), (Sengupta et al., 2010), (Robles-Flores et al., 2021).

Activating mutations in PI3K and Ras and loss-of-function mutations in PTEN and p53 drive hyperactivation of mTORC1 (Robles-Flores et al., 2021) (**Figure 8**). The altered metabolism of tumors also counts for sustained mTORC1 signaling. For instance, glutaminolysis supports mTORC1 activation whereas mTORC1 enhances c-Myc translation that upregulates GLS expression. Indeed, dual inhibition of mTORC1 and GLS limited tumor growth of lung carcinoma xenografts and blocking glutamine influx suppressed mTORC activity and limited tumor growth of colorectal xenografts. Inhibition of a leucine transporter highly expressed in some tumors in combination with rapamycin has shown to limit prostate tumor growth. Furthermore, mTORC1 signaling in tumor cells via c-Myc and HIF-1α is implicated in glycolysis by upregulation of the GLUT1 transporter, hexokinase 2 and PKM2. Some enzymes of the PPP are also upregulated by mTORC1 in cancer cells (Mossmann et al., 2018).

I.3.4 The AMPK pathway

The AMP-activated kinase (AMPK) senses increased levels of AMP and ADP upon nutrient starvation, induces lipolysis to cope with the energetic cellular demands, inhibits mTOR and activates p53 (Robles-Flores et al., 2021) (**Figure 8**). As a bioenergetic sensor, AMPK is allosterically activated by AMP binding to its γ subunit and post-translationally activated by upstream kinases such as liver kinase B1 (LKB1) induced under energy depletion and calcium/calmodulin kinase kinase (CaMKK) induced upon higher concentration of cytosolic calcium. TGF-β-activated kinase 1 (TAK-1) downstream of the TNFα binding and pattern recognition receptor (PRR) engagement leading to NF-κB activation also activates AMPK. These kinases activate AMPK by phosphorylating its catalytic α subunit (Kroemer et al., 2010), (Lin and Hardie, 2018), (Robles-Flores et al., 2021).

The tumor suppressor LKB1 is commonly mutated in lung adenocarcinomas and its genetic ablation has been directly linked to persistent mTORC1 activation due to defective AMPK checkpoint in benign tumoral masses (Shaw and Cantley, 2006), (Robles-Flores et al., 2021). AMPK inhibits mTORC1 through direct activating phosphorylation of TSC2, mechanism that promotes cell survival upon nutrient scarcity and hypoxia (**Figure 8**). AMPK can also phosphorylate Raptor leading to inhibition of the catalytic functions of mTORC1 causing cell

cycle arrest under energy depletion (Sengupta et al., 2010). The LKB1-AMPK signaling negatively control the expression of an enzyme of the pyrimidine biosynthesis. Therefore, loss of LKB1 in KRas-driven NSCLC cells leads to mTORC1 activation and nucleotide synthesis (Mossmann et al., 2018).

Apart from induction of autophagy by AMPK-mediated mTORC1 inhibition, AMPK can contribute itself to the autophagic process by activation of Sirtuin 1 (Sirt1) (Kroemer et al., 2010) (**Figure 8**). Sirt1 is a NAD+-dependent deacetylase promoting autophagy. Positive feedback between AMPK and Sirt1 induces autophagy under nutrient depletion. Deacetylation of LKB1 by Sirt1 increases its kinase activity in the cytoplasm and consequently, AMPK activation, whereas AMPK indirectly increases the levels of NAD+, therefore, supplying cofactors for Sirt1 activity (Kroemer et al., 2010). Hyperactivation of c-Myc and an anabolic metabolism can induce AMPK activation and concomitant activation of p53 which drives mitochondria-dependent apoptosis. AMPK also negatively regulate the expression of c-Myc target genes, although tumor cells overexpressing c-Myc are resistant to those metabolic checkpoints (Dejure and Eilers, 2017), (Robles-Flores et al., 2021).

I.3.5 The integrated stress response

The integrated stress response (ISR) is an evolutionarily conserved and adaptive mechanism induced upon extracellular conditions such as glucose and amino acid deprivation, hypoxia, alterations in the protein homeostasis (or proteostasis), redox status and viral infections (Costa-Mattioli and Walter, 2020) (**Figure 9**). The plasticity displayed upon activation of the ISR endows cells with the capacity to sense homeostatic alterations in the cytoplasm as well as in the lumen of the endoplasmic reticulum (ER) to face and survive challenging extracellular and intrinsic conditions or to induce apoptosis when cell homeostasis cannot be recovered upon persistent or highly intense cellular insults. Therefore, the ISR is implicated in metabolic disorders including cancer. Pharmacological modulators of the ISR have been studied as anti-cancer therapeutic candidates (Pakos-Zebrucka et al., 2016), (Costa-Mattioli and Walter, 2020) (refer to **Table 2**).

The mammalian ISR relies on activation of four serine/threonine kinases, namely, general amino acid control nonderepressible 2 (GCN2), double-stranded RNA-dependent protein kinase (PKR), PKR-like ER kinase (PERK) and heme-regulated inhibitor (HRI) (Costa-Mattioli and Walter, 2020) (**Figure 9**). Subsequent phosphorylation of the translation initiation factor eIF2α results in inhibition of global mRNA translation. However, special mRNAs such as ATF4 will be translated to control the expression of genes which are part of the new transcriptional and translational program leading to cytoprotection or cytotoxicity.

Negative regulatory events when ISR is orchestrated rely on induction of a phosphatase complex that dephosphorylates eIF2α (Costa-Mattioli and Walter, 2020).

eIF2α kinases shared structural features in their catalytic kinase domain as well as activation mechanisms such as dimerization and trans-autophosphorylation upon stress stimuli (Costa-Mattioli and Walter, 2020) (**Figure 9**). GCN2, the most conserved eIF2α kinase is mainly activated upon amino acid scarcity. PERK is a transmembrane ER sensor that control the translational program as part of the unfolded protein response (UPR) activated in part by proteotoxicity-mediated ER stress (refer to section II). Accumulation of misfolded proteins counts as a major stimulus for PERK activation. PKR is mostly activated by double stranded RNA (dsRNA) of viral and cellular origins. HRI is activated upon low concentrations of heme complexes, oxidative and osmotic stresses and protein aggregation. Collectively, eIF2α kinases are patrols of the cellular homeostasis and several alterations trigger their activation in an overlapping-manner in order to ensure cooperative and redundant control of the most optimal translational program upon induction of the ISR (Pakos-Zebrucka et al., 2016), (Costa-Mattioli and Walter, 2020).

Assembly of the initiator tRNA ternary complex (TC) composed of eIF2, GTP and methionine bound to tRNA carrier is disrupted upon phosphorylation of the α subunit of eIF2 (Costa-Mattioli and Walter, 2020) (**Figure 9**). When global translation is attenuated by decreased levels of the TC, mRNAs containing one or more upstream open reading frames (uORFs) at the 5' untranslated region (5'-UTR) are translated irrespective of 5'Cap recognition. Some of the translated mRNAs are the transcription factors ATF4 and ATF5 as well as the pro-apoptotic C/EBP homologous protein (CHOP) and the eIF2 phosphatase GADD34. Translation of GADD34 is part of the negative feedback loop of the ISR that warrants termination when the stimulus is no longer present. Expression of GADD34 reflects the differential transcriptional and translational program executed upon induction of ISR since GADD34 is translated as an uORF-containing mRNAs but it is also transcriptionally upregulated by ATF4 (Pakos-Zebrucka et al., 2016), (Costa-Mattioli and Walter, 2020).

The complex crosstalk among the ISR, autophagy and the UPR dictates the cellular outcome of the ISR depending on the insult (Pakos-Zebrucka et al., 2016). ATF4 induced upon PERK activation upregulates the expression of genes involved in the autophagic process (Kroemer et al., 2010). In addition, ATF4 can positively control genes encoding factors inhibiting mTORC1 activity to trigger autophagy upon nutrient depletion and ER stress. Autophagy as part of the ISR under nutrient deprivation, particularly amino acid depletion is associated with cytoprotection. Recovery of cell homeostasis during ER stress by lowering proteotoxicity caused by an overload of misfolded proteins depends on PERK as a common mediator of the

ISR and UPR. PERK mediated-ISR activation will decreased mRNA translation as an early mechanism promoting cell survival. When cell homeostasis is highly compromised, instead of cellular survival mechanism, ISR contributes to apoptosis. CHOP executes transcriptional upregulation of GADD34 and pro-apoptotic factors of the Bcl2 family such as BIM under irremediable ER stress. Sustained PERK signaling upon chronic ISR also leads to downregulation of inhibitors of apoptosis (Pakos-Zebrucka et al., 2016).

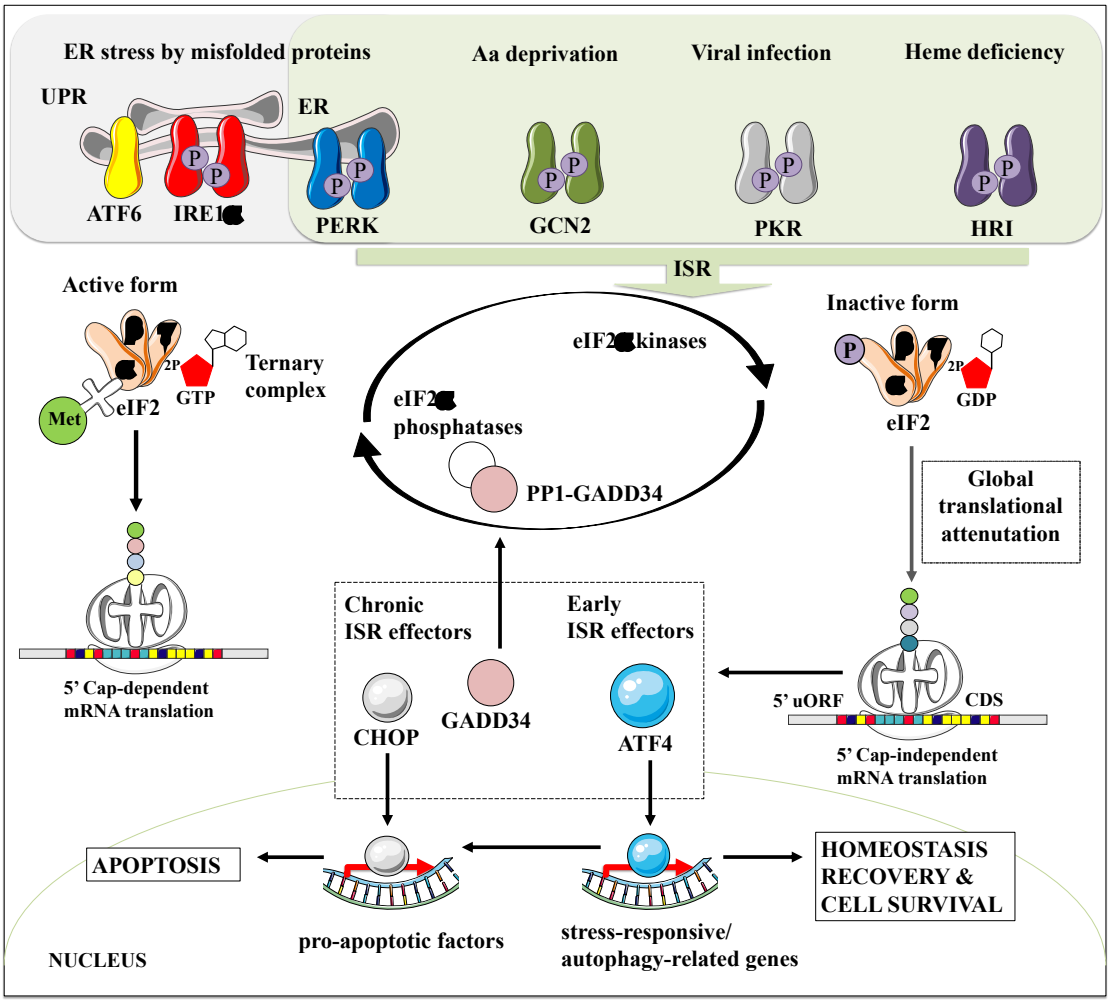

Figure 9. The Integrated Stress Response (ISR), mechanisms and cellular outcomes under early and chronic induction

The ISR is activated upon different stimuli including misfolded proteins and nutrient deprivation leading to phosphorylation of eIF2. Inhibition of eIF2 by phosphorylation leads to attenuation of the global mRNA translation while allows translation of 5' uORF-containing genes such as ATF4 and GADD34. ATF4 is one the downstream targets of the early ISR that promotes cell survival. Upon chronic induction of the ISR, GADD34 and CHOP drive cell apoptosis. ER, endoplasmic reticulum; UPR, unfolded protein response; ATF6, activating transcription factor; IRE1α, inositol-requiring enzyme α; PERK, PKR-like ER kinase; GCN2, general amino acid control nonderepressible 2; PKR, double-stranded RNA-dependent protein kinase; HRI, heme-regulated inhibitor; Aa, amino acid; eIF2, eucaryotic initiation factor 2; met, methionine; ATF4, activating transcription factor 4; CHOP, C/EBP homologous protein; GADD34, DNA damage-inducible 34, CDS, coding sequence.

The ISR is highly implicated in oncogenic processes (Costa-Mattioli and Walter, 2020), (Tian et al., 2021). Oncogenic transformation resulting in increased protein demands beyond the cellular protein folding capacity induces ISR to slowdown translation while warranting cell viability. Indeed, in metastatic prostate cancer models where PERK mediated protein synthesis attenuation, pharmacological inhibition of ISR resulted in apoptosis. Furthermore, growth of c-Myc driven lymphoma in mice was attenuated upon ATF4 silencing whereas animal survival was prolonged. Indeed, tumor cell proliferation and the anabolic metabolism driven by c-Myc was shown to activate GCN2 with concomitant overexpression of ATF4 to reinforce translational attenuation. Deficiency of GCN2 and ATF4 limited growth, finding that might be exploited in combination with amino acid deprivation of malignant tissues. ISR activation in malignant cells might also be activated by anti-cancer interventions contributing to tumor cell survival and chemoresistance (Pakos-Zebrucka et al., 2016), (Costa-Mattioli and Walter, 2020).

Collectively, the ISR clusters molecular signaling events that commonly render eIF2α phosphorylated as the major mechanism leading to mRNA translational attenuation and reprograming as a strategy for cellular homeostatic protection (Costa-Mattioli and Walter, 2020). As noted, some of the eIF2α kinases as the most upstream transducers of the ISR participate in other molecular signaling pathways such the UPR (**Figure 9**). Interestingly, the ISR and the UPR share the common outcome of selective translational mitigation to adapt to diverse environmental and intrinsic factors (Costa-Mattioli and Walter, 2020). The UPR is a molecular avenue with additional mechanisms that cells deploy to keep their homeostasis upon challenging nutritional conditions and proteostatic stress (Hetz et al., 2020).

Table 2. Pharmacological inducers and inhibitors of ISR and ER stress

Compound	Action and mechanism	Reference
CCT020312	Selective PERK induction. No activation of general UPR. Arrest of cell cycle by cyclin depletion. Potential with anti-cancer therapies.	(Pakos-Zebrucka et al., 2016)
Histidinol/Halofuginone/ Asparaginase/Arginine deiminase	GCN2 induction. Halofuginone, inhibition of angiogenesis.	(Pakos-Zebrucka et al., 2016)
Guanabenz/Sephin1	ISR enhancement by inhibiting of eIF2α dephosphorylation via GADD34. Studies on neurodegenerative diseases.	(Costa-Mattioli and Walter, 2020) (Pakos-Zebrucka et al., 2016)
Salubrinal/Sal003	ISR enhancement by inhibiting of eIF2α dephosphorylation via GADD34. Control of viral infections and studies on neurodegenerative diseases and diabetes.	(Costa-Mattioli and Walter, 2020) (Pakos-Zebrucka et al., 2016)
ISRIB	Inhibition of ISR by attenuation of eIF2α phosphorylation. Studies on neurodegenerative pathologies and cognitive and memory disorders.	(Costa-Mattioli and Walter, 2020)
GSK2606414/ GSK2656157	Inhibition of PERK activation by autophosphorylation. Anti-tumoral effects and	(Pakos-Zebrucka et al., 2016)

Compound	Action and mechanism	Reference
	anti-angiogenic activity in pre-clinical mouse cancer models.	
ATP analogs: SP600125/ SyK	Inhibition of GCN2 activation.	(Pakos-Zebrucka et al., 2016)
RPL41 peptide	ISR modulation by enhancement of nuclear to cytoplasmic translocation of phosphorylated ATF4 for proteasomal degradation. Studies on cancer.	(Pakos-Zebrucka et al., 2016)
Tunicamycin	ER stress induction by inhibition of GlcNAc phosphotransferase, enzyme catalizing the transfer of P-GlcNAc from UDP-GlcNAc to dolichol phosphate in the first step for synthesis of the oligosaccharide precursor for N-glycosylation.	(Urano et al., 2000)
Thapsigargin	ER stress induction by inhibition of sarcoplasmatic ER calcium ATPase (SERCA) pump and depletion of calcium in the ER.	(Urano et al., 2000)
DTT	ER stress induction by inhibition of disulfide bond formation.	(Urano et al., 2000)
KIRA6	Allosteric inhibition of IRE1α by ATP-competitive ligand. Inhibition of IRE1α RNAse activity by blocking oligomerization.	(Morita et al., 2017)
STF-083010	Inhibition of IRE1α RNAse activity	(Lerner et al., 2012)
MKC8866/4μ8C/B-I09/	Selective IRE1 RNAse inhibition. Potential with chemotherapy	(Zhao et al., 2018), (Li et al., 2017), (Xie et al., 2018)
Compound 18	Inhibition of IRE1α RNAse activity by blocking oligomerization.	(Morita et al., 2017)
IAX4/IAX6	Selective activation of IRE1α RNAse independent of allosteric activation by targeting IRE1α nucleotide-binding pocket. Induction of ER adaptive proteostasis in a cellular model of Alzheimer's disease.	(Grandjean et al., 2020)

II. The IRE1α signaling in cancer

The ER is a critical organelle for co- and post-translational protein maturation, folding and quality control of over a third of all cellular proteins (Hetz and Papa, 2018). Most of the proteins destined to plasma membrane, ER and GA residents and proteins of the secretory pathway are translated by ER membrane-associated ribosomes facilitating their simultaneous translocation into the ER lumen. The protein maturation processes occurring in the ER include sequential steps that control the tridimensional structure of newly synthesized polypeptides based on protein folding, disulfide bond formation and glycosylation. Quality control relies on the ER-protein associated degradation machinery (ERAD) which is tightly dependent on N-glycosylation and ultimately drives protein ubiquitylation for subsequent degradation by the 26S proteasome (Hetz and Papa, 2018).

Environmental stimuli affecting cell homeostasis count for alteration of the proteostasis inducing ER stress due to glucose deprivation, amino acid starvation and hypoxia (Hetz et al.,

2020). Alterations of calcium homeostasis, lipidic unbalanced in ER membranes and more specifically, point mutations in proteins affecting their folding capabilities represent cellular disturbances inducing ER stress. Accumulation of misfolded proteins can also result from accelerated mRNA translation due to viral infection and accelerated proliferative rate of oncogenic transformed cells or incapability of clearing the misfolded proteins by ERAD (Yoo et al., 2017). Stress induced by lipidic disturbances can result from changes in the protein to lipid ratio of the ER membrane (Covino et al., 2018), (Hetz et al., 2020)

Series of findings since 1977 led to the discovery of the UPR as part of ER stress induced by accumulation of misfolded proteins and under glucose deprivation (Hetz et al., 2020). The UPR attenuates the burden of misfolded proteins to restore cellular homeostasis by decreasing the translational rate, improving protein folding by chaperones and foldases, degrading non-functional newly synthesized proteins by ERAD and increasing lipid synthesis for ER membrane expansion. However, apoptosis is induced by UPR driving a different cell fate under chronic ER stress (Yoo et al., 2017), (Hetz et al., 2020) (**Figure 10**).

II.1 The UPR signaling

UPR is a complex tripartite mechanism driven by transmembrane ER stress sensors described in vertebrates (Hetz and Papa, 2018), (Hetz et al., 2020) (**Figure 10**). These ER stress transducers are 1) protein kinase RNA- (PKR-) like ER kinase (PERK), 2) activating transcription factor 6 (ATF6 α and β) and 3) inositol-requiring enzyme 1 (IRE1α and β) which are kept inactive by binding of immunoglobulin protein (BiP). BiP is a chaperone of the heat shock protein 70 family localized in the ER lumen that binds the ER stress sensors and keeps them in an inactive form until finding of a misfolded protein takes place. The ER stress sensors share structural features including an ER luminal domain that is bound by BiP via its ATPase domain during their inactive monomeric state and a cytoplasmic domain that for IRE1 displays kinase as well as endoribonuclease enzymatic activities (Yoo et al., 2017). BiP chaperone has a substrate-binding domain that senses misfolded proteins. The accepted mechanism for activation of the ER stress transducers is recognition of defective folded proteins by BiP with subsequent release of the luminal domain of the ER sensors. However, direct sensing of misfolded proteins by IRE1α has been proposed in yeast by *in silico* analysis, but not in mammals (Hetz and Papa, 2018), (Hetz et al., 2020).

UPR is activated when N-linked protein glycosylation and disulfide bond formation are perturbed as well as upon depletion of the ER stores of calcium that affects calcium-dependent resident chaperones (Hetz et al., 2020) (**Figure 10**). UPR orchestrates two temporal cellular programs as part of the adaptive output in order to restore proteostasis. Global translational inhibition to avoid further overloading of proteins in the ER and

enhancement of the ERAD machinery for clearing of misfolded proteins count as the first strategy. The second program is based on transcriptional activation of several genes involved in general protein quality control. The latest reaction is accompanied with a selective translational recovery to allow protein synthesis of ER stress responsive mRNAs (Hetz and Papa, 2018), (Hetz et al., 2020).

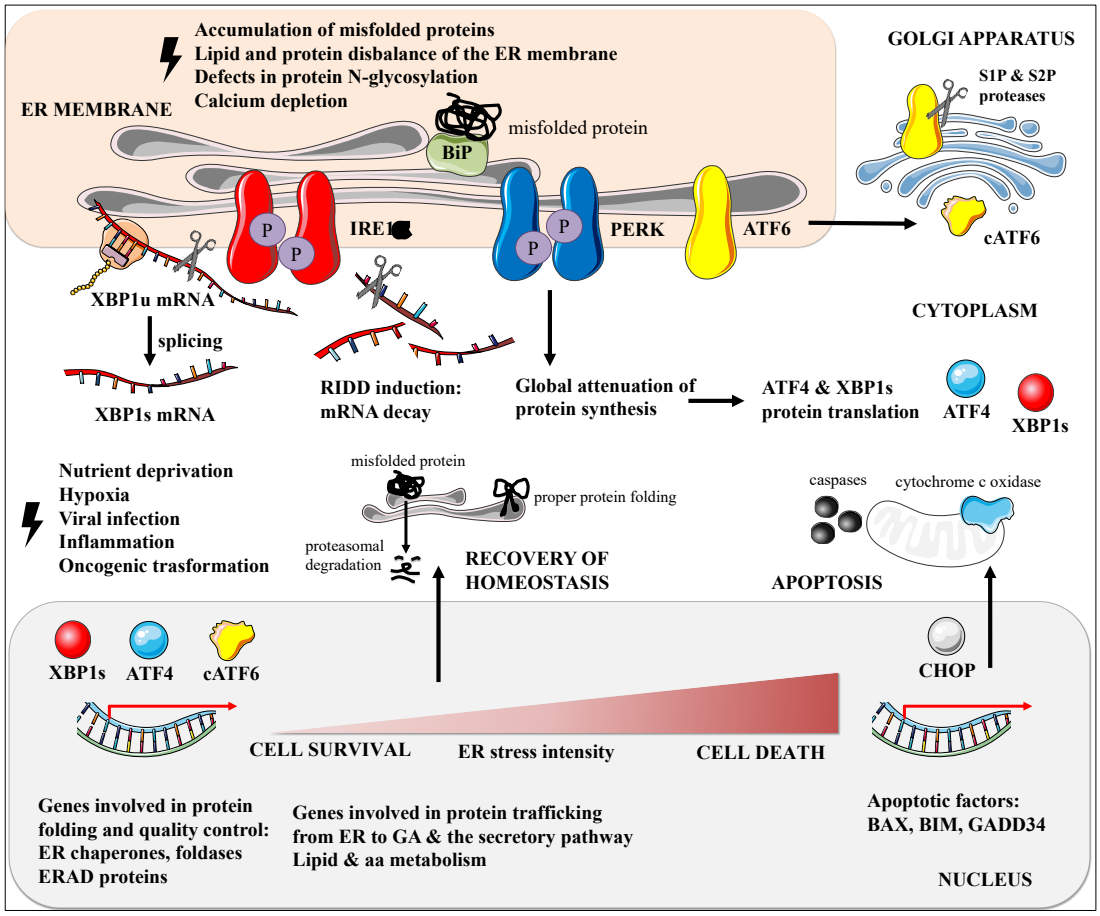

Figure 10. The UPR mechanisms and cellular outcomes under early and chronic induction

The UPR is activated by different stimuli including misfolded proteins, lipidic disturbances, defects in N-glycosylation, calcium depletion, nutrient deprivation and hypoxia. Three ER stress sensors are activated and their downstream targets promote homeostasis recovery and cell survival upon early UPR induction or induce apoptosis upon chronic and intense induction of the UPR. ER, endoplasmic reticulum; BiP, binding immunoglobulin protein; IRE1α, inositol-requiring enzyme α; PERK, PKR-like ER kinase; ATF6, activating transcription factor; S1/2P, site 1/2 proteases; cATF6, cleaved ATF6; XBP1u/s, unspliced and spliced X-box binding protein 1; RIDD, IRE1-dependent decay of RNAs; ATF4, activating transcription factor 4; CHOP, C/EBP homologous protein; GADD34, DNA damage-inducible 34; ERAD, ER-protein associated degradation machinery; aa, amino acid.

II.1.1 The PERK pathway

PERK, a member of the ISR, inactivates eEF2α by phosphorylation to attenuate cap-dependent translation (Hetz and Papa, 2018) (**Figure 10**). As a consequence, the overload of

new synthesized proteins in the ER is decreased. One exception of protein synthesis inhibition is the translation of PERK downstream target, the activating transcription factor 4 (ATF4). ATF4 regulates the expression of UPR responsive genes, including genes involved in restoring cellular homeostasis as well as C/EBP homologous protein (CHOP), an inducer of apoptosis. Induction of either resolving ER stress-genes or pro-apoptotic genes is a fine-tuned equilibrium that depends on the duration and severity of the stimulus. When ER stress is not resolved, ATF4 and CHOP form heterodimers to exacerbate even more the ER stress with concomitant induction of cellular death by apoptosis (Yoo et al., 2017), (Hetz and Papa, 2018), (Hetz et al., 2020).

II.1.2 The ATF6 pathway

ATF6 is a transcription factor that upon release from BiP binding exposes the interaction site with coat protein-II (COP-II) vesicles leading to its translocation into the GA and cleavage by the resident proteases S1P and S2P (Hetz and Papa, 2018), (Hetz et al., 2020) (**Figure 10**). The cleaved active form corresponding to ATF6 cytosolic domain translocates into the nucleus to regulate the expression of several genes including X-box binding protein 1 (XBP1) and genes involved in ERAD. Interestingly, transcriptional induction of XBP1 by ATF6 has been hypothesized to occur as a key step to sustained UPR in a time-dependent fashion (Hetz et al., 2020). The role of ATF6 in regulating the expression of ER chaperones and XBP1 was suggested to occur before XBP1 is activated by splicing and targets specifically other genes to maintain ER stress adaptive mechanisms (Yoshida et al., 2001). In addition, ATF6 and the alternative spliced version of XBP1 can also heterodimerize to regulate the transcriptional program elicited under UPR (Yoo et al., 2017). Activated ATF6 and XBP1 have been suggested to mediate maximal activation of the UPR. This might be an evolutionary advantage in cells expressing both proteins such as mammalian cells since ATF6 homolog has not been found in yeast (Yoshida et al., 2001).

II.1.3 The IRE1α pathway

The most conserved UPR branch from yeast to mammals is triggered by IRE1 (**Figure 10**). IRE1α isoform has been found expressed in all cell types tested (Urano et al., 2000) and the one extensively documented in the literature (Hetz et al., 2020). This serine/threonine kinase has a cytoplasmatic domain with kinase and endoribonuclease activities at the C-terminal of the protein. The kinase domain participates in the trans-autophosphorylation event needed for activation of at least two of these molecules upon dimerization in the ER membrane (Shamu and Walter, 1996). The cytoplasmic kinase domain is linked to the ER luminal domain that senses metabolites, for instance, inositol and probably, unfolded proteins within the ER. Kinase functions of IRE1α as well as its scaffold activity have been described, however, the

most reported function of the protein is linked to its endoribonuclease activity (Hetz et al., 2020).

IRE1α is responsible for activation of XBP1 by alternative splicing of this transcription factor (Shen et al., 2001) (**Figure 10**). Spliced XBP1 (XBP1s) has been described to regulate several genes involved in restoring cell homeostasis under ER stress by forming heterodimers with other transcription factors apart from ATF6. XBP1s-induced genes are involved in protein folding, ERAD, protein secretion and translocation into the ER as well as lipid synthesis. The RNAse activity of IRE1α has also been linked to a process called regulated IRE1-dependent decay of RNAs (RIDD) in which cytosolic and ER-resident mRNAs encoding proteins of the secretory pathway, GA-localized glycosylating enzymes and chaperones are degraded (Han et al., 2009). In addition, microRNAs and ribosomal RNAs are also targeted by RIDD (Hetz and Papa, 2018), (Hetz et al., 2020).

II.1.4 Cell fate under terminal UPR

The crosstalk among all the UPR branches and regulatory networks endow cells with molecular tools to quickly react and adapt to stress (Hetz et al., 2020). For instance, induction of the PERK pathway genetically facilitates ATF6 synthesis. Likewise, active ATF6 regulates the expression of several chaperones, including its own conformational repressor, BiP. Indeed, both XBP1s and ATF6 have been reported to positively regulate the gene expression of BiP as part of a negative feedback loop controlling the activation of ER stress transducers (Yoshida et al., 2001). CHOP induced predominantly as part of the PERK pathway can also be upregulated by IRE1α and ATF6. Furthermore, all the three ER stress transducers are regulated by post-translational modifications as well as interaction with negative and positive cofactors, adaptors and scaffold proteins. The term UPRosome is currently used to describe the protein network and crosstalk with components of other molecular pathway that mediate the different outputs of the UPR (Hetz and Papa, 2018), (Hetz et al., 2020).

Under sustained chronic ER stress, PERK and IRE1α engage the terminal UPR program that instead of resolving the stress, leads to cell apoptosis (Hetz et al., 2020) (**Figure 10**). CHOP, mainly induced under PERK hyperactivation acts as a transcription factor with different partners for upregulation of pro-apoptotic genes as well as suppression of anti-apoptotic factor. GADD34-driven mechanisms as described under chronic ISR is shared with the UPR signaling for induction of apoptosis. The translational program resumes upon dephosphorylation of eEF2α aggravating ER stress and leading to cell death (Li et al., 2014). Re-starting of translation may also depend on ATF4-mediated upregulation of amino acid transporters which activates mTORC1, suppresses autophagy and induces activation of critical components of the translation machinery (Pakos-Zebrucka et al., 2016).

Under IRE1α hyperactivation by cluster formation, the RNAse output of this ER transducer drives RIDD with the consequent massive decay of ER-localized mRNAs (Hetz et al., 2020) (**Figure 10**). mRNA degradation diminishes the ER cargo and protein-folding components which further impair ER stress. In addition, RIDD reduces the levels of some microRNAs that repress pro-apoptotic factors involved in inflammasome formation dependent on caspase 1. Hyperactivation of PERK and IRE1α during terminal UPR induces intrinsic apoptotic pathways (Hetz and Papa, 2018), (Hetz et al., 2020).

II.2 IRE1α, a protein with multiple functions

Sensing misfolded protein in the ER lumen has been the most described signal for activation of IRE1α, however lipid bilayer stress in the ER also triggers the UPR, in special IRE1α (Hetz et al., 2020). IRE1α as an integral protein has a transmembrane domain that allows physical sensing of the mechanical properties of the ER membrane (Covino et al., 2018). Lipid bilayer stress has been reported to activate IRE1α when there is a perturbed ratio of phosphatidylethanolamine to phosphatidylcholine, higher lipid saturation and inositol depletion. In response to inositol depletion and lipid saturation of the ER membrane, IRE1α activation increases membrane lipid biosynthesis leading to a more fluidic ER membrane. The protein-to-lipid ratio of ER membranes has been suggested as a factor driving IRE1α activation. Accumulation of proteins in the ER bilayer rather than in the ER lumen might decrease the lateral diffusion of the membrane, allowing IRE1α molecules being close enough to oligomerize (Covino et al., 2018).

II.2.1 Kinase domain-dependent IREα activity

IRE1α is required for activation of c-Jun N-terminal kinases (JNKs). JNKs, a family of signal transducers of the MAPK pathway were activated upon pharmacological induction of ER stress dependent on the IRE1α kinase domain (Urano et al., 2000). Indeed, overexpression of IRE1α also increased activity of JNK whereas overexpression of a kinase mutant decreased JNK activation. JNK activation was shown to be independent of the PERK pathway upon induction of ER stress. The TNF-receptor associated factor-2 (TRAF2) was identified as an IRE1 kinase domain-binding partner that upon recruitment mediates JNK activation upon ER stress (Urano et al., 2000) (**Figure 11**).

The fine and complex interconnection among ER stress, autophagy and apoptosis under nutrient starvation has been reported to depend on IRE1α-mediated JNK activation (Castillo et al., 2011) (**Figure 11**). Bax inhibitor-1 (BI-1), a conserved ER transmembrane protein suppressing apoptosis mediated by ER calcium release was shown to negatively regulate

autophagy by inhibiting the interaction between IRE1α and TRAF2 under nutrient starvation conditions. BI-1 was shown to physically associate with IRE1α and repress its binding to TRAF2. This correlated with lower JNK activation. Indeed, JNK1 displays a pro-autophagic effect mediated by phosphorylation of the anti-apoptotic factor Bcl-2, dissociation of the complex Beclin1/Bcl-2 and release of Beclin 1 for autophagosome formation (Kroemer et al., 2010). Adult *Drosophila melanogaster* flies showed a longer lifespan after fasting when BI-1 was knocked-down suggesting that at whole-organism level, IRE1α activation induces JNK and may drive autophagy and apoptosis under nutritional deprivation (Castillo et al., 2011).

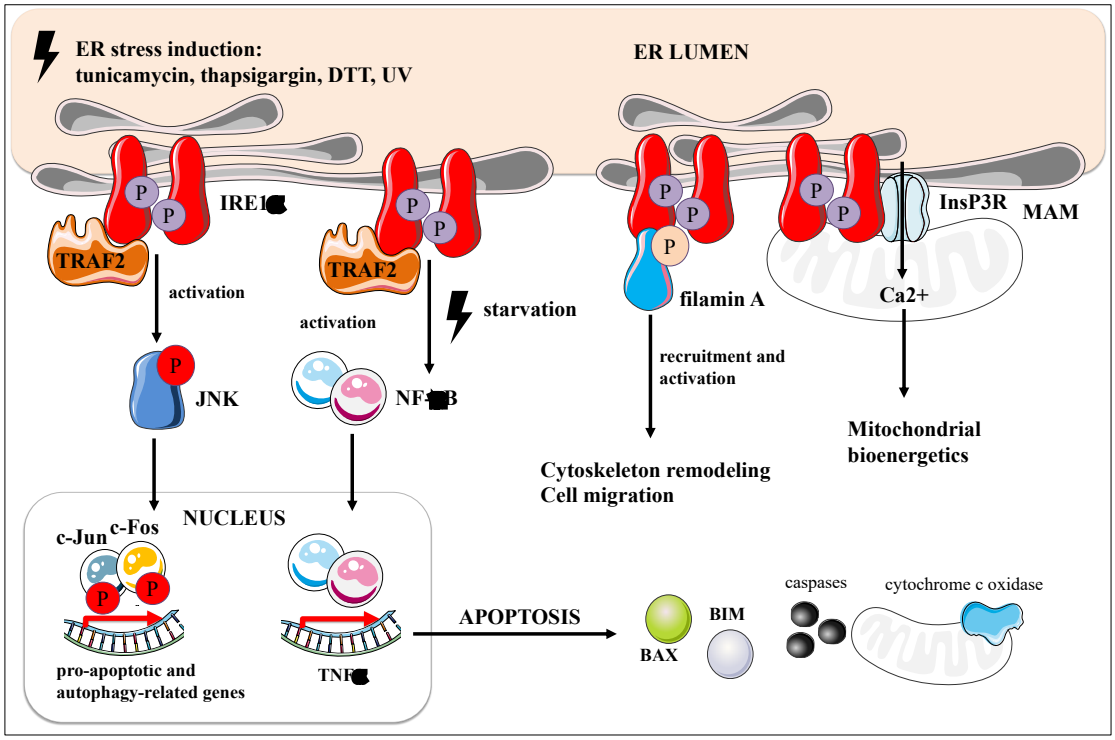

Figure 11. IREα activities dependent on its kinase domain

IREα in a complex with TRAF2 activates JNKs and the NF-κB pathway to drive apoptosis upon ER stress induction. IREα functionating as a scaffold protein interacts with filamin A and InsP3R at MAMs and it is implicated in cytoskeleton remodeling and cell migration as well as mitochondrial bioenergetics. ER, endoplasmic reticulum; DTT, dithiothreitol; UV, ultraviolet light; IRE1α, inositol-requiring enzyme α; TRAF2, TNF-receptor associated factor-2; JNK, c-Jun N-terminal kinases; NF-κB, nuclear factor kappa-light-chain-enhancer of activated B cells; InsP3R, inositol-triphosphate receptors; MAM, mitochondria-associated membranes; BAX, Bcl2 associated X protein; BIM, Bcl2-like protein 11.

IRE1α also activates the NF-κB pathway (Hu et al., 2006) (**Figure 11**). As for JNK activation, IRE1α is involved in activation the NF-κB pathway via physical interaction with TRAF2. Apoptosis induced by ER stress due to IRE1 activation was dependent on NF-κB activation and downstream of TNFα secretion and autocrine signaling. However, NF-κB

activation by ER stress was irrespective of the TNFα-driven signaling. Apoptosis was a result of inhibition of TNFα-induced activation of the NF-κB and JNK pathways due to lower levels of TRAF2 upon ER stress. IREα activity drove NF-κB pathway activation independent of TNFα as well as initiation and amplification of apoptotic mechanisms in ER stressed cells (Hu et al., 2006).

IREα also participates in activation the transcription factor AP1 by induction of members of the MAPK signaling such as JNK and p38. In addition, ERK activation upon ER stress has been shown to involve IREα. Activation of NF-κB and AP1 links the kinase domain-dependent IREα signaling to synthesis and production of cytokines such as IFN-I beyond the role of XBP1s in inducing cytokines by binding to their promoters (Smith, 2018).

IRE1α functions as a scaffold platform for filamin A, an actin-binding protein involved in cytoskeleton remodeling (Urra et al., 2018) (**Figure 11**). The direct physical interaction between these two proteins was shown to occur at the ER irrespective of IRE1α RNAse activity. IRE1α dimer or oligomer formation upon ER stress induction was critical for filamin A phosphorylation and cell migration. Indeed, IRE1α functions as a scaffold for filamin A and at least one of its activating kinases. Involvement of IRE1α in cytoskeleton remodeling and cell migration was confirmed in *Drosophila melanogaster*, *Zebrafish* and in in brain tissue. Therefore, IRE1α may participate in acquisition of metastatic abilities. Cancer dissemination relying on this mechanism will not be affected using pharmacological inhibitors of the IRE1α RNAse activity, a very common approach in cancer research (Urra et al., 2018).

Non-canonical roles of IRE1α functioning as a scaffold at the mitochondria-associated membranes (MAMs) support mitochondrial bioenergetics (Carreras-Sureda et al., 2019) (**Figure 11**). MAMs are the physical bridges communicating the ER and mitochondria. IRE1α accumulated in MAMs participates in the transfer of calcium through inositol-triphosphate receptors (InsP3Rs) from the ER to the mitochondria. Indeed, IRE1α and InsP3R were shown to physically interact at MAMs. IRE1α deficient cells displayed a drop in mitochondrial calcium transfer and concomitant decrease of mitochondrial ATP pool, lower oxygen consumption rate, higher levels of AMPK phosphorylation and increased autophagic flux under nutrient starvation. Splicing of XBP1 was not required for complex formation between IP3R and IRE1α to regulate mitochondrial calcium uptake at basal conditions. At a physiological level, IRE1α kinase mutation in mouse liver tissue showed reduced levels of InsP3R, changes in other MAM-related proteins, TCA metabolites and higher lactic acid (Carreras-Sureda et al., 2019).

II.2.2 IREα RNAse activity

XBP1 is the canonical target of the IREα signaling mediated by its RNAse activity (Hetz et al., 2020) (**Figure 12**). XBP1 mRNA splicing releases an intron containing 26 nucleotides in mammals producing an open reading frame (ORF) shift. The spliced version of XBP1 mRNA (XBP1s) is generated by re-ligation of the fragments by the tRNA ligase RtcB. Cytoplasmatic generation of XBP1s protein occurs during translation of the unspliced mRNA (XBP1 or XBP1u) which is associated with ER-bound ribosomes (Majumder et al., 2012). Pausing of XBP1u translation by docking of the ribosome to the ER membrane allows activated IRE1α to rapidly generate XBP1s mRNA in the cytosol (Hetz and Papa, 2018). Upon early ER stress, XBP1s mRNA accumulates in cytoplasm due to global translational attenuation. The splicing might confer stability to XBP1 avoiding its degradation. When the translational program of some mRNAs is recovered in more advanced UPR, XBP1s is translated while the mRNA is degraded. In this manner, cells immediately respond with sufficient effector protein when protein synthesis resumes while turnover of XBP1s mRNA fines tune the intensity of the signaling (Majumder et al., 2012).

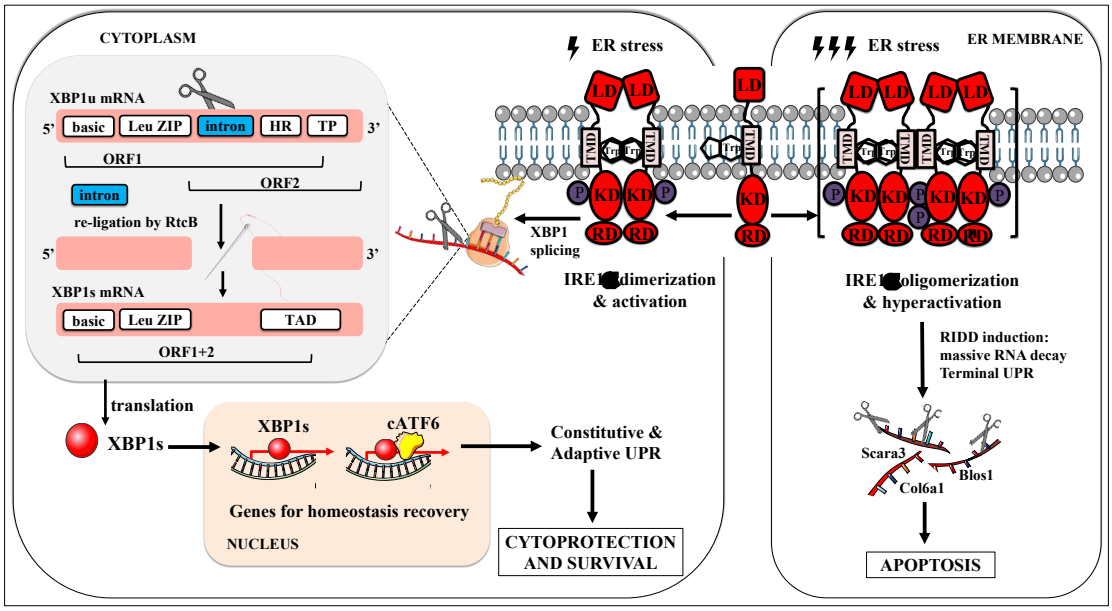

Figure 12. The two branches of the IRE1α RNAse activity

IRE1α drives splicing of XBP1 during early induction of the UPR and massive RNA degradation as part of RIDD during chronic UPR induction. IRE1α dimerization and activation lead to XBP1s activation and to homeostatic recovery and cell survival upon adaptive UPR. IRE1α oligomerization and hyperactivation lead to RIDD induction and apoptosis upon terminal UPR. IRE1α, inositol-requiring enzyme α; XBP1u/s, unspliced and spliced X-box binding protein 1; cATF6, cleaved ATF6; RIDD, IRE1-dependent decay of RNAs; Scara3, Scavenger Receptor Class A Member 3; Blos1, Biogenesis Of Lysosomal Organelles Complex 1 Subunit 1; Col6a1, Collagen Type VI Alpha 1 Chain; LD, luminal domain; KD, kinase domain; RD, RNAse domain; TMD, transmembrane domain; P, phosphate group; basic, basic motif; Leu ZIP, leucine zipper motif; HR, hydrophobic region; TP, translational pausing domain; TAD, transactivation domain; ORF, open reading frame.

This basic leucin zipper transcription factor controls its own transcriptional expression and directly targets several genes involved in ER homeostasis which are constitutively expressed even in the absence of ER stress (Acosta-Alvear et al., 2007) (**Figure 12**). Some of these constitutive UPR genes encode PERK, ATF4, ER resident chaperones such as BiP, DNAJB9, calreticulin and calnexin, members of the disulfide isomerase (PDI) family and components of the protein secretory pathway. Likewise, components of the ERAD pathway and general proteolysis, lipid and fatty acid metabolism, enzymes involved in protein glycosylation, glycolysis, gluconeogenesis and carbohydrate metabolism are also part of the constitutive UPR genes targeted by XBP1s (Acosta-Alvear et al., 2007).

While splicing of XBP1 has been reported to be cytoprotective, RIDD induction is described as a process induced before apoptosis under chronic ER stress (Hetz et al., 2020) (**Figure 12**). The kinase domain of IRE1α has to be functional to allow the RNAse domain being sufficiently active to degrade RNA beyond splicing of XBP1 (Han et al., 2009). Auto-activation of at least two IRE1α molecules by close interaction of their luminal domains in the absent of trans-phosphorylation renders the dimer active only for splicing of XBP1. Oligomerization of IRE1α depending on auto-transphosphorylation enables the two outcomes of the IRE1α RNAse activity, XBP1 splicing and RIDD (Han et al., 2009).

Insulin-producing pancreatic islet β cells are very dependent on the ER machinery (Back and Kaufman, 2012). Therefore, the IRE1α-XBP1 signaling has been extensively reported in the context of type I and type II diabetes mellitus (T1D and T2D). Pro-insulin mRNA is degraded likely by the IRE1α-RIDD pathway upon chronic high glucose stimulation followed by apoptosis in an *in vitro* model of T2D. Hyperglycemia, high demands of insulin and cellular glucolipotoxicity have been linked to ER stress induction and the insulin resistant T2D phenotype (Back and Kaufman, 2012) (**Figure 13**).

IRE1α plays roles in T1D disease onset and progression (Morita et al., 2017) (**Figure 13**). A mouse model of T1D showed that hyperactivation of IRE1α, upregulation of the thioredoxin-binding protein TXNIP as well as reduced insulin mRNA levels in pancreatic β cells are part of the terminal UPR signaling leading to apoptosis and associated with disease initiation. Therefore, treating pre-diabetic mice with pharmacological inhibitors of the IRE1α RNAse activity decreased XBP1s and TXNIP, increased insulin mRNA levels in β cells, decreased glycemia and reverted the pathological phenotype (Morita et al., 2017). Furthermore, upregulation of TXNIP depends on IRE1α-mediated downregulation of microRNA-17 irrespective of XBP1 splicing suggesting that apoptosis is mediated by RIDD induction (Lerner et al., 2012).

The IRE1α-RIDD pathway is implicated in antibody secretion by plasma B cells which are highly dependent on the ER machinery (C.-H. A. Tang et al., 2018) (**Figure 13**). Splenic B cells from XBP1-deficient mice show reduced levels of soluble IgM immunoglobulin upon stimulation with lipopolysaccharide (LPS) which negatively correlated with higher protein expression of IRE1α. Indeed, XBP1 regulates the expression of IRE1α as part of a negative feedback loop. A distinctive phosphorylation site of IRE1α upon LPS stimulation, but no upon tunicamycin treatment induced degradation of canonical RIDD mRNA targets in B cells. Induction of RIDD in B cells by bacterial toxin stimulation was accompanied with reduction of mRNA and protein levels of heavy chains of soluble IgM in a XBP1s independent manner (C.-H. A. Tang et al., 2018).

IRE1α hyperactivation and concomitant RIDD induction have also been reported in splenic $CD8\alpha^+$ DCs (Osorio et al., 2014) (**Figure 13**). This subtype of DCs (cDC1s) displays a high dependency on the IRE1α signaling to control ER homeostasis through constitutive activation of the IRE1α-XBP1 pathway. IRE1α hyperactivation in XBP1 deficient cDC1s was associated with lower cross-presentation of dead cell derived-antigens. Downregulated genes beyond XBP1s targets were found to be RIDD targets such as genes involved in the peptide uptake and processing machinery in the ER for loading onto major histocompatibility complex class I (MHC-I). RIDD induction by IRE1α hyperactivation as a compensatory strategy in XBP1 deficient cDC1s is detrimental for cross-presentation of dead cell-related antigens and therefore, for their T cell-activating functions (Osorio et al., 2014).

The IRE1α-XBP1 pathway maximizes the host innate immunity depending on macrophage-cytokine production against bacterial pathogens engaging Toll-like receptors (TLRs) (Martinon et al., 2010) (**Figure 13**). Upon stimulation of murine macrophages with the TLR4 agonist LPS (lipopolysaccharide), unique activation of the IRE1α pathway was seen among all the UPR branches. XBP1s was shown to play a downstream role upon stimulation of TLRs for sustained production of specific innate immune mediators such as IL-6. Indeed, XBP1s was found to be recruited to the promoters of genes encoding IL-6 and TNFα. TLR2-specific bacterial infection in mice lacking XBP1 in hematopoietic cells produced a higher bacterial burden and less efficient bacterial clearance in the lungs (Martinon et al., 2010).

Hypoxia disrupting ER harmony induces the UPR since protein folding in the ER requires oxygen. Indeed, IRE1α and concomitant JNK-driven autophagy as part of the adaptive ER responses have been induced by hypoxia (Chipurupalli et al., 2019) (**Figure 13**). XBP1s interaction with hypoxia-inducible transcription factor-1, subunit α (HIF-1α) and β-catenin was reported to confer a cellular advantage to cope with reduced oxygen availability (Xia et al., 2019). Increase of HIF-1α and XBP1s in parallel with a reduction of β-catenin levels

occurred upon hypoxia in colon cancer cells. Reduction of the proto-oncogene β-catenin was mediated by ER stress-dependent proteasomal degradation. Lower levels of β-catenin released the inhibition of the HIF-1α-induced transcriptional program while higher levels of XBP1s cooperated with HIF-1α upon hypoxia increasing survival. Therefore, the IRE1α-XBP1 axis synergizes with the cellular response to hypoxia by enhancing HIF-1α program and mediating negative regulation of the β-catenin signaling that is detrimental for cell survival in hypoxic conditions (Xia et al., 2019).

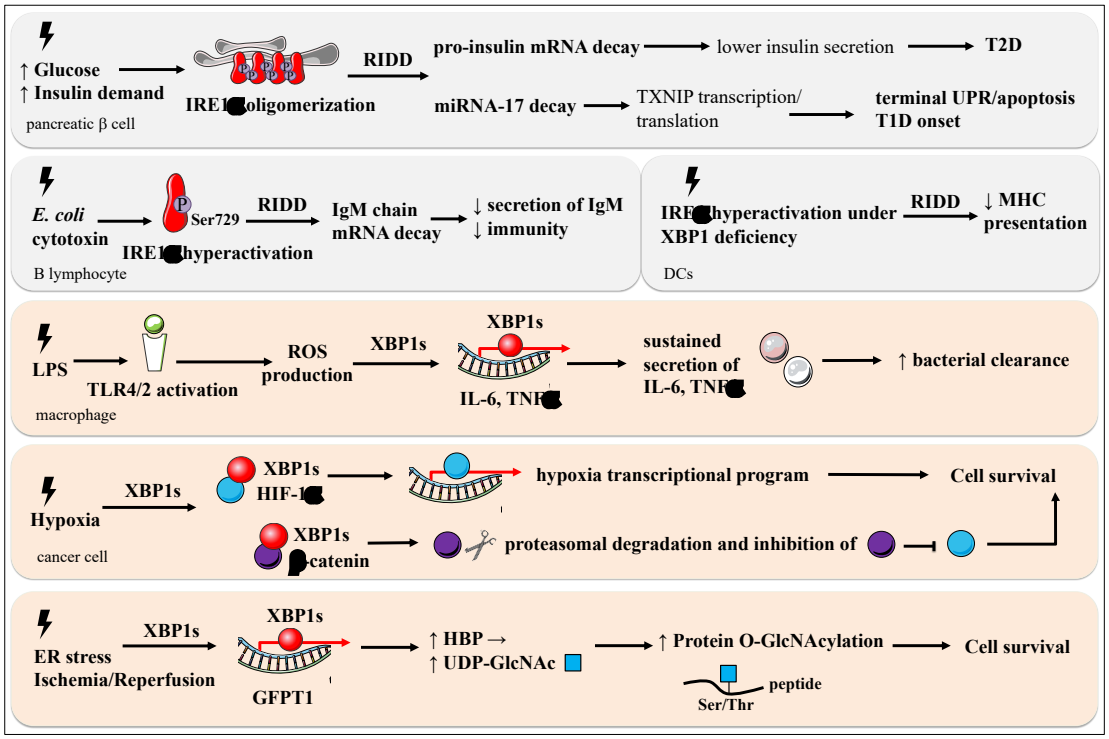

Figure 13. The IRE1α RNAse activities in different cell types, mechanisms of action and cellular outcomes

Different stimuli activate IRE1α in pancreatic β cells, B lymphocytes and DCs leading to RIDD induction upstream of apoptosis, lower antibody secretion and lower MHC-I presentation, respectively. Different stimuli activate IRE1α in macrophages, cancer cells and any cell leading to XBP1 splicing upstream of higher bacterial clearance, oncogene inhibition mediated-cell survival and glycosylation-mediated cell survival, repectively. T1D, T2D, type 1 and type diabetes mellitus; MHC, major histocompatibility complex; DCs, dendritic cells; TLR4/2, Toll-like receptor 4/2; ROS, reactive oxygen species; IL-6, interleukin-6; TNFα, tumor necrosis factor α; HIF-1α, hypoxia inducible factor-1α; HBP, hexosamine biosynthetic pathway; UDP-GlcNAc; uridine diphosphate N-acetylglucosamine; Ser/Thr, serine/threonine.

The IRE1α-XBP1 pathway regulates the HBP (Wang et al., 2014) (**Figure 13**). Upon cardiac ischemia/reperfusion in mice, the infarct region of the heart showed ER stress induction and higher levels of O-GlcNAc modified proteins and enzymes of the HBP. Among them, GFPT1, the first and rate-limiting enzyme of the HBP was found upregulated. Induction of

XBP1s post-reperfusion occurred upstream of the HBP activation. XBP1s was shown to bind the GFPT1 promoter. Indeed, XBP1s is an authentic regulator of the HBP since induction of ER stress with general stimuli caused upregulation of GFPT1 and higher O-GlcNAcylation. Cardioprotective functions of XBP1s upon ischemia/reperfusion in mice overexpressing XBP1s in cardiomyocytes was depending on GFPT1 and O-GlcNAcylation (Wang et al., 2014). The crosstalk between the IRE1α signaling and the HBP also confers survival advantages to *Caenorhabditis elegans* expressing a gain-of-function mutant of GFPT1 by induction of protein quality control processes such as ERAD, proteasomal degradation and autophagy. The increased longevity of GFPT1 mutant worms was completely dependent on the IRE1α-XBP1 signaling (Denzel et al., 2014).

II.3 IRE1α and cancer

Alterations of ER proteostasis have been involved in most hallmarks of cancer (Lhomond et al., 2018), (Hetz et al., 2020). This phenomenon that can be understood considering the high proliferation rate, metabolic demands, secretion capabilities of malignant tissues as well as stressful stimuli coming from the TME. Therefore, the IRE1α signaling pathway has been extensively studied in the context of tumorigenesis and cancer progression and controversial outcomes have been reported. Dual functions of the IRE1α pathway, either pro-tumorigenic or tumor-suppressive have been described in cancer development and progression (Hetz et al., 2020). Cancer type and subtype, oncogenic drivers and dependency of the cell type on the ER machinery and UPRosome dictate the role of this molecular signaling (Rubio-Patiño et al., 2018a). This chapter illustrates the implications of IRE1α in cancer progression mainly in pre-clinical cancer models.

II.3.1 IRE1α in solid tumors

IRE1α pathway modulates the cell secretome, even more in transformed tissues (Gameiro and Struhl, 2018). Non-transformed and transformed breast epithelial cells have shown to inhibit protein synthesis upon glutamine deprivation and during recovery after nutrient depletion. Global translational repression was accompanied by synthesis of ATF4, XBP1s and other ER stress members as well as upregulation of inflammatory factors as part of the selective transcriptional and translation program upon ISR induction. The highest synthesis of inflammatory proteins was seen in transformed cells. The inflammatory response leading to expression of IL-8, IL-6 and CCL20 increased cell migration of transformed cells. Secretion of inflammatory factors might count as mechanism contributing to the metastatic potential of nutrient-depleted tumor. These soluble factors can signal metabolically stressed cells in an

autocrine fashion to pursue a more nutrient-available microenvironment (Gameiro and Struhl, 2018).

Constitutive IRE1α-XBP1 axis has been detected in breast cancer cells, especially in triple negative breast cancer (TNBC) cells (Logue et al., 2018) (**Figure 14**). IRE1α gene signature predictive of the IRE1α activity showed that human breast cancers with high activity had a basal-like with a more mesenchymal-like phenotype, increased invasiveness and a worse clinical outcome. Genes strongly associated with the IRE1α gene signature encode inflammatory factors such as IL-8, IL-6, CXCL1, GM-CSF and TGFβ2. Production and secretion of these cytokines and cell proliferation were reduced upon pharmacological inhibition of the IRE1α RNAse activity with MKC8866. Indeed, blocking these cytokines with neutralizing antibodies decreased proliferation of TNBC cells at the same level that upon treatment with MKC8866 (Logue et al., 2018).

High levels of XBP1s, production of cytokines and clonogenicity were observed in TNBC cells treated with paclitaxel, a common chemotherapeutic for breast cancer (Logue et al., 2018). Inhibition of IRE1α abrogated the tumor-initiating potential of TNBC cells and *in vivo* MKC8866 treatment enhanced the response to chemotherapy. Indeed, combined treatment limited growth of TNBC tumor xenografts and extended mouse survival in comparison to single treatment with paclitaxel. Moreover, continuous IRE1α inhibition seemed to be beneficial after withdrawal of paclitaxel (Logue et al., 2018).

The IRE1α-XBP1 pathway plays pro-tumoral roles by supporting the response to hypoxia in TNBC tumors (Chen et al., 2014) (**Figure 14**). XBP1 silencing in human TNBC cells limited tumor growth and lung metastasis in orthotopic xenografts mouse models as well as decreased tumor incidence of TNBC patient-derived xenografts (PDX). Combination of XBP1 silencing and the chemotherapeutic doxorubicin in TNBC PDXs led to inhibition of tumor relapse. XBP1s as well as HIF-1α were shown to confer tumor-initiating potential to TNBC cells. XBP1s physically interacting with HIF-1α and co-occupying the promoters of HIF-1α targets demonstrated that both factors were necessary for optimal activation of the hypoxic transcriptional program. Therefore, XBP1s regulates the hypoxic transcriptional program orchestrated upon activation of HIF-1α to sustain tumor growth in TNBC mouse models. Furthermore, a high XBP1 gene signature associated with shorter free survival in TNBC patients and XBP1-regulated HIF-1α transcriptional program also associated with a worse clinical outcome in these TNBC patients (Chen et al., 2014).

Activation of IRE1α-XBP1 pathway in breast cancer has been reported to be controlled by c-Myc oncogenic expression since silencing of c-Myc in breast cancer cell lines decreased the

expression of IRE1α and XBP1s (Zhao et al., 2018) (**Figure 14**). Indeed, a high positive correlation between the expression of c-Myc and IRE1α has been seen in breast cancer patients by immunohistochemistry. c-Myc was demonstrated to bind to IRE1α promoter and putative enhancer regions in PDX tumors with high c-Myc expression. Likewise, c-Myc and XBP1s were shown to physically interact in the nucleus and co-occupy the promoter of genes encoding ER-stress related proteins and ERAD components. Unidirectionally, c-Myc was demonstrated to increase the transcriptional activity of XBP1s. Silencing of XBP1s in c-Myc overexpressing cells reduced their clonogenic potential (Zhao et al., 2018).

Inhibition of IRE1α RNAse activity with MKC8866 has shown that tumor growth limitation of orthotopic PDX models correlated with the expression levels of c-Myc in tumors (Zhao et al., 2018). Combined treatment of MKC8866 and the chemotherapeutic docetaxel caused total tumor remission with no relapse after treatment withdrawal. Docetaxel and MKC8866 as monotherapy significantly limited tumor growth of PDX models. The synergic effect of both drugs caused lower proliferation and angiogenesis as well as higher apoptosis induction in tumors. Furthermore, a sensibilization to chemotherapy in the combination treatment was dependent on high c-Myc expression in p53 null-genetically engineered mouse (GEM) models. The combination therapy was associated with higher intra-tumoral infiltration of T lymphocytes and lower recruitment of MDSCs. The combination therapy also reduced the lung metastatic potential of TNBC cells (Zhao et al., 2018).

The IRE1α-XBP1 axis has also been implicated in angiogenesis induction and cancer cell-mediated immunosuppression in TNBC (Harnoss et al., 2020) (**Figure 14**). Silencing of XBP1 or IRE1α limiting tumor growth of subcutaneous xenografts led to reduced expression of VEGF-A. Decreased levels of other pro-angiogenic factors and lower vascular permeabilization were observed in IRE1α-deficient tumors. The IRE1α signaling was implicated in tumor cell-mediated TME remodeling since reduced number of cancer-associated fibroblasts (CAFs) and MDSCs were detected in tumors upon IRE1α inhibition. Indeed, mRNA levels of genes encoding soluble factors involved in recruitment of these stromal cells were downregulated in IRE1α-deficient subcutaneous xenografts (Harnoss et al., 2020).

IRE1α is implicated in the acquisition of a mesenchymal and more aggressive tumor phenotype in PDAC (Genovese et al., 2017) (**Figure 14**). Pancreatic tumor epithelial cells from a Kras-driven PDAC transgenic mouse model escaped senescence upon acquisition of a mesenchymal-like (MS-L) phenotype. The escaper cells exhibited a higher *in vivo* tumor-initiating potential. Downregulation of the Kras signature and target genes of the chromatic remodeler, SMARCB1 in parallel with upregulation of genes involved in cell cycle progression were detected in these cells. Silencing of the tumor suppressor SMARCB1

resulted in higher tumorigenesis, metastatic outgrowth whereas re-expression of SMARCB1 reverted the aggressive mesenchymal phenotype and prolonged survival of PDAC mouse models. Aggressive SMARCB1-deficient tumor cells showed a high protein synthesis rate that led to induction of the IRE1α-XBP1s axis as well as higher c-Myc expression. Malignancy of mesenchymal-like tumors due to attenuation of the original oncogenic signaling driven by Kras and SMARCB1 was dependent on the gain of another oncogenic mechanism driven by c-Myc activation. Genetic suppression of IRE1α in SMARCB1-deficient tumors limited tumor growth, prolonged mouse survival and decreased clonogenicity (Genovese et al., 2017).

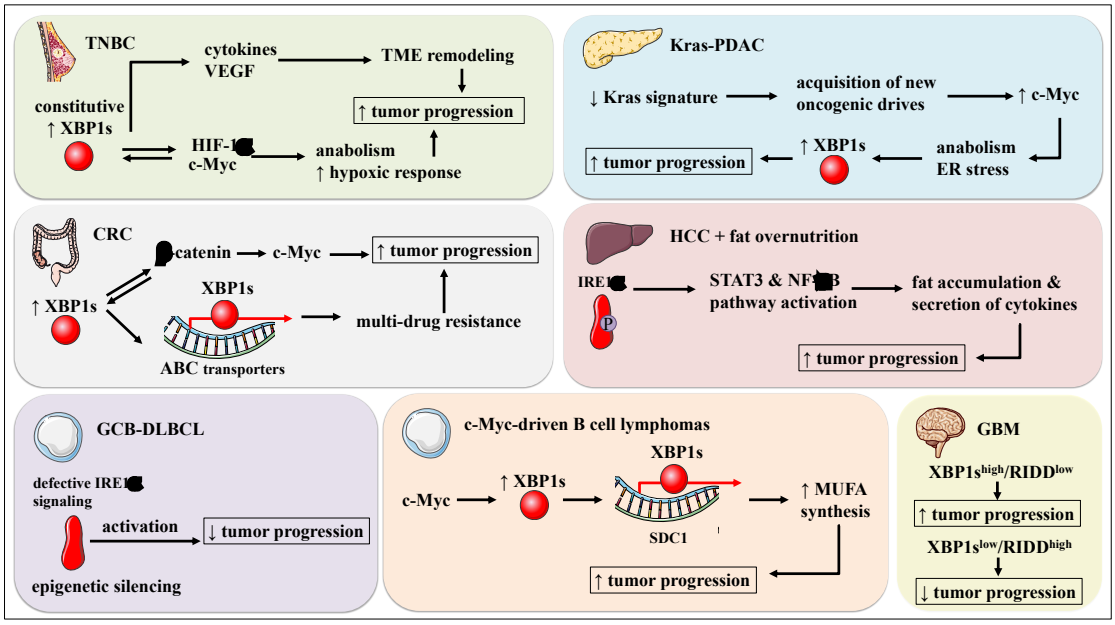

Figure 14. The IRE1α pathway and its mechanisms of action in tumor cells of pre-clinical cancer mouse models

IRE1α activation via XBP1 splicing in TNBC, PDAC, CRC, HCC and c-Myc-driven lymphomas supports tumor progression while IRE1α activation in defective IRE1α-GCB-DLBCL leads to tumor suppression. Uncoupled XBP1s and RIDD induction is associated with tumor progression and suppression, respectively in glioblastoma multiforme. TCNB, triple negative breast cancer; VEGF, vascular endothelial growth factor; TME, tumor microenvironment; PDAC, pancreatic ductal adenocarcinoma; CRC, colorectal carcinoma; ABC, ATP-binding cassette; HCC, hepatocellular carcinoma; GCB-DLBCL, germinal center B cell–like diffuse large B-cell lymphoma; SDC, stearoyl-CoA desaturase 1; MUFA, monounsaturated fatty acids; GBM, glioblastoma multiforme.

The IRE1α-XBP1 pathway has been reported to confer to metastatic disseminated cancer cells (DCCs) the ability to outgrowth in PDAC patients and mouse models (Pommier et al., 2018). DCCs were characterized by loss of epithelial gene expression and lower expression of MHC-I and XBP1s. Once implanted into the liver of pre-immunized mice, DCCs homing the livers

with a quiescent phenotype were unable to form macro-metastasis by the action of T cells. Upon T cell, but not NK cell depletion, DCCs acquired an epithelial phenotype for formation of macro-metastasis while expressing MHC-I. The cell autonomous switch from quiescent to proliferative states in DCCs was depending on XBP1s. XBP1s controlled MHC-I expression in DCCs homing the livers. MHC-I expression on DCCs caused their elimination by $CD8^+$ T cells in pre-immunized mice. In contrast, XBP1 expression in DCCs led to formation of hepatic macro-metastasis by epithelial, proliferating and MHC-I^+ DCCs upon T cell depletion. Therefore, DCCs with a quiescent phenotype downregulate MHC-I to escape immune cell killing by attenuating the IRE1α-XBP1 signaling. The hepatic outgrowth of DCCs with a latent metastasis-initiating potential were processes mediated by reactivation of the IRE1α-XBP1 pathway (Pommier et al., 2018).

Tumor-promoting effects of IRE1α activation through modulation of β-catenin-mediated clonogenicity has been reported in colon carcinoma (Li et al., 2017) (**Figure 14**). IRE1α genetic silencing or pharmacological inhibition of its RNAse activity upon 4μ8C treatment limited subcutaneous tumor growth. IRE1α-silenced tumor xenografts showed a reduction of cell proliferation markers such as β-catenin and β-catenin-regulated genes, cyclin D1 and c-Myc. Abolishing IRE1α expression induced ER stress with subsequent activation of the PERK pathway and translational attenuation of β-catenin. Reduction of β-catenin expression correlated with impaired clonogenicity and cancer stem cell markers. Tumor-protective roles of IRE1α in a β-catenin-mediated manner were also recapitulated in an immunocompetent mouse model of chemical-induced colonic tumorigenesis (Li et al., 2017).

IRE1α independent of its RNAse activity has been link to an oncogenic phenotype enhanced by overnutrition (Wu et al., 2018) (**Figure 14**). Hepatic silencing of IRE1α reduced tumor number and size of a chemical-induced hepatocellular carcinoma mouse model upon high fat diet (HFD). IRE1α-silenced livers displayed hepatocyte apoptosis and reduced proliferation associated with lower expression of STAT3 and its transcriptional targets, c-Myc and HIF-1α. IRE1α played critical roles in the aberrant metabolism and inflammation of obesity-enhanced HCC since liver steatosis and serum and hepatic levels of TNFα and IL-6 were reduced upon IRE1α silencing. Correlating with reduction of inflammatory factors and STAT3 activation, the NF-κB pathway was also impaired. Human HCC tumors displayed higher IRE1α expression than healthy tissue which correlated with STAT3 phosphorylation and poorer patient survival (Wu et al., 2018).

The IRE1α-XBP1 axis as a tumor-protective signaling mediating drug resistance has been shown in colon carcinoma (Gao et al., 2020) (**Figure 14**). Colon carcinoma cells resistant to the chemotherapeutic 5-fluorouracil (5-FU) displayed higher expression of ATP-binding cassette (ABC) transporters. This plasma membrane transporters export drugs out of the cells.

IRE1α silencing or pharmacological inhibition reduced the expression of the transporter ABCB1 while XBP1s was found to bind the ABCB1 promoter. Interestingly, the IRE1α was implicated in multi-drug resistance since inhibition of the IRE1α sensitized 5-FU-resistant cells to treatment with 5-FU and other chemotherapeutics. Indeed, inhibiting IRE1α RNAse activity limited tumor growth of a subcutaneous xenograft mouse model bearing 5-FU-resistant colon carcinoma cells. Synergism when combined with 5-FU chemotherapy was seen depending on reduced levels of ABC transporters (Gao et al., 2020).

The equilibrium between the two different outputs of the IRE1α RNAse activity was shown to dictate tumor brain development (Lhomond et al., 2018) (**Figure 14**). A high IRE1α-gene signature in glioblastoma multiforme (GBM) correlates with shorter patient survival, higher immune response and tumoral invasion markers. Based on XBP1s and RIDD signatures, clustering of tumors revealed that the group of patients with $XBP1s^{high}/RIDD^{low}$ tumors displayed shorter survival, higher expression of markers of tumor invasion, angiogenesis and macrophages than the $XBP1s^{low}/RIDD^{high}$ group. The $XBP1s^{high}/RIDD^{low}$ group was enriched in mesenchymal tumors. A model of antagonizing functions of IRE1α RNAse activity was suggested whereby the IRE1α-XBP1 signaling is positively implicated in tumor malignancy by potentiating tumoral invasion, angiogenesis and immune infiltration whereas the the RIDD axis is more tumor-suppressive. Indeed, primary GBM cells classified as $XBP1s^{high}/RIDD^{low}$ recapitulated a more aggressive tumor phenotype when implanted into mice (Lhomond et al., 2018).

II.3.2 IRE1α in hematological cancer

Anti-tumoral functions of the IRE1α signaling pathway has been reported in diffuse large B-cell lymphoma (DLBCL), specifically, of the germinal center B-cell–like (GCB) subtype (Bujisic et al., 2017). Differentiation of B cells into plasma cells, a process shut-down in GCB-DLBCL, is linked to a high IRE1α-XBP1 signaling. Indeed, plasma cells display a developed ER machinery with sufficient protein folding and maturation capabilities to sustain high secretion of immunoglobulins and cytokines. Therefore, XBP1s as a transcription factor was first described to bind to the X box motif of the HLA-DRα locus encoding the α chain of a variant of MHC class II in a human B lymphoblastic cells (Liou et al., 1990).

Defects in the IRE1α-XBP1 signaling due to IRE1α downregulation was suggested to occur characteristically in GCB-DLBCL (Bujisic et al., 2017) (**Figure 14**). The IRE1α pathway was the only one among the other UPR branches to be impaired. EZH2 histone methyltransferase was found to epigenetically silence IRE1α expression through addition of H3K27me3 marks on its promoter. Interestingly, gain-of-function mutations of EZH2 is a common genetic alteration in GCB-DLBCL. GCB-DLBCL xenografts showed increased transcriptional

expression and higher protein levels of IRE1α upon pharmacological inhibition of EZH2. Epigenetic downregulation of IRE1α by EZH2 was a common oncogenic feature in other types of cancer including cervical cancer. XBP1s displayed a tumor-suppressive function since its overexpression limited tumor growth in subcutaneous xenografts of GCB-DLBCL (Bujisic et al., 2017).

Opposite to the finding in GCB-DLBCL, tumor-promoting functions of the IRE1α-XBP1 axis have been reported in Myc-driven liquid malignancies such as Burkitt's lymphoma (Xie et al., 2018). Pro-tumoral roles of XBP1s was mediated by positive transcriptional regulation of stearoyl-CoA desaturase 1 (SCD1) by binding to its promoter (**Figure 14**). SCD1 is an ER resident protein and the enzyme catalyzing the rate-limiting reaction for synthesis of monounsaturated fatty acids (MUFAs). MUFAs contribute to the fluidic properties of the ER membrane. c-Myc was shown to transcriptionally regulate XBP1 expression by binding to its promoter, to stabilize IRE1α protein and to alter the ER morphology in human B lymphoma cells expressing inducible c-Myc. Indeed, gene expression profiles of Burkitt's lymphoma patients revealed high levels of XBP1s mRNA targets (Xie et al., 2018).

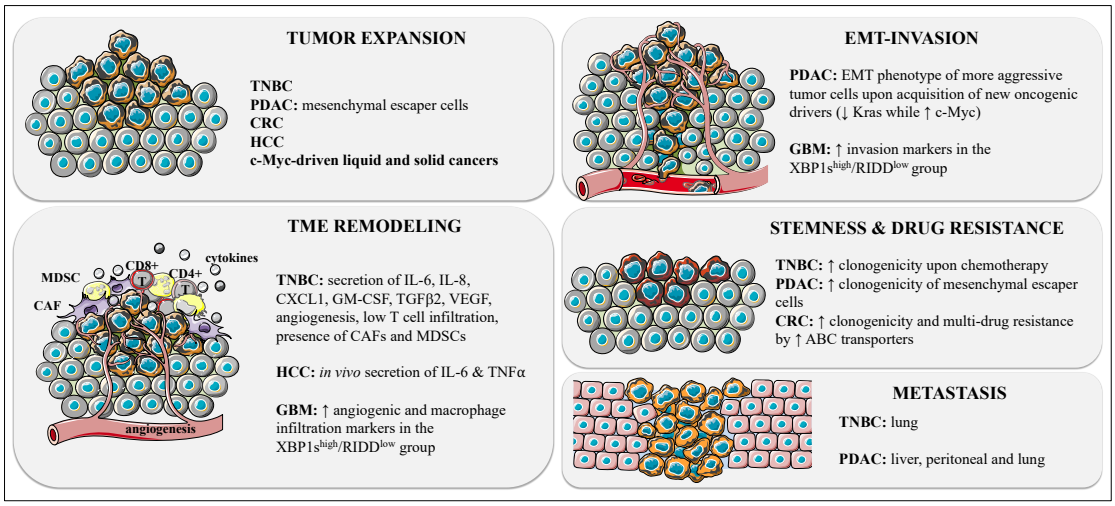

Figure 15. Implication of the IRE1α pathway in the multi-step evolution of different types of cancer

IRE1α activation supports tumor expansion, TME remodeling, EMT and invasion, cancer cell stemness and drug resistance as well as metastasis in TNBC, PDAC, CRC, HCC and c-Myc-driven oncogenic malignancies. TCNB, triple negative breast cancer; PDAC, pancreatic ductal adenocarcinoma; CRC, colorectal carcinoma; HCC, hepatocellular carcinoma; TME, tumor microenvironment; IL, interleukin; CXCL1, chemokine C-X-C motif ligand 1; GM-CSF, granulocyte monocyte-colony stimulating factor; TGFβ2, transforming growth factor β2; VEGF, vascular endothelial growth factor; CAFs, cancer-associated fibroblasts; MDSCs, myeloid-derived suppressor cells; TNFα, tumor necrosis factor α; GBM, glioblastoma multiforme; EMT, epithelial to mesenchymal transition.

Pharmacological inhibition of IRE1α RNAse with B-I09 limited tumor growth of subcutaneous xenograft of high c-Myc human B lymphoma cells (Xie et al., 2018). Indeed, B-I09 treatment decreased SCD1 and *de novo* synthesis of lipids whereas MUFA supplementation rescued the impaired viability of high c-Myc cells caused by B-I09. Tumor-supportive effects of XBP1s downstream of c-Myc-driven tumor progression were extended to N-Myc-driven malignancies such as neuroblastoma. In addition, XBP1 silencing limited tumor growth of subcutaneous xenografts of N-Myc neuroblastoma cells. Combination treatment of the IRE1α inhibitor B-I09 and chemotherapeutics such as doxorubicin or vincristine sensitized human B lymphoma cells to apoptosis. This synergic effect benefited from the reduction in SCD1 protein given by B-I09 (Xie et al., 2018).

Collectively, all these studies illustrate how the IRE1α signaling is involved in the multi-step evolution of neoplastic tissues, mainly by playing tumor-promoting functions (**Figure 15**). Indeed, oncogenic drivers have been shown to deploy the IRE1α pathway as a mechanism to enhance the ER machinery to cope with excessive proteotoxicity due to the high proliferative rate. Likewise, oncogenic drivers activate the IRE1α-XBP1 axis to benefits from the pleiotropic functions of XBP1s which enhances and regulates transcriptional programs supporting tumor cell growth. Ingenious studies have proven that IRE1α plays a role in acquisition of stemness properties conferring mesenchymal phenotypes with higher migration capabilities, invasiveness and tumor-initiating potential. Tumoral aggressiveness supported by the IRE1α pathway have been shown to be activated by c-Myc and to depend on the hypoxic response and secretion of pro-inflammatory factors for TME remodeling and angiogenesis induction. Malignancy supported by IRE1α-XBP1 axis is also implicated in resistance to multiple chemotherapeutics. Opposite to the major described functions of XBP1s, induction of RIDD has been recently described as tumor suppressive (Lhomond et al., 2018).

III. The anti-cancer immunity

The anti-cancer immunosurveillance is orchestrated by different immune cells of the innate and adaptive immunity with cooperative functions. Within the TME, the crosstalk among activating and regulatory immune cells with tumor and other stromal cells dictates immunostimulatory and immunosuppressive phenotypes. Tumor cells play a critical role in shaping the immunological and metabolic features of the TME. While immunologically dying tumor cells can be recognized by immune cells, immune escape mechanisms are often deployed supporting the neoplastic growth. Likewise, metabolic conditions within the TME often dampen the anti-cancer functions of several immune cell population. Therefore, more specialized anti-cancer interventions based on immunotherapy are currently under development and optimization.

III.1 Anti-cancer immunosurveillance and immunosuppression

III.1.1 Cytotoxic T lymphocytes

Naïve mature T lymphocytes expressing a CD8 containing T cell receptor (TCR) undergo clonal expansion upon activation by recognition of TAAs presented by APCs (Raskov et al., 2021) (**Figure 16**). The recognition mechanism implies binding of the TCR to antigenic peptides presented onto major histocompatibility complex class I (MHC-I). The immunological synapse is formed by activated $CD8^+$ T cells via engagement of the TCR, the co-receptor CD8 and adhesion molecules expressed on target cells. A secondary signal mediated with the co-receptor CD28 is needed prior to orchestration of the killing program. Ligands of CD28 such as CD80 and CD86 are highly expressed on professional APCs including macrophages, dendritic cells and B cells. Fully activated $CD8^+$ T cells display higher proliferation and secrete cytokines such as interleukin (IL)-2 (Raskov et al., 2021). $CD8^+$ T cell priming in a TAA-dependent manner occurring in the lymph nodes and tumor infiltration precede the establishment of the immunological synapse between activated effector CTLs and antigen presenting-tumor cells in the TME (Topalian et al., 2016).

Cytotoxic mechanisms of effector $CD8^+$ T cells rely on release of perforin and granzyme at the immunological synapse between CTLs and tumor cells (Raskov et al., 2021) (**Figure 16**). These cytolytic enzymes permeabilize the cell plasma membrane by pore formation to induce apoptosis of the target cells. Alternatively, the Fas ligand expressed on CTLs binds to Fas receptors on target cells inducing apoptosis. CTLs in their naïve and effector states are powerful circulatory patrols of peripheral organs. This property together with their cytotoxic potential, secretion of pro-inflammatory cytokines such as interferon γ (IFNγ) and activation by TAAs make them key immune cells for specific recognition and control of neoplastic masses. However, infiltration of $CD8^+$ T cells into the TME vary depending on the type of tumor. Cold and hot tumors have been defined by the absence and presence of infiltrated CTLs, respectively. A more recent classification considers altered immune-suppressed and altered immune-excluded tumors. The former classification refers to tumors containing few CTLs in the periphery and immunosuppressed by the immune cells including regulatory T cells while the latter classification refers to tumors deprived of CTLs due to a harsh TME (Raskov et al., 2021).

Antigen-experienced effector CTLs develop memory as part of their adaptive immunological features (Han et al., 2020). Memory $CD8^+$ T cells are potent anti-tumor effectors due to their long-lived functions and therefore, persistence during chronic diseases (**Figure 16**). In addition, the long-term T cell-mediated anti-cancer immunity displayed by central memory and memory effector $CD8^+$ T cells has been reported stronger than that of effector T cells in

pre-clinical cancer mouse models. Therefore, the presence of these memory CD8$^+$ T cells has associated with an improved cancer prognosis in humans whereas the proportion of circulatory memory CD8$^+$ T cells relative to total CD8$^+$ T cells has predicted a better response to immune checkpoint blockade. In addition, resident memory CD8$^+$ T cells at barrier sites of mucosal tissues have conferred protection against melanoma by direct killing of tumor cells. This contributes to the loading of DCs with TAA in the TME. DCs carrying tumor antigens can prime naïve CD8$^+$ T cells in lymph nodes, thus potentiating the anti-cancer immune response (Han et al., 2020).

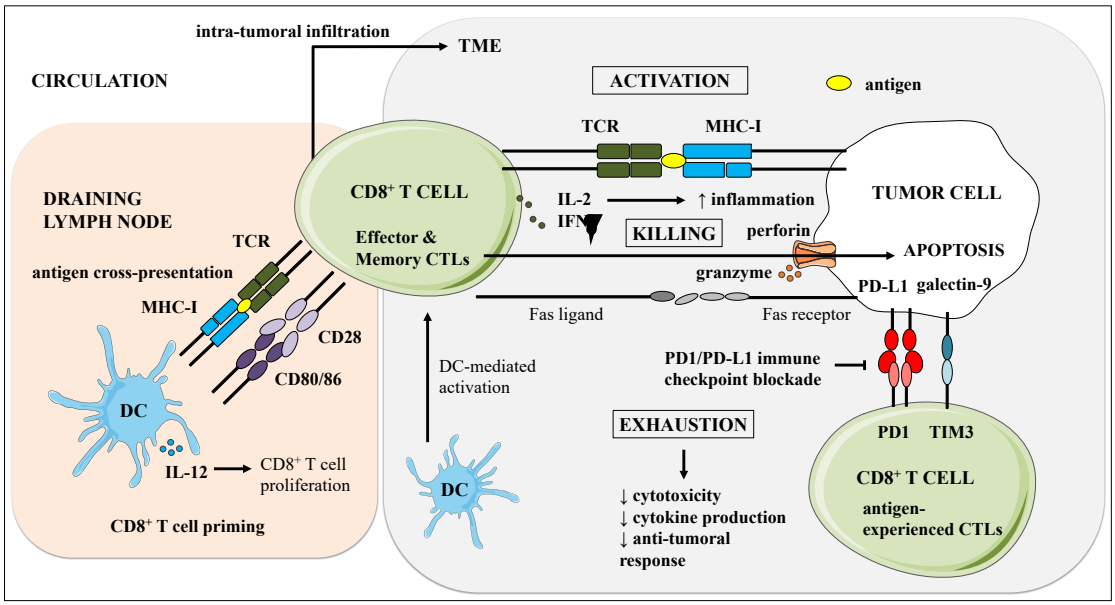

Figure 16. CD8$^+$ T cell, anti-cancer mechanism of action and immune checkpoints

CD8$^+$ T cells are primed and activated by DCs cross-presenting tumor-associated antigens in tumor draining-lymph nodes and within the tumor. Antigen-experienced effector and memory CD8$^+$ T cells are activated by tumor cells presenting antigens onto MHC-I within the TME. Activated effector CD8$^+$T cells orchestrate a killing program by inducing apoptosis in tumor cells via perforin and granzymes and by binding of the Fas ligand to the Fas receptor expressed on tumor cells. Antigen-experienced effector CD8$^+$ T cells undergo exhaustion characterized by higher expression of immune checkpoints on T cells and binding to ligands expressed on tumor cells. TCR, T cell receptor; MHC-I, major histocompatibility complex I; DC, dendritic cell; TME; tumor microenvironment; IFNγ, interferon γ; PD1, programmed cell death protein 1, PD-L1, programmed cell death ligand 1; TIM3, T cell immunoglobulin mucin receptor 3; CAR, chimeric antigen receptor.

Different states of CD8$^+$ T cells include naïve-like, cytotoxic CD8$^+$ T cells and dysfunctional phenotypes in human tumors (van der Leun et al., 2020). The dysfunctional or exhausted states of CD8$^+$ T cells are identified by higher expression of inhibitory molecules such as programmed cell death protein 1 (PD1), cytotoxic T lymphocyte-associated antigen 4 (CTLA4), lymphocyte activation gene 3 protein (LAG3), T cell immunoglobulin mucin receptor 3 (TIM3) and 2B4 (**Figure 16**). These proteins are immune checkpoints to negatively

control the intensity and duration of the immune response avoiding tissue injury and autoimmunity (Dolina et al., 2021). Ligands expressed by APCs, regulatory T cells and tumor cells activate these molecules on $CD8^+$ T cells triggering inhibitory signaling cascades. Exhausted $CD8^+$ T cells display an impaired cytotoxicity and lower secretion of activating and inflammatory cytokines such as tumor necrosis factor (TNF), IL-2 and IFNγ. Cancer patients currently benefits from immune checkpoint blockade (ICB) as anti-cancer immunotherapies aiming to boost the anti-cancer immunosurveillance (van der Leun et al., 2020).

Different expression levels and combinations of the exhaustion markers can define pre-dysfunctional and dysfunctional states as part of a transitional process occurring in intra-tumoral $CD8^+$ T cells undergoing exhaustion (van der Leun et al., 2020). Apart from environmental factors within the TME, continuous exposure of TAAs drives T cell exhaustion. Indeed, activated T cells drive their own disfunction upon persistent triggering of the TCR. Success with ICB in part depends on the dysfunctional profile of tumor-infiltrating T lymphocytes. For instance, in hepatocellular carcinoma-bearing mice, early dysfunctional intra-tumoral $CD8^+$ T cells with tumor reactive functions present at early tumorigenic stages positively responded to PD1 or PD-L1 blockade recovering cytotoxic functions in contrast to late dysfunctional lymphocytes in more advanced tumors (van der Leun et al., 2020).

III.1.2 Helper and regulatory $CD4^+$ T lymphocytes

$CD4^+$ T cells participate in the anti-cancer immune response via different subsets of antigen-experienced cells such as cytotoxic effectors, memory and regulatory (van der Leun et al., 2020). Helper $CD4^+$ T cells can display cytotoxic functions by direct killing of tumor cells via TAA recognition or by modulating the TME. Although this is not the most described functions of helper T cells, $CD4^+$ T cells help to prime CTLs in lymph nodes, therefore, contributing to the effector anti-cancer immunosurveillance (**Figure 17**). This has been described as a second $CD8^+$ T cell-priming step occurring in secondary lymphoid organs depending on $CD4^+$ T cells and DCs. The same DC presenting and cross-presenting MHC-II-destinated antigens onto MHC-I can present antigenic epitopes to both, $CD4^+$ and $CD8^+$ T cells, respectively (Borst et al., 2018).

DCs activating CTLs by cross-presentation need stimulatory membrane-bound signals that occurs by simultaneous antigen presentation to $CD4^+$ T cells for optimal priming of CTLs (Borst et al., 2018) (**Figure 17**). DCs are activated upon binding of CD40 to the CD40 ligand expressed on activated $CD4^+$ T cells. This co-stimulatory signal increases the expression of CD80 and CD86 on DCs enhancing the priming of CTLs via CD28. In addition, $CD4^+$ T cells potentiate the interaction between CD70 expressed on DCs and CD27 on $CD8^+$ T cells. This

binding promotes activation and differentiation of CTLs. This adaptive mechanism for $CD8^+$ T cell priming dependent on $CD4^+$ T cells after the classical and first priming step by DCs alone has shown more potent activation of CTLs. Complementary signals coming from $CD4^+$ T cells seem to confer unique input to DCs priming $CD8^+$ T cells. Indeed, DCs activated as part of innate signals are not able to induce CTL differentiation into memory cells unless they have been in contact with $CD4^+$ T cells. Among the unique features of CTLs primed with the contribution of $CD4^+$ T cells, higher clonal expansion, differentiation into memory $CD8^+$ T cells, higher migratory capacities and tumor infiltration have been reported (Borst et al., 2018).

$CD4^+$ T cells, specifically regulatory T cells (Treg cells) are key modulators of the CTL activity (Ohue and Nishikawa, 2019) (**Figure 17**). Treg cells act through inhibitory mechanisms to maintain the immune response homeostasis by controlling the self-tolerance avoiding allergies and autoimmunity disorders. However, their presence in the TME rather than beneficial suppresses the anti-cancer immune response and associates with impaired control of tumor progression and poor cancer prognosis. Effector Treg cells inhibit DCs maturation in draining lymph nodes and therefore, suppress $CD8^+$ T cell priming in both, the lymph nodes and the TME. Treg cells in contact with self-antigens released by dying tumor cells expand clonally in the TME. Expression of CTLA4 on effector Treg cells mediates immunosuppression by engaging CD80 and CD86 expressed on DCs and blunting the co-stimulatory signal via CD28 needed for $CD8^+$ T cells to become cytotoxic. Indeed, CTLA4 displays a higher affinity for CD80/CD86 than CD28 expressed on $CD8^+$ T cells (Ohue and Nishikawa, 2019). Moreover, intra-tumoral Treg cells show higher activation than circulatory Treg cells based on higher levels of CTLA4 (van der Leun et al., 2020).

Treg cells also display immunosuppressive mechanisms in an antigen-independent manner (Ohue and Nishikawa, 2019) (**Figure 17**). By expressing high levels of CD25 which is the IL-2 receptor α-chain, Treg cells bind with high affinity to IL-2 depriving $CD8^+$ T cells of a cytokine that promotes CTL proliferation. Moreover, secretion of immunosuppressive cytokines such as transforming growth factor (TGF)-β and IL-10 also blunts the activity of effector CTLs. Metabolic immunosuppression is also deployed by Treg cells since binding of CTLA4 to CD80 and CD86 on DCs promotes the expression of metabolic enzymes involved in tryptophane catabolism (Ohue and Nishikawa, 2019). Generation of immunosuppressive tryptophan catabolites within the TME together with depletion of tryptophane hinder effector functions of CTLs (Uyttenhove et al., 2003), (Fallarino et al., 2006). In addition, Treg cells are sensible to oxidative stress and Treg cells undergoing apoptosis by oxidative stress release high content of ATP. ATP catabolism in the TME generates the immunosuppressive metabolite adenosine that negatively impacts on CTL functions. Treg cell depletion in the

TME by CTLA4 blockade has shown to increase the anti-cancer immunosurveillance in pre-clinical mouse cancer models (Ohue and Nishikawa, 2019).

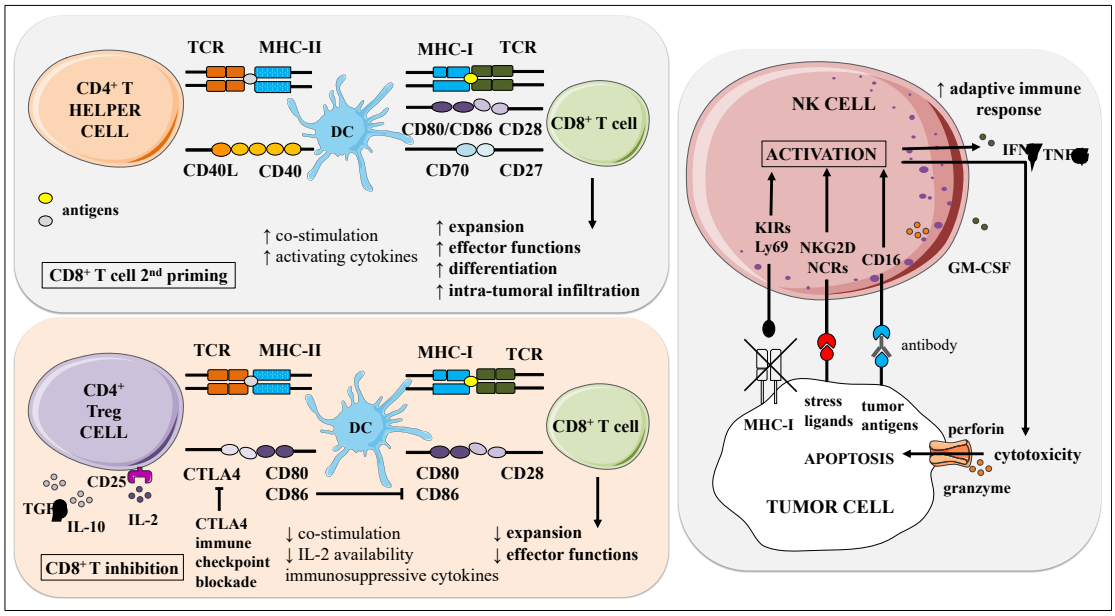

Figure 17. CD4⁺ T helper cells, Treg cells, NK cells and anti-cancer immune mechanisms of action

CD4⁺ helper T cells participate in a second priming event of CD8⁺ T cells mediated by DCs cross-presenting tumor-associated antigens in lymph nodes that induces a more potent activation of CTLs. CD4⁺ Treg cells participates in the negative regulation of antigen-experienced effector CD8⁺ T cells that inhibits CTLs anti-cancer functions within the TME. NK cells are activated upon the absence of MHC-I molecules on tumor cells and upon recognition of activating ligands. Activated NK cells orchestrate a killing program by induction tumor cell apoptosis via perforin and granzymes. TCR, T cell receptor; MHC-I/II, major histocompatibility complex I/II; CD40L, CD40 ligand; DC, dendritic cell; Treg cell, regulatory T cell; CTLA4, cytotoxic T lymphocyte-associated antigen 4; TGFβ, transforming growth factor β; NK cell, natural killer cells; KIRs, killer cell immunoglobulin-like receptors; NCRs, natural cytotoxic receptors; TNFα, tumor necrosis factor α; GM-CSF, granulocyte monocyte-colony stimulating factor; CAR, chimeric antigen receptor.

III.1.3 NK cells

Natural killer (NK) cells are the cytotoxic lymphocytes of the innate immunity that were first described as granular cytotoxic lymphocytes that spontaneously kill tumor cells (Guillerey et al., 2016). Therefore, mechanisms for recognition of cancer cells are not mediated by TAAs presented on MHC. Rather, the lack of MHC-I on tumor cells and the integration of stimulatory and inhibitory signals upon receptor binding determinate the active and inactive states of NK cells (**Figure 17**). By the self-missing mechanism, NK cells are activated upon the absent of MHC-I molecules on any target cells. Consequently, the self-tolerance mediated by stimulation of inhibitory killer cell immunoglobulin-like receptors (KIRs) in humans and Ly69 in mice is lost. This mechanism makes NK cells critical for recognition of tumor cells that downregulate the expression of MHC-I to escape CTL-mediated immunosurveillance.

Likewise, binding of stimulatory receptors such natural cytotoxic receptors (NCRs) and NKG2D to heparan sulphate glycosaminoglycans and damage-associated proteins drives NK cell activation. Damage-associated proteins or stress-induced ligands are commonly expressed by tumor cells. In addition, NK cell recognition mechanisms include binding of CD16 (FcγIIIR) to the Fc region of IgG antibodies opsonizing tumor cells. In that way, NK cells display antibody-dependent cell-mediated cytotoxicity (ADCC). Cytokines such as type I IFN, IL-2, IL-12, IL-15 and IL-18 also count for activation of NK cells (Guillerey et al., 2016).

NK cells have conferred anti-tumoral protection in mouse models of spontaneous tumors (Vivier et al., 2008). Upon activation, effector NK cells display similar cytotoxic mechanism as CTLs such as the release of cytolytic granules containing perforin and granzyme B. In addition, induction of apoptosis of tumor cells can occur by binding to cell death receptors expressed on the target cells since NK cells expressed the Fas ligand and the TNF-related apoptosis-inducing ligand (TRAIL). Since NK cells display low tumor infiltrating capabilities, their anti-cancer effector functions are more potent to control metastatic cells and liquid oncogenic malignancies. A low activity of NK cells in the circulation has been positively associated with the risk of cancer development in humans (Guillerey et al., 2016), (Vivier et al., 2008).

NK cells contribute to innate as well as adaptive immune responses by modulating the activity of T lymphocytes and DCs (Vivier et al., 2008) (**Figure 17**). Indeed, spontaneous cytotoxicity against tumor cells releases tumor antigens that can be cross-presented by DCs. Cytokines secreted by NK cells such as IFNγ, TNFα and granulocyte monocyte colony-stimulating factor (GM-CSF) are involved in DC maturation and maturate DCs can secrete IL-12 reinforcing NK cell effector functions (Vivier et al., 2008). Furthermore, NK cells can secrete chemoattracts to DCs in the TME (Wculek et al., 2020). In lymph nodes, NK cells can potentiate the priming of $CD4^+$ T cells by secreting IFNγ, although cytotoxicity against activated T cells can also take place as an immune homeostatic mechanism. Treg cells secreting TGFβ attenuate the effector functions of NK cells (Vivier et al., 2008). Therefore, potentiating the anti-tumoral effector functions of NK cells by *in vivo* induction with cytokines and agonist antibodies are tested as immunotherapeutic interventions. In addition, the revolution of engineering immune cells with a chimeric antigen receptor (CAR) counts on NK cells for the development of adoptive cell transfer-based immunotherapies (Sivori et al., 2021).

III.1.4 Dendritic cells and macrophages

Dendritic cells (DCs) are the most potent APCs and recognized as the "Nature's adjuvants" (Sabado et al., 2017). DCs elicit as well as regulate naïve and memory T cell immune responses. Conventional and plasmacytoid DCs (cDCs and pDCs, respectively) are the two major subtypes in the circulation, lymphoid organs and peripheral organs, although cDCs display higher migratory capacity. cDCs can be further divided in two subsets such as cDC2 inducing a strong $CD4^+$ T-mediated immunity and cDC1 which are more potent in cross-presentation to $CD8^+$ T cells (Sabado et al., 2017).

Constitutive expression of MHC-II is detected in DCs (Sabado et al., 2017). DC activation and concomitant maturation depends on the acquisition of antigens via recognition of pathogen-associated molecular patterns (PAMPs) and damage-associated molecular patterns (DAMPs) (**Figure 18**). Activation drives upregulation of MHC-I and MHC-II, costimulatory molecules such as CD80 and CD86 as well as production of cytokines. DCs secrete cytokines that modulates immune responses such as IL-12 boosting T cell-mediated responses and IL-12, IL-15 and type I IFN boosting NK cell activities. Maturation of DCs enhances their antigen processing and presentation machinery and migration to lymphoid organs by upregulation of the CCR7 receptor while reducing their phagocytic properties. DCs uptake antigens by several mechanisms including phagocytosis, micropinocytosis, macropinocytosis and endocytosis mediated by receptors including Fc, apoptotic and scavenger receptors. Apart from presenting classical peptides, DCs can present glycopeptides after uptake of glycoconjugates by C- type lectin receptors (Sabado et al., 2017).

The presence of cDC1 within the TME and in tumor-draining lymph nodes is key for priming of $CD8^+$ T cells (Wculek et al., 2020). DCs modulate the CTL-mediated anti-cancer immune response via the formation of an immunological synapse between the $CD8^+$ T cell and DC mediated at first by binding of the TCR to the antigen loaded onto MHC-I. The strength of the synapse depends on co-stimulatory signals such as CD80/CD86 binding to CD28 but also on the interaction between CD137L-CD137, CD40-CD40L and CD70-CD23 (**Figure 18**). CD137L binding induces proliferation of $CD137^+$ T lymphocytes, CD70 binding promotes priming, differentiation and activation of $CD23^+$ T cells and CD40 binding is important for DC reciprocal activation mediated by $CD40L^+$ T cells. DCs also secrete chemoattractants for T cells in the TME such as CXCL9 and CXCL10 (Wculek et al., 2020).

Immunosuppression mediated by DCs expressing programmed cell death ligands (PD-L1/2) attenuates CTL-mediated immune responses (Wculek et al., 2020) (**Figure 18**). Indeed, impaired recruitment, differentiation and survival of DCs into the TME have been observed in human and mouse tumors, in part mediated by lower secretion of the chemoattract CCL4.

Higher content of cDC1 in human tumors positively associates with PD1 ICB responsiveness. Beyond DC activation and mobilization, delivery of neoantigens derived from mutated TAAs alone or in combination with adjuvants and adoptive transfer of autologous antigen-loaded DCs seem to be promising anti-cancer therapies that potentiate NK cell, $CD4^+$ T cell and $CD8^+$ T cell-mediated immune responses (Wculek et al., 2020).

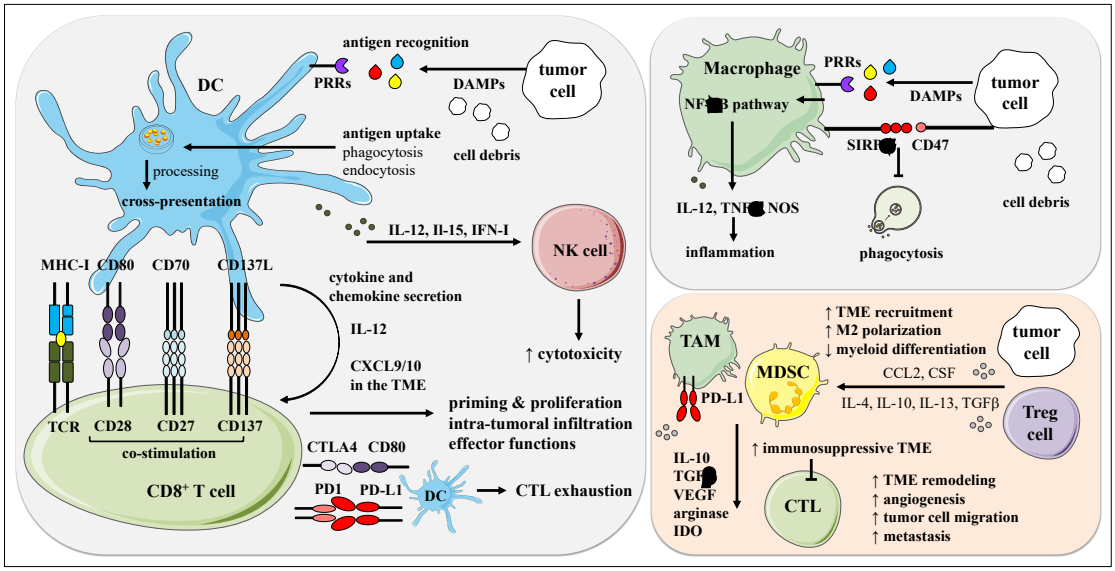

Figure 18. The anti-cancer immune responses of DCs and macrophages. Immunosuppressive responses of TAMs and MDSCs in cancer

DCs are activated upon tumor antigen uptake. Upon activation, release of inflammatory cytokines and chemokines contributes to CTL and NK cell activation. Antigen processing and DC cross-presentation to $CD8^+$ T cells as well as expression of costimulatory molecules mediate $CD8^+$ T cell priming and activation. DCs expressing immune checkpoint ligands drives CTL exhaustion. Macrophages are activated upon tumor antigen recognition and uptake. Macrophage activation leads to release of inflammatory cytokines mediated by NF-κB activation. Phagocytosis of tumor cells by macrophages is inhibited upon activation of the immune checkpoint SIRPα by CD47 expressed on tumor cells. TAMs and MDSCs are induced by cytokines released tumor cells and Treg cells. TAMs and MDSCs induce immunosuppression within the TME and tumor progression by releasing immunosuppressive cytokines and angiogenic factors. DC, dendritic cell, DAMPs, damage-associated molecular patterns; PRRs, pattern recognition receptors; CTL, cytotoxic T cells; NOS, nitric oxide synthase; SIRPα, signal regulatory protein α; TAM, tumor-associated macrophage; MDSC, myeloid-derived suppressor cell; CSF, colony stimulating factor; VEGF, vascular endothelial growth factor; indoleamine 2,3-dioxygenase.

Macrophages are professional phagocytes with antigen-presenting capabilities that can orchestrate an immune response by secreting cytokines and chemokines to attract and activate $CD8^+$ T cells and NK cells (Ruffell and Coussens, 2015) (**Figure 18**). Macrophages are found in the circulation but also as tissue resident cells that in most cases undergo local proliferation in healthy conditions. In cancer, the pool of tissue resident macrophages is replenished by local expansion as well as monocytes recruited from the circulation following chemoattractant

factors such as C-C chemokine ligand 2 (CCL2) and colony-stimulating factor (CSF-1) (Ruffell and Coussens, 2015).

Anti-cancer functions of pro-inflammatory macrophages include secretion of IL-12, inducible nitric oxide synthase (NOS) and TNFα, a cytokine profile that is dependent on induction of the NF-κB pathway (Pathria et al., 2019) (**Figure 18**). The canonical NF-κB (nuclear factor kappa-light-chain-enhancer of activated B cells) pathway is activated in macrophages upon engagement of pattern recognition receptors and cytokine receptors by DAMP-expressing cellular entities and extracellular cytokines (Dorrington and Fraser, 2019). Receptor activation at the plasma membrane leads to phosphorylation of the IKK2 complex that further phosphorylates the inhibitory NF-κB protein IκB. Phosphorylation of IκB induces its proteasomal degradation by polyubiquitination releasing its inhibitory binding to NF-κB subunits forming dimers. Free NF-κB dimers translocate into the nucleus to transcriptionally regulate the expression of several genes including cytokines (Dorrington and Fraser, 2019).

Activation of the PI3K signaling has been shown to be deleterious for the pro-inflammatory state of tumor-associated macrophages (TAMs) (Pathria et al., 2019). Silencing of this pathway has increased the pro-inflammatory profile of macrophages, augmented CTL activity and limited tumor growth and metastasis while increasing animal survival in several cancer mouse models. The anti-cancer phenotype of repolarized TAMs has also been characterized by upregulation of MHC-II and downregulation of immunosuppressive factor such as IL-10, TGFβ, CCL2 and arginase (Pathria et al., 2019).

Before 1970, macrophages were believed to play anti-cancer functions since in vitro studies showed that activated macrophages lyse tumor cells (Pathria et al., 2019). It is now recognized that TAMs are mainly polarized in the TME to play immunosuppressive functions that support tumor growth (Pathria et al., 2019). Accumulation of macrophages in tumors has been associated with poor cancer prognosis and survival (Ruffell and Coussens, 2015), (Cassetta and Pollard, 2018). Still, TAMs are capable of phagocyting tumor cells within the TME of several cancer mouse models upon inhibition of an immune checkpoint triggered by CD47 highly expressed on tumor cells (**Figure 18**). CD47 expressed on any cell is known as the “do not eat me signal” mechanism to keep macrophage self-tolerance. CD47 binding to signal regulatory protein α (SIRPα) on macrophages inhibits phagocytosis, a mechanism of tumor cell immune escape (Pathria et al., 2019).

III.1.5 Tumor-associated macrophages and myeloid-derived suppressor cells

Myeloid-derived cells count as the majority of the immune cell populations in solid tumors (Ruffell and Coussens, 2015). Therefore, targeting the CCL2 receptor CCR2 in pre-clinical

mouse models has shown to control tumor growth depending on a decrease of the immunosuppressive myeloid cells within the tumors and concomitant CTL-mediated anti-cancer response (Pathria et al., 2019). Polarization of TAMs toward an immunosuppressive phenotype in the TME is a process mediated by soluble factors, metabolites, extracellular acidification and hypoxia. This phenotype resembles the anti-inflammatory one displayed by macrophages upon tissue development and repair. Part of the polarizing signals are coming from lymphocytes secreting Th2 cytokines such as IL-4, IL-10, IL-13. Once polarized, TAMs also secrete Th2 cytokines which attenuate anti-cancer immune responses. TAMs producing tumor-promoting soluble factors and extracellular matrix remodelers support tumor survival and chemotherapy resistance (Ruffell and Coussens, 2015) (**Figure 18**).

TAMs have been described to favor angiogenesis by secreting vascular endothelial growth factor-A (VEGF-A), increasing its bioavailability by production of matrix metalloproteinase 9 and inducting VEGF-A production by endothelial cells (Cassetta and Pollard, 2018) (**Figure 18**). Indeed, a subpopulation of TAMs expressing the angiopoietin receptor associates with vessels and its depletion limits tumor growth and metastasis. In addition, TAMs have been shown to inhibit CTLs by *in vitro* nutrient depletion and by *in vivo* upregulation of PD-L1. TAMs also recruit Treg cells to the TME. Pro-metastatic functions of TAMs have been described in pre-clinical cancer mouse models where macrophage depletion decreased the metastatic burden. Furthermore, tumor cells migrate following soluble factors secreted by macrophages (Ruffell and Coussens, 2015), (Cassetta and Pollard, 2018), (Hou et al., 2021).

In contrast to TAMs which are differentiated and mature macrophages, myeloid-derived suppressor cells (MDSCs) derived from cancer-induced myelopoiesis are immature myeloid cells with a natural immunosuppressive activity (Talmadge and Gabrilovich, 2013). Indeed, this immune population of undifferentiated cells with phenotypes similar to monocytes or granulocytes and with immunosuppressive functions are highly detected only under pathological states caused by infection, inflammation and neoplastic growth. MDSCs can be classified as monocytic-MDSCs (Mo-MDSCs) expressing NOS and granulocytic or polymorphonuclear-MDSCs (G or PMN-MDSCs) expressing arginase. The latter subtype is the predominant in most cancer mouse models. MDSCs proliferation is induced by tumors secreting VEGF-A and GM-CSF, G-CSF and M-CSF (Talmadge and Gabrilovich, 2013).

MDSCs inhibit CTL activity and their frequency in the circulation negatively correlates with T cell numbers (Talmadge and Gabrilovich, 2013) (**Figure 18**). Therefore, the presence of MDSCs has been associated with poor cancer prognosis. Indeed, surgical resection of solid tumors has decreased the number of circulating MDSCs and T cell dysfunction. Depletion of MDSCs in cancer mouse models limits tumor growth and metastasis while increasing survival. MDSCs support tumor invasion by secreting proteolytic enzymes such as matrix

metalloproteinases. Likewise, MDSCs are involved in angiogenesis and metastasis. T cell dysfunction mediated by MDSCs has been described dependent on secretion of NOS, ROS, arginase and cyclooxygenase 2 (Talmadge and Gabrilovich, 2013), (Pawelec et al., 2019), (Hou et al., 2021).

III.2 Tumor cells immunogenicity versus immune escape

Apoptosis of malignant cells can be induced by extrinsic signals such as cell death ligands (i.e., Fas ligand, TRAIL and TNFα) expressed by CTLs and NK cells (Hanahan and Weinberg, 2011). Intrinsic danger signals such as DNA damage, cellular stress and disruption of cellular homeostasis associated with oncogene-triggered cancer cell proliferation and anabolism also elicit apoptosis in tumor cells. Extrinsic and intrinsic apoptotic programs converge on the release of cytochrome c from mitochondria to the cytoplasm which leads to caspase activation of caspases 8 and 9 that initiate proteolytic activation of effector caspases such as caspase 3. Dead cells are cleared from the resident tissue by neighboring and phagocytic immune cells without inducing adaptive immune responses (Hanahan and Weinberg, 2011) (**Figure 19**).

As a hallmark of cancer, neoplastic cells avoid apoptosis by p53 loss-of-function mutations, upregulation of anti-apoptotic factors, secretion of growth factors, downregulation of pro-apoptotic members and interruption of the extrinsic death ligand-induced apoptotic pathway (Hanahan and Weinberg, 2011). Therefore, standard anti-cancer drugs are intended to induce apoptosis of tumor cells (Pol et al., 2015). Beyond apoptosis of tumor cells, some anti-cancer cytotoxic drugs are inducers of an immunogenic version of the apoptotic pathway. Immunogenic cell death (ICD) induced by several clinically approved chemotherapeutics such as anthracyclines not only eliminate cancer cells by activating intrinsic apoptosis but amplify tumor cell killing by potentiating adaptive immune responses against dying cells (Pol et al., 2015) (**Figure 19**).

III.2.1 Immunogenic cell death

Tumor cell immunogenicity depends on signals produced by malignant cells that are recognized by the immune system (Garg et al., 2017). Immunogenic cell death (ICD) elicits the recognition of dying tumor cells by DCs and macrophages which can further present TAAs to T lymphocytes to elicit an adaptive anti-cancer immune response (**Figure 19**). DAMP exposition or secretion by stressed, injured or dying tumor cells is detected by PRRs, phagocytosis receptors and purinergic receptors on APCs. DAMPs can be either exposed and highly expressed on the plasma membrane such as calreticulin or secreted into the extracellular matrix such as ATP and high motility group protein B1 (HMGB1) (Krysko et

al., 2012). Recently, secretion of type IFN and extracellular annexin A1 and extracellular nucleic acids have been considered as part of the coordinated ICD mechanisms induced by chemotherapy (Pol et al., 2015), (Garg et al., 2017).

The mechanism of action of several standard care for many cancers such as chemotherapy and radiotherapy is the induction of ICD (Krysko et al., 2012) (**Figure 19**). Indeed, doxorubicin, mitoxantrone and γ-radiation were the first anti-cancer treatments identified as ICD inducers, specifically by induction of ER stress. However, ER stress induction in the absent of ROS production leads to induction of immunologically silent apoptosis. Anti-cancer drugs inducing a strong ICD rely in part in the parallel induction of ER stress and ROS production which promote the expression and secretion of multiple alarmins even at the pre-apoptotic stage (Krysko et al., 2012). Indeed, ICD has been induced in mouse models of $Kras^{G12D}$-driven colorectal carcinoma upon combination treatment with an antibody targeting epidermal growth factor receptor (EGFR) and chemotherapy. ICD was dependent on ER stress induction and DC-mediated phagocytosis. Immunized mice with $CD8^+$ T cells isolated from colorectal carcinoma-bearing mice treated with the combination therapy were more resistant to tumor growth after rechallenging. ICD was described as dependent on suppression of XBP1, a downstream effector of the UPR pathway (Pozzi et al., 2016).

Calreticulin, a calcium-binding and ER resident protein functions as a chaperone and a regulator of calcium levels and signaling (Krysko et al., 2012). Calreticulin exposure as part of the ICD induced in cancer cells under chemotherapy not only mediates tumor cell phagocytosis by APCs but antigen processing and presentation for T cell priming (**Figure 19**). The exposure of calreticulin during ICD occurs in the pre-apoptotic and early apoptotic stages before the cell membrane has been permeabilized (Obeid et al., 2007). Exposure of this alarmin during the pre-apoptotic stage depends on the protein secretory pathway including the transport from the ER to the GA and protein trafficking mediated by PERK and PI3K as well as induction of the pro-apoptotic factors BAX and BAK. However, not all ICD inducers rely on the same molecular pathways for exposure of calreticulin and ICD can also be induced in the mid and late apoptotic stages (Krysko et al., 2012).

Release of ATP during the pre-apoptotic stage depends on the pathways driving calreticulin exposure while ATP secretion during early apoptosis depends on caspases and autophagy induction (Krysko et al., 2012) (**Figure 19**). ATP in the extracellular matrix is detected by purinergic receptors such as P2X7 on DCs. Subsequently, activation of the inflammasome and secretion of IL-1β by DCs take place together with TAA presentation to $CD8^+$ T cells. Beyond ATP as an alarmin, ATP catabolism and generation of adenosine in the extracellular milieu is immunosuppressive rather than immunogenic. Adenosine is generated by ATP hydrolysis by CD39 and CD73 expressed on Treg cells (Krysko et al., 2012).

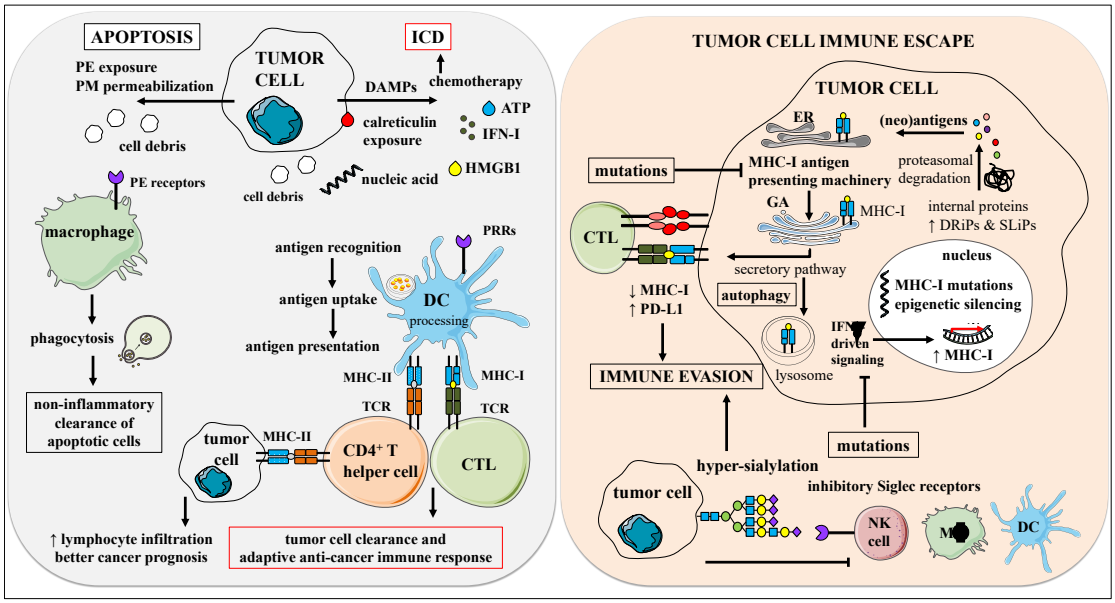

Figure 19. Tumor cell immunogenicity and immune escape mechanisms of tumor cells

ICD of tumor cells elicits an adaptive anti-cancer immune response via recognition of DAMPs by DCs. Activated DCs cross-present and present tumor associated antigens to CD8+ and CD4+ T cells. MHC-II specific expression on tumor cells induce an adaptive anti-cancer immune response by activation of CD4+ T cells. Tumors cells that undergo apoptosis expose PE and permeabilize their membrane. Tumor cell debris is recognized and cleared by macrophages via phagocytosis with not induction of an adaptive immune response. Tumor cells escape immune surveillance by decreasing the surface expression of MHC-I via mutations in genes coding for MHC-I, mutations in genes coding for members of the processing and presenting machinery, mutations in genes of the IFNγ-driven signaling, epigenetic silencing of MHC-I and autophagy of MHC-I. Hyper-sialylation of the tumor cell glycocalyx is another tumor cell immune evasion mechanism that inhibits the effector functions of immune cells via Siglec receptor binding. ICD, immunogenic cell death; PM, plasma membrane; PE, phosphatidylethanolamine; DAMPs, damage-associated molecular patterns; HMGB1; high motility group protein B1; IFN-I, class I interferon; PRRs, pattern recognition receptors; CTL, cytotoxic T cell; DRiPs, defective ribosomal products; SLiPs, short-lived proteins; ER, endoplasmic reticulum; GA, Golgi apparatus; MHC, major histocompatibility complex; Siglec, Sialic acid-binding immunoglobulin-like lectin; Mϕ, macrophage; DC, dendritic cell; NK, natural killer.

HMGB1 is a chromatin binding protein that is secreted as a dead cell-derived antigen by necrotic cells (Krysko et al., 2012). This induces a potent inflammation dependent on neutrophils, monocytes and macrophages. Cancer cells undergoing ICD release HMGB1 during the later stages in a process dependent on caspases (**Figure 19**). The immunogenic role of HMGB1 has been shown in mice immunized with HMGB1-depleted tumor cells which displayed higher tumor burden upon wildtype tumor cell rechallenge. The activity of secreted HMGB1 also depends on the redox status of the extracellular milieu since only an intermediate oxidized form functions as a DAMP inducing pro-inflammatory cytokine secretion (Kazama et al., 2008). Rather than immunogenetic, secretion of HMGB1 can

immunosuppress tumor infiltrating DCs by binding to their inhibitory TIM3 receptors (Krysko et al., 2012).

More recently, tumor-specific expression of MHC-II has been correlated with better cancer prognosis in humans and tumor growth limitation in pre-clinical models (Axelrod et al., 2019) (**Figure 19**). MHC-II molecules which are constitutively expressed on DCs when expressed by tumor cells seem to contribute to tumor cell immunogenicity. Indeed, higher diversity of peptides presented by MHC-II may improve CTL recognition. Apart from MHC-II null tumor cells, tumor cells expressing MHC-II has been described as constitutive or IFNγ-inducible. Tumor specific MHC-II expression and related pathway have been reported in human melanoma, glioma, lymphoma, breast, colon, ovarian, prostate and lung carcinoma. Apart from better survival in some of these cancer patients, tumor-expression of MHC-II associated with higher infiltration of $CD4^+$ and $CD8^+$ T cells. In pre-clinical cancer mouse models, exogenous upregulation of MHC-II limited tumor growth dependent on T cells and irrespective of NK cells. Interestingly, some of these studies have shown that co-stimulatory signals such as CD80 and CD86 are not necessarily needed for tumor regression (Axelrod et al., 2019).

Rather than ICD and MHC-II expression, tumor cells deploy several immune escape mechanisms such as upregulation of the immune checkpoint PD1 ligand (PD-L1), presentation of poor immunogenic antigens and downregulation of MHC-I (Garg et al., 2017). These mechanisms together with an immunosuppressed TME decrease tumor cell immunogenicity and dampen the effects of the ICD (Garg et al., 2017).

III.2.2 Tumor immune escape

Any nucleated cells express on the surface polymorphic glycosylated MHC-I molecules loaded with short peptides containing eight to ten amino acids (Blander, 2018). MHC-I molecules are composed of the constant light chain β2-microglobulin that is non-covalently attached to the heavy α chain. The α chain contains three domains, α1 and α2 form the peptide-binding groove. MHC-I loading with internal peptides derived from the host as well as internalized viruses and bacteria is the classical pathway for antigen presentation whereas cross-presentation refers to MHC-I loading with exogenous proteins taken by endocytosis and phagocytosis. Cancer cells presenting their internal peptides onto MHC-I are sensed by $CD8^+$ T cells and if neoantigens are present, an anti-cancer immune response is elicited (Blander, 2018) (**Figure 19**).

Loading of MHC-I with peptides is a post-translational process occurring in the ER (Blander, 2018) (**Figure 19**). Prior to MHC-I loading, cytoplasmatic proteins are degraded by the

proteosome before peptides are translocated into the ER. While β2-microglobulin is co-translationally translocated into the ER by the Sec61 complex, the α chain is folded in the ER by chaperones such as calnexin and BiP prior to formation of the dimer β2-microglobulin-α chain. The peptide loading complex (PLC) including the peptide transporter associated with antigen processing (TAP), tapasin, the chaperones ERp57 and calreticulin as well as the ER aminopeptidases ERAP1 and ERAP2 associates with the assembled MHC-I molecule. Interactions between MHC-I and the PLC allow MHC-I to bind high affinity peptides prior to export of the complex toward the ER-Golgi apparatus intermediate compartment (ERGIG). Quality control processes occurring in the ER, ERGIG and in the cis-Golgi by tapasin, calreticulin and UDP-glucose:glycoprotein glucosyltransferase (UGT1/UGGT1) warrant that MHC-I is proper folded and loaded with high affinity peptides. Therefore, unfolded, empty or sub-optimally loaded MHC-I with low affinity peptides are retained in these compartments and do not traffic to the plasma membrane (Blander, 2018).

During cancer progression, tumor cells undergo immunoediting because of the intense crosstalk with the anti-cancer immunosurveillance (Dunn et al., 2004). Cancer immunoediting is a process that entails three phases if the first one, elimination of all tumor cells does not occur. Adaptive mechanisms deployed by tumor cells under the pressure of the innate and adaptive immune system allow neoplastic clones to survive and to generate new tumor cell variants which are immune resistant. After this equilibrium phase is reached, immune escape of the tumor cells takes place allowing their uncontrolled proliferation. Immune escape depends on the capacity of tumor cells to be less immunogenic and to reprogram the TME toward an immunosuppressive niche while weakening the anti-cancer immunosurveillance (Dunn et al., 2004).

Lower immunogenic tumor cells downregulate MHC-I to escape sensing by $CD8^+$ T cells (Burr et al., 2019) (**Figure 19**). Mutations in genes encoding members of the MHC-I antigen presenting machinery and the IFNγ response pathway have been described as original as well as acquired tumor resistance strategies. Indeed, the IFNγ-triggered pathway induces MHC-I and PD-L1 expression via activation of the JAK/STAT pathway. Apart from transcriptional downregulation of MHC-I, epigenetic silencing of MHC-I has been recently shown in human cancer cells. Inhibition of the epigenetic silencing upregulated several components of the MHC-I antigen presenting machinery such as proteasomal members, TAP and MHC-I heavy chains. Furthermore, epigenetic repression of MHC-I also occurred upon IFNγ stimulation, fact that led to tumor cell resistance to T cell-mediated cytotoxicity. A poised state of MHC-I by bivalent histone marks (suppressive H3K27me3 and activating H3K4me3) was shown to be conserved in different human cancer cells as well as in stem cells suggesting that tumor

cells deploy an evolutionarily conserved mechanism to acquire immune resistance (Burr et al., 2019).

In cancer cells where MHC-I is not mutated neither downregulated, autophagy has been shown to mediate lower presentation of MHC-I at the cell surface (Yamamoto et al., 2020) (**Figure 19**). In human PDAC cells, MHC-I was shown to accumulate in autophagosomes and to be degraded by lysosomes as part of an autophagic mechanism. Indeed, inhibition of autophagy not only increased surface expression of MHC-I, but potentiated T cell mediated killing as well as limited pancreatic primary and liver metastatic tumor growth in a $CD8^+$ T cell-dependent manner. Autophagy of MHC-I modulated the immunogenicity of ICB-resistant PDAC cells since MHC-I inhibition sensitized tumor-bearing mice to combination ICBs with PD1 and CTL4 (Yamamoto et al., 2020).

Beyond MHC-I expression for CTL recognition, the nature of the presented peptides is critical for activation of T lymphocytes (Wculek et al., 2020) (**Figure 19**). Neoantigens derived from mutated proteins count as immunogenetic epitopes eliciting adaptive anti-cancer immune responses. MHC-I can present peptides generated from defective ribosomal products (DRiPs) and short-lived proteins (SLiPs) (Ruiz Cuevas et al., 2021). Indeed, the MHC-I immunopeptidome of cancer cells is highly abundant in peptides derived from proteins containing non-annotated open reading frames (ORFs) and frame-shifted genes. These non-canonical proteins are more unstable and therefore, contribute less to the cell proteome but they generate five time more MHC-I peptides in human B lymphoma cells than annotated canonical proteins (Ruiz Cuevas et al., 2021). Peptides derived from novel or unannotated ORFs have been shown to be additional sources of tumor-associated antigens in melanoma, chronic lymphocytic leukemia and glioblastoma (Ouspenskaia et al., 2022). Beyond the classical immunopeptidome, glycopeptides can also be presented by MHC-I (O-glycans) and MHC-II (N-glycans) (Wolfert and Boons, 2013). Tumor cells expressing O-glycosylated truncated version of mucin 1 have been suggested to present hypo-glycosylated epitopes on MHC-I that trigger CTL recognition (Wolfert and Boons, 2013).

Hyper-sialylation of the glycocalyx is another tumor cell mechanism of immune evasion (Daly et al., 2019) (**Figure 19**). Sialic acids are self-associated molecular patterns (SAMPs) expressed by heathy cells and help to keep immune tolerance. Sialic acid-binding immunoglobulin-like lectin (Siglec) receptors are expressed by most of the immune cells to mediate the recognition of sialic acid-containing glycoproteins. Most of hematopoietic cells express at least one activating or inhibitory member of the Siglec family. Siglec-7/9 ligands such as mucin-type of O-glycans containing sialic acid residues are highly expressed on colon, renal and cervical carcinomas as well as melanoma and chronic myeloid leukemia. Tumor de-sialylation by intra-tumoral delivery of a sialyltransferase inhibitor limited

melanoma tumor growth in mice dependent on CTL-mediated cytotoxicity, higher infiltration of CTLs and NK cells and lower numbers of Treg cells. Besides, sialylated mucin 1 expressed on breast cancer cells binds to Siglec-9 expressing macrophages inducing an M2 phenotype with an increased expression of PD-L1 and lower capabilities to induce proliferation of $CD8^+$ T cells (Daly et al., 2019).

III.2.3 Metabolic challenges for immune cells in the TME

Apart from immune checkpoint and cytokine-mediated immunosuppression, immune cells experience restrictive and inhibitory metabolic conditions in the TME (O'Neill et al., 2016). Although different immune cell types and subtypes display distinctive nutritional requirements, some metabolic features within the TME have been extensively described to commonly reprogram the anti-tumoral functions of diverse immune cells populations. For instance, glucose scarcity in the TME due to its high consumption by addictive tumor cells limits innate and adaptive anti-cancer activities since activated effector T cells and NK cells are also highly dependent on glucose. Therefore, competition not only for glucose, but for other critical nutrients, metabolites and oxygen apart from immunosuppressive metabolites secreted by cancer cells, stromal cells and immunosuppressive immune cells shape the anti-cancer immunosurveillance (O'Neill et al., 2016) (**Figure 20**).

Activated effector T and NK cells are highly dependent on glucose for production of energy by aerobic glycolysis rather than by TCA cycle-OxPhos metabolism (Bader et al., 2020). Treg cells are more dependent on TCA cycle-OxPhos metabolism relying on fatty acid oxidation for survival. DCs upon stimulation with tumor cells via TLR engagement engage glycolysis and fatty acid synthesis. Tumor resident macrophages displaying an M1 phenotype rely on glycolysis, fatty acid synthesis and amino acid metabolism whereas the M2 phenotype depends on TCA cycle-OxPhos metabolism and fatty acid oxidation. MDSCs when infiltrated in the TME rely more on fatty acid oxidation rather than on glycolysis (Bader et al., 2020). In general, activated effector immune cells with anti-cancer functions seem to rely on rapid production of energy through aerobic glycolysis while long-lived, regulatory and immunosuppressive phenotypes rely on TCA cycle-OxPhos metabolism (A. Wang et al., 2019) (**Figure 20**).

Glucose limitation in the TME has been shown to induce the expression of PD1 in T cells and to impair TCR signaling (Buck et al., 2017). PD1 signaling in T cells is also associated with reduced glycolysis and increased fatty acid oxidation, consequently, accumulation of Treg cells is favored in the TME (Buck et al., 2017). In addition, higher glycolytic rate in tumor cells increases the secretion of colony stimulating factor (CSF) which attracts MDSCs with immunosuppressive effects on T cells (Bader et al., 2020). Aerobic glycolysis by tumor cells

produces a great amount of lactate in the TME. Indeed, the expression of lactate dehydrogenase correlates with tumor progression and severity (Bader et al., 2020). Accumulation of extracellular lactate and lactate uptake by CTLs and NK cells transcriptionally attenuate IFNγ production. Within the acidic TME, CTLs have shown an impaired infiltration and lower anti-cancer effector functions depending on lactate production by tumor cells. Lactate uptake by TAMs has been shown to increase the expression of VEGF and arginase depending of HIF-1α while promoting tumor growth (Buck et al., 2017) (**Figure 20**).

Lactate produced by tumor cells reprograms immune cells and endothelial cells to promote angiogenesis (Bader et al., 2020). Treg cells in the TME benefit from extracellular lactate due their high capacity to metabolize it. Therefore, Treg cell survival is supported by lactate accumulation in the TME (Bader et al., 2020). Glycolytic tumors highly expressing c-Myc have shown to increase the expression of PD1 in Treg cells while decreasing the infiltration of $CD8^+$ T cells (Kumagai et al., 2022). Higher expression of PD1 on Treg cells was depending on lactate uptake via the transporter MCT1. Lactate uptake mediated Treg cell proliferation and immunosuppressive capacity against $CD8^+$ T cells and demonstrated to interfere with the response to PD1 blockade (Kumagai et al., 2022). Beyond lactate accumulation, hypoxia in the TME induces the expression of HIF-1α in TAMs and MDSCs and concomitant induction of PD-L1 leading to T lymphocyte disfunction (Buck et al., 2017). In addition, hypoxia also induces the Treg cell phenotype and their recruitment to the TME. Furthermore, higher production of extracellular adenosine is induced under hypoxia (Buck et al., 2017). Activated Treg cells play a role in converting extracellular ATP to adenosine by highly expressed CD39 and CD73. Adenosine binding to A2A receptors on T cells attenuates their anti-cancer functions (Ohue and Nishikawa, 2019). Prostaglandin E2 generated by tumor cells, TAMs and stromal cells expressing cyclooxygenase 2 is another immunosuppressive metabolite in the TME impairing the anti-cancer functions of NK cells (Melaiu et al., 2019) (**Figure 20**).

Amino acid competition and scarcity in the TME shape the anti-cancer immune response (Bader et al., 2020) (**Figure 20**). Glutamine deprivation has been shown to promote $CD4^+$ T cell differentiation toward a Treg phenotype. Catabolism of arginine by NOS and arginase leads to arginine depletion in the TME which is important for survival, differentiation toward a memory phenotype and anti-cancer functions of $CD8^+$ T cells. Arginine depletion has been associated with accumulation of MDSCs and T cell disfunction in the TME. Indeed, arginase-expressing MDSCs and TAMs contribute to impair T cell cytotoxicity in the TME. Depletion of arginine by arginase rather than by NOS is favored in TMEs with abundant lactate. This has been shown to induce the secretion of tumor-promoting factors by TAMs. On the contrary, arginine catabolism by NOS produces nitric oxide which is associated with a pro-

inflammatory phenotype in macrophages and T cell infiltration into the TME (Pavlova and Thompson, 2016), (Buck et al., 2017), (Bader et al., 2020).

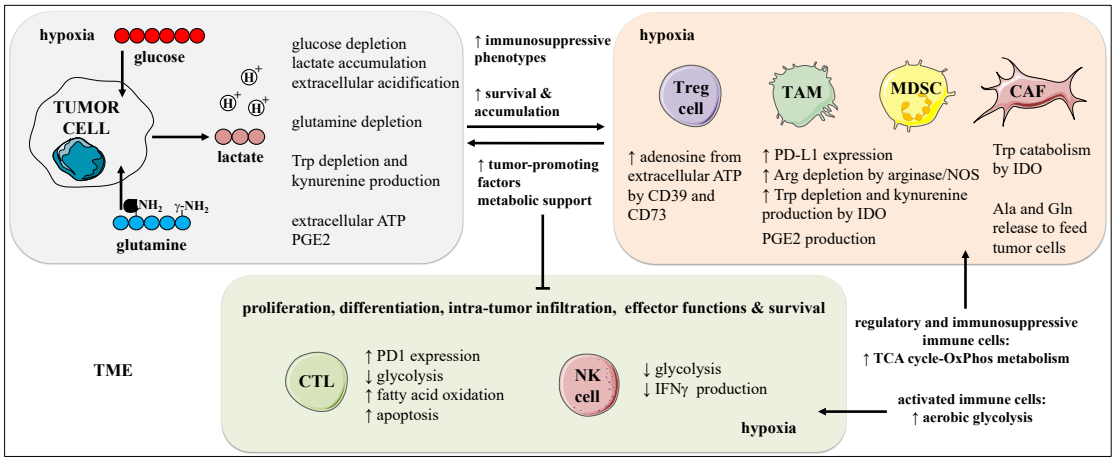

Figure 20. Metabolic challenges for immune cells in the TME

High consumption of glucose, glutamine and depletion of amino acids, production of lactate and acidification by tumor cells in a hypoxic TME challenge the metabolism and functions of immune cells. Treg cells, TAMs, MDSCs and CAFs are attracted to the TME and their survival and functions are potentiated under these conditions. Immunosuppressive immune cells contribute to tumor growth by releasing pro-tumoral soluble factors and depleting amino acids. Effector functions of cytotoxic cells are dampened under extracellular acidification, hypoxia, nutrient deprivation and lactate accumulation, adenosine and PGE2 in the TME. Trp, tryptophan; PGE2, prostaglandin E2; Arg, ariginine; NOS, nitric oxide synthase; IDO, indoleamine 2,3-dioxygenase; Treg cell, regulatory T cell; TAM, tumor-associated macrophage; MDSC, myeloid-derived suppressor cell; CAF, cancer-associated fibroblast; Ala, alanine; Gln, glutamine; TME, tumor microenvironment; TCA, tricarboxylic acid; OxPhos, oxidative phosphorylation.

Cancer cells but also TAMs, MDSCs and cancer-associated fibroblasts (CAFs) upregulate enzymes such as indoleamine 2,3-dioxygenase (IDO) and tryptophan-2, 3-dioxygenase (TDO) responsible for tryptophan catabolism and generation of the byproduct kynurenine (Buck et al., 2017). Besides tryptophan depletion in the local TME, kynurenine blunts T lymphocyte anti-cancer functions by induction of apoptosis and by facilitating the Treg phenotype. Higher activity of IDO has been associated with NK cell dysfunction and proliferation of MDSCs (Bader et al., 2020). CAFs as part of the tumor stroma are reprogramed to support tumor progression. Indeed, CAFs have shown to release alanine and produce glutamine to feed tumor cells (Reina-Campos et al., 2017), (Dey et al., 2021) (**Figure 20**).

III.3 Anti-cancer immunotherapies

Immunotherapy as an intervention to boost the anti-cancer immune response is a promising approach in continuous optimization which has brought successful outcomes in the clinic

(Riley et al., 2019). Immunotherapies represent another angle to attack cancer minimizing the off-target-effects of conventional non-surgical standards of care such as radiotherapy and chemotherapy. After the first clinically approved immunotherapies based on recombinant IFNα in 1986 and IL-2 in 1992, a lot of effort has been made to optimize and generate novel immunotherapeutic approaches. In 2010, the first therapeutic anti-cancer vaccine based on autologous TAA-loaded DCs was approved for prostate cancer. Beyond activating cytokines, agonist antibodies targeting in parallel several stimulatory immune receptors and anti-cancer vaccines, immune checkpoint blockade (ICB) has been developed leading to the clinical approval of CTL4 inhibition for treatment of advanced melanoma in 2011. Since then, new ICBs for PD1, PD-L1 and the novel engineering of chimeric antigen receptor (CAR)-expressing T and NK cells have become the focus of pre-clinical research and clinical trials (Majzner and Mackall, 2018), (Riley et al., 2019), (Parihar et al., 2019), (Depil et al., 2020).

III.3.1 Immune checkpoint blockade

Several PD1 and PD-L1 ICBs are clinically approved for treatment of more than 20 oncogenic malignancies (J. Tang et al., 2018). Indeed, anti-PD1/PD-L1 treatments, as a monotherapy or in combination with anti-CTLA4, chemotherapy, radiotherapy, anti-angiogenic drugs, IDO inhibitors and other anti-cancer agents have been tested in more than a thousand clinical trials (J. Tang et al., 2018). However, up to date, a minority of patients displays long-term anti-cancer protection whereas the majority does not respond to ICB or if they initially do, tumor progression is also possible (Schoenfeld and Hellmann, 2020). To avoid primary resistance, response to ICB is predicted based on the expression of the immune checkpoint within the tumor, the mutational load and immune cell infiltration. Mechanisms for acquired resistance have been suggested such as lower expression of MHC-I, defects in the IFNγ signaling leading to lower expression of MHC-I and PD-L1, decreased expression of immunogenic neoantigens and upregulation of other immune checkpoints (Schoenfeld and Hellmann, 2020).

CTL4 is an early and global immune checkpoint that regulates $CD8^+$ T cell priming and activation via Treg cell functions whereas PD1/PD-L1 immune checkpoint is dominant in tumors with already antigen-experienced immune cells (Topalian et al., 2016). Although tumor cells *per se* can constitutively express PD-L1 due to aberrant oncogenic pathways or mutational gene arrangements, activated effector CTLs secreting IFNγ can potentiate the expression of PD-L1 on APCs and tumor cells within the TME. This mechanism described as adaptive immune resistance is indicative of a strong anti-cancer immunosurveillance in the TME driven by effector $CD8^+$ T cells that upon antigen encounter upregulate PD1. This is followed by PD-L1 upregulation in the TME to control the excessive activity of CTLs.

Therefore, not only the presence of $CD8^+$ T cells at the invasive tumor front in patients has been positively associated with response to PD1 ICB, but PD-L1 expression in tumors is used as a predictive biomarker of a better response to PD1/PD-L1 ICB (Topalian et al., 2016).

The outcome of ICB also depends on targeting immune checkpoints that are commonly expressed in CTLs and Treg cells (Topalian et al., 2016). For instance, PD1 ICB may not only potentiate CTL functions but the immunosuppressive effects of effector $PD1^+$ Treg cells negatively impacting on the anti-cancer effect of the immunotherapy (Ohue and Nishikawa, 2019). Therefore, combinatorial ICB treatments are under optimization. Targeting PD1 and CTL4 in combination showed a better progression-free survival than the monotherapies in melanoma patients. Indeed, this ICB combination has been clinically approved for certain types of melanoma (Topalian et al., 2016). ICB response predictions are optimized over time with the possibility of using oncogenic drivers, mutational load and cancer-associated viruses and the microbiome as biomarkers. Likewise, other immune checkpoints such as TIM3, LAG3, CD39, CD73 and the adenosine receptor A2A have been targeted in clinical trials (Topalian et al., 2016).

III.4 IRE1α and the anti-cancer immune response

Transmissible ER stress from tumor cells to immune cells such as macrophages has been reported (Mahadevan et al., 2011), (Jiang et al., 2020). Although in *in vitro* settings, macrophages displayed ER stress induction with XBP1 splicing when growing in conditioned culture medium from tumor cells that experienced ER stress upon pharmacological induction. Macrophages displaying induction of XBP1s and other UPR branches secreted more cytokines depending of TLR4 sensing (Mahadevan et al., 2011).

The IRE1α-XBP1 signaling has been reported to confer to NK cells not only proliferative advantages, but higher effector functions against tumors and virus (Dong et al., 2019). NK cells upon viral infection in mice showed upregulation of XBP1s (**Figure 21**). Therefore, mice with IRE1α-deficient NK cells showed higher viral titers and shorter survival upon infection. XBP1-deficient NK cells displayed defective expansion in peripheral blood and organs after adoptive transfer. Indeed, XBP1s was demonstrated to bind the c-Myc promoter and positively regulates its expression. In addition, pharmacological inhibition of IRE1α decreased the mitochondrial respiratory capacity of primary human NK cells. Adoptive transfer of IRE1α- or XBP1-deficient NK cells into mice resulted in higher number of melanoma tumors in the lungs (Dong et al., 2019).

Activation of IRE1α in primary bone marrow-derived dendritic cells (BMDCs) in contact with tumor cell lysates played a positive role in cross-presentation to cytotoxic T cells (Medel

et al., 2018). Indeed, inhibition of IRE1α RNAse decreased the production of cytokines and MHC-I/peptide complexes in BMDCs in the presence of melanoma cell lysates. Furthermore, the ability of BMDCs to activate melanoma antigen-specific $CD8^+$ T in the presence of cancer-associated antigens was reduced upon inhibition of IRE1α. Adoptive cell transfer of $CD8^+$ T cells and melanoma cell lysate-stimulated BMDCs expressing an IRE1α RNAse mutant into immunocompetent mice produced defective proliferation of $CD8^+$ T splenocytes (Medel et al., 2018).

Positive impact of the IRE1α signaling on DCs homeostasis and functions has been reported by several studies (Osorio et al., 2014), (Osorio et al., 2018). However, within the tumor milieu, XBP1s has been shown to decrease the anti-tumoral functions of infiltrated DCs in ovarian cancer (Cubillos-Ruiz et al., 2015) (**Figure 21**). Indeed, patient samples of ovarian solid tumors and ascites have shown detectable levels of XBP1s mRNA in DCs which negatively correlated with the number of T lymphocytes. In pre-clinical settings, transplantation of XBP1 deficient BMDCs limited tumor growth in orthotopic models of ovarian cancer. Likewise, lower number of peritoneal tumor masses, significant less ascites accumulation, reduced splenomegaly and prolonged mouse survival were seen in an orthotopic ovarian cancer model of metastasis (Cubillos-Ruiz et al., 2015).

Immunosuppressive metabolic reprogramming of DCs within the TME has been reported to occur by lipid peroxidation (Cubillos-Ruiz et al., 2015) (**Figure 21**). Higher accumulation of lipids, ROS, aldehyde-protein adducts led to downstream induction of XBP1s in intra-tumoral DCs or DCs exposed to ascites. XBP1s induction by lipid peroxidation was implicated in downstream lipogenesis in intra-tumoral DCs since XBP1-deficient DCs displayed lower intracellular triglyceride accumulation. XBP1s induction in intra-tumoral DCs was shown to be deleterious for activation of anti-cancer T lymphocytes. Indeed, ovarian cancer mouse models lacking XBP1 in DCs displayed higher numbers of intra-tumoral T lymphocytes and lower numbers of Treg cells. Adoptive transfer of T cells from ovarian tumor-bearing mice with XBP1-deficient DCs to wildtype ovarian tumor-bearing mice limited tumor growth. Moreover, *in vivo* silencing of either XBP1 or IRE1α by nanoparticle-delivered siRNA targeting DCs extended survival of ovarian tumor-bearing mice (Cubillos-Ruiz et al., 2015).

Activation of the IRE1α pathway has also been reported to modulate TLR-mediated cytokine secretion in macrophages upon bacterial infection in mice and macrophage polarization toward an inflammatory M1-like phenotype (Cubillos-Ruiz et al., 2017). In the context of cancer, the IRE1α pathway is involved in macrophage-mediated extracellular matrix remodeling supporting *in vitro* cancer cell invasion (Yan et al., 2016) (**Figure 21**). The IRE1α-XBP1 axis was triggered by stimulation with anti-inflammatory Th2 cytokines in

bone marrow-derived macrophages (BMDMs). Activation of the transcription factors STAT3 and STAT6 was upstream of XBP1s induction. sXBP1 increased the secretory capacity of BMDMs to export lysosomal proteases such as cathepsins in their inactive forms. Conditioned media from Th2 cytokine-stimulated BMDMs increased the invasion capabilities of a pancreatic neuroendocrine tumor cells whereas IRE1α RNAse inhibition reduced tumor cell invasion (Yan et al., 2016).

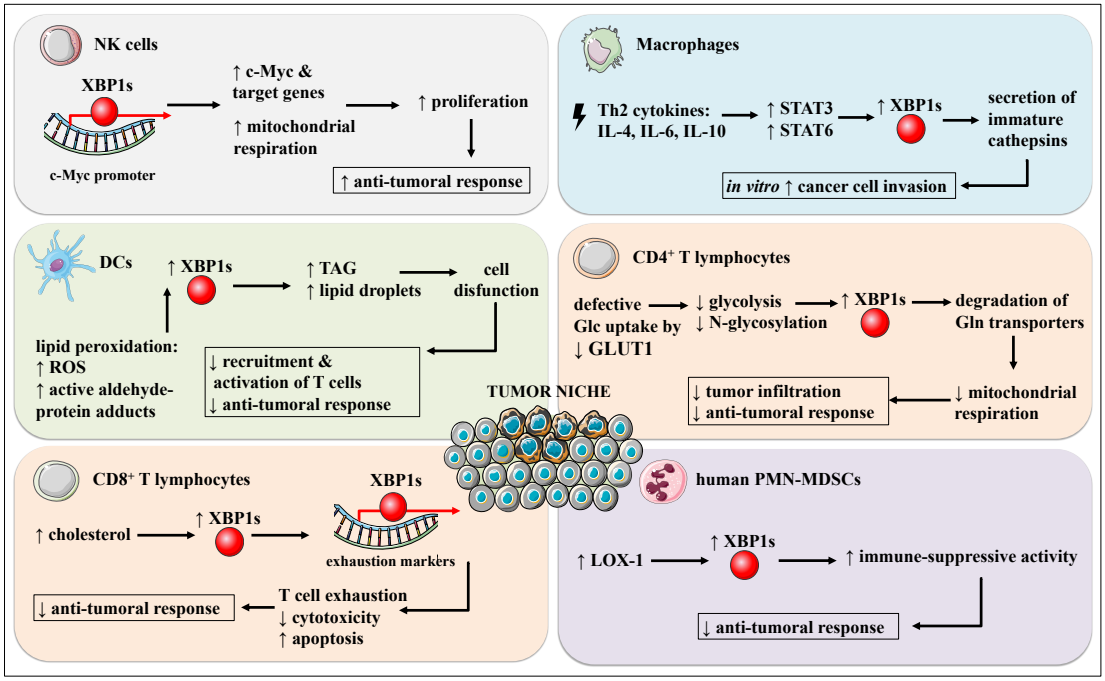

Figure 21. The IRE1α pathway modulates the anti-tumoral functions of immune cells within the TME

IRE1α activation and XBP1 splicing support NK cell proliferation and their anti-cancer effector functions. XBP1 splicing is induced in macrophages exposed to immunosuppressive cytokines and drives secretion of immature cathepsins that increase the tumor cell invasive capabilities in vitro. Induction of XBP1 splicing in DCs and T cells within the TME decreases their tumor infiltration and their anti-cancer effector functions. Induction of XBP1 splicing in human PMN-MDSCs enhances their immunosuppressive functions and dampens the adaptive anti-cancer immune response. NK cells, natural killer cells; DCs, dendritic cells; TAG, triacylglycerides; IL, interleukin; STAT3/6; ROS, reactive oxygen species; GLUT1; glucose transporter 1, PMN-MDSCs, polymorphonuclear-myeloid-derived suppressor cells; LOX-1, oxidized LDL receptor 1.

Activation of IRE1α-XBP1 axis is also implicated in the immune-suppressive effects of malignant TMEs as a typical tumoral mechanism to blunt T lymphocyte-mediated anti-cancer immunosurveillance (Song et al., 2018) (**Figure 21**). Ascites resident T lymphocytes and within the tumors of ovarian cancer patients exhibited higher activation of the IRE1α-XBP1s pathway and an impaired anti-tumoral response. Healthy primary $CD4^+$ T cells treated with ovarian cancer-derived ascites displayed higher and lower expression of XBP1s and the

glucose transporter GLUT1, respectively. Furthermore, ascites-exposed $CD4^+$ T cells displayed defective protein N-glycosylation as well as lower glycolysis and mitochondrial respiration. Indeed, defective glucose uptake was upstream of IRE1α activation. Activated IRE1α mediated degradation of glutamine transporters restricting glutamine uptake and its usage as an energetic substrate. XBP1s induction had a negative impact on the anti-cancer functions of T lymphocytes since XBP1 deficiency in $CD4^+$ T cells limited tumor growth in ovarian cancer mouse models. Likewise, IRE1α deficiency in $CD4^+$ T cells showed decreased peritoneal carcinomatosis and prolonged survival in a mouse model of ovarian cancer (Song et al., 2018).

XBP1s induction in $CD8^+$ T cells by accumulation of cholesterol in the TME has shown to blunt their cytotoxic effects through T cell exhaustion irrespective of the type of cancer (Ma et al., 2019) (**Figure 21**). Exhaustion markers and cholesterol content in $CD8^+$ T cells showed a positive correlation in melanoma cells homing the lungs, in lung and colon carcinomas subcutaneously implanted as well as in colon cancer and myeloma patient samples. Exhausted $CD8^+$ T cells displayed higher apoptosis induction and lower cytotoxicity. Intra-tumoral $CD8^+$ T acquired an exhausted phenotype in parallel with accumulation of cholesterol upon infiltration into the cholesterol-enriched TME of several cancer mouse models. Interestingly, induction of XBP1s by cholesterol was found to induce the expression of exhaustion markers by binding to their gene promoter. Pharmacological inhibition of IRE1α RNAse after adoptive transfer or XBP1 silencing prior to adoptive transfer of $CD8^+$ T cells into tumor-bearing mice strongly reduced the number of melanoma foci in the lungs (Ma et al., 2019).

XBP1s induction defines a granulocyte population with immune-suppressive properties such as polymorphonuclear-myeloid derived suppressor cells (PMN-MDSCs) (Condamine et al., 2016) (**Figure 21**). PMN-MDSCs is the predominant population of suppressor cells in the TME of the majority of human cancer types. Indeed, LOX-1 was a successful biomarker to define the PMN-MDSC population in tumors of non-small cell lung cancer (NSCLC), head and head cancer patients (HNC) and myeloma multiple patients. Upregulation of XBP1s correlated with the expression of LOX-1 in PMN-MDSCs isolated from cancer patients. LOX-1, the oxidized LDL receptor 1 is a scavenger receptor expressed in several cell types such as macrophages and endothelial cells, but not reported in PMN such neutrophils. High expression of LOX-1 in PMN-MDSCs was specific to human cells. PMN-MDSCs from patients displayed an immune-suppressive activity when co-cultured with T cells. Pharmacological inhibition of XBP1s upon general ER stress induction reverted the immune-suppressive phenotype of high LOX-1 PMN-MDSCs cells. LOX-1 upregulation correlated with clinical cancer stage, tumor size and impaired survival in several human cancers and (Condamine et al., 2016).

Collectively, most of these studies implicating the IRE1α pathway in the anti-cancer functions of different populations of immune cells show that activation of IRE1α occurs downstream of soluble factors and metabolic alterations within the TME. Immune cells undergoing metabolic ER stress in the neoplastic niche exhibit impaired anti-tumoral activities leading to tumor growth and progression. In contrast, NK cells rely on XBP1 and c-Myc activation as part of intrinsic mechanisms non-related to the TME. Certainly, the IRE1α pathway is a key modulator of innate and adaptive immune mechanisms orchestrated within oncogenic niches.

RESULTS

ARTICLE 1

IRE1α overexpression in malignant cells is deleterious for tumor progression via the induction of an anti-cancer immune response

Adriana Martinez-Turtos, Rachel Paul, Manuel Grima-Reyes, Hussein Issaoui, Adrien Krug, Rana Mhaidly, Jozef P. Bossowski, Johanna Chiche, Sandrine Marchetti, Els Verhoeyen, Eric Chevet and Jean-Ehrland Ricci. Article under revision

IRE1α overexpression in malignant cells is deleterious for tumor progression via the induction of an anti-cancer immune response

Adriana Martinez-Turtos[1,2], Rachel Paul[1,2], Manuel Grima-Reyes[1,2], Hussein Issaoui[1,2], Adrien Krug[1,2], Rana Mhaidly[1,2], Jozef P. Bossowski[1,2], Johanna Chiche[1,2], Sandrine Marchetti[1,2], Els Verhoeyen[1,2,3], Eric Chevet[4,5] and Jean-Ehrland Ricci[1,2,*]

[1] : Université Côte d'Azur, INSERM, C3M, Nice, France

[2] : Equipe labellisée Ligue Contre le Cancer, Nice, France

[3]: CIRI, Université de Lyon, INSERM U1111, ENS de Lyon, Université Lyon 1, CNRS, UMR 5308, 69007 Lyon, France

[4]: Inserm U1242, Université de Rennes, France.

[5]: Centre de lutte contre le cancer Eugène Marquis, Rennes, France

* corresponding author:

Jean-Ehrland Ricci PhD, Inserm U1065, équipe 3, 151 route de St Antoine de Ginestière, BP 23194, 06204 Nice Cedex 03, France. Phone: +33 4 89 06 43 04; Fax +33 4 89 06 42 21, email: ricci@unice.fr

Abstract

IRE1α is one of the three ER transmembrane transducers of the Unfolded Protein Response (UPR) activated upon endoplasmic reticulum (ER) stress. IRE1α activation has a dual role in cancer as it may be either pro- or anti-tumoral depending on the studied models. Here, we describe that exogenous expression of IRE1α, resulting in IRE1α auto-activation, did not affect cancer cell proliferation *in vitro* but resulted in a tumor-suppressive phenotype in syngeneic immunocompetent mice. Indeed, exogenous expression of IRE1α in murine colorectal and Lewis lung carcinoma cells drastically impaired tumor growth once syngeneic tumor cells were subcutaneously implanted in immunocompetent mice but not in immunodeficient mice. Mechanistically, the *in vivo* protective effect of overexpressing IRE1α in tumor cells was associated with IRE1α RNAse activity driving both XBP1 mRNA splicing and regulated IRE1-dependent decay of RNA (RIDD). We showed that the tumor-suppressive phenotype upon IRE1α overexpression was characterized by the induction of apoptosis in tumor cells in parallel with an enhanced adaptive anti-cancer immunosurveillance. Hence, our work indicates that IRE1α overexpression and/or activation in tumor cells can limit tumor growth in immunocompetent mice and might point towards the need of adjusting the use of IRE1α inhibitors for cancer treatment based on IRE1α expression and activation.

Keywords cancer cancer, UPR, IRE1α, XBP1s, RIDD, anti-cancer immunosurveillance, apoptosis

INTRODUCTION

Nutritional interventions are target of the intense research focused on the treatment of non-communicable diseases including metabolic disorders such as cancer. Indeed, dietary regimens such as caloric restriction, fasting, low carbohydrate, ketogenic as well as low protein and amino acid-restricted diets have shown some benefits to control tumor development and progression in pre-clinical and clinical studies [1, 2]. The nutritional regimens slowing down tumor growth or extending animal survival have been reported as underlying molecular mechanisms: (i) reduction of the insulin-like growth factor-1 (IGF-1)-triggered signaling cascades such as the PI3K/Akt/mTOR pathway, (ii) activation of AMPK, (iii) apoptosis induction, (iv) DNA damage, (v) oxidative stress and (vi) alterations in proteostasis with induction of endoplasmic reticulum (ER) stress in tumor cells [3-5]. Indeed, we have previously reported the protective effect of an isocaloric diet partially reduced in protein (Low PROT diet) in several cancer mouse models. We demonstrated that the Low PROT diet-induced anti-cancer immunosurveillance was mediated, at least in part, via an inositol-requiring enzyme 1α (IRE1α)-dependent signaling pathway [6].

IRE1α is a transducer of the Unfolded Protein Response (UPR). The UPR is canonically activated upon accumulation of improperly folded proteins in the ER but also by disturbances in the ER lipid composition [7, 8]. IRE1α is a type I transmembrane protein exhibiting both kinase and endoribonuclease activities in its cytosolic domain. The IRE1α serine/threonine kinase activity is responsible for its auto-transphosphorylation upon ER stress-dependent IRE1α dimerization, which in turn leads to activation of the IRE1α RNAse activity. Most of the IRE1α signaling outputs have so far been linked to its RNAse activity, first through the non-conventional splicing of XBP1 mRNA, that yields the transcription factor XBP1s, and second through RNA degradation (also called Regulated IRE1 Dependent Decay, RIDD) [9]. The interplay between XBP1s and RIDD is key to control cell life and death decisions driven by ER stress. Beyond these catalytic activities, IRE1α was also recently described to exhibit scaffold functions that were associated with cell migration and calcium signaling [10].

Alteration of ER homeostasis is associated with most cancer hallmarks and IRE1α signaling has been extensively studied in pre-clinical models of solid and hematological cancers. For instance, constitutive activation of the IRE1α-XBP1 signaling in triple negative breast cancer (TNBC) has been reported to play pro-tumorigenic roles in xenografts and genetically modified mouse models through increased cytokine secretion, modulation of cancer cell stemness-like properties, response to hypoxia, induction of angiogenesis, stroma remodeling of the tumor microenvironment (TME), chemotherapy resistance and tumor relapse *in vivo* [11-14]. In pancreatic ductal adenocarcinoma (PDAC) genetic mouse models, IRE1α has also been involved in acquisition of a more aggressive tumor phenotype with mesenchymal-like properties and higher tumor-initiating and metastatic potential [15, 16]. The IRE1α-XBP1 axis has been pro-tumorigenic in colon carcinoma mouse models via cell stemness-related processes [17] and

resistance to chemotherapy in immunodeficient animals [18]. Interestingly, opposite functions of the two IRE1α RNAse activity outputs have been suggested in human glioblastoma and recapitulated in xenograft mouse models of glioblastoma. Indeed, XBP1s and RIDD were described as pro- and anti-tumorigenic, respectively [19]. Tumor-suppressive roles of IRE1α were also documented in hematological cancers such as diffuse large B-cell lymphoma (DLBCL), specifically, of the germinal center B-cell–like (GCB) subtype. Indeed, a defective IRE1α-XBP1 pathway via epigenetic silencing of IRE1α has been recognized as a hallmark of GCB-DLBCL. Therefore, exogenous expression of XBP1s in subcutaneous xenografts of GCB-DLBCL in mice limited tumor growth [20]. In contrast, in other non-Hodgkin's lymphomas such as Burkitt's lymphoma, the IRE1α-XBP1 axis promoted tumor growth [21]. This dual role of the IRE1α signaling in cancer has been also described in different innate as well as adaptive immune cell populations within the TME of several solid oncogenic malignancies [22].

Hence, since IRE1α exerts dual roles in tumor progression, either pro- or anti-tumoral, we sought to investigate the effect of the exogenous expression of IRE1α in tumor cells implanted in immunocompetent mice. We found that overexpression of IRE1α was detrimental for subcutaneous tumor growth of colorectal and Lewis lung carcinomas. Tumors with IRE1α overexpression were characterized by a higher anti-cancer immunosurveillance and tumor cells undergoing apoptosis.

RESULTS

Low Protein diet-dependent tumor protection correlates with IRE1α activation in tumors, higher anti-cancer immunosurveillance and increased synthesis of pro-inflammatory cytokines

To determine how Low PROT diet-induced IRE1α activation was involved in immunosurveillance, immunocompetent BALB/c mice were fed for 7 days with an isocaloric control (CTR) or Low PROT diet prior to subcutaneous (SC) engraftment of syngeneic colorectal carcinoma CT26 cells (**Fig. 1A**). Tumor-bearing mice were kept under diet until sacrifice and tumors were analyzed 15 days post-tumor engraftment. Low PROT tumors were significant smaller than CTR tumors considering tumor volume by caliper measurement and tumor weight after resection (**Fig. 1B**). XBP1s protein levels were higher in Low PROT tumors confirming ER stress induction with activation of the IRE1α pathway (**Fig. 1C**) as we previously described [6]. Immune profiling indicated that tumor-infiltrating lymphocytes (TILs), specifically $CD8^+$ T cells (**Fig. 1D**), tumor-associated macrophages (TAMs) (**Fig. 1E**) and intra-tumoral dendritic cells (DCs, **Fig. 1F**) were enriched in Low PROT tumors. Correlating with higher recruitment of cytotoxic T cells into the TME of Low PROT tumors, a significant increase in the surface expression levels of MHC-I (Major Histocompatibility Complex-I, specifically H2Kd) was detected on isolated tumor cells from Low PROT diet-fed mice (**Fig 1G**). Furthermore, enhanced anti-tumoral effector functions of T lymphocytes from tumor-bearing mice fed the Low PROT diet were also observed by *ex vivo* cytotoxicity assay (**Fig 1H**).

Since the expression of XBP1s was higher in Low PROT tumors and H2Kd was differentially expressed on Low PROT tumor cells, transcript levels of genes encoding members of the antigen processing and presenting machinery as well as proinflammatory factors were quantified in isolated tumor cells. Transcript levels of ERAP1 (Endoplasmic Reticulum Aminopeptidase 1), an ER-resident aminopeptidase, which generates peptide fragments that can be presented by MHC-I were higher in Low PROT tumor cells (**Fig. 1I**). Likewise, TAP1 (Transporter 1, ATP Binding Cassette Subfamily B) which is a member of a transporter complex localized in the ER membrane that shuttles cytoplasmic peptides into the ER to be loaded onto MHC-I was also upregulated in Low PROT tumor cells (**Fig. 1I**). Pro-inflammatory factors including type I interferons, TNF-α and GM-CSF, chemo-attractants (CXCL10, CXCL11, CCL2) and the NK cell-activating cytokine IL-15 were upregulated under Low PROT diet (**Fig. 1J**). These findings indicate that the Low PROT diet regulates gene expression in malignant cells, which might endow them to express more pro-inflammatory soluble factors and increase the antigen processing and presenting machinery that enhances the immunosurveillance of the tumor.

IRE1α overexpression in CT26 cells leads to IRE1α self-activation driving XBP1 mRNA splicing and RIDD induction

To test whether the Low PROT diet-induced immunosurveillance could be linked specifically to IRE1α expression in tumor cells, we overexpressed (OE) IRE1α in CT26 cells. IRE1α OE was confirmed by its higher transcript levels as compared to WT and mock cells (**Fig. 2A**). IRE1α OE resulted in auto-activation as judged by the increase in XBP1 mRNA splicing. Protein levels of IRE1α in OE cells were in accordance with its transcript levels (**Fig. 2B**). IRE1α OE resulted in RNAse activation since XBP1s was increased together with lower transcript levels of the RIDD targets, Blos1 and Col6a1 (**Fig. 2C**). ERAP1 and TAP1 transcripts which were upregulated in Low PROT isolated tumor cells (**Fig. 1I**) were also increased in OE cells as compared to mock cells (**Fig. 2C**). OE cells displayed a proliferative capacity similar to that of control cells (**Fig. 2D**). Even though cell growth was decreased under treatment with tunicamycin (**Fig. 2E**) or 2-deoxyglucose (**Fig. 2F**), two ER stress inducers, OE and mock cells exhibited similar phenotypes. Interestingly, transcript levels of several cytokines that were upregulated in Low PROT tumor cells were not increased in OE cells (**Fig. 2G**), suggesting that Low PROT diet had a wider impact on tumor cells than IRE1α overexpression alone. Hence, exogenous expression of IRE1α in CT26 drives XBP1 mRNA splicing and RIDD with no changes in cell proliferation *in vitro* even under ER stress induction with various pharmacological inducers.

IRE1α-overexpressing tumors display a limited tumor growth, tumor cell apoptosis and higher immune cell infiltration

To evaluate the impact of IRE1α OE on tumor growth and immunogenicity, IRE1α-overexpressing (OE) CT26 cells were subcutaneously engrafted in syngeneic immunocompetent BALB/c mice. IRE1α OE yielded drastic reduction in tumor size when compared to control tumors (**Fig. 3A**). Importantly, this effect was also observed in a subcutaneous syngeneic mouse model of Lewis lung carcinoma since IRE1α-overexpressing (OE) LLC1 cells generated smaller tumors in C57BL/6 mice (**Fig. 3B** and **Fig. S1A**). Prior to *in vivo* engraftment, OE LLC1 cells were generated and validated *in vitro* showing higher transcript levels of IRE1α in parallel with a significant increase of XBP1 mRNA splicing (**Fig. S1A**). IRE1α OE in LLC1 cells did not change their proliferative capacity *in vitro* (**Fig. S1B**). We verified that protein levels of IRE1α and XBP1s were increased in isolated tumor cells from OE CT26 tumor-bearing mice (**Fig. 3C**) and that no significant changes in protein levels of other UPR members, namely, ATF4 and CHOP were observed between mock and OE CT26 tumor cells (**Fig. 3C**). Analysis of isolated CT26 OE tumor cells confirmed the full RNAse activity of IRE1α as judged by the upregulation of XBP1s and downregulation of RIDD targets (**Fig. 3D**). A close characterization of the tumor cells isolated from **Fig 3A**, indicated that OE CT26 tumor cells undergo apoptosis *in vivo* as judged by the increased PARP cleavage (**Fig. 3E**), a canonical caspase substrate, and the increased DEVDase activity

(**Fig. 3F**). Interestingly, in those cells, the extent of RIDD activation appeared much higher (more than 2-fold change) than that of XBP1 mRNA splicing (less than 1.5-fold change) thereby suggesting the forced activation of pro-death RIDD in OE cells. Intra-tumoral immune profiling of OE CT26 tumor-bearing mice revealed higher infiltration of immune cells (**Fig. S2A**). Among them, TILs, specifically $CD3^+$ T cells, cytotoxic $CD8^+$ T cells and helper $CD4^+$ T cells (**Fig. 3G**) were higher in OE CT26 tumors. In addition, tumor-infiltrating NK cells (**Fig. 3H**) and resident TAMs (**Fig. 3I**) were higher in OE tumors. $CD11^+$ resident TAMs were shown to express higher levels of activation markers like MHC-II and CD86 (**Fig. S2B**). Surface expression levels of MHC-I (specifically H2Kd) and CD47 were upregulated and downregulated, respectively, on tumor cells (**Fig. 3J**). This correlated with the upregulation of H2Kd seen on Low PROT tumor cells (**Fig. 1G**). Surface expression of another MHC-I variant of the same haplotype (H2Ld) and the MHC class I-like molecule (H60) did not change in OE cells (**Fig. S2C**). Importantly, isolated $CD3^+$ T cells from the splenocytes of OE tumor-bearing mice displayed higher cytotoxicity when co-cultured *in vitro* with CT26 cells (**Fig. 3K**), indicating a specific adaptive anti-cancer immune response in those mice. Hence, IRE1α overexpression in CT26 and LLC1 tumors is associated with limited tumor progression in immunocompetent mice, via the induction of cell death and a higher immune cell infiltrate.

IRE1α overexpression-associated tumor suppression is mainly dependent on cytotoxic T cells

To document the impact of IRE1α OE on cell death and the adaptive immune response, we injected the CT26 OE cells into immunodeficient Nude mice that lack functional T and B cells. The engraftment of IRE1α OE CT26 cells revealed a trend but not significant impairment of the tumor growth as judged by the tumor weight at endpoint (**Fig. 4A**). We confirmed that IRE1α transcripts were significantly higher in isolated OE CT26 tumor cells which correlated with RNAse activation based on upregulation of XBP1s and downregulation of RIDD targets (**Fig. 4B**). OE CT26 tumor cells isolated from tumor-bearing Nude mice displayed higher caspase activity (**Fig. 4C**). This result recapitulates the enhanced caspase activity observed in OE CT26 tumor-bearing immunocompetent mice (**Fig. 3F**), even if it did not result in a significant reduction in tumor size. Immune profiling showed higher infiltration of NK cells (**Fig. 4D**) as well as resident TAMs expressing MHC-II in OE tumors compared to control tumors (**Fig. 4E**). Although cell surface expression of H2Kd and CD47 did not change, H60, an activating ligand of NK cells, was upregulated on OE tumor cells (**Fig. 4F**). These results suggested that IRE1α overexpression in tumor cells results in cell death induction *in vivo*. However, IRE1α OE-associated cell death was not able to significantly reduce tumor growth in the absence of functional adaptive immune cells, even if other immune cells (such as NK and TAMs) infiltrated the OE tumors (**Fig 4D, 4E**).

DISCUSSION

We have shown that exogenous expression of IRE1α in tumor cells results in an anti-tumoral phenotype in immunocompetent but not in immunodeficient mice (**Fig 3,4**). This finding correlates with the tumor growth limitation observed under Low PROT diet (**Fig. 1**). These tumor-suppressive functions of IRE1α correlated with RIDD induction in tumor cells and with an increase in tumor cell death and higher immune cell infiltrate. We demonstrated that the anti-tumoral phenotype associated with IRE1α overexpression in tumors partially depended on cytotoxic T cells. Beyond the information that the nature of IRE1α activities (XBP1s vs RIDD) is a key factor in regulating tumor growth-associated outputs, our data also suggest that IRE1α expression level on its own could also be a factor to be considered, most likely because it could alter IRE1α scaffolding functions and the subsequent biological outputs. In many cases, pro-tumoral roles of IRE1α are associated with XBP1 mRNA splicing, which when coupled with certain oncogenic drivers copes with the inherent cytotoxicity of rapidly proliferating tissues. In parallel, the expression of XBP1s supports tumor cells in the stressful TME deprived of nutrients and oxygen. Indeed, XBP1s has been shown to confer tumor cells the ability of initiating tumor growth and respond to hypoxia in cooperation with HIF-1α [12]. Hence, XBP1s and its tumor-protective effects might be the result of adaptive ER stress mechanisms induced to support the competitive tumor cell growth.

The tumor-protective roles of the IRE1α-XBP1 axis have been positively associated with the expression of c-Myc in TNBC [13], PDAC [15] as well as in high c-Myc human B lymphomas and N-Myc-driven human neuroblastoma [21]. This is an important point to take into consideration because depending on the oncogenic driver, signaling pathways supporting the tumor proliferative capacity and anabolic metabolism will vary among different cell and cancer types. Therefore, tumors expressing high levels of c-Myc and XBP1s such as TNBC will benefit from the inhibition of this signaling axis. Altogether, the oncogenic drivers, the type of cancer, the immunocompetence of cancer animal models and subcutaneous or orthotopic tumors may count for the dual role of the IRE1α pathway in cancer. Considering the transformed cell lines used in our study, genomic characterization of colorectal carcinoma CT26 cells has shown homozygous mutation of Kras at $G^{12}D$, homozygous deletion of Cdkn2a and no mutations but high expression of Myc, p53, Mdm2, HIF1-α and Nras [25]. In Lewis lung carcinoma LLC1 cells, heterozygous Kras mutation at $G^{12}C$ is present [26]. This might count for the tumor-suppressive roles of IRE1α overexpression in these cells since the oncogenic driver is Kras and not c-Myc and the IRE1α is mostly oriented towards RIDD rather than XBP1s.

Exogenous expression of IRE1α in our model resulted in a full induction of its endoribonuclease activity with no changes in the *in vitro* cell proliferative capacity even upon extra ER and nutritional stresses. Despite the robustness of IRE1α-overexpressing cells in *in vitro* settings, *in vivo* implanted cells within the restrictive TME displayed an impaired growth. In this regard, XBP1 splicing and RIDD

induction when uncoupled have been reported to be tumor-protective and tumor-suppressive, respectively [19]. Therefore, we can hypothesize that higher levels of RIDD induction as compared to XBP1 splicing in tumor cells growing *in vivo* could be responsible for driving terminal UPR with induction of apoptosis in IRE1α-overexpressing cells. Indeed, tumor cells undergoing apoptosis was a common feature of the immunocompetent and the immunodeficient cancer mouse models. Certainly, most studies define IRE1α activation based on XBP1 splicing but, selective as well as massive degradation of some mRNAs and miRNAs, could also dictate tumor growth progression.

Irrespective of tumor cells undergoing apoptosis, an enhanced anti-cancer immune response was seen in IRE1α-overexpressing tumors. The less aggressive tumor phenotype might be a combination of endogenous apoptosis induced by toxic IRE1α exogenous expression in tumor cells growing *in vivo* and an anti-cancer immune response elicited by the immunogenic tumor cell death. Likewise, a potent anti-cancer immunosurveillance elicited by plasma membrane and soluble factors secreted by tumor cells at early stages during tumor progression cannot be ruled out. Indeed, MHC-I was upregulated in tumor cells from tumor-bearing immunocompetent mice in parallel with a downregulation of CD47, inducing the 'don't eat me' signal for macrophages. In addition, in immunodeficient mice, H60, an activating ligand of NK cell receptors was found upregulated. We can hypothesize that in the absence of functional T cells in Nude mice, cytotoxic NK cells played a major role in controlling tumor growth [27]. Therefore, modulation of immune markers on tumor cells overexpressing IRE1α and consequent activation of immune cells cannot be ruled out.

We consistently recapitulated tumor-suppressive phenotypes under a Low PROT diet and upon exogenous expression of IRE1α in tumor cells. However, the molecular mechanisms underlying these anti-tumorigenic effects might be different. For instance, the Low PROT diet modulated the synthesis of several pro-inflammatory factors in tumor cells while IRE1α-overexpression in CT26 cells did not change the transcript levels of these cytokines and chemo-attractants, which might correlate with a RIDD characteristic. Common features between the nutritional and genetic models include higher expression of genes coding for members of the antigen processing and presenting machinery and indeed, upregulation of MHC-I on tumor cells in both models. Despite the distinctive features of each model (nutritional vs genetic), this study shows that overexpression of IRE1α and the subsequent nature of its RNAse signaling outputs towards XBP1s or RIDD should be carefully considered to design proper anti-cancer treatments to potentiate scaffolding functions and RIDD induction that may in turn sensitize tumor cells to apoptosis.

Acknowledgements

We gratefully acknowledge the Centre Méditerranéen de Médecine Moléculaire (C3M) animal facility. We thank PhD. Camila Rubio-Patiño for her intellectual support. This work has been supported by la Ligue Nationale Contre le Cancer “Equipe Labellisée”, la Fondation ARC pour la Recherche sur le Cancer, by Institut National du Cancer (INCa PLBIO) and le Cancéropôle PACA and l’Agence Nationale de la Recherche (LABEX SIGNALIFE ANR-11- LABX-0028-01). This project has received funding from the European Union’s Horizon 2020 research and innovation program under the Marie Skłodowska-Curie grant agreement No. 766214 (Meta-Can). A.M.T was supported by la Fondation pour la Recherche Médicale (FRM) grant No. FDT202012010714.

Author contributions

A.M-T performed most of the research described herein and was assisted by R.P-B, M.G-R, H.I, R.M, E.V, J.P.B. and A.K. E.V, S.M J.C and M.G.R provided intellectual input and experimental designs. E.C provided invaluable reagents and inputs. J-E.R designed the research, secured funding and wrote the manuscript.

Competing Interests

Authors declare no conflict of interests.

MATERIALES AND METHODS

Mice

All animal experiments were performed according to the guidelines of the Institutional Animal Care and Use Committee and the regional ethics committee (approval references PEA-503 and PEA 673). All experiments used age-matched five-week-old female littermates. WT syngeneic BALB/c and C57BL/6 mice as well as Nude mice were obtained from ENVIGO and housed in our animal facility (C3M-Nice, France). When specified, mice were fed isocaloric diets purchased from ENVIGO: Control (CTR: TD.130931) and Low Protein diet reduced in protein (Low PROT -25%: TD.130933). The caloric composition of these diets (% of energy provided by carbohydrate: protein: fat content) was the following: CTR - (70.9% : 19.5% : 9.6%) and Low PROT -25% - (73.7% : 14.9% : 11.5%), see [6]. Mice were fed the specified diets for seven days prior to subcutaneous engraftment of tumor cells. WT syngeneic BALB/c and Nude mice were subcutaneously engrafted with $0.75x10^6$ CT26 cells while C57BL/6 mice were subcutaneously engrafted with $0.5x10^6$ LLC1. After subcutaneous engraftment of CT26 and LLC1 cells, mice were inspected every two days for tumor development. Tumor growth was monitored by caliper measurement following the equation $(width^2 \times length)/2$. Animals were sacrificed when at least a tumor reached 1000 mm^3.

Cell lines and cell culture conditions

CT26 cells were obtained from the ATCC (#CRL-2638) and cultured in RPMI-1640 medium (Gibco) supplemented with 10% fetal bovine serum (FBS), 1% penicillin-streptomycin (5000 U/mL) (Gibco) and 1% sodium pyruvate (Gibco). LL/2 (LLC1) cells were obtained from the ECACC (#90020104) and cultured in DMEM (Gibco) supplemented with 10% FBS. All cell lines were mycoplasma free. CT26 and LLC1 cells were seeded and cultured for 48 h prior to cell engraftment into mice and for validation of IRE1α expression and activity by RT-qPCR. CT26 and LLC1 cells were treated with tunicamycin at 1 μg/mL for 16 h after cell culture for 24 h. For cell growth experiments, CT26 cells were seeded and 24 h post-seeding, tunicamycin (Sigma-Aldrich) or 2-deoxyglucose (Sigma-Aldrich) were added at the indicated concentrations for a total cell culture of 96 h. All experiments were performed in duplicates or triplicates. All cell lines were incubated at 37 ºC in a 5% CO^2 atmosphere.

Generation of mock and IRE1α-overexpressing cells

A lentiviral vector coding for human IRE1α (hERN1) and GFP under the control of the SFFV promoter was designed (pLV[Exp]-SFFV>SalI/hERN1[NM_001433.5](ns)}:T2A/SalI:EGFP) and purchased from VectorBuilder (VB201207-1387mct). This lentiviral vector was used to generate the control vector expressing only GFP. In summary, the lentiviral vector was designed to contain SalI restriction sites upstream of the insert (hERN1) and downstream of the T2A sequence. Enzymatic digestion with

SalI and re-ligation at 16 ºC for 16 h yielded the control plasmid coding for GFP under the control of the SFFV promoter. For generating transduced cells, self-inactivating viruses were generated by transient transfection of 293T cells (ATCC, #CRL-1573) and tittered as described previously [23]. Briefly, using the classical calcium phosphate method, the envelope plasmid VSV-G (3 μg) was co-transfected with 8.6 μg of Gag-Pol packaging plasmid (psPAX2, Adgene, #12260) and 8.6 μg of the empty lentiviral vector coding for GFP or the lentiviral vector coding for hERN1α (VB201207-1387mct). Eighteen hours after transfection, the medium was replaced by Opti-MEM supplemented with 1% HEPES (Invitrogen). Viral supernatants were harvested 48 h after transfection and filtered with a 0.45 μm filter. The vectors were concentrated at low speed by overnight centrifugation of the viral supernatants at 3000 g and 4 ºC. Viral particles were titered in CT26 and LLC1 cells. CT26 and LLC1 cells were transduced with viruses at a multiplicity of infection (MOI) equivalent to 1. Cells were seeded ($8x10^4$ cells) in 6-well culture plates overnight prior to virus addition to the cell culture media. Cells were kept in the same media up to 48 h before medium refreshment and cell expansion. Transduced cells were sorted (SONY sorter SH800, Sony Biotechnology) based on GFP expression, resulting in >95% purity. Exogenous expression of hIRE1α was verified by RT-qPCR and immunoblotting.

Quantitative Reverse Transcription-PCR (RT-qPCR) analysis

For *in vitro* cultured cells, cells seeded for 48 h were detached with trypsin-EDTA 0.25% (Gibco) and collected. Cell pellets were lysed in tryzol prior to RNA extraction with chloroform. Reverse transcription was performed using the Omniscript RT Kit (Qiagen, #205113). Quantitative-PCR was performed with Power SYBR Green PCR master mix (Applied Biosystems, Life Technologies, # 4367659) using the Step One real-time PCR systems (Applied Biosystems) following the manufacturers' instructions. For whole tumor, a piece of the frozen tissue was cut and mechanically disrupted in tryzol using a Pre-cellys 24 tissue homogenizer (Bertin Instruments) (3 x 30 s, 6500 x *g*). For analysis of only tumor cells from tumor-bearing mice, tumors were enzymatically digested with the Tumor Dissociation Kit for mouse (Miltenyi Biotec, #130-096-730) yielding a single tumor cell suspension. Tumor cells were magnetically isolated using the Tumor Cell Isolation kit for mouse (Miltenyi Biotec, 130-110-187) following the manufacturers' instructions. In brief, dissociated tumors were incubated with a depletion cocktail for 15 min and after magnetic isolation using an AutoMACS Pro Separator (Miltenyi Biotec), the negative and positive fractions containing tumor cells and stromal cells, respectively, were frozen either as a dry pellet or in 10% DMSO-containing FBS.

The following primers for mouse sequences were used for SYBR Green qPCR:

Gene	**Primer sequences (forward 5'-3' / reverse 5'-3')**	**Source**
ERN1	AGAGAAGCAGCAGACTTTGTC GTTTTGGTGTCGTACATGGTGA	This paper

Gene	Primer sequences (forward 5'-3' / reverse 5'-3')	Source
XBP1u	GAGTCCGCAGCACTCAGACT GTGTCAGAGTCCATGGGAAGA	Villeneuve et al., 2010
XBP1s	GCTGAGTCCGCAGCAGGTG GTGTCAGAGTCCATGGGAAGA	Villeneuve et al., 2010
Scara3	TGACAGGGATGTACTGTGTGT TGCAAAGATAGGTTCTTCTGGC	This paper
Blos1	CAAGGAGCTGCAGGAGAAGA GCCTGGTTGAAGTTCTCCAC	This paper
Col6a1	TGCTCAACATGAAGCAGACC TTGAGGGAGAAAGCTCTGGA	This paper
IFNα	AGCAGATCCAGAAGGCTCAA GGAGGGTTGTATTCCAAGCA	This paper
IFNβ	GCAGCTGAATGGAAAGATCA TGGCAAAGGCAGTGTAACTC	This paper
IFNγ	TCAAGTGGCATAGATGTGGAAGAA TGGCTCTGCAGGATTTTCATG	This paper
TNFα	CCCTCACACTCAGATCATCTTCT GCTACGACGTGGGCTACAG	This paper
CXCL10	CCAAGTGCTGCCGTCATTTTC GGCTCGCAGGGATGATTTCAA	This paper
CXCL11	GGCTTCCTTATGTTCAAACAGGG GCCGTTACTCGGGTAAATTACA	This paper
CCL2	TTAAAAACCTGGATCGGAACCAA GCATTAGCTTCAGATTTACGGGT	This paper
GM-CSF	TCGTCTCTAACGAGTTCTCCTT CGTAGACCCTGCTCGAATATCT	This paper
IL15	ACATCCATCTCGTGCTACTTGT GCCTCTGTTTTAGGGAGACCT	This paper
Rn18S	GTAACCCGTTGAACCCCATT CCATCCAATCGGTAGTAGCG	This paper
Rplp0	AGATTCGGGATATGCTGTTGGC TCGGGTCCTAGACCAGTGTTC	This paper

ERN1 primers were designed to recognize mouse and human sequences. The housekeeping genes Rn18S and Rplp0 were used as control for RNA quality and normalization. All analyses were performed in technical triplicates and melting curve analysis was performed for SYBR Green to control product quality and specificity.

Western Blot Analysis

For whole tumors, pieces of tumor tissue were cut and mechanically disrupted in a protease inhibitor-containing RIPA buffer using a Pre-cellys 24 tissue homogenizer (Bertin Instruments) (3 x 30 s, 6500 x *g*). Magnetically isolated tumor cells (Tumor Cell Isolation kit for mouse (Miltenyi Biotec, 130-110-187) were lysed in a protease inhibitor-containing RIPA buffer. Protein lyses were quantified and standardized (Pierce BCA protein assay kit, Thermo Scientific, #23225), immunoblots were developed using the Amersham ECL Prime Western Blotting Detection Reagent (Cytiva, #RPN2236) and visualized with ImageQuant LAS 4000 (GE Healthcare, Life Science). The following antibodies were used for immunoblotting:

Antibody	**Source**	**Identifier**
Rabbit monoclonal anti-IRE1α	Cell Signaling	3294; RRID:AB_823545
Mouse monoclonal anti-XBP1	Santa Cruz	sc-8015; RRID:AB_628449
Mouse monoclonal anti-CHOP	Cell Signaling	2895; RRID:AB_2089254
Rabbit monoclonal anti-ATF4	Cell Signaling	11815; RRID:AB_2616025
Rabbit polyclonal anti-PARP	Cell Signaling	9542, RRID:AB_2160739
Mouse monoclonal anti-ERK2	Santa Cruz	sc-1647; RRID:AB_627547

Flow Cytometry Analysis

CT26 tumors were dissociated with the mouse Tumor Dissociation Kit (Miltenyi Biotec, #130-096-730) yielding a single cell suspension. Stained samples were analyzed with a MACSQuant Analyzer 10 (Miltenyi Biotec). The following fluorochrome-conjugated anti-mouse antibodies were used for flow cytometry and isolation of $CD3^+$ splenocytes:

Antibody	**Source**	**Identifier (cat #, RRID)**
APC-eFluor 780 anti-CD45.2	eBioscience, Thermo Fisher Scientific	47-0454-80, RRID:AB_1272211
PE anti-H-2Kd	BD Biosciences	553566, RRID:AB_394924
PE anti-H-2Ld/H-2Db	BioLegend	114507, RRID:AB_313588
PE-Cyanine7 anti-CD274 (PD-L1, B7-H1)	eBioscience, Thermo Fisher Scientific	25-5982-82, RRID:AB_2573509
APC anti-H60a	REAfinity, Miltenyi Biotec	130-108-847, RRID:AB_2651975
PE-Vio770 anti-CD47	REAfinity, Miltenyi Biotec	130-103-105, RRID:AB_2659751
APC anti-CD3	BioLegend	Cat# 100236, RRID:AB_2561456
PE-Vio770 anti-CD8a	REAfinity, Miltenyi Biotec	130-119-123, RRID:AB_2733250
V450 anti-CD4	BD Biosciences	560468, RRID:AB_1645271
CD152 Antibody, anti-mouse, PE	Miltenyi Biotec	130-102-570, RRID:AB_2655252
PE-Vio770 anti-CD49b	Miltenyi Biotec	130-105-402, RRID:AB_2660461

Antibody	Source	Identifier (cat #, RRID)
Brilliant Violet 42 anti-CD64 (FcgammaRI)	BioLegend	139309, RRID:AB_2562694
PE anti-MERTK (Mer)	Biolegend	151505, RRID:AB_2617036
Alexa Fluor 647 anti-I-A/I-E	Biolegend	107617, RRID:AB_493526
PE-Cyanine7 anti-CD86 (B7-2)	eBioscience, Thermo Fisher Scientific	25-0862-82, RRID:AB_2573372
eFluor 450 anti-F4/80	eBioscience, Thermo Fisher Scientific	48-4801-82, RRID:AB_1548747
PE/Cy7 anti-CD11c	BD Biosciences	558079, RRID:AB_647251
FITC anti-CD11b	BD Biosciences	553310, RRID:AB_394774
PE anti-CD11c	BD Bioscience	557401, RRID:AB_396684
PE anti-annexin V	Miltenyi Biotec	130-118-499
FITC anti-CD19	Miltenyi Biotec	130-102-494, RRID:AB_2661108
FITC anti-CD45R (B220)	REAfinity, Miltenyi Biotec	130-110-708, RRID:AB_2658274)
FITC anti-CD49b	Miltenyi Biotec	130-102-258, RRID:AB_2660456
FITC anti-Ter-119	REAfinity, BD Biosciences	130-112-719, RRID:AB_2654114

Intra-tumoral infiltration of immune cell populations was calculated as a percentage from the whole tumor. Tumor-infiltrating lymphocytes (TILs) were defined as followed: $CD3^+$ TILs ($CD3^+/CD45^+$), $CD8^+$ TILs ($CD8^+/CD3^+$) and $CD4^+$ TILs ($CD4^+/CD3^+$). Infiltrating NK cells were defined as $CD49b^+/CD3^-/CD45^+$. TAMs were defined as $CD86^+/CD11c^+/CD11b^+/F4/80^+/CD45^+$ in CTR and Low PROT tumors while resident TMAs were defined as $CD64^+/Mertk^+/CD45^+$ cells in mock and OE tumors.

Cytotoxicity Assay

Spleens were manually smashed and filtered through a 40 μm strainer to obtain a single cell suspension of splenocytes. $CD3^+$ cells were depleted by magnetic isolation using an autoMACS Pro Separator (Miltenyi Biotec) after staining with FITC-conjugated antibodies against CD19 (Miltenyi, #130-102-494), CD45R (Miltenyi, #130-110-708), CD49b (Miltenyi, #130-102-258), CD11b (BD Bioscience, #553310) and Ter-119 (Miltenyi, #130-112-719). The resulting purified cells were co-cultured with CT26 cells at a ratio 5:1 in the presence of IL-2 (1 ng/mL, Miltenyi Biotec #130-094-055) for 4 h at 37ºC. Cell death of CT26 cells was monitored by $DAPI^+$ staining by flow cytometry (MACSQuant Analyzer 10, Miltenyi Biotec).

Cell death measurement

Cell death was analyzed either by DEVDase activity or 4',6-diamidino-2-phenylindole staining (DAPI, Sigma-Aldrich #D9542) staining. To measure apoptosis in isolated tumor cells, the activity of

DEVDases was assayed as described previously [24] with some modifications. Briefly, cells were lysed in a lysis buffer (50 mM HEPES [pH 7.4], 150 mM NaCl, 20 mM EDTA, 0.2 % NP40, 2 μg/mL aprotinin, 1 mM PMSF, and 10 μg/mL leupeptin). Protein lysates were quantified and standardized (Pierce BCA protein assay kit, Thermo Scientific, #23225) and loaded into a black 96-well plate (CellStar) in the presence of 0.2 mmol/L of the caspase-3 substrate Ac-DEVD-AMC (Enzo LifeScience, ALX-260-031-M005) diluted in the lysis buffer containing 10 mmol/L DTT. Caspase activity was determined either in the absence or presence of 1 mmol/L Ac-DEVD- CHO (Enzo LifeScience, ALX-260-030-M001) using a fluoroscan recording the emission fluorescence at 460 nm (Fluoroskan Ascent, Thermo Scientific). The specific DEVDase activity was calculated as the change in fluorescence per minute.

Statistical analysis

Graphs and statistical tests were generated using Prism v.8 (GraphPad software, Inc.). Differences in calculated means between groups were assessed by two-tailed, unpaired Student's t tests. A p-value less than 0.05 was considered significant.

REFERENCES

1 Levesque S, Pol JG, Ferrere G, Galluzzi L, Zitvogel L, Kroemer G. Trial watch: dietary interventions for cancer therapy. *Oncoimmunology* 2019; 8: 1591878.

2 Kanarek N, Petrova B, Sabatini DM. Dietary modifications for enhanced cancer therapy. *Nature* 2020; 579: 507-517.

3 Tajan M, Vousden KH. Dietary Approaches to Cancer Therapy. *Cancer Cell* 2020; 37: 767-785.

4 Sahu N, Dela Cruz D, Gao M, Sandoval W, Haverty PM, Liu J *et al*. Proline Starvation Induces Unresolved ER Stress and Hinders mTORC1-Dependent Tumorigenesis. *Cell metabolism* 2016; 24: 753-761.

5 Meynet O, Ricci JE. Caloric restriction and cancer: molecular mechanisms and clinical implications. *Trends in molecular medicine* 2014; 20: 419-427.

6 Rubio-Patino C, Bossowski JP, De Donatis GM, Mondragon L, Villa E, Aira LE *et al*. Low-Protein Diet Induces IRE1alpha-Dependent Anticancer Immunosurveillance. *Cell metabolism* 2018; 27: 828-842 e827.

7 Halbleib K, Pesek K, Covino R, Hofbauer HF, Wunnicke D, Hanelt I *et al*. Activation of the Unfolded Protein Response by Lipid Bilayer Stress. *Mol Cell* 2017; 67: 673-684 e678.

8 Covino R, Hummer G, Ernst R. Integrated Functions of Membrane Property Sensors and a Hidden Side of the Unfolded Protein Response. *Mol Cell* 2018; 71: 458-467.

9 Hetz C, Axten JM, Patterson JB. Pharmacological targeting of the unfolded protein response for disease intervention. *Nature chemical biology* 2019; 15: 764-775.

10 Carreras-Sureda A, Jana F, Urra H, Durand S, Mortenson DE, Sagredo A *et al*. Non-canonical function of IRE1alpha determines mitochondria-associated endoplasmic reticulum composition to control calcium transfer and bioenergetics. *Nature cell biology* 2019; 21: 755-767.

11 Logue SE, McGrath EP, Cleary P, Greene S, Mnich K, Almanza A *et al*. Inhibition of IRE1 RNase activity modulates the tumor cell secretome and enhances response to chemotherapy. *Nat Commun* 2018; 9: 3267.

12 Chen X, Iliopoulos D, Zhang Q, Tang Q, Greenblatt MB, Hatziapostolou M *et al*. XBP1 promotes triple-negative breast cancer by controlling the HIF1alpha pathway. *Nature* 2014; 508: 103-107.

13 Zhao N, Cao J, Xu L, Tang Q, Dobrolecki LE, Lv X *et al*. Pharmacological targeting of MYC-regulated IRE1/XBP1 pathway suppresses MYC-driven breast cancer. *J Clin Invest* 2018; 128: 1283-1299.

14 Harnoss JM, Le Thomas A, Reichelt M, Guttman O, Wu TD, Marsters SA *et al*. IRE1alpha Disruption in Triple-Negative Breast Cancer Cooperates with Antiangiogenic Therapy by Reversing ER Stress Adaptation and Remodeling the Tumor Microenvironment. *Cancer Res* 2020; 80: 2368-2379.

15 Genovese G, Carugo A, Tepper J, Robinson FS, Li L, Svelto M *et al*. Synthetic vulnerabilities of mesenchymal subpopulations in pancreatic cancer. *Nature* 2017; 542: 362-366.

16 Robinson CM, Talty A, Logue SE, Mnich K, Gorman AM, Samali A. An Emerging Role for the Unfolded Protein Response in Pancreatic Cancer. *Cancers (Basel)* 2021; 13.

17 Li XX, Zhang HS, Xu YM, Zhang RJ, Chen Y, Fan L *et al*. Knockdown of IRE1alpha inhibits colonic tumorigenesis through decreasing beta-catenin and IRE1alpha targeting suppresses colon cancer cells. *Oncogene* 2017; 36: 6738-6746.

18 Gao Q, Li XX, Xu YM, Zhang JZ, Rong SD, Qin YQ *et al*. IRE1alpha-targeting downregulates ABC transporters and overcomes drug resistance of colon cancer cells. *Cancer Lett* 2020; 476: 67-74.

19 Lhomond S, Avril T, Dejeans N, Voutetakis K, Doultsinos D, McMahon M *et al*. Dual IRE1 RNase functions dictate glioblastoma development. *EMBO Mol Med* 2018: in press.

20 Bujisic B, De Gassart A, Tallant R, Demaria O, Zaffalon L, Chelbi S *et al*. Impairment of both IRE1 expression and XBP1 activation is a hallmark of GCB DLBCL and contributes to tumor growth. *Blood* 2017; 129: 2420-2428.

21 Xie H, Tang CH, Song JH, Mancuso A, Del Valle JR, Cao J *et al*. IRE1alpha RNase-dependent lipid homeostasis promotes survival in Myc-transformed cancers. *J Clin Invest* 2018; 128: 1300-1316.

22 Rubio-Patino C, Bossowski JP, Chevet E, Ricci JE. Reshaping the Immune Tumor Microenvironment Through IRE1 Signaling. *Trends in molecular medicine* 2018; 24: 607-614.

23 Frecha C, Fusil F, Cosset FL, Verhoeyen E. In vivo gene delivery into hCD34+ cells in a humanized mouse model. *Methods Mol Biol* 2011; 737: 367-390.

24 Villa E, Proics E, Rubio-Patino C, Obba S, Zunino B, Bossowski JP *et al*. Parkin-Independent Mitophagy Controls Chemotherapeutic Response in Cancer Cells. *Cell Rep* 2017; 20: 2846-2859.

25 Castle JC, Loewer M, Boegel S, de Graaf J, Bender C, Tadmor AD *et al*. Immunomic, genomic and transcriptomic characterization of CT26 colorectal carcinoma. *BMC Genomics* 2014; 15: 190.

26 Agalioti T, Giannou AD, Krontira AC, Kanellakis NI, Kati D, Vreka M *et al*. Mutant KRAS promotes malignant pleural effusion formation. *Nat Commun* 2017; 8: 15205.

27 Obiedat A, Seidel E, Mahameed M, Berhani O, Tsukerman P, Voutetakis K *et al*. Transcription of the NKG2D ligand MICA is suppressed by the IRE1/XBP1 pathway of the unfolded protein response through the regulation of E2F1. *FASEB J* 2019; 33: 3481-3495.

FIGURE LEGENDS

Figure 1. Low PROT diet limits tumor growth, activates the IRE1α pathway, increases the anti-cancer immunosurveillance and the synthesis of inflammatory genes.

A. Immunocompetent BALB/c mice fed a control (CTR) or Low Protein (Low PROT) diet for seven days were engrafted with syngeneic colorectal carcinoma CT26 cells. **B.** Subcutaneous (SC) tumor growth curve and tumor weight at endpoint (CTR, n=5 and Low PROT, n=6). **C.** Protein expression of IRE1α and XBP1s in whole tumors isolated from B. **D, E, F.** Percentage of $CD8^+$ TILs, TAMs and DCs from whole tumor presented in B, as quantified by flow cytometry (CTR, n=4 and Low PROT, n=5). **G.** Surface expression levels (MFI) of H2Kd determined by FACS analysis on live and isolated tumor cells (CTR, n=4 and Low PROT, n=4). **H.** Percentage of dead CT26 cells co-cultured with $CD3^+$ T splenocytes isolated from tumor-bearing mice (from B) for *ex vivo* cytotoxicity assay. **I.** Transcript levels in isolated tumor cells of proteins involved in the antigenic peptide shuttle into the ER and peptide loading onto MHC-I as quantified by RT-qPCR. **J.** Transcript levels in isolated tumor cells from B of type I and II interferons, cytokines and chemokine ligands.

Bars represent mean ± SD (or SEM for panel B) and each data point represent a biological replicate. Statistical differences were determined by two-tailed, unpaired Student's t-test. In vivo experiments are representative of several performed.

Figure 2. IRE1α-overexpressing CT26 cells display a functional IRE1α protein with an enhanced endoribonuclease activity.

A. Transcript expression levels of ERN1 and XBP1s/u in WT, mock and IRE1α-overexpressing (OE) CT26 cells in basal conditions and under tunicamycin 1 μg/mL for 16 hours (biological triplicates of a single experiment). **B.** Protein expression levels of IRE1α and CHOP were determined by immunoblotting in WT, mock or OE CT26 cells in basal conditions and under tunicamycin 1 μg/mL for 16 hours (representation of one out of three independent experiments). ERK2 is used as a loading control. **C.** Transcript levels of hERN1, XBP1s/u, RIDD targets, ERAP1 and TAP1 in mock and OE CT26 cells were quantified by RT-qPCR (combined data of three independent experiments). **D.** Cell growth of mock and OE CT26 cells (combined data of three independent experiments). **E.** Cell growth of mock and OE CT26 cells when treated with indicated doses of tunicamycin (biological triplicates of a single experiment). **F.** Cell growth of mock and OE CT26 cells when treated with indicated doses of 2-DG (biological triplicates). **G.** Transcript expression of type I and II interferons, ligands of chemokines and cytokines in mock and OE CT26 cells as quantified by RT-qPCR (technical triplicates of a single experiment).

Bars and data points of the cell growth curves represent mean ± SD. Statistical differences were determined by two-tailed, unpaired Student's t-test.

Figure 3. IRE1α overexpression in CT26 tumor cells limits tumor growth in immuno-competent syngeneic mice.

A. Subcutaneous (SC) tumor growth curve and tumor weight at endpoint of immunocompetent BALB/c mice engrafted with mock and IRE1α-overexpressing (OE) CT26 cells (n=5 per group). **B.** Tumor weight at endpoint of immunocompetent C57BL/6 mice subcutaneously engrafted with mock and IRE1α-overexpressing (OE) LLC1 cells (n=8 per group). **C.** Protein expression levels of IRE1α, XBP1s and other UPR components (CHOP, ATF4) in isolated tumor cells from CT26 tumor-bearing mice (presented in A). ERK2 is used as a loading control. **D.** Transcript expression levels of IRE1α, XBP1s/u and RIDD targets (Scara3, Blos1, Col6a1) in isolated tumor cells from CT26 tumor-bearing mice and quantified by RT-qPCR. **E.** Protein expression levels of PARP and cleaved PARP in isolated tumor cells from CT26 tumor-bearing mice. ERK2 is used as a loading control **F.** Caspase (DEVDase) activity in isolated tumor cells from CT26 tumor-bearing mice. **G.** Percentage of $CD3^+$ TILs, $CD8^+$ TILs and $CD4^+$ TILs from whole CT26 tumors were quantified by flow cytometry. **H, I.** Percentage of resident TAMs and tumor-infiltrating NK cells from whole CT26 tumors were quantified by flow cytometry. **J.** Surface expression levels (MFI) of immune markers on live $GFP^+/CD45^-$ CT26 tumor cells were quantified by flow cytometry. **K.** $CD3^+$ T splenocytes were isolated from mice bearing mock or OE-CT26 tumors (from A) and incubated with WT CT26 for 4 hours (ratio 5 T cells for 1 CT26 cell). The ability of T cells to kill tumoral cells was determined by flow cytometry.

Bars represent mean ± SD and each data point represents biological replicates. Statistical differences were determined by two-tailed, unpaired Student's t-test. In vivo experiments are representative of at least two performed.

Figure 4. IRE1α overexpression in CT26 tumor cells limits tumor growth mainly dependent on T cells.

A. Subcutaneous (SC) tumor growth curve and tumor weight at endpoint of immunodeficient Nude mice engrafted with mock (n=7) and IRE1α-overexpressing (OE) CT26 cells (n=5). **B.** Transcript expression levels of IRE1α, XBP1s/u and RIDD targets in isolated tumor cells from tumor-bearing mice were quantified by RT-qPCR. **C.** Caspase (DEVDase) activity in isolated tumor cells from tumor-bearing mice presented in A. **D, E.** Percentage of resident TAMs and tumor-infiltrating NK cells from whole tumors were quantified by flow cytometry. **F.** Surface expression levels (MFI) of immune markers on live $GFP^+/CD45^-$ tumor cells were quantified by flow cytometry.

Bars represent mean ± SD and each data point represents biological replicates. Statistical differences were determined by two-tailed, unpaired Student's t-test. In vivo experiments are representative of two performed.

SUPPLEMENTARY FIGURE LEGENDS

Figure S1. Characterization of LLC1 cells overexpressing IRE1α.

A. Transcript levels of IRE1α and XBP1s/u in mock and IRE1α-overexpressing (OE) LLC1 cells in basal conditions and upon treatment with tunicamycin 1 μg/mL for 16 h hours (technical triplicates of a single experiment). **B.** *in vitro* cell growth of mock and OE LLC1 cells over 72 hours (biological triplicates of a single experiment).

Bars represent mean ± SD. Data points of the cell growth curve represent mean ± SD. Statistical differences were determined by two-tailed, unpaired Student's t-test.

Figure S2. Immune profiling of mock- or OE-CT26 tumors grown in syngeneic BALB/c mice.

A. Percentage of tumor-infiltrating immune cells measure in whole tumors of mock- or OE-CT26 tumor-bearing BALB/c mice (n=5). **B.** Surface expression levels (MFI) of activation markers on resident $CD11c^+$ TAMs ($CD64^+$/$Mertk^+$/$CD45^+$) in the tumor presented in A. **C.** Surface expression levels (MFI) of immune markers on live GFP^+/$CD45^-$ CT26 tumor cells were quantified by flow cytometry from tumors presented in A.

Bars represent mean ± SD and each data point represents biological replicates. Statistical differences were determined by two-tailed, unpaired Student's t-test.

FIGURE 1

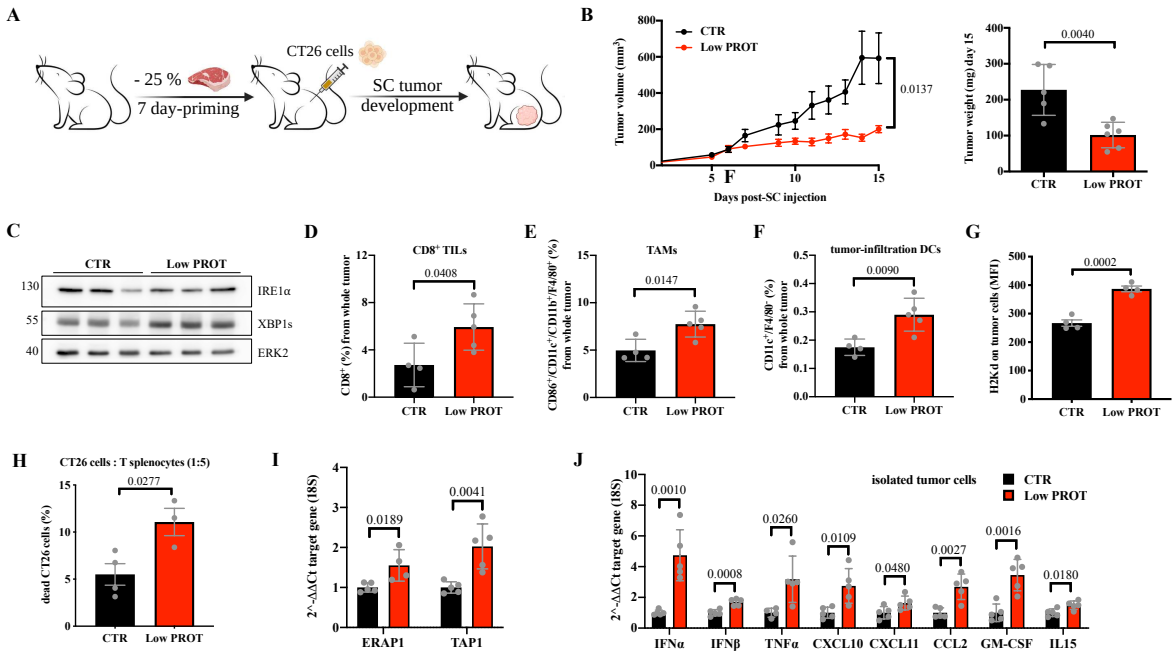
A
- 25 %
7 day-priming
CT26 cells
SC tumor development
B
CTR
Low PROT
Tumor volume (mm³)
Days post-SC injection
0.0137
Tumor weight (mg) day 15
0.0040
C
CTR
Low PROT
IRE1α
XBP1s
ERK2
D
CD8⁺ TILs
CD8⁺ (%) from whole tumor
0.0408
E
TAMs
CD86⁺/CD11c⁺/CD11b⁺/F4/80⁺ (%) from whole tumor
0.0147
F
tumor-infiltration DCs
CD11c⁺/F4/80⁺ (%) from whole tumor
0.0090
G
H2Kd on tumor cells (MFI)
0.0002
H
CT26 cells : T splenocytes (1:5)
dead CT26 cells (%)
0.0277
I
2^-ΔΔCt target gene (18S)
ERAP1
TAP1
0.0189
0.0041
J
isolated tumor cells
CTR
Low PROT
IFNα
IFNβ
TNFα
CXCL10
CXCL11
CCL2
GM-CSF
IL15
0.0010
0.0008
0.0260
0.0109
0.0480
0.0027
0.0016
0.0180

FIGURE 2

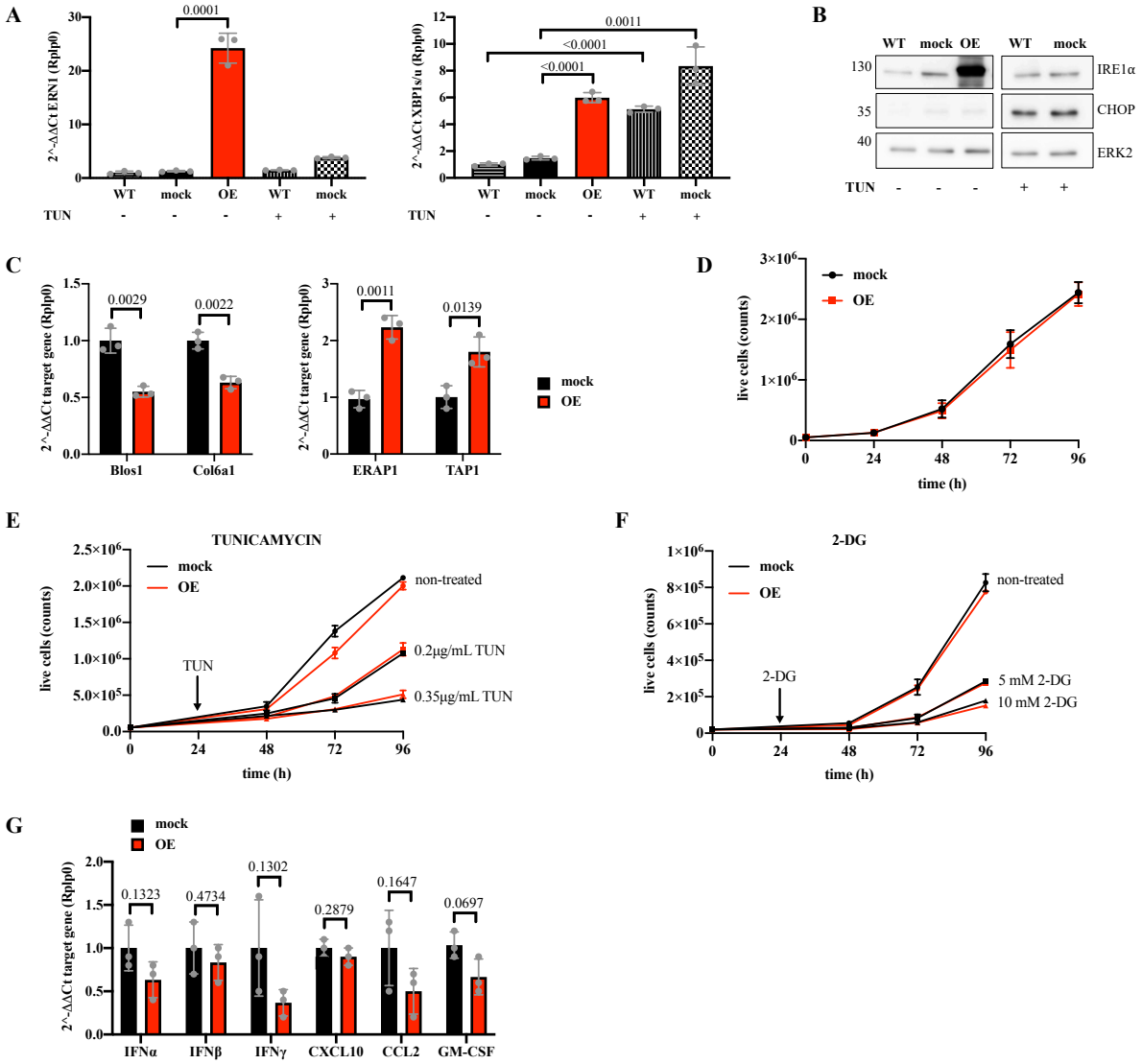
A
2^-ΔΔCt ERN1 (Rplp0)
0.0001
WT mock OE WT mock
TUN - - - + +
2^-ΔΔCt XBP1s/u (Rplp0)
0.0011
<0.0001
<0.0001
WT mock OE WT mock
TUN - - - + +
B
WT mock OE WT mock
130
35
40
IRE1α
CHOP
ERK2
TUN - - - + +
C
2^-ΔΔCt target gene (Rplp0)
0.0029
0.0022
Blos1
Col6a1
0.0011
0.0139
ERAP1
TAP1
mock
OE
D
live cells (counts)
mock
OE
time (h)
E
TUNICAMYCIN
live cells (counts)
mock
OE
non-treated
0.2µg/mL TUN
0.35µg/mL TUN
TUN
time (h)
F
2-DG
live cells (counts)
mock
OE
non-treated
5 mM 2-DG
10 mM 2-DG
2-DG
time (h)
G
mock
OE
2^-ΔΔCt target gene (Rplp0)
0.1323
0.4734
0.1302
0.2879
0.1647
0.0697
IFNα
IFNβ
IFNγ
CXCL10
CCL2
GM-CSF

FIGURE 3

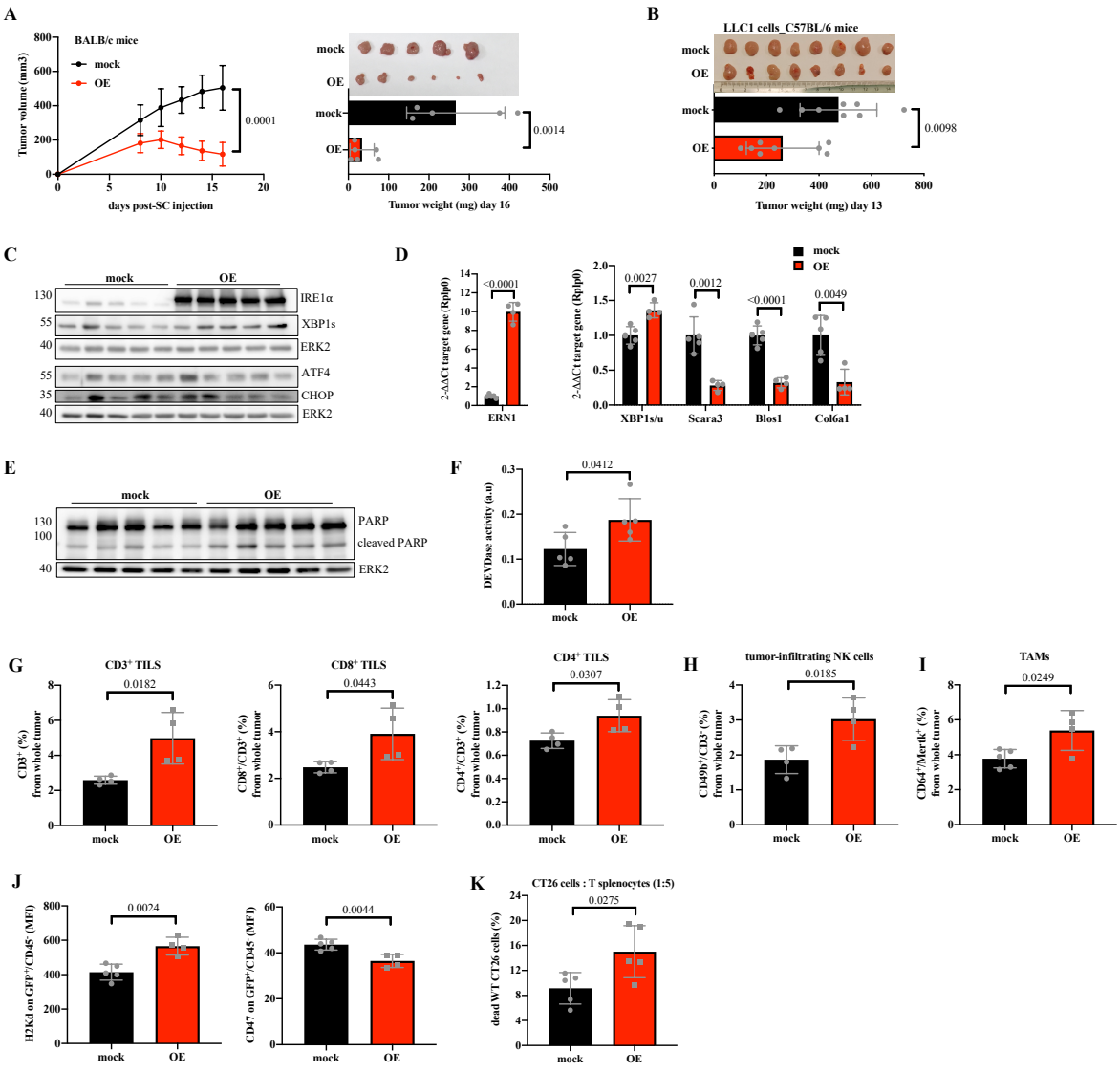
A
BALB/c mice
mock
OE
Tumor volume (mm3)
days post-SC injection
0.0001
Tumor weight (mg) day 16
0.0014
B
LLC1 cells_C57BL/6 mice
Tumor weight (mg) day 13
0.0098
C
mock
OE
IRE1α
XBP1s
ERK2
ATF4
CHOP
D
2-ΔΔCt target gene (Rplp0)
ERN1
XBP1s/u
Scara3
Blos1
Col6a1
E
PARP
cleaved PARP
F
DEVDase activity (a.u)
0.0412
G
CD3+ TILS
0.0182
CD8+ TILS
0.0443
CD4+ TILS
0.0307
H
tumor-infiltrating NK cells
0.0185
I
TAMs
0.0249
J
0.0024
0.0044
K
CT26 cells : T splenocytes (1:5)
0.0275

FIGURE 4

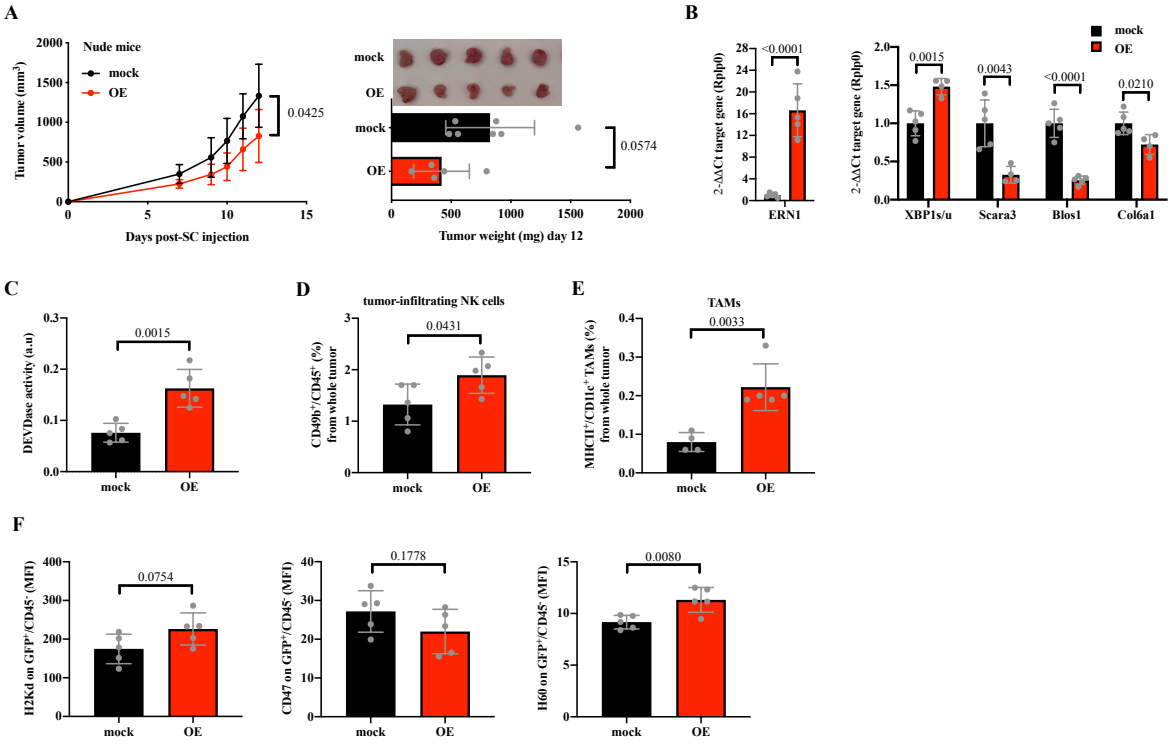
A
Nude mice
mock
OE
Tumor volume (mm3)
Days post-SC injection
0.0425
mock
OE
mock
OE
0.0574
Tumor weight (mg) day 12
B
mock
OE
2-ΔΔCt target gene (Rplp0)
<0.0001
ERN1
0.0015
0.0043
<0.0001
0.0210
XBP1s/u
Scara3
Blos1
Col6a1
C
DEVDase activity (a.u)
0.0015
mock
OE
D
tumor-infiltrating NK cells
CD49b+/CD45+ (%) from whole tumor
0.0431
mock
OE
E
TAMs
MHCII+/CD11c+ TAMs (%) from whole tumor
0.0033
mock
OE
F
H2Kd on GFP+/CD45- (MFI)
0.0754
mock
OE
CD47 on GFP+/CD45- (MFI)
0.1778
mock
OE
H60 on GFP+/CD45- (MFI)
0.0080
mock
OE

SUPPLEMENTARY FIGURE 1

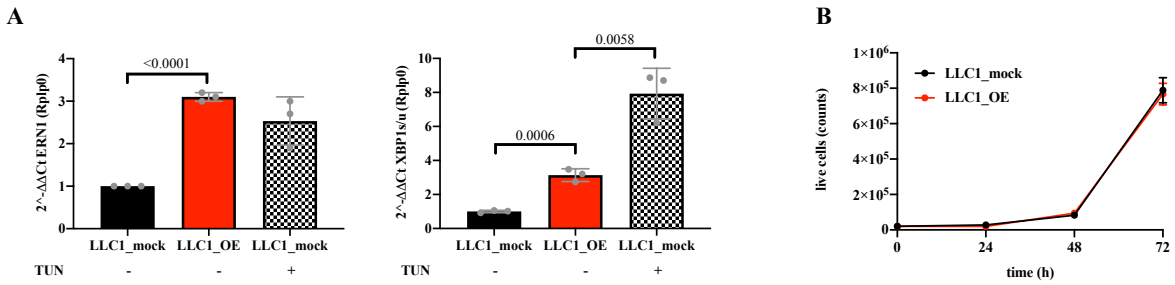

SUPPLEMENTARY FIGURE 2

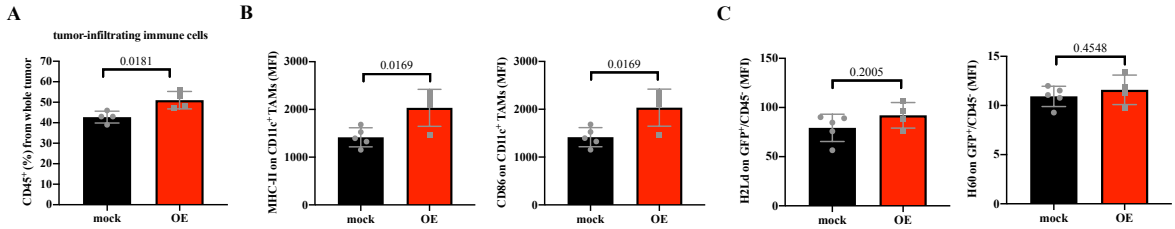

PRELIMINARY RESULTS

Preliminary results are presented in a scientific journal format.

The tumor suppressive effect of a low protein diet might be mediated by glycosylation in malignant cells leading to increased immunosurveillance

Adriana Martinez-Turtos, Manuel Grima-Reyes, Hussein Issaoui, Adrien Krug, Ivan Nemazanny, Johanna Chiche, Rachel Paul, Sandrine Marchetti, Ifat Abramovich, Mohamed Abdel-Mohsen, Eyal Gottlieb, Nao Yamakawa, Els Verhoeyen and Jean-Ehrland Ricci
Ongoing research project

The tumor suppressive effect of a low protein diet might be mediated by glycosylation in malignant cells leading to increased immunosurveillance

Adriana Martinez-Turtos[1,2], Manuel Grima-Reyes[1,2], Hussein Issaoui[1,2], Adrien Krug[1,2], Ivan Nemazanny[3], Johanna Chiche[1,2], Rachel Paul[1,2], Sandrine Marchetti[1,2], Ifat Abramovich[4], Mohamed Abdel-Mohsen[5], Eyal Gottlieb[4], Nao Yamakawa[6], Els Verhoeyen[1,2,7] and Jean-Ehrland Ricci[1,2,*]

1 Université Côte d'Azur, INSERM, C3M, Nice, France

2 Equipe labellisée Ligue Contre le Cancer, Nice, France

3 Platforme d'étude du metabolism, SFR-Necker, Inserm US 24 - CNRS UMS 3633, Paris, France

4 Ruth and Bruce Rappaport Faculty of Medicine, Technion e Israel Institute of Technology, Haifa, Israel

5 The Wistar Institute, Philadelphia, Pennsylvania, United States of America

6 Plateforme d'Analyses des Glycoconjugués, CNRS Université de Lille, Villeneuve d'Ascq, France.

7 CIRI, Université de Lyon, INSERM U1111, ENS de Lyon, Université Lyon1, CNRS, UMR 5308, Lyon, France

* corresponding author: Jean-Ehrland Ricci PhD, Inserm U1065, équipe 3, 151 route de St Antoine de Ginestière, BP 23194, 06204 Nice Cedex 03, France. Phone: +33 4 89 06 43 04; Fax +33 4 89 06 42 21, email: ricci@unice.fr

Abstract

Some nutritional regimens as therapeutic interventions have shown anti-cancer benefits. We recently reported that an isocaloric diet reduced in proteins (Low PROT diet) limited tumor growth through a T cell-mediated anti-cancer immune response. However, how this diet alters the immunogenicity of tumor cells remains to be found. Here, using metabolomics characterization of tumors, we observed that the levels of uridine diphosphate N-acetylhexosamines, UDP-HexNAc(s) and uridine diphosphate hexoses, UDP-Hex(s) were higher in tumors from mice fed the Low PROT diet as compared to tumors from mice fed a control diet. UDP-HexNAc(s) and UDP-Hex(s) are common substrates for N- and O-glycosylation as well as O-GlcNAcylation of proteins. Aberrant glycosylation contributing to most hallmarks of cancer is known to modulate the immune response. We observed that the increase in uridine diphosphate N-acetylglucosamine (UDP-GlcNAc) was not linked to *de novo* synthesis but correlated with transcriptional downregulation of O-GlcNAc transferase (OGT) and O-GlcNAcase (OGA), two major regulators of UDP-GlcNAc levels beyond the hexosamine biosynthetic pathway (HBP). In addition, changes in glycosylated structures that have been reported in more immunogenic tumors were detected on Low PROT tumor cells. In conclusion, we have found that a Low PROT diet resulted in differential glycosylation patterns in tumoral cells, therefore representing a possible mechanism underlying tumor cell immunogenicity under this protein-restricted dietary regimen.

Keywords cancer, low protein diet, anti-cancer immune response, UDP-HexNAc, glycosylation, OGT, OGA, tumor immunogenicity

INTRODUCTION

Anti-cancer therapies have benefited from nutritional interventions to improve response to the treatment while minimizing side effects and improving life quality and survival (Tajan and Vousden, 2020), (Kanarek et al., 2020). We have previously reported that an isocaloric diet reduced in a 25% of proteins (Low PROT diet) limited tumor growth in several cancer mouse models. The protein-restricted dietary formula was designed to keep the same amount of calories by a compensatory increased of carbohydrates and lipids. The tumor-suppressive effect of the Low PROT diet depended on a stronger anti-cancer immune response mediated by cytotoxic T cells (Rubio-Patiño et al., 2018). Here, we aimed to decipher tumor metabolic alterations associated with enhanced anti-cancer immunosurveillance under the Low PROT diet.

We have found that uridine-diphosphate (UDP)-sugars were more abundant in tumors of mice fed the Low PROT diet. Uridine diphosphate N-acetylhexosamines, UDP-HexNAc(s) and uridine diphosphate hexoses, UDP-Hex(s) are common substrates fueling glycosylation reactions mediating N- and O-glycosylation of extracellular and surface proteins as well as O-GlcNAcylation of intracellular proteins (Pinho and Reis, 2015), (Reily et al., 2019). Aberrant glycosylation has been reported to contribute to most hallmarks of cancer (Chandler et al., 2019), (Li et al., 2016), (Song et al., 2020), (Arnold et al., 2020). Disturbances in the hexosamine biosynthetic pathway (HBP) for *de novo* synthesis of uridine diphosphate N-acetylglucosamine (UDP-GlcNAc) (Kim et al., 2020), (Chokchaitaweesuk et al., 2019), (Akella et al., 2019) as well as deregulation of major enzymatic regulators, O-GlcNAc transferase (OGT) and O-GlcNAcase (OGA) (Liu et al., 2018), (Phoomak et al., 2018) are mechanisms underlying aberrant glycosylation in cancer. The cytoplasmic abundance of UDP-GlcNAc is dictated by its rate of synthesis and consumption. Beyond the HBP and the UDP-GlcNAc salvage pathway governing the synthesis of this metabolite, OGT consumes UDP-GlcNAc for post-translational O-GlcNAcylation of proteins and OGA releases GlcNAc from O-GlcNAcylated proteins. Therefore, OGT and OGA tightly control the free pool of UDP-GlcNAc (Yang and Qian, 2017), (Lee et al., 2021).

In the present work, we found that the Low PROT diet does not change the global metabolism of tumors but resulted in an increase of the tumoral levels of UDP-HexNAc(s) and UDP-NAc(s). Along with more abundant UDP-sugars, OGT and OGA were found transcriptional downregulated. Glycosylated structures of the tumor cell glycocalyx that have been associated with more immunogenic tumors (Ghasempour and Freeman, 2021) were found differentially changed on the surface of tumor cells from mice fed the Low PROT diet. Our preliminary results therefore suggest that differential glycosylation processes associated with unbalanced levels of UDP-sugars and deregulation of UDP-GlcNAc master regulators, OGT and OGA are possible mechanisms underlying tumor cell immunogenicity under low PROT diet.

RESULTS

A low PROT diet increases UDP-HexNAc and UDP-Hex levels in tumors

To unravel the metabolic alterations associated with a stronger immune response under the Low PROT diet (Rubio-Patiño et al., 2018), *in vivo* steady state metabolomics analysis and stable isotope carbon tracing of universally labeled glucose were performed in tumor-bearing mice (**Fig. 1A**).

We chose to analyze the effect of the low PROT diet at earlier stages during tumor progression avoiding metabolic differences related to the tumor size. Indeed, the mid-term *in vivo* experiment allowed us to make a non-biased comparison of metabolic features between CTR and low PROT tumors avoiding limited nutrients and oxygen availability when comparing bigger versus smaller tumors at later stages during tumor progression. Therefore, mice were sacrificed 11-12 days post-tumor cell engraftment when tumors displayed a small but similar volume in CTR and Low PROT groups of mice. A trend to upregulate MHC-I on tumor cells and a significant higher infiltration of $CD8^+$ T cells were observed in Low PROT tumors at this earlier stage of tumor development (Fig. S1A), suggesting that modifications of tumor cell interaction with the immune system induced under Low PROT diet were already present.

Targeted steady-state metabolomics analysis of polar metabolites showed that the levels of 148 metabolites do not fully discriminate between CTR and low PROT tumors by principal component analysis (PCA) despite dietary protein reduction (**Fig. 1B**). This result fits with the mouse phenotype observed under a partial (-25%) reduction of dietary protein content which is characterized by the same body weight and food intake as its control counterpart (Rubio-Patiño et al., 2018). Among the 25 most discriminant tumoral metabolites, uridine diphosphate-N-acetylhexosamines (UDP-HexAc) and uridine diphosphate-hexoses (UDP-Hex) were significant higher in Low PROT tumors (**Fig. 1C**). HPLC-MS detection of glucose (Glc) and galactose (Gal) does not discriminate between them. Therefore, UDP-HexNAc refers to a metabolite mix composed of UDP-GlcNAc and UDP-GalNAc whereas UDP-Hex clusters UDP-Glc and UDP-Gal. Other discriminant metabolites included fatty acids, nucleotides and amino acids (**Fig. 1C**). We focused our attention on the nucleotide sugars UDP-HexAc and UDP-Hex due to their implications in protein glycosylation, ER stress, tumor cell immunogenicity and immune response (Pinho and Reis, 2015), (Wang et al., 2014), (Rudd et al., 2001), (Li et al., 2016). Total levels of UDP-HexNAc and UDP-Hex were higher in Low PROT tumors in steady-state but not in livers of corresponding mice reflecting the specificity of this phenomenon (**Fig. 1D**).

Since UDP-GlcNAc and UDP-Glc are synthesized from glucose, we traced the incorporation of labeled carbons derived from [U-$^{13}C_6$]-Glucose into these metabolites. In the case of UDP-GlcNAc, *de novo* synthesis from glucose is driven by the HBP (**Fig. 1E**). Levels of UDP-HexNAc M+6 and UDP-Hex M+6 were not different between CTR and Low PROT tumors (**Fig. 1F**) indicating that the higher total level of UDP-HexNAc is unlikely to be a consequence of increased *de novo* synthesis from glucose due to an enhanced flux rate through the HBP. Importantly, tumoral levels of [U-$^{13}C_6$]-Glucose of mice

supplemented with this tracer were roughly 50% (**Fig. S1B**), enrichment that allows tracking the incorporation of glucose-derived labeled carbons into downstream metabolites (Jang et al., 2018). Despite this tracer enrichment in tumoral tissue, the contribution of isopologues M+6 to the total levels of UDP-HexNAc and UDP-Hex were 2% (**Fig. S1C**) and 8-15% (**Fig. S1D**), respectively, in tumors. The low levels of UDP-HexNAc M+6 may reflect the 2 to 3% contribution of intracellular glucose to the HBP (Marshall et al., 1991). Like in tumors, the contribution of isotopologues M+6 to the total levels of UDP-HexNAc and UDP-Hex was low in livers. Despite this low ^{13}C labeling, UDP-HexNAc M+6 was higher in Low PROT livers (**Fig. S1C**) suggesting that the *de novo* synthesis of UDP-HexNAc can be detected upon *in vivo* tracing of labelled glucose. Total levels of other nucleotide sugars such as GDP-mannose (**Fig. S1E**) and CMP-sialic acid (CMP-Neu5Ac) (**Fig. S1F**) were unaltered in tumors.

To monitor whether higher total levels of UDP-HexNAc in Low PROT tumors could be associated with the GlcNAc salvage pathway and the activity of OGA fueling the HBP at the level of GlcNAc 6-phosphate (**Fig. 1E**), the levels of GlcNAc were measured. We did not observe any changes in total levels of GlcNAc between CTR and Low PROT tumors (**Fig. S1G**) indicating that the release of GlcNAc derived from the recycling of glycosylated proteins cannot explain higher levels of UDP-GlcNAc. Monitoring the levels of glucosamine as another carbon source fueling the HBP at the level of glucosamine 6-phosphate (**Fig. 1E**) revealed that glucosamine was higher in Low PROT tumors (**Fig. S1H**).

Altogether, these results show that the Low PROT diet associates with higher tumoral levels of UDP-HexNAc and UDP-Hex. The [U-$^{13}C_6$]-Glucose tracing did not allow to confirm neither rule out *de novo* synthesis by the HBP. We therefore decided to find out whether higher levels of these nucleotide sugars may be a consequence of accumulation rather than *de novo* synthesis in tumors.

Tumor cells under Low PROT diet downregulate OGT and OGA and display distinctive glycosylated structures

Beyond *de novo* synthesis, the cytoplasmic levels of UDP-GlcNAc are governed by the activity of OGT and OGA (**Fig. 2A**). In addition, the levels of UDP-GlcNAc and UDP-GalNAc as well as the levels of UDP-Glc and UDP-Gal are tightly connected since these nucleotide sugars can be converted from glucose to galactose and *vice versa* by reciprocal epimerization (Akella et al., 2019). All these nucleotide sugars participate in N- as well as O-glycosylation of proteins and synthesis of glycosaminoglycans destinated either to the extracellular matrix or the cell surface. In addition, UDP-GlcNAc is also incorporated as a unique saccharide moiety onto serine/threonine residues of proteins by a O-GlcNAcylation reaction catalyzed by OGT (Ong et al., 2018).

To check whether key enzymes involved in UDP-GlcNAc synthesis, consumption and release from glycosylated proteins were deregulated, transcript levels of the enzyme catalyzing the first rate-limiting step of the HBP, GFPT1 as well as OGT and OGA were measured in isolated tumor cells from tumor-

bearing mice fed the CTR or Low PROT diet. Whereas the levels of glutamine-fructose-6-phosphate transaminase 1 (GFPT1) were unaltered (**Fig. 2B**), OGT (**Fig. 2C**) and OGA (**Fig. 2D**) were downregulated in tumor cells from mice fed the Low PROT diet. No changes in the transcript levels of GFPT1 was consistent with the unaltered levels of UDP-HexNAc M+6 that we observed upon ^{13}C glucose tracing. This may indicate that *de novo* synthesis from glucose is not potentiated by the Low PROT diet while accumulation of UDP-GlcNAc could be a consequence of lower expression of OGT. Indeed, OGT is a master regulator of the free pool of UDP-GlcNAc due to its high affinity for this nucleotide sugar as compared to some organelle-resident UDP-GlcNAc transferases and UDP-GlcNAc transporters localized in the endoplasmic reticulum and Golgi apparatus (Haltiwanger et al., 1992), (Biwi et al., 2018). Of note, positive correlations of OGT and OGA transcript expression have been described in several types of cancer including colorectal carcinoma, lung, breast and prostate cancers (Qian et al., 2018). Rather than genomic alterations of OGT and OGA in several cancers, transcriptional reciprocal regulation between OGT and OGA has been demonstrated in PDAC cells. Human PDAC tissues have shown higher expression of OGT and OGA transcript and proteins (Qian et al., 2018).

Pursuing downstream effects of higher levels of UDP-HexNAc and UDP-Hex in tumors, proteins modified with O-GlcNAcylation, global N-glycan structures and surface glycoconjugates were analyzed. While O-GlcNAcylated proteins in whole tumors did not display different levels under Low PROT diet (**Fig. 2E**), certain N-glycans structures from isolated Low PROT tumor cells showed differential abundance (**Fig. 2F**) by mass spectrometry analysis. N-glycan profiling of isolated tumor cells by glycomics detected 15 different structures including three high oligo-mannose and twelve complex bi-antenna and tri-antenna type of N-glycan trees. The mature complex N-linked glycans which are more diverse were relatively lower abundant than precursor oligo mannose structures likely due to the detection of global N-glycans in whole tumor cells (**Fig. 2F**). Clustering based on glycan branching and sialylation revealed that complex bi-antenna type of N-glycans were relatively less abundant while sialylated complex type of N-glycans were relatively more represented in Low PROT tumor cells (**Fig. 2G**). Detection of glycoconjugates expressed on the surface of isolated tumor cells by a lectin microarray containing 96 lectins (**Table 1**) revealed that three lectins mediated a differential binding to the glycocalyx of tumor cells isolated from CTR and Low PROT diet-fed mice. While rPAIL recognizing Tn antigens (mucin type of O-glycans) was lower detected, rGC2 (Lewis antigens of the blood group system) and rGRFT (Man) were higher in Low PROT tumor cells (**Fig. 2H**).

Altogether, these results suggest that a Low PROT diet might differentially impact on glycosylation processes in tumor cells in association with higher levels of UDP-HexNAc and UDP-Hex in tumors, possibly due to the deregulation of OGT and OGA expression in tumor cells.

Discussion of these preliminary results is part of the Discussion and Perspectives section of the thesis

Table 1. Lectin microarray containing 96 lectins for detection of surface glycoconjugates

* indicates differential detection on Low PROT tumor cells

#	Name	#	Name	#	Name	#	Name
1	LFA	25	rCGL2	49	rBC2LA	73	STL
2	WGA	26	PHAE	50	AOL	74	rGal3C
3	PVL	27	GSLII	51	AAL	75	rLSLN
4	MAL	28	rSRL	52	rAAL	76	rCGL3
5	MAH	29	UDA	53	rPAIIL	77	PNA
6	ACG	30	PWM	54	rRSIIL	78	ACA
7	rACG	31	rF17AG	55	rPTL	79	HEA
8	rGal8N	32	rGRFT*	56	PSA	80	ABA
9	SNA	33	NPA	57	LCA	81	Jacalin
10	SSA	34	ConA	58	rAOL	82	MPA
11	TJAI	35	GNA	59	rBC2LCN	83	HPA
12	rPSL1a	36	HHL	60	LTL	84	VVA
13	ADA	37	ASA	61	UEAI	85	DBA
14	PHAL	38	DBAI	62	TJAII	86	SBA
15	DSA	39	CCA	63	MCA	87	rPPL
16	TxLcI	40	Heltuba	64	FLAG-EW29Ch	88	rCNL
17	ECA	41	rHeltuba	65	PTLI	89	rXCL
18	RCA120	42	Ricinus communis	66	GSLIA4	90	VVAI
19	rGal7	43	VVAII	67	rGC2*	91	WFA
20	rGal9N	44	rOrysata	68	GSLIB4	92	rABA
21	rGal9C	45	rPALa	69	rMOA	93	rDiscoidin I
22	rC14	46	rBanana	70	EEL	94	DBAIII
23	rDiscoidin II	47	rCalsepa	71	rPAIL*	95	rMalectin
24	BPL	48	rRSL	72	LEL	96	CSA

MATERIALES AND METHODS

Experimental models and subject details

Mice

All animal experiments were performed according to the guidelines of the Institutional Animal Care and Use Committee and the regional ethics committee (approval references PEA-503). All experiments used age-matched five-week-old female littermates. WT syngeneic BALB/c were obtained from ENVIGO and housed in our animal facility (C3M-Nice, France).

Mice were fed isocaloric diets purchased from ENVIGO: Control (CTR: TD.130931) and Low Protein diet reduced in a 25% (Low PROT -25%: TD.130933). The caloric composition of these diets (% of energy provided by carbohydrate: protein: fat content) was the following: CTR - (70.9% : 19.5% : 9.6%) and Low PROT -25% - (73.7% : 14.9% : 11.5%). Mice were fed the specified diet for seven days prior to subcutaneous engraftment of tumor cells. Control diet from ENVIGO was designed to contain the same composition in term of energy and nutritional sources than the standard diet provided by the animal facility.

WT syngeneic BALB/c mice were subcutaneously engrafted with $0.75x10^6$ CT26 cells. After subcutaneous engraftment of CT26 cells, mice were inspected every two days for tumor development. Tumor growth was monitored by caliper measurement following the equation ($width^2$ x length)/2. Animals were sacrificed when at least a tumor reached 1000 mm^3 except for *in vivo* metabolomics and isotope tracing experiments in which mice were sacrificed 12 days post-subcutaneous injection of tumor cells.

Cell lines and cell culture conditions

CT26 cells were obtained from the ATCC (#CRL-2638) and cultured in RPMI-1640 medium (Gibco) supplemented with 10% fetal bovine serum (FBS), 1% penicillin-streptomycin (5000 U/mL) (Gibco) and 1% sodium pyruvate (Gibco). CT26 cells were mycoplasma free and were incubated at 37 ºC in a 5% CO^2 atmosphere.

Method details

In vivo stable isotope tracing

For steady-state metabolomics, blood was collected from the tail vein of tumor-bearing BALB/c mice prior to sacrifice and organ resection. Tumors and livers were harvested and immediately frozen in liquid nitrogen. For ^{13}C isotope tracing, blood was collected from the tail vein of tumor-bearing prior to administration of the tracer, immediately and 40 min after the first injection. [U-$^{13}C_6$]-Glucose (D-GLUCOSE (U-$^{13}C^6$, 99%), # CLM-1396, Cambridge Isotope Laboratories, Inc.) was administered to the mice via two consecutive intra-peritoneal discrete bolus injections (1 g/kg mouse weight in 200 µl

of sterile NaCl 0.9%) separated by a 20 min interval. After the second injection of the tracer, mice were immediately sacrificed by cervical dislocation. Tumors and livers were resected and frozen in liquid nitrogen. Plasma was isolated by centrifugation at 6000 x g for 2 min and frozen in liquid nitrogen. Animals had access to food during the experiments. All the collected samples were stored at -80°C for further LC-MS-based metabolomics analyses.

Targeted LC-MS metabolite analyses

For tissues, frozen samples were homogenized using a stainless-steel tissue grinder (1292, BioSpec Products) and 10 mg of tissue powder were used for metabolite extraction. For metabolomic analysis, the extraction solution for polar metabolites was composed of 50% methanol, 30% acetonitrile (ACN) and 20 % water. The volume of the extraction solution was adjusted to the cell number (1 mL per $1x10^6$ cells). Plasma was diluted 20 folds with the same extraction solution. After addition of the extraction solution, samples were vortexed for 5 min at 4 °C and centrifuged at 16000 x *g* for 15 min at 4 °C. The supernatants were collected and stored at -80 °C. LC-MS analyses were conducted on a QExactive Plus Orbitrap mass spectrometer equipped with an Ion Max source and a HESI II probe coupled to a Dionex UltiMate 3000 UPLC system (Thermo). External mass calibration was performed using a standard calibration mixture as recommended by the manufacturer. Samples were injected onto a ZIC-pHILIC column (150 mm × 2.1 mm; i.d. 5 µm) with a guard column (20 mm × 2.1 mm; i.d. 5 µm) (Millipore) for LC separation. For chromatographic separation, buffer A (20 mM ammonium carbonate, 0.1% ammonium hydroxide, pH 9.2) and buffer B (ACN) were used. The chromatographic gradient was run at a flow rate of 0.200 µl min^{-1} as follows: 0-20 min, linear gradient from 80% to 20% of buffer B; 20-20.5 min, linear gradient from 20% to80 % of buffer B; 20.5–28 min, 80% buffer B. The mass spectrometer was operated in full scan, polarity switching mode with the spray voltage set to 2.5 kV and the heated capillary held at 320 °C. The sheath gas flow was set to 20 units, the auxiliary gas flow to 5 units and the sweep gas flow to 0 units. The metabolites were detected across a mass range of 75-1,000 *m*/*z* at a resolution of 35000 (at 200 *m*/*z*) with the automatic gain control target at 10^6 and the maximum injection time at 250 ms. Lock masses were used to ensure mass accuracy below 5 ppm. Data acquisition and peak integration of metabolites and isopologues was performed with a Thermo Xcalibur software (Thermo). Metabolites were identified by the exact mass of each singly charged ion and by the known retention time on the HPLC column.

Quantitative Reverse Transcription-PCR (RT-qPCR) analysis

For analysis of only tumor cells from tumor-bearing mice, tumor were enzymatically digested with the Tumor Dissociation Kit for mouse (Miltenyi Biotec, #130-096-730) yielding a single cell suspension. Tumor cells were magnetically isolated using the Tumor Cell Isolation kit for mouse (Miltenyi Biotec, 130-110-187) following the manufacturers' instructions. In brief, dissociated tumors were incubated with a depletion cocktail for 15 min and after magnetic isolation using an AutoMACS Pro Separator

(Miltenyi Biotec), the tumor cell-containing fraction was frozen either as a dry pellet or in 10% DMSO-containing FBS. Cell pellets were lysed in tryzol prior to RNA extraction with chloroform. Reverse transcription was performed using the Omniscript RT Kit (Qiagen, #205113). Quantitative-PCR was performed with Power SYBR Green PCR master mix (Applied Biosystems, Life Technologies, # 4367659) using the Step One real-time PCR systems (Applied Biosystems) following the manufacturers' instructions.

The following primers for mouse sequences were used for SYBR Green qPCR:

Gene	Primer sequences (forward 5'-3' / reverse 5'-3')	Source
Gfpt1	TGGTGTGCGGAGTGAACATAA GTGTGCTCTATCACGGCACTT	This paper
Ogt	GACGCAACCAAACTTTGCAGT TCAAGGGTGACAGCCTTTTCA	This paper
Oga	AGCGAAGATGGCAGAGGAGT CCGTGCTCGTAAGGAAGGTA	This paper
Rplp0	AGATTCGGGATATGCTGTTGGC TCGGGTCCTAGACCAGTGTTC	This paper

The housekeeping gene Rplp0 was used as control for RNA quality and normalization. All analyses were performed in technical triplicates and melting curve analysis was performed to control product quality and specificity.

Western Blot Analysis

For whole tumors, pieces of tumor tissue were cut and mechanically disrupted in RIPA buffer containing protease inhibitors and PUGNAC (Sigma Aldrich, # A7229) using a Pre-cellys 24 tissue homogenizer (Bertin Instruments) (3 x 30 s, 6500 x *g*). Protein lyses were quantified and standardized (Pierce BCA protein assay kit, Thermo Scientific, #23225), immunoblots were developed using the Amersham ECL Prime Western Blotting Detection Reagent (Cytiva, #RPN2236) and visualized with ImageQuant LAS 4000 (GE Healthcare, Life Science). The following antibodies were used for immunoblotting:

Antibody	Source	Identifier
Mouse monoclonal anti-O-GlcNAc (CTD110.6)	Cell Signaling	9875; RRID:AB_10950973

N-glycan purification and structural analysis by glycomics

Magnetically isolated tumor cells were frozen as a dry pellet. Dry material was sequentially extracted three times by chloroform/methanol (2:1, v/v) and chloro- form/methanol (1:2, v/v). Pellets containing the glycoprotein fraction were suspended in Tris/HCl and centrifuged at low speed. Supernatant was precipitated with 70% cold ethanol overnight and centrifuged at 1200 × g. Total glycoprotein fraction was resuspended in a solution of 6 M guanidinium chloride and 5 mM EDTA in 0.1 M Tris/HCl, pH 8, and agitated for 4 h at 4 °C. Dithiothreitol was then added to a final concentration of 20 mM and

incubated for 5 h at 37 °C, followed by addition of iodoacetamide to a final concentration of 50 mM and further incubated overnight in the dark at room temperature. Reduced/alkylated sample was dialyzed against water at 4 °C for 3 days and lyophilized. The recovered protein samples were then sequentially digested by TPCK-treated trypsin for 5 h and chymotrypsin overnight at 37 °C, in 50 mM ammonium bicarbonate buffer, pH 8.4. Crude peptide fraction was separated from hydrophilic components on a C18 Sep-Pak cartridge (Waters) equilibrated in 5% acetic acid by extensive washing in the same solvent and eluted with a step gradient of 20%, 40%, and 60% propanol in 5% acetic acid. Pooled propanol fraction was dried and subjected to Peptide-N-glycosidase F (Roche) digestion in 50 mM ammonium bicarbonate buffer pH 8.4, overnight at 37 °C. The released N- glycans were separated from peptides using the same C18 Sep-Pak procedure as described above.

Following their purification, N-linked glycans were permethylated using the NaOH/dimethyl sulfoxide reagent (Ciucanu and Kerek, 1984). The per- methylated derivatives were then extracted in chloroform and repeatedly washed with water. MALDI-QIT-TOF spectra were acquired on 4800 Proteomics Analyzer mass spectrometer (Applied Biosystems, Framingham, MA, USA) in reflecton positive or negative mode by delayed extraction using an acceleration mode of 20 kV, a pulse delay of 200 ns and grid voltage of 66%. Samples were prepared by mixing directly on the target 1 μL of oligosaccharide solution (1–5 pmol) with 1 μL of 2,5 dihydroxybenzoic acid matrix solution (10 mg/mL in CH_3OH/H_2O, 50/50, vol/vol). Between 50 and 100 scans were averaged for every spectrum. Glycosylated structures were deduced based on the m/z peak in the spectrum.

For comparison between CTR and Low PROT groups, all glycans were relatively quantified as percentages of all identified glycan within each sample by integrating corresponding MALDI-MS signals from three technical replicates (Aoki et al., 2007), (Yamakawa et al., 2018).

Lectin microarray

The surface glycome of isolated tumor cells was profiled by a lectin microarray containing a panel of 96 immobilized lectins (Table 2). To analyse multiple glycan structures, plasma membrane proteins were labeled with Cy3 and the same protein was hybridized to the lectin microarray. The resulting chips were scanned for fluorescence intensity on each lectin-coated spot using an evanescent-field fluorescence scanner GlycoStation Reader (GlycoTechnica Ltd.). Data were normalized using the global normalization method.

Table 2. Lectin, species, origin and glycan-binding specificities of the 96 lectin microarray.

Name	Species	Origin	Specificity[1,2]
LFA	*Limax flavus*	Natural	Sia
WGA	Triticum vulgaris	Natural	(GlcNAc)n, polySia
PVL	*Psathyrella velutina*	Natural	Sia, GlcNAc
MAL	Maackia amurensis	Natural	α2-3Sia
MAH	Maackia amurensis	Natural	α2-3Sia
ACG	Agrocybe cylindracea	Natural	α2-3Sia

Name	Species	Origin	Specificity[1,2]
rACG	*Agrocybe cylindracea*	Recombinant	α2-3Sia
rGal8N	*Homo sapiens*	Recombinant	α2-3Sia
SNA	Sambucus nigra	Natural	α2-6Sia
SSA	Sambucus sieboldiana	Natural	α2-6Sia
TJAI	Trichosanthes japonica	Natural	α2-6Sia
rPSL1a	*Polyporus squamosus*	*E.coli*	α2-6Sia
ADA	*Allomyrina dichtoma*	Natural	α2-6Sia, Forssman, A, B
PHAL	Phaseolus vulgaris	Natural	GlcNAcβ1-6Man (Tetraantenna)
DSA	Datura stramonium	Natural	GlcNAcβ1-6Man (Tetraantenna)
TxLcI	Tulipa gesneriana	Natural	Mannose/GalNac
ECA	Erythrina cristagalli	Natural	βGal
RCA120	Ricinus communis	Natural	βGal
rGal7	*Homo sapiens*	Recombinant	Type1 LacNAc, chondroitin polymer
rGal9N	*Homo sapiens*	Recombinant	GalNAcα1-4Gal (A), PolyLacNAc
rGal9C	*Homo sapiens*	Recombinant	PolyLacNAc, Branched LacNAc
rC14	*Gallus gallus domesticus*	Recombinant	Branched LacNAc
rDiscoidin II	*Dictyostelium dicodeum*	Recombinant	LacNAc, Galβ1-3GalNAc (T), GalNAc (Tn)
BPL	Bauhinia purpurea alba	Natural	Galβ1-3GlcNAc(GalNAc), α/βGalNAc
rCGL2	*Homo sapiens*	Recombinant	GalNAcα1-3Gal (A), PolyLacNAc
PHAE	Phaseolus vulgaris	Natural	bisecting GlcNAc
GSLII	Griffonia simplicifolia	Natural	GlcNAcβ1-4Man
rSRL	*Sclerotium rolfsii*	Recombinant	Core1,3, agalacto N-glycan
UDA	Urtica dioica	Natural	(GlcNAc)n
PWM	Phytolacca americana	Natural	(GlcNAc)n
rF17AG	*Escherichia coli*	Natural	GlcNAc
rGRFT*	*Griffithia sp.*	Recombinant	Man
NPA	Narcissus pseudonarcissus	Natural	Manα1-3Man
ConA	Canavalia ensiformis	Natural	M3, Manα1-2Manα1-3(Manα1-6)Man, GlcNAcβ1-2Manα1-3(Manα1-6)Man
GNA	Galanthus nivalis	Natural	Manα1-3Man, Manα1-6Man
HHL	Hippeastrum hybrid	Natural	Manα1-3Man, Manα1-6Man
ASA	*Allium sativum*	Natural	Galβ1-4GlcNAcβ1-2Man
DBAI	*Dioscorea batatas*	Natural	High-man
CCA	*Castanea crenata*	Natural	Galactosylated N-glycans up to triantenna
Heltuba	*Helianthus t uberosus*	Natural	Manα1-3Man
rHeltuba	*Helianthus tuberosus*	Recombinant	Manα1-3Man
VVAII	*Vicia villosa*	Natural	Man, Agalacto
rOrysata	*Oryza sativa*	Recombinant	Manα1-3Man, High man, biantenna
rPALa	*Phlebodium aureum*	Recombinant	Man5, biantenna
rBanana	*Musa acuminata*	Recombinant	Manα1-2Manα1-3(6)Man
rCalsepa	Calystegia sepium	Recombinant	Biantenna with bisecting GlcNAc
rRSL	*Ralstonia solanacearum*	Recombinant	αMan, α1-2Fuc (H), α1-3Fuc (Le^x), α1-4Fuc (Le^a)
rBC2LA	*Burkholderia cenocepacia*	Recombinant	αMan, High-man
AOL	Aspergillus oryzae	Recombinant	α1-2Fuc (H), α1-3Fuc (Le^x), α1-3Fuc (Le^a)
AAL	Aleuria aurantia	Natural	α1-6Fuc (Core), α1-2Fuc (H), α1-3Fuc (Le^x), α1-3Fuc (Le^a)
rAAL	*Aleuria aurantia*	Recombinant	α1-2Fuc (H), α1-3Fuc (Le^x), α1-3Fuc (Le^a)
rPAIIL	*Pseudomonas aeruginosa*	Recombinant	αMan, α1-2Fuc (H), α1-3Fuc (Le^x), α1-4Fuc (Le^a)
rRSIIL	*Ralstonia solanacearum*	Recombinant	α1-2Fuc (H), α1-3Fuc (Le^x), α1-3Fuc (Le^a)
rPTL	*Pholiota terrestris*	Recombinant	α1-6Fuc

Name	Species	Origin	Specificity[1,2]
PSA	Pisum sativum	Natural	α1-6Fuc up to biantenna
LCA	Lens culinaris	Natural	α1-6Fuc up to biantenna
rAOL	*Aspergillus oryzae*	Recombinant	α1-6Fuc (Core), α1-2Fuc (H), α1-3Fuc (Le^x), α1-3Fuc (Le^a)
rBC2LCN	*Burkholderia cenocepacia*	Recombinant	Fuc α1-2Galβ1-3GlcNAc (GalNAc)
LTL	Lotus tetragonolobus	Natural	Fuc (Le^x,Le^y)
UEAI	Ulex europaeus	Natural	α1-2Fuc
TJAII	Trichosanthes japonica	Natural	α1-2Fuc
MCA	*Momordica charantia*	Natural	α1-2Fuc
FLAG-EW29Ch	Earthworth	Recombinant	6-sulfo-galactose
PTLI	Psophocarpus tetragonolobus	Natural	αGalNAc (A, Tn)
GSLIA4	Griffonia simplicifolia	Natural	αGalNAc (A, Tn)
rGC2*	*Geodia cydonium*	Recombinant	α1-2Fuc (H), αGalNAc (A), αGal (B)
GSLIB4	Griffonia simplicifolia	Natural	αGal (B)
rMOA	*Marasmius oreades*	Recombinant	αGal (B)
EEL	Euonymus europaeus	Natural	αGal (B)
rPAIL*	*Pseudomonas aeruginosa*	Recombinant	α,βGal, αGalNAc (Tn)
LEL	Lycopersicon esculentum	Natural	Polylactosamine, (GlcNAc)n
STL	Solanum tuberosum	Natural	Polylactosamine, (GlcNAc)n
rGal3C	*Homo sapiens*	Recombinant	LacNAc, polylactosamine
rLSLN	*Laetiporus sulphureus*	Recombinant	LacNAc, polylactosamine
rCGL3	*Coprinopsis cinerea*	Recombinant	LacDiNAc
PNA	Arachis hypogaea	Natural	Galβ1-3GalNAc (T)
ACA	Amaranthus caudatus	Natural	Galβ1-3GalNAc (T)
HEA	*Hericium erinaceum*	Natural	Galβ1-3GalNAc (T)
ABA	Agarics bisporus	Natural	Galβ1-3GalNAc (T), GlcNAc
Jacalin	Artocarpus integrifolia	Natural	Galβ1-3GalNAc (T), GalNAcα (Tn)
MPA	Maclura pomifera	Natural	Galβ1-3GalNAc (T), GalNAcα (Tn)
HPA	Helix pomatia	Natural	αGalNAc (A, Tn)
VVA	Vicia villosa	Natural	α,βGalNAc (A, Tn, LacDiNAc)
DBA	Dolichos biflorus	Natural	α,βGalNAc (A, Tn, LacDiNAc)
SBA	*Glycine max*	Natural	α,β GalNAc (A, Tn, LacDiNAc)
rPPL	*Pleurocybella porrigens*	Recombinant	α,β GalNAc (A, Tn, LacDiNAc)
rCNL	*Clitocybe nebularis*	Recombinant	α,β GalNAc (A, Tn, LacDiNAc)
rXCL	*Xerocomus chrysenteron*	Recombinant	Core1,3, agalacto N-glycan
VVAI	*Vicia villosa*	Natural	GalNAc β 1-3(4)Gal
WFA	Wisteria floribunda	Natural	Terminal GalNAc, LacDiNAc
rABA	*Agarics bisporus*	Recombinant	Gal β 1-3GalNAc (T), GlcNAc
rDiscoidin I	*Dictyostelium Discodeum*	Recombinant	Gal
DBAIII	*Dioscorea batatas*	Natural	Maltose
rMalectin	*Homo sapiens*	Recombinant	Glcα1-2Glc
CSA	*Oncorhynchus keta*	Natural	Rhamnose, Galα1-4Gal

[1]Abbreviations: Gal (D-galactose), GalNAc (N-acetyl-galactosamine), GlcNAc (*N*-acetylglucosamine), Fuc (L-fucose), Glc (D-glucose), Sia (Sialic acid), LacNAc (N-acetyl-lactosamine). Between brakers, T (antigen T), Tn (antigen Tn), Le (Lewis antigen), Le^a (Lewis antigen A), Le^b (Lewis antigen B), Le^x (Lewis antigen X), Le^y (Lewis antigen Y), A (Antigen A), B (Antigen B), H (Antigen H)

[2]Specificity data were obtained by frontal affinity chromatography and glycoconjugate microarray

Quantification and statistical analysis

Principal Component Analysis (PCA) and heatmap plots of steady state levels of 148 metabolites were performed with Metaboanalyst 5.0. Briefly, no data filtering and normalization of the data by auto-scaling were applied. The clustering was performed based on the abundance of tumoral metabolites. PCA plots show the 95 % confidence regions of each group. Data was not corrected for the presence of the naturally occurring ^{13}C stable isotopes.

Graphs and statistical tests were generated using Prism v.8 (GraphPad software, Inc.). Differences in calculated means between groups were assessed by two-tailed, unpaired Student's t tests. A p-value lower than 0.05 was considered significant.

REFERENCES

Akella, N.M., Ciraku, L., Reginato, M.J., 2019. Fueling the fire: emerging role of the hexosamine biosynthetic pathway in cancer. BMC Biology 17, 52. https://doi.org/10.1186/s12915-019-0671-3

Aoki, K., Perlman, M., Lim, J.-M., Cantu, R., Wells, L., Tiemeyer, M., 2007. Dynamic developmental elaboration of N-linked glycan complexity in the Drosophila melanogaster embryo. J Biol Chem 282, 9127–9142. https://doi.org/10.1074/jbc.M606711200

Arnold, J.M., Gu, F., Ambati, C.R., Rasaily, U., Ramirez-Pena, E., Joseph, R., Manikkam, M., San Martin, R., Charles, C., Pan, Y., Chatterjee, S.S., Den Hollander, P., Zhang, W., Nagi, C., Sikora, A.G., Rowley, D., Putluri, N., Zhang, X.H.-F., Karanam, B., Mani, S.A., Sreekumar, A., 2020. UDP-glucose 6-dehydrogenase regulates hyaluronic acid production and promotes breast cancer progression. Oncogene 39, 3089–3101. https://doi.org/10.1038/s41388-019-0885-4

Biwi, J., Biot, C., Guerardel, Y., Vercoutter-Edouart, A.-S., Lefebvre, T., 2018. The Many Ways by Which O-GlcNAcylation May Orchestrate the Diversity of Complex Glycosylations. Molecules 23, E2858. https://doi.org/10.3390/molecules23112858

Chandler, K.B., Costello, C.E., Rahimi, N., 2019. Glycosylation in the Tumor Microenvironment: Implications for Tumor Angiogenesis and Metastasis. Cells 8. https://doi.org/10.3390/cells8060544

Chokchaitaweesuk, C., Kobayashi, T., Izumikawa, T., Itano, N., 2019. Enhanced hexosamine metabolism drives metabolic and signaling networks involving hyaluronan production and O-GlcNAcylation to exacerbate breast cancer. Cell Death Dis 10, 1–15. https://doi.org/10.1038/s41419-019-2034-y

Ciucanu, I., Kerek, F., 1984. A simple and rapid method for the permethylation of carbohydrates. Carbohydrate Research 131, 209–217. https://doi.org/10.1016/0008-6215(84)85242-8

Ghasempour, S., Freeman, S.A., 2021. The glycocalyx and immune evasion in cancer. FEBS J. https://doi.org/10.1111/febs.16236

Haltiwanger, R.S., Blomberg, M.A., Hart, G.W., 1992. Glycosylation of nuclear and cytoplasmic proteins. Purification and characterization of a uridine diphospho-N-acetylglucosamine:polypeptide beta-N-acetylglucosaminyltransferase. J Biol Chem 267, 9005–9013.

Jang, C., Chen, L., Rabinowitz, J.D., 2018. Metabolomics and Isotope Tracing. Cell 173, 822–837. https://doi.org/10.1016/j.cell.2018.03.055

Kanarek, N., Petrova, B., Sabatini, D.M., 2020. Dietary modifications for enhanced cancer therapy. Nature 579, 507–517. https://doi.org/10.1038/s41586-020-2124-0

Kim, Jiyeon, Lee, H.M., Cai, F., Ko, B., Yang, C., Lieu, E.L., Muhammad, N., Rhyne, S., Li, K., Haloul, M., Gu, W., Faubert, B., Kaushik, A.K., Cai, L., Kasiri, S., Marriam, U., Nham, K., Girard, L., Wang, H., Sun, X., Kim, James, Minna, J.D., Unsal-Kacmaz, K., DeBerardinis, R.J., 2020. The hexosamine biosynthesis pathway is a targetable liability in KRAS/LKB1 mutant lung cancer. Nat Metab 2, 1401–1412. https://doi.org/10.1038/s42255-020-00316-0

Lee, J.B., Pyo, K.-H., Kim, H.R., 2021. Role and Function of O-GlcNAcylation in Cancer. Cancers (Basel) 13, 5365. https://doi.org/10.3390/cancers13215365

Li, C.-W., Lim, S.-O., Xia, W., Lee, H.-H., Chan, L.-C., Kuo, C.-W., Khoo, K.-H., Chang, S.-S., Cha, J.-H., Kim, T., Hsu, J.L., Wu, Y., Hsu, J.-M., Yamaguchi, H., Ding, Q., Wang, Y., Yao, J., Lee, C.-C., Wu, H.-J., Sahin, A.A., Allison, J.P., Yu, D., Hortobagyi, G.N., Hung, M.-C., 2016. Glycosylation and stabilization of programmed death ligand-1 suppresses T-cell activity. Nat Commun 7, 12632. https://doi.org/10.1038/ncomms12632

Liu, Y., Cao, Y., Pan, X., Shi, M., Wu, Q., Huang, T., Jiang, H., Li, W., Zhang, J., 2018. O-GlcNAc elevation through activation of the hexosamine biosynthetic pathway enhances cancer cell chemoresistance. Cell Death Dis 9, 1–12. https://doi.org/10.1038/s41419-018-0522-0

Marshall, S., Bacote, V., Traxinger, R.R., 1991. Discovery of a metabolic pathway mediating glucose-induced desensitization of the glucose transport system. Role of hexosamine biosynthesis in the induction of insulin resistance. J Biol Chem 266, 4706–4712.

Ong, Q., Han, W., Yang, X., 2018. O-GlcNAc as an Integrator of Signaling Pathways. Front Endocrinol (Lausanne) 9. https://doi.org/10.3389/fendo.2018.00599

Phoomak, C., Silsirivanit, A., Park, D., Sawanyawisuth, K., Vaeteewoottacharn, K., Wongkham, C., Lam, E.W.-F., Pairojkul, C., Lebrilla, C.B., Wongkham, S., 2018. O-GlcNAcylation mediates metastasis of cholangiocarcinoma through FOXO3 and MAN1A1. Oncogene 37, 5648–5665. https://doi.org/10.1038/s41388-018-0366-1

Pinho, S.S., Reis, C.A., 2015. Glycosylation in cancer: mechanisms and clinical implications. Nat Rev Cancer 15, 540–555. https://doi.org/10.1038/nrc3982

Qian, K., Wang, S., Fu, M., Zhou, J., Singh, J.P., Li, M.-D., Yang, Y., Zhang, K., Wu, J., Nie, Y., Ruan, H.-B., Yang, X., 2018. Transcriptional regulation of O-GlcNAc homeostasis is disrupted in pancreatic cancer. J Biol Chem 293, 13989–14000. https://doi.org/10.1074/jbc.RA118.004709

Reily, C., Stewart, T.J., Renfrow, M.B., Novak, J., 2019. Glycosylation in health and disease. Nat Rev Nephrol 15, 346–366. https://doi.org/10.1038/s41581-019-0129-4

Rubio-Patiño, C., Bossowski, J.P., De Donatis, G.M., Mondragón, L., Villa, E., Aira, L.E., Chiche, J., Mhaidly, R., Lebeaupin, C., Marchetti, S., Voutetakis, K., Chatziioannou, A., Castelli, F.A., Lamourette, P., Chu-Van, E., Fenaille, F., Avril, T., Passeron, T., Patterson, J.B., Verhoeyen, E., Bailly-Maitre, B., Chevet, E., Ricci, J.-E., 2018. Low-Protein Diet Induces IRE1α-Dependent Anticancer Immunosurveillance. Cell Metab. 27, 828-842.e7. https://doi.org/10.1016/j.cmet.2018.02.009

Rudd, P.M., Elliott, T., Cresswell, P., Wilson, I.A., Dwek, R.A., 2001. Glycosylation and the immune system. Science 291, 2370–2376. https://doi.org/10.1126/science.291.5512.2370

Song, X., Zhou, Z., Li, H., Xue, Y., Lu, X., Bahar, I., Kepp, O., Hung, M.-C., Kroemer, G., Wan, Y., 2020. Pharmacologic Suppression of B7-H4 Glycosylation Restores Antitumor Immunity in Immune-Cold Breast Cancers. Cancer Discov 10, 1872–1893. https://doi.org/10.1158/2159-8290.CD-20-0402

Tajan, M., Vousden, K.H., 2020. Dietary Approaches to Cancer Therapy. Cancer Cell. https://doi.org/10.1016/j.ccell.2020.04.005

Wang, Z.V., Deng, Y., Gao, N., Pedrozo, Z., Li, D.L., Morales, C.R., Criollo, A., Luo, X., Tan, W., Jiang, N., Lehrman, M.A., Rothermel, B.A., Lee, A.-H., Lavandero, S., Mammen, P.P.A., Ferdous, A., Gillette, T.G., Scherer, P.E., Hill, J.A., 2014. Spliced X-Box Binding Protein 1 Couples the Unfolded Protein Response to Hexosamine Biosynthetic Pathway. Cell 156, 1179–1192. https://doi.org/10.1016/j.cell.2014.01.014

Yamakawa, N., Vanbeselaere, J., Chang, L.-Y., Yu, S.-Y., Ducrocq, L., Harduin-Lepers, A., Kurata, J., Aoki-Kinoshita, K.F., Sato, C., Khoo, K.-H., Kitajima, K., Guerardel, Y., 2018. Systems glycomics of adult zebrafish identifies organ-specific sialylation and glycosylation patterns. Nat Commun 9, 4647. https://doi.org/10.1038/s41467-018-06950-3

Yang, X., Qian, K., 2017. Protein O-GlcNAcylation: emerging mechanisms and functions. Nat Rev Mol Cell Biol 18, 452–465. https://doi.org/10.1038/nrm.2017.22

FIGURE LEGENDS

Figure 1. UDP-HexNAc and UDP-Hex are more abundant in tumors of mice fed a Low PROT diet.

A. Protocol for *in vivo* steady state and [U-$^{13}C_6$]-Glucose tracing-based metabolomics in immunocompetent mice bearing syngeneic CT26 colorectal carcinoma subcutaneous tumors. **B.** Principal Component Analysis (PCA) plot of steady state metabolites of CTR (n=4) and Low PROT (n=4) tumor-bearing mice. The clustering was performed based on the levels of 148 metabolites quantified by HPLC-MS. **C.** Heatmap of the 25 most discriminant metabolites at steady state between CTR (n=4) and low PROT tumors (n=4). **D.** Steady state levels of UDP-HexNAc and UDP-Hex in whole tumors and livers. **E.** Scheme of the metabolic reactions for *de novo* synthesis of UDP-GlcNAc from [U-$^{13}C_6$]-Glucose by the HBP and the salvage pathway. Reaction for *de novo* synthesis of UDP-Glc from [U-$^{13}C_6$]-Glucose. **F.** Tumoral levels of UDP-HexNAc M+6 and UDP-Hex M+6 (CTR, n=5; Low PROT, n=5) upon [U-$^{13}C_6$]-Glucose. PCA and heatmap plots were generated with Metabolanalyst 5.0. Bars represent mean ± SD and each data point represents biological replicates. Statistical differences were determined by two-tailed, unpaired Student's t-test. GFPT1, glutamine-fructose-6-phosphate aminotransferase; GNPNAT1, glucosamine-phosphate N-acetyltransferase 1; NAGK, N-acetylglucosamine kinase; GlcNAc, N-acetylglucosamine; PGM3, phosphoglucomutase 3; UAP1, UDP-N-acetylhexosamine pyrophosphorylase; UDP-GlcNAc, uridine diphosphate N-acetylglucosamine; HK, hexokinase; PGM, phosphoglucomutase; UGP, UTP pyrophosphorylase, UDP-Glc, uridine diphosphate glucose.

Figure 2. OGT and OGA are transcriptionally downregulated and levels of glycosylated structures are perturbed in tumor cells isolated from Low PROT diet-fed mice.

A. Scheme representing the control of OGT and OGA on the cytoplasmic levels UDP-GlcNAc. UDP-HexNAc and UDP-Hex interconversion and their input to protein glycosylation occurring in the endoplasmic reticulum and Golgi apparatus. **B. C. D.** transcript levels of GFPT1, OGT and OGA in isolated tumor cells from mice fed a CTR (n=5) or Low PROT (n=5) diet. **E.** Levels of O-GlcNAcylated proteins in whole tumors of mice fed a a CTR (n=4) or Low PROT (n=4) diet. **F.** N-glycan profile of isolated tumor cells from CT26-tumor bearing mice fed a CTR (n=4) or Low PROT (n=4) diet as detected by glycomics. **G.** Relative enrichment of bi-antenna and complex sialylated N-glycan structures in isolated tumor cells from tumor-bearing mice were measured by glycomics. **H.** Levels of lectin binding to the glycocalyx of isolated tumor cells from mice fed a CTR (n=3) or Low PROT (n=3) diet measured by a lectin microarray. Bars represent mean ± SD and each data point represents biological replicates. Statistical differences were determined by two-tailed, unpaired Student's t-test.

SUPPLEMENTARY FIGURE LEGEND

Figure S1. Tumoral total levels, isotopologue contribution and isotopologue levels of UDP-sugars in tumors and livers upon [U-$^{13}C_6$]-Glucose. Steady-state levels of nucleotide sugars, GlcNAc and glucosamine in tumor-bearing mice fed a Low PROT diet.

A. MHC-I surface expression (MFI) on tumor cells and $CD8^+$ TILs (%) in CT26 tumor-bearing Balb/c mice were measured by flow cytometry at day 11 post-subcutaneous engraftment. **B.** Fractional enrichment of [U-$^{13}C_6$]-Glucose in plasma, tumors and livers of tumor-bearing mice fed a CTR (n=5) or Low PROT (n=5) diet. **C.** Isotopologue contribution to UDP-HexNAc total levels in whole tumors and livers and levels of UDP-HexNAc M+6 in livers upon [U-$^{13}C_6$]-Glucose tracing. **D.** Isotopologue contribution to UDP-Hex total levels in whole tumors and livers and levels of UDP-Hex M+6 in livers upon [U-$^{13}C_6$]-Glucose tracing. p values in isotopologue enrichment plot represent statistical difference of total levels of the metabolite. **E. F.** Tumoral steady state levels of GDP-Man and CMP-Neu5Ac in tumors. **G.** Tumoral steady-state levels of GlcNAc. **H.** Tumoral steady-state levels of glucosamine. Bars represent mean ± SD and each data point represents biological replicates. Statistical differences were determined by two-tailed, unpaired Student's t-test.

FIGURE 1

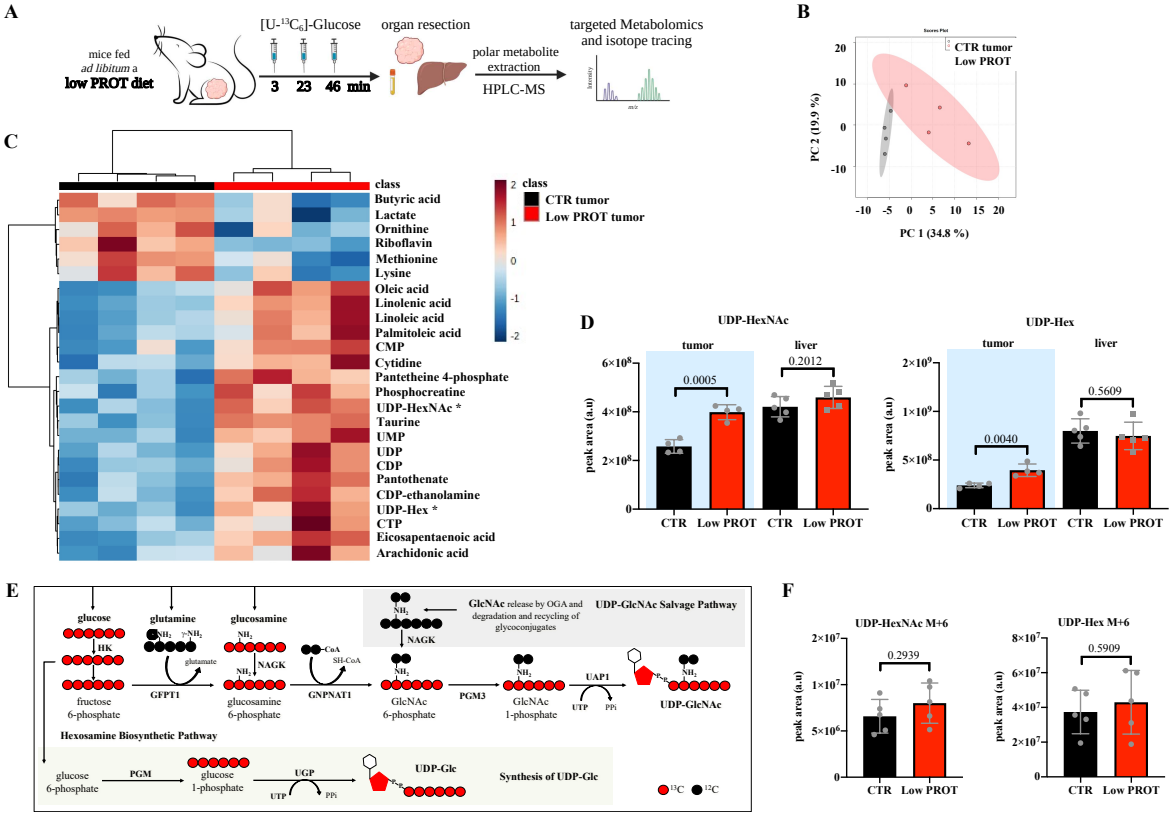
A
mice fed
ad libitum a
low PROT diet
[U-13C6]-Glucose
3 23 46 min
organ resection
polar metabolite
extraction
HPLC-MS
targeted Metabolomics
and isotope tracing
B
CTR tumor
Low PROT
PC 2 (19.9 %)
PC 1 (34.8 %)
C
class
CTR tumor
Low PROT tumor
Butyric acid
Lactate
Ornithine
Riboflavin
Methionine
Lysine
Oleic acid
Linolenic acid
Linoleic acid
Palmitoleic acid
CMP
Cytidine
Pantetheine 4-phosphate
Phosphocreatine
UDP-HexNAc *
Taurine
UMP
UDP
CDP
Pantothenate
CDP-ethanolamine
UDP-Hex *
CTP
Eicosapentaenoic acid
Arachidonic acid
D
UDP-HexNAc
UDP-Hex
tumor
liver
peak area (a.u)
0.0005
0.2012
0.0040
0.5609
CTR
Low PROT
E
glucose
glutamine
glucosamine
HK
GFPT1
NAGK
GNPNAT1
PGM3
UAP1
UTP
fructose
6-phosphate
glucosamine
6-phosphate
GlcNAc
6-phosphate
GlcNAc
1-phosphate
UDP-GlcNAc
GlcNAc release by OGA and
degradation and recycling of
glycoconjugates
UDP-GlcNAc Salvage Pathway
Hexosamine Biosynthetic Pathway
glucose
6-phosphate
PGM
glucose
1-phosphate
UGP
UDP-Glc
Synthesis of UDP-Glc
F
UDP-HexNAc M+6
UDP-Hex M+6
0.2939
0.5909

FIGURE 2

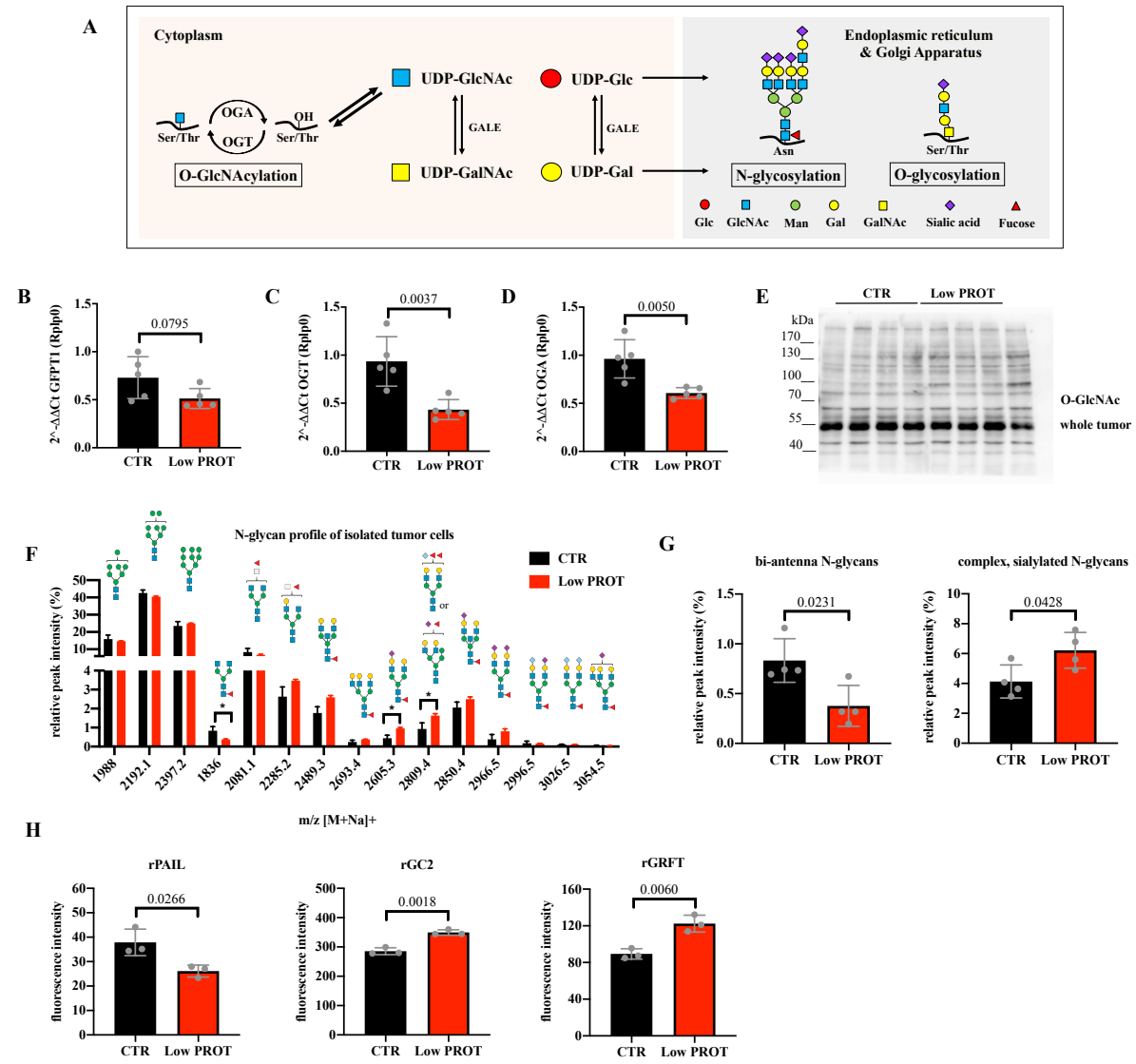
A
Cytoplasm
Endoplasmic reticulum & Golgi Apparatus
UDP-GlcNAc
UDP-Glc
UDP-GalNAc
UDP-Gal
GALE
GALE
OGA
OGT
OH
Ser/Thr
Ser/Thr
O-GlcNAcylation
Asn
N-glycosylation
Ser/Thr
O-glycosylation
Glc
GlcNAc
Man
Gal
GalNAc
Sialic acid
Fucose
B
2^-ΔΔCt GFPT1 (Rplp0)
0.0795
CTR
Low PROT
C
2^-ΔΔCt OGT (Rplp0)
0.0037
CTR
Low PROT
D
2^-ΔΔCt OGA (Rplp0)
0.0050
CTR
Low PROT
E
CTR
Low PROT
kDa
170
130
100
70
55
40
O-GlcNAc
whole tumor
F
N-glycan profile of isolated tumor cells
CTR
Low PROT
relative peak intensity (%)
1988
2192.1
2397.2
1836
2081.1
2285.2
2489.3
2693.4
2605.3
2809.4
2850.4
2966.5
2996.5
3026.5
3054.5
m/z [M+Na]+
G
bi-antenna N-glycans
0.0231
relative peak intensity (%)
CTR
Low PROT
complex, sialylated N-glycans
0.0428
relative peak intensity (%)
CTR
Low PROT
H
rPAIL
0.0266
fluorescence intensity
CTR
Low PROT
rGC2
0.0018
fluorescence intensity
CTR
Low PROT
rGRFT
0.0060
fluorescence intensity
CTR
Low PROT

SUPPLEMENTARY FIGURE 1

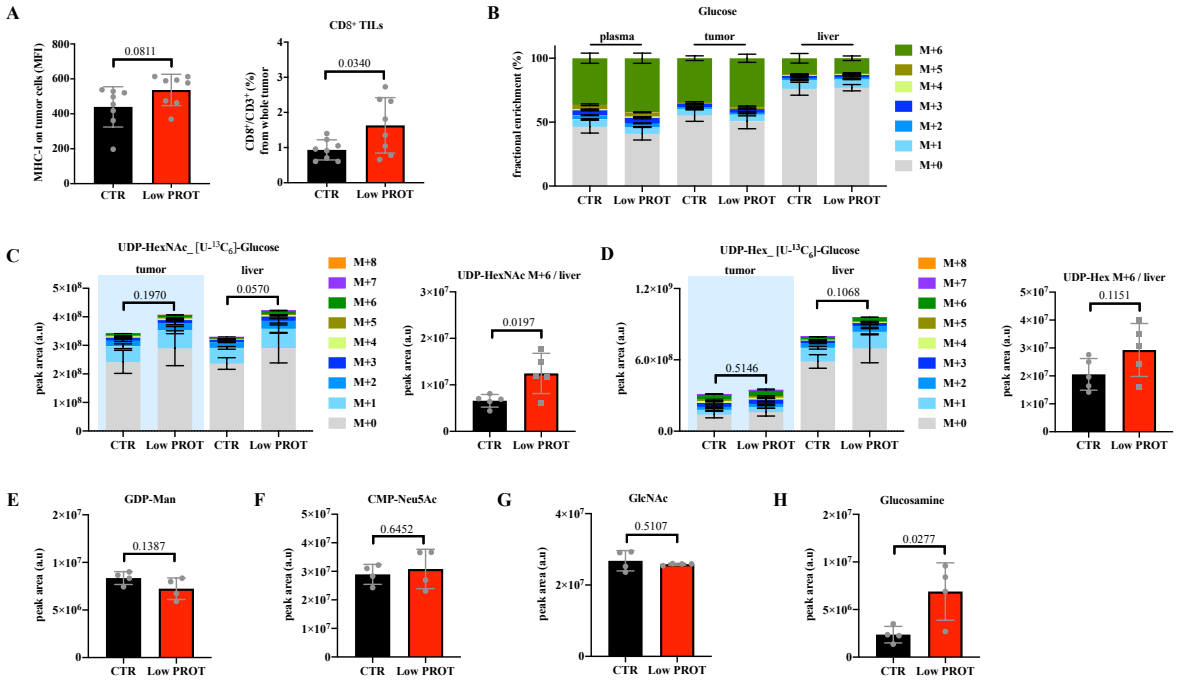

DISCUSSION AND PERSPECTIVES

IRE1α bifunctionality in cancer has been reported in several solid and liquid tumors. Most of the roles of the IRE1α signaling have been described as tumor-promoting not only for tumor expansion but for TME remodeling, angiogenesis, epithelial-to-mesenchymal transition, metastasis and anti-cancer drug resistance. We have previously shown that the tumor-suppressive effects of a Low PROT diet was dependent on the IRE1α pathway (Rubio-Patiño et al., 2018b). In agreement with these findings, we have recently found that exogenous expression of IRE1α in tumor cells limited tumor growth in immunocompetent mouse models of colorectal and lung carcinomas (**Article 1, Figure 3**).

Noteworthy, the anti-tumoral phenotype observed upon exogenous expression of IRE1α is limited to subcutaneous tumor models in our study. To confirm whether the tumor-suppressive effects associated with IRE1α overexpression in malignant cells occur irrespective of the tumor model, tumors growing in the tissue of origin should be monitored. Overexpression of IRE1α either in tumors orthotopically implanted or in transgenic mice spontaneously developing tumors with inducible IRE1α expression in malignant cells are alternatives that could be tested. Subcutaneous tumors that share the same location beyond their type and genetics might resemble more to each other than to orthotopically growing tumors. Subcutaneous implanted tumors of different types of cancer share similar TMEs and largely differ from the parental TME of orthotopic tumors (Kim et al., 2021), (Cai et al., 2022).

IRE1α overexpression in tumor cells led to self-activation of its full RNAse activity (**Article 1, Figure 2**). XBP1 splicing as well as RIDD induction were shown to be enhanced in IRE1α-overexpressing cells. Despite no alteration in the proliferation rate of *in vitro* cultured IRE1α-overexpressing cells (**Article 1, Figure 2**), these cells displayed a disadvantage while growing *in vivo*. Apart from a higher anti-cancer immunosurveillance based on higher intra-tumoral levels of CTLs, NK cells and resident TMAs (Pathria et al., 2019) (**Article 1, Figure 3**), tumor cells undergoing apoptosis were detected in IRE1α-overexpressing tumors in immunocompetent as well as immunodeficient mice (**Article 1, Figure 3 and Figure 4**). As compared to the tumor-suppressive effects of a Low PROT diet (Rubio-Patiño et al., 2018b) (**Article 1, Figure 1**), IRE1α overexpression limited tumor growth partially dependent on cytotoxic T cells and with not induction of cytokines and chemokines in tumor cells. Therefore, different molecular mechanisms underlie the anti-tumoral effects of the Low PROT diet and IRE1α exogenous expression in malignant cells.

One of the factors that may contribute to the different anti-tumoral phenotypes driven by the Low PROT diet and the exogenous expression of IRE1α is the levels of induction of RIDD in the two tumor models. To prove that induction of apoptosis in IRE1α-overexpressing cells

growing *in vivo* is mediated by RIDD induction, exogenous expression of an IRE1α RNAse domain mutant (N906A or K907A) and a kinase mutant (I642G) that can be activated with 1NM-PP1 could be performed in CT26 cells. The IRE1α kinase mutant (I642G) is inducible by binding to 1NM-PP1, a cell-permeable adenosine nucleotide that functions as an allosteric activator of the kinase domain. The IRE1α mutant (I642G) auto-transphosphorylates and splices XBP1 but is unable to induce RIDD (Han et al., 2009). Whether *in vivo* apoptosis is induced in WT IRE1α-overexpressing cells by RIDD induction, exogenous expression of the two IRE1α mutants in CT26 cells is not expected to limit tumor growth upon tumor cell engraftment into immunocompetent mice. However, exogenous expression of the IRE1α kinase mutant (I642G) and activation upon supplementation with 1NM-PP1 may have an unexpected tumor phenotype when implanted into mice since the capacity to splice XBP1 would be retained in these genetically engineered tumor cells. We have not tried only induction of XBP1s in CT26 cells prior to tumor implantation into mice. The tumor phenotypes driven by exogenous expression of WT and the two IRE1α mutants can be useful to distinguish between the two IRE1α RNAse outcomes and potential IRE1α kinase and scaffold activities in our cancer mouse model. However, the feasibility of *in vivo* supplementation of tumor-bearing mice with 1NM-PP1 must be evaluated.

Another factor that may contribute to differences between our nutritional and genetic tumor models is changes in the microbiota induced by the Low PROT diet. The gut microbiome is a critical regulator of the physiological metabolism and the immune system (Tajan and Vousden, 2020). Diet is a direct modulator of the gut microbiome and the microflora is implicated in nutrient processing and synthesis of certain metabolites that contribute to physiological processes implicated in tumorigenesis. Indeed, patients with colorectal carcinoma (CRC) show differences in the gut microbiome as compared to healthy individuals. Consumption of animal protein has been associated with higher abundance of mucin-degrading bacteria impairing the gut barrier functions that contribute to carcinogenic processes including changes in the expression of oncogenes and tumor suppressors, hyperplasia and hyperproliferation of the colonic epithelium. Furthermore, consumption of essential polyunsaturated fatty acids (PUFAs) such as omega-3 fatty acids has been associated with anti-cancer effects in CRC patients. In mouse models, dietary intake of omega-3 fatty acids associates with higher content of anti-inflammatory bacteria that can promote anti-cancer immunity and synergize with immunotherapy (Song and Chan, 2019). Indeed, certain gut commensal bacteria detected under ketogenic diet have been associated with a positive response to immune checkpoint blockade by potentiating an anti-cancer adaptive immune response depending on higher activity and infiltration of $CD8^+$ T cells and lower Treg cells in tumors (Routy et al., 2018), (Tajan and Vousden, 2020).

As a proof of concept of the anti-tumoral phenotype driven by exogenous expression of WT IRE1α in tumor cells, rescue *in vivo* experiments could be performed. By knocking down IRE1α in IRE1α-overexpressing cells, we could expect that engraftment of these cells into immunocompetent mice rescue the tumor growth to the levels of WT cells. Importantly, knockdown of IRE1α in IRE1α-overexpressing cells should result in IRE1α expression levels similar to that of WT cells. As a pharmacological alternative, induction of IRE1α in WT CT26 tumor-bearing mice with a specific pharmacological activator of IRE1α might help to confirm the anti-tumoral impact of activating IRE1α in tumor cells (Raymundo et al., 2020), (Grandjean et al., 2020). Although, systemic activation of IRE1α by pharmacological induction might affect the whole TME yielding a different tumor phenotype.

I. IRE1α overexpression in tumor cells is deleterious for cancer progression irrespective of GFPT1, OGT and OGA transcriptional downregulation

We observed that under Low PROT diet, malignant cells display transcriptional downregulation of OGT and OGA with not changes in GFPT1, the rate-limiting enzyme of the hexosamine biosynthetic pathway (HBP) (**Preliminary results, Figure 2B, 2C, 2D**). To determine whether the IRE1α signaling is associated with regulation of the HBP as well as OGT and OGA, transcript levels of these enzymes were measured in IRE1α-overexpressing (OE) malignant cells isolated from tumor-bearing mice. GFPT1 was found upregulated in OE cells (**Figure 22A**) while not changes in OGT (**Figure 22B**) and OGA (**Figure 22C**) transcripts were detected between mock and OE cells. Upregulation of GFPT1 is expected in OE tumor cells since XBP1s has been described to bind the GFPT1 promoter and drive its transcriptional upregulation as a bona fide mechanism induced upon different cellular stresses (Wang et al., 2014), (Denzel et al., 2014). However, GFPT1 upregulation was not seen in Low PROT tumors cells (**Preliminary results, Figure 2B**) which suggests that IRE1α activation induced by the Low PROT diet may not impact on the HBP.

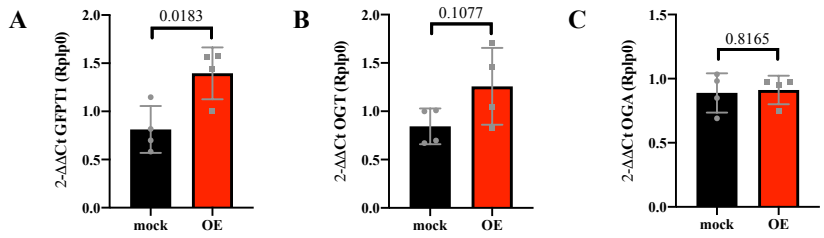

Figure 22. Exogenous expression of IRE1α in malignant cells of tumor-bearing mice does not impact of the transcript levels of OGT and OGA

Transcript levels of GFPT1, OGT and OGA in magnetically isolated tumor cells from mock (n=4) and OE (n=4) tumor-bearing mice measured by RT-qPCR.

Not changes in OGT and OGA transcripts in OE tumor cells (**Figure 22B, 22C**) may indicate that the downregulation of OGT and OGA observed in tumor cells under Low PROT diet (**Preliminary results, Figure 2C, 2D**) is either upstream of IRE1α activation in tumor cells or independent of the IRE1α signaling. Importantly, at this stage a post-translational regulation of OGT and OGA cannot be ruled out since protein levels of these enzymes and their activities were not measured in OE cells. Certainly, the transcriptional downregulation of OGT and OGA in Low PROT tumor cells as changes that could explain higher total levels of UDP-sugars under Low PROT diet is not a mechanism recapitulated upon IRE1α overexpression in isolated tumor cells. This could count as a distinctive mechanism induced upstream or irrespective of IRE1α activation under Low PROT diet. Measuring tumoral levels of UDP-HexNAc(s) and UDP-Hex(s) in OE tumors by metabolomics would be informative of IRE1α-mediated induction of the HBP for *de novo* synthesis of UDP-GlcNAc.

II. A tumor-suppressive low protein diet induces putative differential glycosylation in malignant cells (Preliminary results)

Our preliminary results have shown that UDP-HexNAc(s) and UDP-Hex(s) are more abundant in Low PROT tumors (**Preliminary results, Figure 1D**). We focused on the nucleotides sugar among other tumoral metabolites that were differentially abundant (**Preliminary results, Figure 1C**) because these UDP-sugars are substrates for glycosylation of proteins. The link among glycosylation, ER stress and the immune response is extensively documented in oncogenic malignancies (Pinho and Reis, 2015), (Xu et al., 2017).

Among the other metabolites that were discriminant between tumors of CTR or Low PROT diet-fed mice (**Preliminary results, Figure 1C**), CMP, CDP, CTP, UMP and UDP were more abundant in Low PROT tumors. This could be a result of either higher synthesis or lower consumption. Further analysis of their ^{13}C labeling upon [U-$^{13}C_6$]-Glucose tracing might bring insights into their potential synthesis from glucose.

In consistency with the reduction in dietary protein content, methionine and lysine, two EAAs were lower in Low PROT tumors (**Preliminary results, Figure 1C**). Studies with protein-restricted diets have shown that the levels of amino acids are buffered in plasma at expense of muscle atrophy (Kanarek et al., 2020). Although, an isocaloric protein-free diet has shown to decrease the levels of most amino acids in plasma while slightly decreasing the animal body weight (Adibi et al., 1973). Key organs are fed by circulating amino acids coming from muscle and other organs such as the liver and the small intestine under dietary protein restriction. Levels of amino acids in plasma have been found increased rather than reduced under full deprivation of each of the essential amino acids in the diet (Kamata et al., 2014).

This could explain why in our study, levels of amino acids in plasma were unaltered (data non-shown) and only two EAAs were decreased in tumors under a partial reduction of dietary proteins.

Deprivation of amino acids within the tumor microenvironment by reduction of amino acids at the organism level is hard to achieve without causing toxicity (Kanarek et al., 2020). Due to the risk of cachexia under caloric restriction, our protein restricted diet was designed to be isocaloric. Partial reduction of dietary proteins did not affect mouse body weight neither food intake arguing for not perturbations in global animal physiology as compared to other studies depleting essential amino acids and causing body weight loss and reduced food consumption (Kamata et al., 2014) . It is likely that circulating amino acids derived from minimal protein catabolism or *de novo synthesis* by the skeletal muscle, liver and other organs supply the tumor under nutritional protein reduction. In agreement with the reduction of methionine in Low PROT tumors, dietary methionine reduction has been shown to limit tumor growth of Ras-driven colorectal carcinoma PDX mouse models and to sensibilize tumor-bearing mice to chemotherapy and radiotherapy (Gao et al., 2019).

Interestingly, Low PROT tumors were also characterized by higher abundance of some fatty acids (**Preliminary results, Figure 1C**). Four out of these six lipids that were increased in Low PROT tumors are essential polyunsaturated fatty acids (PUFAs) including linolenic acid, linoleic acid, eicosapentanoic acid and arachidonic acid while oleic acid and palmitoleic acid are monounsaturated fatty acids that can be endogenously synthesized (Dierge et al., 2021). The higher abundance of essential PUFAs might reflect the composition of the isocaloric Low PROT diet that has a compensatory increased in 20% of lipids in order to be isocaloric and to compensate for the reduction in proteins. PUFAs such as linoleate, arachidonate, linolenate and eicosapentaenoate have been shown to accumulate within lipid droplets of tumor cells grown in acidic media (Dierge et al., 2021). Uptake of exogenous PUFAs by tumor cells growing in 3D spheroids has shown to drive cancer cell cytotoxicity by ferroptosis (Dierge et al., 2021). Therefore, in our study, higher fat content in the Low PROT diet might potentiate the uptake of extracellular fatty acids by tumor cells.

Higher abundance of two non-essential fatty acids (Morigny et al., 2021) correlates with the higher levels of pantothenate and pantetheine 4-phosphate in Low PROT tumors (**Preliminary results, Figure 1C**). The latest metabolites are needed for synthesis of coenzyme A, a critical cofactor for synthesis as well as catabolism of fatty acids via acetyl-CoA (Bourgin et al., 2022). Indeed, pantothenic acid (vitamin B5) has been reported to display immunostimulatory effects upon PD-L1 blockade in a colorectal carcinoma mouse model and to potentiate the effects of cytotoxic T cells (Bourgin et al., 2022). CDP-ethanolamine, an intermediate of the synthesis of phosphatidylethanolamine (PE) was also

higher in Low PROT tumors. PE, one of the most abundant phospholipids is enriched in the plasma membrane and the inner mitochondrial membrane (Garlapati et al., 2021). In a mouse model of prostate cancer, oral supplementation with a precursor of PE limited tumor growth by decreasing membrane fluidity and the expression of GLUT1 on the cell surface resulting in metabolic stress, mitochondrial disfunction, lipolysis, autophagy and ultimately, apoptosis (Garlapati et al., 2021).

Whether these metabolic features of the Low PROT nutritional regimen beyond dietary reduction of amino acids impacts on tumor cell immunogenicity is an open question and deserves to be further explored. How tumor cells compensate for the dietary reduction of amino acids by *de novo* synthesis or uptake from the extracellular milieu can be interesting to study as an adaptive strategy of tumors growing under a protein-restricted diet. A deep metabolic understanding of the tumoral metabolism under Low PROT diet should consider the lower steady-state levels of lactate which may indicate lower tumor cell dependency for aerobic glycolysis (**Preliminary results, Figure 1C**), although the levels of lactate M+3 upon [U-$^{13}C_6$]-Glucose tracing were not lower in Low PROT tumors (**Figure 23A**). Whether higher abundance of dietary fat in the Low PROT nutritional formula is associated with higher uptake of fatty acids by tumors and whether these fatty acids are used for lipogenesis or fatty acid oxidation (FAO) within tumors are open questions. Likewise, whether the higher tumoral abundance of fatty acids is a consequence of catabolizing stored TAG within lipid droplets can also be explored. Certainly, higher fat content in the Low PROT diet might potentiate ketogenesis in the liver since the steady-state levels of 3-hydroxybutyric acid were significantly higher in the liver while a trend for higher abundance of this the ketone body was detected in plasma and tumors (**Figure 23B**). Uptake of 3-hydroxybutyric acid by tumor cells may serve either as an energetic fuel or as a modulator of intracellular signaling pathways (Puchalska and Crawford, 2017).

Whether tumor cells under Low PROT diet uptake fatty acids (FA) and either burn fat by FAO or synthesize phospholipids and TAG for lipid storage can be monitored by measure the levels of expression FA transporters and several enzymes involved in fatty acid catabolism and lipogenesis. Attractive candidates to be measured include CD36, a FA transporter, enzymes participating in TAG synthesis such as long-chain fatty acid-CoA ligase (ACSL), glycerol-3-phosphate acyltransferase (GPAT), 1-acylglycerol-3-phosphate O-acyltransferase (AGPAT) and diglyceride acyltransferase (DGAT) and enzymes participating in FAO such as carnitine palmitoyltransferase 1A (CPT1A), the rate-limiting enzyme of FAO and medium-chain acyl-CoA dehydrogenase (MCAD), enzyme that catalyzes the first-step for oxidation of medium-chain fatty acids (Loo et al., 2021), (Puca et al., 2021).

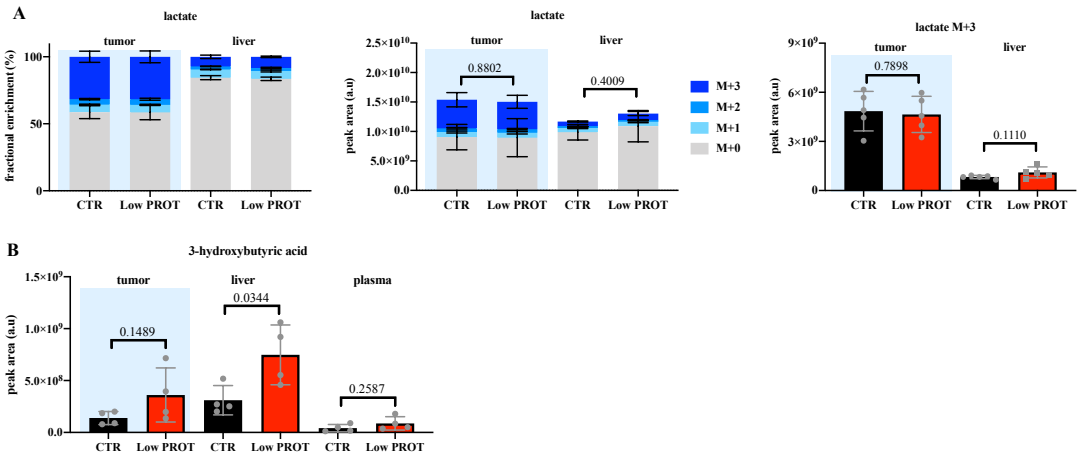

Figure 23. Lactate levels upon [U-$^{13}C_6$]-Glucose tracing and steady-state levels of 3-hydroxybutyric acid

A. Fractional enrichment, isopologue contribution to total levels of lactate and levels of lactate M+3 in tumor and liver upon [U-$^{13}C_6$]-Glucose tracing in tumor-bearing mice fed a CTR (n=5) or Low PROT (n=5) diet. B. Steady-state levels of 3-hydroxybutyric acid in tumor, liver and plasma of tumor-bearing mice fed a CTR (n=4) or Low PROT (n=4) diet measured by mass spectrometry.

II.1 Finding the sources of UDP-sugars in Low PROT tumors

UDP-GlcNAc is synthesized from glucose, glutamine, acetyl-CoA and nucleotides as part of the HBP (**Preliminary results, Figure 1E**) for glycosylation of proteins and synthesis of glycosaminoglycans such as hyaluronan (Akella et al., 2019). Therefore, UDP-GlcNAc has been considered a nutritional sensor since its *de novo* synthesis depends on key energetic and building block metabolites. Thus, UDP-GlcNAc synthetic rate reflects cellular nutritional availability (Chiaradonna et al., 2018). Although UDP-HexNAc(s) content was more abundant in Low PROT tumors (**Preliminary results, Figure 1D**), a higher flux rate through the HBP was not seen by [U-$^{13}C_6$]-Glucose tracing. An enhanced HBP from glucose is expected to yield higher levels of the isotopologue M+6 (**Preliminary results, Figure 1E**) which was not detected in Low PROT tumors (**Preliminary results, Figure 1F**). Likewise, higher synthesis of UDP-Glc from [U-$^{13}C_6$]-Glucose was not detected in Low PROT tumors (**Preliminary results, Figure 1F**).

Another way of fueling the HBP is via the GlcNAc salvage pathway that bypasses the first reaction of the HBP by channeling free GlcNAc for generation of GlcNAc 6-phosphate (**Preliminary results, Figure 1E**) (Campbell et al., 2021). Tumoral levels of GlcNAc were monitored but no differences were observed between groups (**Preliminary results, Figure S1G**). The expression of the enzyme NAGK could be quantified to monitor whether GlcNAc is channeled into the HBP by the salvage pathway.

Higher flux rate of the HBP from glucosamine is plausible since total levels of glucosamine were higher in Low PROT tumors (**Preliminary results, Figure S1H**). However, glucosamine fueling the HBP for higher synthesis of UDP-GlcNAc can only be confirmed by tracing ^{13}C labeled glucosamine. The activity of GFPT1 and NAGK can be assayed by ^{13}C labeled glucose and ^{13}C labeled glucosamine, respectively, by quantifying the ^{13}C labeling of the common product of both reactions, glucosamine 6-phosphate (Akella et al., 2019) (**Preliminary results, Figure 1E**). In addition, the expression of glucose transporters functioning for uptake of glucosamine such as GLUT1/2/4 (Uldry et al., 2002) as well as the expression of NAGK, the enzyme channeling glucosamine into the HBP could be measured (Akella et al., 2019). Expression levels of the second rate-limiting enzyme of the HBP, UAP1 catalyzing the last step of the pathway by addition of UTP and generation of the high energy sugar donor UDP-GlcNAc (Lam et al., 2021) can also be measured.

Interestingly, the higher total levels of UDP-HexNAc(s) and UDP-Hex(s) in Low PROT tumors (**Preliminary results, Figure 1D**) were lost upon ^{13}C labeled glucose tracing (**Preliminary results, Figure S1C, S1D**). This could be explained by the acute effects of the tracer when administrated by discrete bolus instead of by infusion (Fernández-García et al., 2020), (Grima-Reyes et al., 2021). Excessive supplementation of the labeled nutrient, in this case glucose, may affect the levels of downstream metabolites derived from the tracer. Indeed, disturbances of the physiological metabolism are expected by discrete administration of the tracer (Grima-Reyes et al., 2021). A tracer enrichment in plasma between 10 to 30% has been recommended to avoid challenging the global metabolism of the animal (Jang et al., 2018). Therefore, the steady-state levels of these nucleotide sugars in tumor-bearing mice not challenged with the tracer reflect a more reliable tumoral abundance in non-perturbed physiological conditions (**Preliminary results, Figure 1D**).

As higher steady-state levels of UDP-HexNAc(s) could not be explained by a higher flux of the HBP from labeled glucose and in the absence of glucosamine tracing, transcriptional expression of critical enzymes regulating the levels of UDP-GlcNAc were quantified in tumor cells (**Preliminary results, Figure 2B, 2C, 2D**). Rather than changes in GFPT1, OGT and OGA were found downregulated. Downregulation of OGT and a lower activity could explain accumulation of UDP-GlcNAc and higher levels of UDP-GalNAc due to epimerization between these nucleotide sugars (**Preliminary results, Figure 2A**). Likewise, UDP-Glc and UDP-Gal can be generated from the accumulated UDP-GlcNAc as it has been reported in liver of mice supplemented with oral GlcNAc (Ryczko et al., 2016). UDP-GlcNAc can also fuel the pools of other nucleotide sugars such as GDP-Man and CMP-Neu5Ac (Akella et al., 2019). However, the levels of these nucleotide sugars were not found altered in Low PROT tumors (**Preliminary results, Figure S1E, S1F**). To verify that downregulation of OGT and

OGA also occur at the protein level, we will measure OGT and OGA protein expression in isolated tumor cells by Western blot.

II.2 The multiple fates of UDP-HexNAc(s) and UDP-Hex(as) in tumor cells

OGT mediates the incorporation of a unique moiety of GlcNAc from UDP-GlcNAc into the serine/threonine residues of proteins while OGA catalyzes the removal of GlcNAc from O-GlcNAcylated proteins (Yang and Qian, 2017). OGT-mediated O-GlcNAcylation of cytoplasmic, nuclear and mitochondrial proteins in contrast to N- and O-glycosylation is commonly reported to regulate the activity of intracellular proteins as phosphorylation does (Parker et al., 2021). Indeed, phosphorylation and O-GlcNAcylation as post-translational modifications can compete for common sites within a protein and therefore, fine-tune intracellular signaling pathways. O-GlcNAcylation plays regulatory roles controlling the activity and localization of several target proteins involved in gene expression and metabolism (Parker et al., 2021).

Despite the transcriptional downregulation of OGT and OGA, no obvious changes in the levels of O-GlcNAcylated proteins were detected when comparing whole tumors of CTR and Low PROT diet-fed mice (**Preliminary results, Fig. 2E**). To verify this finding, we will measure O-GlcNAcylated proteins in isolated tumor cells since detection of O-GlcNAcylation in the whole tumor may mask slight differences between tumor cells from CTR and Low PROT diet-fed mice.

II.2.1 Putative roles of OGT and OGA lower expression in Low PROT tumor cells

The transcriptional downregulation of OGT and OGA that we observed in the less aggressive Low PROT tumors (**Preliminary results, Figure 2C and 2D)** is in line with the tumor-protective roles of OGT that have been described in several types of cancer (Lam et al., 2021). Upregulation of OGT via the PI3K-mTOR-cMyc pathway (Sodi et al., 2015) and its interplay with glycolysis, HIF-1α and ER stress (Ferrer et al., 2014) have been observed in breast cancer. OGT via induction of the oncogenic transcription factor FOXM1 and synthesis of metalloproteinases has been involved in breast cancer aggressiveness and metastasis (Ferrer et al., 2017). OGT upregulation has been connected with aerobic glycolysis and metastasis in prostate cancer (Lynch et al., 2012). O-GlcNAcylation levels have positively correlated with hepatocellular carcinoma recurrence (Zhu et al., 2012). OGT upregulation has been detected in cholangiocarcinoma (CCA) and associated with poor survival (Phoomak et al., 2012). Upregulation of OGT and higher levels of O-GlcNAcylation have been also reported in colorectal carcinoma and associated with EMT (Steenackers et al., 2016), tumor-initiating potential (Guo et al., 2017) and metastasis (Jiang et al., 2019).

We have not found an association among higher levels of UDP-HexNAc(s) (**Preliminary results, Figure 1D**), the HBP (**Preliminary results, Figure 1F, 2B**) and O-GlcNAcylation of proteins. Instead, we have observed a negative correlation between the levels of UDP-sugars (**Preliminary results, Figure 1D**) and OGT/OGA mRNA levels (**Preliminary results, Figure 2C, 2D**) with not appreciable changes in protein O-GlcNAcylation levels (**Preliminary results, Figure 2E**). Most reports associating OGT with cancer progression describe a link between O-GlcNAcylation and the HBP. For instance, enhanced O-GlcNAcylation associated with higher flux of the HBP has been shown to be part of the metabolic reprogramming of more aggressive and metastatic lung tumors (Kim et al., 2020). Non-small-cell lung cancer (NSCLC) cells driven by oncogenic Kras and loss-of-function mutation in LKB1 *de novo* synthesized UDP-GlcNAc through an enhanced HBP dependent on GFPT. Higher O-GlcNAcylation as well as upregulation of complex type of N-glycans on the surface of tumor cells conferred survival advantages to co-mutant tumor cells. Inhibition of GFPT limited tumor growth in Kras/LKB1-driven NSCLC xenografts and in a GEM mouse model (Kim et al., 2020). Considering this evidence and our findings, no appreciable changes in the HBP and O-GlcNAcylation levels occurring under the Low PROT diet match with the less aggressive tumor phenotype driven by nutritional protein restriction.

O-GlcNAcylation and the HBP have been involved in the intrinsic and acquired chemotherapy resistance of human breast, hepatocellular carcinoma, leukemia and cervical tumor cells (Liu et al., 2018). The resistance phenotype was characterized by activation of Akt, subsequent induction of XBP1s and upregulation of GFPT. Higher expression and activity of GFPT1 led to higher levels of UDP-HexNAc. Higher O-GlcNAcylation under chemotherapy led to O-GlcNAcylated caspases displaying a decreased apoptotic activity in resistance cells. As a positive feedback mechanism, Akt activation was also dependent on O-GlcNAcylation. Inhibition of OGT sensibilized tumor cells to chemotherapies by decreasing the pro-survival signals and increasing the activity of caspases whereas OGT overexpression rescued the resistant phenotype (Liu et al., 2018). On the contrary, O-GlcNAcylation and stabilization of thymidylate synthase has been shown to sensitize colorectal carcinoma to 5-FU treatment. Therefore, treating tumor-bearing mice with an OGA inhibitor in combination with 5-FU had a synergic effect in this cancer mouse model (Very et al., 2022).

As OGT and OGA display metabolic roles, a link between the Low PROT diet and OGT/OGA deregulation (**Preliminary results, Figure 2C, 2D**) is plausible. Although an impact of dietary protein reduction on OGT and OGA expression could be expected, numerous reports have already described a link between OGT regulation and lipid metabolism. As the Low PROT diet contains more fat and FAs are more abundant in Low PROT tumors (**Preliminary results, Figure 1C**), a connection between OGT/OGA

deregulation and lipid metabolism in tumor cells might be possible. For instance, OGT and OGA cycling has been reported to control the response to insulin by inhibiting Akt via O-GlcNAcylation as well as other downstream effectors of the insulin signaling as a negative feedback mechanism (Yang et al., 2008). When exogenously expressed, OGT induces hepatic insulin resistance and concomitant gluconeogenesis, glycogen depletion and inhibition of lipogenesis in the liver. In this context, OGT downregulated several regulators of lipid synthesis including sterol regulatory element-binding protein-1 (SREBP-1) and its downstream targets with not changes in genes involved in fatty acid oxidation such as CPT1A and MCAD (Yang et al., 2008).

As OGT and OGA are temporally and physiologically regulated by substrate availability and hormones, their transient activities do not necessarily match with changes in the intracellular levels of free UDP-GlcNAc (Yang and Qian, 2017. Indeed, there is not a linear correlation between nutritional availability and OGT/OGA cycling. O-GlcNAcylation of proteins cannot be considered a readout of higher nutrient flux through the HBP since under nutrient scarcity, O-GlcNAcylation is also elevated and regulated by glucagon. In addition, mutual regulation of OGT and OGA occurs transcriptionally, but post-translational modifications including O-GlcNAcylation of both proteins also seem to play a role (Yang and Qian, 2017). Mutual transcriptional regulation between OGT and OGA occurs since exogenous expression of OGA increases OGT mRNA levels while knockdown of OGA decreases OGT expression in hepatocytes (Qian et al., 2018). In addition, OGT knockdown decreased OGA mRNA levels while OGT exogenous expression did not lead to OGA upregulation (Qian et al., 2018). Therefore, mutual downregulation of OGT and OGA not necessarily has to be linked with global changes of the O-GlcNAcylated proteome in our study (**Preliminary results, Figure 2E**) but instead, to O-GlcNAcylation of specific target proteins. Indeed, expression of OGT not correlating with augmented global O-GlcNAcylation of intracellular proteins has been reported in TNBC tumor cells (Chokchaitaweesuk et al., 2019).

Higher expression of OGT has been associated with carcinogenesis mediated by fat overnutrition as in fatty liver (NAFLD)-associated hepatocellular carcinoma (HCC) patients (Xu et al., 2017). Indeed, exogenous expression of OGT enhanced tumor growth whereas OGT knockdown reduced primary tumor growth in the liver and lung metastasis. The tumor-promoting role of OGT was associated with upregulation of fatty acid synthase (FASN), increased levels of palmitic acid, downstream induction of ER stress with IRE1α activation and induction of JNK/c-Jun and NF-κB/TNFα pathways. Higher HCC cell viability upon OGT upregulation was decreased by inhibiting ER stress (Xu et al., 2017).

As we have found downregulation of OGT mRNA in tumor cells under an isocaloric Low PROT diet with a compensatory increase in fat, we can hypothesize that by a negative feedback loop, higher levels of fatty acids in Low PROT tumors (**Preliminary results, Figure 1C**) might induce transcriptional downregulation of OGT in tumor cells (**Preliminary results, Figure 2C**). Alterations in amino acids levels due to the nutritional protein restriction might also count as metabolic alterations that could drive OGT/OGA deregulation independent of IRE1α activation in tumor cells (**Article 1, Figure 1C**), (Rubio-Patiño et al., 2018b). This hypothesis (**Figure 27**) fits the unaltered expression levels of OGT and OGA in IRE1α-overexpressing tumor cells from tumor-bearing mice (**Figure 22**). Downregulation of OGT may lead to lower OGA mRNA levels by their reciprocal regulation (**Preliminary results, Figure 2D**) and concomitant accumulation of UDP-GlcNAc and derived UDP-sugars (**Preliminary results, Figure 1D**) irrespective of the HBP (**Preliminary results, Figure 1F**).

Other evidence connecting the pro-tumoral roles of OGT with lipid metabolism has been reported in breast cancer (Sodi et al., 2018). OGT suppression decreased the levels of free fatty acids and lipid droplets. These changes associated with reduced expression of SREBP-1 and lipogenic enzymes including fatty acid synthase (FASN) and ATP citrate lyase (ACLY). Indeed, OGT knockdown limited tumor growth of breast xenografts whereas exogenous expression of SREBP-1 rescued tumor growth (Sodi et al., 2018). Beyond SREBP-1 regulation, O-GlcNAcylation of serine/arginine-rich protein-specific kinase 2 (SRPK2) has been shown to induce mRNA splicing of lipogenic genes in human breast cancer cells (Tan et al., 2021). Induced lipogenic genes such FASN and ACLY associated with higher levels of fatty acids and cholesterol. Tumor growth of subcutaneous xenografts were rescued in SRPK2 KO cells upon exogenous expression of wildtype SRPK2 but not upon ectopic expression of O-GlcNAcylation deficient SRPK2 mutants (Tan et al., 2021).

To determine the effects of OGT and OGA downregulation in tumor cells, we initiated the generation of OGT and OGA stable knockdown CT26 cells. Knockdown cells have been generated to first monitor whether partial silencing of OGT and OGA is cytotoxic and whether full genetic silencing is feasible in term of cell viability. The cell phenotype based on the levels of downregulation of OGT and OGA, effects of downregulation of one of these genes in the expression of the other one and cell proliferative capacity will be characterized prior to subcutaneous transplantation of OGT and OGA knockdown CT26 cells into immunocompetent mice.

II.2.2 Hyaluronic acid as a product or source of UDP-sugars in Low PROT tumors

Downstream of higher levels of UDP-GlcNAc and UDP-Glc in Low PROT tumors (**Fig. 1D, Preliminary results**), synthesis of hyaluronic acid (HA) could be potentiated. Although, rather than tumor-suppressive, HA has been described to support angiogenesis, EMT and metastasis in different types of cancers including colorectal carcinoma (Caon et al., 2020), (Ghasempour and Freeman, 2021). Accumulation of HA in the TME does not only depends on higher *de novo* synthesis by hyaluronan synthases (HAS) integral proteins of the plasma membrane but on substrate availability (Caon et al., 2020). Indeed, in TNBC mouse models, an enhanced HBP via upregulation of GFPT was observed in parallel with increased levels of O-GlcNAcylation and HA production (Chokchaitaweesuk et al., 2019). Higher HA production was also dependent on HAS2 upregulation. HAS2 deficiency limited breast tumor growth while diminishing cancer-stem cell (CSC) features such as tumor-initiating potential and chemotherapy resistance. Silencing of both HAS2 and GFPT1 synergized in decreasing the CSC potential of breast tumor cells. Indeed, co-expression of GFPT and HAS2 was negatively correlated with cancer survival of breast cancer patients. O-GlcNAcylation was shown to play overlapping and also different roles as that of HA production in cancer progression (Chokchaitaweesuk et al., 2019).

Accumulation of UDP-GlcNAc, UDP-Glc, UDP-glucuronic acid (UDP-GlcUA) and HA has been reported in breast cancer biopsies correlating with higher transcript levels of GFPT (Arnold et al., 2020). As mRNA levels of HAS were unaltered, higher HA production in breast tumors was suggested to be a result of higher substrate availability via an enhanced HBP (Oikari et al., 2018). Furthermore, UDP-glucose 6-dehydrogenase (UGDH), the enzyme catalyzing the synthesis of UDP-GlcUA from UDP-Glc has been found upregulated in TNBC patients and associated with tumor aggressiveness. Lower HA production by silencing UGDH in tumor cells limited tumor growth of breast cancer xenografts. In addition, UGDH silencing increased the expression of several genes involved in lipid catabolism (Arnold et al., 2020). Based on this evidence, whether UDP-sugars in Low PROT tumors are destinated to HA production does not correlate with the tumor-promoting roles described for HA.

On the contrary, HA positively impacting on the immune system has been described in DCs derived from CRC patients. Treating DCs with low molecular weight (LMW) HA fragments increased their activation (Caon et al., 2020) and their potential to activate T lymphocyte proliferation (Rizzo et al., 2014). Likewise, higher DC migration capabilities toward lymph nodes was observed in a mouse model of CRC xenograft (Rizzo et al., 2014). Whether production of LMW HA is a consequence of the accumulation of UDP-sugars in our study,

enhancement of the anti-cancer immune response by changes in the extracellular matrix within the Low PROT TME is a plausible mechanism.

Rather than UDP-sugars as substrates for HA production, accumulation of UDP-sugars in tumor cells as a consequence of HA uptake from the TME has been described in pancreatic cancer (Kim et al., 2021). LMW HA feeding pancreatic tumor cells rescued their impaired proliferation upon GFPT1 deficiency by fueling the HBP through the GlcNAc salvage pathway mediated by NAGK. *In vitro* cultured pancreatic tumor cells as well as orthotopic tumors were susceptible to GFPT1 deficiency whereas subcutaneous tumors were insensible. These differences were attributed to higher deposition of HA in the TME of subcutaneous tumors. HA uptake via macropinocytosis by pancreatic tumor cells reverted the decrease in clonogenicity, cell proliferation and O-GlcNAcylation levels upon GFPT1 silencing (Kim et al., 2021). Therefore, HA deposition in the TME and uptake by tumor cells might count as a mechanism for accumulation of UDP-sugars in tumor cells under Low PROT diet.

Tumor-suppressive roles of UDP-sugars beyond their contribution to glycosylation processes have been reported in lung cancer (X. Wang et al., 2019). Higher UGDH mRNA levels in human lung cancer tissues correlated with malignancy and UGDH knockdown reduced lung metastasis in mouse xenografts. Interestingly, higher UGDH-depending migrating capabilities of lung cancer cells were beyond synthesis of HA. UGDH consuming UDP-Glc was demonstrated to increase the mRNA stability of SNAIL, an EMT- related transcription factor. UDP-Glc was shown to be tumor-suppressive by binding and inhibiting an RNA-binding protein stabilizing SNAIL mRNA. Therefore, UDP-Glc supplementation reduced lung metastasis while increasing survival of tumor-bearing mice. Migration and metastasis of lung tumor cells were shown to be dependent on UDP-Glc consumption by the activity of UGDH irrespective of HA synthesis (X. Wang et al., 2019).

Altogether, this evidence stimulates to measure levels of HA in Low PROT tumors by histological staining with HA binding proteins.

II.2.3 N- and O-glycosylation in Low PROT tumor cells

N- and O-glycosylation depends on UDP-HexNAc(s) and UDP-Hex(s) (**Preliminary results, Figure 2A**). These glycosylation events start co-translationally in the ER and continue post-translationally in the the GA as part of the secretory pathway (Stanley, 2011). Therefore, ER stress and glycosylation are tightly related (Vincenz and Hartl, 2014). N-glycosylation which depends on the incorporation of GlcNAc from the UDP-GlcNAc free pool to asparagine residues of proteins also rely on the incorporation of glucose from UDP-Glc for synthesis of immature glycosylated proteins in the ER (Reily et al., 2019). N-glycosylated proteins carry glycan trees that acquire a mature and definitive structure in the GA after modification by

removal and addition of sugar residues from the precursor structure (Reily et al., 2019). O-glycosylation of proteins containing mucin-like motifs rely mainly in the incorporation at first of GalNAc from UPD-GalNAc to serine or threonine residues of proteins (Chandler et al., 2019). Subsequent addition of other sugar residues including GlcNAc determine the structure and length of the O-type of glycans (Chandler et al., 2019), (Reily et al., 2019).

The global N-glycan profile of isolated tumor cells from Low PROT diet-fed mice showed that among 15 identified N-glycan structures, few of them changed their levels as detected by glycomics (**Preliminary results, Figure 2F**). Lower and higher relative levels of complex non-sialylated bi-antenna and sialylated type of N-glycans, respectively were detected in Low PROT tumor cells (**Preliminary results, Figure 2G**). Higher branched type of N-linked glycans expressed on the cell surface of colorectal tumors (M. C. Silva et al., 2020) and higher sialylation of the tumor glycocalyx (Büll et al., 2014), (Moffett et al., 2021) have been described as tumor cell mechanisms for immune invasion and chemotherapy resistance. Opposite to this evidence, we found higher relative abundance of global sialylated structures including membranous and intracellular glycans in the less aggressive tumor phenotype driven by the Low PROT diet. In our study, the glycan structures detected by glycomics can be derived from the intracellular compartment as well as the plasma membrane since subcellular fractionation of isolated tumor cells was not performed prior to mass spectrometry. In addition, glycan detection by glycomics is more favorable for smaller glycan trees since larger structures are underestimate due to their lower ionization and detector response of the mass spectrometer (Yamakawa et al., 2018). Therefore, a partial N-glycan profile might be provided by glycomics.

N- and O-glycosylation confers to target proteins protection against proteolytic cleavage, solubility, stability and specific features. Indeed, glycan epitopes of glycosylated proteins confer distinctive immunological features when these proteins are expressed on the cell surface. For instance, MHC-I is N-glycosylated for proper folding, maturation, transport to the cell surface and likely recognition by the $CD8^+$ T cell receptor (Ryan and Cobb, 2012). Likewise, branched N-glycosylation of PD-L1 confers protein stability as well as T cell inhibitory properties (Li et al., 2016). As the glycomics approach was performed in whole cell lysates, we decided to detect glycosylation on the tumor cell surface with lectin staining. The glycocalyx of tumor cells was screened by a lectin microarray containing 96 lectins (**Preliminary results, Table 1**). Lectins are carbohydrate-binding proteins that recognize with low affinity glycan epitopes on glycoconjugates (Chandler et al., 2019). Out of 96 lectins, three lectins were differentially detected between CTR and Low PROT tumors cells (**Preliminary results, Figure 2H**).

rPAIL, a lectin recognizing α,βGal and αGalNAc (Tn antigen) (**Preliminary results, Table 2**) was lower detected in Low PROT tumor cells (**Preliminary results, Figure 2H**). However, other lectins that have the ability to bind the αGalNAc moiety of Tn antigens such as HPA, VVA, DBA, SBA, rPPL and rCNL (**Preliminary results, Table 2**) did not show any significant differences in staining of membranous glycoconjugates on isolated tumor cells from CTR or Low PROT diet-fed mice (data non-shown). Therefore, whether Tn antigens are lower expressed in Low PROT tumor cells must be confirmed by specific antibodies recognizing Tn antigens. Although we cannot warrant that alterations of Tn antigens on the tumor cell glycocalyx occur under Low PROT diet, this is a promising hint since Tn antigen exposure is a common aberrant glycosylation in several types of cancer including colorectal carcinoma (Rømer et al., 2021), (Ghasempour and Freeman, 2021). Therefore, lower exposure of Tn antigens on tumor cells under Low PROT diet correlates with a less aggressive tumor phenotype.

More than 80% of surface or secreted proteins are O-glycosylated (Rømer et al., 2021). Tumor cells expressing aberrant glycosylated O-linked mucins are very common. For instance, enrichment of Tn antigens (GalNAc-α-1-O-Ser/Thr) as well as sialylation of Tn antigens have been reported in tumor cells (Moffett et al., 2021). Truncation of these structures not allowing for elongated O-glycan trees from the core structure detailed above is a common feature of glycosylated proteins at the tumor cell surface. Deregulation of GalNAc transferases and competition for the same substrates by different glycosyltransferases underlie the synthesis of these truncated O-glycan structures. Truncated O-glycosylated epitopes exposed on the tumor cell surface count as neo-antigens. Mutations in the chaperone of the T antigen synthase potentiate the synthesis of Tn antigens over T antigens (Galβ-1-3GalNAc-α-1-O-Ser/Thr) as well as the generation of sialyl-Tn antigens (STn) by upregulation of the sialyltransferase ST6GalNAc-I (Pinho and Reis, 2015). Likewise, Lewis epitopes including determinant of the blood groups are also glycosylated structures present not only on proteins, but in lipids. These epitopes can be sialylated and have been reported as tumor markers on the cell surface or in the circulation (Reily et al., 2019).

Most of the FDA-approved cancer biomarkers detected by antibodies are indeed glycoconjugates (Rømer et al., 2021). In this regard, the Tn antigen has been considered a pan-marker of human cancer in contrast to the T antigen that is expressed on cancer cells but also in healthy tissues. Cell surface exposition of truncated O-glycans has been associated with perturbances in cell differentiation, invasion and adhesion in mouse models of gastrointestinal cancers. Furthermore, surface expression of truncated O-glycans correlates with impaired cancer prognosis of colorectal carcinoma patients. Higher and heterogeneous

expression of Tn antigens within single tumors has been reported in human colon, breast, lung, pancreatic and skin cancers. Expression of Tn antigens has been positively associated with co-occurrence of the STn and T antigens. Interestingly, PDX of 13 types of cancers including CRC displayed Tn antigen expression on tumor cells indicating maintenance of truncated O-glycan structures upon tumor transplantation (Rømer et al., 2021).

The interaction between tumor cells and stromal cells including immune and endothelial cells is highly mediated by O-glycosylated epitopes as well as N-glycosylated proteins expressed on tumor cells and lectins expressed by stromal cells (Chandler et al., 2019). Naturally expressed lectins recognizing glycan structures on the tumor glycocalyx are potentiated or inhibited depending on the aberrant glycosylation on tumor proteins and lipids. Animal lectins include galectins which bind to galactose residues and selectins which recognize sialylated and fucosylated glycan structures. For instance, E- and P-selectins expressed by endothelial cells recognize sialylated Lewis X epitopes on N-glycosylated proteins expressed by tumor cells of several types of cancers including colon carcinoma. Galectin-3 expressed on endothelial cells bind to mucin-type of O-glycans such as the T antigen on mucin-1 (MUC1) on tumor cells contributing to rolling and extravasation. Therefore, glycosylation on tumor cells as well as on endothelial cells within the TME is a key modulator of angiogenesis and metastasis (Chandler et al., 2019).

Tumor cells expressing galectin-1 bind the VEGFR bearing branched N-type of glycans expressed by endothelial cells (Croci et al., 2014). This has been shown to be a compensatory mechanism through a glycosylation-mediated signaling inducing angiogenesis upon VEGF blockage and therefore, resistance to VEGF anti-cancer therapies (Croci et al., 2014). Another naturally occurring lectins that predominantly attenuate innate and adaptive immune responses are Siglec receptors with different binding specificities for sialylated structures (De Bousser et al., 2020), (Lübbers et al., 2018).

Under healthy conditions, membrane-bound mucins are a protective barrier of epithelial cells against pathogens and injury. Mucins also inhibit inflammation (Bhatia et al., 2019), (Ghasempour and Freeman, 2021). Mucins expressing O-type of glycans but also N-type of glycans on the surface of tumor cells can bind ICAM-1 expressed on T lymphocytes leading to T cell tolerance and avoiding tumor-associated antigen recognition. In addition, mucins on tumor cells bind inhibitory Siglec receptors on APCs provoking suppression. MUC16, an ovarian cancer marker downregulates CD16 and other activating receptors on NK cells, thus dampening their cytotoxic functions. MUC4 on pancreatic tumor cells has been involved in apoptosis of $CD8^+$ T cells. Aberrant glycosylation of mucins on tumor cells contributes to metastasis by potentiating tumor cell migration by binding to selectin-expressing leukocytes and platelets and inhibiting immune cell recognition. High expression of MUC1 associates

with tumor invasion and metastasis as well as activation of the NF-κB pathway and higher activity of matrix metalloproteinases (Bhatia et al., 2019).

rGC2 recognizing α1-2Fuc (antigen H), αGalNAc (antigen A) and αGal (antigen B) was higher detected on Low PROT tumor cells (**Preliminary results, Figure 2H**). Other lectins binding to α1-2Fuc (antigen H) such as rRSL, AOL, AAL, rPAIIL, rRSIIL, UEAI, TJAII and MCA (**Preliminary results, Table 2**) did not change between CTR and Low PROT groups. In addition, lectins recognizing the other glycan motifs αGalNAc (antigen A) and αGal (antigen B) such as PTLI, GSLIA4 and HPA as well as GSLI4B, rMOA and EEL did not change either (data non-shown). Thus, we cannot confirm an increase of the glycan structures recognized by rGC2 based on the binding of other lectins with redundant specificities. Therefore, whether there is more exposure of these Lewis antigens must be confirmed by antibody staining. Noteworthy, higher surface expression of Lewis antigen A (Le^a) has been detected by immunofluorescence on colon heathy mucosa while the neoplastic tissue lacked Le^a expression (Aronica et al., 2017). This would correlate with putative higher expression of Le^a on Low PROT tumor cells.

Our lectin microarray data showed higher binding of rGRFT recognizing terminal mannose residues on Low PROT tumor cells (**Preliminary results, Figure 2H**). Other lectins binding to high oligo mannose mediated by linkage specificity such as ConA, GNA, DBAI, HHL, NPA and Heltuba (**Preliminary results, Table 2**) were not changing between CTR and Low PROT groups (data non-shown). However, rBanana and rOrysata detecting mannose residues displayed a trend for higher binding to Low PROT tumor cells (**Figure 24**) as rGRFT does. No changes in the majority of lectin recognizing mannose residues might be explained by their linkage-mediated recognition as compared to rGRFT that binds terminal mannose irrespective of their sugar bonds. Whether oligo mannose N-type of glycans are higher exposed by Low PROT tumor cells is not associated with decreased binding of lectins recognizing complex N-types of glycans such as PHA-L and DSA (data non-shown). Lectins binding to sialic acid (in a α2-3 and α2-6 linkage) such as MAL, MAH, ACG, SNA, SSA, TJAI were unaltered.

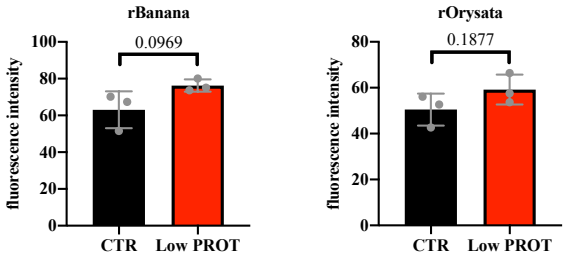

Figure 24. Levels of lectins recognizing mannose residues on the glycocalyx of tumor cells

Tumor cells were isolated from mice fed a CTR (n=3) or a Low PROT diet (n=3).

Importantly, higher oligo mannose type of N-glycans on Low PROT tumor cells detected by the lectin array do not correlate with the global N-glycan profile by glycomics that showed higher relative abundance of complex and sialylated structures in Low PROT tumor cells with not changes in high oligo mannose N-glycans (**Preliminary results, Figure 2F**). High oligo mannose structures are more common of intracellular immature proteins along the glyco-editing process occurring from the ER to the GA as part of the protein secretory pathway. The high abundance of these precursors in whole tumor cells as detected by mass spectrometry might mask slight changes in high oligo mannose structures expressed on the cell surface. Therefore, although not correlating with the N-glycan profile of whole cellular proteins as detected by mass spectrometry, higher surface expression of oligo mannose might be possible as indicated by the lectin array. This is promising hint since reports on colorectal carcinoma describe this type of N-linked glycosylation as immunostimulatory (M. C. Silva et al., 2020).

Higher levels of complex branched N-glycans have been detected on human colorectal carcinoma (CRC) tissues in association with carcinogenesis progression while negatively correlating with Treg cell markers (M. C. Silva et al., 2020). Branched N-glycans are generated by the action of the N-acetylglucosaminyltransferase V (GnT-V) and GnT-V mRNA levels correlated with CRC progression. Complex branched N-glycan expressed on the tumor cell surface were shown to be tumor-protective by inhibiting immune recognition. Branched N-glycans functioning as immune checkpoints suppressed the $CD4^+$ T cell activating functions of APC cells and cytokine secretion. Immunosuppression was mediated by lower binding of lectins expressed on APCs such as DC-SING. DC-SING recognition of high mannose containing-glycosylated structures on tumor cells was masked by exposition of branched N-glycans attenuating lectin binding and DC activation. Indeed, pharmacological inhibition of N-glycan branching as well as genetic silencing of GnT-V limited tumor growth in immunocompetent mice in an immune response dependent manner (M. C. Silva et al., 2020).

Despite this evidence in CRC, higher exposition of high oligo mannose rather than branched type of N-glycans was determinant for the metastatic potential of cholangiocarcinoma (CCA) cells. In addition, a crosstalk between O-GlcNAcylation and N-glycosylation has been shown to mediate this process. High mannose type of N-glycans were enriched on the cell membrane in metastatic CCA cells and downregulated upon inhibition of O-GlcNAcylation as compared to parental cells. Higher expression of oligo mannose N-glycans in metastatic CCA cells conferred advantages for migration. Accumulation of high oligo mannose N-glycans was associated with α1,2-mannosidase IA (MAN1A1) downregulation mediated by O-GlcNAcylation of FOXO3. MAN1A1 is a mannosidase operating in the GA to trim mannose

residues for generation of hybrid and complex N-glycans and its expression is controlled by the transcription factor FOXO3. Indeed, a positive correlation among metastasis, O-GlcNAcylation, high mannose N-glycans and a negative association with MAN1A1 protein expression was confirmed in human CCA tissues (Phoomak et al., 2018).

Altogether, the glycomics and the lectin binding approaches brought different hints about the glycans structures that can be differentially abundant in Low PROT tumor cells. As the identification of global N-glycan structures in whole cell lysates by glycomics may be biased by the abundance of intracellular immature N-glycoconjugates, we will determinate whether there is higher surface exposition of oligo mannose N-type of glycans by individual lectin staining measured by flow cytometry. In addition, using specific antibodies for Tn antigens would be more suitable than lectin staining due to the cross specificity of the lectins for several glycans. Measure the levels of expression of the glycosyltransferases and glycosylases involved in synthesis of high mannose N-glycans and Tn antigens as well as nucleotide sugar transporters at membranous compartments would be also informative to drive conclusion about these putative changes in the glycocalyx of Low PROT tumor cells. In addition, the expression of membrane-bound mucins can also be measured since MUC1, MUC4 and MUC16 have been reported to contribute to cancer.

In a cytotoxic assay, *ex vivo* glycosidase treatment of isolated tumor cells prior to co-culture with T splenocytes from tumor-bearing mice can be performed to link modifications of the tumor cell glycocalyx with the anti-cancer immune response. Glycosidases catalyzing the removal of high oligo mannose (Endo H) and complex type of N-glycans (PNGase F) as well as O-glycans (O-glycosidases) from the tumor cell surface are deglycosylation treatments that deserve to be tested. Likewise, removal of terminal sugar residues such as sialic acid, galactose and fucose moieties can bring insight into the composition of the tumor cell glycocalyx that contribute to the establishment of the immunological synapse between tumor cells and T lymphocytes. Cytotoxic assays with NK cells as well as efferocytosis assays with BMDCs upon glycosidase treatment of isolated tumors might broaden the repertory of immune cells that interact with cancer cells and are modulated via the tumor glycocalyx.

III. Pursuing differential glycosylation in surface immune markers higher expressed on Low PROT tumor cells

Changes in glycosylation on immune markers that were found upregulated on tumor cells under Low PROT diet were monitored. Mouse MHC-I (H2Kd haplotype) that is higher expressed on tumor cells under Low PROT diet (**Article, Figure 1G**) displays three N glycosylation sites as reported by UniProtKB (P01902) including Asn at positions 107, 197

and 277. To check whether H2Kd displays differential glycosylation patterns under Low PROT diet, whole tumors were treated with glycosidases that are specific for different glycan structures (Fig. 24A). Peptide-N-glycosidase F (PNGase F) is an amidase cleaving N-glycans trees by recognizing the core GlcNAc moiety attached to the Asn residue of a protein while Endoglycosidase H (Endo H) cleaves between the two innermost GlcNAc residues of N-linked high mannose and hybrid glycans containing at least five mannose residues (Stanley, 2011) (**Figure 25A**).

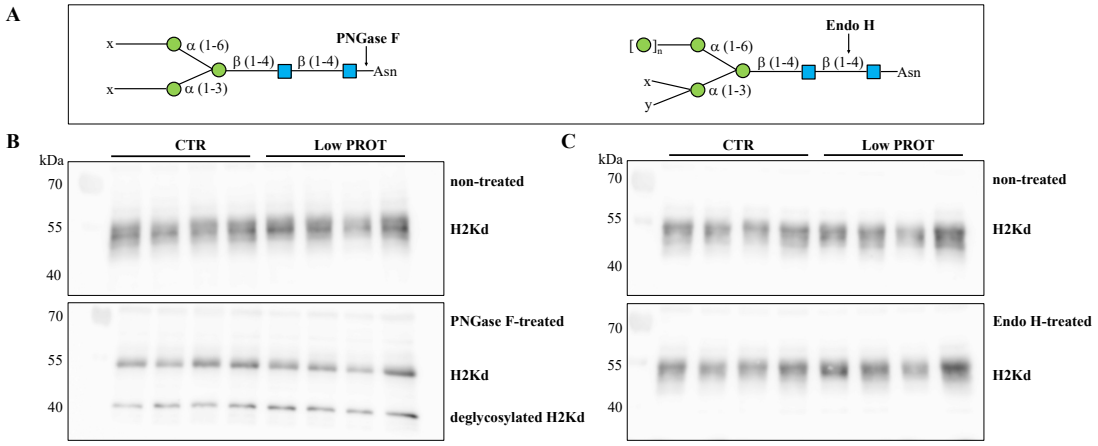

Figure 25. MHC-I is N-glycosylated

A. Scheme of the glycan specificity and cleavage site of PNGase F and Endo H based on the Glycoproteomics Technical Guide from New England Biolab. Asn, asparagine; blue square, GlcNAc; green circle, mannose; X, any sugar. B. Cell lysates treated with PNGase F (250 U and 80 U/ µg of protein) at 37 °C for 1 h. C. Cell lysates treated with Endo H (80 U/ µg of protein) at 37 °C for 1 h. Whole tumors from mice fed a CTR (n=4) or Low PROT diet (n=4) were used for glycosidase digestion.

Digestion of whole tumor lysates with PNGase F partially deglycosylated H2Kd (**Figure 25B**). The H2Kd signal of control samples appearing around 55 kDa became a sharper band at the same size while a second lower band was newly generated upon treatment. The lower band appearing around 40 kDa is likely to be the deglycosylated form of H2Kd which is reported to have a peptide molecular weight of 41 kDa by UniProtKB. However, the remaining band that appears around 55 kDa after PNGase F treatment might correspond to glycosylated forms of H2Kd that likely contain core α (1-3) fucose attached to the first GlcNAc moiety. PNGase F is not able to cleave if fucose is present. Whether H2Kd is only decorated with N-glycan structures, PNGase A treatment should fully deglycosylate H2Kd containing core fucose moieties. In contrast to PNGase F, H2Kd was insensible to digestion with Endo H (**Figure 25C**) revealing that H2Kd does not bear high oligo mannose structures which are more common of immature H2Kd proteins along their folding process in the ER

(Rudd et al., 2001). PNGase A treatment will be tested prior to detection of H2Kd in tumors. As a positive control, *in vitro* cultured tumor cells treated with tunicamycin must be included as a reference of fully deglycosylated H2Kd.

As compared to the role of glycosylation in MHC-I protein folding and antigenic peptide loading, knowledge of the mature N-glycan structures on MHC-I and their roles at the cell surface is more limited (Ryan and Cobb, 2012). Human MHC-I molecules have been described as bearing fucose-containing-sialylated complex (bi- and tri-antenna) types of N-glycans. In addition, high mannose structures have been detected in a lower expressed allotype which might be more critical for NK cell recognition (Ryan and Cobb, 2012). A more recent study has shown that sialylation of MHC-I on human DCs impairs its stability at the plasma membrane and associates with higher protein turnover and lower MHC-I half-life (Z. Silva et al., 2020). Desialylation of DCs increased their activating functions when co-cultured with autologous T lymphocytes based on higher synthesis of IFNγ by T cells. Desialylation, indeed, decreased the molecular weight of the heavy α chain of MHC-I with slight but appreciable changes in its molecular weight as visualized by Western blot. Importantly, desialylation of human colorectal adenocarcinoma cells did not increase the surface expression of MHC-I indicating that sialic acid on MHC-I expressed by these tumor cells if present it is not affecting MHC-I protein stability (Z. Silva et al., 2020). Beyond MHC-I glycosylation, antigenic glycopeptides containing mono- and disaccharide structures presented by MHC molecules have been identified in melanoma and leukemic cells (Moffett et al., 2021). Therefore, glycan modification not affecting the antigen processing and presenting machinery also contribute to immune recognition of tumor cells (Moffett et al., 2021).

In addition to MHC-I, PD-L1 was also higher expressed on Low PROT tumor cells (**Figure 26A**), likely as a consequence of IFNγ exposition within the TME (Topalian et al., 2016). Different to MHC-I, PD-L1 was fully deglycosylated upon PNGase F treatment (**Figure 26B**) as it has extensively described that PD-L1 bears complex types of N-glycans (Lee et al., 2019). It seems that PD-L1 does not contain core fucose moieties that limit the digestion with PNGase F. PD-L1 was insensible to treatment with Endo H (**Figure 26C**) confirming the presence of complex N-glycans on this immune marker. By searching in UniProtKB (Q9EP73), five N-linked glycosylation sites have been reported for mouse PD-L1 including Asn at positions 35, 191, 199, 218 and 236 while for human PD-L1 four N-glycosylation has been reported at Asn 35, 192, 200 and 219 (Li et al., 2016). Glycosylated human PD-L1 has been detected as a smear by Western blot with a molecular weight between 40 and 50 kDa (Li et al., 2016) reflecting fewer N-glycosylation sites as compared to mouse PD-L1 that appears between 55 and 70 kDa in our study (**Figure 26B, 26C**). The deglycosylated form of PD-L1

upon PNGase F digestion appears as a sharp band between 35 and 40 kDa which is near to the reported peptide molecular weight of 33 kDa and consistent with the molecular weight of deglycosylated human PD-L1 (Li et al., 2016).

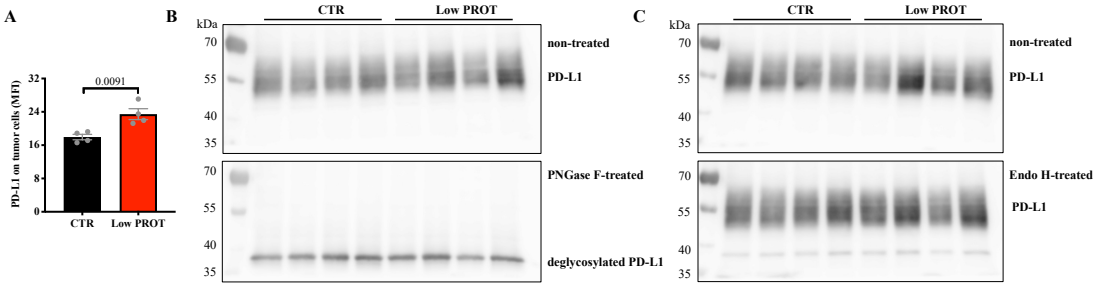

Figure 26. PD-L1 is fully N-glycosylated

A. Surface expression levels (MFI) of PD-L1 on tumor cells from mice fed a CTR (n=4) or a Low PROT (n=4) diet as detected by flow cytometry. B. Cell lysates were treated with PNGase F (80 U/ µg of protein) at 37 ℃ for 1 h. C. Cell lysates were treated with 1 µL of Endo H 80 U/ µg of protein) at 37 ℃ for 1 h. Whole tumors from mice fed a CTR (n=4) or Low PROT diet (n=4) were used for glycosidase digestion.

Detection of H2Kd and PD-L1 in non-treated samples (**Figure 25 and Figure 26**) showed that differences in molecular weight due to distinctive glycosylation trees between CTR and Low PROT tumors cannot be appreciated by Western blot. Indeed, detection of differential glycosylation patterns relying on differences in molecular weight requires massive changes of the glycan structures or changes in several glycan trees on the same protein depending on the number of glycosylation sites. Upon treatment with PNGase F, the deglycosylated form of H2Kd was slightly stronger in Low PROT than in CTR tumors. This might suggest that core fucose moieties at the N-glycan trees are likely less predominant under Low PROT diet. Treatment with other O-glycosidases beyond PNGase A might bring insight into O-glycan modifications of H2Kd, although this has not been reported.

PD-L1 expression is regulated at transcriptional, post-transcriptional, post-translational and extracellular levels (Cha et al., 2019). PD-L1 protein PTM-mediated stability is dependent on N-glycosylation. As for MHC-I and other secreted proteins along the secretory pathway, PD-L1 glycosylation starts in the ER for proper protein folding. Interaction with PD1 is mediated by poly-N-acetyllactosamine extensions on some N-glycosylation sites (Cha et al., 2019). In human tumor cells, PD-L1 has been demonstrated to carry extensive complex type of N-glycans in the extracellular domain while not bearing O-glycans (Li et al., 2016). Glycosylated PD-L1 was shown to be stable for at least 16 h as compared to the fully deglycosylated form that was stable only for 4 h. Glycosylation of PD-L1 confers protection

against proteasomal degradation enhanced by GSK3β-mediated phosphorylation and subsequent ubiquitination. GSK3β-mediated PD-L1 destabilization has been shown to confer less immunosuppressive properties to breast tumor cells orthotopically implanted in immunocompetent mice while enhancing the infiltration of activated CTLs (Li et al., 2016).

Altogether, although we did not observe obvious changes in glycosylation on MHC-I and PD-L1 by Western blot, glycosylation of these immune markers is critical for their stability, expression on the cell surface and functions. Therefore, alternative to digestion with PNGase F or PNGase A that remove whole N-glycans, digestion with exoglycosidases such as neuraminidases removing terminal sialic acids, galactosidases, mannosidases and fucosidases with different specificities for the glycosidic linkage may provide insights of the glycan tree composition of H2Kd and PD-L1. However, visualization of changes upon removal of these saccharide moieties may result challenging by Western blot. As an alternative, glycoproteomics of purified H2Kd and PD-L1 may provide information of the glycan tree composition with the pitfall that the longest glycan structures can be missed out from the glycan profile. In addition, other immune markers that can be differentially expressed on Low PROT tumor cells are potential glyco-candidates that can be studied.

IV. Perspectives, a working model

As a **working model** (**Figure 27**), we suggest that beyond dietary reduction of proteins, higher abundance of fatty acids in Low PROT tumors might lead to transcriptional downregulation of OGT and OGA in tumor cells. The link between lipid metabolism and OGT activity has been commonly reported. However, dietary protein reduction could also be the trigger of OGT and OGA deregulation. To test whether higher dietary fat is connected to OGT/OGA downregulation, a tailored isocaloric diet can be designed increasing the content of fat in 20% while reducing carbohydrates and maintaining the same protein content. Decreased expression of OGT and OGA might be a consequence of a negative feedback mechanism to attenuate lipid synthesis since OGT has been shown to induce lipogenesis in several cancer mouse models. Lower expression of OGT and OGA might be linked to accumulation of UDP-GlcNAc which in turn leads to higher abundance of UDP-GalNAc and UDP-Glc. Accumulation of these nucleotide sugars could be involved in disturbances of glycosylation processes driven differential N- or O-glycosylation as well as putative synthesis of HA in Low PROT tumor cells. Noteworthy, HA deposition in the TME may also count for accumulation of UDP-GlcNAc and UDP-Glc in Low PROT tumors.

Differential glycosylation might be involved in higher tumor cell immunogenicity under Low PROT diet mediated by higher cell surface exposition of oligo mannose N-glycans and lower O-linked Tn epitopes. In parallel, the protein-restricted diet and likely independent of

OGT/OGA downregulation could activate the IRE1α pathway via lower levels of amino acids (Sahu et al., 2016) or by lipidic disturbances of the ER membrane. It is also plausible that the IRE1α signaling might be enhanced by higher content of UDP-sugars that can accumulate in the cytoplasm and the ER. IRE1α activation might have a positive impact on tumor cell tumorigenicity in a glycosylation-independent or dependent manner.

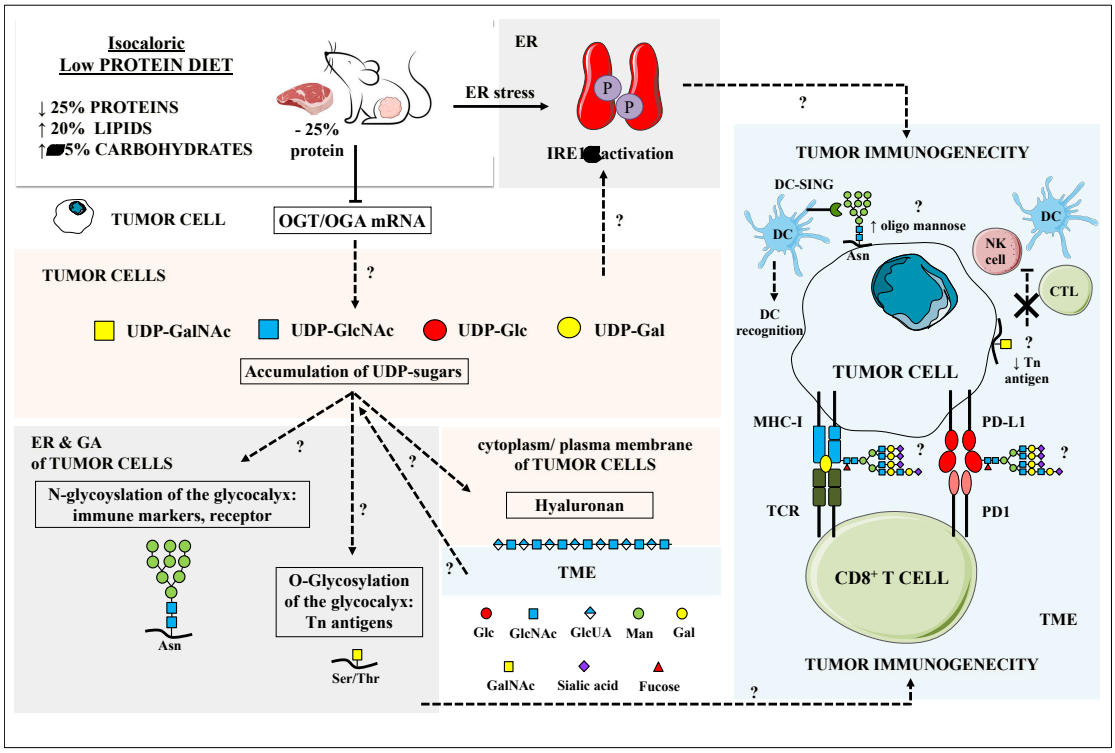

Figure 27. Hypothetic effects of the Low PROT diet on tumor cell immunogenicity

The Low PROT diet induces activation of the IRE1α pathway and transcriptional downregulation of OGT and OGA in tumor cells. Tumoral accumulation of UDP-sugars downstream of OGT/OGA lower expression can result in differential glycosylation of the tumor cell glycocalyx and HA production. Putative changes in tumor cell glycosylation associated with OGT and OGA downregulation and IRE1α activation may positively impact on tumor cell immunogenicity. Dashed lines and question marks represent putative cellular processes occurring within tumor cells, at the tumor cell surface and at the immunological synapse between tumor cells and immune cells within the TME. OGT, O-GlcNAc transferase; OGA, O-GlcNAcase; IRE1α, inositol-requiring protein 1α; ER, endoplasmic reticulum; GA, Golgi apparatus; CTL, cytotoxic T cell; DC, dendritic cell; NK cell, natural killer cell; Glc, glucose; GlcNAc, N-acetylglucosamine; GlcUA; glucuronic acid; Man, mannose; Gal, galactose; GalNAc, N-acetylgalactosamine

BIBLIOGRAPHY

Acosta-Alvear, D., Zhou, Y., Blais, A., Tsikitis, M., Lents, N.H., Arias, C., Lennon, C.J., Kluger, Y., Dynlacht, B.D., 2007. XBP1 Controls Diverse Cell Type- and Condition-Specific Transcriptional Regulatory Networks. Mol. Cell 27, 53–66. https://doi.org/10.1016/j.molcel.2007.06.011

Adibi, S.A., Modesto, T.A., Morse, E.L., Amin, P.M., 1973. Amino acid levels in plasma, liver, and skeletal muscle during protein deprivation. Am. J. Physiol. 225, 408–414. https://doi.org/10.1152/ajplegacy.1973.225.2.408

Akella, N.M., Ciraku, L., Reginato, M.J., 2019. Fueling the fire: emerging role of the hexosamine biosynthetic pathway in cancer. BMC Biol. 17, 52. https://doi.org/10.1186/s12915-019-0671-3

Antoniewicz, M.R., 2018. A guide to 13C metabolic flux analysis for the cancer biologist. Exp. Mol. Med. 50, 19. https://doi.org/10.1038/s12276-018-0060-y

Arnold, J.M., Gu, F., Ambati, C.R., Rasaily, U., Ramirez-Pena, E., Joseph, R., Manikkam, M., San Martin, R., Charles, C., Pan, Y., Chatterjee, S.S., Den Hollander, P., Zhang, W., Nagi, C., Sikora, A.G., Rowley, D., Putluri, N., Zhang, X.H.-F., Karanam, B., Mani, S.A., Sreekumar, A., 2020. UDP-glucose 6-dehydrogenase regulates hyaluronic acid production and promotes breast cancer progression. Oncogene 39, 3089–3101. https://doi.org/10.1038/s41388-019-0885-4

Aronica, A., Avagliano, L., Caretti, A., Tosi, D., Bulfamante, G.P., Trinchera, M., 2017. Unexpected distribution of CA19.9 and other type 1 chain Lewis antigens in normal and cancer tissues of colon and pancreas: Importance of the detection method and role of glycosyltransferase regulation. Biochim. Biophys. Acta BBA - Gen. Subj. 1861, 3210–3220. https://doi.org/10.1016/j.bbagen.2016.08.005

Axelrod, M.L., Cook, R.S., Johnson, D.B., Balko, J.M., 2019. Biological Consequences of MHC-II Expression by Tumor Cells in Cancer. Clin. Cancer Res. Off. J. Am. Assoc. Cancer Res. 25, 2392–2402. https://doi.org/10.1158/1078-0432.CCR-18-3200

Back, S.H., Kaufman, R.J., 2012. Endoplasmic Reticulum Stress and Type 2 Diabetes. Annu. Rev. Biochem. 81, 767–793. https://doi.org/10.1146/annurev-biochem-072909-095555

Bader, J.E., Voss, K., Rathmell, J.C., 2020. Targeting Metabolism to Improve the Tumor Microenvironment for Cancer Immunotherapy. Mol. Cell 78, 1019–1033. https://doi.org/10.1016/j.molcel.2020.05.034

Bhatia, R., Gautam, S.K., Cannon, A., Thompson, C., Hall, B.R., Aithal, A., Banerjee, K., Jain, M., Solheim, J.C., Kumar, S., Batra, S.K., 2019. Cancer-associated mucins: role in immune modulation and metastasis. Cancer Metastasis Rev. 38, 223–236. https://doi.org/10.1007/s10555-018-09775-0

Biwi, J., Biot, C., Guerardel, Y., Vercoutter-Edouart, A.-S., Lefebvre, T., 2018. The Many Ways by Which O-GlcNAcylation May Orchestrate the Diversity of Complex Glycosylations. Mol. Basel Switz. 23, E2858. https://doi.org/10.3390/molecules23112858

Blander, J.M., 2018. Regulation of the Cell Biology of Antigen Cross-Presentation. Annu. Rev. Immunol. 36, 717–753. https://doi.org/10.1146/annurev-immunol-041015-055523

Borst, J., Ahrends, T., Bąbała, N., Melief, C.J.M., Kastenmüller, W., 2018. CD4+ T cell help in cancer immunology and immunotherapy. Nat. Rev. Immunol. 18, 635–647. https://doi.org/10.1038/s41577-018-0044-0

Bourgin, M., Kepp, O., Kroemer, G., 2022. Immunostimulatory effects of vitamin B5 improve anticancer immunotherapy. Oncoimmunology 11, 2031500. https://doi.org/10.1080/2162402X.2022.2031500

Brandhorst, S., Wei, M., Hwang, S., Morgan, T.E., Longo, V.D., 2013. Short-term calorie and protein restriction provide partial protection from chemotoxicity but do not delay glioma progression. Exp. Gerontol., Calorie Restriction and Fasting; Challenges and Future Directions for Research 48, 1120–1128. https://doi.org/10.1016/j.exger.2013.02.016

Bray, F., Ferlay, J., Soerjomataram, I., Siegel, R.L., Torre, L.A., Jemal, A., 2018. Global cancer statistics 2018: GLOBOCAN estimates of incidence and mortality worldwide for 36 cancers in 185 countries. CA. Cancer J. Clin. 68, 394–424. https://doi.org/10.3322/caac.21492

Buck, M.D., Sowell, R.T., Kaech, S.M., Pearce, E.L., 2017. Metabolic Instruction of Immunity. Cell 169, 570–586. https://doi.org/10.1016/j.cell.2017.04.004

Bujisic, B., De Gassart, A., Tallant, R., Demaria, O., Zaffalon, L., Chelbi, S., Gilliet, M., Bertoni, F., Martinon, F., 2017. Impairment of both IRE1 expression and XBP1 activation is a hallmark of GCB DLBCL and contributes to tumor growth. Blood 129, 2420–2428. https://doi.org/10.1182/blood-2016-09-741348

Büll, C., Stoel, M.A., den Brok, M.H., Adema, G.J., 2014. Sialic acids sweeten a tumor's life. Cancer Res. 74, 3199–3204. https://doi.org/10.1158/0008-5472.CAN-14-0728

Buono, R., Longo, V.D., 2018. Starvation, Stress Resistance, and Cancer. Trends Endocrinol. Metab. 29, 271–280. https://doi.org/10.1016/j.tem.2018.01.008

Burr, M.L., Sparbier, C.E., Chan, K.L., Chan, Y.-C., Kersbergen, A., Lam, E.Y.N., Azidis-Yates, E., Vassiliadis, D., Bell, C.C., Gilan, O., Jackson, S., Tan, L., Wong, S.Q., Hollizeck, S., Michalak, E.M., Siddle, H.V., McCabe, M.T., Prinjha, R.K., Guerra, G.R., Solomon, B.J., Sandhu, S., Dawson, S.-J., Beavis, P.A., Tothill, R.W., Cullinane, C., Lehner, P.J., Sutherland, K.D., Dawson, M.A., 2019. An Evolutionarily Conserved Function of Polycomb Silences the MHC Class I Antigen Presentation Pathway and Enables Immune Evasion in Cancer. Cancer Cell 36, 385-401.e8. https://doi.org/10.1016/j.ccell.2019.08.008

Cai, Y., Chen, T., Liu, J., Peng, S., Liu, H., Lv, M., Ding, Z., Zhou, Z., Li, L., Zeng, S., Xiao, E., 2022. Orthotopic Versus Allotopic Implantation: Comparison of Radiological and Pathological Characteristics. J. Magn. Reson. Imaging JMRI 55, 1133–1140. https://doi.org/10.1002/jmri.27940

Campbell, S., Mesaros, C., Izzo, L., Affronti, H., Noji, M., Schaffer, B.E., Tsang, T., Sun, K., Trefely, S., Kruijning, S., Blenis, J., Blair, I.A., Wellen, K.E., 2021. Glutamine deprivation triggers NAGK-dependent hexosamine salvage. eLife 10, e62644. https://doi.org/10.7554/eLife.62644

Caon, I., Bartolini, B., Parnigoni, A., Caravà, E., Moretto, P., Viola, M., Karousou, E., Vigetti, D., Passi, A., 2020. Revisiting the hallmarks of cancer: The role of hyaluronan. Semin. Cancer Biol. 62, 9–19. https://doi.org/10.1016/j.semcancer.2019.07.007

Carreras-Sureda, A., Jaña, F., Urra, H., Durand, S., Mortenson, D.E., Sagredo, A., Bustos, G., Hazari, Y., Ramos-Fernández, E., Sassano, M.L., Pihán, P., Vliet, A.R. van, González-Quiroz, M., Torres, A.K., Tapia-Rojas, C., Kerkhofs, M., Vicente, R., Kaufman, R.J., Inestrosa, N.C., Gonzalez-Billault, C., Wiseman, R.L., Agostinis, P., Bultynck, G., Court, F.A., Kroemer, G., Cárdenas, J.C., Hetz, C., 2019. Non-canonical function of IRE1α determines mitochondria-associated endoplasmic

reticulum composition to control calcium transfer and bioenergetics. Nat. Cell Biol. 21, 755–767. https://doi.org/10.1038/s41556-019-0329-y

Cassetta, L., Pollard, J.W., 2018. Targeting macrophages: therapeutic approaches in cancer. Nat. Rev. Drug Discov. 17, 887–904. https://doi.org/10.1038/nrd.2018.169

Castillo, K., Rojas-Rivera, D., Lisbona, F., Caballero, B., Nassif, M., Court, F.A., Schuck, S., Ibar, C., Walter, P., Sierralta, J., Glavic, A., Hetz, C., 2011. BAX inhibitor-1 regulates autophagy by controlling the IRE1α branch of the unfolded protein response. EMBO J. 30, 4465–4478. https://doi.org/10.1038/emboj.2011.318

Cha, J.-H., Chan, L.-C., Li, C.-W., Hsu, J.L., Hung, M.-C., 2019. Mechanisms Controlling PD-L1 Expression in Cancer. Mol. Cell 76, 359–370. https://doi.org/10.1016/j.molcel.2019.09.030

Chandler, K.B., Costello, C.E., Rahimi, N., 2019. Glycosylation in the Tumor Microenvironment: Implications for Tumor Angiogenesis and Metastasis. Cells 8. https://doi.org/10.3390/cells8060544

Chen, X., Iliopoulos, D., Zhang, Q., Tang, Q., Greenblatt, M.B., Hatziapostolou, M., Lim, E., Tam, W.L., Ni, M., Chen, Y., Mai, J., Shen, H., Hu, D.Z., Adoro, S., Hu, B., Song, M., Tan, C., Landis, M.D., Ferrari, M., Shin, S.J., Brown, M., Chang, J.C., Liu, X.S., Glimcher, L.H., 2014. XBP1 promotes triple-negative breast cancer by controlling the HIF1α pathway. Nature 508, 103–107. https://doi.org/10.1038/nature13119

Chiaradonna, F., Ricciardiello, F., Palorini, R., 2018. The Nutrient-Sensing Hexosamine Biosynthetic Pathway as the Hub of Cancer Metabolic Rewiring. Cells 7. https://doi.org/10.3390/cells7060053

Chipurupalli, S., Kannan, E., Tergaonkar, V., D'Andrea, R., Robinson, N., 2019. Hypoxia Induced ER Stress Response as an Adaptive Mechanism in Cancer. Int. J. Mol. Sci. 20. https://doi.org/10.3390/ijms20030749

Chokchaitaweesuk, C., Kobayashi, T., Izumikawa, T., Itano, N., 2019. Enhanced hexosamine metabolism drives metabolic and signaling networks involving hyaluronan production and O-GlcNAcylation to exacerbate breast cancer. Cell Death Dis. 10, 1–15. https://doi.org/10.1038/s41419-019-2034-y

Condamine, T., Dominguez, G.A., Youn, J.-I., Kossenkov, A.V., Mony, S., Alicea-Torres, K., Tcyganov, E., Hashimoto, A., Nefedova, Y., Lin, C., Partlova, S., Garfall, A., Vogl, D.T., Xu, X., Knight, S.C., Malietzis, G., Lee, G.H., Eruslanov, E., Albelda, S.M., Wang, X., Mehta, J.L., Bewtra, M., Rustgi, A., Hockstein, N., Witt, R., Masters, G., Nam, B., Smirnov, D., Sepulveda, M.A., Gabrilovich, D.I., 2016. Lectin-type oxidized LDL receptor-1 distinguishes population of human polymorphonuclear myeloid-derived suppressor cells in cancer patients. Sci. Immunol. 1. https://doi.org/10.1126/sciimmunol.aaf8943

Costa-Mattioli, M., Walter, P., 2020. The integrated stress response: From mechanism to disease. Science 368. https://doi.org/10.1126/science.aat5314

Covino, R., Hummer, G., Ernst, R., 2018. Integrated Functions of Membrane Property Sensors and a Hidden Side of the Unfolded Protein Response. Mol. Cell 71, 458–467. https://doi.org/10.1016/j.molcel.2018.07.019

Croci, D.O., Cerliani, J.P., Dalotto-Moreno, T., Méndez-Huergo, S.P., Mascanfroni, I.D., Dergan-Dylon, S., Toscano, M.A., Caramelo, J.J., García-Vallejo, J.J., Ouyang, J., Mesri, E.A., Junttila, M.R., Bais, C., Shipp, M.A., Salatino, M., Rabinovich, G.A., 2014. Glycosylation-dependent lectin-receptor interactions preserve angiogenesis in anti-VEGF refractory tumors. Cell 156, 744–758. https://doi.org/10.1016/j.cell.2014.01.043

Cubillos-Ruiz, J.R., Bettigole, S.E., Glimcher, L.H., 2017. Tumorigenic and Immunosuppressive Effects of Endoplasmic Reticulum Stress in Cancer. Cell 168, 692–706. https://doi.org/10.1016/j.cell.2016.12.004

Cubillos-Ruiz, J.R., Silberman, P.C., Rutkowski, M.R., Chopra, S., Perales-Puchalt, A., Song, M., Zhang, S., Bettigole, S.E., Gupta, D., Holcomb, K., Ellenson, L.H., Caputo, T., Lee, A.-H., Conejo-Garcia, J.R., Glimcher, L.H., 2015. ER Stress Sensor XBP1 Controls Anti-tumor Immunity by Disrupting Dendritic Cell Homeostasis. Cell 161, 1527–1538. https://doi.org/10.1016/j.cell.2015.05.025

Daly, J., Carlsten, M., O'Dwyer, M., 2019. Sugar Free: Novel Immunotherapeutic Approaches Targeting Siglecs and Sialic Acids to Enhance Natural Killer Cell Cytotoxicity Against Cancer. Front. Immunol. 10, 1047. https://doi.org/10.3389/fimmu.2019.01047

De Bousser, E., Meuris, L., Callewaert, N., Festjens, N., 2020. Human T cell glycosylation and implications on immune therapy for cancer. Hum. Vaccines Immunother. 16, 2374–2388. https://doi.org/10.1080/21645515.2020.1730658

De Feyter, H.M., Behar, K.L., Rao, J.U., Madden-Hennessey, K., Ip, K.L., Hyder, F., Drewes, L.R., Geschwind, J.-F., de Graaf, R.A., Rothman, D.L., 2016. A ketogenic diet increases transport and oxidation of ketone bodies in RG2 and 9L gliomas without affecting tumor growth. Neuro-Oncol. 18, 1079–1087. https://doi.org/10.1093/neuonc/now088

de Groot, S., Lugtenberg, R.T., Cohen, D., Welters, M.J.P., Ehsan, I., Vreeswijk, M.P.G., Smit, V.T.H.B.M., de Graaf, H., Heijns, J.B., Portielje, J.E.A., van de Wouw, A.J., Imholz, A.L.T., Kessels, L.W., Vrijaldenhoven, S., Baars, A., Kranenbarg, E.M.-K., Carpentier, M.D., Putter, H., van der Hoeven, J.J.M., Nortier, J.W.R., Longo, V.D., Pijl, H., Kroep, J.R., Dutch Breast Cancer Research Group (BOOG), 2020. Fasting mimicking diet as an adjunct to neoadjuvant chemotherapy for breast cancer in the multicentre randomized phase 2 DIRECT trial. Nat. Commun. 11, 3083. https://doi.org/10.1038/s41467-020-16138-3

Dejure, F.R., Eilers, M., 2017. MYC and tumor metabolism: chicken and egg. EMBO J. 36, 3409–3420. https://doi.org/10.15252/embj.201796438

Denzel, M.S., Storm, N.J., Gutschmidt, A., Baddi, R., Hinze, Y., Jarosch, E., Sommer, T., Hoppe, T., Antebi, A., 2014. Hexosamine pathway metabolites enhance protein quality control and prolong life. Cell 156, 1167–1178. https://doi.org/10.1016/j.cell.2014.01.061

Depil, S., Duchateau, P., Grupp, S.A., Mufti, G., Poirot, L., 2020. 'Off-the-shelf' allogeneic CAR T cells: development and challenges. Nat. Rev. Drug Discov. 19, 185–199. https://doi.org/10.1038/s41573-019-0051-2

Dey, P., Kimmelman, A.C., DePinho, R.A., 2021. Metabolic Codependencies in the Tumor Microenvironment. Cancer Discov. 11, 1067–1081. https://doi.org/10.1158/2159-8290.CD-20-1211

Dierge, E., Debock, E., Guilbaud, C., Corbet, C., Mignolet, E., Mignard, L., Bastien, E., Dessy, C., Larondelle, Y., Feron, O., 2021. Peroxidation of n-3 and n-6 polyunsaturated fatty acids in the acidic tumor environment leads to ferroptosis-mediated anticancer effects. Cell Metab. 33, 1701-1715.e5. https://doi.org/10.1016/j.cmet.2021.05.016

Dolina, J.S., Van Braeckel-Budimir, N., Thomas, G.D., Salek-Ardakani, S., 2021. CD8+ T Cell Exhaustion in Cancer. Front. Immunol. 12, 715234. https://doi.org/10.3389/fimmu.2021.715234

Dong, H., Adams, N.M., Xu, Y., Cao, J., Allan, D.S.J., Carlyle, J.R., Chen, X., Sun, J.C., Glimcher, L.H., 2019. The IRE1 ER stress sensor activates natural killer cell immunity in part by regulating c-Myc. Nat. Immunol. 20, 865–878. https://doi.org/10.1038/s41590-019-0388-z

Dorrington, M.G., Fraser, I.D.C., 2019. NF-κB Signaling in Macrophages: Dynamics, Crosstalk, and Signal Integration. Front. Immunol. 10, 705. https://doi.org/10.3389/fimmu.2019.00705

Drosten, M., Barbacid, M., 2020. Targeting the MAPK Pathway in KRAS-Driven Tumors. Cancer Cell 37, 543–550. https://doi.org/10.1016/j.ccell.2020.03.013

Dunn, G.P., Old, L.J., Schreiber, R.D., 2004. The three Es of cancer immunoediting. Annu. Rev. Immunol. 22, 329–360. https://doi.org/10.1146/annurev.immunol.22.012703.104803

Fallarino, F., Grohmann, U., You, S., McGrath, B.C., Cavener, D.R., Vacca, C., Orabona, C., Bianchi, R., Belladonna, M.L., Volpi, C., Santamaria, P., Fioretti, M.C., Puccetti, P., 2006. The Combined Effects of Tryptophan Starvation and Tryptophan Catabolites Down-Regulate T Cell Receptor ζ-Chain and Induce a Regulatory Phenotype in Naive T Cells. J. Immunol. 176, 6752–6761. https://doi.org/10.4049/jimmunol.176.11.6752

Fang, J.Y., Richardson, B.C., 2005. The MAPK signalling pathways and colorectal cancer. Lancet Oncol. 6, 322–327. https://doi.org/10.1016/S1470-2045(05)70168-6

Faubert, B., DeBerardinis, R.J., 2017. Analyzing Tumor Metabolism In Vivo. Annu. Rev. Cancer Biol. 1, 99–117. https://doi.org/10.1146/annurev-cancerbio-050216-121954

Faubert, B., Solmonson, A., DeBerardinis, R.J., 2020. Metabolic reprogramming and cancer progression. Science 368. https://doi.org/10.1126/science.aaw5473

Fernández-García, J., Altea-Manzano, P., Pranzini, E., Fendt, S.-M., 2020. Stable Isotopes for Tracing Mammalian-Cell Metabolism In Vivo. Trends Biochem. Sci. 45, 185–201. https://doi.org/10.1016/j.tibs.2019.12.002

Ferrer, C.M., Lu, T.Y., Bacigalupa, Z.A., Katsetos, C.D., Sinclair, D.A., Reginato, M.J., 2017. O-GlcNAcylation regulates breast cancer metastasis via SIRT1 modulation of FOXM1 pathway. Oncogene 36, 559–569. https://doi.org/10.1038/onc.2016.228

Ferrer, C.M., Lynch, T.P., Sodi, V.L., Falcone, J.N., Schwab, L.P., Peacock, D.L., Vocadlo, D.J., Seagroves, T.N., Reginato, M.J., 2014. O-GlcNAcylation Regulates Cancer Metabolism and Survival Stress Signaling via Regulation of the HIF-1 Pathway. Mol. Cell 54, 820–831. https://doi.org/10.1016/j.molcel.2014.04.026

Fontana, L., Adelaiye, R.M., Rastelli, A.L., Miles, K.M., Ciamporcero, E., Longo, V.D., Nguyen, H., Vessella, R., Pili, R., 2013. Dietary protein restriction inhibits tumor growth in human xenograft models. Oncotarget 4, 2451–2461. https://doi.org/10.18632/oncotarget.1586

Gameiro, P.A., Struhl, K., 2018. Nutrient Deprivation Elicits a Transcriptional and Translational Inflammatory Response Coupled to Decreased Protein Synthesis. Cell Rep. 24, 1415–1424. https://doi.org/10.1016/j.celrep.2018.07.021

Gao, Q., Li, X., Xu, Y., Zhang, J., Rong, S., Qin, Y., Fang, J., 2020. IRE1α-targeting downregulates ABC transporters and overcomes drug resistance of colon cancer cells. Cancer Lett. 476, 67–74. https://doi.org/10.1016/j.canlet.2020.02.007

Gao, X., Sanderson, S.M., Dai, Z., Reid, M.A., Cooper, D.E., Lu, M., Richie, J.P., Ciccarella, A., Calcagnotto, A., Mikhael, P.G., Mentch, S.J., Liu, J., Ables, G., Kirsch, D.G., Hsu, D.S., Nichenametla, S.N., Locasale, J.W., 2019. Dietary methionine influences

therapy in mouse cancer models and alters human metabolism. Nature 572, 397–401. https://doi.org/10.1038/s41586-019-1437-3

Garcia-Bermudez, J., Williams, R.T., Guarecuco, R., Birsoy, K., 2020. Targeting extracellular nutrient dependencies of cancer cells. Mol. Metab., Cancer Metabolism 33, 67–82. https://doi.org/10.1016/j.molmet.2019.11.011

Garg, A.D., More, S., Rufo, N., Mece, O., Sassano, M.L., Agostinis, P., Zitvogel, L., Kroemer, G., Galluzzi, L., 2017. Trial watch: Immunogenic cell death induction by anticancer chemotherapeutics. OncoImmunology 6, e1386829. https://doi.org/10.1080/2162402X.2017.1386829

Garlapati, C., Joshi, S., Turaga, R.C., Mishra, M., Reid, M.D., Kapoor, S., Artinian, L., Rehder, V., Aneja, R., 2021. Monoethanolamine-induced glucose deprivation promotes apoptosis through metabolic rewiring in prostate cancer. Theranostics 11, 9089–9106. https://doi.org/10.7150/thno.62724

Genovese, G., Carugo, A., Tepper, J., Robinson, F.S., Li, L., Svelto, M., Nezi, L., Corti, D., Minelli, R., Pettazzoni, P., Gutschner, T., Wu, C.-C., Seth, S., Akdemir, K.C., Leo, E., Amin, S., Molin, M.D., Ying, H., Kwong, L.N., Colla, S., Takahashi, K., Ghosh, P., Giuliani, V., Muller, F., Dey, P., Jiang, S., Garvey, J., Liu, C.-G., Zhang, J., Heffernan, T.P., Toniatti, C., Fleming, J.B., Goggins, M.G., Wood, L.D., Sgambato, A., Agaimy, A., Maitra, A., Roberts, C.W.M., Wang, H., Viale, A., DePinho, R.A., Draetta, G.F., Chin, L., 2017. Synthetic vulnerabilities of mesenchymal subpopulations in pancreatic cancer. Nature 542, 362–366. https://doi.org/10.1038/nature21064

Ghasempour, S., Freeman, S.A., 2021. The glycocalyx and immune evasion in cancer. FEBS J. https://doi.org/10.1111/febs.16236

Grandjean, J.M.D., Madhavan, A., Cech, L., Seguinot, B.O., Paxman, R.J., Smith, E., Scampavia, L., Powers, E.T., Cooley, C.B., Plate, L., Spicer, T.P., Kelly, J.W., Wiseman, R.L., 2020. Pharmacologic IRE1/XBP1s activation confers targeted ER proteostasis reprogramming. Nat. Chem. Biol. 16, 1052–1061. https://doi.org/10.1038/s41589-020-0584-z

Grima-Reyes, M., Martinez-Turtos, A., Abramovich, I., Gottlieb, E., Chiche, J., Ricci, J.-E., 2021. Physiological impact of in vivo stable isotope tracing on cancer metabolism. Mol. Metab. 53, 101294. https://doi.org/10.1016/j.molmet.2021.101294

Guillerey, C., Huntington, N.D., Smyth, M.J., 2016. Targeting natural killer cells in cancer immunotherapy. Nat. Immunol. 17, 1025–1036. https://doi.org/10.1038/ni.3518

Guo, H., Zhang, B., Nairn, A.V., Nagy, T., Moremen, K.W., Buckhaults, P., Pierce, M., 2017. O-Linked N-Acetylglucosamine (O-GlcNAc) Expression Levels Epigenetically Regulate Colon Cancer Tumorigenesis by Affecting the Cancer Stem Cell Compartment via Modulating Expression of Transcriptional Factor MYBL1*. J. Biol. Chem. 292, 4123–4137. https://doi.org/10.1074/jbc.M116.763201

Han, D., Lerner, A.G., Vande Walle, L., Upton, J.-P., Xu, W., Hagen, A., Backes, B.J., Oakes, S.A., Papa, F.R., 2009. IRE1alpha kinase activation modes control alternate endoribonuclease outputs to determine divergent cell fates. Cell 138, 562–575. https://doi.org/10.1016/j.cell.2009.07.017

Han, J., Khatwani, N., Searles, T.G., Turk, M.J., Angeles, C.V., 2020. Memory CD8+ T cell responses to cancer. Semin. Immunol. 49, 101435. https://doi.org/10.1016/j.smim.2020.101435

Hanahan, D., 2022. Hallmarks of Cancer: New Dimensions. Cancer Discov. 12, 31–46. https://doi.org/10.1158/2159-8290.CD-21-1059

Hanahan, D., Weinberg, R.A., 2011. Hallmarks of cancer: the next generation. Cell 144, 646–674. https://doi.org/10.1016/j.cell.2011.02.013

Hanover, J.A., Chen, W., Bond, M.R., 2018. O-GlcNAc in cancer: An Oncometabolism-fueled vicious cycle. J. Bioenerg. Biomembr. 50, 155–173. https://doi.org/10.1007/s10863-018-9751-2

Harnoss, J.M., Le Thomas, A., Reichelt, M., Guttman, O., Wu, T.D., Marsters, S.A., Shemorry, A., Lawrence, D.A., Kan, D., Segal, E., Merchant, M., Totpal, K., Crocker, L.M., Mesh, K., Dohse, M., Solon, M., Modrusan, Z., Rudolph, J., Koeppen, H., Walter, P., Ashkenazi, A., 2020. IRE1α disruption in triple-negative breast cancer cooperates with anti-angiogenic therapy by reversing ER stress adaptation and remodeling the tumor microenvironment. Cancer Res. https://doi.org/10.1158/0008-5472.CAN-19-3108

Hetz, C., Papa, F.R., 2018. The Unfolded Protein Response and Cell Fate Control. Mol. Cell 69, 169–181. https://doi.org/10.1016/j.molcel.2017.06.017

Hetz, C., Zhang, K., Kaufman, R.J., 2020. Mechanisms, regulation and functions of the unfolded protein response. Nat. Rev. Mol. Cell Biol. 21, 421–438. https://doi.org/10.1038/s41580-020-0250-z

Hosios, A.M., Hecht, V.C., Danai, L.V., Johnson, M.O., Rathmell, J.C., Steinhauser, M.L., Manalis, S.R., Vander Heiden, M.G., 2016. Amino acids rather than glucose account for the majority of cell mass in proliferating mammalian cells. Dev. Cell 36, 540–549. https://doi.org/10.1016/j.devcel.2016.02.012

Hou, J., Karin, M., Sun, B., 2021. Targeting cancer-promoting inflammation - have anti-inflammatory therapies come of age? Nat. Rev. Clin. Oncol. 18, 261–279. https://doi.org/10.1038/s41571-020-00459-9

Hu, P., Han, Z., Couvillon, A.D., Kaufman, R.J., Exton, J.H., 2006. Autocrine Tumor Necrosis Factor Alpha Links Endoplasmic Reticulum Stress to the Membrane Death Receptor Pathway through IRE1α-Mediated NF-κB Activation and Down-Regulation of TRAF2 Expression. Mol. Cell. Biol. 26, 3071–3084. https://doi.org/10.1128/MCB.26.8.3071-3084.2006

Hui, S., Cowan, A.J., Zeng, X., Yang, L., TeSlaa, T., Li, X., Bartman, C., Zhang, Z., Jang, C., Wang, L., Lu, W., Rojas, J., Baur, J., Rabinowitz, J.D., 2020. Quantitative Fluxomics of Circulating Metabolites. Cell Metab. 32, 676-688.e4. https://doi.org/10.1016/j.cmet.2020.07.013

Jang, C., Chen, L., Rabinowitz, J.D., 2018. Metabolomics and Isotope Tracing. Cell 173, 822–837. https://doi.org/10.1016/j.cell.2018.03.055

Jiang, M., Xu, B., Li, X., Shang, Y., Chu, Y., Wang, W., Chen, D., Wu, N., Hu, S., Zhang, S., Li, M., Wu, K., Yang, X., Liang, J., Nie, Y., Fan, D., 2019. O-GlcNAcylation promotes colorectal cancer metastasis via the miR-101-O-GlcNAc/EZH2 regulatory feedback circuit. Oncogene 38, 301–316. https://doi.org/10.1038/s41388-018-0435-5

Jiang, Z., Zhang, G., Huang, L., Yuan, Y., Wu, C., Li, Y., 2020. Transmissible Endoplasmic Reticulum Stress: A Novel Perspective on Tumor Immunity. Front. Cell Dev. Biol. 8, 846. https://doi.org/10.3389/fcell.2020.00846

Kamata, S., Yamamoto, J., Kamijo, K., Ochiai, T., Morita, T., Yoshitomi, Y., Hagiya, Y., Kubota, M., Ohkubo, R., Kawaguchi, M., Himi, T., Kasahara, T., Ishii, I., 2014. Dietary deprivation of each essential amino acid induces differential systemic adaptive responses in mice. Mol. Nutr. Food Res. 58, 1309–1321. https://doi.org/10.1002/mnfr.201300758

Kanarek, N., Petrova, B., Sabatini, D.M., 2020. Dietary modifications for enhanced cancer therapy. Nature 579, 507–517. https://doi.org/10.1038/s41586-020-2124-0

Kaushik, A.K., DeBerardinis, R.J., 2018. Applications of Metabolomics to Study Cancer Metabolism. Biochim. Biophys. Acta Rev. Cancer 1870, 2–14. https://doi.org/10.1016/j.bbcan.2018.04.009

Kazama, H., Ricci, J.-E., Herndon, J.M., Hoppe, G., Green, D.R., Ferguson, T.A., 2008. Induction of immunological tolerance by apoptotic cells requires caspase-dependent oxidation of high-mobility group box-1 protein. Immunity 29, 21–32. https://doi.org/10.1016/j.immuni.2008.05.013

Keum, N., Giovannucci, E., 2019. Global burden of colorectal cancer: emerging trends, risk factors and prevention strategies. Nat. Rev. Gastroenterol. Hepatol. 16, 713–732. https://doi.org/10.1038/s41575-019-0189-8

Kim, Jiyeon, Lee, H.M., Cai, F., Ko, B., Yang, C., Lieu, E.L., Muhammad, N., Rhyne, S., Li, K., Haloul, M., Gu, W., Faubert, B., Kaushik, A.K., Cai, L., Kasiri, S., Marriam, U., Nham, K., Girard, L., Wang, H., Sun, X., Kim, James, Minna, J.D., Unsal-Kacmaz, K., DeBerardinis, R.J., 2020. The hexosamine biosynthesis pathway is a targetable liability in KRAS/LKB1 mutant lung cancer. Nat. Metab. 2, 1401–1412. https://doi.org/10.1038/s42255-020-00316-0

Kim, P.K., Halbrook, C.J., Kerk, S.A., Radyk, M., Wisner, S., Kremer, D.M., Sajjakulnukit, P., Andren, A., Hou, S.W., Trivedi, A., Thurston, G., Anand, A., Yan, L., Salamanca-Cardona, L., Welling, S.D., Zhang, L., Pratt, M.R., Keshari, K.R., Ying, H., Lyssiotis, C.A., 2021. Hyaluronic acid fuels pancreatic cancer cell growth. eLife 10, e62645. https://doi.org/10.7554/eLife.62645

Klement, R.J., 2020. Addressing the controversial role of ketogenic diets in cancer treatment. Expert Rev. Anticancer Ther. 1–4. https://doi.org/10.1080/14737140.2020.1747438

Klement, R.J., 2017. Beneficial effects of ketogenic diets for cancer patients: a realist review with focus on evidence and confirmation. Med. Oncol. Northwood Lond. Engl. 34, 132. https://doi.org/10.1007/s12032-017-0991-5

Koppenol, W.H., Bounds, P.L., Dang, C.V., 2011. Otto Warburg's contributions to current concepts of cancer metabolism. Nat. Rev. Cancer 11, 325–337. https://doi.org/10.1038/nrc3038

Kroemer, G., Mariño, G., Levine, B., 2010. Autophagy and the integrated stress response. Mol. Cell 40, 280–293. https://doi.org/10.1016/j.molcel.2010.09.023

Krysko, D.V., Garg, A.D., Kaczmarek, A., Krysko, O., Agostinis, P., Vandenabeele, P., 2012. Immunogenic cell death and DAMPs in cancer therapy. Nat. Rev. Cancer 12, 860–875. https://doi.org/10.1038/nrc3380

Kumagai, S., Koyama, S., Itahashi, K., Tanegashima, T., Lin, Y.-T., Togashi, Y., Kamada, T., Irie, T., Okumura, G., Kono, H., Ito, D., Fujii, R., Watanabe, S., Sai, A., Fukuoka, S., Sugiyama, E., Watanabe, G., Owari, T., Nishinakamura, H., Sugiyama, D., Maeda, Y., Kawazoe, A., Yukami, H., Chida, K., Ohara, Y., Yoshida, T., Shinno, Y., Takeyasu, Y., Shirasawa, M., Nakama, K., Aokage, K., Suzuki, J., Ishii, G., Kuwata, T., Sakamoto, N., Kawazu, M., Ueno, T., Mori, T., Yamazaki, N., Tsuboi, M., Yatabe, Y., Kinoshita, T., Doi, T., Shitara, K., Mano, H., Nishikawa, H., 2022. Lactic acid promotes PD-1 expression in regulatory T cells in highly glycolytic tumor microenvironments. Cancer Cell 40, 201-218.e9. https://doi.org/10.1016/j.ccell.2022.01.001

Kurmi, K., Haigis, M.C., 2020. Nitrogen Metabolism in Cancer and Immunity. Trends Cell Biol. 30, 408–424. https://doi.org/10.1016/j.tcb.2020.02.005

Lam, C., Low, J.-Y., Tran, P.T., Wang, H., 2021. The hexosamine biosynthetic pathway and cancer: Current knowledge and future therapeutic strategies. Cancer Lett. 503, 11–18. https://doi.org/10.1016/j.canlet.2021.01.010

Lane, A.N., Higashi, R.M., Fan, T.W.-M., 2020. Metabolic reprogramming in tumors: Contributions of the tumor microenvironment. Genes Dis. 7, 185–198. https://doi.org/10.1016/j.gendis.2019.10.007

Lee, C., Raffaghello, L., Brandhorst, S., Safdie, F.M., Bianchi, G., Martin-Montalvo, A., Pistoia, V., Wei, M., Hwang, S., Merlino, A., Emionite, L., Cabo, R. de, Longo, V.D., 2012. Fasting Cycles Retard Growth of Tumors and Sensitize a Range of Cancer Cell Types to Chemotherapy. Sci. Transl. Med. 4, 124ra27-124ra27. https://doi.org/10.1126/scitranslmed.3003293

Lee, H.-H., Wang, Y.-N., Xia, W., Chen, C.-H., Rau, K.-M., Ye, L., Wei, Y., Chou, C.-K., Wang, S.-C., Yan, M., Tu, C.-Y., Hsia, T.-C., Chiang, S.-F., Chao, K.S.C., Wistuba, I.I., Hsu, J.L., Hortobagyi, G.N., Hung, M.-C., 2019. Removal of N-Linked Glycosylation Enhances PD-L1 Detection and Predicts Anti-PD-1/PD-L1 Therapeutic Efficacy. Cancer Cell 36, 168-178.e4. https://doi.org/10.1016/j.ccell.2019.06.008

Lee, M.B., Hill, C.M., Bitto, A., Kaeberlein, M., 2021. Antiaging diets: Separating fact from fiction. Science 374, eabe7365. https://doi.org/10.1126/science.abe7365

Lerner, A.G., Upton, J.-P., Praveen, P.V.K., Ghosh, R., Nakagawa, Y., Igbaria, A., Shen, S., Nguyen, V., Backes, B.J., Heiman, M., Heintz, N., Greengard, P., Hui, S., Tang, Q., Trusina, A., Oakes, S.A., Papa, F.R., 2012. IRE1α Induces Thioredoxin-Interacting Protein to Activate the NLRP3 Inflammasome and Promote Programmed Cell Death under Irremediable ER Stress. Cell Metab. 16, 250–264. https://doi.org/10.1016/j.cmet.2012.07.007

Lévesque, S., Pol, J.G., Ferrere, G., Galluzzi, L., Zitvogel, L., Kroemer, G., 2019. Trial watch: dietary interventions for cancer therapy. Oncoimmunology 8, 1591878. https://doi.org/10.1080/2162402X.2019.1591878

Levine, M.E., Suarez, J.A., Brandhorst, S., Balasubramanian, P., Cheng, C.-W., Madia, F., Fontana, L., Mirisola, M.G., Guevara-Aguirre, J., Wan, J., Passarino, G., Kennedy, B.K., Wei, M., Cohen, P., Crimmins, E.M., Longo, V.D., 2014. Low Protein Intake Is Associated with a Major Reduction in IGF-1, Cancer, and Overall Mortality in the 65 and Younger but Not Older Population. Cell Metab. 19, 407–417. https://doi.org/10.1016/j.cmet.2014.02.006

Lhomond, S., Avril, T., Dejeans, N., Voutetakis, K., Doultsinos, D., McMahon, M., Pineau, R., Obacz, J., Papadodima, O., Jouan, F., Bourien, H., Logotheti, M., Jégou, G., Pallares-Lupon, N., Schmit, K., Le Reste, P.-J., Etcheverry, A., Mosser, J., Barroso, K., Vauléon, E., Maurel, M., Samali, A., Patterson, J.B., Pluquet, O., Hetz, C., Quillien, V., Chatziioannou, A., Chevet, E., 2018. Dual IRE1 RNase functions dictate glioblastoma development. EMBO Mol. Med. 10. https://doi.org/10.15252/emmm.201707929

Li, C.-W., Lim, S.-O., Xia, W., Lee, H.-H., Chan, L.-C., Kuo, C.-W., Khoo, K.-H., Chang, S.-S., Cha, J.-H., Kim, T., Hsu, J.L., Wu, Y., Hsu, J.-M., Yamaguchi, H., Ding, Q., Wang, Y., Yao, J., Lee, C.-C., Wu, H.-J., Sahin, A.A., Allison, J.P., Yu, D., Hortobagyi, G.N., Hung, M.-C., 2016. Glycosylation and stabilization of programmed death ligand-1 suppresses T-cell activity. Nat. Commun. 7, 12632. https://doi.org/10.1038/ncomms12632

Li, X., Shepard, H.M., Cowell, J.A., Zhao, C., Osgood, R.J., Rosengren, S., Blouw, B., Garrovillo, S.A., Pagel, M.D., Whatcott, C.J., Han, H., Von Hoff, D.D., Taverna, D.M., LaBarre, M.J., Maneval, D.C., Thompson, C.B., 2018. Parallel Accumulation of Tumor Hyaluronan, Collagen, and Other Drivers of Tumor Progression. Clin. Cancer Res. Off. J. Am. Assoc. Cancer Res. 24, 4798–4807. https://doi.org/10.1158/1078-0432.CCR-17-3284

Li, X.-X., Zhang, H.-S., Xu, Y.-M., Zhang, R.-J., Chen, Y., Fan, L., Qin, Y.-Q., Liu, Y., Li, M., Fang, J., 2017. Knockdown of IRE1α inhibits colonic tumorigenesis through decreasing β-catenin and IRE1α targeting suppresses colon cancer cells. Oncogene 36, 6738–6746. https://doi.org/10.1038/onc.2017.284

Li, Y., Guo, Y., Tang, J., Jiang, J., Chen, Z., 2014. New insights into the roles of CHOP-induced apoptosis in ER stress. Acta Biochim. Biophys. Sin. 46, 629–640. https://doi.org/10.1093/abbs/gmu048

Lin, S.-C., Hardie, D.G., 2018. AMPK: Sensing Glucose as well as Cellular Energy Status. Cell Metab. 27, 299–313. https://doi.org/10.1016/j.cmet.2017.10.009

Liou, H.C., Boothby, M.R., Finn, P.W., Davidon, R., Nabavi, N., Zeleznik-Le, N.J., Ting, J.P., Glimcher, L.H., 1990. A new member of the leucine zipper class of proteins that binds to the HLA DR alpha promoter. Science 247, 1581–1584. https://doi.org/10.1126/science.2321018

Liu, Y., Cao, Y., Pan, X., Shi, M., Wu, Q., Huang, T., Jiang, H., Li, W., Zhang, J., 2018. O-GlcNAc elevation through activation of the hexosamine biosynthetic pathway enhances cancer cell chemoresistance. Cell Death Dis. 9, 1–12. https://doi.org/10.1038/s41419-018-0522-0

Logue, S.E., McGrath, E.P., Cleary, P., Greene, S., Mnich, K., Almanza, A., Chevet, E., Dwyer, R.M., Oommen, A., Legembre, P., Godey, F., Madden, E.C., Leuzzi, B., Obacz, J., Zeng, Q., Patterson, J.B., Jäger, R., Gorman, A.M., Samali, A., 2018. Inhibition of IRE1 RNase activity modulates the tumor cell secretome and enhances response to chemotherapy. Nat. Commun. 9, 3267. https://doi.org/10.1038/s41467-018-05763-8

Loo, S.Y., Toh, L.P., Xie, W.H., Pathak, E., Tan, W., Ma, S., Lee, M.Y., Shatishwaran, S., Yeo, J.Z.Z., Yuan, J., Ho, Y.Y., Peh, E.K.L., Muniandy, M., Torta, F., Chan, J., Tan, T.J., Sim, Y., Tan, V., Tan, B., Madhukumar, P., Yong, W.S., Ong, K.W., Wong, C.Y., Tan, P.H., Yap, Y.S., Deng, L.-W., Dent, R., Foo, R., Wenk, M.R., Lee, S.C., Ho, Y.S., Lim, E.H., Tam, W.L., 2021. Fatty acid oxidation is a druggable gateway regulating cellular plasticity for driving metastasis in breast cancer. Sci. Adv. 7, eabh2443. https://doi.org/10.1126/sciadv.abh2443

Lübbers, J., Rodríguez, E., van Kooyk, Y., 2018. Modulation of Immune Tolerance via Siglec-Sialic Acid Interactions. Front. Immunol. 9, 2807. https://doi.org/10.3389/fimmu.2018.02807

Ludwig, D.S., Willett, W.C., Volek, J.S., Neuhouser, M.L., 2018. Dietary fat: From foe to friend? Science 362, 764–770. https://doi.org/10.1126/science.aau2096

Lukey, M.J., Katt, W.P., Cerione, R.A., 2017. Targeting amino acid metabolism for cancer therapy. Drug Discov. Today 22, 796–804. https://doi.org/10.1016/j.drudis.2016.12.003

Lv, M., Zhu, X., Wang, H., Wang, F., Guan, W., 2014. Roles of caloric restriction, ketogenic diet and intermittent fasting during initiation, progression and metastasis of cancer in animal models: a systematic review and meta-analysis. PloS One 9, e115147. https://doi.org/10.1371/journal.pone.0115147

Lynch, T.P., Ferrer, C.M., Jackson, S.R., Shahriari, K.S., Vosseller, K., Reginato, M.J., 2012. Critical Role of O-Linked β-N-Acetylglucosamine Transferase in Prostate Cancer Invasion, Angiogenesis, and Metastasis*. J. Biol. Chem. 287, 11070–11081. https://doi.org/10.1074/jbc.M111.302547

Ma, X., Bi, E., Lu, Y., Su, P., Huang, C., Liu, L., Wang, Q., Yang, M., Kalady, M.F., Qian, J., Zhang, A., Gupte, A.A., Hamilton, D.J., Zheng, C., Yi, Q., 2019. Cholesterol Induces

CD8+ T Cell Exhaustion in the Tumor Microenvironment. Cell Metab. 30, 143-156.e5. https://doi.org/10.1016/j.cmet.2019.04.002

Maddocks, O.D.K., Athineos, D., Cheung, E.C., Lee, P., Zhang, T., Broek, N.J.F. van den, Mackay, G.M., Labuschagne, C.F., Gay, D., Kruiswijk, F., Blagih, J., Vincent, D.F., Campbell, K.J., Ceteci, F., Sansom, O.J., Blyth, K., Vousden, K.H., 2017. Modulating the therapeutic response of tumours to dietary serine and glycine starvation. Nature 544, 372–376. https://doi.org/10.1038/nature22056

Mahadevan, N.R., Rodvold, J., Sepulveda, H., Rossi, S., Drew, A.F., Zanetti, M., 2011. Transmission of endoplasmic reticulum stress and pro-inflammation from tumor cells to myeloid cells. Proc. Natl. Acad. Sci. 108, 6561–6566. https://doi.org/10.1073/pnas.1008942108

Majumder, M., Huang, C., Snider, M.D., Komar, A.A., Tanaka, J., Kaufman, R.J., Krokowski, D., Hatzoglou, M., 2012. A novel feedback loop regulates the response to endoplasmic reticulum stress via the cooperation of cytoplasmic splicing and mRNA translation. Mol. Cell. Biol. 32, 992–1003. https://doi.org/10.1128/MCB.06665-11

Majzner, R.G., Mackall, C.L., 2018. Tumor Antigen Escape from CAR T-cell Therapy. Cancer Discov. 8, 1219–1226. https://doi.org/10.1158/2159-8290.CD-18-0442

Marshall, S., Bacote, V., Traxinger, R.R., 1991. Discovery of a metabolic pathway mediating glucose-induced desensitization of the glucose transport system. Role of hexosamine biosynthesis in the induction of insulin resistance. J. Biol. Chem. 266, 4706–4712.

Martinon, F., Chen, X., Lee, A.-H., Glimcher, L.H., 2010. TLR activation of the transcription factor XBP1 regulates innate immune responses in macrophages. Nat. Immunol. 11, 411–418. https://doi.org/10.1038/ni.1857

Masclef, L., Dehennaut, V., Mortuaire, M., Schulz, C., Leturcq, M., Lefebvre, T., Vercoutter-Edouart, A.-S., 2019. Cyclin D1 Stability Is Partly Controlled by O-GlcNAcylation. Front. Endocrinol. 10, 106. https://doi.org/10.3389/fendo.2019.00106

Mattison, J.A., Colman, R.J., Beasley, T.M., Allison, D.B., Kemnitz, J.W., Roth, G.S., Ingram, D.K., Weindruch, R., de Cabo, R., Anderson, R.M., 2017. Caloric restriction improves health and survival of rhesus monkeys. Nat. Commun. 8, 14063. https://doi.org/10.1038/ncomms14063

Mattson, M.P., Longo, V.D., Harvie, M., 2017. Impact of intermittent fasting on health and disease processes. Ageing Res. Rev. 39, 46–58. https://doi.org/10.1016/j.arr.2016.10.005

Medel, B., Costoya, C., Fernandez, D., Pereda, C., Lladser, A., Sauma, D., Pacheco, R., Iwawaki, T., Salazar-Onfray, F., Osorio, F., 2018. IRE1α Activation in Bone Marrow-Derived Dendritic Cells Modulates Innate Recognition of Melanoma Cells and Favors CD8+ T Cell Priming. Front. Immunol. 9, 3050. https://doi.org/10.3389/fimmu.2018.03050

Melaiu, O., Lucarini, V., Cifaldi, L., Fruci, D., 2019. Influence of the Tumor Microenvironment on NK Cell Function in Solid Tumors. Front. Immunol. 10, 3038. https://doi.org/10.3389/fimmu.2019.03038

Méndez-Lucas, A., Lin, W., Driscoll, P.C., Legrave, N., Novellasdemunt, L., Xie, C., Charles, M., Wilson, Z., Jones, N.P., Rayport, S., Rodríguez-Justo, M., Li, V., MacRae, J.I., Hay, N., Chen, X., Yuneva, M., 2020. Identifying strategies to target the metabolic flexibility of tumours. Nat. Metab. 2, 335–350. https://doi.org/10.1038/s42255-020-0195-8

Meynet, O., Zunino, B., Happo, L., Pradelli, L.A., Chiche, J., Jacquin, M.A., Mondragón, L., Tanti, J.-F., Taillan, B., Garnier, G., Reverso-Meinietti, J., Mounier, N., Michiels, J.-F., Michalak, E.M., Carles, M., Scott, C.L., Ricci, J.-E., 2013. Caloric restriction

modulates Mcl-1 expression and sensitizes lymphomas to BH3 mimetic in mice. Blood 122, 2402–2411. https://doi.org/10.1182/blood-2013-01-478651

Moffett, S., Shiao, T.C., Mousavifar, L., Mignani, S., Roy, R., 2021. Aberrant glycosylation patterns on cancer cells: Therapeutic opportunities for glycodendrimers/metallodendrimers oncology. Wiley Interdiscip. Rev. Nanomed. Nanobiotechnol. 13, e1659. https://doi.org/10.1002/wnan.1659

Morigny, P., Boucher, J., Arner, P., Langin, D., 2021. Lipid and glucose metabolism in white adipocytes: pathways, dysfunction and therapeutics. Nat. Rev. Endocrinol. 17, 276–295. https://doi.org/10.1038/s41574-021-00471-8

Morita, S., Villalta, S.A., Feldman, H.C., Register, A.C., Rosenthal, W., Hoffmann-Petersen, I.T., Mehdizadeh, M., Ghosh, R., Wang, L., Colon-Negron, K., Meza-Acevedo, R., Backes, B.J., Maly, D.J., Bluestone, J.A., Papa, F.R., 2017. Targeting ABL-IRE1α Signaling Spares ER-Stressed Pancreatic β Cells to Reverse Autoimmune Diabetes. Cell Metab. 25, 883-897.e8. https://doi.org/10.1016/j.cmet.2017.03.018

Mossmann, D., Park, S., Hall, M.N., 2018. mTOR signalling and cellular metabolism are mutual determinants in cancer. Nat. Rev. Cancer 18, 744–757. https://doi.org/10.1038/s41568-018-0074-8

Mozaffarian, D., Rosenberg, I., Uauy, R., 2018. History of modern nutrition science—implications for current research, dietary guidelines, and food policy. BMJ 361. https://doi.org/10.1136/bmj.k2392

Munkley, J., Elliott, D.J., 2016. Hallmarks of glycosylation in cancer. Oncotarget 7, 35478–35489. https://doi.org/10.18632/oncotarget.8155

Obeid, M., Tesniere, A., Ghiringhelli, F., Fimia, G.M., Apetoh, L., Perfettini, J.-L., Castedo, M., Mignot, G., Panaretakis, T., Casares, N., Métivier, D., Larochette, N., van Endert, P., Ciccosanti, F., Piacentini, M., Zitvogel, L., Kroemer, G., 2007. Calreticulin exposure dictates the immunogenicity of cancer cell death. Nat. Med. 13, 54–61. https://doi.org/10.1038/nm1523

O'Flanagan, C.H., Smith, L.A., McDonell, S.B., Hursting, S.D., 2017. When less may be more: calorie restriction and response to cancer therapy. BMC Med. 15. https://doi.org/10.1186/s12916-017-0873-x

Ohue, Y., Nishikawa, H., 2019. Regulatory T (Treg) cells in cancer: Can Treg cells be a new therapeutic target? Cancer Sci. 110, 2080–2089. https://doi.org/10.1111/cas.14069

Oikari, S., Kettunen, T., Tiainen, S., Häyrinen, J., Masarwah, A., Sudah, M., Sutela, A., Vanninen, R., Tammi, M., Auvinen, P., 2018. UDP-sugar accumulation drives hyaluronan synthesis in breast cancer. Matrix Biol. J. Int. Soc. Matrix Biol. 67, 63–74. https://doi.org/10.1016/j.matbio.2017.12.015

O'Neill, L.A.J., Kishton, R.J., Rathmell, J., 2016. A guide to immunometabolism for immunologists. Nat. Rev. Immunol. 16, 553–565. https://doi.org/10.1038/nri.2016.70

Orillion, A., Damayanti, N.P., Shen, L., Adelaiye-Ogala, R., Affronti, H., Elbanna, M., Chintala, S., Ciesielski, M., Fontana, L., Kao, C., Elzey, B.D., Ratliff, T.L., Nelson, D.E., Smiraglia, D., Abrams, S.I., Pili, R., 2018. Dietary Protein Restriction Reprograms Tumor-Associated Macrophages and Enhances Immunotherapy. Clin. Cancer Res. Off. J. Am. Assoc. Cancer Res. 24, 6383–6395. https://doi.org/10.1158/1078-0432.CCR-18-0980

Osorio, F., Lambrecht, B.N., Janssens, S., 2018. Antigen presentation unfolded: identifying convergence points between the UPR and antigen presentation pathways. Curr. Opin. Immunol. 52, 100–107. https://doi.org/10.1016/j.coi.2018.04.020

Osorio, F., Tavernier, S.J., Hoffmann, E., Saeys, Y., Martens, L., Vetters, J., Delrue, I., Rycke, R.D., Parthoens, E., Pouliot, P., Iwawaki, T., Janssens, S., Lambrecht, B.N., 2014. The unfolded-protein-response sensor IRE-1α regulates the function of CD8α + dendritic cells. Nat. Immunol. 15, 248–257. https://doi.org/10.1038/ni.2808

Ouspenskaia, T., Law, T., Clauser, K.R., Klaeger, S., Sarkizova, S., Aguet, F., Li, B., Christian, E., Knisbacher, B.A., Le, P.M., Hartigan, C.R., Keshishian, H., Apffel, A., Oliveira, G., Zhang, W., Chen, S., Chow, Y.T., Ji, Z., Jungreis, I., Shukla, S.A., Justesen, S., Bachireddy, P., Kellis, M., Getz, G., Hacohen, N., Keskin, D.B., Carr, S.A., Wu, C.J., Regev, A., 2022. Unannotated proteins expand the MHC-I-restricted immunopeptidome in cancer. Nat. Biotechnol. 40, 209–217. https://doi.org/10.1038/s41587-021-01021-3

Pakos-Zebrucka, K., Koryga, I., Mnich, K., Ljujic, M., Samali, A., Gorman, A.M., 2016. The integrated stress response. EMBO Rep. 17, 1374–1395. https://doi.org/10.15252/embr.201642195

Parihar, R., Rivas, C., Huynh, M., Omer, B., Lapteva, N., Metelitsa, L.S., Gottschalk, S.M., Rooney, C.M., 2019. NK Cells Expressing a Chimeric Activating Receptor Eliminate MDSCs and Rescue Impaired CAR-T Cell Activity against Solid Tumors. Cancer Immunol. Res. 7, 363–375. https://doi.org/10.1158/2326-6066.CIR-18-0572

Parker, M.P., Peterson, K.R., Slawson, C., 2021. O-GlcNAcylation and O-GlcNAc Cycling Regulate Gene Transcription: Emerging Roles in Cancer. Cancers 13, 1666. https://doi.org/10.3390/cancers13071666

Pathria, P., Louis, T.L., Varner, J.A., 2019. Targeting Tumor-Associated Macrophages in Cancer. Trends Immunol. 40, 310–327. https://doi.org/10.1016/j.it.2019.02.003

Pavlova, N.N., Thompson, C.B., 2016. The Emerging Hallmarks of Cancer Metabolism. Cell Metab. 23, 27–47. https://doi.org/10.1016/j.cmet.2015.12.006

Pawelec, G., Verschoor, C.P., Ostrand-Rosenberg, S., 2019. Myeloid-Derived Suppressor Cells: Not Only in Tumor Immunity. Front. Immunol. 10, 1099. https://doi.org/10.3389/fimmu.2019.01099

Phoomak, C., Silsirivanit, A., Park, D., Sawanyawisuth, K., Vaeteewoottacharn, K., Wongkham, C., Lam, E.W.-F., Pairojkul, C., Lebrilla, C.B., Wongkham, S., 2018. O-GlcNAcylation mediates metastasis of cholangiocarcinoma through FOXO3 and MAN1A1. Oncogene 37, 5648–5665. https://doi.org/10.1038/s41388-018-0366-1

Phoomak, C., Silsirivanit, A., Wongkham, C., Sripa, B., Puapairoj, A., Wongkham, S., 2012. Overexpression of O-GlcNAc-Transferase Associates with Aggressiveness of Mass-Forming Cholangiocarcinoma. Asian Pac. J. Cancer Prev. 13, 101–105. https://doi.org/10.7314/APJCP.2012.13.KKSuppl.101

Pinho, S.S., Reis, C.A., 2015. Glycosylation in cancer: mechanisms and clinical implications. Nat. Rev. Cancer 15, 540–555. https://doi.org/10.1038/nrc3982

Pol, J., Vacchelli, E., Aranda, F., Castoldi, F., Eggermont, A., Cremer, I., Sautès-Fridman, C., Fucikova, J., Galon, J., Spisek, R., Tartour, E., Zitvogel, L., Kroemer, G., Galluzzi, L., 2015. Trial Watch: Immunogenic cell death inducers for anticancer chemotherapy. Oncoimmunology 4. https://doi.org/10.1080/2162402X.2015.1008866

Pommier, A., Anaparthy, N., Memos, N., Kelley, Z.L., Gouronnec, A., Yan, R., Auffray, C., Albrengues, J., Egeblad, M., Iacobuzio-Donahue, C.A., Lyons, S.K., Fearon, D.T., 2018. Unresolved endoplasmic reticulum stress engenders immune-resistant, latent pancreatic cancer metastases. Science 360. https://doi.org/10.1126/science.aao4908

Pozzi, C., Cuomo, A., Spadoni, I., Magni, E., Silvola, A., Conte, A., Sigismund, S., Ravenda, P.S., Bonaldi, T., Zampino, M.G., Cancelliere, C., Fiore, P.P.D., Bardelli, A., Penna, G., Rescigno, M., 2016. The EGFR-specific antibody cetuximab combined with

chemotherapy triggers immunogenic cell death. Nat. Med. 22, 624–631. https://doi.org/10.1038/nm.4078

Puca, F., Yu, F., Bartolacci, C., Pettazzoni, P., Carugo, A., Huang-Hobbs, E., Liu, J., Zanca, C., Carbone, F., Del Poggetto, E., Gumin, J., Dasgupta, P., Seth, S., Srinivasan, S., Lang, F.F., Sulman, E.P., Lorenzi, P.L., Tan, L., Shan, M., Tolstyka, Z.P., Kachman, M., Zhang, L., Gao, S., Deem, A.K., Genovese, G., Scaglioni, P.P., Lyssiotis, C.A., Viale, A., Draetta, G.F., 2021. Medium-Chain Acyl-CoA Dehydrogenase Protects Mitochondria from Lipid Peroxidation in Glioblastoma. Cancer Discov. 11, 2904–2923. https://doi.org/10.1158/2159-8290.CD-20-1437

Puchalska, P., Crawford, P.A., 2017. Multi-dimensional roles of ketone bodies in fuel metabolism, signaling, and therapeutics. Cell Metab. 25, 262–284. https://doi.org/10.1016/j.cmet.2016.12.022

Qian, K., Wang, S., Fu, M., Zhou, J., Singh, J.P., Li, M.-D., Yang, Y., Zhang, K., Wu, J., Nie, Y., Ruan, H.-B., Yang, X., 2018. Transcriptional regulation of O-GlcNAc homeostasis is disrupted in pancreatic cancer. J. Biol. Chem. 293, 13989–14000. https://doi.org/10.1074/jbc.RA118.004709

Raskov, H., Orhan, A., Christensen, J.P., Gögenur, I., 2021. Cytotoxic CD8+ T cells in cancer and cancer immunotherapy. Br. J. Cancer 124, 359–367. https://doi.org/10.1038/s41416-020-01048-4

Raymundo, D.P., Doultsinos, D., Guillory, X., Carlesso, A., Eriksson, L.A., Chevet, E., 2020. Pharmacological Targeting of IRE1 in Cancer. Trends Cancer 6, 1018–1030. https://doi.org/10.1016/j.trecan.2020.07.006

Reily, C., Stewart, T.J., Renfrow, M.B., Novak, J., 2019. Glycosylation in health and disease. Nat. Rev. Nephrol. 15, 346–366. https://doi.org/10.1038/s41581-019-0129-4

Reina-Campos, M., Moscat, J., Diaz-Meco, M., 2017. Metabolism shapes the tumor microenvironment. Curr. Opin. Cell Biol. 48, 47–53. https://doi.org/10.1016/j.ceb.2017.05.006

Riley, R.S., June, C.H., Langer, R., Mitchell, M.J., 2019. Delivery technologies for cancer immunotherapy. Nat. Rev. Drug Discov. 18, 175–196. https://doi.org/10.1038/s41573-018-0006-z

Rizzo, M., Bayo, J., Piccioni, F., Malvicini, M., Fiore, E., Peixoto, E., García, M.G., Aquino, J.B., Campaña, A.G., Podestá, G., Terres, M., Andriani, O., Alaniz, L., Mazzolini, G., 2014. Low Molecular Weight Hyaluronan-Pulsed Human Dendritic Cells Showed Increased Migration Capacity and Induced Resistance to Tumor Chemoattraction. PLOS ONE 9, e107944. https://doi.org/10.1371/journal.pone.0107944

Roberts, P.J., Der, C.J., 2007. Targeting the Raf-MEK-ERK mitogen-activated protein kinase cascade for the treatment of cancer. Oncogene 26, 3291–3310. https://doi.org/10.1038/sj.onc.1210422

Robles-Flores, M., Moreno-Londoño, A.P., Castañeda-Patlán, M.C., 2021. Signaling Pathways Involved in Nutrient Sensing Control in Cancer Stem Cells: An Overview. Front. Endocrinol. 12, 627745. https://doi.org/10.3389/fendo.2021.627745

Rømer, T.B., Aasted, M.K.M., Dabelsteen, S., Groen, A., Schnabel, J., Tan, E., Pedersen, J.W., Haue, A.D., Wandall, H.H., 2021. Mapping of truncated O-glycans in cancers of epithelial and non-epithelial origin. Br. J. Cancer 125, 1239–1250. https://doi.org/10.1038/s41416-021-01530-7

Routy, B., Gopalakrishnan, V., Daillère, R., Zitvogel, L., Wargo, J.A., Kroemer, G., 2018. The gut microbiota influences anticancer immunosurveillance and general health. Nat. Rev. Clin. Oncol. 15, 382–396. https://doi.org/10.1038/s41571-018-0006-2

Rubio-Patiño, C., Bossowski, J.P., Chevet, E., Ricci, J.-E., 2018a. Reshaping the Immune Tumor Microenvironment Through IRE1 Signaling. Trends Mol. Med. 24, 607–614. https://doi.org/10.1016/j.molmed.2018.05.005

Rubio-Patiño, C., Bossowski, J.P., De Donatis, G.M., Mondragón, L., Villa, E., Aira, L.E., Chiche, J., Mhaidly, R., Lebeaupin, C., Marchetti, S., Voutetakis, K., Chatziioannou, A., Castelli, F.A., Lamourette, P., Chu-Van, E., Fenaille, F., Avril, T., Passeron, T., Patterson, J.B., Verhoeyen, E., Bailly-Maitre, B., Chevet, E., Ricci, J.-E., 2018b. Low-Protein Diet Induces IRE1α-Dependent Anticancer Immunosurveillance. Cell Metab. 27, 828-842.e7. https://doi.org/10.1016/j.cmet.2018.02.009

Rubio-Patiño, C., Bossowski, J.P., Villa, E., Mondragón, L., Zunino, B., Proïcs, E., Chiche, J., Bost, F., Verhoeyen, E., Ricci, J.-E., 2016. Low carbohydrate diet prevents Mcl-1-mediated resistance to BH3-mimetics. Oncotarget 7, 73270–73279. https://doi.org/10.18632/oncotarget.12309

Rudd, P.M., Elliott, T., Cresswell, P., Wilson, I.A., Dwek, R.A., 2001. Glycosylation and the immune system. Science 291, 2370–2376. https://doi.org/10.1126/science.291.5512.2370

Ruffell, B., Coussens, L.M., 2015. Macrophages and therapeutic resistance in cancer. Cancer Cell 27, 462–472. https://doi.org/10.1016/j.ccell.2015.02.015

Ruiz Cuevas, M.V., Hardy, M.-P., Hollý, J., Bonneil, É., Durette, C., Courcelles, M., Lanoix, J., Côté, C., Staudt, L.M., Lemieux, S., Thibault, P., Perreault, C., Yewdell, J.W., 2021. Most non-canonical proteins uniquely populate the proteome or immunopeptidome. Cell Rep. 34, 108815. https://doi.org/10.1016/j.celrep.2021.108815

Ryan, S.O., Cobb, B.A., 2012. Roles for major histocompatibility complex glycosylation in immune function. Semin. Immunopathol. 34, 425–441. https://doi.org/10.1007/s00281-012-0309-9

Ryczko, M.C., Pawling, J., Chen, R., Abdel Rahman, A.M., Yau, K., Copeland, J.K., Zhang, C., Surendra, A., Guttman, D.S., Figeys, D., Dennis, J.W., 2016. Metabolic Reprogramming by Hexosamine Biosynthetic and Golgi N-Glycan Branching Pathways. Sci. Rep. 6, 23043. https://doi.org/10.1038/srep23043

Sabado, R.L., Balan, S., Bhardwaj, N., 2017. Dendritic cell-based immunotherapy. Cell Res. 27, 74–95. https://doi.org/10.1038/cr.2016.157

Sahu, N., Dela Cruz, D., Gao, M., Sandoval, W., Haverty, P.M., Liu, J., Stephan, J.-P., Haley, B., Classon, M., Hatzivassiliou, G., Settleman, J., 2016. Proline Starvation Induces Unresolved ER Stress and Hinders mTORC1-Dependent Tumorigenesis. Cell Metab. 24, 753–761. https://doi.org/10.1016/j.cmet.2016.08.008

Schoenfeld, A.J., Hellmann, M.D., 2020. Acquired Resistance to Immune Checkpoint Inhibitors. Cancer Cell 37, 443–455. https://doi.org/10.1016/j.ccell.2020.03.017

Sengupta, S., Peterson, T.R., Sabatini, D.M., 2010. Regulation of the mTOR Complex 1 Pathway by Nutrients, Growth Factors, and Stress. Mol. Cell 40, 310–322. https://doi.org/10.1016/j.molcel.2010.09.026

Shamu, C.E., Walter, P., 1996. Oligomerization and phosphorylation of the Ire1p kinase during intracellular signaling from the endoplasmic reticulum to the nucleus. EMBO J. 15, 3028–3039.

Shaw, R.J., Cantley, L.C., 2006. Ras, PI(3)K and mTOR signalling controls tumour cell growth. Nature 441, 424–430. https://doi.org/10.1038/nature04869

Shen, X., Ellis, R.E., Lee, K., Liu, C.-Y., Yang, K., Solomon, A., Yoshida, H., Morimoto, R., Kurnit, D.M., Mori, K., Kaufman, R.J., 2001. Complementary Signaling Pathways

Regulate the Unfolded Protein Response and Are Required for C. elegans Development. Cell 107, 893–903. https://doi.org/10.1016/S0092-8674(01)00612-2

Shukla, S.K., Gebregiworgis, T., Purohit, V., Chaika, N.V., Gunda, V., Radhakrishnan, P., Mehla, K., Pipinos, I.I., Powers, R., Yu, F., Singh, P.K., 2014. Metabolic reprogramming induced by ketone bodies diminishes pancreatic cancer cachexia. Cancer Metab. 2, 18. https://doi.org/10.1186/2049-3002-2-18

Silva, M.C., Fernandes, Â., Oliveira, M., Resende, C., Correia, A., de-Freitas-Junior, J.C., Lavelle, A., Andrade-da-Costa, J., Leander, M., Xavier-Ferreira, H., Bessa, J., Pereira, C., Henrique, R.M., Carneiro, F., Dinis-Ribeiro, M., Marcos-Pinto, R., Lima, M., Lepenies, B., Sokol, H., Machado, J.C., Vilanova, M., Pinho, S.S., 2020. Glycans as Immune Checkpoints: Removal of Branched N-glycans Enhances Immune Recognition Preventing Cancer Progression. Cancer Immunol. Res. 8, 1407–1425. https://doi.org/10.1158/2326-6066.CIR-20-0264

Silva, Z., Ferro, T., Almeida, D., Soares, H., Ferreira, J.A., Deschepper, F.M., Hensbergen, P.J., Pirro, M., van Vliet, S.J., Springer, S., Videira, P.A., 2020. MHC Class I Stability is Modulated by Cell Surface Sialylation in Human Dendritic Cells. Pharmaceutics 12, E249. https://doi.org/10.3390/pharmaceutics12030249

Sivori, S., Pende, D., Quatrini, L., Pietra, G., Della Chiesa, M., Vacca, P., Tumino, N., Moretta, F., Mingari, M.C., Locatelli, F., Moretta, L., 2021. NK cells and ILCs in tumor immunotherapy. Mol. Aspects Med. 80, 100870. https://doi.org/10.1016/j.mam.2020.100870

Smith, J.A., 2018. Regulation of Cytokine Production by the Unfolded Protein Response; Implications for Infection and Autoimmunity. Front. Immunol. 9, 422. https://doi.org/10.3389/fimmu.2018.00422

Sodi, V.L., Bacigalupa, Z.A., Ferrer, C.M., Lee, J.V., Gocal, W.A., Mukhopadhyay, D., Wellen, K.E., Ivan, M., Reginato, M.J., 2018. Nutrient sensor O-GlcNAc transferase controls cancer lipid metabolism via SREBP-1 regulation. Oncogene 37, 924–934. https://doi.org/10.1038/onc.2017.395

Sodi, V.L., Khaku, S., Krutilina, R., Schwab, L.P., Vocadlo, D.J., Seagroves, T.N., Reginato, M.J., 2015. MTOR/MYCAxis regulates O-GlcNAc transferase expression and O-GlcN acylation in breast cancer. Mol. Cancer Res. 13, 923–933. https://doi.org/10.1158/1541-7786.MCR-14-0536

Soldati, L., Di Renzo, L., Jirillo, E., Ascierto, P.A., Marincola, F.M., De Lorenzo, A., 2018. The influence of diet on anti-cancer immune responsiveness. J. Transl. Med. 16, 75. https://doi.org/10.1186/s12967-018-1448-0

Song, M., Chan, A.T., 2019. Environmental Factors, Gut Microbiota, and Colorectal Cancer Prevention. Clin. Gastroenterol. Hepatol. Off. Clin. Pract. J. Am. Gastroenterol. Assoc. 17, 275–289. https://doi.org/10.1016/j.cgh.2018.07.012

Song, M., Sandoval, T.A., Chae, C.-S., Chopra, S., Tan, C., Rutkowski, M.R., Raundhal, M., Chaurio, R.A., Payne, K.K., Konrad, C., Bettigole, S.E., Shin, H.R., Crowley, M.J.P., Cerliani, J.P., Kossenkov, A.V., Motorykin, I., Zhang, S., Manfredi, G., Zamarin, D., Holcomb, K., Rodriguez, P.C., Rabinovich, G.A., Conejo-Garcia, J.R., Glimcher, L.H., Cubillos-Ruiz, J.R., 2018. IRE1α-XBP1 controls T cell function in ovarian cancer by regulating mitochondrial activity. Nature 562, 423–428. https://doi.org/10.1038/s41586-018-0597-x

Štambuk, T., Klasić, M., Zoldoš, V., Lauc, G., 2021. N-glycans as functional effectors of genetic and epigenetic disease risk. Mol. Aspects Med. 79, 100891. https://doi.org/10.1016/j.mam.2020.100891

Stanley, P., 2011. Golgi Glycosylation. Cold Spring Harb. Perspect. Biol. 3, a005199. https://doi.org/10.1101/cshperspect.a005199

Steenackers, A., Olivier-Van Stichelen, S., Baldini, S.F., Dehennaut, V., Toillon, R.-A., Le Bourhis, X., El Yazidi-Belkoura, I., Lefebvre, T., 2016. Silencing the nucleocytoplasmic O-GlcNAc transferase reduces proliferation, adhesion, and migration of cancer and fetal human colon cell lines. Front. Endocrinol. 7. https://doi.org/10.3389/fendo.2016.00046

Sung, H., Ferlay, J., Siegel, R.L., Laversanne, M., Soerjomataram, I., Jemal, A., Bray, F., 2021. Global Cancer Statistics 2020: GLOBOCAN Estimates of Incidence and Mortality Worldwide for 36 Cancers in 185 Countries. CA. Cancer J. Clin. 71, 209–249. https://doi.org/10.3322/caac.21660

Tajan, M., Vousden, K.H., 2020. Dietary Approaches to Cancer Therapy. Cancer Cell. https://doi.org/10.1016/j.ccell.2020.04.005

Talmadge, J.E., Gabrilovich, D.I., 2013. History of myeloid-derived suppressor cells. Nat. Rev. Cancer 13, 739–752. https://doi.org/10.1038/nrc3581

Tan, W., Jiang, P., Zhang, W., Hu, Z., Lin, S., Chen, L., Li, Y., Peng, C., Li, Z., Sun, A., Chen, Y., Zhu, W., Xue, Y., Yao, Y., Li, X., Song, Q., He, F., Qin, W., Pei, H., 2021. Posttranscriptional regulation of de novo lipogenesis by glucose-induced O-GlcNAcylation. Mol. Cell 81, 1890-1904.e7. https://doi.org/10.1016/j.molcel.2021.02.009

Tang, C.-H.A., Chang, S., Paton, A.W., Paton, J.C., Gabrilovich, D.I., Ploegh, H.L., Del Valle, J.R., Hu, C.-C.A., 2018. Phosphorylation of IRE1 at S729 regulates RIDD in B cells and antibody production after immunization. J. Cell Biol. 217, 1739–1755. https://doi.org/10.1083/jcb.201709137

Tang, J., Yu, J.X., Hubbard-Lucey, V.M., Neftelinov, S.T., Hodge, J.P., Lin, Y., 2018. The clinical trial landscape for PD1/PDL1 immune checkpoint inhibitors. Nat. Rev. Drug Discov. 17, 854–855. https://doi.org/10.1038/nrd.2018.210

Terrell, E.M., Morrison, D.K., 2019. Ras-Mediated Activation of the Raf Family Kinases. Cold Spring Harb. Perspect. Med. 9, a033746. https://doi.org/10.1101/cshperspect.a033746

TeSlaa, T., Bartman, C.R., Jankowski, C.S.R., Zhang, Z., Xu, X., Xing, X., Wang, L., Lu, W., Hui, S., Rabinowitz, J.D., 2021. The Source of Glycolytic Intermediates in Mammalian Tissues. Cell Metab. 33, 367-378.e5. https://doi.org/10.1016/j.cmet.2020.12.020

Tian, X., Zhang, S., Zhou, L., Seyhan, A.A., Hernandez Borrero, L., Zhang, Y., El-Deiry, W.S., 2021. Targeting the Integrated Stress Response in Cancer Therapy. Front. Pharmacol. 12, 747837. https://doi.org/10.3389/fphar.2021.747837

Topalian, S.L., Taube, J.M., Anders, R.A., Pardoll, D.M., 2016. Mechanism-driven biomarkers to guide immune checkpoint blockade in cancer therapy. Nat. Rev. Cancer 16, 275–287. https://doi.org/10.1038/nrc.2016.36

Uldry, M., Ibberson, M., Hosokawa, M., Thorens, B., 2002. GLUT2 is a high affinity glucosamine transporter. FEBS Lett. 524, 199–203. https://doi.org/10.1016/s0014-5793(02)03058-2

Urano, F., Wang, X., Bertolotti, A., Zhang, Y., Chung, P., Harding, H.P., Ron, D., 2000. Coupling of Stress in the ER to Activation of JNK Protein Kinases by Transmembrane Protein Kinase IRE1. Science 287, 664–666. https://doi.org/10.1126/science.287.5453.664

Urra, H., Henriquez, D.R., Cánovas, J., Villarroel-Campos, D., Carreras-Sureda, A., Pulgar, E., Molina, E., Hazari, Y.M., Limia, C.M., Alvarez-Rojas, S., Figueroa, R., Vidal, R.L., Rodriguez, D.A., Rivera, C.A., Court, F.A., Couve, A., Qi, L., Chevet, E., Akai, R., Iwawaki, T., Concha, M.L., Glavic, Á., Gonzalez-Billault, C., Hetz, C., 2018. IRE1α governs cytoskeleton remodelling and cell migration through a direct interaction with filamin A. Nat. Cell Biol. 20, 942–953. https://doi.org/10.1038/s41556-018-0141-0

Uyttenhove, C., Pilotte, L., Théate, I., Stroobant, V., Colau, D., Parmentier, N., Boon, T., Van den Eynde, B.J., 2003. Evidence for a tumoral immune resistance mechanism based on tryptophan degradation by indoleamine 2,3-dioxygenase. Nat. Med. 9, 1269–1274. https://doi.org/10.1038/nm934

van der Leun, A.M., Thommen, D.S., Schumacher, T.N., 2020. CD8+ T cell states in human cancer: insights from single-cell analysis. Nat. Rev. Cancer 20, 218–232. https://doi.org/10.1038/s41568-019-0235-4

Vander Heiden, M.G., DeBerardinis, R.J., 2017. Understanding the Intersections between Metabolism and Cancer Biology. Cell 168, 657–669. https://doi.org/10.1016/j.cell.2016.12.039

Vernieri, C., Fucà, G., Ligorio, F., Huber, V., Vingiani, A., Iannelli, F., Raimondi, A., Rinchai, D., Frigè, G., Belfiore, A., Lalli, L., Chiodoni, C., Cancila, V., Zanardi, F., Ajazi, A., Cortellino, S., Vallacchi, V., Squarcina, P., Cova, A., Pesce, S., Frati, P., Mall, R., Corsetto, P.A., Rizzo, A.M., Ferraris, C., Folli, S., Garassino, M.C., Capri, G., Bianchi, G., Colombo, M.P., Minucci, S., Foiani, M., Longo, V.D., Apolone, G., Torri, V., Pruneri, G., Bedognetti, D., Rivoltini, L., de Braud, F., 2022. Fasting-Mimicking Diet Is Safe and Reshapes Metabolism and Antitumor Immunity in Patients with Cancer. Cancer Discov. 12, 90–107. https://doi.org/10.1158/2159-8290.CD-21-0030

Very, N., Hardivillé, S., Decourcelle, A., Thévenet, J., Djouina, M., Page, A., Vergoten, G., Schulz, C., Kerr-Conte, J., Lefebvre, T., Dehennaut, V., El Yazidi-Belkoura, I., 2022. Thymidylate synthase O-GlcNAcylation: a molecular mechanism of 5-FU sensitization in colorectal cancer. Oncogene 41, 745–756. https://doi.org/10.1038/s41388-021-02121-9

Vincenz, L., Hartl, F.U., 2014. Sugarcoating ER Stress. Cell 156, 1125–1127. https://doi.org/10.1016/j.cell.2014.02.035

Vivier, E., Tomasello, E., Baratin, M., Walzer, T., Ugolini, S., 2008. Functions of natural killer cells. Nat. Immunol. 9, 503–510. https://doi.org/10.1038/ni1582

Wang, A., Luan, H.H., Medzhitov, R., 2019. An evolutionary perspective on immunometabolism. Science 363. https://doi.org/10.1126/science.aar3932

Wang, X., Liu, R., Zhu, W., Chu, H., Yu, H., Wei, P., Wu, X., Zhu, H., Gao, H., Liang, J., Li, G., Yang, W., 2019. UDP-glucose accelerates SNAI1 mRNA decay and impairs lung cancer metastasis. Nature 571, 127–131. https://doi.org/10.1038/s41586-019-1340-y

Wang, Z.V., Deng, Y., Gao, N., Pedrozo, Z., Li, D.L., Morales, C.R., Criollo, A., Luo, X., Tan, W., Jiang, N., Lehrman, M.A., Rothermel, B.A., Lee, A.-H., Lavandero, S., Mammen, P.P.A., Ferdous, A., Gillette, T.G., Scherer, P.E., Hill, J.A., 2014. Spliced X-Box Binding Protein 1 Couples the Unfolded Protein Response to Hexosamine Biosynthetic Pathway. Cell 156, 1179–1192. https://doi.org/10.1016/j.cell.2014.01.014

Wculek, S.K., Cueto, F.J., Mujal, A.M., Melero, I., Krummel, M.F., Sancho, D., 2020. Dendritic cells in cancer immunology and immunotherapy. Nat. Rev. Immunol. 20, 7–24. https://doi.org/10.1038/s41577-019-0210-z

Weber, D.D., Aminzadeh-Gohari, S., Tulipan, J., Catalano, L., Feichtinger, R.G., Kofler, B., 2020. Ketogenic diet in the treatment of cancer – Where do we stand? Mol. Metab., Cancer Metabolism 33, 102–121. https://doi.org/10.1016/j.molmet.2019.06.026

Wolfert, M.A., Boons, G.-J., 2013. Adaptive immune activation: glycosylation does matter. Nat. Chem. Biol. 9, 776–784. https://doi.org/10.1038/nchembio.1403

Wu, Y., Shan, B., Dai, J., Xia, Z., Cai, J., Chen, T., Lv, S., Feng, Y., Zheng, L., Wang, Y., Liu, Jianfeng, Fang, J., Xie, D., Rui, L., Liu, Jianmiao, Liu, Y., 2018. Dual role for inositol-requiring enzyme 1α in promoting the development of hepatocellular carcinoma during diet-induced obesity in mice. Hepatology 68, 533–546. https://doi.org/10.1002/hep.29871

Xia, Z., Wu, S., Wei, X., Liao, Y., Yi, P., Liu, Y., Liu, Jianmiao, Liu, Jianfeng, 2019. Hypoxic ER stress suppresses β-catenin expression and promotes cooperation between the transcription factors XBP1 and HIF1α for cell survival. J. Biol. Chem. jbc.RA119.008353. https://doi.org/10.1074/jbc.RA119.008353

Xie, H., Tang, C.-H.A., Song, J.H., Mancuso, A., Del Valle, J.R., Cao, J., Xiang, Y., Dang, C.V., Lan, R., Sanchez, D.J., Keith, B., Hu, C.-C.A., Simon, M.C., 2018. IRE1α RNase-dependent lipid homeostasis promotes survival in Myc-transformed cancers. J. Clin. Invest. 128, 1300–1316. https://doi.org/10.1172/JCI95864

Xu, W., Zhang, X., Wu, J., Fu, L., Liu, K., Liu, D., Chen, G.G., Lai, P.B., Wong, N., Yu, J., 2017. O-GlcNAc transferase promotes fatty liver-associated liver cancer through inducing palmitic acid and activating endoplasmic reticulum stress. J. Hepatol. 67, 310–320. https://doi.org/10.1016/j.jhep.2017.03.017

Yamakawa, N., Vanbeselaere, J., Chang, L.-Y., Yu, S.-Y., Ducrocq, L., Harduin-Lepers, A., Kurata, J., Aoki-Kinoshita, K.F., Sato, C., Khoo, K.-H., Kitajima, K., Guerardel, Y., 2018. Systems glycomics of adult zebrafish identifies organ-specific sialylation and glycosylation patterns. Nat. Commun. 9, 4647. https://doi.org/10.1038/s41467-018-06950-3

Yamamoto, K., Venida, A., Yano, J., Biancur, D.E., Kakiuchi, M., Gupta, S., Sohn, A.S.W., Mukhopadhyay, S., Lin, E.Y., Parker, S.J., Banh, R.S., Paulo, J.A., Wen, K.W., Debnath, J., Kim, G.E., Mancias, J.D., Fearon, D.T., Perera, R.M., Kimmelman, A.C., 2020. Autophagy promotes immune evasion of pancreatic cancer by degrading MHC-I. Nature 1–6. https://doi.org/10.1038/s41586-020-2229-5

Yan, D., Wang, H.-W., Bowman, R.L., Joyce, J.A., 2016. STAT3 and STAT6 Signaling Pathways Synergize to Promote Cathepsin Secretion from Macrophages via IRE1α Activation. Cell Rep. 16, 2914–2927. https://doi.org/10.1016/j.celrep.2016.08.035

Yang, X., Ongusaha, P.P., Miles, P.D., Havstad, J.C., Zhang, F., So, W.V., Kudlow, J.E., Michell, R.H., Olefsky, J.M., Field, S.J., Evans, R.M., 2008. Phosphoinositide signalling links O-GlcNAc transferase to insulin resistance. Nature 451, 964–969. https://doi.org/10.1038/nature06668

Yang, X., Qian, K., 2017. Protein O-GlcNAcylation: emerging mechanisms and functions. Nat. Rev. Mol. Cell Biol. 18, 452–465. https://doi.org/10.1038/nrm.2017.22

Yin, J., Ren, W., Huang, X., Li, T., Yin, Y., 2018. Protein restriction and cancer. Biochim. Biophys. Acta Rev. Cancer 1869, 256–262. https://doi.org/10.1016/j.bbcan.2018.03.004

Yoo, Y.S., Han, H.G., Jeon, Y.J., 2017. Unfolded Protein Response of the Endoplasmic Reticulum in Tumor Progression and Immunogenicity. Oxid. Med. Cell. Longev. 2017, 2969271. https://doi.org/10.1155/2017/2969271

Yoshida, H., Matsui, T., Yamamoto, A., Okada, T., Mori, K., 2001. XBP1 mRNA Is Induced by ATF6 and Spliced by IRE1 in Response to ER Stress to Produce a Highly Active

Transcription Factor. Cell 107, 881–891. https://doi.org/10.1016/S0092-8674(01)00611-0

Zhang, J., Pavlova, N.N., Thompson, C.B., 2017. Cancer cell metabolism: the essential role of the nonessential amino acid, glutamine. EMBO J. 36, 1302–1315. https://doi.org/10.15252/embj.201696151

Zhao, N., Cao, J., Xu, L., Tang, Q., Dobrolecki, L.E., Lv, X., Talukdar, M., Lu, Y., Wang, X., Hu, D.Z., Shi, Q., Xiang, Y., Wang, Y., Liu, X., Bu, W., Jiang, Y., Li, M., Gong, Y., Sun, Z., Ying, H., Yuan, B., Lin, X., Feng, X.-H., Hartig, S.M., Li, F., Shen, H., Chen, Y., Han, L., Zeng, Q., Patterson, J.B., Kaipparettu, B.A., Putluri, N., Sicheri, F., Rosen, J.M., Lewis, M.T., Chen, X., 2018. Pharmacological targeting of MYC-regulated IRE1/XBP1 pathway suppresses MYC-driven breast cancer. J. Clin. Invest. 128, 1283–1299. https://doi.org/10.1172/JCI95873

Zhu, Q., Zhou, L., Yang, Z., Lai, M., Xie, H., Wu, L., Xing, C., Zhang, F., Zheng, S., 2012. O-GlcNAcylation plays a role in tumor recurrence of hepatocellular carcinoma following liver transplantation. Med. Oncol. 29, 985–993. https://doi.org/10.1007/s12032-011-9912-1

ANNEX

REVIEW 1

Grima-Reyes, M., **Martinez-Turtos, A**., Abramovich, I., Gottlieb, E., Chiche, J., Ricci, J.-E., 2021. Physiological impact of in vivo stable isotope tracing on cancer metabolism. Mol Metab 53, 101294. https://doi.org/10.1016/j.molmet.2021.101294

Review

MOLECULAR METABOLISM

Physiological impact of *in vivo* stable isotope tracing on cancer metabolism

Manuel Grima-Reyes [1,2,4], Adriana Martinez-Turtos [1,2,4], Ifat Abramovich [3], Eyal Gottlieb [3], Johanna Chiche [1,2,5], Jean-Ehrland Ricci [1,2,*,5]

ABSTRACT

Background: There is growing interest in the analysis of tumor metabolism to identify cancer-specific metabolic vulnerabilities and therapeutic targets. Finding of such candidate metabolic pathways mainly relies on the highly sensitive identification and quantitation of numerous metabolites and metabolic fluxes using metabolomics and isotope tracing analyses. However, nutritional requirements and metabolic routes used by cancer cells cultivated *in vitro* do not always reflect the metabolic demands of malignant cells within the tumor milieu. Therefore, to understand how the metabolism of tumor cells in its physiological environment differs from that of normal cells, these analyses must be performed *in vivo*.
Scope of Review: This review covers the physiological impact of the exogenous administration of a stable isotope tracer into cancer animal models. We discuss specific aspects of *in vivo* isotope tracing protocols based on discrete bolus injections of a labeled metabolite: the tracer administration *per se* and the fasting period prior to it. In addition, we illustrate the complex physiological scenarios that arise when studying tumor metabolism — by isotopic labeling in animal models fed with a specific amino acid restricted diet. Finally, we provide strategies to minimize these limitations.
Major Conclusions: There is growing evidence that metabolic dependencies in cancers are influenced by tissue environment, cancer lineage, and genetic events. An increasing number of studies describe discrepancies in tumor metabolic dependencies when studied in *in vitro* settings or *in vivo* models, including cancer patients. Therefore, in-depth *in vivo* profiling of tumor metabolic routes within the appropriate pathophysiological environment will be key to identify relevant alterations that contribute to cancer onset and progression.

Keywords Stable isotope tracing; Tracer administration; Interorgan exchange; Fasting; Tumor metabolism

1. INTRODUCTION

Metabolic reprogramming has been recognized as a hallmark of cancer [1,2]. The challenge of expanding our understanding of major cancer metabolic features and specific metabolic dependencies requires sophisticated approaches, such as metabolomics. Metabolomics allows the identification and relative quantitation of numerous metabolites by mass spectrometry coupled to gas or liquid chromatography (GC/LC-MS). Other techniques such as magnetic resonance spectroscopy enable metabolite identification and quantification, but at a lower scale [3]. Metabolomics endows cancer researchers with a high-resolution tool for the quantification of absolute and relative abundances of metabolite pools in malignant tissues and biofluids surrounding the tumoral mass [4]. Levels of these small molecules provide hints of which metabolic pathways have been aberrantly altered during oncogenic transformation [5].
Stable isotope resolved metabolomics allows to monitor how labeled metabolic sources contribute to bioenergetic, biosynthetic, and/or redox pathways that sustain tumoral tissues in their transformed state (Figure 1). Depending on the intracellular metabolic labeling, isotope tracing helps to infer metabolite interconversion, a feature that cannot be perceived by steady state metabolomics [6]. Tracing the incorporation of stable isotopes of carbon (^{13}C), nitrogen (^{15}N), or hydrogen (^{2}H) from isotopically labeled nutrients (tracers) into downstream tissue metabolites is considered the state-of-the-art approach to study cancer metabolism [7]. This methodology determines the isotopic composition of metabolites based on the differences in atomic masses. For instance, the heavy stable isotope of carbon (^{13}C) has a molecular mass increased by a unit (M+1) as compared to the most naturally abundant carbon isotope (^{12}C). These differences in nominal masses allow to distinguish the fully labeled glucose with six heavier carbons (M+6) from unlabeled glucose (M+0). Therefore, tracing a stable labeled nutrient into downstream metabolites allows to follow the cascade of chemical reactions by which nutrient catabolism or anabolism is increased or decreased. Aberrant metabolite uptake or secretion from tissues can also be estimated by isotopic labeling.

[1]Université Côte d'Azur, INSERM, C3M, Nice, France [2]Equipe labellisée LIGUE Contre le Cancer, Nice, France [3]Ruth and Bruce Rappaport Faculty of Medicine, Technion — Israel Institute of Technology, Haifa, Israel

[4] Manuel Grima-Reyes and Adriana Martinez-Turtos are co-first authors.
[5] Johanna Chiche and Jean-Ehrland Ricci are co-last authors.

*Corresponding author. Inserm U1065, Équipe 3, 151 Route de St Antoine de Ginestière, BP 23194, 06204, Nice Cedex 03, France. Fax +33 4 89 06 42 21. E-mail: ricci@unice.fr (J.-E. Ricci).

Received May 10, 2021 • Revision received June 30, 2021 • Accepted July 8, 2021 • Available online 10 July 2021

https://doi.org/10.1016/j.molmet.2021.101294

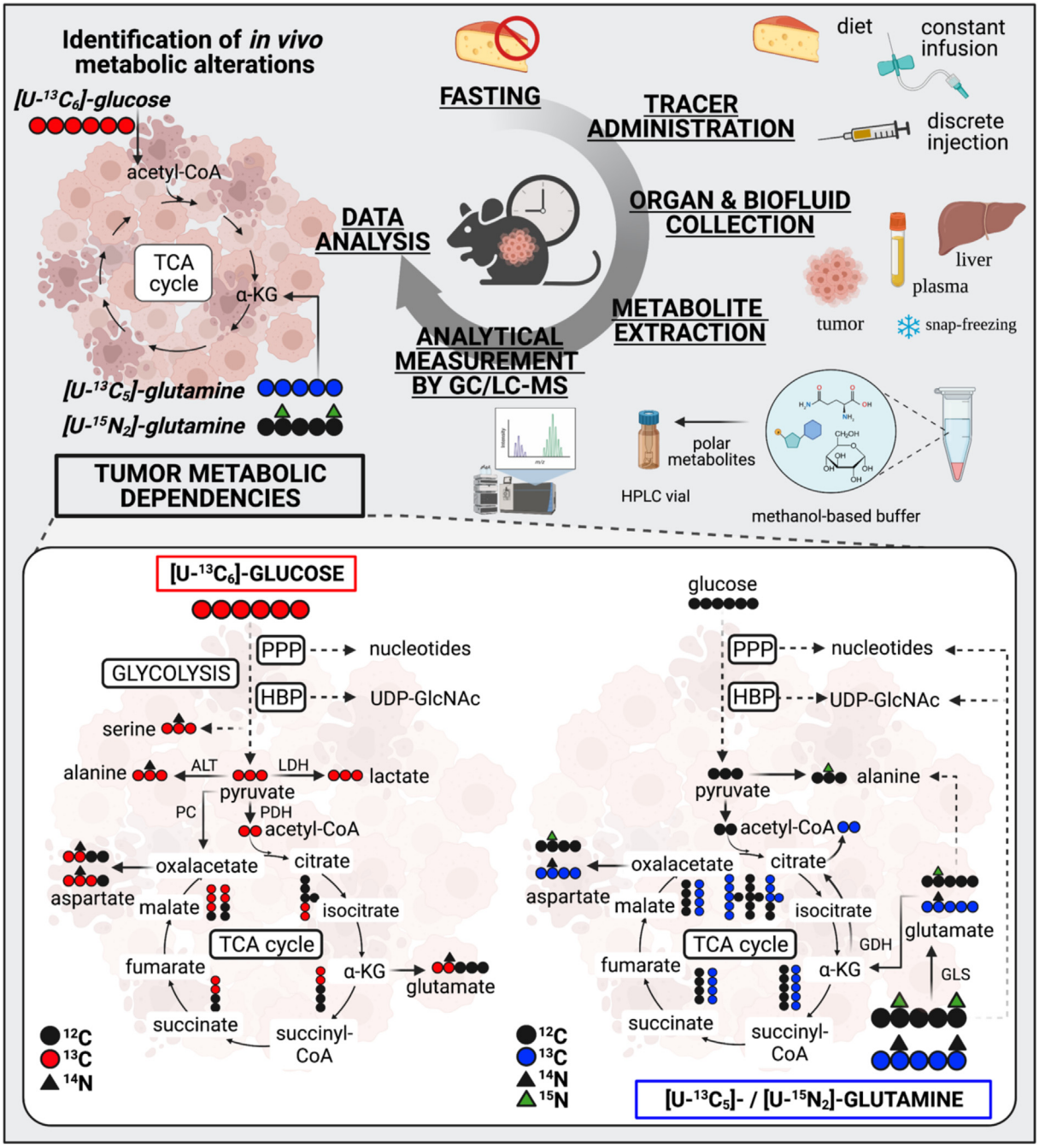

Figure 1: Time course steps of *in vivo* stable isotope tracing approaches. Lower panel, carbon, and nitrogen fate of labeled glucose and glutamine in main metabolic pathways. PPP, pentose phosphate pathway; HBP, hexosamine biosynthetic pathway; TCA, tricarboxylic acid cycle; ALT, alanine aminotransferase; LDH, lactate dehydrogenase; PDH, pyruvate dehydrogenase; PC, pyruvate carboxylase; GLS, glutaminase; and GDH, glutamate dehydrogenase. Created with BioRender.com.

Tumors usually reside in a poorly vascularized microenvironment under nutritional conditions that significantly differ from those found in cell culture media [8,9]. Therefore, cancer cells growing *in vitro* do not necessarily display the same metabolic phenotype as the intact tumor. For instance, Ras-driven lung tumors in mice are more dependent on glucose to fuel the tricarboxylic acid (TCA) cycle and less dependent on glutamine compared to their *in vitro* counterpart cell lines [10]. Nutritional availabilities and metabolite exchange between stromal and cancer cells also determine how tumor cells will metabolically adapt to competitively growth and survive [3]. Therefore, *in vivo* tracer-based metabolomics is the most authentic approach for studying the nutritional requirements and metabolic reprograming of intact malignant tissues. For instance, tracing the incorporation of uniformly carbon labeled glucose, ([U—$^{13}C_6$]-glucose), into downstream metabolites has expanded our notions of how glucose is metabolized in tumoral tissues (Figure 1). However, preferential glucose contribution to the TCA cycle through the activity of pyruvate carboxylase (PC) — as compared to the activity of

pyruvate dehydrogenase (PDH) — has been reported in mouse models of lung cancer and breast cancer-derived lung metastasis. The differential labeling patterns of TCA cycle intermediates arising from reactions catalyzed by PC and PDH in the presence of [U−$^{13}C_6$]-glucose have allowed to estimate the relative activity of the former enzymes for anaplerotic replenishment of the TCA cycle in these tumors [11,12]. *De novo* serine biosynthesis from fully carbon-labeled glucose has been demonstrated to preferentially occur in lung metastases of breast cancer as compared to primary tumors by quantitation of serine M+3 [13]. [U−$^{13}C_5$]-glutamine fueling the TCA cycle through glutaminase activity has been demonstrated by the labeling pattern of glutamate M+5 and TCA cycle intermediates. The latest metabolic pathway has been shown to preferentially occur in *in vitro* culture of lung tumor cells as compared to lung tumors growing in mice [10]. In addition, KRAS mutant/LKB1 deleted-driven lung cancer cells labeled with $^{15}N_1$-amide-glutamine display a high flux through the hexosamine biosynthetic pathway reflected by an increase in the detection of ^{15}N-UDP-GlcNAC [14] (also refer to Table 1 for more examples and details). Beyond preclinical research, stable isotope labeling to study cancer metabolism in patients highlighted that glucose does not only yield energy by aerobic glycolysis, but is also terminally oxidized in several types of tumors. Moreover, radioisotope labeled nutrients, such as the glucose analogue ^{18}FDG (Fluorodeoxyglucose), are commonly used for cancer diagnosis and follow-up treatment by positron emission tomography [3].

New insights into the metabolic reprograming of tumors have been acquired by continuously improving isotope tracing approaches. Broadly, typical experimental designs include the following: (i) food deprivation of animal models before tracer administration, (ii) tracer supplementation, (iii) collection of tissues and biofluids of interest (iv), metabolite extraction from samples, (v) analytical measurement of metabolites by GC/LC-MS, and (vi) chromatographic peak integration and data analysis (Figure 1, upper panel). Importantly, although ^{13}C, ^{15}N, and ^{2}H stable isotopes occur naturally at a very low level, their natural abundance can impact the isotopic composition of metabolites and confound the labeling derived from the tracer. For instance, one of the most common isotopic tracing relies on ^{13}C, which displays a natural abundance of 1.07%. Therefore, correcting the natural abundance of stable isotopes deserves attention when rigorously analyzing the fractional enrichment of downstream metabolites [15].

In this review, we will discuss how tracer supplementation impacts global physiology and how this might confound the interpretation of metabolic processes occurring in healthy and transformed tissues. Likewise, fasting before tracing supplementation can trigger an adaptive metabolism in mice; a topic that will be addressed to broaden our understanding of its potential impact on animal physiology and tumor metabolism. We will illustrate these two sections with metabolomic data from stable isotope tracing by discrete bolus administration in cancer mouse models. Complex scenarios that arise when metabolic reprograming is studied by isotope tracing in nutritional-restricted mice will be also covered.

2. DOES *IN VIVO* TRACER ADMINISTRATION CHALLENGE PHYSIOLOGICAL METABOLISM?

Studying *in vivo* cancer-specific metabolic pathways in animal models by stable isotope tracing is challenging at several steps of the procedure, including the very first step i.e., tracer delivery for optimal enrichment in tumor cells. To avoid substantial disruption of the physiological homeostasis upon tracer delivery, an isotopic enrichment equivalent to 10−30% of the total circulating pool of the tracer is recommended. This will enable downstream labeling patterns without excessive impact on the bloodstream concentration of the given metabolite [4]. To deliver a tracer, several administration methods have been successfully developed and optimized.

Performed on conscious mice, single or multiple discrete boluses by intraperitoneal (i.p) or intravenous (i.v) injections or gavage provoke intense and transient tracer boosts in the bloodstream that might complicate/hinder data analysis and interpretations [16,17]. The unnatural systemic metabolic effects caused by bolus include glucose spikes [16], likely causing increases in insulin secretion following each [U−$^{13}C_6$]-glucose injection. Repeated mice handling to deliver the tracer through discrete bolus also leads to acute stress responses which affect the whole-body metabolism [18]. Nevertheless, this tracer administration method is simple to perform and does not require the use of anesthesia, an advantage when considering the influence of anesthetics on cellular energy metabolism [19].

Continuous tracer infusion through the tail vein of sedated animals are advantageous because it allows a mild and continuous tracer delivery to achieve a stable concentration permitting robust evaluation of steady-state labeling of metabolic pathways in tissues of interest. Compared to this, tracer infusion through catheterization of the jugular vein on conscious immobile mice hold similar advantages to reach metabolic steady state, without the disadvantage related to the use of anesthetics. Importantly, infusion through a jugular vein catheter requires specialized surgical skills and expertise.

From a physiological point of view, tracer delivery by feeding animals with a solid or liquid diet containing the labeled nutrient is simple and advantageous — because the tracer is absorbed over time reaching physiological levels while not disturbing mouse feeding habits. Furthermore, it minimizes the metabolic response to stress induced by animal handling. Although this tracer delivery method is emerging as a promising strategy to perform *in vivo* stable isotope tracing, it is not often used because of limitations such as the strict control of the animal feeding behavior, long tracing periods, and a substantial economic outlay [20,21]. To date, the most commonly used procedures to deliver labeled nutrients are constant intravenous infusions and single or multiple discrete boluses (i.v, i. p, or gavage) (please refer to Table 1). As reviewed by Fernández-García et al. [7], the advantages and disadvantages of each method should be *a priori* understood to choose the best option according to the specific scientific question. Delivering an exogenous nutrient into an animal is not trivial, and depending on the administration method, it entails notable inherent technical limitations that may directly complicate the analysis of metabolomic data and interpretation of tumor metabolic phenotypes. Some of them have not been extensively covered in the literature, leaving a gap in our basic knowledge and much more space for improvement. Here, we focused on (i) the disruption of physiological homeostasis after bolus injections and (ii) the tissue-specific conversion of the tracer from one isotopologue to another and into its downstream metabolites.

2.1. Disruption of physiological homeostasis upon tracer administration

Although very few studies have reported results on this technical aspect, it is widely accepted that a discrete bolus of labeled nutrients causes intense and transient tracer peaks in the bloodstream as shown in mouse and human studies [16,17]. Such phenomenon has not been sufficiently described in the literature and deserves further attention because it can mislead the interpretation of tumor metabolic

Table 1 — Compilation of *in vivo* GC/LC-MS-based stable isotope tracing studies using labeled glucose, glutamine, and lactate in cancer mouse models.

Tracer administration	Fasting	Experimental details	Metabolic analysis	Ref
[^{13}C]-glucose				
Ad libitum liquid diet	None	[U−$^{13}C_6$]-glucose in liquid diet for 18 h	Fractional enrichment of intra-tumoral metabolites in NSCLC PDX models versus *ex vivo* tissue cultures	[20]
Infusion	Diurnal fasting of 6 h	[U−$^{13}C_6$]-glucose at 30 and 20 mg/kg/min for 6 h through the jugular vein and carotid artery in free-moving mice, anesthesia for mouse sacrifice	Glucose contribution to the TCA cycle in Ras-driven NSCLC tumors and tumor-derived cell lines	[10]
Infusion	Unspecified	[U−$^{13}C_6$]-glucose at 30 mg/kg/min for 6 h through the jugular vein	Pyruvate carboxylase activity estimation by differences between malate M+3 and succinate M+3 in breast cancer tumors and derived lung metastases	[12]
Infusion	Unspecified	[U−$^{13}C_6$]-glucose at 30 mg/kg/min for 6 h through the jugular vein	Proline catabolism by the activity of proline dehydrogenase in breast primary tumors and derived lung metastasis	[49]
Infusion	Nocturnal fasting of 16 h	[U−$^{13}C_6$]-glucose at approximately 540 mg/kg/min for 1 min by initial bolus followed by 11 mg/kg/min for 3 h through the tail vein under anesthesia [$^{13}C_3$]-lactate at 36 mg/kg/min for 10 min by initial bolus followed by 6 mg/kg/min for 3 h	Contribution of circulating lactate to glycolytic intermediates and the TCA cycle by co-infusion of fully labeled glucose and positional labeled lactate in tumors of human NSCLC xenografts in mice	[28]
Infusion	Nocturnal fasting	[U−$^{13}C_6$]-glucose at 1 mg/kg/min (after a 5 min priming) for 2 h through the jugular vein	Contribution of circulating glucose to the TCA cycle in colorectal tumors under anti-metabolic treatments	[50]
Infusion	Fasting of 6 h	[U−$^{13}C_6$]-glucose at 20 mg/kg/min for 3 h through the jugular vein in free-moving mice	Glucose oxidation and acetate production in primary soft tissue sarcoma mouse models	[51]
Infusion	Fasting of 16 h	[U−$^{13}C_6$]-glucose and [$^{13}C_{1,2}$]-glucose at 412.5 mg/kg for 1 min by initial bolus followed by 8 mg/kg/min for 3 h through the tail vein under anesthesia	Contribution of glucose to pyruvate and lactate Relative glucose flux through glycolysis over the PPP (ratio lactate M+2/M+1)	[52]
Infusion	Unspecified	[U−$^{13}C_6$]-glucose at 30 mg/kg/min for 6 h through the jugular vein	Glucose contribution to *de novo* biosynthesis of serine in primary breast cancer tumors and derived lung metastases	[13]
Discrete bolus	Unspecified	[U−$^{13}C_6$]-glucose at approximately 1 g/kg every 15 min for 1 h through the tail vein	Glucose entry to the TCA cycle by pyruvate carboxylase in a NSCLC mouse xenograft	[11]
Discrete bolus	Unspecified	[U−$^{13}C_6$]-glucose at 1 g/kg for 22 min through the tail vein [U−$^{13}C_5$]-glutamine at 0.15 g/kg	Glucose contribution to *de novo* synthesis of glutamine by glutamine synthetase in glioblastoma PDX mouse models	[23]
[^{13}C]-glutamine and [^{15}N]-glutamine				
Infusion	Unspecified	[U−$^{13}C_5$]-glutamine at 1.9 mg/kg/min for 4 h through the intra-carotid artery under anesthesia	Uptake of circulating glutamine by tumor cells in glioblastoma PDX mouse models	[23]
Infusion	Diurnal fasting of 6 h	[U−$^{13}C_5$]-glutamine at 2.0 mg/kg/min and 3.7 mg/kg/min for 6 h through the jugular vein and the carotid artery in free-moving mice, anesthesia for mouse sacrifice	Glutamine contribution to the TCA cycle in Ras-driven NSCLC tumors and tumor-derived cell lines	[10]
Infusion	Fasting of 16 h	[U−$^{13}C_5$]-glutamine at 172.5 mg/kg for 1 min by initial bolus followed by 2.88 mg/min/kg for 5 h through the tail vein under anesthesia	Contribution of glutamine to the TCA cycle intermediates in melanoma PDX mouse models	[52]
Infusion	Nocturnal fasting of 16 h	[γ-^{15}N]-glutamine at 300 mg/kg for 1 min by initial bolus followed by 5 mg/kg/min for 5 h through the tail vein under anesthesia	Glutamine γ-nitrogen contribution to the HBP by detection of UDP-HexNAc M+1 in tumors of subcutaneous lung xenograft mouse models	[14]
Discrete bolus	Unspecified	[γ-^{15}N]-glutamine at 700 mg/kg for 2 h and 4 h by intra-peritoneal injection	Contribution of glutamine-derived γ-nitrogen to orotate and dihydroorotate synthesis in subcutaneous Hela xenograft and breast tumors	[53]
Discrete bolus	Unspecified	[U−$^{13}C_5$]-glutamine and [U−$^{15}N_2$]-glutamine at 100 mg/kg for 10 min through the tail vein	Glutamine contribution to glutathione and pyrimidine nucleotide synthesis in chemotherapy-resistant AML tumors. *In vivo* and *in vitro* different usage of aspartate by AML cells	[17]
[^{13}C]-lactate				
Infusion	Fasting of 16 h	[$^{13}C_2$]-lactate at 15 mg/kg/min by initial bolus followed by 0.2 mg/kg/min for 2 h through the tail vein under anesthesia	Contribution of circulating lactate to the TCA cycle and glutamine by detection of malate M+1 in subcutaneous mouse xenografts of NSCLC	[16]

NSCLC, Nonsmall cell lung carcinoma; PDX, patient-derived xenograft; PPP, pentose phosphate pathway; HBP, hexosamine biosynthetic pathway.

phenotypes. Therefore, we have explored the extent to which tracer delivery through multiple discrete boluses could stimulate physiological metabolism and cause global metabolic changes in plasma.

In vivo stable isotope tracing by two discrete bolus injections was performed on tumor-bearing mice. Glucose and glutamine are two of the most abundant metabolites in plasma and they play critical functions in the metabolism of tumors; therefore, we decided to perform *in vivo* tracing by two successive intraperitoneal injections at a 20 min interval with the following stable isotope tracers: [U−$^{13}C_6$]-glucose or [U−$^{13}C_5$]-glutamine. Carbon-labeled glucose delivery caused global changes in the circulating metabolome of tumor-bearing mice, as shown by principal component analysis (PCA) (Figure 2A). Interestingly, glucose and many free fatty acids appear among the top 15 significantly discriminant metabolites, which hint at variations in the systemic energetic metabolism upon discrete administration of exogenous glucose (Figure 2B). Similarly, global changes in the circulating

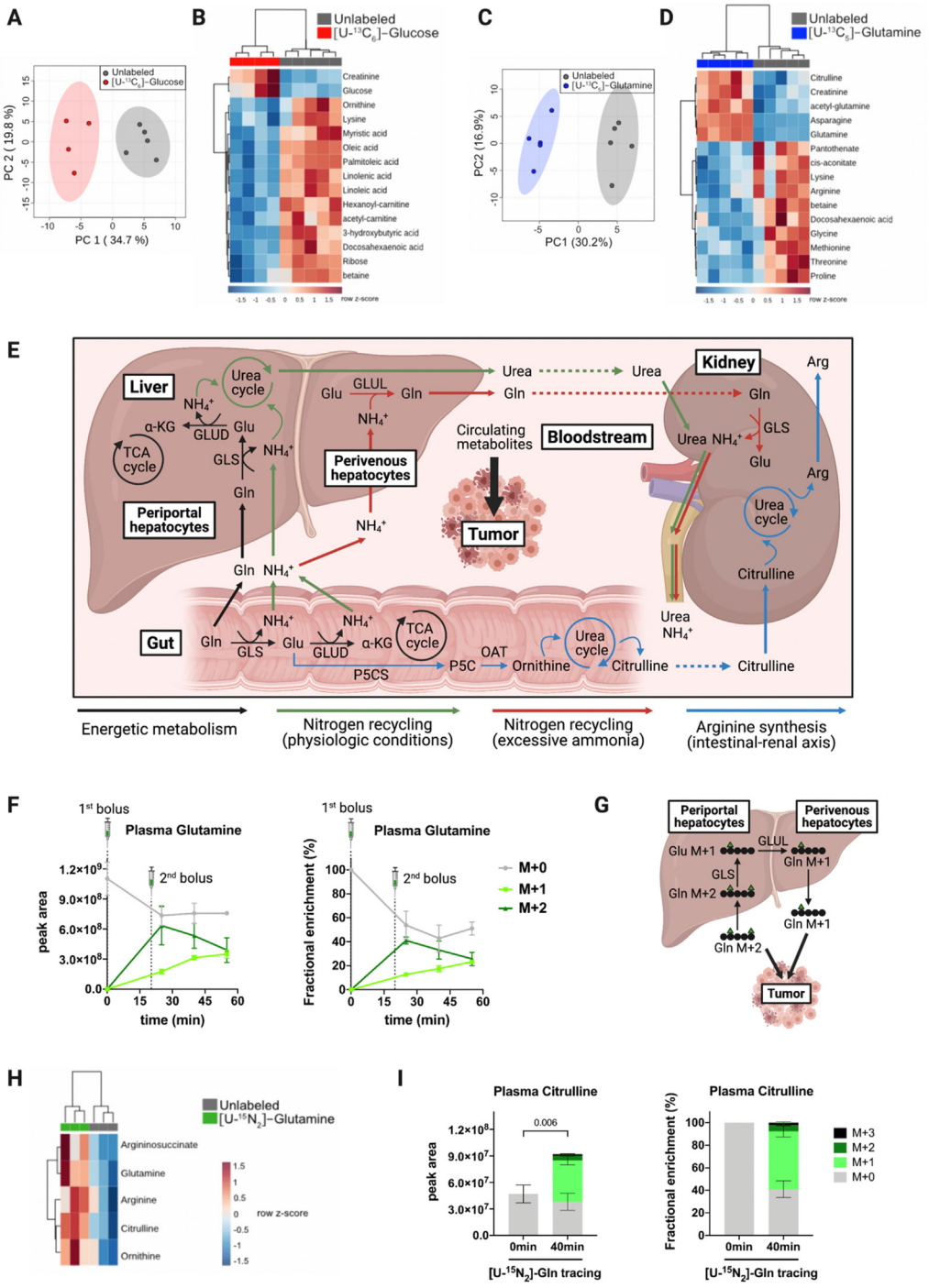

Figure 2: Impact of tracer administration on physiological homeostasis and interorgan exchange fluxes. A,C. Principal component analysis (PCA) plots of the circulating metabolome from tumor-bearing mice traced with [U−$^{13}C_6$]-glucose (n = 4) and [U−$^{13}C_5$]-glutamine (n = 5) *versus* unlabeled control mice (n = 5), respectively. The clustering has been performed based on 97 metabolites that were detectable and quantifiable in plasma with the LC-MS method used. **B,D.** Heatmap with the top 15 discriminant metabolites led to the clustering showed in panels A and C, respectively. Mice were intraperitoneally injected with two boluses separated by a 20-min interval of [U−$^{13}C_6$]-glucose (1 g/kg) and [U−$^{13}C_5$]-glutamine (0.3 g/kg). Blood was collected from the tail vein, 40 min after the first tracer injection. **E.** Schematic representation of the main glutamine interorgan exchange fluxes occurring in mammals and their impact on circulating metabolites that can be further taken up by tumors. **F.** Kinetics of M+0, M+1, and M+2 glutamine levels in plasma on [U−$^{15}N_2$]-glutamine tracing. Results are shown as peak areas (left panel) and fractional enrichment (right panel). Tumor-free mice were intraperitoneally injected with two boluses separated by a 20-min interval of [U−$^{15}N_2$]-glutamine (0.3 g/kg) and blood was collected from the tail vein at 0 min (n = 3), 25 min (n = 3), 40 min (n = 3), and 55 min (n = 3) after the first tracer injection. **G.** Schematic representation of the hypothetical conversion of circulating glutamine M+2 into glutamine M+1 on [U−$^{15}N_2$]-glutamine tracing. **H.** Heatmap representing changes in glutamine, argininosuccinate, arginine, citrulline, and ornithine levels in the plasma of tumor-free mice after 40 min of [U−$^{15}N_2$]-glutamine tracing (n = 3) compared to unlabeled mice (n = 3). **I.** Citrulline isotopologues in the plasma of tumor-free mice after 40 min of [U−$^{15}N_2$]-glutamine tracing (n = 3) *versus* unlabeled mice (n = 3). Results are shown as peak areas (left panel) and fractional enrichment (right panel). Results have been corrected for the presence of naturally occurring ^{13}C stable isotopes using Metabolite AutoPlotter, a free online tool for metabolomics data processing [43]. Bars represent mean ± SD. Statistical differences were determined by two-tailed Student's t-test. α-KG, α-ketoglutarate; Arg, arginine; Gln, glutamine; Glu, glutamate; GLS, glutaminase; GLUD, glutamate dehydrogenase; GLUL, glutamate-ammonia ligase; NH_4^+, ammonium; OAT, ornithine aminotransferase; P5CS, pyrroline-5-carboxylate synthase; and TCA, tricarboxylic acid. Created with BioRender.com.

metabolome of tumor-bearing mice were observed upon the delivery of carbon-labeled glutamine (Figure 2C). Glutamine, other amino acids, and urea cycle intermediates were among the top 15 significantly discriminant metabolites, suggesting alterations in the physiological metabolism of nitrogen upon discrete administration of exogenous glutamine (Figure 2D). These preliminary results indicate that discrete administration of exogenous nutritional sources can cause global changes in the circulating metabolome and possibly in the tumor metabolism, which could lead to misleading interpretations of tumor metabolic phenotypes.

Importantly, we cannot extrapolate to which extent plasma metabolic alterations induced by discrete bolus might impact the tumor metabolism. In cancer animal models, the nutrient composition of the plasma differs from that of the tumor interstitial fluid (TIF). Concentrations of a specific nutrient can either be increased, decreased, or unchanged in TIF compared to the plasma of a mouse with pancreatic cancer [22]. Depending on the nutrients modulated in plasma after tracer bolus, those alterations might not be mirrored in tumors. This will also be dictated by tumor-specific metabolic dependencies [10]. It could be argued that both the number of injections and the tracer doses we used are higher compared to other studies [23,24]. However, there are also examples in the literature where the total amount of [U−$^{13}C_6$]-glucose and [U−$^{13}C_5$]-glutamine injected is similar or even higher than what we have used [11,25,26]. Therefore, we encourage the scientific community studying cancer metabolism through *in vivo* stable isotope tracing to assess whether the delivery of a given tracer induces substantial changes not only in the tumor metabolome, but also in the circulating metabolome. Ideally, analysis of the tumor interstitial fluid metabolome would be even more informative. The experimental protocols thus could be optimized (e.g., lowering tracer concentration and/or doing single instead of multiple boluses) to minimize alterations in the physiological levels of the labeled source without compromising the isotopic enrichment required to track downstream metabolic reactions. As proposed by Yuan et al. [26], measuring glycemia throughout [U−$^{13}C_6$] glucose tracing experiments will be helpful to establish the optimal conditions. Similar real-time measurements of plasma glutamine concentration during tracer administration can also be considered using specific enzymatic analyzers.

2.2. Interorgan exchange fluxes of the tracer: a [U−^{15}N]-glutamine case study

Owing to its role as an energetic substrate for mammalian tissues, glucose has been traditionally recognized as the main source of interorgan circulatory fluxes. However, recent elegant studies have shown that up to 37 metabolites are sufficiently concentrated in mouse plasma to substantially contribute to interorgan fluxes. Constant infusion is the best technical option to achieve the isotopic steady state, facilitating the interpretation of complex labeling patterns derived from the interorgan exchange of the tracer. Metabolic flux analysis (MFA), which aims to model complex metabolic networks only if steady-state isotopic labeling is achieved highlighted that circulating lactate has the highest circulatory flux and is a major carbon source for TCA cycle anaplerosis in most mammalian organs and certain tumor entities [27,28]. However, MFA is based on mathematical assumptions and simplifications of interconnected metabolic networks that sometimesan mislead interpretations [29].

It cannot be excluded that interorgan exchanges of labeled sources other than glucose-derived metabolites occur. When studying tumor metabolism, considering the interorgan exchange of the tracer is crucial — as the resulting tracer and its downstream metabolites may complicate plasma and tumor labeling patterns. This might be of high importance if occurring at the level of nutrients to which cancer cells are addicted, because it could bring confusing interpretations of tumor metabolic phenotypes. Here, we aimed to recapitulate the importance of metabolic compartmentalization and the main interorgan exchange fluxes occurring in mammals to sustain physiological homeostasis [27,30–32]. We will focus on the interorgan fluxes derived from glutamine metabolism (summarized in Figure 2E), the most abundant amino acid in plasma, and one of the most common substrates used to study tumor metabolism through *in vivo* stable isotope tracing (refer to Table 1).

Apart from its contribution to nucleotides and protein synthesis, glutamine is involved in many metabolic pathways to sustain the physiological functions of mammalian tissues [33]. Therefore, glutamine has a high interorgan exchange flux (Figure 2E). Dietary glutamine is absorbed by the gut, where it is subsequently deaminated into glutamate and α-ketoglutarate (α-KG) to fuel the TCA cycle and sustain the energetic demands of enterocytes and colonocytes [34]. Beyond the gut, glutaminolysis supports TCA cycle anaplerosis in almost every organ, with a particularly high contribution in the pancreas [27].

Glutamine carbons also fuel anabolic pathways [33] leading to production of glucose and glycolytic intermediates not only in gluconeogenic tissues (liver, kidney), but also in other organs, such as the pancreas [32]. In addition, the incorporation of glutamine to both glycolytic and TCA cycle intermediates provides a carbon skeleton for synthesis of several nonessential amino acids (NEAAs). Glutamine carbons also contribute to the synthesis of glutathione, proline, and arginine; the latest through a pathway that involves the intestinal–renal axis [35–37]. Briefly, glutamine-derived glutamate is converted into pyrroline-5-carboxylate (P5C) in the small intestine, which serves as a precursor for the synthesis of ornithine, an intermediate of the urea cycle. Therefore, glutamine fuels the urea cycle in the gut, which in turn releases citrulline into the portal vein that is further taken up by the kidney for *de novo* biosynthesis of arginine [38,39] (Figure 2E).

The amide and amine groups of glutamine substantially contribute to the physiological metabolism of nitrogen [33]. The amide group is incorporated into the synthesis of asparagine, nucleotides, hexosamines, and nicotinamide adenine dinucleotide (NAD). Similarly, the amine group serves for the synthesis of several NEAAs (e.g., aspartate, alanine, and serine) through glutamate transamination. The highly active nitrogen metabolism in mammalian tissues generates considerable amounts of ammonium, which is toxic. Therefore, mammalian organs (mainly the liver and the kidney) act in concert to recycle ammonium under diverse physiological conditions [39,40].

Liver zonation regulates ammonium recycling through compartmentalization of glutamine metabolism (Figure 2E). Under physiological conditions, periportal hepatocytes extract glutamine from the portal vein and subsequently catabolize it into glutamate and α-KG. Glutaminolysis in periportal hepatocytes generates a carbon skeleton to fuel the TCA cycle and produce two ammonium molecules that are recycled as urea by the urea cycle [39]. The urea produced in periportal hepatocytes is then released into the bloodstream and transported to the kidneys, where it is eliminated through the urine. The liver is the only mammalian organ with a full urea cycle, and therefore, it also recycles ammonium derived from the nitrogen metabolism of other tissues. In perivenous hepatocytes, glutamate generated in periportal hepatocytes is taken up and converted into glutamine through the recycling of ammonium. When ammonium is excessively concentrated in plasma, this glutamine–glutamate–glutamine cycle in the liver is enhanced to maximize its recycling [39,41,42].

Physiological glutamine interorgan exchanges can be illustrated with *in vivo* [U−$^{15}N_2$]-glutamine tracing, which we performed in tumor-free mice through two discrete bolus injections. Importantly, a transient equilibrium between labeled and unlabeled glutamine was reached at least 30 min after the second bolus of [U−$^{15}N_2$]-glutamine. Nevertheless, a switch from M+2 to M+1 glutamine (the latest being the main circulating isotopologue) occurred in a time-dependent manner (Figure 2F) [43]. Such an unexpected and quick phenomenon (25 min after the first bolus injection) suggests a tissue-specific conversion of [U−$^{15}N_2$]-glutamine through the glutamine−glutamate−glutamine cycle between periportal and perivenous hepatocytes (Figure 2E, G). As the excessive intake of dietary protein or amino acids has been shown to increase renal ammonium excretion [40], we hypothesized that [U−$^{15}N_2$]-glutamine administration might stimulate glutaminolysis, and concomitantly, ammonium production. Therefore, this would activate ammonium recycling through the glutamine−glutamate−glutamine cycle in the liver, leading to the mix of circulating glutamine isotopologues that we observed.

Glutamine is highly taken up and metabolized by certain tumor types such as glioma and liver tumors [44,45]. Although not formally proved, it is likely that the presence of substantial glutamine in the bloodstream following two discrete [U−$^{15}N_2$]-glutamine boluses can alter the labeling patterns of glutamine addicted tumors. However, the position of the labeled nitrogen in circulating glutamine M+1 remains unresolved: Do we have a mix or only a specific $^{15}N_1$-glutamine isotopomer ($^{15}N_1$-amine- and/or $^{15}N_1$-amide-glutamine)? Since liquid chromatography coupled to tandem mass spectrometry (LC-MS-MS) was not performed, we cannot illustrate the isotopomer distribution of the glutamine M+1 isotopologue. Nevertheless, we hypothesized that conversion of glutamine M+2 into M+1 might occur in the liver (Figure 2F) [43]; thus the labeled nitrogen of glutamine M+1 should correspond to its amine-group (Figure 2G). In this case, the relative abundance of the metabolites that incorporate the ^{15}N-amide-group of glutamine would be under-estimated; possibly leading to false conclusions. Normalization according to the percentage of plasma glutamine M+2 enrichment would be a solution to correct the loss of labeled amide. However, this requires the achievement of a circulating isotopic steady state, which is not reached through tracer administration by bolus (es).

Physiological [U−$^{15}N_2$]-glutamine interorgan exchanges can also lead to the presence of other circulating labeled metabolites. For instance, glutaminolysis would generate an excess of labeled ammonium in the bloodstream. Although ammonium is physiologically recycled in the liver and excreted by the kidney through urine, this does not account for complete elimination [40]. Therefore, in the context of cancer, circulating labeled ammonium might be taken up and metabolically recycled by tumors through ammonium assimilating enzymes [46]. Reinforcing the hypothesis of a dynamic nitrogen metabolism upon [U−$^{15}N_2$]-glutamine administration, we observed increased levels of all urea cycle intermediates in the plasma of mice after 40 min of tracing (maximal glutamine abundance) (Figure 2H). Furthermore, consistent with the physiological synthesis of arginine through the intestinal−renal axis (Figure 2E), total levels of plasma citrulline were significantly higher and substantial levels of labeled citrulline were detected in circulation after 40 min of [U−$^{15}N_2$]-glutamine tracing (Figure 2I) [43]. Further *in vivo* isotope tracing experiments are required to refine the proposed hypothetical mechanism of interorgan exchange that might occur after discrete bolus administration of nitrogen-labeled glutamine.

It is also important to mention that if instead of tracing [U−$^{15}N_2$]-glutamine we had traced [U−$^{13}C_5$]-glutamine, we would have never observed the fast time-dependent conversion of one glutamine isotopologue to another in the bloodstream — because the carbon skeleton is maintained throughout this physiological glutamine−glutamate−glutamine cycle (Figure 2G). Therefore, the choice of the tracer is an important factor to consider according to the biological model used and the specific scientific question raised, when designing *in vivo* stable isotope tracing protocols.

Whether glutamine interorgan exchange might occur following continuous infusion of [U−$^{15}N_2$]-glutamine still needs to be addressed. Nevertheless, it seems plausible that this phenomenon is likely to be exacerbated by discrete administration methods, which do not allow for a constant supply of the tracer and require injections of the tracer at high concentrations and/or multiple boluses (refer to Table 1).

Although we cannot extend our results to other tracers, the interorgan exchange of circulating nutrients other than glutamine has been already reported in mammals [30−32]. Whether the resulting labeled metabolites in the bloodstream can alter tumor labeling patterns might depend on the avidity of cancer cells for this given nutrient. Recently, a glucose−alanine cycle between tumor and liver has been reported in a zebrafish melanoma model [47]. After considering the potential impact of delivering a tracer by discrete bolus, optimization of experimental settings would help to minimize the isotopic labeling of the tracer derived from an interorgan exchange, as it naturally happens. In our case, shortening the [U−$^{15}N_2$]-glutamine tracing period partially prevented the conversion of glutamine M+2 into glutamine M+1 without impacting tracer enrichment in the bloodstream (Figure 2F). Other parameters such as the route of administration might influence plasma and tumor labeling patterns. For instance, the route used to administer ^{13}C-labeled fructose has been shown to impact the way it is metabolized [48]. Therefore, it would be of interest to investigate whether delivering a given tracer through different discrete administration methods (oral, i. p, i. v) influences the outcome of the experiment. Finally, another parameter to consider is the fasting period that is usually performed before constant tracer infusions (refer to Table 1). However, the impact of fasting when performing *in vivo* stable isotope tracing has not been fully addressed and it will be considered in the following section.

3. TO BE FASTED OR NOT TO BE FASTED? THE PARADIGM OF FASTING IN ISOTOPE TRACING

Fasting of animal models before tracer administration is commonly included as part of most *in vivo* isotope tracing protocols despite any consensus. Fasting is expected to maximize tissue uptake of the labeled metabolite and minimize fluctuations in the concentration of plasma and tissue metabolites caused by variable feeding behaviors among animals fed *ad libitum*. This common practice might be analogous to the routine overnight fasting required in the clinic before measuring serum biochemical variables in humans (glycemia, cholesterol, for instance). Interestingly, changing this clinical standard to a more practical nonfasting blood sampling when measuring the lipidic profile has been effective for predictions of cardiovascular disease risk in humans [54].

In the case of *in vivo* stable isotope tracing, fasting is not intended to change animal metabolism, but to provide a basal postabsorptive metabolic state as has been described in humans [55]. Indeed, intraoperative [$^{13}U-C_6$]-glucose infusions for metabolomic analysis of resected tumors and biopsies from adults and children with different types of cancer have been performed under fasting as required by a surgical intervention [16,56,57]. In the context of cancer research on animal models, rigorous studies to experimentally determine the

optimal fasting duration to achieve a basal metabolic state in mice have not been undertaken yet. Interestingly, in stable isotope tracing studies, mice commonly undergo fasting periods that last longer than the clinical standard for human blood sampling. Whether mice deprived of food for 8h and longer are just fasted or rather starved is to be determined. Beyond the fasting duration, mice are also commonly fasted during their active night cycle, a practice that disrupts their natural feeding-fasting rhythm.

Few recent studies have investigated metabolite fluxes in fasted and fed states by independently infusing several labeled metabolites. However, analysis of total metabolite levels in plasma and tissue beyond labeling enrichment has not been reported [31,32]. Here, we discuss (i) the major systemic effects of fasting in mice and (ii) the impact of fasting on the levels of tumoral metabolites upon discrete bolus injections of fully carbon-labeled glucose. The latter topic will be illustrated with our metabolomics and tracing data.

3.1. Adaptive metabolism to food deprivation in mammals

Metabolic plasticity in fed, postabsorptive, and fasted states allows organisms to adjust their metabolic demands to nutrient availability (Figure 3A). In humans, the smooth metabolic transition from fed to fasted state is regulated by insulin, glucagon, and other hormones. Major changes after two or three days of fasting are glucose and nonesterified fatty acid release into plasma because of hepatic glycogenolysis and lipolysis in adipose tissue [58]. When hepatic glycogen stores are depleted, gluconeogenesis remains as the main hepatic pathway producing circulating glucose [59]. In accordance with this adaptive metabolism in humans, mice undergoing diurnal fasting for 8 h use glycogenolysis and gluconeogenesis for synthesis of glycolytic intermediates in most organs [32]. Indeed, gluconeogenesis has been shown to contribute more than glycogenolysis to circulating glucose, whereas glycogen stands out as a major contributor of glycolytic intermediates in mice fasted for 8 h [32].

Mice fasted for 8 h display higher glycogen breakdown in most organs to fuel tissue energetic demands as compared to fed animals. Gluconeogenesis contribution to circulating glucose and TCA cycle intermediates also occur in the liver and extrahepatic tissues of mice fasted for 8 h. Among the gluconeogenic substrates, lactate and glycerol contribute the most to circulating glucose and the TCA cycle in tissues. Major differences between 8 h-fasted and refed mice come from increased glycerol usage for the production of circulating glucose in fasted animals. This correlates with a key metabolic feature of the fasted state, i.e., the catabolism of triglycerides producing free pools of glycerol for gluconeogenesis [32]. In mice fasted for 8.5 h, glycerol followed by alanine and fatty acids made a higher direct contribution to circulating glucose than in fed mice [31]. Glucose conversion to circulating lactate (the Cori cycle) for subsequent lactate oxidation by tissues has been described as the main flux dictating carbohydrate oxidation irrespective of 8 h-fasting and refeeding in mice [32]. Apart from the Cori cycle with a flux rate notably decreased in fasted mice, other major circulating metabolite fluxes are not significantly perturbated after food deprivation for 8 h [31]. Overall, when a steady-state labeling is reached after the infusion of tracers other than glucose and fructose, fasting does not significantly change animal tissue nutrients consumption [31]. Besides adipose tissue and muscle, minor changes in tissue nutrient usage occurred in fasted mice for 8 h. The analysis of the specific labeled nutrient contribution to tissue metabolites along with the determination of total metabolite levels in plasma and tissue will bring novel notions of systemic and organ-specific changes because due to fasting.

Carbohydrate oxidation from dietary glucose constitutes the main source of energy production upon feeding. Mice refed during the night after diurnal fasting have shown two-fold higher carbohydrate oxidation and glucose turnover from the circulation as compared to fasted animals [32]. In the fasted state, energetic demands are satisfied from different substrates as compared to the fed state. As the availability of dietary glucose drops over the fasting period, there is a gradual switch from carbohydrate to fatty acid oxidation. Fatty acid oxidation in the liver not only yields energy for hepatic demands, but also produces alternative fuels such as ketone species by ketogenesis [59]. Circulating ketone species are taken up by extrahepatic tissues such as the brain, heart, and skeletal muscle for production of energy by terminal oxidation [60]. Indeed, the human circulating metabolome during starvation is characterized by high levels of ketone species, unsaturated long-chain fatty acids, and acylcarnitines along with ketogenic amino acids and their catabolites. Most of these metabolites reach significantly higher levels after two days of fasting in humans [58].

Mice fasted for 8.5 h during the day showed an augmented contribution of fatty acids to tissue TCA cycle intermediates as compared to fed animals. In addition, fatty acids were the major direct contributors to circulating D-β-hydroxybutyrate (D-βOHB), the most abundant ketone body. The direct contribution of this ketone to the tissue TCA cycle was higher in the fasted state. Thus, systemic carbohydrate and fat contribution to tissue TCA cycle stand out as the major metabolic phenomena differentiating fasted and fed states, respectively. Signs of this metabolic switch have been observed in mice fasted for 8.5 h [31]. Fasting, as a physiological challenge, elicits an evolutionarily conserved and adaptive metabolic mechanism characterized by a gradual switch in substrate usage to cope with energetic demands when dietary glucose becomes scarcer over time (Figure 3A).

3.2. Impact of fasting for *in vivo* stable isotope tracing on mouse physiology

Most of the stable isotope tracing studies in cancer mouse models in the previous years show variability in experimental setups with respect to fasting duration and timing (refer to Table 1). Several studies infusing glucose, glutamine, and lactate have reported fasting periods of 6 or 16 h [10,14,16,28,50–52]. For those studies where the fasting time was detailed, both diurnal and nocturnal fasting appeared as options. Despite the absence of consensus, overnight fasting for 16 h is the most common practice. Interestingly, one of the most recent tracing studies in healthy mice has reported that diurnal fasted animals for 8 h display a respiratory exchange ratio (RER) that decreased from 0.9 to 0.8 after 2 h of fasting. As a measure of carbon oxidation, RER was below 0.8 after 4 h of fasting onset, reflecting definitive fat burning [31]. Therefore, fasting for 16 h is expected to induce metabolic adaptations that rely on fatty acid oxidation for energy production. Another critical aspect of fasting beyond its duration is associated with its daily timing. Since mice are nocturnal mammals consuming food mainly in their active night cycle, an imposed nocturnal fasting disrupts their natural feeding-fasting cycle. Under normal conditions, the systemic circadian clock couples brain and systemic signals with the organism behavior to anticipate and adapt nutrient availability to energetic demands along the day–night cycle. Food intake and digestion along with carbohydrate and fat oxidation, as well as daily oscillations of the local and global metabolism are transcriptionally and hormonally regulated by the circadian clock [61]. Environmental desynchronization of the feeding-fasting rhythm of mice with their natural wake–sleep cycle might lead to metabolic alterations [61,62], whereas reinforcing the natural circadian rhythm with night-restricted feeding and diurnal fasting provides better control of physiological metabolic

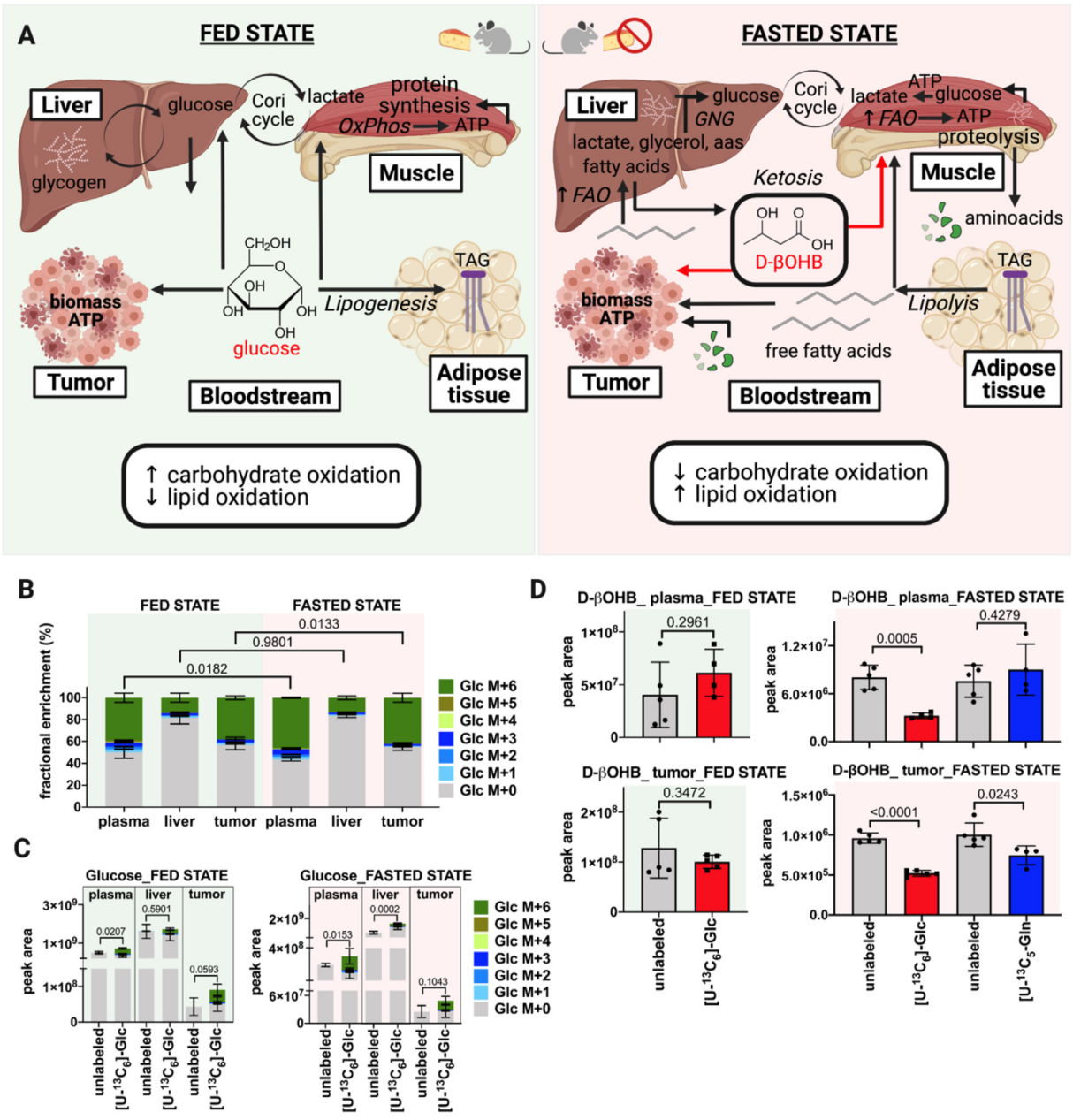

Figure 3: Metabolic plasticity during feeding and fasting. A. Schematic representation of the systemic metabolic phenomena occurring in fed and fasted states. Glycogen breakdown, gluconeogenesis, fatty acid release by lipolysis, and systemic switch from carbohydrate to lipid oxidation during the transit from fed to fasted states. Systemic changes impact tumoral metabolism depending on the availability of energetic substrates. **B.** Fractional enrichment of ^{13}C-labeled glucose in plasma, liver, and tumor of fasted (n = 4–5) and fed mice (n = 4–5) on [U−$^{13}C_6$]-glucose administration. **C.** Peak area of glucose isotopologues in plasma, liver, and tumor of fasted (n = 4–5) and fed mice (n = 4–5) traced with [U−$^{13}C_6$]-glucose *versus* their respective unlabeled control mice (n = 4–5). [U−$^{13}C_6$]-glucose (1 g/kg) was administered by two intraperitoneal boluses separated by a 20-min interval in 3 h-fasted and fed tumor-bearing mice. Blood was collected from the tail vein 40 min after the first tracer injection. Results have been corrected for the presence of naturally occurring ^{13}C stable isotopes using Metabolite AutoPlotter, a free online tool for metabolomics data processing [43]. **D.** Total levels of D-β-hydroxybutyrate in plasma and tumor of fed and fasted mice traced with [U−$^{13}C_6$]-glucose (1 g/kg) and [U−$^{13}C_5$]-glutamine (0.3 g/kg) *versus* their respective unlabeled control mice (n = 4–5). Bars represent mean ± SD. Statistical differences were determined by the two-tailed Student's t-test. OxPhos, oxidative phosphorylation; FAO, fatty acid oxidation; TAG, triglycerides; D-βOHB, D-β-hydroxybutyrate. Created with BioRender.com.

parameters [62,63]. Mice undergoing diurnal or nocturnal fasting for only a day display perturbations in the circadian rhythmic expression of more than 80% of hepatic transcripts as compared to mice fed *ad libitum* [64]. Therefore, it is rational to argue that food deprivation for 16 h overnight before tracer administration entails not only a prolonged period of fasting, but also circadian metabolic perturbations. These potential physiological alterations should be experimentally determined and considered for *in vivo* stable isotope tracing experiments.

It is still unclear whether diurnal fasting impacts tracer enrichment in the bloodstream and global or tumor metabolism. Some suggestions can be made from our metabolomics studies. Subcutaneous tumor-bearing mice fasted in the morning for 3 h or fed *ad libitum* were

supplemented with [U−$^{13}C_6$]-glucose by discrete boluses (Figure 3B) [43]. Tracer enrichment in the circulation was slightly and significantly lower in fed mice compared to fasted animals, although sufficiently high (40%) to detect labeling into downstream metabolites (Figure 3B) [43]. Whereas levels of [U-$^{13}C_6$]-glucose were not different in the liver, labeled glucose in tumors mimicked circulating levels of the tracer. Heterogeneity among samples did not stand out as a parameter that was dramatically changed between fasted and fed state. Thus, in terms of tracer enrichment, a diurnal fasting period of 3 h when performing glucose tracing by discrete boluses does not bring apparent benefits.

Administration of [U−$^{13}C_6$]-glucose increased total levels of glucose in plasma and tumor irrespective of fasted and fed state (Figure 3C) [43]. In the liver, total glucose levels upon tracer administration were increased in the fasted state, but not in fed mice despite similar enrichment of labeled glucose (Figure 3B) [43]. These higher levels of hepatic glucose correlate with higher levels of circulating glucose following its exogenous administration, and likely, with an augmented hepatic appetite for sugar upon its availability.

Total levels of circulating D-β-hydroxybutyrate (D-βOHB) were significantly decreased in fasted mice on supplementation with [U−$^{13}C_6$]-glucose, but not with [U−$^{13}C_5$]-glutamine (Figure 3D, upper panel). As glucose is the preferential energetic substrate at a systemic level, these results may indicate a ketogenic status that is not ameliorated by a less favorite source of energy, glutamine. Circulating levels of this ketone body did not change in fed mice irrespective of labeled glucose administration. In tumors, the abundance of D-βOHB was significantly decreased after labeled glucose supplementation and to a lesser extent upon labeled glutamine administration in fasted mice (Figure 3D, lower panel). No changes were observed in plasma and tumors of fed animals irrespective of labeled glucose administration. As a ketone body, D-βOHB could be synthesized at higher levels by its main producer, the liver, exported to the circulation and taken up by the tumor as an alternative energetic fuel in fasted mice. We cannot exclude that D-βOHB could also be produced at a higher extent by the tumor itself [60]. Irrespective of the source of this ketone body, reduced levels of intratumoral D-βOHB in fasted mice are likely associated with the exogenous administration of labeled glucose and glutamine. Therefore, fasting might impact tumoral metabolism by favoring the use of alternative energetic fuels such as ketones due to food deprivation. Even though tracer supplementation decreased intratumoral levels of D-βOHB to different degrees depending on the labeled nutrient exogenously administrated, terminal oxidation of D-βOHB through oxidative phosphorylation might still occur in fasted mice upon tracing as compared to fed animals. Tracing the fate of labeled carbons in fasted mice might partially reflect a gradual switch from ketone to tracer oxidation in tumors rather than a basal metabolic usage of the labeled nutrient by transformed tissues.

Metabolic alterations associated with fasting and subsequent tracer supplementation by discrete bolus cannot be ruled out. Beyond tracer supplementation-associated disturbances of the animal physiology, nonoptimized fasting periods may contribute to systemic and tissue-specific metabolic alterations. We encourage, as a rational alternative, (i) to perform *in vivo* stable isotope tracing experiments in fasted and fed mice to determine the optimal conditions in a cancer animal model of interest. *In vivo* tracing without prior fasting would not only be experimentally simpler, but also advantageous. If fasting is experimentally proven to be beneficial for *in vivo* tracing in cancer animal models, we suggest (ii) diurnal and short-term food restriction in mice. Considering that fasting might impact animal physiology and stable isotope tracing, it is intriguing to consider whether tracing in mice depleted of certain nutrients will lead to confounding interpretations. Such a complex scenario will be illustrated in the next section, focusing on mice under amino acid-restricted diets or amino acid-depleting antimetabolic drugs.

4. IMPACT OF AMINO ACID RESTRICTION APPROACHES ON *IN VIVO* STABLE ISOTOPE TRACING

Amino acids (AAs) not only serve as building blocks for protein synthesis, but also provide carbons and nitrogen atoms for anabolic reactions, energy production, regulation of the redox balance as well as epigenetic and post-transcriptional gene expression. Therefore, beyond their widely known glucose dependence, it is now well-established that cancer cells are also addicted to nonessential amino acids (NEAAs) to sustain tumor growth [65,66]. As a consequence, the classification of AAs as essential and nonessential does not properly reflect tumor dependencies and several NEAAs have been reclassified as conditionally essential in the context of cancer [67,68].

The AA requirements of cancer cells are dependent on several factors irrespective of their oncogenic mutations. However, both extracellular (i.e., in the TME) and intracellular AA availability dictate the dependency of tumors for certain AAs. In this sense, some tumors are dependent on *de novo* biosynthesis of the NEAAs that are present at very low concentrations in plasma, such as aspartate [69,70]. Similarly, some AAs (e.g., glutamine, and serine) are spatially depleted within the TME of certain cancer types [22], rendering tumors dependent on *de novo* biosynthesis [71] or extracellular protein scavenging [72,73]. In addition, conditionally essential AAs can also be *de novo* synthesized at insufficient concentrations to satisfy tumor needs, which partly explains the avidity of cancer cells for exogenous sources of such AAs. Moreover, some tumors are auxotrophic for certain NEAAs since epigenetic modifications suppress the expression of key metabolic enzymes involved in their *de novo* biosynthesis. For instance, the gene encoding for the asparagine synthetase (ASNS) enzyme is commonly silenced in acute lymphoblastic leukemia (ALL), rendering ALL cells auxotrophic for asparagine [74]. Similarly, several cancers are deficient for the urea cycle enzyme, argininosuccinate synthase (ASS1), which appears to be a metabolic advantage by diverting aspartate into *de novo* pyrimidine synthesis [75], but renders ASS1-deficient cancer cells auxotrophic for arginine [76].

Targeting the addiction of tumors for certain AAs appears to be a promising anticancer therapeutic strategy. In this context, AA dietary modifications are emerging as a potential approach to exploit the AA dependencies of tumors to enhance anticancer therapies [77,78]. For instance, tumor growth inhibition and sensitization to chemo- and radiotherapy have been observed in several mouse cancer mouse models fed a low-methionine diet [79]. Interestingly, dietary restriction of certain NEAAs has also shown antitumoral effects. For instance, serine/glycine-free diets have been efficient in reducing tumor growth in several xenografts and autochthonous mouse cancer models driven by different mutations [80,81]. More recently, limiting asparagine bioavailability through dietary restriction has been shown to reduce the metastatic potential of an orthotopic breast cancer mouse model [82]. Going a step further, it would be of great interest to study tumor metabolism in mouse cancer models under AA-restricted diets. Understanding how cancer cells adapt their metabolism to sustain tumor growth will help to identify and tackle the potential mechanisms of resistance occurring on AA restriction. In *in vitro* settings, stable isotope tracing appears to be a valuable tool to follow the metabolic adaptations of cancer cells deprived of specific AAs. [U−$^{13}C_6$]-glucose tracing *in vitro* has shown that *de novo* serine synthesis is induced by

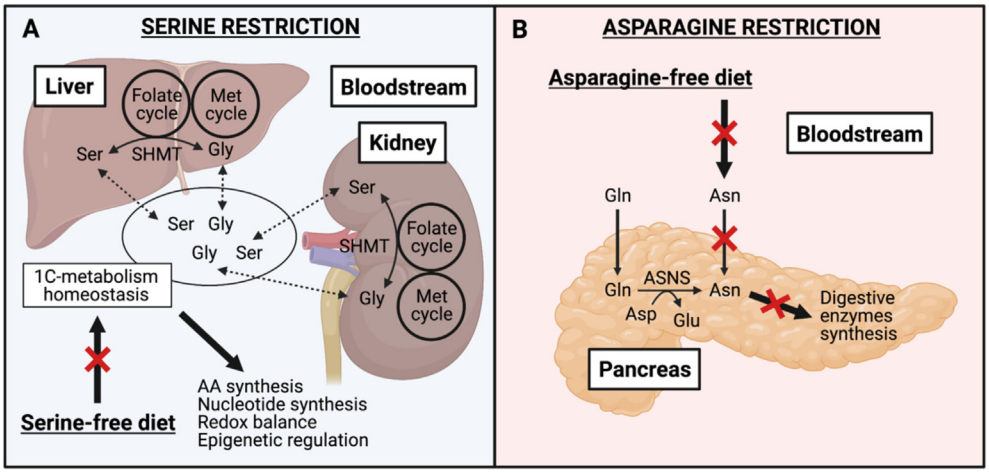

Figure 4: Impact of systemic AA restriction in the physiological metabolism of healthy tissues. A. Physiological functions of 1C-metabolism; the role of the liver and the kidney in the maintenance of its homeostasis and potential impact of serine-free diets. **B.** Pancreas dependence on asparagine uptake and *de novo* production for the synthesis of digestive enzymes and the potential impact of asparagine-free diets. 1C, one-carbon; AA, amino acid; Asn, asparagine; ASNS, asparagine synthetase; Asp, aspartate; Gln, glutamine; Glu, glutamate; Gly, glycine; Met, methionine; Ser, Serine; and SHMT, serine hydroxymethyltransferase. Created with BioRender.com.

cancer cells under serine-deprived conditions. As a consequence, the combination of dietary serine restriction and pharmacological inhibition of phosphoglycerate dehydrogenase (PHGDH), a rate-limiting enzyme in the serine biosynthetic pathway, has shown antitumoral effects on mouse cancer models resistant to each treatment alone [81,83]. Indeed, *in vivo* [U—$^{13}C_6$]-glucose tracing has not been performed to directly prove increased *de novo* serine synthesis in tumors of mice fed with a serine-free diet. However, very few studies have applied *in vivo* stable isotope tracing to unravel tumor metabolism in animals upon AA restriction or any other antimetabolic treatment [17,84,85]. In addition, many of these studies have limited the use of *in vivo* stable isotope tracing to assess the efficacy of enzymatic inhibitors, without exploring potential tumor metabolic adaptations in response to a given anti-metabolic treatment [86—88]. Based on the scarcity of these studies, we hypothesized that the physiological consequences of systemic AA deprivation might lead to a very complex isotopic scenario in the TME that challenges the interpretation of tumor labeling patterns. At a physiological level, it is not trivial to starve tumors of AAs without impacting the systemic metabolism. The depletion of circulating AAs disrupts the AA physiological homeostasis, which is dictated by the organ-specific metabolite turnover [30]. To illustrate this point, serine and glycine are highly interconverted both in the kidney and the liver, contributing to the systemic homeostasis of one-carbon metabolism, which supports important physiological processes (e.g., nucleotide and amino acid synthesis, redox balance, epigenetic regulation) [30,39,40,89,90] (Figure 4A). Despite being the organ expressing the highest levels of ASNS [91—93], the pancreas is addicted to exogenous sources of asparagine, a feature that is reflected by asparagine enrichment in digestive enzymes synthesized by pancreatic acinar cells as compared to the global proteome [94] (Figure 4B). Therefore, targeting tumor nutritional requirements using specific AA restriction strategies may also impact the metabolism of nontumoral tissues, especially those with specific AA metabolic functions, a phenomenon that might disturb the composition of the circulating metabolome. While plasma AA levels of tumor-bearing mice have been shown to remain highly constant even upon protein deprivation — partly owing to muscle atrophy to maintain a constant supply of EAAs in mammalian organs [78,95] — it is reasonable to argue that upon AA dietary restriction, the organism will undergo adaptative responses to sustain its physiologic metabolic functions. Based on the metabolic alterations observed on tracer administration (Figure 2), we hypothesized that performing *in vivo* stable isotope tracing on mouse cancer models fed with an AA-restricted diet might stimulate systemic adaptative responses leading to specific interorgan exchange and conversion of the labeled source. In this scenario, the interpretation of tumor labeling patterns would become particularly challenging, which might explain the lack of such studies in the literature.

5. CONCLUSIONS & PERSPECTIVES

Despite the apparent difficulty of studying the metabolism of nutritional-restricted tumors by *in vivo* stable isotope tracing, we strongly believe that this is a necessary step to deeply understand the metabolic adaptations leading to treatment escape and tumor relapse. Therefore, we encourage the scientific community to address this hot topic. As previously described, careful selection of the tracer, optimization of its concentration, administration method, and duration of the tracing period will be key to designing protocols that can address specific scientific questions and obtain interpretable results. Thus, an exhaustive bibliographic study of the physiological adaptative responses occurring upon restriction of specific metabolites followed by an experimental optimization in the cancer animal model of interest will be required. Importantly, most tumor entities are composed of various cell types including cancer cells (evolving in hypoxic or oxygenated areas) and stromal cells (fibroblasts, immune, and endothelial cells). There is extensive evidence of cross-talk between cancer cells and stromal cells to sustain tumor metabolism [23,96—100]. Consequently, each cell-specific population contributes to the metabolic profile of the tumor *in vivo* [101,102]. When performing *in vivo* stable isotope tracing, these different populations might metabolize tracer, providing labeled metabolites independent of the circulation, another complex scenario that might resemble the interorgan exchange of labeled nutrients. Determining the metabolic features of cancer cells and different cell populations within the TME have been challenging till now; because the time needed to isolate the different cell populations is incompatible with the stability of the

metabolites that have a rapid turnover [96]. Tracing labeled nutrients (for instance, [U−$^{13}C_6$]-glucose) into macromolecules with a lower turnover than metabolites has been proposed as an elegant solution to dissect cell-type specific metabolism in pancreatic adenocarcinomas [103].

FUNDING SOURCES

This project has received funding from the European Union's Horizon 2020 research and innovation program under the Marie Skłodowska-Curie grant agreement No 766214 (META-CAN), by La Ligue Contre le Cancer, le Cancéropole PACA, l'Inserm and the Agence Nationale de la Recherche (LABEX SIGNALIFE ANR-11- LABX-0028-01). JC obtained a grant from la Fondation ARC.

ACKNOWLEDGMENTS

We thank Dr. I. Nemazanyy (Platforme d'étude du metabolism, SFR-Necker, Inserm US 24 - CNRS UMS 3633, Paris, France) for LC-MS metabolomics analyses and helpful discussions.

CONFLICT OF INTEREST

None declared.

REFERENCES

[1] Hanahan, D., Weinberg, R.A., 2011. Hallmarks of cancer: the next generation. Cell 144(5):646−674. https://doi.org/10.1016/j.cell.2011.02.013.

[2] Pavlova, N.N., Thompson, C.B., 2016. The emerging hallmarks of cancer metabolism. Cell Metabolism 23(1):27−47. https://doi.org/10.1016/j.cmet.2015.12.006.

[3] Faubert, B., DeBerardinis, R.J., 2017. Analyzing tumor metabolism *in vivo*. Annual Review of Cancer Biology 1(1):99−117. https://doi.org/10.1146/annurev-cancerbio-050216-121954.

[4] Jang, C., Chen, L., Rabinowitz, J.D., 2018. Metabolomics and isotope tracing. Cell 173(4):822−837. https://doi.org/10.1016/j.cell.2018.03.055.

[5] Kaushik, A.K., DeBerardinis, R.J., 2018. Applications of Metabolomics to Study Cancer Metabolism. Biochimica et Biophysica Acta. Reviews on Cancer 1870(1):2−14. https://doi.org/10.1016/j.bbcan.2018.04.009.

[6] Buescher, J.M., Antoniewicz, M.R., Boros, L.G., Burgess, S.C., Brunengraber, H., Clish, C.B., et al., 2015. A roadmap for interpreting 13C metabolite labeling patterns from cells. Current Opinion in Biotechnology 34:189−201. https://doi.org/10.1016/j.copbio.2015.02.003.

[7] Fernández-García, J., Altea-Manzano, P., Pranzini, E., Fendt, S.-M., 2020. Stable isotopes for tracing mammalian-cell metabolism *in vivo*. Trends in Biochemical Sciences 45(3):185−201. https://doi.org/10.1016/j.tibs.2019.12.002.

[8] Vande Voorde, J., Ackermann, T., Pfetzer, N., Sumpton, D., Mackay, G., Kalna, G., et al., 2019. Improving the metabolic fidelity of cancer models with a physiological cell culture medium. Science Advances 5(1):eaau7314. https://doi.org/10.1126/sciadv.aau7314.

[9] Rossiter, N.J., Huggler, K.S., Adelmann, C.H., Keys, H.R., Soens, R.W., Sabatini, D.M., et al., 2021. CRISPR screens in physiologic medium reveal conditionally essential genes in human cells. Cell Metabolism 33(6):1248−1263. https://doi.org/10.1016/j.cmet.2021.02.005 e9.

[10] Davidson, S.M., Papagiannakopoulos, T., Olenchock, B.A., Heyman, J.E., Keibler, M.A., Luengo, A., et al., 2016. Environment impacts the metabolic dependencies of ras-driven non-small cell lung cancer. Cell Metabolism 23(3):517−528. https://doi.org/10.1016/j.cmet.2016.01.007.

[11] Sellers, K., Fox, M.P., Bousamra, M., Slone, S.P., Higashi, R.M., Miller, D.M., et al., 2015. Pyruvate carboxylase is critical for non-small-cell lung cancer proliferation. Journal of Clinical Investigation 125(2):687−698. https://doi.org/10.1172/JCI72873.

[12] Christen, S., Lorendeau, D., Schmieder, R., Broekaert, D., Metzger, K., Veys, K., et al., 2016. Breast cancer-derived lung metastases show increased pyruvate carboxylase-dependent anaplerosis. Cell Reports 17(3):837−848. https://doi.org/10.1016/j.celrep.2016.09.042.

[13] Rinaldi, G., Pranzini, E., Van Elsen, J., Broekaert, D., Funk, C.M., Planque, M., et al., 2021. *In vivo* evidence for serine biosynthesis-defined sensitivity of lung metastasis, but not of primary breast tumors, to mTORC1 inhibition. Molecular Cell 81(2):386−397. https://doi.org/10.1016/j.molcel.2020.11.027 e7.

[14] Kim, J., Lee, H.M., Cai, F., Ko, B., Yang, C., Lieu, E.L., et al., 2020. The hexosamine biosynthesis pathway is a targetable liability in KRAS/LKB1 mutant lung cancer. Nature Metabolism 2(12):1401−1412. https://doi.org/10.1038/s42255-020-00316-0.

[15] Su, X., Lu, W., Rabinowitz, J.D., 2017. Metabolite spectral accuracy on orbitraps. Analytical Chemistry 89(11):5940−5948. https://doi.org/10.1021/acs.analchem.7b00396.

[16] Hensley, C.T., Faubert, B., Yuan, Q., Lev-Cohain, N., Jin, E., Kim, J., et al., 2016. Metabolic heterogeneity in human lung tumors. Cell 164(4):681−694. https://doi.org/10.1016/j.cell.2015.12.034.

[17] van Gastel, N., Spinelli, J.B., Sharda, A., Schajnovitz, A., Baryawno, N., Rhee, C., et al., 2020. Induction of a timed metabolic collapse to overcome cancer chemoresistance. Cell Metabolism 32(3):391−403. https://doi.org/10.1016/j.cmet.2020.07.009 e6.

[18] Lønbro, S., Wiggins, J.M., Wittenborn, T., Elming, P.B., Rice, L., Pampo, C., et al., 2019. Reliability of blood lactate as a measure of exercise intensity in different strains of mice during forced treadmill running. PloS One 14(5):e0215584. https://doi.org/10.1371/journal.pone.0215584.

[19] La Monaca, E., Fodale, V., 2012. Effects of anesthetics on mitochondrial signaling and function. Current Drug Safety 7(2):126−139. https://doi.org/10.2174/157488612802715681.

[20] Sun, R.C., Fan, T.W.-M., Deng, P., Higashi, R.M., Lane, A.N., Le, A.-T., et al., 2017. Noninvasive liquid diet delivery of stable isotopes into mouse models for deep metabolic network tracing. Nature Communications 8(1):1646. https://doi.org/10.1038/s41467-017-01518-z.

[21] Williams, H.C., Piron, M.A., Nation, G.K., Walsh, A.E., Young, L.E.A., Sun, R.C., et al., 2020. Oral gavage delivery of stable isotope tracer for in vivo metabolomics. Metabolites 10(12). https://doi.org/10.3390/metabo10120501.

[22] Sullivan, M.R., Danai, L.V., Lewis, C.A., Chan, S.H., Gui, D.Y., Kunchok, T., et al., 2019. Quantification of microenvironmental metabolites in murine cancers reveals determinants of tumor nutrient availability. ELife 8. https://doi.org/10.7554/eLife.44235.

[23] Tardito, S., Oudin, A., Ahmed, S.U., Fack, F., Keunen, O., Zheng, L., et al., 2015. Glutamine synthetase activity fuels nucleotide biosynthesis and supports growth of glutamine-restricted glioblastoma. Nature Cell Biology 17(12):1556−1568. https://doi.org/10.1038/ncb3272.

[24] Méndez-Lucas, A., Lin, W., Driscoll, P.C., Legrave, N., Novellasdemunt, L., Xie, C., et al., 2020. Identifying strategies to target the metabolic flexibility of tumours. Nature Metabolism 2(4):335−350. https://doi.org/10.1038/s42255-020-0195-8.

[25] Lane, A.N., Yan, J., Fan, T.W.-M., 2015. 13C tracer studies of metabolism in mouse tumor xenografts. Bio-protocol 5(22). https://doi.org/10.21769/bioprotoc.1650.

[26] Yuan, M., Kremer, D.M., Huang, H., Breitkopf, S.B., Ben-Sahra, I., Manning, B.D., et al., 2019. Ex vivo and in vivo stable isotope labelling of central carbon metabolism and related pathways with analysis by LC−MS/MS. Nature Protocols 14(2):313−330. https://doi.org/10.1038/s41596-018-0102-x.

[27] Hui, S., Ghergurovich, J.M., Morscher, R.J., Jang, C., Teng, X., Lu, W., et al., 2017. Glucose feeds the TCA cycle via circulating lactate. Nature 551(7678): 115–118. https://doi.org/10.1038/nature24057.

[28] Faubert, B., Li, K.Y., Cai, L., Hensley, C.T., Kim, J., Zacharias, L.G., et al., 2017. Lactate metabolism in human lung tumors. Cell 171(2):358–371. https://doi.org/10.1016/j.cell.2017.09.019 e9.

[29] Antoniewicz, M.R., 2018. A guide to 13C metabolic flux analysis for the cancer biologist. Experimental & Molecular Medicine 50(4):1–13. https://doi.org/10.1038/s12276-018-0060-y.

[30] Jang, C., Hui, S., Zeng, X., Cowan, A.J., Wang, L., Chen, L., et al., 2019. Metabolite exchange between mammalian organs quantified in pigs. Cell Metabolism 30(3):594–606. https://doi.org/10.1016/j.cmet.2019.06.002 e3.

[31] Hui, S., Cowan, A.J., Zeng, X., Yang, L., TeSlaa, T., Li, X., et al., 2020. Quantitative fluxomics of circulating metabolites. Cell Metabolism 32(4): 676–688. https://doi.org/10.1016/j.cmet.2020.07.013 e4.

[32] TeSlaa, T., Bartman, C.R., Jankowski, C.S.R., Zhang, Z., Xu, X., Xing, X., et al., 2021. The source of glycolytic intermediates in mammalian tissues. Cell Metabolism 33(2):367–378. https://doi.org/10.1016/j.cmet.2020.12.020 e5.

[33] Wu, G., 2009. Amino acids: metabolism, functions, and nutrition. Amino Acids 37(1):1–17. https://doi.org/10.1007/s00726-009-0269-0.

[34] Beaumont, M., Blachier, F., 2020. Amino acids in intestinal physiology and health. Advances in Experimental Medicine & Biology 1265:1–20. https://doi.org/10.1007/978-3-030-45328-2_1.

[35] Brosnan, M.E., Brosnan, J.T., 2004. Renal arginine metabolism. Journal of Nutrition 134(10 Suppl):2791S–2795S. https://doi.org/10.1093/jn/134.10.2791S discussion 2796S-2797S.

[36] van de Poll, M.C.G., Soeters, P.B., Deutz, N.E.P., Fearon, K.C.H., Dejong, C.H.C., 2004. Renal metabolism of amino acids: its role in interorgan amino acid exchange. American Journal of Clinical Nutrition 79(2):185–197. https://doi.org/10.1093/ajcn/79.2.185.

[37] Buijs, N., Brinkmann, S.J.H., Oosterink, J.E., Luttikhold, J., Schierbeek, H., Wisselink, W., et al., 2014. Intravenous glutamine supplementation enhances renal de novo arginine synthesis in humans: a stable isotope study. American Journal of Clinical Nutrition 100(5):1385–1391. https://doi.org/10.3945/ajcn.113.081547.

[38] van de Poll, M.C.G., Siroen, M.P.C., van Leeuwen, P.A.M., Soeters, P.B., Melis, G.C., Boelens, P.G., et al., 2007. Interorgan amino acid exchange in humans: consequences for arginine and citrulline metabolism. American Journal of Clinical Nutrition 85(1):167–172. https://doi.org/10.1093/ajcn/85.1.167.

[39] Hou, Y., Hu, S., Li, X., He, W., Wu, G., 2020. Amino acid metabolism in the liver: nutritional and physiological significance. Advances in Experimental Medicine & Biology 1265:21–37. https://doi.org/10.1007/978-3-030-45328-2_2.

[40] Li, X., Zheng, S., Wu, G., 2020. Amino acid metabolism in the kidneys: nutritional and physiological significance. Advances in Experimental Medicine & Biology 1265:71–95. https://doi.org/10.1007/978-3-030-45328-2_5.

[41] Brosnan, J.T., 2003. Interorgan amino acid transport and its regulation. Journal of Nutrition 133(6 Suppl 1):2068S–2072S. https://doi.org/10.1093/jn/133.6.2068S.

[42] Hakvoort, T.B.M., He, Y., Kulik, W., Vermeulen, J.L.M., Duijst, S., Ruijter, J.M., et al., 2017. Pivotal role of glutamine synthetase in ammonia detoxification. Hepatology 65(1):281–293. https://doi.org/10.1002/hep.28852.

[43] Pietzke, M., Vazquez, A., 2020. Metabolite AutoPlotter - an application to process and visualise metabolite data in the web browser. Cancer & Metabolism 8:15. https://doi.org/10.1186/s40170-020-00220-x.

[44] Yuneva, M.O., Fan, T.W.M., Allen, T.D., Higashi, R.M., Ferraris, D.V., Tsukamoto, T., et al., 2012. The metabolic profile of tumors depends on both the responsible genetic lesion and tissue type. Cell Metabolism 15(2):157–170. https://doi.org/10.1016/j.cmet.2011.12.015.

[45] Venneti, S., Dunphy, M.P., Zhang, H., Pitter, K.L., Zanzonico, P., Campos, C., et al., 2015. Glutamine-based PET imaging facilitates enhanced metabolic evaluation of gliomas *in vivo*. Science Translational Medicine 7(274):274ra17. https://doi.org/10.1126/scitranslmed.aaa1009.

[46] Spinelli, J.B., Yoon, H., Ringel, A.E., Jeanfavre, S., Clish, C.B., Haigis, M.C., 2017. Metabolic recycling of ammonia via glutamate dehydrogenase supports breast cancer biomass. Science (New York, N.Y 358(6365):941–946. https://doi.org/10.1126/science.aam9305.

[47] Naser, F.J., Jackstadt, M.M., Fowle-Grider, R., Spalding, J.L., Cho, K., Stancliffe, E., et al., 2021. Isotope tracing in adult zebrafish reveals alanine cycling between melanoma and liver. Cell Metabolism. https://doi.org/10.1016/j.cmet.2021.04.014.

[48] Jang, C., Hui, S., Lu, W., Cowan, A.J., Morscher, R.J., Lee, G., et al., 2018. The small intestine converts dietary fructose into glucose and organic acids. Cell Metabolism 27(2):351–361. https://doi.org/10.1016/j.cmet.2017.12.016 e3.

[49] Elia, I., Broekaert, D., Christen, S., Boon, R., Radaelli, E., Orth, M.F., et al., 2017. Proline metabolism supports metastasis formation and could be inhibited to selectively target metastasizing cancer cells. Nature Communications 8(1):15267. https://doi.org/10.1038/ncomms15267.

[50] Wang, Y., Nasiri, A.R., Damsky, W.E., Perry, C.J., Zhang, X.-M., Rabin-Court, A., et al., 2018. Uncoupling hepatic oxidative phosphorylation reduces tumor growth in two murine models of colon cancer. Cell Reports 24(1):47–55. https://doi.org/10.1016/j.celrep.2018.06.008.

[51] Liu, X., Cooper, D.E., Cluntun, A.A., Warmoes, M.O., Zhao, S., Reid, M.A., et al., 2018. Acetate production from glucose and coupling to mitochondrial metabolism in mammals. Cell 175(2):502–513. https://doi.org/10.1016/j.cell.2018.08.040 e13.

[52] Tasdogan, A., Faubert, B., Ramesh, V., Ubellacker, J.M., Shen, B., Solmonson, A., et al., 2020. Metabolic heterogeneity confers differences in melanoma metastatic potential. Nature 577(7788):115–120. https://doi.org/10.1038/s41586-019-1847-2.

[53] Wang, Y., Bai, C., Ruan, Y., Liu, M., Chu, Q., Qiu, L., et al., 2019. Coordinative metabolism of glutamine carbon and nitrogen in proliferating cancer cells under hypoxia. Nature Communications 10(1):201. https://doi.org/10.1038/s41467-018-08033-9.

[54] Nordestgaard, B.G., Langsted, A., Mora, S., Kolovou, G., Baum, H., Bruckert, E., et al., 2016. Fasting is not routinely required for determination of a lipid profile: clinical and laboratory implications including flagging at desirable concentration cut-points-a joint consensus statement from the European Atherosclerosis Society and European Federation of Clinical Chemistry and Laboratory Medicine. European Heart Journal 37(25):1944–1958. https://doi.org/10.1093/eurheartj/ehw152.

[55] Tuvdendorj, D., Chinkes, D.L., Bahadorani, J., Zhang, X., Sheffield-Moore, M., Killewich, L.A., et al., 2014. Comparison of bolus injection and constant infusion methods for measuring muscle protein fractional synthesis rate in humans. Metabolism - Clinical and Experimental 63(12):1562–1567. https://doi.org/10.1016/j.metabol.2014.09.009.

[56] Maher, E.A., Marin-Valencia, I., Bachoo, R.M., Mashimo, T., Raisanen, J., Hatanpaa, K.J., et al., 2012. Metabolism of [U-13 C]glucose in human brain tumors *in vivo*. NMR in Biomedicine 25(11):1234–1244. https://doi.org/10.1002/nbm.2794.

[57] Johnston, K., Pachnis, P., Tasdogan, A., Faubert, B., Zacharias, L.G., Vu, H.S., et al., 2021. Isotope tracing reveals glycolysis and oxidative metabolism in childhood tumors of multiple histologies. Medicine (New York, N.Y.) vol. 2(4):395–410. https://doi.org/10.1016/j.medj.2021.01.002.

[58] Steinhauser, M.L., Olenchock, B.A., O'Keefe, J., Lun, M., Pierce, K.A., Lee, H., et al., 2018. The circulating metabolome of human starvation. JCI Insight 3(16). https://doi.org/10.1172/jci.insight.121434.

[59] Soeters, M.R., Soeters, P.B., Schooneman, M.G., Houten, S.M., Romijn, J.A., 2012. Adaptive reciprocity of lipid and glucose metabolism in human short-

term starvation. American Journal of Physiology. Endocrinology and Metabolism 303(12):E1397—E1407. https://doi.org/10.1152/ajpendo.00397.2012.

[60] Puchalska, P., Crawford, P.A., 2017. Multi-dimensional roles of ketone bodies in fuel metabolism, signaling, and therapeutics. Cell Metabolism 25(2):262—284. https://doi.org/10.1016/j.cmet.2016.12.022.

[61] Brown, S.A., 2016. Circadian metabolism: from mechanisms to metabolomics and medicine. Trends in Endocrinology and Metabolism: Trends in Endocrinology and Metabolism 27(6):415—426. https://doi.org/10.1016/j.tem.2016.03.015.

[62] Zarrinpar, A., Chaix, A., Panda, S., 2016. Daily eating patterns and their impact on health and disease. Trends in Endocrinology and Metabolism: Trends in Endocrinology and Metabolism 27(2):69—83. https://doi.org/10.1016/j.tem.2015.11.007.

[63] Adamovich, Y., Rousso-Noori, L., Zwighaft, Z., Neufeld-Cohen, A., Golik, M., Kraut-Cohen, J., et al., 2014. Circadian clocks and feeding time regulate the oscillations and levels of hepatic triglycerides. Cell Metabolism 19(2):319—330. https://doi.org/10.1016/j.cmet.2013.12.016.

[64] Vollmers, C., Gill, S., DiTacchio, L., Pulivarthy, S.R., Le, H.D., Panda, S., 2009. Time of feeding and the intrinsic circadian clock drive rhythms in hepatic gene expression. Proceedings of the National Academy of Sciences 106(50):21453—21458. https://doi.org/10.1073/pnas.0909591106.

[65] Choi, B.-H., Coloff, J.L., 2019. The diverse functions of non-essential amino acids in cancer. Cancers 11(5). https://doi.org/10.3390/cancers11050675.

[66] Lieu, E.L., Nguyen, T., Rhyne, S., Kim, J., 2020. Amino acids in cancer. Experimental & Molecular Medicine 52(1):15—30. https://doi.org/10.1038/s12276-020-0375-3.

[67] Reeds, P.J., 2000. Dispensable and indispensable amino acids for humans. Journal of Nutrition 130(7):1835S. https://doi.org/10.1093/jn/130.7.1835S, 40S.

[68] Lacey, J.M., Wilmore, D.W., 1990. Is glutamine a conditionally essential amino acid? Nutrition Reviews 48(8):297—309 https://doi.org/10.1111/j.1753-4887.1990.tb02967.x.

[69] Birsoy, K., Wang, T., Chen, W.W., Freinkman, E., Abu-Remaileh, M., Sabatini, D.M., 2015. An essential role of the mitochondrial electron transport chain in cell proliferation is to enable aspartate synthesis. Cell 162(3):540—551. https://doi.org/10.1016/j.cell.2015.07.016.

[70] Sullivan, L.B., Gui, D.Y., Hosios, A.M., Bush, L.N., Freinkman, E., Vander Heiden, M.G., 2015. Supporting aspartate biosynthesis is an essential function of respiration in proliferating cells. Cell 162(3):552—563. https://doi.org/10.1016/j.cell.2015.07.017.

[71] Sullivan, M.R., Mattaini, K.R., Dennstedt, E.A., Nguyen, A.A., Sivanand, S., Reilly, M.F., et al., 2019. Increased serine synthesis provides an advantage for tumors arising in tissues where serine levels are limiting. Cell Metabolism 29(6):1410—1421. https://doi.org/10.1016/j.cmet.2019.02.015 e4.

[72] Commisso, C., Davidson, S.M., Soydaner-Azeloglu, R.G., Parker, S.J., Kamphorst, J.J., Hackett, S., et al., 2013. Macropinocytosis of protein is an amino acid supply route in Ras-transformed cells. Nature 497(7451):633—637. https://doi.org/10.1038/nature12138.

[73] Kamphorst, J.J., Nofal, M., Commisso, C., Hackett, S.R., Lu, W., Grabocka, E., et al., 2015. Human pancreatic cancer tumors are nutrient poor and tumor cells actively scavenge extracellular protein. Cancer Research 75(3):544—553. https://doi.org/10.1158/0008-5472.CAN-14-2211.

[74] Chiu, M., Taurino, G., Bianchi, M.G., Kilberg, M.S., Bussolati, O., 2019. Asparagine synthetase in cancer: beyond acute lymphoblastic leukemia. Frontiers in Oncology 9:1480. https://doi.org/10.3389/fonc.2019.01480.

[75] Rabinovich, S., Adler, L., Yizhak, K., Sarver, A., Silberman, A., Agron, S., et al., 2015. Diversion of aspartate in ASS1-deficient tumours fosters de novo pyrimidine synthesis. Nature 527(7578):379—383. https://doi.org/10.1038/nature15529.

[76] Patil, M.D., Bhaumik, J., Babykutty, S., Banerjee, U.C., Fukumura, D., 2016. Arginine dependence of tumor cells: targeting a chink in cancer's armor. Oncogene 35(38):4957—4972. https://doi.org/10.1038/onc.2016.37.

[77] Garcia-Bermudez, J., Williams, R.T., Guarecuco, R., Birsoy, K., 2020. Targeting extracellular nutrient dependencies of cancer cells. Molecular Metabolism 33:67—82. https://doi.org/10.1016/j.molmet.2019.11.011.

[78] Kanarek, N., Petrova, B., Sabatini, D.M., 2020. Dietary modifications for enhanced cancer therapy. Nature 579(7800):507—517. https://doi.org/10.1038/s41586-020-2124-0.

[79] Gao, X., Sanderson, S.M., Dai, Z., Reid, M.A., Cooper, D.E., Lu, M., et al., 2019. Dietary methionine influences therapy in mouse cancer models and alters human metabolism. Nature 572(7769):397—401. https://doi.org/10.1038/s41586-019-1437-3.

[80] Maddocks, O.D.K., Berkers, C.R., Mason, S.M., Zheng, L., Blyth, K., Gottlieb, E., et al., 2013. Serine starvation induces stress and p53-dependent metabolic remodelling in cancer cells. Nature 493(7433):542—546. https://doi.org/10.1038/nature11743.

[81] Maddocks, O.D.K., Athineos, D., Cheung, E.C., Lee, P., Zhang, T., van den Broek, N.J.F., et al., 2017. Modulating the therapeutic response of tumours to dietary serine and glycine starvation. Nature 544(7650):372—376. https://doi.org/10.1038/nature22056.

[82] Knott, S.R.V., Wagenblast, E., Khan, S., Kim, S.Y., Soto, M., Wagner, M., et al., 2018. Asparagine bioavailability governs metastasis in a model of breast cancer. Nature 554(7692):378—381. https://doi.org/10.1038/nature25465.

[83] Tajan, M., Hennequart, M., Cheung, E.C., Zani, F., Hock, A.K., Legrave, N., et al., 2021. Serine synthesis pathway inhibition cooperates with dietary serine and glycine limitation for cancer therapy. Nature Communications 12(1):366. https://doi.org/10.1038/s41467-020-20223-y.

[84] Leone, R.D., Zhao, L., Englert, J.M., Sun, I.-M., Oh, M.-H., Sun, I.-H., et al., 2019. Glutamine blockade induces divergent metabolic programs to overcome tumor immune evasion. Science (New York, N.Y 366(6468):1013—1021. https://doi.org/10.1126/science.aav2588.

[85] Ren, L., Ruiz-Rodado, V., Dowdy, T., Huang, S., Issaq, S.H., Beck, J., et al., 2020. Glutaminase-1 (GLS1) inhibition limits metastatic progression in osteosarcoma. Cancer & Metabolism 8:4. https://doi.org/10.1186/s40170-020-0209-8.

[86] Pacold, M.E., Brimacombe, K.R., Chan, S.H., Rohde, J.M., Lewis, C.A., Swier, L.J.Y.M., et al., 2016. A PHGDH inhibitor reveals coordination of serine synthesis and one-carbon unit fate. Nature Chemical Biology 12(6):452—458. https://doi.org/10.1038/nchembio.2070.

[87] Ngo, B., Kim, E., Osorio-Vasquez, V., Doll, S., Bustraan, S., Liang, R.J., et al., 2020. Limited environmental serine and Glycine confer brain metastasis sensitivity to PHGDH inhibition. Cancer Discovery 10(9):1352—1373. https://doi.org/10.1158/2159-8290.CD-19-1228.

[88] García-Cañaveras, J.C., Lancho, O., Ducker, G.S., Ghergurovich, J.M., Xu, X., da Silva-Diz, V., et al., 2021. SHMT inhibition is effective and synergizes with methotrexate in T-cell acute lymphoblastic leukemia. Leukemia 35(2):377—388. https://doi.org/10.1038/s41375-020-0845-6.

[89] Neis, E.P.J.G., Sabrkhany, S., Hundscheid, I., Schellekens, D., Lenaerts, K., Olde Damink, S.W., et al., 2017. Human splanchnic amino-acid metabolism. Amino Acids 49(1):161—172. https://doi.org/10.1007/s00726-016-2344-7.

[90] Ducker, G.S., Rabinowitz, J.D., 2017. One-carbon metabolism in health and disease. Cell Metabolism 25(1):27—42. https://doi.org/10.1016/j.cmet.2016.08.009.

[91] Milman, H.A., Cooney, D.A., 1974. The distribution of L-asparagine synthetase in the principal organs of several mammalian and avian species. Biochemical Journal 142(1):27—35. https://doi.org/10.1042/bj1420027.

[92] Milman, H.A., Cooney, D.A., Young, D.M., 1979. Role of pancreatic L-asparagine synthetase in homeostasis of L-asparagine. American Journal of Physiology 236(6):E746—E753. https://doi.org/10.1152/ajpendo.1979.236.6.E746.

[93] Mukherjee, A., Ahmed, N., Rose, F.T., Ahmad, A.N., Javed, T.A., Wen, L., et al., 2020. Asparagine synthetase is highly expressed at baseline in the pancreas through heightened PERK signaling. Cellular and Molecular Gastroenterology and Hepatology 9(1):1—13. https://doi.org/10.1016/j.jcmgh.2019.08.003.

[94] Tsai, C.-Y., Kilberg, M.S., Husain, S.Z., 2020. The role of asparagine synthetase on nutrient metabolism in pancreatic disease. Pancreatology: official Journal of the International Association of Pancreatology (IAP) 20(6):1029—1034. https://doi.org/10.1016/j.pan.2020.08.002 [et Al.].

[95] Bröer, S., Bröer, A., 2017. Amino acid homeostasis and signalling in mammalian cells and organisms. Biochemical Journal 474(12):1935—1963. https://doi.org/10.1042/BCJ20160822.

[96] Lau, A.N., Vander Heiden, M.G., 2020. Metabolism in the tumor microenvironment. Annual Review of Cell Biology 4(1):17—40. https://doi.org/10.1146/annurev-cancerbio-030419-033333.

[97] Zhang, W., Trachootham, D., Liu, J., Chen, G., Pelicano, H., Garcia-Prieto, C., et al., 2012. Stromal control of cystine metabolism promotes cancer cell survival in chronic lymphocytic leukaemia. Nature Cell Biology 14(3):276—286. https://doi.org/10.1038/ncb2432.

[98] Sousa, C.M., Biancur, D.E., Wang, X., Halbrook, C.J., Sherman, M.H., Zhang, L., et al., 2016. Pancreatic stellate cells support tumour metabolism through autophagic alanine secretion. Nature 536(7617):479—483. https://doi.org/10.1038/nature19084.

[99] Bertero, T., Oldham, W.M., Grasset, E.M., Bourget, I., Boulter, E., Pisano, S., et al., 2019. Tumor-stroma mechanics coordinate amino acid availability to sustain tumor growth and malignancy. Cell Metabolism 29(1):124—140. https://doi.org/10.1016/j.cmet.2018.09.012 e10.

[100] Banh, R.S., Biancur, D.E., Yamamoto, K., Sohn, A.S.W., Walters, B., Kuljanin, M., et al., 2020. Neurons release serine to support mRNA translation in pancreatic cancer. Cell 183(5):1202—1218. https://doi.org/10.1016/j.cell.2020.10.016 e25.

[101] Ghergurovich, J.M., Lang, J.D., Levin, M.K., Briones, N., Facista, S.J., Mueller, C., et al., 2021. Local production of lactate, ribose phosphate, and amino acids by human triple-negative breast cancer. Medicine 2(6):736—754. https://doi.org/10.1016/j.medj.2021.03.009 e6.

[102] Reinfeld, B.I., Madden, M.Z., Wolf, M.M., Chytil, A., Bader, J.E., Patterson, A.R., et al., 2021. Cell-programmed nutrient partitioning in the tumour microenvironment. Nature 593(7858):282—288. https://doi.org/10.1038/s41586-021-03442-1.

[103] Lau, A.N., Li, Z., Danai, L.V., Westermark, A.M., Darnell, A.M., Ferreira, R., et al., 2020. Dissecting cell-type-specific metabolism in pancreatic ductal adenocarcinoma. ELife 9. https://doi.org/10.7554/eLife.56782.

REVIEW 2

Krug, A., **Martinez-Turtos, A**., Verhoeyen, E., 2021. Importance of T, NK, CAR T and CAR NK Cell Metabolic Fitness for Effective Anti-Cancer Therapy: A Continuous Learning Process Allowing the Optimization of T, NK and CAR-Based Anti-Cancer Therapies. Cancers (Basel) 14, 183. https://doi.org/10.3390/cancers14010183

cancers

MDPI

Review

Importance of T, NK, CAR T and CAR NK Cell Metabolic Fitness for Effective Anti-Cancer Therapy: A Continuous Learning Process Allowing the Optimization of T, NK and CAR-Based Anti-Cancer Therapies

Adrien Krug [1,†], Adriana Martinez-Turtos [1,†] and Els Verhoeyen [1,2,*]

[1] Université Côte d'Azur, INSERM, C3M, 06204 Nice, France; adrien.krug@etu.univ-cotedazur.fr (A.K.); Adrianna.MARTINEZ-TURTOS@univ-cotedazur.fr (A.M.-T.)
[2] CIRI, Université de Lyon, INSERM U1111, ENS de Lyon, Université Lyon1, CNRS, UMR 5308, 69007 Lyon, France
* Correspondence: els.verhoeyen@unice.fr or els.verhoeyen@ens-lyon.fr; Tel.: +33-4-72728731
† These authors contributed equally to this work and are listed in alphabetical order.

Simple Summary: Cancer treatments are evolving at a very rapid pace. Some of the most novel anti-cancer medicines under development rely on the modification of immune cells in order to transform them into potent tumor-killing cells. However, the tumor microenvironment (TME) is competing for nutrients with these harnessed immune cells and therefore paralyzes their metabolic effective and active anti-cancer activities. Here we describe strategies to overcome these hurdles imposed on immune cell activity, which lead to therapeutic approaches to enhance metabolic fitness of the patient's immune system with the objective to improve their anti-cancer capacity.

Abstract: Chimeric antigen receptor (CAR) T and CAR NK cell therapies opened new avenues for cancer treatment. Although original successes of CAR T and CAR NK cells for the treatment of hematological malignancies were extraordinary, several obstacles have since been revealed, in particular their use for the treatment of solid cancers. The tumor microenvironment (TME) is competing for nutrients with T and NK cells and their CAR-expressing counterparts, paralyzing their metabolic effective and active states. Consequently, this can lead to alterations in their anti-tumoral capacity and persistence in vivo. High glucose uptake and the depletion of key amino acids by the TME can deprive T and NK cells of energy and building blocks, which turns them into a state of anergy, where they are unable to exert cytotoxic activity against cancer cells. This is especially true in the context of an immune-suppressive TME. In order to re-invigorate the T, NK, CAR T and CAR NK cell-mediated antitumor response, the field is now attempting to understand how metabolic pathways might change T and NK responses and functions, as well as those from their CAR-expressing partners. This revealed ways to metabolically rewire these cells by using metabolic enhancers or optimizing pre-infusion in vitro cultures of these cells. Importantly, next-generation CAR T and CAR NK products might include in the future the necessary metabolic requirements by improving their design, manufacturing process and other parameters. This will allow the overcoming of current limitations due to their interaction with the suppressive TME. In a clinical setting, this might improve their anti-cancer effector activity in synergy with immunotherapies. In this review, we discuss how the tumor cells and TME interfere with T and NK cell metabolic requirements. This may potentially lead to therapeutic approaches that enhance the metabolic fitness of CAR T and CAR NK cells, with the objective to improve their anti-cancer capacity.

Keywords: T cell; NK cell; CAR T cell; CAR NK cell; metabolism; glycolysis; OXPHOS; immunotherapy; cancer therapy

Citation: Krug, A.; Martinez-Turtos, A.; Verhoeyen, E. Importance of T, NK, CAR T and CAR NK Cell Metabolic Fitness for Effective Anti-Cancer Therapy: A Continuous Learning Process Allowing the Optimization of T, NK and CAR-Based Anti-Cancer Therapies. *Cancers* **2022**, *14*, 183. https://doi.org/10.3390/cancers14010183

Academic Editor: Izumi Horikawa

Received: 16 November 2021
Accepted: 29 December 2021
Published: 30 December 2021

1. T Cell and CAR T Cell Metabolism Plays a Major Role in Anti-Cancer Immunity

1.1. T Cell Metabolism in a "Healthy" Environment

T cells are major components of the adaptive immune system. CD4+ cells, as well as CD8+ T cells, function as effectors of the immune system. T cells continuously screen lymphoid and peripheral tissues such as the spleen and lymph nodes for antigens (peptides or lipids) that are presented by the major histocompatibility complex (MHC) of antigen-presenting cells (APCs). APCs include macrophages, dendritic cells and B cells. When T cells recognize a specific antigen from pathogens or tumor cells through their TCR, they start to expand and migrate to the diseased tissues, where they exert their effector functions by killing infected or malignant cells. In order to perform these effector functions, T cells undergo complex molecular changes. Once the TCR is engaged, protein tyrosine kinases phosphorylate tyrosine residues situated in the cytoplasmic tail of the TCR, which then binds to various signaling molecules that activate multiple transcription factors that transform naïve T cells into effector T cells [1].

This requires an extensive "metabolic reprogramming" of T cells in order to provide the energy and building blocks for their clonal expansion and to ensure their anti-cancer activity. Some of the earlier studies on immunometabolism of human T cells were published in the context of HIV. HIV-1 mainly infects CD4+ T cells and accumulation. The evidence has brought to light the association between T cell metabolism reprogramming and HIV-1 pathogenesis [2,3]. Recently, metabolic reprogramming of T cells was proposed as an approach for HIV cure and HIV reservoir eradication [4]. Resting T cells in our bloodstream rely mainly on oxidative phosphorylation (OXPHOS) and fatty acid oxidation in the mitochondria to generate enough ATP, which sustains their homeostasis. Upon antigen encounter, they rapidly start to increase glucose and amino acid (aa) uptake, which alters their metabolism to glycolysis, by increasing the activity of multiple kinases (Phosphoinositide 3-kinase (PI3K)/Protein kinase B (AKT)/mammalian target of rapamycin (mTOR) [5–9]. For example, activation of mTOR promotes glycolysis through the upregulation of the major regulator c-Myc and hypoxia-inducible factor 1 α (HIF1α) [10,11]. Glucose uses mainly the glucose transporter 1 (GLUT1) transporter for its uptake, whereas aa such as glutamine uses large amino acid transporter 1 (LAT1), serotonin N-acetyltransferase (SNAT-1,-2) and ASC amino acid transporter 2 (ASCT2) [12–14]. In human and mouse T cells, antigen exposure that requires a co-stimulatory signal through CD28 [15,16] results in activation of the central metabolic regulator mTOR, which boosts the GLUT1 transporter ensuring increased glucose uptake [17–19].

Glucose is first metabolized into pyruvate, which according to the T cell activation state, follows a different metabolic pathway. Resting T cells convert pyruvate to acetyl-CoA for mitochondrial respiration. Interleukin 7 (IL-7) is the main survival cytokine required for the maintenance of these cells as it upregulates GLUT1 for glucose uptake [20,21]. In contrast, antigen-stimulated T cells increase their glucose uptake 18-fold, compared to resting T cells [22], and preferentially convert the resulting pyruvate into lactate, which is then secreted via the monocarboxylate lactate transporters (MCT), MCT1 and MCT4 [16,23,24]. Of note, pyruvate can also be directly imported by the MCTs [25]. This process is called "aerobic glycolysis" and permits a more rapid metabolism of incoming glucose to pyruvate. This occurs by rapid regeneration of the cofactor NAD+, while at the same time, provides many precursors for aa, protein and lipid synthesis that are all required by rapidly dividing cells. Additionally, increased glycolytic flux also increases the expression of effector molecules and requires high rate glycolytic enzymes, such as GAPDH, which is then unable to exercise non-glycolytic functions, including interferon γ (INFγ) inhibition at the mRNA level [26]. In parallel, activated murine and human T cells also continue to some extent their mitochondrial metabolism because some of the pyruvates from glycolysis can enter into the mitochondria and is converted into acetyl-CoA, which enters the tricarboxylic acid (TCA) cycle to produce carbon dioxide and water, but also drives the electron transport chain to produce ATP and reactive oxygen species (ROS) [27–29].

An essential aa such as glutamine is required for T cell proliferation [13,16,27]. Activated T cells upregulate glutamine transporters and glutaminolytic enzymes, which metabolize glutamine to α-ketoglutarate that fuels the TCA cycle [16]. T cell proliferation is not only sustained by ATP generation but also by ROS production, which stabilizes effector molecule expression and redox homeostasis in murine T cells [29,30]. Moreover, inhibition of the mitochondrial transport chain in murine T cells and hematopoietic stem cells renders them functionally incompetent in vivo, underlining the importance of mitochondrial function in these cells [29,31]. Importantly, it was recently revealed that intermediate products of the TCA cycle are implicated in histone modification, thereby modulating gene transcription and function of several genes, important for T cell fitness [30,32,33]. It is important to note that in the activation phase, effector T cells use mainly aerobic glycolysis. However, once they become memory T cells, they adapt again to OXPHOS metabolism, as shown in the context of murine T cells [34]. Subsequently, once they are repeatedly challenged, murine T cells, as well as human T cells, rapidly undergo a reactivation by adapting their metabolism [35,36].

We further focus on the T cell immunometabolism and function in the context of cancer and cancer treatment, focusing on chimeric antigen receptor (CAR) T cell immunotherapy.

1.2. T Cells Metabolism in the "Tumor" Microenvironment (Figure 1)

T cell therapies are very effective for hematopoietic malignancies [37–40]. However, for solid tumors, this is not the case since the metabolic environment can be very immunosuppressive, reverting murine and human T cells into a nonfunctional exhausted phenotype [41–43]. Uncovering these immune-metabolic hurdles will be essential for a more rational design of future cancer therapies. Acidity, low oxygen levels (hypoxia), suppressive metabolites and low nutrient availability encountered in the tumor microenvironment (TME) can severely suppress therapeutic T cell effector function. This was previously not considered in the context of clinical trials. However, it now represents a major concern in the field of immunotherapy and has encouraged an extensive field of research. Tumor cells rely strongly on glycolysis for their energy (ATP) production. Strangely enough, it has become clear that tumors cells still have the capacity to use OXPHOS, which is a metabolic pathway that generates more ATP. However, cancer cells use mainly glucose for fueling glycolysis, even in the presence of sufficient oxygen. This phenomenon, called aerobic glycolysis, was discovered by Warburg (Warburg effect; [44–48]). Glycolysis leads to strong tumor cell proliferation that depletes the TME of nutrients for the T infiltrating lymphocytes (TILs) and also produces immunosuppressive metabolites [26,49]. However, as indicated above, T cells can make a sudden switch in their metabolism from oxidative phosphorylation to glycolysis in order to exert their effector function [6,26]. This actually means that activated/effector T cells adapt an anaerobic glycolytic metabolic program in a similar manner to highly proliferating cancer cells [5]. Thus, T cells and cancer cells are in continuous competition for the same nutrients to sustain themselves (Figure 1). Importantly, T cell metabolic requirements can vary with the type of solid tumor. Indeed, glucose uptake by tumors and the TME results in glucose deprivation for T cells. Additionally, the byproduct lactate is extremely immunosuppressive, which leads to the acidification of the tumor environment [50–52], weakening CD8+ T cell effector functions, proliferation and cytokine production both in the murine and human context [53,54]. In the TME, T cells are often subjected to hypoxia, leading to the inhibition of mitochondrial function, a decrease in reactive oxygen species (ROS) and ATP levels, which paralyze effector T cells both in the murine and human context [55].

Another important mechanism by which cancer cells inhibit T cell effector functions is through the expression of ligands to immune checkpoint molecules such as programmed cell death 1 (PD-1) and cytotoxic T lymphocyte-associated protein 4 (CTLA-4), which are highly upregulated on the surface of activated T cells. PD-1 and CTLA-4 engagement inhibit mTOR function through the protein phosphatase 2A (PP2A) and SH2-domain-containing tyrosine phosphatase 2 (SHP-S) signaling, respectively [56–60]. It was shown that that co-inhibitory immune checkpoint blockade (e.g., anti-PD-1, anti-CTLA-4) reduced glucose

uptake by the tumor cells reinstating glucose availability for the T cells. This might, in part, explain the success of this kind of immunotherapy [61]. T-cell immunoglobulin and mucin domain-3 (TIM3), another co-inhibitory molecule, can activate mTOR; however, the mechanism by which this occurs has yet to be revealed [62]. In the TME, regulatory T cells and myeloid-derived suppressor cells (MDSCs) can secrete factors such as transforming growth factor β (TGFβ) and Indoleamine-pyrrole 2,3-dioxygenase (IDO), which reduce human T cell function by mTOR suppression [63]. Furthermore, IL10, IL35 and adenosine can severely affect human effector T cell activity [64].

In the TME, only low levels of amino acids remain available for T cells. For example, glutamine is a primary energy source for tumor cells; however, low levels of glutamine are detrimental for T cell activation and function [12,14]. The aa arginine is also essential for human T cell function and is strongly depleted from the TME because it also becomes consumed by the cancer cells [65–67].

TIL and chimeric antigen receptor (CAR) T cells are clearly subjected to the same challenges in the TME that inhibit effector T cell metabolism and function. Below, we introduce this novel immunotherapy consisting of presenting newly engineered CARs on T cells. In order to reveal how to improve immunotherapies by reactivating TILs as well as CAR T cells or protecting them against the hostile TME, we address the different components in the TME that contribute to the changes in T effector metabolism in more detail and how one could therapeutically interfere with these obstacles to revert the exhausted T cells or CAR T cells into potent anti-cancer effector T cells.

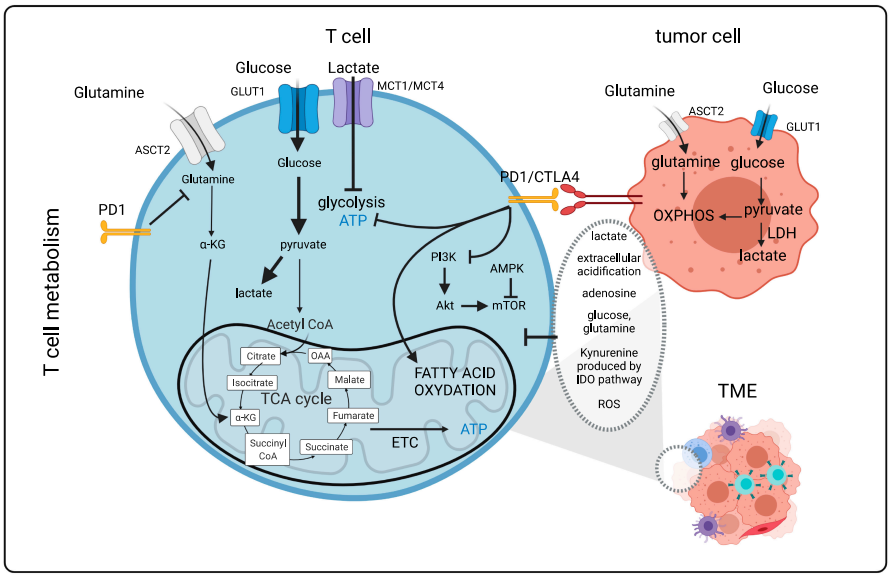

Figure 1. T cell metabolism in the tumor microenvironment. Naïve T cells rely mainly on oxidative metabolism. Following activation with an antigen, T cells switch to a glycolytic metabolism by activation of the mTOR pathway. This metabolic program supports effector T cell functions. If antigen stimulation persists long term, such as in the tumor environment, inhibitory receptors such as PD1 and CTLA4 can rewire T cell metabolism by reducing glycolysis and glutaminolysis, which weakens effector functions. Other factors in the TME contributing to the exhausted state of T cells include low levels of oxygen, low levels of tryptophan metabolized into kynurenine by IDO, low levels of arginine, high levels of lactate and resulting acidification and strong competition of T cells with cancer cells for glucose and glutamine. PD1: Programmed cell death 1; CTLA4: cytotoxic T-lymphocyte-associated protein 4; ASCT2: ASC amino-acid transporter 2; GLUT1: glucose transporter 1; OAA: Oxaloacetate; α-KG: α-Ketoglutarate; AMPK: Adenosine monophosphate kiinase; LDH: Lactate dehydrogenase; TME: Tumor microenvironment; Akt: Protein kinase B; mTOR: mammalian target of rapamycin; ATP: Adenosine triphosphate; ROS: Reactive oxygen species; PI3K: Phosphoinositide 3-kinase; IDO: Indoleamine-pyrrole 2,3-dioxygenase; ETC: Electron transport chain; TCA: Tricarboxylic acid; CoA: Coenzyme A. Figure generated with Biorender.com (accessed on 15 November 2021).

1.3. CAR T Cells for Anticancer Treatment: Latest Developments

In cancer, particularly in the context of hematological tumors, T cells are also used as a therapeutic tool. In this type of immunotherapy, the patient's T cells are genetically engineered ex vivo to express a CAR that recognizes a specific antigen present on the surface of the tumor cells. After reinfusion of these cells in the patient's circulation, the binding between the CAR T cells and the cancer cells induces a cytotoxic response. One example of this therapy currently being used in clinics is for the treatment of advanced B-cell lymphomas, resulting in complete remission in 30 to 40 % of the patients. Importantly, it needs to be emphasized that CAR T cells are used last in line as a therapeutic strategy to suppress tumor cells. This means that the T cells are often isolated from the patients after various treatments, including chemotherapy that can alter the metabolic phenotype of the T cells (mitochondrial damage and metabolic alterations) [68]. Therefore, metabolism is an important aspect in the conception and the anti-tumoral activity of a CAR T cell.

1.3.1. Continuous Improvements in the CAR Design to Stir CAR T Cell Metabolism (Figure 2)

The CAR incorporated at the surface of T cells has a T cell receptor (TCR)-like structure. The extracellular part consists of a single variable chain fragment (scFv) of an antibody that recognizes the antigen present on the cancer cell surface. The transmembrane and intracellular parts contain co-stimulatory domains that permit the amplification of the signaling and, thus, the response of the T cell following binding to the tumor antigen. In the first-generation CAR T cell design, CD3ζ was the only signaling domain used, but in the following generations, CD28 and/or 4-1BB (CD137) co-stimulatory domains were added to this structure. The choice of these domains is also important for the metabolic status and the survival of the CAR T cells. It was observed in patients that the use of 4-1BB permitted a persistence of CAR T cells in time, without exhaustion of those CAR T cells, via the stimulation of the noncanonical nuclear factor kappa B (NF-κB) pathway [69]. In contrast, the CD28 costimulatory domain does not permit the cells to survive longer than 30 days in the patients [70–73]. This phenomenon can be explained by the fact that the 4-1BB promotes improved mitochondrial function so that T cells can rely on mitochondrial respiration as their energy source, which promotes the survival of central memory T cells by the activation of adenosine monophosphate kinase (AMPK), as demonstrated in mice [74]. When the CD28 co-stimulatory domain was included in the CAR, patient T cells were relying more on glycolysis (via activation of the PI3K/AKT/mTOR axis), which pushed their differentiation towards effector memory T cells [75,76]. Following antigen recognition by the CAR, CD28 stimulated GLUT1 via the PI3K/AKT pathway, linked to the mTOR/Myc pathways, which are also implicated in amino acid/lipid metabolism [17,19]. These data underline the importance of the choice of the co-stimulatory domain to shape CAR T cell metabolism and permit short-term or long-term anti-tumor efficacy. As for CAR T cells, TIL performance also depends strongly on the metabolic status of the malignancy and the TME.

Cytokines also play a role in the metabolic shape of the CAR T cells (see Section 1.3.2). Indeed, the fourth CAR T cell generation, also known as "TRUCKS" (T-cell redirected for unrestricted cytokine-mediated killing), has a transgenic cytokine expression system that improves their expansion and persistence in vivo via metabolic changes [77]. The cytokines employed in this strategy are interleukin 12 (IL12), IL15 and IL18. IL15 can, for example, lower the glycolysis level in human CAR T cells via a decrease in mTOR complex 1 (mTORC1) activity, whilst OXPHOS levels/respiratory capacity and expression of fatty acid oxidation-related genes are increased in these cells. This metabolic phenotype allows the human CAR T cells to have a stem cell memory behavior with higher cell proliferation and in vivo longevity [78]. More recent fifth-generation CAR T cells express a sub-unit of the IL2 receptor (IL2RB) between the stimulatory domains (CD3ζ and CD28/4-1BB). Since IL2RB presents a binding site for STAT3, the cells can activate the JAK-STAT pathway, following the antigen recognition, which leads to a higher proliferation rate. Moreover,

these human CAR T cells seem to have a stronger anti-cancer activity against leukemic cells [79].

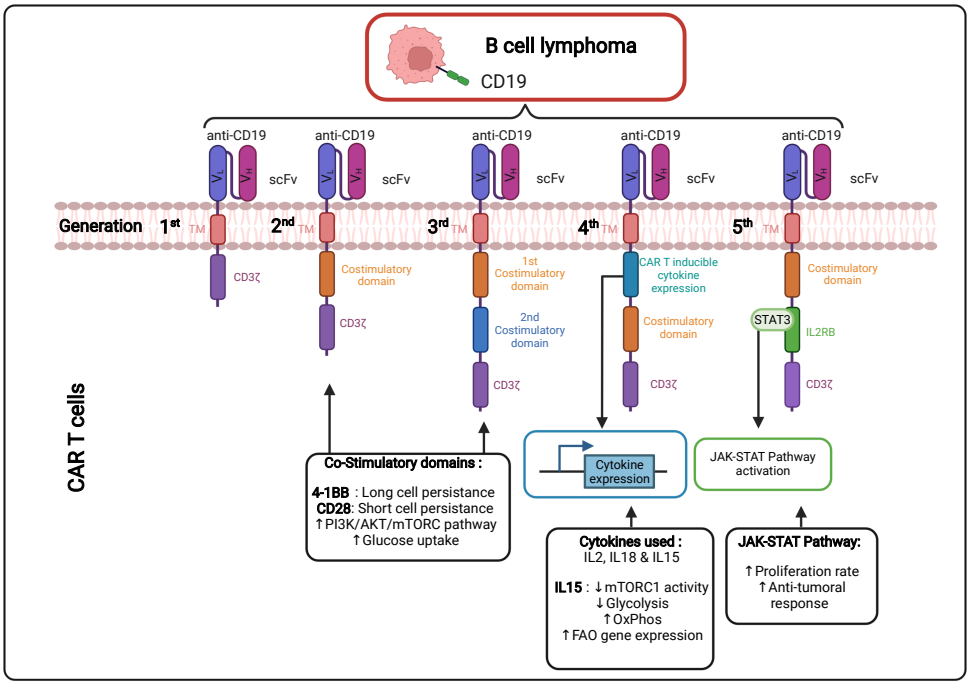

Figure 2. Different generations of CAR T cells and their signaling pathways. TM: Transmembrane; scFv: Single-chain variable Fragment; V_L: Variable Light chain; V_H: Variable Heavy chain; IL2RB: interleukin 2 Receptor B; mTORC: mammalian target of rapamycin complex; FAO: Fatty Acid Oxidation; JAK-STAT: Janus Kinase-Signal Transducers and Activators of Transcription; PI3K: Phosphoinositide 3-kinase; Akt: Protein kinase; CART: Chimeric Antigen Receptor T cell. Figure generated.

1.3.2. Ex Vivo Expansion of CAR T Cells to Manipulate Their Metabolism

As they are immune cells and similar to TILs, CAR T cells are highly sensitive to metabolic changes in their environment, which can influence their survival and their functionality. When cultured ex vivo, CAR T cells are often cultured in the presence of supra-physiological nutrient levels in order to generate enough cells for reinfusion. This also means that the cytotoxic efficiency is compromised when changing from an overdosed medium to a nutrient restrictive microenvironment. Thus, the composition of expansion media plays an important role in the process of CAR T cell generation and needs to be optimized in order to facilitate the transition between the ex vivo expansion and in vivo adaptation. For example, carnosine, an amine poorly present in sera, when added to the medium, facilitates human T cell transduction and their in vivo engraftment by switching the main metabolic state from glycolysis to OXPHOS, which allowed a better anti-tumoral response [80]. Currently, expansion media rely essentially either on fetal bovine serum (FBS) or human serum (HS), which does not take into account some blood fractions, which might highly compromise human CAR T cell fitness [81].

The effect of cytokines on T cell metabolism is only beginning to be explored in the field. Survival cytokines, IL2 and IL7, promote glycolysis in T cells [21,82], while IL-15 promotes their mitochondrial biogenesis [36]. TGFβ seems to suppress both glycolysis and mitochondrial respiration. Therefore, the choice of cytokines or growth factors in the media for CAR T cell expansion might be crucial for their in vivo adaptation.

It is therefore important to be aware that the ex vivo expansion of these CAR T cells is a tricky step in the process and can be limiting and compromise treatment efficacy. Several research teams are currently trying to improve CAR T cell therapy by circumventing the ex vivo expansion step and directly generating CAR T cells in vivo. In recent studies, lentiviral

vectors specifically recognizing the $CD3^+$ or even the $CD8^+$ human T cells were used to generate efficiently anti-CD19 CAR T cells directly in vivo and were able to wipe out the targeted healthy and malignant B cells in humanized mouse models [83–87]. Although this still needs to be evaluated, one can speculate that these in vivo generated CAR T cells might expand in their proper environment and maintain their metabolic fitness in vivo.

More recently, an elegant strategy to overcome in vivo CAR T cell exhaustion has been reported with better outcomes than PD-1/PD-L1 blockade, which can improve T cell functions but do not change the epigenetic reprogramming associated with T cell exhaustion. The approach is based on inducing a transient rest in CAR signaling and, therefore, temporally blocking the sustained CAR T cell activation that leads to exhaustion [88]. This approach made use of temporal downregulation of the surface expression of the CAR by inducing its degradation by pharmacological treatments. The tunable control of CAR expression levels not only improved CAR T cell anti-tumoral functions in vivo in terms of intensity and duration but also led to non-exhausted T cells with a memory-like phenotype in xenograft mouse models of leukemia and osteosarcoma. Interestingly, the already established exhaustion of CAR T cells can even be reverted after a transient rest of the CAR signaling [88].

1.4. Importance of Nutrients, Metabolites for T/CAR T Cell Metabolism, Survival and Function (Figure 1)

Currently, in the clinic, CAR T cells are essentially used as a therapeutic strategy for hematopoietic malignancies. Unfortunately, the efficiency of this technique is extremely poor to non-existent when it comes to a solid tumor. This can be explained by the low number of known specific antigens in these types of cancers. Furthermore, the TME can, by its composition, affect the metabolic phenotype of these cells, and even a slight change in its composition can alter T cell functionality and survival [89,90], as described in Section 1.1.

1.4.1. Glucose Availability in the Tumor Environment

Glucose is the key element for which T cells and cancer cells compete and is therefore limited in the TME. This is a critical metabolite for energy production via metabolic pathways such as glycolysis and OXPHOS. Indeed, once activated, effector T cells increase their glucose uptake via a higher expression of the glucose transporter GLUT1, which permits higher use of glycolysis compared to OXPHOS. The important consumption of glucose by tumor cells, therefore, favors a decrease in glycolysis in immune cells such as T effector cells, thereby reducing their proliferation and cytokine production [54,61].

Interestingly, a side effect of reduced glucose availability also leads to the apparition of memory T cells with higher OXPHOS respiration in a human context [91]. Therefore, recent investigations have tried to use glucose restriction to enhance CAR T cell persistence and response. Indeed, in a lymphoma mouse model, $CD8^+$ effector T cells that underwent a transient glucose restriction displayed a higher cell proliferation and persistence in the blood and induced improved tumor clearance. Moreover, effector cytokines such as IFNγ and granzyme B were released at higher amounts from these cells [92]. Currently, the use of glucose restriction in the process of CAR T development in the clinic might still be risky and needs further investigation. However, it is possible that by substituting glucose with other carbohydrates such as galactose, we might improve CAR T cell generation and production in the future.

Alternatively, Qiu et al. revealed that under glucose restriction, acetate was able to rescue effector T cells functions. They showed that exhausted human and murine T cells could be epigenetically remodeled and reactivated by acetate, and this resulted in enhanced INFγ gene transcription and cytokine production [33]. Therefore, interfering with metabolism using acetate might be of therapeutic benefit.

1.4.2. Lactate, a Side Product of Tumor Cell Glycolysis

Other immunosuppressive metabolites are present in this TME. As tumor cells generally rely on glycolysis, lactate is one of these elements. Glycolysis causes greater amounts of lactate production, which leads to acidification in the TME. This influences the murine T cell effector function in terms of cytolytic capacity and cytokine production [93]. Lactate reduces the anti-tumoral response by impairing NAD+ recycling and therefore blocking the enzymatic reactions, involving glyceraldehyde 3-phosphate dehydrogenase and 3-phosphoglycerate dehydrogenase, which promotes the differentiation of murine T lymphocytes in regulatory T cells (Treg) [94]. Lactate also functions as an oncometabolite, which polarizes macrophages to the M2 type and maintains Treg cells in a low glucose TME [94–96].

In order to reduce these high levels of lactate in the TME, Mane et al. also used an inhibitor of the lactate Dehydrogenase (LDH), which, when combined with a CAR T cell therapy, reduced the tumor growth in a murine prostate xenograft cancer model treated with human CAR T cells [97,98]. Of note, human CAR T cells might, in the context of a murine tumor, show lower activity. Lactate induced TME acidification and rendered TILs incapable of IL2 and INFγ production and increased the number of regulatory T cells in humans [99,100]. Unsurprisingly, the inhibition of LDH restored human effector T cell proliferation and function [101]. In another approach, Renner et al. [102] used an inhibitor (diclofenac) of the lactate transporters MCT1 and MCT4 to reduce the efflux of lactate from the tumor into the TME. Due to the diclofenac treatment effector, T cells remained functional and were able to control tumor growth. In addition, this drug, which targets glycolysis, also improved immunotherapy outcomes.

1.4.3. Limited Amino Acid Availability

Glutamine is an important essential metabolite and the most abundant aa in blood. Upon TCR signaling, T cells highly express aa transporters and increase their glutamine uptake. Glutamine is a major fuel for metabolic pathways in active T cells [103]. Therefore, glutamine is an important metabolic element for effector T cells and also for tumor cells. Hence, many cancer cell types over-express ASCT2, the main glutamine transporter, which induces a reduction in the glutamine pool that is available for T cells in the TME. Indeed, targeting glutamine uptake in a human cancer xenograft mouse model resulted in reduced tumor development [104]. Therefore, the availability of glutamine is an important element for anti-tumoral response by promoting T cell proliferation and cytokine production [105]. As expected, Leone et al. [106] demonstrated that glutamine blockade in tumor-bearing mice reduced mitochondrial and glycolytic metabolism in cancer cells, which in turn reduced hypoxia, acidification and nutrient depletion in the TME. In contrast, in effector T cells, glutamine blockade induced upregulation of oxidative metabolism and an activated phenotype with effector function [106]. This differential response upon interference with glutamine metabolism between cancer and T cells in a mouse model might be of therapeutic benefit for tumors but needs further investigation. Unexpectedly, one interesting study showed that the restriction of glutamine metabolism during the TCR stimulation led to reduced exhaustion and increased anti-tumor activity in T cells [107]. More in depth studies are needed to reveal the importance of glutamine in different types of cancers and infiltrating T cells.

Other aa play an important role in the competition between tumor and healthy cells. Tryptophan is an essential aa that is also important for the production of certain molecules required by effector T cells. Contrary to glutamine, its catabolism produces several metabolites through the kynurenine pathway that reduce the TCR response and favor T cell apoptosis in humans as wells as in mice [108]. The IDO enzyme that catalyzes the conversion of tryptophan into kynurenine was found to be upregulated in murine cancer cells [109] and is linked to an inhibition of the glycolytic pathway in T cells, which reduces the anti-tumoral response of effector T cells [110]. Therapeutic inhibition of IDO in cancer might therefore restore T cell function [111].

Arginine is essential for protein synthesis and is also involved in immunometabolism through its metabolites such as Nitrite Oxide and polyamines [112]. Similar to glutamine, a lack of arginine in the TME impaired murine T cell function [113] and activation of human and murine T cells, especially through the decrease in activation markers expression such as CD25/CD28 [114,115]. Indeed, higher levels of arginine have been linked to improved survival of memory T cells and anti-tumoral response [112].

1.4.4. Hypoxia in the TME Has Important Effects on TIL Infiltration and Function

Lactate secretion and high glycolytic activity in the tumor cells are linked to a hostile hypoxic environment in the TME. The importance of oxygen availability for T cells was shown by supplying oxygen to tumor-bearing mice, which led to increased T cell infiltration and improved tumor regression [116,117]. This hypoxic state triggers the transcription factor HIF1α in T cells, which is also stabilized by T cell activation and favors glycolysis by upregulation of GLUT1 expression and some other enzymes and regulators. Hypoxia also induces a higher production and release of reactive oxygen species (ROS) that impair T cell mitochondrial functions and induce T cell exhaustion in mice [118,119]. In order to bypass this problem, recent work in the CAR T cell field showed that it is now possible to generate T cells that will express the CAR only in hypoxic conditions. Hence in normoxia, the CAR is degraded, but once in hypoxic conditions, the CAR is stabilized at the cell surface in a murine solid tumor model, and all the pathways required for an effective anti-tumoral response remain active [120].

In hypoxic tumors, adenosine is a major immunosuppressive factor that limits the function of murine as well as human T cells in the TME via activation of the adenosine A_{2A} receptor ($A_{2A}R$) [121,122]. In this regard, CAR T cells deficient for the $A_{2A}R$ were engineered, which became insensitive to high adenosine levels and maintained cytokine production, activation of the JAK-STAT signaling pathway and anti-tumor functions [123].

1.4.5. Cholesterol

Cholesterol uptake by TILs in the TME activates their endoplasmatic reticulum (ER) stress response and the inositol requiring enzyme 1α (IRE-1α) signaling pathway, which induces inhibitory receptor expression on murine and human TILs and, as a consequence, their exhaustion [124]. A new mechanism by which the antitumor response of mouse CD8 T cells can be potentiated through modulating cholesterol metabolism was reported. Inhibiting cholesterol esterification in T cells by genetic ablation or pharmacological inhibition of ACAT1, a key cholesterol esterification enzyme, led to potentiated effector function and enhanced proliferation of CD8 but not CD4 T cells. This is due to the increase in the plasma membrane cholesterol level of CD8 T cells, which causes enhanced T-cell receptor clustering and signaling as well as a more efficient formation of the immunological synapse [125]. Cholesterol metabolism still needs to be further studied in order to explain these effects on anti-cancer T cell response.

1.4.6. Mitochondria in T Lymphocytes Infiltrating the TME

Mitochondria are essential for T cells in terms of energy, biosynthesis of macromolecules in order to sustain their clonal expansion and also for T cell effector function. Once activated, effector T cells undergo dramatic mitochondrial remodeling to sustain their functions [29]. However, T cells lose mitochondrial function and mass when they infiltrate the TME. This process coincides with the upregulation of co-inhibitory checkpoint molecules [42]. Furthermore, this process is accompanied by the repression of the transcriptional co-activator peroxisome proliferator-activated receptor-gamma coactivator 1α (PGC1α) that is essential for mitochondrial biogenesis. In accordance, overexpression of PGC1α rescued intratumoral T cell metabolism and improved T cell effector function in a melanoma mouse model [126]. Therefore, increasing mitochondrial mass and quality may armor T cells to resist the hostile tumor environment.

1.5. Immune Checkpoint Molecules and T Cell Metabolism in the TME (Figure 1)

Immune checkpoint molecules (ICM) are co-inhibitory receptors expressed by T cells that are essential for preventing autoimmunity or immunopathologies. However, in the context of tumors, they can tune down anti-tumor responses of T cells. Checkpoint molecules and their ligands are expressed by multiple cells in the TME, which can impact the T cell metabolism and efficiency in a more direct manner. Upon antigen stimulation, costimulatory signals such as CD28 are essential for human and murine T cell activation, glycolysis and mitochondrial activity [17,127]. In contrast, ICM such as PD-1 and CTLA-4 revert this process by switching human T cell metabolism and reducing T cell effector functions [128].

Targeting immune checkpoint receptors such and CTLA-4, PD-1 and PD-1 ligand in blood malignancies has proven to be efficient. However, several patients relapsed, and the efficacy in solid tumors was not as successful. Programmed death-1 (PD-1) is a major regulator of T cell exhaustion; thus, human T cells stimulated with a PD-1 Ligand reduced their glucose uptake and used neither glycolysis nor catabolism of glutamine. Conversely, these cells express a higher rate of Fatty Acid Oxidation and lipolysis [129]. PD-1 signaling is also linked to a reduction in the expression of the proto-oncogene cMyc and reduced activity of the PI3K/Akt/mTOR pathway [130]. However, Chang et al. [61] showed that signaling through PD-L1 in tumor cells promotes glycolysis. Antibody-mediated blockade of PD-L1 reduced tumor glycolysis rate and restored the level of glucose in the TME, and consequently improved anti-cancer T cell effector function [61], which might be potentiated by the metformin-induced reduction in tumor hypoxia [42]. Additionally, it was shown that increasing phosphoenolpyruvate (PEP) levels in tumor-reactive T cells through overexpression of PEP carboxykinase 1 (PCK1) in T cells restored their anti-cancer T cell activity that counteracted the low levels of glucose in the TME [49]. Importantly, PD-1 was shown to inhibit PGC1α, inducing a reduction in glycolysis and loss of mitochondrial mass in TILs. In accordance with this observation, this TIL phenotype was reverted by PGC-1α overexpression [42,126].

In order to overcome this dampening of T cell function through immune checkpoints in the TME, CAR T cells have been engineered, in which inhibitory receptors were removed [131–136] or that express costimulatory signals or secrete factors that can re-activate the immune system, such as inhibitors or cytokines. This was demonstrated in mice xenografted with human tumors as also in murine cancer models [137,138]. One of these immune-stimulating cytokines is IL12P70, which was reported to increase CAR T cell activity [139–141]. Sachdeva et al. [142] used an elegant procedure to achieve two objectives at once by gene editing of CAR T cells, in which they inserted the IL12P70 expression cassette into the PDCD1 locus (coding for PD-1). In this way, PDCD1 regulatory elements control the secretion of IL12P70, which will only be expressed with the CAR T cells encountering the tumor antigen. This concomitantly led to the abolition of PD-1 expression. These IL12 secreting human CAR T cells knock-out (KO) for PDCD1 increased significantly antitumor activity in a patient-derived xenograft mouse model compared to CAR T cells KO for PDCD1 alone or CAR T cell counterparts [142]. These results might be explained by the controlled IL12P70 secretion [139–141,143].

Similar to PD-1, CTLA-4 is also important in the process of tumoral immune escape by inhibiting CD28-costimulation in effector T cells and therefore preventing activation-induced glycolysis [144]. By blocking CTLA-4 mediated signaling, T cell stimulation and metabolism can be reverted to glycolysis again by reviving PI3K/Akt/mTOR signaling and turning T cells back into potent effector cells.

Upon engagement, TIM3, another ICM, leads to reduced glycolysis and GLUT1 expression and might also inhibit glutaminolysis [145], while the ICM, lymphocyte activation gene 3 (LAG3) negatively regulates mitochondrial metabolism [146]. TIM3 and LAG3 are highly expressed by exhausted T cells [147–150].

Unfortunately, from the clinical point of view, tumor cells stimulate not only these immune blockades but also secrete immunosuppressive cytokines and enzymes. It is for this reason that in certain tumors, an inhibitor of the immune blockade should be

accompanied by inhibitors of these pathways [151], as reviewed by Tabana et al. [152]. Therapeutic interference with these metabolic regulatory molecules may affect biosynthesis and epigenetic marks that influence T cell function and fate. This is discussed in detail in the next section.

1.6. Epigenetics Influences the Metabolic Response of T and CAR T Cells (Figure 3)

In recent years it has become clear that epigenetic remodeling plays a major role in T cell immunometabolism and differentiation, as shown in a murine context [153,154]. Several types of epigenetic events were revealed: DNA modification (e.g., by methylation), histone modification, non-coding RNA (ncRNA)-associated modifications and chromatin organization/condensation. The different epigenetic modifications in T/CAR T cells and their importance for T cell physiology have recently drawn a lot of attention and initiated a new field of research.

DNA modification and, more precisely, methylation generally occur to silence a gene expression, e.g., effector genes are often methylated in naïve/memory T cells and demethylated in effector T cells. Therefore, DNA methyltransferases (DNMTs) are highly active in exhausted T cells. Their inhibition therefore can lead to a reduction in T cell exhaustion and an increase in less differentiated T cells [155]. Interestingly, glucose restriction by itself, for example, can reduce the expression and the activity of epigenetic enzymes such as the methyl transferase enhancer of zeste homolog 2 (EZH2), leading to reduced cytokine expression and mouse cytotoxic T lymphocyte (CTL) exhaustion [156,157].

Imprinting of the "histone code" is an essential mechanism of gene regulation. The core histone proteins undergo post-translational modification relying on metabolites and cofactors, resulting in epigenetic remodeling of genomic regions in the T cells. Therefore, in CAR T cells, anti-tumoral or pro-tumoral elements might be modulated by epigenetic modification. It is indeed possible to target cell metabolism in order to impact epigenetics. For example, S-adenosylmethionine (SAM), a metabolite synthetized from methionine and a methyl donor, can modulate the methylation of DNA and histones. The upregulation of the methionine transporter SLC43A2 in cancer cells results in TILs deprived of methionine, which in turn results in decreased histone methylation and cytokine production in both murine and human T cells [158]. It is, however, not yet clear whether methionine restriction or supplementation might be of benefit as an anti-cancer treatment [158].

α-ketoglutarate, fuel for the TCA cycle derived from glutamine metabolism, regulates demethylation in aerobic conditions [159,160]. Thus, the use of an α-ketoglutarate-dependent demethylation inhibitor such as S2HG facilitates the apparition of central memory $CD8^+$ T cells. Alternatively, inhibition of glutamine metabolism may decrease α-ketoglutarate and, as a result, increase a hypermethylation state of the DNA in murine T cells [106,161].

In a mouse tumor context, the histone acetylation marks differ strongly between effector and exhausted T cells [162]. Metabolites such as acetyl-CoA, propionyl-CoA and succinyl-CoA are involved in this process and lead, for example, to H3K17 acetylation of introns, a characteristic of exhausted T cells [126,163]. Memory and effector T cells show higher histone acetylation at the INFγ promoter compared to naïve T cells and exhausted T cells [43,162]. In accordance with this, providing acetate in a glucose-deprived TME can induce histone acetylation in T cells, thereby restoring their effector function [92].

Conversely, histones deacetylation enhanced T cell effector function and anti-tumoral response. Histone acetylation inhibitors were further used to avoid T cell exhaustion. Thus, nicotinamide adenine dinucleotide (NAD^+) generated from glycolysis can change the cell fate via its regulation of sirtuins that are NAD^+-dependent deacetylases [164]. These sirtuins can modulate cellular metabolism. For instance, in human $CD8^+$ T cells, some sirtuins can maintain the FOXO1 protein stability that promotes OXPHOS metabolism in resting cells. However, they also can regulate cell proliferation via the deacetylation of p65, a subunit of NF-κB [165,166].

Even high levels of lactate can lead to histone modification, also called "lactylation" that is implicated in metabolic changes in macrophages, but its role in T cells remains to be determined even though it can be triggered by metabolic enzymes, such as lactate dehydrogenase, that play important roles in T cell life [167].

In view of the tight interconnection between metabolism and epigenetic modifications in CD8+ T cells differentiation, effector functions and exhaustion, particularly in the TME, it will be essential to try to therapeutically interfere with these processes, as suggested in a recent review by Van Acker et al. [168].

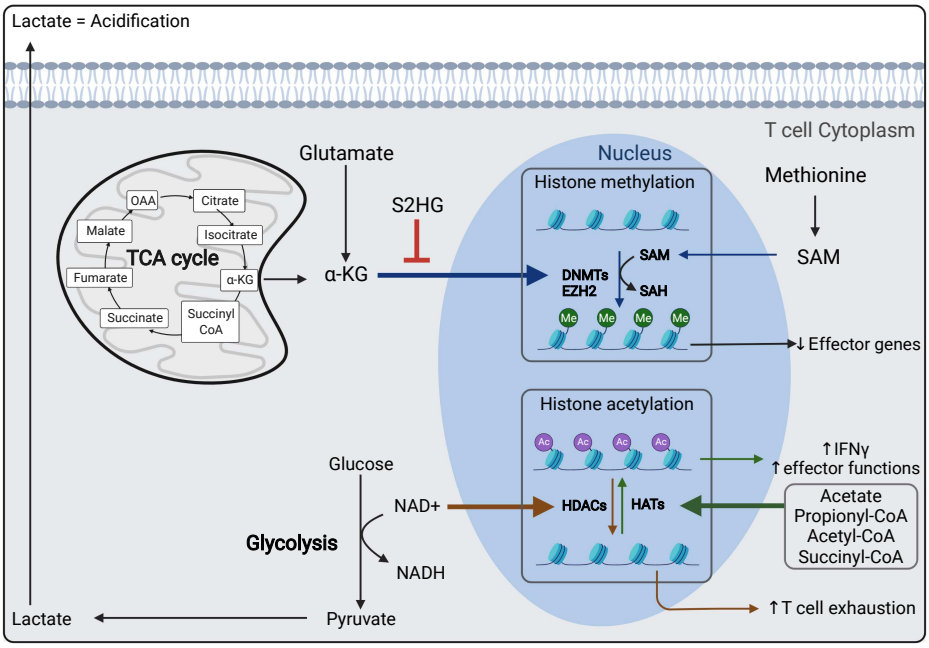

Figure 3. Immunometabolism shapes the epigenome of T cells. Here several of these epigenetic modifying pathways and metabolites influencing histone modification are outlined. OAA: Oxaloacetate; a-KG: a-Ketoglutarate; S2HG: S-2-hydroxyglutarate; DNMTs: DNA methyltransferase; EZH2: Enhancer of zeste homolog 2; SAM: S-adenosyl methionine; SAH: S-adenosyl homocysteine; NAD+: Nicotinamide adenine dinucleotide; NADH: Nicotinamide adenine dinucleotide hydrogen; HDACs: Histone deacetylases; HATs: Histone acetyltransferase. Figure generated by Biorender.com (accessed on 15 November 2021).

2. NK and CAR NK Cell-Based Therapies for a First-Line Anti-Cancer Immune Response

In contrast to T lymphocytes, natural killer cells are the granular effector lymphocytes of the innate immune system. Therefore, recognition mechanisms of damaged cells are MHC-independent, and the absence of MHC on any cell elicits the killing program in NK cells. Rather than recognizing specific antigenic peptides on the cell surface, NK cells bind ligands expressed on cells that are infected by viruses, bacteria and parasites or transformed by oncogenes [169]. Once the cytotoxic program is engaged, secretion of cytolytic enzyme-containing granules occurs, as well as production of IFNγ which promotes inflammation. Indeed, NK cells are responsible for a direct and non-primed cell killing, with an early onset during the immune response, orchestrated upon pathogen infection as well as tumor development and progression. Activation of NK cells is the consequence of soluble and membrane-bound signals that come from other immune cells, such as antigen-presenting cells (APCs) and damaged cells. Ligand-binding by a large spectrum of stimulatory and inhibitory receptors on NK cells underlies the self-tolerance and cytotoxic responses displayed by these granular lymphocytes [170]. Even though NK lymphocytes have been classified as part of the innate immune response, memory NK cells have recently been reported [171]. These long-lived memory NK cells and similar

NK memory-like phenotypes were described upon infection with human cytomegalovirus (CMV) and upon in vitro treatment with several inflammatory cytokines [170].

2.1. NK Cells Display Unique Anti-Cancer Immunosurveillance Mechanisms (Figure 4)

In the context of cancer, NK cells were described to follow two mechanisms for the recognition of oncogenic cellular entities [172,173]. Firstly, by the so-called "self-missing" recognition, malignant cells deprived of MHC (major histocompatibility complex) class I molecules do not signal to the inhibitory receptors, KIRs (killer cell immunoglobulin-like receptors) that are expressed on NK cells, which do not become activated [170,174,175]. The second mechanism relies on the activation of stimulatory receptors on NK cells such as natural cytotoxicity receptors (NCRs) and NKG2D (natural killer group 2D, a C-type lectin-like receptor), which generally bind to heparan sulfate glycosaminoglycans, damage-associated proteins or stress ligands expressed on the surface of cancer cells [176]. Likewise, tumor cells also express ligands binding to immune checkpoint molecules expressed on NK cells, which are in part also expressed on T cells (e.g., PD-1, LAG3, 2B4, T cell immunoreceptor with Ig and ITIM domains (TIGIT)), warranting immune escape from these natural killers [7,177]. As effector lymphocytes, NK cells can kill tumor cells by themselves by directly secreting cytolytic enzymes such as perforin and granzymes. Antibody-dependent cell-mediated cytotoxicity (ADCC) is another mechanism orchestrated by NK cells that directly target tumor cells via CD16 (FcγIIIR) binding to IgG antibodies recognizing tumor-associated antigens (TAAs) [178,179]. Once CD16 expressed on NK cells is engaged, tumor cell killing occurs via secretion of cytolytic granules. At a slower pace but still direct, NK cells can induce tumor cell death once death receptor ligands encounter their cognate receptor (e.g., Fas (CD95) and tumor necrosis factor-related apoptosis-inducing ligand (TRAIL)) on transformed cells. Indirectly, NK cells can secrete a rich repertory of soluble factors including IFNγ, tumor necrosis factor α (TNFα) and granulocyte-macrophage colony-stimulating factor (GM-CSF) that beyond contributing to the establishment of adaptive immune responses dependent on APCs, T and B lymphocytes can induce necrosis of tumor cells [170].

Due to their cytotoxic functions without pre-immunization, these cytotoxic immune cells represent a promising avenue for anti-cancer therapies. For instance, in vivo activation of NK cells using cytokine treatments (e.g., IL2, IL12, IL15, IL18 and IL21) has been investigated in several types of mouse cancer models and human cancers [180–183]. Furthermore, the use of antibodies to potentiate ADCC as well as to inhibit NK cell immune checkpoints, with similar immunotherapies used for effector T cells activation, are other alternatives that have been tested in mouse cancer models [2]. Antibodies that strengthen ADCC by NK cells include engineered versions that recognize tumor antigens in parallel with a stronger binding to CD16 [184]. In addition, antibodies to activate stimulatory receptors such as 4-1BB in combination with antibodies targeting TAAs are also part of therapeutic strategies under investigation [185]. Direct in vivo activation of NK cells using blocking antibodies against KIRs [186], the inhibitory receptor NKG2A [187] and immune checkpoints have also been tested in vitro as well as in pre-clinical studies and clinical trials of different types of cancer, showing that their potential benefits still need optimization. More sophisticated antibody-based approaches to potentiate in vivo NK cytotoxicity use bi- and tri-specific killer engagers that target TAAs and at the same time bind to NK receptors such as NKG2D, CD16 and IL15 cross-linking moieties [170,188].

Owing to the NK cell contribution to adaptive immune responses and the fact that they do not need to be of autologous origin, NK cells are used for adoptive cell transfer-based anticancer therapies. Sources of either allogeneic or autologous NK cells include peripheral blood and cord blood (CB). However, NK cells can also be derived from hematopoietic stem cells, embryonic stem cells and induced pluripotent stem cells (IPSC). Indeed, autologous, but mainly haploidentical allogeneic NK cells, have been used in clinical trials not only for hematological malignancies [189–192] and also for solid tumors in patients with recurrent ovarian and breast cancer [193], non-small cell lung carcinoma [194] and digestive cancers [195] as well as metastatic melanoma and renal carcinoma [196]. However,

the efficacy of NK cell-based immunotherapy for the treatment of solid cancers is rather poor, as NK cells not only need to expand in vivo following adoptive transfer but also infiltrate the tumoral mass and remain activated despite the immunosuppressive conditions of the TME [197]. NK cells derived from umbilical CB are poorer in cytotoxicity but can be expanded more easily and activated with cytokine treatments. Indeed, stem cell-derived NK cells have already been used in pre-clinical studies and clinical trials of liquid malignancies [198]. Evidently, NK cell lines generated from malignant NK cells represent the most expandable sources of NK cells, with the additional benefit of facilitating genetic engineering. Indeed, genetically engineered NK-92 cells are part of ongoing human clinical trials [172]. The most efficient source of NK cells for adoptive cell transfer in terms of cost, delays, cell expansion, in vivo persistence and anti-cancer cytotoxicity is still under investigation, but the most recent evidence indicates that stem cell-derived NK cells are a promising off-the-shelf alternative for anti-cancer therapies.

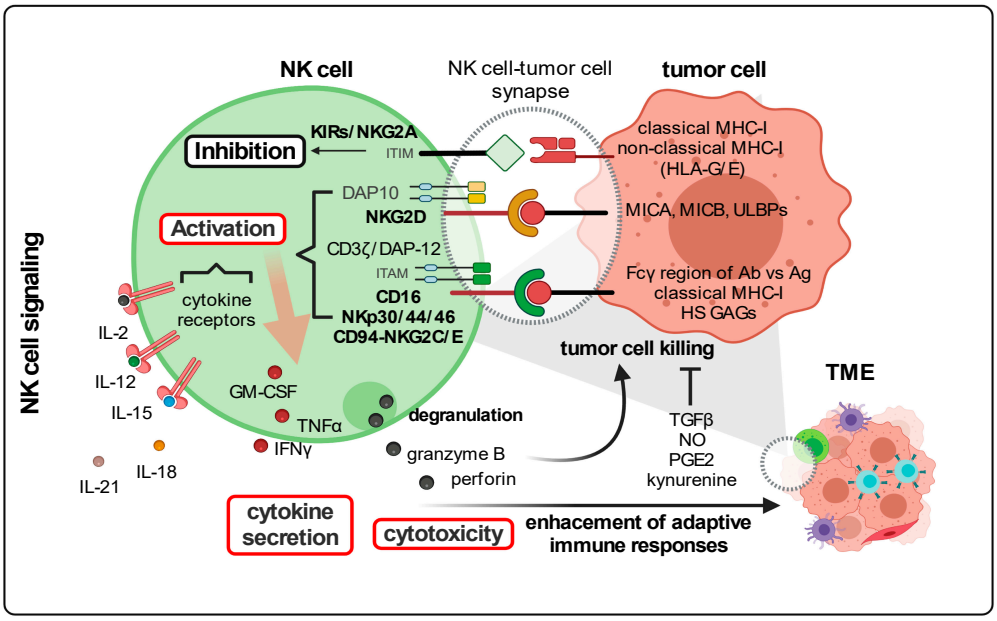

Figure 4. Simplified overview of the human NK cell-tumor cell synapse. Tumor cells signal to inhibitory and activating receptors expressed on NK cells. The binding of KIRs and NKG2A to MHC-I molecules leads to NK cell inhibition; engagement of NKG2D, NKp30/44/46, NKG2C/E and CD16; and drives the activation of NK cells. Upon receptor engagement, inhibitory signaling is mediated by ITIM motifs. Activating signaling can be ITAM-dependent and ITAM-independent. Activating receptors commonly form complexes with adaptor molecules such as DAP10 and DAP12 that trigger the activating signaling cascade. In addition to NK cell activation mediated by receptor engagement, cytokines also stimulate NK cells. Total NK cell activation is characterized by the production of inflammatory cytokines and degranulation, which leads to the release of cytolytic granules containing perforin and granzyme B. Lytic enzymes released at the synapse between NK cells and tumor cells warrant tumor cell clearance. Cytokines secreted by NK cells strengthen adaptive immune responses depending on several soluble factors within the TME such as TGFβ, NO, PGE2 and L-kynurenine that are secreted by tumor and stromal cells, limit the killing of tumor cells by NK cells. KIRs: Killer cell Immunoglobulin-like receptors; DAP: DNAX-activating protein; ITIM: Immunoreceptor tyrosine-based inhibitory motifs; ITAM: Immunoreceptor tyrosine-based activation Motifs; MHC-I: Major Histocompatibility Complex I; HLA: Human Leukocyte Antigen; MICA, MICB: MHC class I chain-related protein A and B; ULBPs: UL16 binding proteins; HS GAGs: Heparan Sulfate Glycosaminoglycans; Ab: Antibody; Ag: Antigen; GM-CSF: Granulocyte monocyte-colony stimulating fFactor; TNFα: Tumor cecrosis factor α; IFNγ: Interferon γ; IL: interleukin; TGFβ: Transforming growth factor β; NO: Nitric oxide; PGE2: Prostaglandin E2; TME: Tumor microenvironment. Figure generated with Biorender.com (accessed on 15 November 2021).

Genetic modifications of NK cells irrespective of their source were performed despite the poor performance of gene delivery achieved into these cells [199]. NK cells lacking CD16 were modified to express this receptor [200], and other NK cell lines were engineered to synthesize IL15 [201]. Furthermore, more specific targeting of tumor cells was pursued by engineering NK cells to recognize TAAs, cellular entities known as CAR NK cells [202,203]. In contrast to T cells that have the property of recognizing TAAs via MHC-I, receptors targeting tumoral antigens are not normally expressed on NK cells. Therefore, engineering CAR for NK cells so that they can recognize specific tumoral antigens is a powerful tool that allows the use of cytotoxic effectors in immunotherapy beyond CAR T cells. Similar to CAR T cells, CAR NK cell design has evolved towards third- and fourth-generation CARs that not only include the CD3ζ chain but also other co-stimulatory molecules such as 4-1BB, DAP-12 and CD28 as part of the activating intracellular domain. The design of the extracellular domain of the CAR in NK cells depends on the type of cancer. For instance, CAR NK cells have already been generated to recognize CD19+/CD20+ B-cell acute lymphoblastic leukemia and chronic lymphocytic leukemia [204,205], CD33+ acute myeloid leukemia [206], CD138+ multiple myeloma [207], CD5+ T cell lymphoma [208], GD2+ neuroblastoma [209], GPA7+ melanoma [210], EGFR+/HER-2+ glioblastoma [211], EpCAM+/HER-2+ breast [201], CD24+/HER-2+ ovarian [212] ROBO-1+ pancreatic [213] and MUC-1+ carcinomas, including colorectal cancer [214].

2.2. The Metabolism of Activated NK Cells in a "Healthy" Environment (Figure 4)

Apart from stimulatory and inhibitory signaling at the synapse of NK cells and target cells, the metabolism of NK cells also governs how these granulocytes will proliferate, maturate and function. A low basal metabolic rate, in terms of fluxes through glycolysis and OXPHOS, is a feature of resting or quiescent murine NK cells. For acute NK cell responses, this low metabolic rate is still sufficient for the production of IFNγ in NK cells, upon short-term in vitro stimulation with cytokines or via receptor binding because inhibition of these metabolic pathways limits the production of IFNγ. However, NK cells also participate in immune responses over extended periods, not only displaying cytotoxic functions but also sustaining adaptive immune responses. Prolonged stimulation of murine and human NK cells with different cocktails of cytokines not only activates them but also increases glycolysis and OXPHOS. Augmented glucose uptake and glycolytic rate in activated NK cells are accompanied by increased expression of glucose transporters and glycolytic enzymes [215]. Indeed, upregulation of the glucose transporter GLUT1 was reported in cytokine-stimulated NK cells, which correlated with their increased effector functions, production of IFNγ and granzyme B and NK cell proliferation [216]. Cytokine stimulation was also reported to augment the expression of amino acid transporters [28,197]. Likewise, an augmented OXPHOS in activated NK cells correlates with the higher mitochondrial mass observed in NK effectors during in vivo CMV infection. Upon stimulation, different subtypes of circulating NK cells ($CD56^{bright}$ and $CD56^{dim}$), as well as tissue-resident NK granulocytes, underwent an increase in the energetic metabolism although to different extents [215]. The importance of glycolysis for NK cell effector functions was demonstrated by administrating 2-deoxyglucose (2-DG), a metabolic inhibitor of glycolysis, into mice infected with mouse CMV. Mice treated with 2-DG showed impaired virus clearance and consequently higher viral titers [217].

When active, NK cells rely on glucose to fulfill energetic and biosynthetic demands. Indeed, glucose metabolism and consequently the production of lactate is sustained by pyruvate entering the TCA cycle, which produces citrate in the mitochondria. However, citrate is not further metabolized through the TCA cycle but rather exported to the cytoplasm and converted into malate. This reaction yields NAD+, a cofactor that is needed to sustain glycolysis. In turn, cytosolic malate enters the mitochondria as a carrier of electrons to yield NADH, which fuels the electron transport chain for ATP synthesis. This exchange of mitochondrial citrate by cytosolic malate is known as the citrate–malate shuttle (CMS) and serves to sustain glycolysis as well as the electron transport chain in mitochondria [215].

The glucose dependency of activated NK cells for glycolysis and OXPHOS was reflected by glutaminolysis inhibition, which did not limit OXPHOS nor the effector functions of these granulocytes. Indeed, OXPHOS was shown to be sustained, to a greater extent, by the CMS compared to glutaminolysis in stimulated NK cells [218].

Metabolism of NK cells has been associated with the activity mTOR [219]. mTOR was shown to be involved in the metabolic changes during NK cell maturation but also during the activation of mature NK cells. Similar to T cells, mTOR activity gradually decreased in the transit from the pre-NK to mature NK cell state in order to sustain proliferation and differentiation. Indeed, mature and resting NK cells displayed the lower activity of this master regulator of the cell metabolism. However, activation of NK cells was accompanied by an increase in the activity of mTOR [220]. Indeed, when treated with the classical mTOR inhibitor, rapamycin, mice infected with CMV displayed NK cells with limited proliferative capacity, less production of IFNγ, lower cytotoxicity and consequently higher viral load. Notably, in vitro activated NK cells with different combinations of cytokines or receptor engagement have a variable dependency on mTOR activity to increase glycolysis. Noteworthy, mTOR activity in NK cells is highly dependent on the levels of the amino acids glutamine and leucine [215].

Memory-like NK cells (ML-NK cells) have been described in mice and humans upon infection with CMV as virus-specific effectors that persist after infection [221]. These "adaptive" NK cells are self-renewable and generate pools of NK cells with higher effector functions following a second activation. Interestingly, these so-called adaptive NK cells rely on mitochondrial fitness and OXPHOS to exert an anti-viral and possibly also an anti-cancer program. Indeed, the establishment of mouse memory-like NK cells was reported to depend on the capacity of NK cells to recover a maximal mitochondrial function. This process is achieved upon removal of damaged mitochondria by mitophagy in rapidly proliferating NK cells [215]. Interestingly, this type of NK cells was also described to execute an anti-tumoral killing program with a higher production of INFγ and cytotoxicity and this for a longer period upon reactivation.

The metabolic program of activated NK cells is not only sustained by mTOR but also by other metabolic regulators such as sterol regulatory element-binding proteins (SREBPs) and cMyc. Interestingly, a non-canonical function of SREBPs that is unrelated to the synthesis of fatty acids and cholesterol was described in IL2/ IL12 stimulated NK cells, which rely on glucose to increase their biomass [222]. Increased proliferation, glycolysis and OXPHOS in stimulated NK cells were dependent on SREBPs, as pharmacological inhibition of SREBPs abolished these changes but did not affect mTOR activation. SREBPs transcriptionally regulate the expression of the mitochondrial citrate transporter and cytosolic malate across the mitochondrial membrane and also regulate the expression of the first enzyme, which catalyzes the cytoplasmic conversion of citrate into malate, which is the ATP citrate lyase. Therefore, these two proteins are critical for the citrate–malate shuttle (CMS). By tracing-based metabolomic analysis, the majority of the citrate detected in stimulated NK cells was cytosolic, and therefore generated by the CMS. The importance of SREBPs in mediating NK cell metabolism and cytotoxicity was demonstrated by in vivo inhibition of SREBPs in melanoma tumor-bearing mice upon adoptive NK cell transfer as it abolished their anti-tumoral effect [222].

Inhibition of SREBPs in cytokine-stimulated NK cells reduces NK cell cytotoxicity to a greater extent compared to the inhibition of mTOR with rapamycin, indicating that SREBPs play a unique role in NK function [223]. Indeed, SREBPs control cMyc expression in mouse NK cells stimulated with IL2 and IL12 as inhibition of SREBPs decreased the protein expression of cMyc. cMyc is known to control the transcriptional expression of the rate-limiting enzyme of de novo polyamine synthesis, ornithine decarboxylase (ODC1). Upon inhibition of SREBPs, ODC1 transcript levels were decreased as well as several polyamines in cytokine-activated NK cells. Inhibition of de novo polyamine synthesis resulted in lower proliferation, glycolytic and OXPHOS rates and less production of IFNγ and granzyme B. However, the activation of NK cells with polyamine addition was not

able to rescue the metabolic and cytotoxic defects in NK cells that are caused by SREBP inhibition. Instead, this rescue occurred via the production of IFNγ and granzyme B. Polyamines participate in a post-translational modification known as hypusination that occurs in a translation initiation factor. Inhibition of SREBPs was shown to decrease the transcript levels of one of the enzymes involved in hypusination. Inhibition of hypusination decreased NK cell proliferation, OXPHOS rate, production of cytokines as well as NK cell-mediated cytotoxicity. Therefore, as part of SREBPs and cMyc downstream signaling and apart from SREBP regulation of the energetic metabolism, de novo polyamine synthesis and hypusination seem to be downstream pathways that contribute to the optimal performance of cytokine-stimulated NK cells [223].

Upon stimulation with IL2 and IL12, cMyc, an anabolic transcription factor, was upregulated at the transcript and protein levels in IL15-expanded splenic mouse NK cells. However, the expression of hypoxia-inducible factor-1α (HIF-1α) was not critically modulated by cytokine stimulation. NK cell stimulation increased the expression of the transferrin receptor CD71, glycolytic and OXPHOS rates, as well as mitochondrial mass in a cMyc-dependent and a HIF-1α-independent manner. These metabolic responses in stimulated NK cells were accompanied by increased production of IFNγ and granzyme B. Interestingly, initial cMyc upregulation upon stimulation with IL2 and IL12 was mTOR-dependent for cytokine stimulation less than 18 h and fully independent of Akt-driven signaling. Blocking the highly expressed aa transporter SLC7A5 reduced the expression of cMyc, mTOR activity, energetic metabolism and cytokine production in activated NK cells. While this aa antiporter extrudes mostly glutamine for uptake of some other amino acids such as leucine, only glutamine availability controlled cMyc expression in stimulated NK cells independently of mTOR activity. Therefore, cMyc expression in NK cells was dependent on the SLC7A5 transporter and glutamine, pointing out that high expression of cMyc requires not only rapid translation machinery but also sufficiently available aa. Indeed, the role of glutamine in NK cell responses was shown to be independent of fueling the TCA cycle for OXPHOS, which was consistent with the reliance of activated NK cells on the CMS. Glutamine was shown to be critical not as an energetic fuel but as an aa that is needed for the upregulation of cMyc. In this regard, glutamine deprivation but not inhibition of glutaminolysis dramatically reduced OXPHOS and glycolytic rates, as well as cytokine production and in vitro cytotoxicity of NK cells against tumor cells [218]. This is not exactly the same for T cells residing in the TME (see point 1.2.3)

2.3. NK Cells Are Metabolically Challenged within the TME (Figure 5)

Similar to other stromal cells infiltrating the TME of solid malignancies, also equivalent to T cells, NK cells experience metabolic challenges that could impair their cytotoxic functions. For example, glucose restriction occurs due to sugar-devouring tumor cells. Indeed, the TME should be viewed as an area with specific cellular entities, nutrient and oxygen availability, and soluble factors that will shape the functions of already resident and newly incoming cells. For instance, some of the immunosuppressive signals from tumor and stromal cells exert metabolic changes in NK cells that induce their exhaustion. NK cell exhaustion could be detrimental to controlling tumor progression. One example includes the combination of TGFβ with IL2 that not only downregulates the expression of several activating receptors on NK cells but also decreases OXPHOS in activated NK cells, thereby reducing their proliferation and cytotoxic responses [197,224]. TGFβ was reported to limit NK cell metabolism by inhibiting mTOR [225]. Sources of TGFβ within the TME include regulatory T lymphocytes (Treg), M2 macrophages, cancer-associated fibroblasts (CAF) and tumor cells. For instance, TGFβ-secreting Treg cells negatively impact NK cells via the activation of the NK receptor CD69.

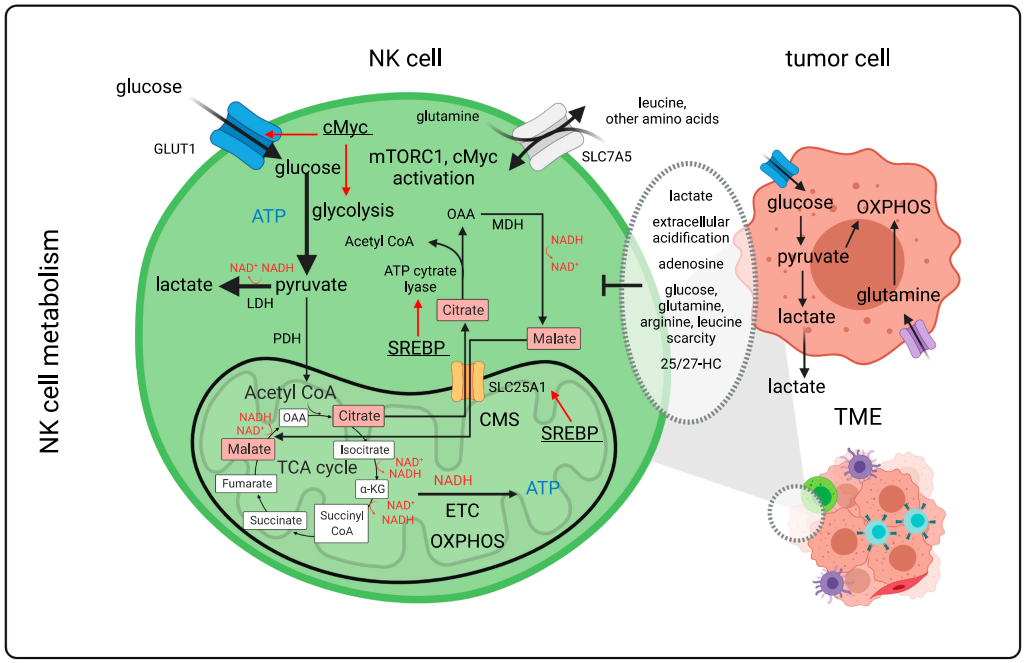

Figure 5. NK cell metabolism upon activation and challenges within the TME. NK cells rely on glucose to sustain glycolysis and OXPHOS for the production of energy. The citrate–malate shuttle between mitochondrial citrate and cytosolic malate provides sufficient reducing equivalents in the cytoplasm to sustain glycolysis and glycolytic ATP production while generating lactate. The citrate–malate shuttle also generates NADH molecules in the mitochondria apart from the ones that are generated by the tricarboxylic acid during OXPHOS. NADH molecules are oxidized by the electron transport chain to produce ATP. Upon NK cell activation, SREBPs transcriptionally controls the expression of the malate–citrate antiporter SLC25A1 and the ATP citrate lyase. In activated NK cells, the glucose transporter Glut1 is upregulated as well as the aa transporter SLC7A5. The exchange of intracellular glutamine for other aa, such as leucine through SLC7A5, increases the intracellular aa availability that is required to activate mTORC1 and enhance cMyc expression. cMyc transcriptionally controls glycolysis as well as the expression of the glucose transporter GLUT1. NK cells at the synapse with tumor cells and within the tumor microenvironment encounter extracellular acidification. This is mediated by a higher content of lactate secreted by tumor cells, inhibitory metabolites such as adenosine, limited availability of glucose and aa such as glutamine, arginine and leucine, as well as soluble inhibitors of SREBPs such as 25/27-HC. LDH, lactate dehydrogenase; PHD, pyruvate dehydrogenase; TCA, tricarboxylic acid; OAA, oxalacetate; α-KG, α-ketoglutarate; ETC, electron transport chain; OXPHOS, oxidative phosphorylation; CMS, citrate–malate shuttle; SREBPs, sterol regulatory element-binding proteins; mTORC1, mammalian target of rapamycin complex 1; MDH, malate dehydrogenase; 25/27-HC, hydroxycholesterol; TME, tumor microenvironment. aa, amino acid. Figure generated by Biorender.com (accessed on 15 November 2021).

2.3.1. The Hypoxic Tumor Environment and NK Cell Function

Several metabolic aspects of the TME were shown to alter NK cell functions. For example, higher levels of adenosine, as a tumor-derived metabolite produced by ATP and AMP that are released by tumor cells in a hypoxic microenvironment, limited NK cell functions similar to T cell functions when adenosine was bound to adenosine receptors expressed on NK cells. Adenosine was reported to decrease OXPHOS and glycolysis of human NK cells, stimulated with IL2 plus IL15, which reduced their cytotoxicity [226]. A hypoxic TME was also suggested to shape NK cell metabolism. Some studies showed that hypoxia could reduce but not entirely abolish NK cell functions. Activation of HIF-1α mediates the transcriptional regulation of glycolytic genes, which might be critical for NK cells in order to keep their cytotoxic effects in a low oxygen environment. However,

evidence is controversial since hypoxia also decreased the expression of several activating NK cell receptors such as NKp30, NKp46 and NKG2D [197]. Moreover, a hypoxic TME leads to granzyme B degradation in NK cells through autophagy [224].

2.3.2. Effect of the Metabolite Lactate and Other Metabolites on NK Cell Performance

Our understanding of NK cell metabolism has mainly progressed in the past ten years since immunometabolism was mostly studied in T lymphocytes and myeloid cells [8]. Lactate is one of the metabolites that is readily generated by tumor cells and was shown to blunt the anticancer immune surveillance of NK cells and of T cells, as mentioned earlier. Indeed, local secretion of lactate by tumor cells within the TME of murine melanoma and pancreatic adenocarcinoma models was associated with less infiltration of NK cells, which produced lower levels of IFNγ and granzyme B. In vitro stimulated NK cells did not only secrete lower levels of IFNγ but also reduced levels of IFNγ transcripts when treated with lactic acid or cultured in low pH conditions. Upregulation of nuclear factor of activated T cells (NFAT), a transcription factor controlling IFNγ expression during NK cell activation was also found to be inhibited upon lactic acid treatment and led to apoptosis of NK cells. Extracellular lactic acid was shown to be taken up by NK cells, which caused intracellular acidification and a drop in ATP levels. Therefore, immune cell evasion in these cancer models was dependent on the levels of expression of lactate dehydrogenase A (LDHA) in tumor cells and the levels of lactate within the TME, which dampened the cytotoxic effects of NK cells [53]. Another study in colorectal carcinoma patients found that when the carcinoma metastasized to the liver, lactate was produced, which in turn causes intra-cellular acidification of intra-tumoral NK cells. Additionally, NK cells residing in the liver displayed mitochondrial dysfunction and underwent apoptosis [215].

The NK cell-tumor synapse was described as an energetically demanding connection. Indeed, there is mitochondrial polarization in NK cells to the site of tumor cell docking. This is accompanied by a reduction in the mitochondrial membrane potential of NK cells when the tumor cell is targeted as a reflection of an energy-consuming mechanism [227,228]. Alterations of the glycolytic pathway were described in intra-tumoral NK cells. In a lung cancer mouse model, NK cells displayed a reduced glycolytic rate, which correlated with lower effector functions. Interestingly, fructose-1,6-biphosphatase, an enzyme of gluconeogenesis, was found to be upregulated in these NK cells, in accordance with glycolysis inhibition and an improved NK cell anti-cancer activity upon inhibition of this enzyme [229]. In addition, metabolic alterations can be caused by inhibition of SREBPs, major transcription factors that mediate higher glycolytic rates, cytotoxicity and cytokine production in cytokine-stimulated NK cells. Indeed, higher levels of naturally occurring SREBP inhibitors such as 25- and 27-hydroxycholesterol were found in tumors of patients with breast, gastric or colorectal carcinomas [197]. These compounds are synthesized from cholesterol by enzymes upregulated in macrophages and some tumors [215].

2.3.3. Limited Amino Acid Availability in the TME

Other metabolic challenges encountered by NK cells within the nutrient-deprived TME include reduced aa availability. Although reported in vitro, human NK cell lines and primary cells display lower proliferative capacity and IFNγ production when arginine levels are low. Furthermore, the absence of leucine in the culture media inhibited the mTOR pathway in NK cells. Aside from the aa requirements of NK cells, the production of certain aa byproducts can modulate NK metabolism. In myeloid cells, arginine catabolism that occurred as a result of inducible nitric oxide synthase (iNOS) upregulated the yield of nitric oxide. Nitric oxide in the TME impairs NK cell-mediated ADCC, and the inhibition of iNOS or the depletion of myeloid-derived suppressor cells (MDSCs) was shown to revert NK cell cytotoxicity [230]. Furthermore, myeloid cells also upregulated arginase, an enzyme that catabolizes arginine and depletes this aa in the TME. In addition, L-kynurenine, which is a byproduct of tryptophan degradation and is catalyzed by IDO, was described to inhibit the proliferative capacity of NK cells. A similar scenario was reported for T cells in the

TME. This also leads to the upregulation of activating NK cell receptors (i.e., NKp46 and NKG2D) and cytokine synthesis [231]. Activated NK cells display high levels of the L-kynurenine transporter across the cell membrane, and these granulocytes are at high risk of undergoing inhibition by this catabolite within the TME [215]. Apart from producing immunosuppressive catabolites, IDO depletes tryptophan in the TME and therefore reduces the availability of this essential aa [8]. Prostaglandin E2 (PGE2) is another metabolite that NK cells can encounter within the TME. PEG2 is synthesized by cyclooxygenases that can be expressed not only in tumor cells but also in tumor-associated macrophages (TAM) and other stromal cells. PGE2 is known as a critical modulator of NK cellular functions. For instance, PGE2, once bound to EP2 and EP4 receptors on NK cells, can decrease the expression of several activating NK cell receptors such as NKp30, NKp44, NKp46 and NKG2D. In TMEs where PGE2 is secreted, NK cell cytotoxicity is impaired. PEG2 blocking was shown to improve NK cell effector functions in a mouse model of metastatic breast cancer. Likewise, a positive outcome when using inhibitors of cyclooxygenase 2 in several solid malignancies was reported [232].

Recently, the effect of glutathione on NK cell cytotoxicity was described. Pharmacologically blocking the formation of epigenetic enzymatic complexes that contain the demethylase LSD1 did not only decrease the viability of NK cells but also OXPHOS respiration, which had a lesser effect on T cells. In correlation, mitophagy with ROS production and reduced glycolysis were also demonstrated. The oxidative stress and impaired viability were rescued by glutathione supplementation, and the cytotoxic effect of NK cells was also partially reinstalled. This occurred upon scaffolding LSD1 inhibition, despite not reversing the impaired energetic metabolism. Therefore, the redox status of NK cells seems to be crucial for their cytotoxicity, even when their energy metabolism is affected. Improvement of the anticancer effector functions of NK cells beyond an optimal energetic metabolism was suggested with nutritional supplementation of glutathione [233].

2.3.4. Targeting the Metabolism in the TME to Re-Establish NK Effector Function

Boosting NK cell effector functions by targeting the metabolism within the TME is a promising avenue for anticancer therapies. However, this is not an easy task when considering that metabolic pathways are not exclusive to tumor cells and that targeting them might also affect stromal cells [234]. Despite this, several strategies were suggested to overcome the metabolic challenges that NK cells encounter when fighting cancer cells in liquid as well as solid malignancies. For example, chemotherapy-induced tumor cell death might diminish the amount of glucose consumed by tumor cells. Consequently, NK cells may benefit from a TME that is less deprived of glucose. Inhibitors of glutaminase, which reduce the entry of glutamine into the TCA cycle in tumor cells, might increase glutamine availability in the TME in order to activate mTOR and induce cMyc translation in NK cells. Treatment with inhibitors of the glycogen synthase kinase 3 (GSK3) in order to avoid cMyc degradation might retain NK cells in their active state. Indeed, GSK3 inhibitors were described to increase the antitumor cytotoxic functions of NK cells [234]. These strategies could also be applied in combination with adoptive NK cell transfer. In the context of CAR NK cells, it is fair to consider whether there are versions of CARs that increase NK cell effector functions by making them more metabolically fit and resistant in order to fight malignant cells.

2.4. How Can CAR NK Cells Persist, Remain Cytotoxic and Metabolically Fit in TME?

When considering adoptive cell transfer, CAR NK cells were developed as an alternative to CAR T cell-based therapy, as several side effects can occur when delivering genetically modified T lymphocytes. Some of the limitations associated with CAR T cell immunotherapy include graft-versus-host disease (GVHD), cytokine release syndrome (CRS) and immune cell-associated neurotoxicity (ICAN) [235]. Although not very well established, CAR NK cells are believed to be less prone to causing GVHD because of the strong regulation of their self-tolerance for healthy as well as "self" tissue, which are

mediated by inhibitory NK receptors. As part of innate immunity, NK cells do not generate antigen-specific clones as compared to T cells. In addition, NK cells present different properties to elicit the production of myeloid-derived cytokines that might generate an inflammatory storm. Apart from side effects that are minimized with CAR NK cells, these biological entities carry a broad spectrum of activating receptors, which might warrant CAR NK cell activation, even though tumor cells undergo immune-editing and lose the antigen to which the CAR is specific [236]. CAR NK cells as artificial effector lymphocytes can display CAR-dependent and CAR-independent mechanisms of action, a property that makes them valuable for immunotherapy. Indeed, the first clinical trial (NCT03056339) for CD19-targeting CAR NK cells derived from CB in refractory B cell lymphoma patients reported a positive clinical response in more than 50 % of the individuals with no signs of the above-mentioned side effects [237].

Metabolic interventions to improve the immunosurveillance of tumor-infiltrating immune cells have not yet been explored to the same extent compared to targeting tumor cells with antimetabolic drugs. Indeed, targeting metabolism within the TME is another avenue that is currently being investigated in combination with classical immunotherapy but primarily in the context of T cells. For instance, in melanoma, neutralizing the acidic pH of the TME with oral bicarbonate showed improved tumor growth control in combination with anti-PD-1 treatment. Likewise, oral bicarbonate, in combination with adoptive T cell transfer, extended the survival of tumor-bearing mice [238,239]. Other strategies focused on glucose and lactate metabolism in tumor cells [49,240–243]; however, targeting these metabolic pathways exclusively in malignant cells remains a challenge and is still in progress [80,244,245]. Currently, the following are being investigated and refined: targeting glutamine metabolism in tumor cells [106,246], arginine metabolism in myeloid cells [247], tryptophan metabolism in the TME [248], lipid metabolism in both, tumor [207] and immune cell populations [249] and disruption of signaling pathways activated by nutrient availability and oxygen content (i.e., mTORC1 [250,251], AMPK [252], HIF-1α [234,253,254]). Of note, most of these studies include T or CAR T cells.

When focusing on enhancing the anticancer performance of NK cells beyond CAR engineering in order to target different TAAs and stress ligands, different CAR constructs were designed to improve NK cell-intrinsic activation pathways and trafficking. Likewise, there are CAR versions that intend to reduce the tumor cell heterogeneity within solid TMEs. These CAR versions generate NK cells, which target NKG2D-expressing cancer stem cells and immune checkpoint expressing tumor cells that evade T cell recognition. Furthermore, CAR NK cells were generated to avoid immunosuppressive signals within the tumor, such as TGFβ [214]. How all these CAR constructs contribute to NK cell metabolic fitness remains to be fully interrogated. To our knowledge, genetic modifications that potentiate the metabolism of CAR NK cells have not yet been reported. One major obstacle when using primary NK cells in immunotherapy is the lack of an efficient gene transfer method. Recently, though, two independent studies showed that this hurdle could be overcome by changing the vesicular stomatitis G (VSV-G) envelope glycoprotein (gp) at the surface of a lentiviral vector (LV) by a baboon retroviral envelope gp [255,256]. These new LVs ensured up to 80 % genetic modification of activated NK cells [199,257] and were shown to generate functional CAR-expressing NKs. Another study also showed high-level CAR delivery into NK cells by employing an α-retroviral vector system [258]. These results will pave the way to progress CAR NK cell therapy to the clinic.

In the following section, we illustrate with the few available studies how evaluating the metabolic fitness of CAR NK cells may provide a better in vitro validation of NK cell performance prior to pre-clinical and clinical testing. Much of the knowledge about NK cell dysfunctions is based on pathologies such as obesity. It is very well established that NK cells from obese mice do not respond efficiently to viral infections. This is indicated by fewer cytotoxic responses and a lower number in the circulation, and a number of factors that make these cells less effective against tumors [223]. Immune dysfunction due to obesity has been associated with a lower energetic metabolism in NK cells upon cytokine stimulation.

Indeed, lipid accumulation mediated by peroxisome proliferator-activated receptor (PPAR) downregulates cMyc expression, mTOR activity and decreases the rates of glycolysis and OXPHOS in NK cells, which limits their anticancer response [259]. The chronic low-grade inflammation underlying obesity occurs as a result of inflammatory soluble factors secreted by adipocytes and adipocyte-associated macrophages. This inflammatory niche resembles the inflammatory TME of several solid tumors. Local microenvironments with such characteristics induce MDSCs, an immune cell population that is common in oncogenic malignancies and also detected in obese mice driven [260]. Therefore, CAR NK cells were designed to target not only tumor cells but also MDSCs within the TME. MDSC-containing TMEs are often immunosuppressive due to the presence of mediators such as TGFβ that, for instance, downregulates the expression of NKG2D co-adapter molecules on NK cells. A CAR targeting NKG2D ligands was designed to express a fusion protein containing the extracellular domain of the activating NK receptor NKG2D and the CD3ζ chain of cytotoxic T cells as the intracellular domain. NKG2D ligands are not only expressed by damaged and hypoxic tumor cells but also by intra-tumoral MDSCs. This makes NKG2D a suitable receptor for dual targeting in solid malignancies [261]. NKG2D CAR NK cells artificially and constitutively express a functional activating receptor that naturally is usually reduced in the TME. NK cells modified with this CAR displayed higher NKG2D-mediated cytotoxicity in vitro against tumor cells expressing NKG2D ligands. Importantly, this stronger cytotoxicity was retained irrespective of the presence of TGFβ and NKG2D soluble ligands in the cell culture medium, which are components of in vivo TMEs that limit NKG2D signaling. NKG2D CAR NK cells also displayed enhanced cytotoxicity against autologous NK2GD ligand-expressing MDSCs (Figure 6). CAR NK cells were able to limit tumor growth in a xenograft model that was generated by engrafting MDSC and GD2+ neuroblastoma cells, which did not express NKG2D ligands. Importantly, a significant tumor growth control was dependent on the elimination of NKG2D ligand-expressing MDSCs rather than directly targeting tumor cells. These engineered CAR NK cells did not react against NKG2D ligand-expressing autologous T cells as compared to the NKG2D CAR T cells, further demonstrating the safety of the adoptive CAR NK cell-based immunotherapy in terms of GVHD [261].

Memory-like (ML) or adaptive NK cells in humans were reported to display distinctive metabolic features when compared to non-adaptive NK cells. Aside from having an augmented mitochondrial mass, mitochondrial membrane potential and OXPHOS rates, mTOR activation is more enhanced upon CD16 engagement as compared to classical human NK cells in their ML counterparts [215]. This metabolic fitness has not yet been reported as the cause of higher cytotoxicity against tumor cells for longer periods. A recent study, however, clearly shows that ML NK cells were not only suitable for adoptive cell transfer but can also be engineered with a CAR and displayed improved tumor control compared to conventional CAR NK cells. Indeed, engineering ML NK cells derived from PB with a CAR targeting CD19 has shown to improve IFNγ production, degranulation (CD107a+) and cytotoxicity in vitro when co-cultured with NK-cell resistant lymphoma cells as compared to conventional CAR NK cells. This was confirmed in vivo [236].

Other alternatives to expand human NK cells are currently being tested in order to obtain metabolically fit CAR NK cells with stronger cytotoxic responses for clinical application. For instance, expansion of NK cells was performed under co-culture conditions using irradiated feeder B cells that were genetically modified to express membrane-bound IL21 and none or low levels of MHC-I. Expansion in the presence of IL2 and IL15 and a CD19 CAR encoding retroviral vector yielded metabolically fit CAR NK cells. These feeder B cells proved to be advantageous for NK and CD19 CAR NK cell proliferation, purity and reduced their apoptosis. CD19 CAR NK cells expanded using IL21-expressing feeder B cells were more cytotoxic against CD19+ lymphoma cells and displayed higher tumor burden control in two lymphoma xenograft models [262]. CD19 CAR NK cells that were expanded using IL21^{+} feeder B cells upregulated genes involved in aa metabolism and glycolysis, while genes involved in NK cell activation, differentiation and cell-to-cell adhe-

sion were downregulated, reflecting a less differentiated state. Higher glucose uptake was also confirmed in feeder B cell-expanded NK cells. Moreover, genes coding for cell death receptors and cognate ligands were downregulated upon expansion, indicating that these NK cells were less prone to undergo cell death. Furthermore, some transcription factors and signaling proteins that are downregulated in the ML NK cell phenotype were expressed at lower levels when using the feeder B cell expansion system. This highlighted that the resulting NK cells had a potentiated adaptive phenotype that resembled ML NK cells. Furthermore, several metabolic genes such as cMyc, SLC7A5, transferrin receptor (TFRC), serine sulfhydrase (CBS), phosphoserine phosphatase (PSPH), phosphoserine aminotransferase 1 (PSAT1) and genes contributing to the CMS, malate dehydrogenase 1 (MDH1) and pyruvate dehydrogenase (PDHA1) were all upregulated. This study, therefore, described a novel human NK cell expansion system that was superior in generating allogeneic CAR NK cells with an ML NK cell phenotype. This phenotype marked by enriched expression of metabolic genes was associated with rapid cell proliferation without inducing exhaustion. This highlights the feasibility of CAR NK cell-based immunotherapies, as CB banks are readily available [262].

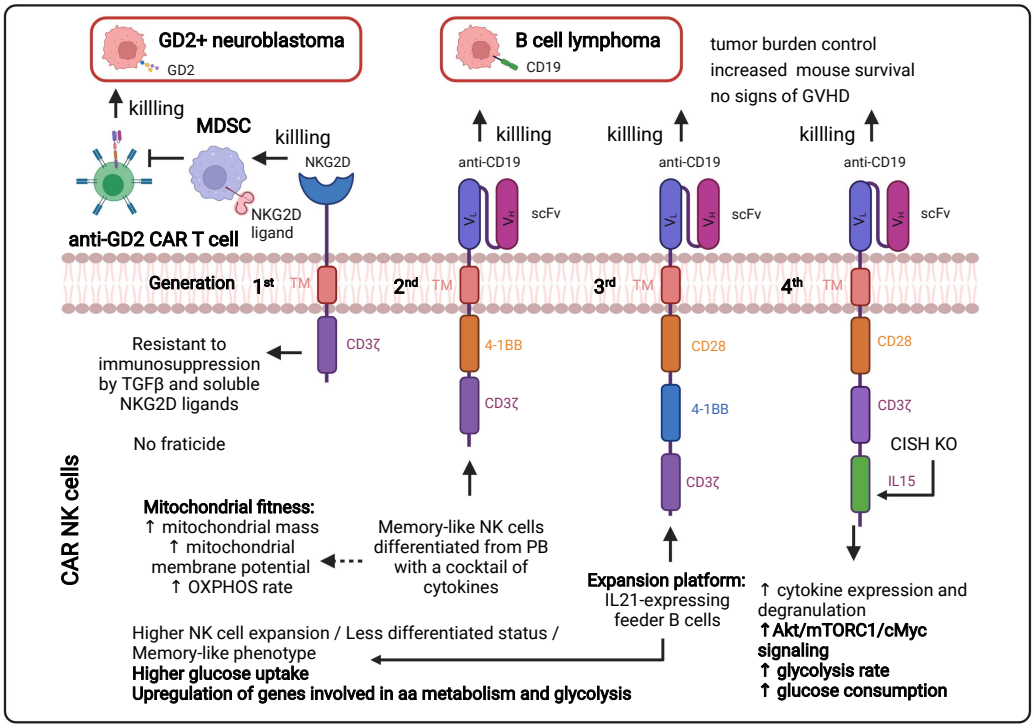

Figure 6. Overview of CAR NK cell generations. Depicted designs are representative of CAR NK cells resistant to challenges within the tumor microenvironment that limit NK cell metabolism and CAR NK cells with reported improvement of metabolic features. MDSCs, myeloid-derived suppressor cells; TGFβ, transforming growth factor β; tCD19, truncated CD19; GVHD, graft-versus-host disease; OXPHOS, oxidative phosphorylation; aa, amino acid. Figure generated by Biorender.com (accessed on 15 November 2021).

Recently, the fourth generation of CAR NK cells was developed to express an anti-CD19 CAR, specific for B cell lymphoma and IL15 (Figure 6). Moreover, these so-called armored CAR NK cells were further modified to inhibit an NK immune checkpoint. The genetic modification is based on knocking-out *CISH*, a gene coding for the cytokine-inducible SH2-containing protein (CIS). CIS is activated as part of a negative feedback mechanism induced by IL2 and IL15 stimulation [263]. Targeting this cytokine immune checkpoint improved the metabolic fitness of NK cells that were derived from CB. These CAR NK cells, when co-cultured with lymphoma cells, displayed a higher Akt/mTOR/cMyc signaling

and glycolysis, which was confirmed by increased extracellular acidification. These IL15 secreting anti-CD19 CAR NK cells were more cytotoxic in vitro and persisted longer in mice when *CISH* was silenced. Adoptive transfer of these *CISH* KO CAR NK cells significantly prolonged the survival of a lymphoma mouse model. This innovative way of specifically improving CAR NK cell immunotherapy is due to the synergism of combining specific tumor cell targeting and cytokine activation by the NK cells themselves while abolishing the cytokine-associated negative feedback. Secretion of IL15 by CAR NK cells gives them a therapeutic advantage since some TMEs are poor in IL15. Importantly, these CAR NK cells are also equipped with a suicide gene that allows inducing apoptosis if adoptive cell transfer results toxic in the clinic [264].

3. Perspectives

Currently, the field is investigating the missing links between the proof of concept of innovative strategies in order to overcome current limitations in CAR T/NK cells and their translation into the clinic. Among these hurdles, CAR T/NK cells encounter immune responses, inhibitory signals, metabolic changes from the tumor cells and tumor microenvironment, toxic side-effects and loss of long-term persistence, among others. The field is actively attempting to find solutions to these obstacles by multiple innovative approaches. These approaches include gene editing techniques and in vivo generation of CAR T cells [265] in an attempt to improve the accessibility of the CAR T cell therapy to more patients. In the future, improved mice models that mimic human hematopoiesis and immune response more closely [266] will assist the field with addressing pertinent unanswered questions. Below, we discuss some novel research avenues in the CAR T/NK field.

3.1. "Off the Shelf" Universal CAR T Cells

T cell and CAR T cell therapies currently rely on autologous T cell transfer, which requires patient-specific manufacturing. This is a costly process and can lead to heterogeneous products from one patient to another. Therefore, huge efforts are invested into generating allogeneic T cells, which have strong anti-cancer potency that is not rejected by the patient's immune system. One strategy for universal CAR T cell generation is to eliminate the endogenous TCR, resulting in the sole expression of a CAR on the T cell [131,267–269].

Universal anti-CD19 CAR T cells were developed by gene editing strategies to knock out the constant region of the TCRα chain and the CD52 gene, in order to make the CAR T cells resistant to an anti-CD52 antibody that is used for the treatment of B-cell chronic lymphocyte leukemia (Quasim et al. 2017). The treatment of two children with aggressive B-ALL with this universal CAR T was effective. More strategies for the generation of universal CAR T cells as described by Morgan et al. [270].

Mo et al. [271] used an elegant approach based on the fact that recipient T and NK cells, upon allogeneic CAR T cell infusion, may upregulate co-stimulation receptors such as 4-1BB, while resting T cells will not. Therefore, they engineered therapeutic T cells carrying an anti-CD19 CAR together with an allogeneic defense receptor exposing 4-1BB Ligand at their surface, which was shown to eliminate the recipient T cells and NK cells that reacted against this CAR T cell graft. Here, it is obvious that large metabolic changes are involved and that we might need to rewire these universal CAR T cells to make them even more potent and persisting long-term.

Pluripotent stem cells, such as human induced pluripotent stem cells (hiPSCs), can provide an unlimited T cell source for CAR T cell development, with the potential of generating off-the-shelf T cell products. T-iPSCs (iPSC-derived T cells) are phenotypically defined, expandable, easily genetically manipulated and are as functional as their physiological T cell counterparts. The combination of iPSC and CAR technologies provides an exciting opportunity for oncology and greatly facilitates cell-based therapy for cancer patients.

However, T-iPSCs, in combination with CARs, are at the early stage of development and need further pre-clinical and clinical investigation (for review, see [272]).

3.2. Combining CAR T and CAR NK Cells to Increase Their Anti-Tumor Activity

The most recent studies on CAR NK cells reflect that evaluation of CAR NK cell effectivity for immunotherapy cannot only rely on the assessment of effector functions, including cell killing and production of cytokines. Other parameters such as cell phenotype as well as metabolic features are critical when testing the in vitro efficacy of CAR NK and T cells. Therefore, immunotherapy pursuing to enhance T and NK cell effector functions in parallel with the objective to minimize cancer immune-evasion is beginning to yield promising results [7]. Recently, CAR T and CAR NK cells were combined to pursue this objective. For example, adoptive NKG2D CAR NK cell transfer enhanced tumor infiltration of GD2 CAR T cells that were delivered after CAR NK cell education into a subcutaneous xenograft containing neuroblastoma cells and MDSCs. In contrast to CAR T cells, which demonstrated an impaired infiltration in MDSC-containing tumors in the absence of CAR NK cell education, CAR NK cells homed into the tumor core, irrespective of the presence of MDSCs in the tumoral mass. GD2 CAR T cells were also able to limit tumor growth and increase survival in the presence of MDSCs in mice educated with CAR NK cells. Therefore, NKG2D CAR NK cells that did not directly target neuroblastoma cells due to their lack of NKG2D ligand contributed to limiting tumor growth by eliminating NKG2D+ MDSCs and increasing infiltration of neuroblastoma-targeting CAR T cells [261]. Therefore, this study demonstrated the synergism of combining CAR T and NK cell therapy for improved control of tumor progression.

3.3. NKT Cells, the Natural Hybrids of T and NK Cells at the Cutting Edge of CAR Therapies

The potential of combining T and NK adoptive cell transfer as immunotherapy might rely on the mechanisms of malignant cell recognition by T and NK cells. Whereas higher expression of MHC-I leads to stronger activation of T cells, the presence of MHC-I molecules inhibits NK cell targeting. Indeed, natural killer T cells (NKT cells) at the border of T and NK lymphocytes represent an immune population with mixed mechanisms for target cell recognition. NKT cells constitute a subgroup of T lymphocytes, which expresses some NK cell markers. Similar to T cells, NKT cells express a TCR, which is restricted to glycolipid antigens and not peptides. Glycolipid antigens are presented on CD1 molecules, which are MHC-like and expressed by hepatocytes, adipocytes and professional APCs that present microbial antigens to T lymphocytes [177,273].

NKT cells were shown to possess higher glycolytic capacity compared to T lymphocytes upon TCR engagement [177]. These so-called “innate-like T lymphocytes” are activated by T cell-like mechanisms via TCR engagement. In parallel, an active or inhibited state also depends on the engagement of the NK cell receptors expressed on NKT cells. Indeed, activation via TCR binding to glycolipids presented by CD1 was suggested to be interrupted by KIR ligation. Although NKT cells display the capacity to kill tumor cells in a CD1-dependent manner, the role of NKT cells in vivo has mainly been described as regulatory. The secretion of a repertory of cytokines by NKT cells positively or negatively contributes to T and NK cell generation and activation [273]. NKT cells with a morphology resembling NK cells because of their granularity and a low nucleus-to-cytoplasm ratio combine unique characteristics of T and NK cells. However, low numbers, anergy and the NKT cell switch from Th1- to an immunosuppressive Th2-like phenotype were observed in cancer patients. Therefore, injection of the activating glycosphingolipid α-galactosylceramide was attempted as immunotherapy. Likewise, adoptive cell transfer of autologous ex vivo activated NKT cells was studied in clinical trials. CAR NKT cells targeting different oncogenic malignancies were also tested in pre-clinical models [274]. These attempts did not result in high efficacy or preventing and reversing anergy, and maintenance of the Th1-like phenotype has therefore been suggested to boost NKT tumor killing [274]. These attempts

did not result in high efficacy; therefore, preventing and reversing anergy and maintenance of the Th1-like phenotype were suggested to boost the NKT tumor killing [273].

Additionally, CAR primary NKT cells were designed to target GD2 ganglioside-positive neuroblastoma cells. The intracellular CAR domain included the CD3ζ chain, CD28 and 4-1BB sequences. The GD2 CAR NKT cells were more persistent than unmodified NKT cells in a metastatic neuroblastoma xenograft model. In addition, serum levels of IFNγ and GM-CSF post-adoptive cell transfer were higher, indicating that the CAR design was effective in polarizing NKT cells into the Th1-phenotype. Furthermore, when adoptively and repeatedly transferred to immunodeficient mice with developing neuroblastoma metastasis, these CAR NKT cells not only delayed the metastatic growth but also significantly increased animal survival. Indeed, CAR NKT cells had the advantage to infiltrate neuroblastoma tissues and displayed no signs of GVHD, compared to CAR T cells [274]. In addition, NKT cells were shown to co-localize in tumors with TAMs. Indeed, NKT cells have the potential to target glycolipid-expressing TAMs via CD1 recognition. Therefore, CAR NKT cells are not only specific for tumor cells but can also shape the TME by making it less immunosuppressive. A more advanced version of this CAR was engineered to express IL15. These GD2.CD28.IL15 CAR NKT cells that target neuroblastoma indicated encouraging results in pre-clinical cancer models and were chosen for an initial clinical trial. In a pre-clinical setup, this design improved in vivo persistence and tumor infiltration, as well as limiting to a greater extent the tumor growth, compared to GD2 CAR NKT cells that do not express IL15 [275]. Furthermore, CD19 CAR NKT cells were also generated and tested in a B lymphoma mouse model. CAR design, including CD62L, was successful in generating CAR NKT cells that were able to control B cell lymphoma growth [176]. However, how we can metabolically interfere with this in order to increase the CAR NKT potency in vivo is currently unknown.

4. Conclusions

One of the major advantages of CAR NK over CAR T cells consists in the fact that NK cells can be used as an off-the-shelf product, while CAR T cells can only be used in an autologous setting in order to avoid GVHD. Currently, the generation of CAR T cells though is slow and very expensive. For this reason, universal CAR T cells using gene-editing technologies [270] are under development in order to allow their use in an allogeneic setting. However, in the TME, both NK cells and T cells encounter similar metabolic challenges but also distinct ones that impede their anti-cancer function. These similar or distinct general and metabolic features for both NK and T cells are listed in Table 1, in which we made a side-by-side comparison, including metabolic intervention strategies that are currently explored. Further identifying key cellular and molecular mechanisms that regulate NK and T cell metabolism will reveal new and exciting strategies to engineer innovative CAR NK and T cells in order to overcome the immunosuppressive TME and promote longevity and metabolic and functional fitness.

In summary, multiple strategies to improve the metabolic fitness of CAR T and CAR NK cells in the tumor environment are being explored. Moreover, the first results demonstrated that it might be useful to combine both cell types as described above to overcome the hurdles in the hostile tumors and TME. Even if improved off-the-shelf CAR-expressing T and NK cells reduced the costs of this cell-based immunotherapy, in the future, it would be of vital importance to generate metabolically fit CAR NK and T cells directly in vivo [265].

Table 1. Comparison between T and NK cell recognition mechanisms, metabolic features, approaches to improve effectivity of adoptive cell transfer, CAR designs boosting their metabolism and strategies to improve metabolic fitness of CAR-expressing cells.

Features	Active Effector T Cell	Active Effector NK Cell
Immune cell activation mechanisms	TCR engagement via recognition of peptides onto MHC-I in target cells [7]	No requirement of MHC-I on target cells, activation through stimulatory receptors [172]
Energetic metabolism	aerobic glycolysis and OXPHOS via the TCA cycle [7,20].	aerobic glycolysis and OXPHOS via the CMS [215]
Metabolic phenotype	glycolytic [7]	glycolytic [215]
Energetic sources	glucose and glutamine [20]	glucose [215]
Metabolic regulators	PI3K/Akt/mTORC1 pathway cMyc, HIF-1α, glutamine [7]	mTORC1 dependent on and independent of PI3K/Akt pathway cMyc, SREBP, glutamine [215]
Metabolism of memory (-like) phenotype	OXPHOS [34]	OXPHOS [215]
Metabolic approaches to enhance immune cell metabolism, effector functions and persistence upon adoptive cell transfer	In vivo inhibition of the lactate transporters MCT1 and MCT4 by diclofenac in a melanoma mouse model renders tumors sensible to PD1 blockade [102]	Pharmacological inhibition of SREBPs in a melanoma mouse model controls tumor burden [222]
	Glucose restriction for expansion of CD8 T+ cells prior to adoptive transfer into a lymphoma mouse model drives better tumor burden control [92]	Ex vivo pharmacological inhibition of fructose-1,6-biphosphatase in infiltrating NK cells from lung tumors in mice enhances glycolysis in vitro and in vivo tumor control upon adoptive cell transfer [229]
	In vitro and ex vivo administration of acetate in glucose-restricted CD8+ T cells and exhausted T cells, respectively, increases cytokine expression. Silencing of the acetyl-CoA synthetase controls better the tumor burden of a lymphoma mouse model [33]	
	Overexpression of PEP carboxykinase 1 [49] and PGC1α [42] in T cells transferred into melanoma-bearing mice lead to higher tumor cytotoxicity.	Pharmacological inhibition of GSK3 in NK cells from PB expanded with IL15 increases maturation and tumor cytotoxicity in mouse model of ovarian cancer [276]
	Oral bicarbonate in tumor-bearing mice controls tumor growth upon PD1 and/or CTL4 blockade and upon adoptive T cell transfer in melanoma-bearing mice [234]	
Advantages of adoptive CAR-expressing cell transfer as a therapy	Commercial approval of several CAR T cell therapies by the FDA [277] T cells are more suitable for bioengineering by classical viral vector transduction [257]	No need for cells of autologous origin [172] Less prone to GVHD [172]
CAR designs and metabolic fitness	4-1BB-containing CAR: OXPHOS metabolism [75] and longer in vivo persistence [72] CD28-containing CAR: glycolytic metabolism [75] and shorter in vivo persistence [72]	NKG2D-expressing CAR resistant to the immune and metabolic suppressor TGFβ drives MDSCs clearance and better tumor burden control of CAR T cells targeting neuroblastoma in mice [261].
	Hypoxia-inducible CAR expression for better tumor control in mouse models of ovarian cancer and neck and head cancer [120]	IL15-expressing CAR increases in vivo persistence and survival of a lymphoma mouse model [278]
Metabolic strategies to improve fitness of CAR-expressing cells in the TME	IL15 stimulation of CAR T cells reduces glycolysis, increases OXPHOS and FAO genes and leads to a stem cell memory phenotype, high proliferation, longer in vivo persistence, tumor burden control and survival of a lymphoma model [78]	Cytokine-induced memory-like (ML) NK cells modified with a CAR displayed better tumor burden control in lymphoma mouse models as compared to conventional CAR NK cells and ML NK cells [236]
	LDH depletion in prostate tumors improved cancer growth control by CAR T cells [98]	Genetic deletion of the IL15 immune checkpoint in IL15-expressing CAR NK cells increases mTOR and cMyc pathways, glycolytic rates and survival of a lymphoma model [264]
	$A_{2A}R$ deficiency in mouse and human CAR T cells improved tumor burden control in breast and ovarian cancer mouse models, respectively [123]	NK cell expansion with IL21-expressing feeder cells increases the expression of several metabolic genes, glucose uptake and promotes a less differentiated phenotype while enhancing tumor cytotoxicity in lymphoma mouse models [262]
	PD1 silencing and expression of IL12 in PD1 deficient CAR T cells increased survival of a lymphoma xenograft mouse model [142]	

Author Contributions: E.V., A.K., and A.M.-T. contributed to original draft preparation, including original figure construct, review and editing of the manuscript. All authors have read and agreed to the published version of the manuscript.

Funding: This work was supported by the "Fondation ARC pour la Recherche sur le Cancer" and "the Agence Nationale de la Recherche". We also acknowledge the support from the Canceropôle

PACA, Institut National du Cancer (INCA) and Conseil Régional PACA. A.K. received a scholarship from the French Ministry of Research. A.M.-T. received a scholarship from the META-CAN European network and the "Fondation pour la recherche médicale" (FRM).

Acknowledgments: We thank Ana Popovic and Manuel Grima Reyes for reviewing and editing the publication.

Conflicts of Interest: The authors have no conflict of interest to declare.

References

1. Shah, K.; Al-Haidari, A.; Sun, J.; Kazi, J.U. T cell receptor (TCR) signaling in health and disease. *Signal Transduct. Target. Ther.* **2021**, *6*, 412. [CrossRef] [PubMed]
2. Palmer, C.S.; Duette, G.A.; Wagner, M.C.E.; Henstridge, D.C.; Saleh, S.; Pereira, C.; Zhou, J.; Simar, D.; Lewin, S.R.; Ostrowski, M.; et al. Metabolically active CD4+ T cells expressing Glut1 and OX40 preferentially harbor HIV during in vitro infection. *FEBS Lett.* **2017**, *591*, 3319–3332. [CrossRef] [PubMed]
3. Palmer, C.S.; Ostrowski, M.; Gouillou, M.; Tsai, L.; Yu, D.; Zhou, J.; Henstridge, D.C.; Maisa, A.; Hearps, A.C.; Lewin, S.R.; et al. Increased glucose metabolic activity is associated with CD4+ T-cell activation and depletion during chronic HIV infection. *AIDS* **2014**, *28*, 297–309. [CrossRef]
4. Kang, S.; Tang, H. HIV-1 Infection and Glucose Metabolism Reprogramming of T Cells: Another Approach Toward Functional Cure and Reservoir Eradication. *Front. Immunol.* **2020**, *11*, 572677. [CrossRef] [PubMed]
5. Andrejeva, G.; Rathmell, J.C. Similarities and Distinctions of Cancer and Immune Metabolism in Inflammation and Tumors. *Cell Metab.* **2017**, *26*, 49–70. [CrossRef]
6. Ma, E.H.; Verway, M.J.; Johnson, R.M.; Roy, D.G.; Steadman, M.; Hayes, S.; Williams, K.S.; Sheldon, R.D.; Samborska, B.; Kosinski, P.A.; et al. Metabolic Profiling Using Stable Isotope Tracing Reveals Distinct Patterns of Glucose Utilization by Physiologically Activated CD8+ T Cells. *Immunity* **2019**, *51*, 856–870.e5. [CrossRef]
7. Menk, A.V.; Scharping, N.E.; Moreci, R.S.; Zeng, X.; Guy, C.; Salvatore, S.; Bae, H.; Xie, J.; Young, H.A.; Wendell, S.G.; et al. Early TCR Signaling Induces Rapid Aerobic Glycolysis Enabling Distinct Acute T Cell Effector Functions. *Cell Rep.* **2018**, *22*, 1509–1521. [CrossRef]
8. Pearce, E.L.; Pearce, E.J. Metabolic Pathways in Immune Cell Activation and Quiescence. *Immunity* **2013**, *38*, 633–643. [CrossRef]
9. Roy, S.; Rizvi, Z.A.; Awasthi, A. Metabolic Checkpoints in Differentiation of Helper T Cells in Tissue Inflammation. *Front. Immunol.* **2019**, *9*, 3036. [CrossRef]
10. Doedens, A.L.; Phan, A.T.; Stradner, M.H.; Fujimoto, J.K.; Nguyen, J.V.; Yang, E.; Johnson, R.S.; Goldrath, A.W. Hypoxia-inducible factors enhance the effector responses of $CD8^+$ T cells to persistent antigen. *Nat. Immunol.* **2013**, *14*, 1173–1182. [CrossRef]
11. Michalek, R.D.; Gerriets, V.A.; Jacobs, S.R.; Macintyre, A.N.; MacIver, N.J.; Mason, E.F.; Sullivan, S.A.; Nichols, A.G.; Rathmell, J.C. Cutting Edge: Distinct Glycolytic and Lipid Oxidative Metabolic Programs Are Essential for Effector and Regulatory CD4+ T Cell Subsets. *J. Immunol.* **2011**, *186*, 3299–3303. [CrossRef]
12. Carr, E.L.; Kelman, A.; Wu, G.S.; Gopaul, R.; Senkevitch, E.; Aghvanyan, A.; Turay, A.M.; Frauwirth, K.A. Glutamine Uptake and Metabolism Are Coordinately Regulated by ERK/MAPK during T Lymphocyte Activation. *J. Immunol.* **2010**, *185*, 1037–1044. [CrossRef]
13. Nakaya, M.; Xiao, Y.; Zhou, X.; Chang, J.-H.; Chang, M.; Cheng, X.; Blonska, M.; Lin, X.; Sun, S.-C. Inflammatory T Cell Responses Rely on Amino Acid Transporter ASCT2 Facilitation of Glutamine Uptake and mTORC1 Kinase Activation. *Immunity* **2014**, *40*, 692–705. [CrossRef]
14. Sinclair, L.V.; Rolf, J.; Emslie, E.; Shi, Y.-B.; Taylor, P.M.; Cantrell, D.A. Control of amino-acid transport by antigen receptors coordinates the metabolic reprogramming essential for T cell differentiation. *Nat. Immunol.* **2013**, *14*, 500–508. [CrossRef]
15. Boomer, J.S.; Green, J.M. An Enigmatic Tail of CD28 Signaling. *Cold Spring Harb. Perspect. Biol.* **2010**, *2*, a002436. [CrossRef]
16. Wang, R.; Dillon, C.P.; Shi, L.Z.; Milasta, S.; Carter, R.; Finkelstein, D.; McCormick, L.L.; Fitzgerald, P.; Chi, H.; Munger, J.; et al. The Transcription Factor Myc Controls Metabolic Reprogramming upon T Lymphocyte Activation. *Immunity* **2011**, *35*, 871–882. [CrossRef]
17. Frauwirth, K.A.; Riley, J.L.; Harris, M.H.; Parry, R.V.; Rathmell, J.C.; Plas, D.R.; Elstrom, R.L.; June, C.; Thompson, C.B. The CD28 Signaling Pathway Regulates Glucose Metabolism. *Immunity* **2002**, *16*, 769–777. [CrossRef]
18. West, E.E.; Kolev, M.; Kemper, C. Complement and the Regulation of T Cell Responses. *Annu. Rev. Immunol.* **2018**, *36*, 309–338. [CrossRef] [PubMed]
19. Wieman, H.L.; Wofford, J.A.; Rathmell, J.C. Cytokine Stimulation Promotes Glucose Uptake via Phosphatidylinositol-3 Kinase/Akt Regulation of Glut1 Activity and Trafficking. *Mol. Biol. Cell* **2007**, *18*, 1437–1446. [CrossRef] [PubMed]
20. Fox, C.J.; Hammerman, P.S.; Thompson, C.B. Fuel feeds function: Energy metabolism and the T-cell response. *Nat. Rev. Immunol.* **2005**, *5*, 844–852. [CrossRef] [PubMed]
21. Wofford, J.A.; Wieman, H.L.; Jacobs, S.R.; Zhao, Y.; Rathmell, J.C. IL-7 promotes Glut1 trafficking and glucose uptake via STAT5-mediated activation of Akt to support T-cell survival. *Blood* **2008**, *111*, 2101–2111. [CrossRef]

22. Macintyre, A.N.; Gerriets, V.A.; Nichols, A.G.; Michalek, R.D.; Rudolph, M.C.; DeOliveira, D.; Anderson, S.M.; Abel, E.D.; Chen, B.J.; Hale, L.P.; et al. The Glucose Transporter Glut1 Is Selectively Essential for CD4 T Cell Activation and Effector Function. *Cell Metab.* **2014**, *20*, 61–72. [CrossRef] [PubMed]
23. Jacobs, S.R.; Herman, C.E.; MacIver, N.J.; Wofford, J.A.; Wieman, H.L.; Hammen, J.J.; Rathmell, J.C. Glucose Uptake Is Limiting in T Cell Activation and Requires CD28-Mediated Akt-Dependent and Independent Pathways. *J. Immunol.* **2008**, *180*, 4476–4486. [CrossRef]
24. Murray, C.M.; Hutchinson, R.; Bantick, J.R.; Belfield, G.P.; Benjamin, A.D.; Brazma, D.; Bundick, R.V.; Cook, I.D.; Craggs, R.I.; Edwards, S.; et al. Monocarboxylate transporter MCT1 is a target for immunosuppression. *Nat. Chem. Biol.* **2005**, *1*, 371–376. [CrossRef] [PubMed]
25. Ryuge, A.; Kosugi, T.; Maeda, K.; Banno, R.; Gou, Y.; Zaitsu, K.; Ito, T.; Sato, Y.; Hirayama, A.; Tsubota, S.; et al. Basigin deficiency prevents anaplerosis and ameliorates insulin resistance and hepatosteatosis. *JCI Insight* **2021**, *6*. [CrossRef] [PubMed]
26. Chang, C.-H.; Curtis, J.D.; Maggi, L.B.; Faubert, B.; Villarino, A.V.; O'Sullivan, D.; Huang, S.C.-C.; van der Windt, G.J.W.; Blagih, J.; Qiu, J.; et al. Posttranscriptional Control of T Cell Effector Function by Aerobic Glycolysis. *Cell* **2013**, *153*, 1239–1251. [CrossRef]
27. Blagih, J.; Coulombe, F.; Vincent, E.E.; Dupuy, F.; Galicia-Vazquez, G.; Yurchenko, E.; Raissi, T.C.; van der Windt, G.J.; Viollet, B.; Pearce, E.L.; et al. The Energy Sensor AMPK Regulates T Cell Metabolic Adaptation and Effector Responses in vivo. *Immunity* **2015**, *42*, 41–54. [CrossRef] [PubMed]
28. Buck, M.D.; O'Sullivan, D.; Geltink, R.I.K.; Curtis, J.D.; Chang, C.-H.; Sanin, D.E.; Qiu, J.; Kretz, O.; Braas, D.; Van Der Windt, G.J.; et al. Mitochondrial Dynamics Controls T Cell Fate through Metabolic Programming. *Cell* **2016**, *166*, 63–76. [CrossRef]
29. Sena, L.A.; Li, S.; Jairaman, A.; Prakriya, M.; Ezponda, T.; Hildeman, D.A.; Wang, C.-R.; Schumacker, P.T.; Licht, J.D.; Perlman, H.; et al. Mitochondria Are Required for Antigen-Specific T Cell Activation through Reactive Oxygen Species Signaling. *Immunity* **2013**, *38*, 225–236. [CrossRef]
30. Bailis, W.; Shyer, J.A.; Zhao, J.; García-Cañaveras, J.C.; Al Khazal, F.J.; Qu, R.; Steach, H.R.; Bielecki, P.; Khan, O.; Jackson, R.; et al. Distinct modes of mitochondrial metabolism uncouple T cell differentiation and function. *Nature* **2019**, *571*, 403–407. [CrossRef]
31. Ansó, E.; Weinberg, S.E.; Diebold, L.P.; Thompson, B.J.; Malinge, S.; Schumacker, P.T.; Liu, X.; Zhang, Y.; Shao, Z.; Steadman, M.; et al. The mitochondrial respiratory chain is essential for haematopoietic stem cell function. *Nat. Cell Biol.* **2017**, *19*, 614–625. [CrossRef]
32. Balmer, M.L.; Ma, E.H.; Bantug, G.R.; Grählert, J.; Pfister, S.; Glatter, T.; Jauch, A.; Dimeloe, S.; Slack, E.; Dehio, P.; et al. Memory CD8 + T Cells Require Increased Concentrations of Acetate Induced by Stress for Optimal Function. *Immunity* **2016**, *44*, 1312–1324. [CrossRef] [PubMed]
33. Qiu, J.; Villa, M.; Sanin, D.E.; Buck, M.D.; O'Sullivan, D.; Ching, R.; Matsushita, M.; Grzes, K.M.; Winkler, F.; Chang, C.-H.; et al. Acetate Promotes T Cell Effector Function during Glucose Restriction. *Cell Rep.* **2019**, *27*, 2063–2074.e5. [CrossRef] [PubMed]
34. Van Der Windt, G.J.W.; Everts, B.; Chang, C.-H.; Curtis, J.D.; Freitas, T.C.; Amiel, E.; Pearce, E.J.; Pearce, E.L. Mitochondrial Respiratory Capacity Is a Critical Regulator of CD8+ T Cell Memory Development. *Immunity* **2012**, *36*, 68–78. [CrossRef] [PubMed]
35. Gubser, P.M.; Bantug, G.R.; Razik, L.; Fischer, M.; Dimeloe, S.; Hoenger, G.; Müller-Durovic, B.; Jauch, A.; Hess, C. Rapid effector function of memory CD8+ T cells requires an immediate-early glycolytic switch. *Nat. Immunol.* **2013**, *14*, 1064–1072. [CrossRef] [PubMed]
36. Van der Windt, G.J.W.; O'Sullivan, D.; Everts, B.; Huang, S.C.-C.; Buck, M.D.; Curtis, J.D.; Chang, C.-H.; Smith, A.M.; Ai, T.; Faubert, B.; et al. CD8 memory T cells have a bioenergetic advantage that underlies their rapid recall ability. *Proc. Natl. Acad. Sci. USA* **2013**, *110*, 14336–14341. [CrossRef] [PubMed]
37. Maude, S.L.; Laetsch, T.W.; Buechner, J.; Rives, S.; Boyer, M.; Bittencourt, H.; Bader, P.; Verneris, M.R.; Stefanski, H.E.; Myers, G.D.; et al. Tisagenlecleucel in Children and Young Adults with B-Cell Lymphoblastic Leukemia. *N. Engl. J. Med.* **2018**, *378*, 439–448. [CrossRef] [PubMed]
38. Neelapu, S.S.; Locke, F.L.; Bartlett, N.L.; Lekakis, L.J.; Miklos, D.B.; Jacobson, C.A.; Braunschweig, I.; Oluwole, O.O.; Siddiqi, T.; Lin, Y.; et al. Axicabtagene Ciloleucel CAR T-Cell Therapy in Refractory Large B-Cell Lymphoma. *N. Engl. J. Med.* **2017**, *377*, 2531–2544. [CrossRef]
39. Park, J.H.; Rivière, I.; Gonen, M.; Wang, X.; Sénéchal, B.; Curran, K.J.; Sauter, C.; Wang, Y.; Santomasso, B.; Mead, E.; et al. Long-Term Follow-up of CD19 CAR Therapy in Acute Lymphoblastic Leukemia. *N. Engl. J. Med.* **2018**, *378*, 449–459. [CrossRef]
40. Turtle, C.J.; Hay, K.A.; Hanafi, L.-A.; Li, D.; Cherian, S.; Chen, X.; Wood, B.; Lozanski, A.; Byrd, J.C.; Heimfeld, S.; et al. Durable Molecular Remissions in Chronic Lymphocytic Leukemia Treated With CD19-Specific Chimeric Antigen Receptor–Modified T Cells After Failure of Ibrutinib. *J. Clin. Oncol.* **2017**, *35*, 3010–3020. [CrossRef]
41. Chamoto, K.; Chowdhury, P.S.; Kumar, A.; Sonomura, K.; Matsuda, F.; Fagarasan, S.; Honjo, T. Mitochondrial activation chemicals synergize with surface receptor PD-1 blockade for T cell-dependent antitumor activity. *Proc. Natl. Acad. Sci. USA* **2017**, *114*, E761–E770. [CrossRef]
42. Scharping, N.E.; Menk, A.V.; Moreci, R.S.; Whetstone, R.D.; Dadey, R.E.; Watkins, S.C.; Ferris, R.L.; Delgoffe, G.M. The Tumor Microenvironment Represses T Cell Mitochondrial Biogenesis to Drive Intratumoral T Cell Metabolic Insufficiency and Dysfunction. *Immunity* **2016**, *45*, 701–703. [CrossRef] [PubMed]

43. Siska, P.J.; Beckermann, K.E.; Mason, F.M.; Andrejeva, G.; Greenplate, A.R.; Sendor, A.B.; Chiang, Y.-C.J.; Corona, A.L.; Gemta, L.F.; Vincent, B.G.; et al. Mitochondrial dysregulation and glycolytic insufficiency functionally impair CD8 T cells infiltrating human renal cell carcinoma. *JCI Insight* **2017**, *2*. [CrossRef] [PubMed]
44. DeBerardinis, R.J.; Chandel, N.S. We need to talk about the Warburg effect. *Nat. Metab.* **2020**, *2*, 127–129. [CrossRef] [PubMed]
45. Fantin, V.R.; St-Pierre, J.; Leder, P. Attenuation of LDH-A expression uncovers a link between glycolysis, mitochondrial physiology, and tumor maintenance. *Cancer Cell* **2006**, *9*, 425–434. [CrossRef] [PubMed]
46. Koppenol, W.H.; Bounds, P.L.; Dang, C.V. Otto Warburg's contributions to current concepts of cancer metabolism. *Nat. Rev. Cancer* **2011**, *11*, 325–337. [CrossRef]
47. Patra, K.C.; Wang, Q.; Bhaskar, P.T.; Miller, L.; Wang, Z.; Wheaton, W.; Chandel, N.; Laakso, M.; Muller, W.J.; Allen, E.L.; et al. Hexokinase 2 Is Required for Tumor Initiation and Maintenance and Its Systemic Deletion Is Therapeutic in Mouse Models of Cancer. *Cancer Cell* **2013**, *24*, 213–228. [CrossRef] [PubMed]
48. Warburg, O.; Wind, F.; Negelein, E. The metabolism of tumors in the body. *J. Gen. Physiol.* **1927**, *8*, 519–530. [CrossRef]
49. Ho, P.-C.; Bihuniak, J.D.; Macintyre, A.N.; Staron, M.; Liu, X.; Amezquita, R.; Tsui, Y.-C.; Cui, G.; Micevic, G.; Perales, J.C.; et al. Phosphoenolpyruvate Is a Metabolic Checkpoint of Anti-tumor T Cell Responses. *Cell* **2015**, *162*, 1217–1228. [CrossRef] [PubMed]
50. Choi, S.Y.C.; Collins, C.C.; Gout, P.W.; Wang, Y. Cancer-generated lactic acid: A regulatory, immunosuppressive metabolite? *J. Pathol.* **2013**, *230*, 350–355. [CrossRef]
51. Helmlinger, G.; Sckell, A.; Dellian, M.; Forbes, N.S.; Jain, R.K. Acid production in glycolysis-impaired tumors provides new insights into tumor metabolism. *Clin. Cancer Res.* **2002**, *8*, 1284–1291.
52. Kato, Y.; Ozawa, S.; Miyamoto, C.; Maehata, Y.; Suzuki, A.; Maeda, T.; Baba, Y. Acidic extracellular microenvironment and cancer. *Cancer Cell Int.* **2013**, *13*, 89. [CrossRef]
53. Brand, A.; Singer, K.; Koehl, G.E.; Kolitzus, M.; Schoenhammer, G.; Thiel, A.; Matos, C.; Bruss, C.; Klobuch, S.; Peter, K.; et al. LDHA-Associated Lactic Acid Production Blunts Tumor Immunosurveillance by T and NK Cells. *Cell Metab.* **2016**, *24*, 657–671. [CrossRef]
54. Cham, C.M.; Driessens, G.; O'Keefe, J.P.; Gajewski, T.F. Glucose deprivation inhibits multiple key gene expression events and effector functions in CD8+ T cells. *Eur. J. Immunol.* **2008**, *38*, 2438–2450. [CrossRef]
55. McNamee, E.N.; Johnson, D.K.; Homann, D.; Clambey, E.T. Hypoxia and hypoxia-inducible factors as regulators of T cell development, differentiation, and function. *Immunol. Res.* **2012**, *55*, 58–70. [CrossRef] [PubMed]
56. Chemnitz, J.M.; Parry, R.V.; Nichols, K.E.; June, C.H.; Riley, J.L. SHP-1 and SHP-2 Associate with Immunoreceptor Tyrosine-Based Switch Motif of Programmed Death 1 upon Primary Human T Cell Stimulation, but Only Receptor Ligation Prevents T Cell Activation. *J. Immunol.* **2004**, *173*, 945–954. [CrossRef] [PubMed]
57. Staron, M.M.; Gray, S.M.; Marshall, H.D.; Parish, I.A.; Chen, J.H.; Perry, C.J.; Cui, G.; Li, M.O.; Kaech, S.M. The Transcription Factor FoxO1 Sustains Expression of the Inhibitory Receptor PD-1 and Survival of Antiviral CD8+ T Cells during Chronic Infection. *Immunity* **2014**, *41*, 802–814. [CrossRef] [PubMed]
58. Teft, W.A.; Chau, T.A.; Madrenas, J. Structure-Function analysis of the CTLA-4 interaction with PP2A. *BMC Immunol.* **2009**, *10*, 23. [CrossRef]
59. Wlodarchak, N.; Xing, Y. PP2A as a master regulator of the cell cycle. *Crit. Rev. Biochem. Mol. Biol.* **2016**, *51*, 162–184. [CrossRef] [PubMed]
60. Zhang, S.Q.; Tsiaras, W.G.; Araki, T.; Wen, G.; Minichiello, L.; Klein, R.; Neel, B.G. Receptor-Specific Regulation of Phosphatidylinositol 3′-Kinase Activation by the Protein Tyrosine Phosphatase Shp2. *Mol. Cell. Biol.* **2002**, *22*, 4062–4072. [CrossRef]
61. Chang, C.-H.; Qiu, J.; O'Sullivan, D.; Buck, M.D.; Noguchi, T.; Curtis, J.D.; Chen, Q.; Gindin, M.; Gubin, M.M.; Van Der Windt, G.J.W.; et al. Metabolic Competition in the Tumor Microenvironment Is a Driver of Cancer Progression. *Cell* **2015**, *162*, 1229–1241. [CrossRef] [PubMed]
62. Lee, J.; Su, E.W.; Zhu, C.; Hainline, S.; Phuah, J.; Moroco, J.A.; Smithgall, T.E.; Kuchroo, V.K.; Kane, L.P. Phosphotyrosine-Dependent Coupling of Tim-3 to T-Cell Receptor Signaling Pathways. *Mol. Cell. Biol.* **2011**, *31*, 3963–3974. [CrossRef] [PubMed]
63. Platten, M.; Wick, W.; Van den Eynde, B.J. Tryptophan Catabolism in Cancer: Beyond IDO and Tryptophan Depletion. *Cancer Res.* **2012**, *72*, 5435–5440. [CrossRef]
64. Mastelic-Gavillet, B.; Rodrigo, B.N.; Décombaz, L.; Wang, H.; Ercolano, G.; Ahmed, R.; Lozano, L.E.; Ianaro, A.; Derré, L.; Valerio, M.; et al. Adenosine mediates functional and metabolic suppression of peripheral and tumor-infiltrating CD8+ T cells. *J. Immunother. Cancer* **2019**, *7*, 257. [CrossRef]
65. Fultang, L.; Booth, S.; Yogev, O.; da Costa, B.M.; Tubb, V.; Panetti, S.; Stavrou, V.; Scarpa, U.; Jankevics, A.; Lloyd, G.; et al. Metabolic engineering against the arginine microenvironment enhances CAR-T cell proliferation and therapeutic activity. *Blood* **2020**, *136*, 1155–1160. [CrossRef]
66. Lind, D.S. Arginine and Cancer. *J. Nutr.* **2004**, *134*, 2837S–2841S. [CrossRef]
67. Munder, M. Arginase: An emerging key player in the mammalian immune system. *Mov. Disord.* **2009**, *158*, 638–651. [CrossRef] [PubMed]
68. Das, R.K.; O'Connor, R.S.; Grupp, S.A.; Barrett, D.M. Lingering effects of chemotherapy on mature T cells impair proliferation. *Blood Adv.* **2020**, *4*, 4653–4664. [CrossRef]
69. Philipson, B.I.; O'Connor, R.S.; May, M.J.; June, C.H.; Albelda, S.M.; Milone, M.C. 4-1BB costimulation promotes CAR T cell survival through noncanonical NF-κB signaling. *Sci. Signal.* **2020**, *13*. [CrossRef]

70. Brentjens, R.J.; Davila, M.L.; Riviere, I.; Park, J.; Wang, X.; Cowell, L.G.; Bartido, S.; Stefanski, J.; Taylor, C.; Olszewska, M.; et al. CD19-Targeted T Cells Rapidly Induce Molecular Remissions in Adults with Chemotherapy-Refractory Acute Lymphoblastic Leukemia. *Sci. Transl. Med.* **2013**, *5*, 177ra38. [CrossRef]
71. Lee, D.W.; Kochenderfer, J.N.; Stetler-Stevenson, M.; Cui, Y.K.; Delbrook, C.; Feldman, S.A.; Fry, T.J.; Orentas, R.; Sabatino, M.; Shah, N.N.; et al. T cells expressing CD19 chimeric antigen receptors for acute lymphoblastic leukaemia in children and young adults: A phase 1 dose-escalation trial. *Lancet* **2015**, *385*, 517–528. [CrossRef]
72. Long, A.H.; Haso, W.M.; Shern, J.F.; Wanhainen, K.M.; Murgai, M.; Ingaramo, M.; Smith, J.P.; Walker, A.J.; Kohler, M.E.; Venkateshwara, V.R.; et al. 4-1BB costimulation ameliorates T cell exhaustion induced by tonic signaling of chimeric antigen receptors. *Nat. Med.* **2015**, *21*, 581–590. [CrossRef]
73. Porter, D.L.; Hwang, W.-T.; Frey, N.V.; Lacey, S.F.; Shaw, P.A.; Loren, A.W.; Bagg, A.; Marcucci, K.T.; Shen, A.; Gonzalez, V.; et al. Chimeric antigen receptor T cells persist and induce sustained remissions in relapsed refractory chronic lymphocytic leukemia. *Sci. Transl. Med.* **2015**, *7*, 303ra139. [CrossRef]
74. Choi, B.K.; Lee, D.Y.; Lee, D.G.; Kim, Y.H.; Kim, S.-H.; Oh, H.S.; Han, C.; Kwon, B.S. 4-1BB signaling activates glucose and fatty acid metabolism to enhance CD8+ T cell proliferation. *Cell. Mol. Immunol.* **2016**, *14*, 748–757. [CrossRef]
75. Kawalekar, O.U.; O'Connor, R.S.; Fraietta, J.A.; Guo, L.; Mcgettigan, S.E.; Posey, A.D.; Patel, P.R.; Guedan, S.; Scholler, J.; Keith, B.; et al. Distinct Signaling of Coreceptors Regulates Specific Metabolism Pathways and Impacts Memory Development in CAR T Cells. *Immunity* **2016**, *44*, 380–390. [CrossRef]
76. Zeng, H.; Cohen, S.; Guy, C.; Shrestha, S.; Neale, G.; Brown, S.A.; Cloer, C.; Kishton, R.J.; Gao, X.; Youngblood, B.; et al. mTORC1 and mTORC2 Kinase Signaling and Glucose Metabolism Drive Follicular Helper T Cell Differentiation. *Immunity* **2016**, *45*, 540–554. [CrossRef]
77. Petersen, C.T.; Krenciute, G. Next Generation CAR T Cells for the Immunotherapy of High-Grade Glioma. *Front. Oncol.* **2019**, *9*, 69. [CrossRef] [PubMed]
78. Alizadeh, D.; Wong, R.A.; Yang, X.; Wang, D.; Pecoraro, J.R.; Kuo, C.-F.; Aguilar, B.; Qi, Y.; Ann, D.K.; Starr, R.; et al. IL15 Enhances CAR-T Cell Antitumor Activity by Reducing mTORC1 Activity and Preserving Their Stem Cell Memory Phenotype. *Cancer Immunol. Res.* **2019**, *7*, 759–772. [CrossRef]
79. Kagoya, Y.; Tanaka, S.; Guo, T.; Anczurowski, M.; Wang, C.-H.; Saso, K.; Butler, M.O.; Minden, M.D.; Hirano, N. A novel chimeric antigen receptor containing a JAK–STAT signaling domain mediates superior antitumor effects. *Nat. Med.* **2018**, *24*, 352–359. [CrossRef] [PubMed]
80. Sukumar, M.; Liu, J.; Ji, Y.; Subramanian, M.; Crompton, J.G.; Yu, Z.; Roychoudhuri, R.; Palmer, D.C.; Muranski, P.; Karoly, E.D.; et al. Inhibiting glycolytic metabolism enhances CD8+ T cell memory and antitumor function. *J. Clin. Investig.* **2013**, *123*, 4479–4488. [CrossRef] [PubMed]
81. Ghassemi, S.; Martinez-Becerra, F.J.; Master, A.M.; Richman, S.A.; Heo, D.; Leferovich, J.; Tu, Y.; García-Cañaveras, J.C.; Ayari, A.; Lu, Y.; et al. Enhancing Chimeric Antigen Receptor T Cell Anti-tumor Function through Advanced Media Design. *Mol. Ther. Methods Clin. Dev.* **2020**, *18*, 595–606. [CrossRef] [PubMed]
82. Preston, G.C.; Sinclair, L.V.; Kaskar, A.; Hukelmann, J.L.; Navarro, M.N.; Ferrero, I.; Macdonald, H.R.; Cowling, V.H.; Cantrell, D.A. Single cell tuning of Myc expression by antigen receptor signal strength and interleukin-2 in T lymphocytes. *EMBO J.* **2015**, *34*, 2008–2024. [CrossRef] [PubMed]
83. Agarwal, S.; Weidner, T.; Thalheimer, F.B.; Buchholz, C.J. In vivo generated human CAR T cells eradicate tumor cells. *OncoImmunology* **2019**, *8*, e1671761. [CrossRef]
84. Frank, A.M.; Braun, A.H.; Scheib, L.; Agarwal, S.; Schneider, I.C.; Fusil, F.; Perian, S.; Sahin, U.; Thalheimer, F.B.; Verhoeyen, E.; et al. Combining T-cell-specific activation and in vivo gene delivery through CD3-targeted lentiviral vectors. *Blood Adv.* **2020**, *4*, 5702–5715.
85. Mhaidly, R.; Verhoeyen, E. Humanized Mice Are Precious Tools for Preclinical Evaluation of CAR T and CAR NK Cell Therapies. *Cancers* **2020**, *12*, 1915. [CrossRef] [PubMed]
86. Pfeiffer, A.; Thalheimer, F.B.; Hartmann, S.; Frank, A.M.; Bender, R.R.; Danisch, S.; Costa, C.; Wels, W.S.; Modlich, U.; Stripecke, R.; et al. In vivo generation of human CD 19- CAR T cells results in B-cell depletion and signs of cytokine release syndrome. *EMBO Mol. Med.* **2018**, *10*, e9158. [CrossRef] [PubMed]
87. Weidner, T.; Agarwal, S.; Perian, S.; Fusil, F.; Braun, G.; Hartmann, J.; Verhoeyen, E.; Buchholz, C.J. Genetic in vivo engineering of human T lymphocytes in mouse models. *Nat. Protoc.* **2021**, *16*, 3210–3240. [CrossRef]
88. Weber, E.W.; Parker, K.R.; Sotillo, E.; Lynn, R.C.; Anbunathan, H.; Lattin, J.; Good, Z.; Belk, J.A.; Daniel, B.; Klysz, D.; et al. Transient rest restores functionality in exhausted CAR-T cells through epigenetic remodeling. *Science* **2021**, *372*. [CrossRef]
89. Finlay, D.K.; Rosenzweig, E.; Sinclair, L.V.; Carmen, F.C.; Hukelmann, J.L.; Rolf, J.; Panteleyev, A.A.; Okkenhaug, K.; Cantrell, D.A. PDK1 regulation of mTOR and hypoxia-inducible factor 1 integrate metabolism and migration of CD8+ T cells. *J. Exp. Med.* **2012**, *209*, 2441–2453. [CrossRef]
90. Kedia-Mehta, N.; Finlay, D.K. Competition for nutrients and its role in controlling immune responses. *Nat. Commun.* **2019**, *10*, 2123. [CrossRef]
91. Greiner, E.F.; Guppy, M.; Brand, K. Glucose is essential for proliferation and the glycolytic enzyme induction that provokes a transition to glycolytic energy production. *J. Biol. Chem.* **1994**, *269*, 31484–31490. [CrossRef]

92. Geltink, R.I.K.; Edwards-Hicks, J.; Apostolova, P.; O'Sullivan, D.; Sanin, D.E.; Patterson, A.E.; Puleston, D.J.; Ligthart, N.A.M.; Buescher, J.M.; Grzes, K.M.; et al. Metabolic conditioning of CD8+ effector T cells for adoptive cell therapy. *Nat. Metab.* **2020**, *2*, 703–716. [CrossRef] [PubMed]
93. Díaz, F.E.; Dantas, E.; Geffner, J. Unravelling the Interplay between Extracellular Acidosis and Immune Cells. *Mediat. Inflamm.* **2018**, *2018*, 1218297. [CrossRef]
94. Angelin, A.; Gil-De-Gómez, L.; Dahiya, S.; Jiao, J.; Guo, L.; Levine, M.H.; Wang, Z.; Quinn, W.J., II; Kopinski, P.K.; Wang, L.; et al. Foxp3 Reprograms T Cell Metabolism to Function in Low-Glucose, High-Lactate Environments. *Cell Metab.* **2017**, *25*, 1282–1293.e7. [CrossRef]
95. Colegio, O.R.; Chu, N.-Q.; Szabo, A.L.; Chu, T.; Rhebergen, A.M.; Jairam, V.; Cyrus, N.; Brokowski, C.E.; Eisenbarth, S.C.; Phillips, G.M.; et al. Functional polarization of tumour-associated macrophages by tumour-derived lactic acid. *Nature* **2014**, *513*, 559–563. [CrossRef]
96. Haas, R.; Smith, J.; Rocher-Ros, V.; Nadkarni, S.; Montero-Melendez, T.; D'Acquisto, F.; Bland, E.J.; Bombardieri, M.; Pitzalis, C.; Perretti, M.; et al. Lactate Regulates Metabolic and Pro-inflammatory Circuits in Control of T Cell Migration and Effector Functions. *PLoS Biol.* **2015**, *13*, e1002202. [CrossRef]
97. Hermans, D.; Gautam, S.; García-Cañaveras, J.C.; Gromer, D.; Mitra, S.; Spolski, R.; Li, P.; Christensen, S.; Nguyen, R.; Lin, J.-X.; et al. Lactate dehydrogenase inhibition synergizes with IL-21 to promote CD8+T cell stemness and antitumor immunity. *Proc. Natl. Acad. Sci. USA* **2020**, *117*, 6047–6055. [CrossRef]
98. Mane, M.M.; Cohen, I.J.; Ackerstaff, E.; Shalaby, K.; Ijoma, J.N.; Ko, M.; Maeda, M.; Albeg, A.S.; Vemuri, K.; Satagopan, J.; et al. Lactate Dehydrogenase A Depletion Alters MyC-CaP Tumor Metabolism, Microenvironment, and CAR T Cell Therapy. *Mol. Ther. Oncolytics* **2020**, *18*, 382–395. [CrossRef]
99. Comito, G.; Iscaro, A.; Bacci, M.; Morandi, A.; Ippolito, L.; Parri, M.; Montagnani, I.; Raspollini, M.R.; Serni, S.; Simeoni, L.; et al. Lactate modulates CD4+ T-cell polarization and induces an immunosuppressive environment, which sustains prostate carcinoma progression via TLR8/miR21 axis. *Oncogene* **2019**, *38*, 3681–3695. [CrossRef]
100. Fischer, K.; Hoffmann, P.; Voelkl, S.; Meidenbauer, N.; Ammer, J.; Edinger, M.; Gottfried, E.; Schwarz, S.; Rothe, G.; Hoves, S.; et al. Inhibitory effect of tumor cell–derived lactic acid on human T cells. *Blood* **2007**, *109*, 3812–3819. [CrossRef]
101. Ping, W.; Senyan, H.; Li, G.; Yan, C.; Long, L. Increased Lactate in Gastric Cancer Tumor-Infiltrating Lymphocytes Is Related to Impaired T Cell Function Due to miR-34a Deregulated Lactate Dehydrogenase A. *Cell. Physiol. Biochem.* **2018**, *49*, 828–836. [CrossRef] [PubMed]
102. Renner, K.; Bruss, C.; Schnell, A.; Koehl, G.; Becker, H.M.; Fante, M.; Menevse, A.-N.; Kauer, N.; Blazquez, R.; Hacker, L.; et al. Restricting Glycolysis Preserves T Cell Effector Functions and Augments Checkpoint Therapy. *Cell Rep.* **2019**, *29*, 135–150.e9. [CrossRef]
103. Newsholme, E.A.; Crabtree, B.; Ardawi, M.S.M. Glutamine metabolism in lymphocytes: Its biochemical, physiological and clinical importance. *Q. J. Exp. Physiol.* **1985**, *70*, 473–489. [CrossRef] [PubMed]
104. Wang, Q.; Hardie, R.A.; Hoy, A.J.; Van Geldermalsen, M.; Gao, D.; Fazli, L.; Sadowski, M.C.; Balaban, S.; Schreuder, M.; Nagarajah, R.; et al. Targeting ASCT2 -mediated glutamine uptake blocks prostate cancer growth and tumour development. *J. Pathol.* **2015**, *236*, 278–289. [CrossRef] [PubMed]
105. Hammami, I.; Chen, J.; Bronte, V.; DeCrescenzo, G.; Jolicoeur, M. l-glutamine is a key parameter in the immunosuppression phenomenon. *Biochem. Biophys. Res. Commun.* **2012**, *425*, 724–729. [CrossRef] [PubMed]
106. Leone, R.D.; Zhao, L.; Englert, J.M.; Sun, I.-M.; Oh, M.-H.; Arwood, M.L.; Bettencourt, I.A.; Patel, C.H.; Wen, J.; Tam, A.; et al. Glutamine blockade induces divergent metabolic programs to overcome tumor immune evasion. *Science* **2019**, *366*, 1013–1021. [CrossRef]
107. Nabe, S.; Yamada, T.; Suzuki, J.; Toriyama, K.; Yasuoka, T.; Kuwahara, M.; Shiraishi, A.; Takenaka, K.; Yasukawa, M.; Yamashita, M. Reinforce the antitumor activity of CD 8 + T cells via glutamine restriction. *Cancer Sci.* **2018**, *109*, 3737–3750. [CrossRef]
108. Liu, M.; Wang, X.; Wang, L.; Ma, X.; Gong, Z.; Zhang, S.; Li, Y. Targeting the IDO1 pathway in cancer: From bench to bedside. *J. Hematol. Oncol.* **2018**, *11*, 100. [CrossRef]
109. Wainwright, D.A.; Balyasnikova, I.V.; Chang, A.L.; Ahmed, A.U.; Moon, K.-S.; Auffinger, B.; Tobias, A.L.; Han, Y.; Lesniak, M.S. IDO Expression in Brain Tumors Increases the Recruitment of Regulatory T Cells and Negatively Impacts Survival. *Clin. Cancer Res.* **2012**, *18*, 6110–6121. [CrossRef]
110. Munn, D.H.; Mellor, A.L. Indoleamine 2,3 dioxygenase and metabolic control of immune responses. *Trends Immunol.* **2012**, *34*, 137–143. [CrossRef]
111. Prendergast, G.C.; Malachowski, W.J.; Mondal, A.; Scherle, P.; Muller, A.J. Indoleamine 2,3-Dioxygenase and Its Therapeutic Inhibition in Cancer. *Int. Rev. Cell Mol. Biol.* **2018**, *336*, 175–203. [CrossRef]
112. Geiger, R.; Rieckmann, J.C.; Wolf, T.; Basso, C.; Feng, Y.; Fuhrer, T.; Kogadeeva, M.; Picotti, P.; Meissner, F.; Mann, M.; et al. L-Arginine Modulates T Cell Metabolism and Enhances Survival and Anti-tumor Activity. *Cell* **2016**, *167*, 829–842.e13. [CrossRef] [PubMed]
113. Fletcher, M.; Ramirez, M.E.; Sierra, R.A.; Raber, P.; Thevenot, P.; Al-Khami, A.A.; Sanchez-Pino, D.; Hernandez, C.; Wyczechowska, D.D.; Ochoa, A.C.; et al. l-Arginine Depletion Blunts Antitumor T-cell Responses by Inducing Myeloid-Derived Suppressor Cells. *Cancer Res.* **2014**, *75*, 275–283. [CrossRef]

114. Rodriguez, P.C.; Quiceno, D.G.; Zabaleta, J.; Ortiz, B.; Zea, A.H.; Piazuelo, M.B.; Delgado, A.; Correa, P.; Brayer, J.; Sotomayor, E.M.; et al. Arginase I Production in the Tumor Microenvironment by Mature Myeloid Cells Inhibits T-Cell Receptor Expression and Antigen-Specific T-Cell Responses. *Cancer Res.* **2004**, *64*, 5839–5849. [CrossRef]
115. Rodriguez, P.C.; Zea, A.H.; DeSalvo, J.; Culotta, K.S.; Zabaleta, J.; Quiceno, D.G.; Ochoa, J.B.; Ochoa, A.C. l-Arginine Consumption by Macrophages Modulates the Expression of CD3ζ Chain in T Lymphocytes. *J. Immunol.* **2003**, *171*, 1232–1239. [CrossRef]
116. Hatfield, S.M.; Kjaergaard, J.; Lukashev, D.; Schreiber, T.H.; Belikoff, B.; Abbott, R.; Sethumadhavan, S.; Philbrook, P.; Ko, K.; Cannici, R.; et al. Immunological mechanisms of the antitumor effects of supplemental oxygenation. *Sci. Transl. Med.* **2015**, *7*, 277ra30. [CrossRef]
117. Shi, L.Z.; Wang, R.; Huang, G.; Vogel, P.; Neale, G.; Green, D.R.; Chi, H. HIF1α–dependent glycolytic pathway orchestrates a metabolic checkpoint for the differentiation of TH17 and Treg cells. *J. Exp. Med.* **2011**, *208*, 1367–1376. [CrossRef]
118. Riera-Domingo, C.; Audigé, A.; Granja, S.; Cheng, W.-C.; Ho, P.-C.; Baltazar, F.; Stockmann, C.; Mazzone, M. Immunity, Hypoxia, and Metabolism–the Ménage à Trois of Cancer: Implications for Immunotherapy. *Physiol. Rev.* **2020**, *100*, 1–102. [CrossRef] [PubMed]
119. Scharping, N.E.; Rivadeneira, D.B.; Menk, A.V.; Vignali, P.D.A.; Ford, B.R.; Rittenhouse, N.L.; Peralta, R.; Wang, Y.; Wang, Y.; DePeaux, K.; et al. Mitochondrial stress induced by continuous stimulation under hypoxia rapidly drives T cell exhaustion. *Nat. Immunol.* **2021**, *22*, 205–215. [CrossRef] [PubMed]
120. Kosti, P.; Opzoomer, J.W.; Larios-Martinez, K.I.; Henley-Smith, R.; Scudamore, C.L.; Okesola, M.; Taher, M.Y.M.; Davies, D.M.; Muliaditan, T.; Larcombe-Young, D.; et al. Hypoxia-sensing CAR T cells provide safety and efficacy in treating solid tumors. *Cell Rep. Med.* **2021**, *2*, 100227. [CrossRef] [PubMed]
121. Ohta, A.; Gorelik, E.; Prasad, S.J.; Ronchese, F.; Lukashev, D.; Wong, M.K.K.; Huang, X.; Caldwell, S.; Liu, K.; Smith, P.; et al. A2A adenosine receptor protects tumors from antitumor T cells. *Proc. Natl. Acad. Sci. USA* **2006**, *103*, 13132–13137. [CrossRef]
122. Sitkovsky, M.V. Lessons from the A2A Adenosine Receptor Antagonist–Enabled Tumor Regression and Survival in Patients with Treatment-Refractory Renal Cell Cancer. *Cancer Discov.* **2020**, *10*, 16–19. [CrossRef]
123. Giuffrida, L.; Sek, K.; Henderson, M.A.; Lai, J.; Chen, A.X.Y.; Meyran, D.; Todd, K.L.; Petley, E.V.; Mardiana, S.; Mølck, C.; et al. CRISPR/Cas9 mediated deletion of the adenosine A2A receptor enhances CAR T cell efficacy. *Nat. Commun.* **2021**, *12*, 3236. [CrossRef] [PubMed]
124. Ma, X.; Bi, E.; Lu, Y.; Su, P.; Huang, C.; Liu, L.; Wang, Q.; Yang, M.; Kalady, M.F.; Qian, J.; et al. Cholesterol Induces CD8+ T Cell Exhaustion in the Tumor Microenvironment. *Cell Metab.* **2019**, *30*, 143–156.e5. [CrossRef] [PubMed]
125. Yang, W.; Bai, Y.; Xiong, Y.; Zhang, J.; Chen, S.; Zheng, X.; Meng, X.; Li, L.; Wang, J.; Xu, C.; et al. Potentiating the antitumour response of CD8+ T cells by modulating cholesterol metabolism. *Nature* **2016**, *531*, 651–655. [CrossRef]
126. Bengsch, B.; Johnson, A.L.; Kurachi, M.; Odorizzi, P.M.; Pauken, K.E.; Attanasio, J.; Stelekati, E.; McLane, L.M.; Paley, M.A.; Delgoffe, G.M.; et al. Bioenergetic Insufficiencies Due to Metabolic Alterations Regulated by the Inhibitory Receptor PD-1 Are an Early Driver of CD8 + T Cell Exhaustion. *Immunity* **2016**, *45*, 358–373. [CrossRef] [PubMed]
127. Geltink, R.K.; O'Sullivan, D.; Corrado, M.; Bremser, A.; Buck, M.D.; Buescher, J.M.; Firat, E.; Zhu, X.; Niedermann, G.; Caputa, G.; et al. Mitochondrial Priming by CD28. *Cell* **2017**, *171*, 385–397.e11. [CrossRef] [PubMed]
128. Parry, R.V.; Chemnitz, J.M.; Frauwirth, K.A.; Lanfranco, A.R.; Braunstein, I.; Kobayashi, S.V.; Linsley, P.S.; Thompson, C.B.; Riley, J.L. CTLA-4 and PD-1 Receptors Inhibit T-Cell Activation by Distinct Mechanisms. *Mol. Cell. Biol.* **2005**, *25*, 9543–9553. [CrossRef] [PubMed]
129. Patsoukis, N.; Bardhan, K.; Chatterjee, P.; Sari, D.; Liu, B.; Bell, L.N.; Karoly, E.D.; Freeman, G.J.; Petkova, V.; Seth, P.; et al. PD-1 alters T-cell metabolic reprogramming by inhibiting glycolysis and promoting lipolysis and fatty acid oxidation. *Nat. Commun.* **2015**, *6*, 6692. [CrossRef]
130. Waickman, A.T.; Powell, J.D. mTOR, metabolism, and the regulation of T-cell differentiation and function. *Immunol. Rev.* **2012**, *249*, 43–58. [CrossRef]
131. Ren, J.; Liu, X.; Fang, C.; Jiang, S.; June, C.H.; Zhao, Y. Multiplex Genome Editing to Generate Universal CAR T Cells Resistant to PD1 Inhibition. *Clin. Cancer Res.* **2016**, *23*, 2255–2266. [CrossRef]
132. Zhao, Z.; Shi, L.; Zhang, W.; Han, J.; Zhang, S.; Fu, Z.; Cai, J. CRISPR knock out of programmed cell death protein 1 enhances anti-tumor activity of cytotoxic T lymphocytes. *Oncotarget* **2017**, *9*, 5208–5215. [CrossRef] [PubMed]
133. Rupp, L.J.; Schumann, K.; Roybal, K.T.; Gate, R.E.; Chun, J.Y.; Lim, W.A.; Marson, A. CRISPR/Cas9-mediated PD-1 disruption enhances anti-tumor efficacy of human chimeric antigen receptor T cells. *Sci. Rep.* **2017**, *7*, 737. [CrossRef] [PubMed]
134. Guo, X.; Jiang, H.; Shi, B.; Zhou, M.; Zhang, H.; Shi, Z.; Du, G.; Luo, H.; Wu, X.; Wang, Y.; et al. Disruption of PD-1 Enhanced the Anti-tumor Activity of Chimeric Antigen Receptor T Cells Against Hepatocellular Carcinoma. *Front. Pharmacol.* **2018**, *9*, 1118. [CrossRef]
135. Pomeroy, E.J.; Hunzeker, J.T.; Kluesner, M.G.; Lahr, W.S.; Smeester, B.A.; Crosby, M.R.; Lonetree, C.-L.; Yamamoto, K.; Bendzick, L.; Miller, J.S.; et al. A Genetically Engineered Primary Human Natural Killer Cell Platform for Cancer Immunotherapy. *Mol. Ther.* **2019**, *28*, 52–63. [CrossRef]
136. Zhang, Y.; Zhang, X.; Cheng, C.; Mu, W.; Liu, X.; Li, N.; Wei, X.; Liu, X.; Xia, C.; Wang, H. CRISPR-Cas9 mediated LAG-3 disruption in CAR-T cells. *Front. Med.* **2017**, *11*, 554–562. [CrossRef]

137. Suarez, E.R.; de Chang, K.; Sun, J.; Sui, J.; Freeman, G.J.; Signoretti, S.; Zhu, Q.; Marasco, W.A. Chimeric antigen receptor T cells secreting anti-PD-L1 antibodies more effectively regress renal cell carcinoma in a humanized mouse model. *Oncotarget* **2016**, *7*, 34341–34355. [CrossRef] [PubMed]
138. Yeku, O.O.; Purdon, T.J.; Koneru, M.; Spriggs, D.; Brentjens, R.J. Armored CAR T cells enhance antitumor efficacy and overcome the tumor microenvironment. *Sci. Rep.* **2017**, *7*, 10541. [CrossRef]
139. Chmielewski, M.; Kopecky, C.; Hombach, A.A.; Abken, H. IL-12 Release by Engineered T Cells Expressing Chimeric Antigen Receptors Can Effectively Muster an Antigen-Independent Macrophage Response on Tumor Cells That Have Shut Down Tumor Antigen Expression. *Cancer Res.* **2011**, *71*, 5697–5706. [CrossRef]
140. Kerkar, S.P.; Muranski, P.; Kaiser, A.; Boni, A.; Sanchez-Perez, L.; Yu, Z.; Palmer, D.C.; Reger, R.N.; Borman, Z.A.; Zhang, L.; et al. Tumor-Specific CD8+ T Cells Expressing Interleukin-12 Eradicate Established Cancers in Lymphodepleted Hosts. *Cancer Res.* **2010**, *70*, 6725–6734. [CrossRef]
141. Pegram, H.J.; Lee, J.C.; Hayman, E.G.; Imperato, G.H.; Tedder, T.F.; Sadelain, M.; Brentjens, R.J. Tumor-targeted T cells modified to secrete IL-12 eradicate systemic tumors without need for prior conditioning. *Blood* **2012**, *119*, 4133–4141. [CrossRef] [PubMed]
142. Sachdeva, M.; Busser, B.W.; Temburni, S.; Jahangiri, B.; Gautron, A.-S.; Maréchal, A.; Juillerat, A.; Williams, A.; Depil, S.; Duchateau, P.; et al. Repurposing endogenous immune pathways to tailor and control chimeric antigen receptor T cell functionality. *Nat. Commun.* **2019**, *10*, 5100. [CrossRef] [PubMed]
143. Chmielewski, M.; Abken, H. CAR T cells transform to trucks: Chimeric antigen receptor–redirected T cells engineered to deliver inducible IL-12 modulate the tumour stroma to combat cancer. *Cancer Immunol. Immunother.* **2012**, *61*, 1269–1277. [CrossRef]
144. McCoy, K.D.; Le Gros, G. The role of CTLA-4 in the regulation of T cell immune responses. *Immunol. Cell Biol.* **1999**, *77*, 1–10. [CrossRef]
145. Lee, M.J.; Yun, S.J.; Lee, B.; Jeong, E.; Yoon, G.; Kim, K.; Park, S. Association of TIM-3 expression with glucose metabolism in Jurkat T cells. *BMC Immunol.* **2020**, *21*, 48. [CrossRef] [PubMed]
146. Previte, D.M.; Martins, C.P.; O'Connor, E.C.; Marre, M.L.; Coudriet, G.M.; Beck, N.W.; Menk, A.V.; Wright, R.H.; Tse, H.M.; Delgoffe, G.M.; et al. Lymphocyte Activation Gene-3 Maintains Mitochondrial and Metabolic Quiescence in Naive CD4+ T Cells. *Cell Rep.* **2019**, *27*, 129–141.e4. [CrossRef]
147. Andrews, L.P.; Marciscano, A.E.; Drake, C.G.; Vignali, D.A.A. LAG3 (CD223) as a cancer immunotherapy target. *Immunol. Rev.* **2017**, *276*, 80–96. [CrossRef]
148. Cai, G.; Anumanthan, A.; Brown, J.A.; Greenfield, E.A.; Zhu, B.; Freeman, G.J. CD160 inhibits activation of human CD4+ T cells through interaction with herpesvirus entry mediator. *Nat. Immunol.* **2008**, *9*, 176–185. [CrossRef] [PubMed]
149. Pauken, K.E.; Wherry, E.J. Overcoming T cell exhaustion in infection and cancer. *Trends Immunol.* **2015**, *36*, 265–276. [CrossRef] [PubMed]
150. Phan, A.T.; Goldrath, A.W.; Glass, C.K. Metabolic and Epigenetic Coordination of T Cell and Macrophage Immunity. *Immunity* **2017**, *46*, 714–729. [CrossRef]
151. Ye, Y.; Wang, J.; Hu, Q.; Hochu, G.M.; Xin, H.; Wang, C.; Gu, Z. Synergistic Transcutaneous Immunotherapy Enhances Antitumor Immune Responses through Delivery of Checkpoint Inhibitors. *ACS Nano* **2016**, *10*, 8956–8963. [CrossRef] [PubMed]
152. Tabana, Y.; Moon, T.C.; Siraki, A.; Elahi, S.; Barakat, K. Reversing T-cell exhaustion in immunotherapy: A review on current approaches and limitations. *Expert Opin. Ther. Targets* **2021**, *25*, 347–363. [CrossRef] [PubMed]
153. Fonseca, R.; Beura, L.K.; Quarnstrom, C.F.; Ghoneim, H.E.; Fan, Y.; Zebley, C.C.; Scott, M.C.; Fares-Frederickson, N.J.; Wijeyesinghe, S.; Thompson, E.A.; et al. Developmental plasticity allows outside-in immune responses by resident memory T cells. *Nat. Immunol.* **2020**, *21*, 412–421. [CrossRef] [PubMed]
154. Zebley, C.C.; Gottschalk, S.; Youngblood, B. Rewriting History: Epigenetic Reprogramming of CD8+ T Cell Differentiation to Enhance Immunotherapy. *Trends Immunol.* **2020**, *41*, 665–675. [CrossRef]
155. Ghoneim, H.E.; Fan, Y.; Moustaki, A.; Abdelsamed, H.A.; Dash, P.; Dogra, P.; Carter, R.; Awad, W.; Neale, G.; Thomas, P.G.; et al. De Novo Epigenetic Programs Inhibit PD-1 Blockade-Mediated T Cell Rejuvenation. *Cell* **2017**, *170*, 142–157.e19. [CrossRef] [PubMed]
156. Koss, B.; Shields, B.D.; Taylor, E.M.; Storey, A.J.; Byrum, S.D.; Gies, A.J.; Washam, C.L.; Choudhury, S.R.; Ahn, J.H.; Uryu, H.; et al. Epigenetic Control of Cdkn2a.Arf Protects Tumor-Infiltrating Lymphocytes from Metabolic Exhaustion. *Cancer Res.* **2020**, *80*, 4707–4719. [CrossRef]
157. Zhao, E.; Maj, T.; Kryczek, I.; Li, W.; Wu, K.; Zhao, L.; Wei, S.; Crespo, J.; Wan, S.; Vatan, L.; et al. Cancer mediates effector T cell dysfunction by targeting microRNAs and EZH2 via glycolysis restriction. *Nat. Immunol.* **2015**, *17*, 95–103. [CrossRef]
158. Bian, Y.; Li, W.; Kremer, D.M.; Sajjakulnukit, P.; Li, S.; Crespo, J.; Nwosu, Z.C.; Zhang, L.; Czerwonka, A.; Pawłowska, A.; et al. Cancer SLC43A2 alters T cell methionine metabolism and histone methylation. *Nature* **2020**, *585*, 277–282. [CrossRef]
159. Roy, D.G.; Chen, J.; Mamane, V.; Ma, E.H.; Muhire, B.M.; Sheldon, R.D.; Shorstova, T.; Koning, R.; Johnson, R.M.; Esaulova, E.; et al. Methionine Metabolism Shapes T Helper Cell Responses through Regulation of Epigenetic Reprogramming. *Cell Metab.* **2020**, *31*, 250–266.e9. [CrossRef]
160. Schvartzman, J.M.; Thompson, C.B.; Finley, L.W.S. Metabolic regulation of chromatin modifications and gene expression. *J. Cell Biol.* **2018**, *217*, 2247–2259. [CrossRef]

161. Johnson, M.O.; Wolf, M.M.; Madden, M.Z.; Andrejeva, G.; Sugiura, A.; Contreras, D.C.; Maseda, D.; Liberti, M.V.; Paz, K.; Kishton, R.J.; et al. Distinct Regulation of Th17 and Th1 Cell Differentiation by Glutaminase-Dependent Metabolism. *Cell* **2018**, *175*, 1780–1795.e19. [CrossRef] [PubMed]
162. Peng, M.; Yin, N.; Chhangawala, S.; Xu, K.; Leslie, C.S.; Li, M.O. Aerobic glycolysis promotes T helper 1 cell differentiation through an epigenetic mechanism. *Science* **2016**, *354*, 481–484. [CrossRef] [PubMed]
163. McDonnell, E.; Crown, S.B.; Fox, D.B.; Kitir, B.; Ilkayeva, O.R.; Olsen, C.A.; Grimsrud, P.A.; Hirschey, M.D. Lipids Reprogram Metabolism to Become a Major Carbon Source for Histone Acetylation. *Cell Rep.* **2016**, *17*, 1463–1472. [CrossRef]
164. Navas, L.E.; Carnero, A. NAD+ metabolism, stemness, the immune response, and cancer. *Signal Transduct. Target. Ther.* **2021**, *6*, 2. [CrossRef]
165. Jeng, M.Y.; Hull, P.A.; Fei, M.; Kwon, H.-S.; Tsou, C.-L.; Kasler, H.; Ng, C.-P.; Gordon, D.E.; Johnson, J.; Krogan, N.; et al. Metabolic reprogramming of human CD8+ memory T cells through loss of SIRT1. *J. Exp. Med.* **2017**, *215*, 51–62. [CrossRef] [PubMed]
166. Kwon, H.-S.; Brent, M.M.; Getachew, R.; Jayakumar, P.; Chen, L.-F.; Schnolzer, M.; McBurney, M.W.; Marmorstein, R.; Greene, W.C.; Ott, M. Human Immunodeficiency Virus Type 1 Tat Protein Inhibits the SIRT1 Deacetylase and Induces T Cell Hyperactivation. *Cell Host Microbe* **2008**, *3*, 158–167. [CrossRef]
167. Zhang, D.; Tang, Z.; Huang, H.; Zhou, G.; Cui, C.; Weng, Y.; Liu, W.; Kim, S.; Lee, S.; Perez-Neut, M.; et al. Metabolic regulation of gene expression by histone lactylation. *Nature* **2019**, *574*, 575–580. [CrossRef] [PubMed]
168. Van Acker, H.H.; Ma, S.; Scolaro, T.; Kaech, S.M.; Mazzone, M. How metabolism bridles cytotoxic CD8+ T cells through epigenetic modifications. *Trends Immunol.* **2021**, *42*, 401–417. [CrossRef]
169. Vivier, E.; Nunès, J.A.; Vély, F. Natural Killer Cell Signaling Pathways. *Science* **2004**, *306*, 1517–1519. [CrossRef]
170. Fang, F.; Xiao, W.; Tian, Z. NK cell-based immunotherapy for cancer. *Semin. Immunol.* **2017**, *31*, 37–54. [CrossRef]
171. Gardiner, C.M.; Finlay, D.K. What Fuels Natural Killers? Metabolism and NK Cell Responses. *Front. Immunol.* **2017**, *8*, 367. [CrossRef]
172. Myers, J.A.; Miller, J.S. Exploring the NK cell platform for cancer immunotherapy. *Nat. Rev. Clin. Oncol.* **2020**, *18*, 85–100. [CrossRef]
173. Sivori, S.; Pende, D.; Quatrini, L.; Pietra, G.; Della Chiesa, M.; Vacca, P.; Tumino, N.; Moretta, F.; Mingari, M.C.; Locatelli, F.; et al. NK cells and ILCs in tumor immunotherapy. *Mol. Asp. Med.* **2020**, *80*, 100870. [CrossRef]
174. Ljunggren, H.-G.; Kärre, K. In search of the 'missing self': MHC molecules and NK cell recognition. *Immunol. Today* **1990**, *11*, 237–244. [CrossRef]
175. Morandi, F.; Pistoia, V. Interactions between HLA-G and HLA-E in Physiological and Pathological Conditions. *Front. Immunol.* **2014**, *5*, 394. [CrossRef]
176. Bollino, D.; Webb, T.J. Chimeric antigen receptor–engineered natural killer and natural killer T cells for cancer immunotherapy. *Transl. Res.* **2017**, *187*, 32–43. [CrossRef]
177. Wu, S.-Y.; Fu, T.; Jiang, Y.-Z.; Shao, Z.-M. Natural killer cells in cancer biology and therapy. *Mol. Cancer* **2020**, *19*, 120. [CrossRef]
178. Caligiuri, M.A. Human natural killer cells. *Blood* **2008**, *112*, 461–469. [CrossRef]
179. Clynes, R.A.; Towers, T.L.; Presta, L.G.; Ravetch, J.V. Inhibitory Fc receptors modulate in vivo cytoxicity against tumor targets. *Nat. Med.* **2000**, *6*, 443–446. [CrossRef]
180. Conlon, K.C.; Lugli, E.; Welles, H.C.; Rosenberg, S.A.; Fojo, A.T.; Morris, J.C.; Fleisher, T.A.; Dubois, S.P.; Perera, L.P.; Stewart, D.M.; et al. Redistribution, Hyperproliferation, Activation of Natural Killer Cells and CD8 T Cells, and Cytokine Production During First-in-Human Clinical Trial of Recombinant Human Interleukin-15 in Patients With Cancer. *J. Clin. Oncol.* **2015**, *33*, 74–82. [CrossRef]
181. Fallon, J.; Tighe, R.; Kradjian, G.; Guzman, W.; Bernhardt, A.; Neuteboom, B.; Lan, Y.; Sabzevari, H.; Schlom, J.; Greiner, J.W. The immunocytokine NHS-IL12 as a potential cancer therapeutic. *Oncotarget* **2014**, *5*, 1869–1884. [CrossRef]
182. Floros, T.; Tarhini, A.A. Anticancer Cytokines: Biology and Clinical Effects of Interferon-α2, Interleukin (IL)-2, IL-15, IL-21, and IL-12. *Semin. Oncol.* **2015**, *42*, 539–548. [CrossRef]
183. Srivastava, S.; Pelloso, D.; Feng, H.; Voiles, L.; Lewis, D.; Haskova, Z.; Whitacre, M.; Trulli, S.; Chen, Y.-J.; Toso, J.; et al. Effects of interleukin-18 on natural killer cells: Costimulation of activation through Fc receptors for immunoglobulin. *Cancer Immunol. Immunother.* **2013**, *62*, 1073–1082. [CrossRef]
184. Koerner, S.P.; André, M.C.; Leibold, J.S.; Kousis, P.C.; Kübler, A.; Pal, M.; Haen, S.; Bühring, H.-J.; Grosse-Hovest, L.; Jung, G.; et al. An Fc-optimized CD133 antibody for induction of NK cell reactivity against myeloid leukemia. *Leukemia* **2016**, *31*, 459–469. [CrossRef]
185. Kohrt, H.E.; Houot, R.; Weiskopf, K.; Goldstein, M.J.; Scheeren, F.; Czerwinski, D.; Colevas, A.D.; Weng, W.-K.; Clarke, M.F.; Carlson, R.W.; et al. Stimulation of natural killer cells with a CD137-specific antibody enhances trastuzumab efficacy in xenotransplant models of breast cancer. *J. Clin. Investig.* **2012**, *122*, 1066–1075. [CrossRef]
186. Romagné, F.; André, P.; Spee, P.; Zahn, S.; Anfossi, N.; Gauthier, L.; Capanni, M.; Ruggeri, L.; Benson, D.M., Jr.; Blaser, B.W.; et al. Preclinical characterization of 1-7F9, a novel human anti–KIR receptor therapeutic antibody that augments natural killer–mediated killing of tumor cells. *Blood* **2009**, *114*, 2667–2677. [CrossRef] [PubMed]
187. Ruggeri, L.; Urbani, E.; André, P.; Mancusi, A.; Tosti, A.; Topini, F.; Bléry, M.; Animobono, L.; Romagné, F.; Wagtmann, N.; et al. Effects of anti-NKG2A antibody administration on leukemia and normal hematopoietic cells. *Haematologica* **2015**, *101*, 626–633. [CrossRef]

188. Wu, J.; Fu, J.; Zhang, M.; Liu, D. AFM13: A first-in-class tetravalent bispecific anti-CD30/CD16A antibody for NK cell-mediated immunotherapy. *J. Hematol. Oncol.* **2015**, *8*, 96. [CrossRef]
189. Bachanova, V.; Burns, L.J.; McKenna, D.H.; Curtsinger, J.; Panoskaltsis-Mortari, A.; Lindgren, B.R.; Cooley, S.; Weisdorf, D.; Miller, J.S. Allogeneic natural killer cells for refractory lymphoma. *Cancer Immunol. Immunother.* **2010**, *59*, 1739–1744. [CrossRef] [PubMed]
190. Klingemann, H.; Grodman, C.; Cutler, E.; Duque, M.; Kadidlo, D.; Klein, A.K.; Sprague, K.A.; Miller, K.B.; Comenzo, R.L.; Kewalramani, T.; et al. Autologous stem cell transplant recipients tolerate haploidentical related-donor natural killer cell-enriched infusions. *Transfusion* **2012**, *53*, 412–418. [CrossRef] [PubMed]
191. Romee, R.; Rosario, M.; Berrien-Elliott, M.M.; Wagner, J.A.; Jewell, B.A.; Schappe, T.; Leong, J.W.; Abdel-Latif, S.; Schneider, S.E.; Willey, S.; et al. Cytokine-induced memory-like natural killer cells exhibit enhanced responses against myeloid leukemia. *Sci. Transl. Med.* **2016**, *8*, 357ra123. [CrossRef]
192. Rubnitz, J.E.; Inaba, H.; Ribeiro, R.C.; Pounds, S.; Rooney, B.; Bell, T.; Pui, C.-H.; Leung, W. NKAML: A Pilot Study to Determine the Safety and Feasibility of Haploidentical Natural Killer Cell Transplantation in Childhood Acute Myeloid Leukemia. *J. Clin. Oncol.* **2010**, *28*, 955–959. [CrossRef]
193. Geller, M.A.; Cooley, S.; Judson, P.L.; Ghebre, R.; Carson, L.F.; Argenta, P.A.; Jonson, A.L.; Panoskaltsis-Mortari, A.; Curtsinger, J.; McKenna, D.; et al. A phase II study of allogeneic natural killer cell therapy to treat patients with recurrent ovarian and breast cancer. *Cytotherapy* **2011**, *13*, 98–107. [CrossRef]
194. Iliopoulou, E.G.; Kountourakis, P.; Karamouzis, M.V.; Doufexis, D.; Ardavanis, A.; Baxevanis, C.N.; Rigatos, G.; Papamichail, M.; Perez, S.A. A phase I trial of adoptive transfer of allogeneic natural killer cells in patients with advanced non-small cell lung cancer. *Cancer Immunol. Immunother.* **2010**, *59*, 1781–1789. [CrossRef] [PubMed]
195. Sakamoto, N.; Ishikawa, T.; Kokura, S.; Okayama, T.; Oka, K.; Ideno, M.; Sakai, F.; Kato, A.; Tanabe, M.; Enoki, T.; et al. Phase I clinical trial of autologous NK cell therapy using novel expansion method in patients with advanced digestive cancer. *J. Transl. Med.* **2015**, *13*, 277. [CrossRef] [PubMed]
196. Parkhurst, M.R.; Riley, J.P.; Dudley, M.E.; Rosenberg, S.A. Adoptive Transfer of Autologous Natural Killer Cells Leads to High Levels of Circulating Natural Killer Cells but Does Not Mediate Tumor Regression. *Clin. Cancer Res.* **2011**, *17*, 6287–6297. [CrossRef]
197. Terrén, I.; Orrantia, A.; Vitallé, J.; Zenarruzabeitia, O.; Borrego, F. NK Cell Metabolism and Tumor Microenvironment. *Front. Immunol.* **2019**, *10*, 2278. [CrossRef] [PubMed]
198. Dolstra, H.; Roeven, M.W.H.; Spanholtz, J.; Hangalapura, B.N.; Tordoir, M.; Maas, F.; Leenders, M.; Bohme, F.; Kok, N.; Trilsbeek, C.; et al. Successful Transfer of Umbilical Cord Blood CD34+ Hematopoietic Stem and Progenitor-derived NK Cells in Older Acute Myeloid Leukemia Patients. *Clin. Cancer Res.* **2017**, *23*, 4107–4118. [CrossRef]
199. Colamartino, A.B.L.; Lemieux, W.; Bifsha, P.; Nicoletti, S.; Chakravarti, N.; Sanz, J.; Roméro, H.; Selleri, S.; Béland, K.; Guiot, M.; et al. Efficient and Robust NK-Cell Transduction With Baboon Envelope Pseudotyped Lentivector. *Front. Immunol.* **2019**, *10*, 2873. [CrossRef]
200. Jochems, C.; Hodge, J.W.; Fantini, M.; Fujii, R.; Maurice, Y.M., II; Greiner, J.W.; Padget, M.R.; Tritsch, S.R.; Tsang, K.Y.; Campbell, K.S.; et al. An NK cell line (haNK) expressing high levels of granzyme and engineered to express the high affinity CD16 allele. *Oncotarget* **2016**, *7*, 86359–86373. [CrossRef]
201. Sahm, C.; Schönfeld, K.; Wels, W.S. Expression of IL-15 in NK cells results in rapid enrichment and selective cytotoxicity of gene-modified effectors that carry a tumor-specific antigen receptor. *Cancer Immunol. Immunother.* **2012**, *61*, 1451–1461. [CrossRef]
202. Schirrmann, T.; Pecher, G. Human natural killer cell line modified with a chimeric immunoglobulin T-cell receptor gene leads to tumor growth inhibition in vivo. *Cancer Gene Ther.* **2002**, *9*, 390–398. [CrossRef] [PubMed]
203. Uherek, C.; Tonn, T.; Uherek, B.; Becker, S.; Schnierle, B.; Klingemann, H.-G.; Wels, W. Retargeting of natural killer–cell cytolytic activity to ErbB2-expressing cancer cells results in efficient and selective tumor cell destruction. *Blood* **2002**, *100*, 1265–1273. [CrossRef] [PubMed]
204. Müller, T.; Uherek, C.; Maki, G.; Chow, K.U.; Schimpf, A.; Klingemann, H.-G.; Tonn, T.; Wels, W.S. Expression of a CD20-specific chimeric antigen receptor enhances cytotoxic activity of NK cells and overcomes NK-resistance of lymphoma and leukemia cells. *Cancer Immunol. Immunother.* **2007**, *57*, 411–423. [CrossRef]
205. Shimasaki, N.; Fujisaki, H.; Cho, D.; Masselli, M.; Lockey, T.; Eldridge, P.; Leung, W.; Campana, D. A clinically adaptable method to enhance the cytotoxicity of natural killer cells against B-cell malignancies. *Cytotherapy* **2012**, *14*, 830–840. [CrossRef]
206. Tang, X.; Yang, L.; Li, Z.; Nalin, A.P.; Dai, H.; Xu, T.; Yin, J.; You, F.; Zhu, M.; Shen, W.; et al. First-in-man clinical trial of CAR NK-92 cells: Safety test of CD33-CAR NK-92 cells in patients with relapsed and refractory acute myeloid leukemia. *Am. J. Cancer Res.* **2018**, *8*, 1083–1089. [PubMed]
207. Jiang, L.; Fang, X.; Wang, H.; Li, D.; Wang, X. Ovarian Cancer-Intrinsic Fatty Acid Synthase Prevents Anti-tumor Immunity by Disrupting Tumor-Infiltrating Dendritic Cells. *Front. Immunol.* **2018**, *9*, 2927. [CrossRef]
208. Xu, Y.; Liu, Q.; Zhong, M.; Wang, Z.; Chen, Z.; Zhang, Y.; Xing, H.; Tian, Z.; Tang, K.; Liao, X.; et al. 2B4 costimulatory domain enhancing cytotoxic ability of anti-CD5 chimeric antigen receptor engineered natural killer cells against T cell malignancies. *J. Hematol. Oncol.* **2019**, *12*, 491. [CrossRef] [PubMed]

209. Altvater, B.; Landmeier, S.; Pscherer, S.; Temme, J.; Schweer, K.; Kailayangiri, S.; Campana, D.; Juergens, H.; Pule, M.; Rossig, C. 2B4 (CD244) Signaling by Recombinant Antigen-specific Chimeric Receptors Costimulates Natural Killer Cell Activation to Leukemia and Neuroblastoma Cells. *Clin. Cancer Res.* **2009**, *15*, 4857–4866. [CrossRef]
210. Zhang, G.; Liu, R.; Zhu, X.; Wang, L.; Ma, J.; Han, H.; Wang, X.; Zhang, G.; He, W.; Wang, W.; et al. Retargeting NK-92 for anti-melanoma activity by a TCR-like single-domain antibody. *Immunol. Cell Biol.* **2013**, *91*, 615–624. [CrossRef]
211. Han, J.; Chu, J.; Chan, W.K.; Zhang, J.; Wang, Y.; Cohen, J.B.; Victor, A.; Meisen, W.H.; Kim, S.-H.; Grandi, P.; et al. CAR-Engineered NK Cells Targeting Wild-Type EGFR and EGFRvIII Enhance Killing of Glioblastoma and Patient-Derived Glioblastoma Stem Cells. *Sci. Rep.* **2015**, *5*, 11483. [CrossRef]
212. Kruschinski, A.; Moosmann, A.; Poschke, I.; Norell, H.; Chmielewski, M.; Seliger, B.; Kiessling, R.; Blankenstein, T.; Abken, H.; Charo, J. Engineering antigen-specific primary human NK cells against HER-2 positive carcinomas. *Proc. Natl. Acad. Sci. USA* **2008**, *105*, 17481–17486. [CrossRef]
213. Li, C.; Yang, N.; Li, H.; Wang, Z. Robo1-specific chimeric antigen receptor natural killer cell therapy for pancreatic ductal adenocarcinoma with liver metastasis. *J. Cancer Res. Ther.* **2020**, *16*, 393–396. [CrossRef]
214. Wrona, E.; Borowiec, M.; Potemski, P. CAR-NK Cells in the Treatment of Solid Tumors. *Int. J. Mol. Sci.* **2021**, *22*, 5899. [CrossRef]
215. O'Brien, K.L.; Finlay, D.K. Immunometabolism and natural killer cell responses. *Nat. Rev. Immunol.* **2019**, *19*, 282–290. [CrossRef] [PubMed]
216. Keating, S.E.; Bittencourt, V.Z.; Loftus, R.M.; Keane, C.; Brennan, K.; Finlay, D.K.; Gardiner, C.M. Metabolic Reprogramming Supports IFN-γ Production by CD56bright NK Cells. *J. Immunol.* **2016**, *196*, 2552–2560. [CrossRef]
217. Mah-Som, A.Y.; Rashidi, A.; Keppel, M.P.; Saucier, N.; Moore, E.K.; Alinger, J.B.; Tripathy, S.K.; Agarwal, S.K.; Jeng, E.K.; Wong, H.C.; et al. Glycolytic requirement for NK cell cytotoxicity and cytomegalovirus control. *JCI Insight* **2017**, *2*, e95128. [CrossRef]
218. Loftus, R.M.; Assmann, N.; Kedia-Mehta, N.; O'Brien, K.L.; Garcia, A.; Gillespie, C.; Hukelmann, J.L.; Oefner, P.J.; Lamond, A.I.; Gardiner, C.M.; et al. Amino acid-dependent cMyc expression is essential for NK cell metabolic and functional responses in mice. *Nat. Commun.* **2018**, *9*, 2341. [CrossRef]
219. Donnelly, R.P.; Loftus, R.M.; Keating, S.E.; Liou, K.T.; Biron, C.A.; Gardiner, C.M.; Finlay, D.K. mTORC1-Dependent Metabolic Reprogramming Is a Prerequisite for NK Cell Effector Function. *J. Immunol.* **2014**, *193*, 4477–4484. [CrossRef]
220. Marçais, A.; Cherfils-Vicini, J.; Viant, C.; Degouve, S.; Viel, S.; Fenis, A.; Rabilloud, J.; Mayol, K.; Tavares, A.; Bienvenu, J.; et al. The metabolic checkpoint kinase mTOR is essential for IL-15 signaling during the development and activation of NK cells. *Nat. Immunol.* **2014**, *15*, 749–757. [CrossRef]
221. Sun, J.C.; Beilke, J.N.; Lanier, L.L. Adaptive immune features of natural killer cells. *Nature* **2009**, *457*, 557–561. [CrossRef]
222. Assmann, N.; O'Brien, K.L.; Donnelly, R.P.; Dyck, L.; Zaiatz-Bittencourt, V.; Loftus, R.M.; Heinrich, P.; Oefner, P.J.; Lynch, L.; Gardiner, C.M.; et al. Srebp-controlled glucose metabolism is essential for NK cell functional responses. *Nat. Immunol.* **2017**, *18*, 1197–1206. [CrossRef]
223. O'Brien, K.L.; Assmann, N.; O'Connor, E.; Keane, C.; Walls, J.; Choi, C.; Oefner, P.J.; Gardiner, C.M.; Dettmer, K.; Finlay, D.K. De novo polyamine synthesis supports metabolic and functional responses in activated murine NK cells. *Eur. J. Immunol.* **2020**, *51*, 91–102. [CrossRef]
224. Saetersmoen, M.L.; Hammer, Q.; Valamehr, B.; Kaufman, D.S.; Malmberg, K.-J. Off-the-shelf cell therapy with induced pluripotent stem cell-derived natural killer cells. *Semin. Immunopathol.* **2018**, *41*, 59–68. [CrossRef]
225. Viel, S.; Marçais, A.; Guimaraes, F.S.-F.; Loftus, R.; Rabilloud, J.; Grau, M.; Degouve, S.; Djebali, S.; Sanlaville, A.; Charrier, E.; et al. TGF-β inhibits the activation and functions of NK cells by repressing the mTOR pathway. *Sci. Signal.* **2016**, *9*, ra19. [CrossRef]
226. Chambers, A.M.; Wang, J.; Lupo, K.B.; Yu, H.; Lanman, N.M.A.; Matosevic, S. Adenosinergic Signaling Alters Natural Killer Cell Functional Responses. *Front. Immunol.* **2018**, *9*, 2533. [CrossRef]
227. Abarca-Rojano, E.; Muñiz-Hernández, S.; Moreno-Altamirano, M.M.B.; Mondragón-Flores, R.; Enriquez-Rincón, F.; Sánchez-García, F.J. Re-organization of mitochondria at the NK cell immune synapse. *Immunol. Lett.* **2009**, *122*, 18–25. [CrossRef]
228. Netter, P.; Anft, M.; Watzl, C. Termination of the Activating NK Cell Immunological Synapse Is an Active and Regulated Process. *J. Immunol.* **2017**, *199*, 2528–2535. [CrossRef]
229. Cong, J.; Wang, X.; Zheng, X.; Wang, D.; Fu, B.; Sun, R.; Tian, Z.; Wei, H. Dysfunction of Natural Killer Cells by FBP1-Induced Inhibition of Glycolysis during Lung Cancer Progression. *Cell Metab.* **2018**, *28*, 243–255.e5. [CrossRef]
230. Stiff, A.; Trikha, P.; Mundy-Bosse, B.L.; McMichael, E.L.; Mace, T.A.; Benner, B.; Kendra, K.; Campbell, A.; Gautam, S.; Abood, D.; et al. Nitric Oxide Production by Myeloid-Derived Suppressor Cells Plays a Role in Impairing Fc Receptor–Mediated Natural Killer Cell Function. *Clin. Cancer Res.* **2018**, *24*, 1891–1904. [CrossRef]
231. Della Chiesa, M.; Carlomagno, S.; Frumento, G.; Balsamo, M.; Cantoni, C.; Conte, R.; Moretta, L.; Moretta, A.; Vitale, M. The tryptophan catabolite l-kynurenine inhibits the surface expression of NKp46- and NKG2D-activating receptors and regulates NK-cell function. *Blood* **2006**, *108*, 4118–4125. [CrossRef]
232. Melaiu, O.; Lucarini, V.; Cifaldi, L.; Fruci, D. Influence of the Tumor Microenvironment on NK Cell Function in Solid Tumors. *Front. Immunol.* **2020**, *10*, 3038. [CrossRef]
233. Bailey, C.P.; Figueroa, M.; Gangadharan, A.; Lee, D.A.; Chandra, J. Scaffolding LSD1 Inhibitors Impair NK Cell Metabolism and Cytotoxic Function Through Depletion of Glutathione. *Front. Immunol.* **2020**, *11*, 2196. [CrossRef]
234. Bader, J.E.; Voss, K.; Rathmell, J.C. Targeting Metabolism to Improve the Tumor Microenvironment for Cancer Immunotherapy. *Mol. Cell* **2020**, *78*, 1019–1033. [CrossRef]

235. Xie, G.; Dong, H.; Liang, Y.; Ham, J.D.; Rizwan, R.; Chen, J. CAR-NK cells: A promising cellular immunotherapy for cancer. *EBioMedicine* **2020**, *59*, 102975. [CrossRef]
236. Gang, M.; Marin, N.D.; Wong, P.; Neal, C.C.; Marsala, L.; Foster, M.; Schappe, T.; Meng, W.; Tran, J.; Schaettler, M.; et al. CAR-modified memory-like NK cells exhibit potent responses to NK-resistant lymphomas. *Blood* **2020**, *136*, 2308–2318. [CrossRef]
237. Liu, E.; Marin, D.; Banerjee, P.; Macapinlac, H.A.; Thompson, P.; Basar, R.; Kerbauy, L.N.; Overman, B.; Thall, P.; Kaplan, M.; et al. Use of CAR-Transduced Natural Killer Cells in CD19-Positive Lymphoid Tumors. *N. Engl. J. Med.* **2020**, *382*, 545–553. [CrossRef]
238. Koltai, T. Cancer: Fundamentals behind pH targeting and the double-edged approach. *OncoTargets Ther.* **2016**, *9*, 6343–6360. [CrossRef]
239. Kouidhi, S.; Ayed, F.B.; Elgaaied, A.B. Targeting Tumor Metabolism: A New Challenge to Improve Immunotherapy. *Front. Immunol.* **2018**, *9*, 353. [CrossRef]
240. Faubert, B.; Li, K.Y.; Cai, L.; Hensley, C.T.; Kim, J.; Zacharias, L.G.; Yang, C.; Do, Q.N.; Doucette, S.; Burguete, D.; et al. Lactate Metabolism in Human Lung Tumors. *Cell* **2017**, *171*, 358–371.e9. [CrossRef]
241. Feichtinger, R.G.; Lang, R. Targeting L-Lactate Metabolism to Overcome Resistance to Immune Therapy of Melanoma and Other Tumor Entities. *J. Oncol.* **2019**, *2019*, 2084195. [CrossRef]
242. Yeung, C.; Gibson, A.E.; Issaq, S.H.; Oshima, N.; Baumgart, J.T.; Edessa, L.D.; Rai, G.; Urban, D.J.; Johnson, M.S.; Benavides, G.A.; et al. Targeting Glycolysis through Inhibition of Lactate Dehydrogenase Impairs Tumor Growth in Preclinical Models of Ewing Sarcoma. *Cancer Res.* **2019**, *79*, 5060–5073. [CrossRef] [PubMed]
243. Zhang, D.; Li, J.; Wang, F.; Hu, J.; Wang, S.; Sun, Y. 2-Deoxy-D-glucose targeting of glucose metabolism in cancer cells as a potential therapy. *Cancer Lett.* **2014**, *355*, 176–183. [CrossRef]
244. Benjamin, D.; Robay, D.; Hindupur, S.K.; Pohlmann, J.; Colombi, M.; El-Shemerly, M.Y.; Maira, S.-M.; Moroni, C.; Lane, H.A.; Hall, M.N. Dual Inhibition of the Lactate Transporters MCT1 and MCT4 Is Synthetic Lethal with Metformin due to NAD+ Depletion in Cancer Cells. *Cell Rep.* **2018**, *25*, 3047–3058.e4. [CrossRef]
245. Chirasani, S.R.; Leukel, P.; Gottfried, E.; Hochrein, J.; Stadler, K.; Neumann, B.; Oefner, P.J.; Gronwald, W.; Bogdahn, U.; Hau, P.; et al. Diclofenac inhibits lactate formation and efficiently counteracts local immune suppression in a murine glioma model. *Int. J. Cancer* **2012**, *132*, 843–853. [CrossRef] [PubMed]
246. Oh, M.-H.; Sun, I.-H.; Zhao, L.; Leone, R.D.; Sun, I.M.; Xu, W.; Collins, S.L.; Tam, A.J.; Blosser, R.L.; Patel, C.H.; et al. Targeting glutamine metabolism enhances tumor-specific immunity by modulating suppressive myeloid cells. *J. Clin. Investig.* **2020**, *130*, 3865–3884. [CrossRef]
247. Miret, J.J.; Kirschmeier, P.; Koyama, S.; Zhu, M.; Li, Y.Y.; Naito, Y.; Wu, M.; Malladi, V.S.; Huang, W.; Walker, W.; et al. Suppression of Myeloid Cell Arginase Activity leads to Therapeutic Response in a NSCLC Mouse Model by Activating Anti-Tumor Immunity. *J. Immunother. Cancer* **2019**, *7*, 32. [CrossRef]
248. Labadie, B.W.; Bao, R.; Luke, J.J. Reimagining IDO Pathway Inhibition in Cancer Immunotherapy via Downstream Focus on the Tryptophan–Kynurenine–Aryl Hydrocarbon Axis. *Clin. Cancer Res.* **2018**, *25*, 1462–1471. [CrossRef] [PubMed]
249. Herber, D.L.; Cao, W.; Nefedova, Y.; Novitskiy, S.V.; Nagaraj, S.; Tyurin, V.A.; Corzo, A.; Cho, H.-I.; Celis, E.; Lennox, B.; et al. Lipid accumulation and dendritic cell dysfunction in cancer. *Nat. Med.* **2010**, *16*, 880–886. [CrossRef]
250. Chaoul, N.; Fayolle, C.; Desrues, B.; Oberkampf, M.; Tang, A.; Ladant, D.; Leclerc, C. Rapamycin Impairs Antitumor CD8+ T-cell Responses and Vaccine-Induced Tumor Eradication. *Cancer Res.* **2015**, *75*, 3279–3291. [CrossRef]
251. Mao, Y.; van Hoef, V.; Zhang, X.; Wennerberg, E.; Lorent, J.; Witt, K.; Masvidal, L.; Liang, S.; Murray, S.; Larsson, O.; et al. IL-15 activates mTOR and primes stress-activated gene expression leading to prolonged antitumor capacity of NK cells. *Blood* **2016**, *128*, 1475–1489. [CrossRef]
252. Eikawa, S.; Nishida, M.; Mizukami, S.; Yamazaki, C.; Nakayama, E.; Udono, H. Immune-mediated antitumor effect by type 2 diabetes drug, metformin. *Proc. Natl. Acad. Sci. USA* **2015**, *112*, 1809–1814. [CrossRef]
253. Chang, D.-K.; Moniz, R.J.; Xu, Z.; Sun, J.; Signoretti, S.; Zhu, Q.; Marasco, W.A. Human anti-CAIX antibodies mediate immune cell inhibition of renal cell carcinoma in vitro and in a humanized mouse model in vivo. *Mol. Cancer* **2015**, *14*, 119. [CrossRef]
254. Cui, J.; Zhang, Q.; Song, Q.; Wang, H.; Dmitriev, P.; Sun, M.Y.; Cao, X.; Wang, Y.; Guo, L.; Indig, I.H.; et al. Targeting hypoxia downstream signaling protein, CAIX, for CAR T-cell therapy against glioblastoma. *Neuro-Oncology* **2019**, *21*, 1436–1446. [CrossRef]
255. Bernadin, O.; Amirache, F.; Girard-Gagnepain, A.; Moirangthem, R.D.; Lévy, C.; Ma, K.; Costa, C.; Negre, D.; Reimann, C.; Fenard, D.; et al. Baboon envelope LVs efficiently transduced human adult, fetal, and progenitor T cells and corrected SCID-X1 T-cell deficiency. *Blood Adv.* **2019**, *3*, 461–475. [CrossRef]
256. Girard-Gagnepain, A.; Amirache, F.; Costa, C.; Lévy, C.; Frecha, C.; Fusil, F.; Negre, D.; Lavillette, D.; Cosset, F.-L.; Verhoeyen, E. Baboon envelope pseudotyped LVs outperform VSV-G-LVs for gene transfer into early-cytokine-stimulated and resting HSCs. *Blood* **2014**, *124*, 1221–1231. [CrossRef]
257. Bari, R.; Granzin, M.; Tsang, K.S.; Roy, A.; Krueger, W.; Orentas, R.; Schneider, D.; Pfeifer, R.; Moeker, N.; Verhoeyen, E.; et al. A Distinct Subset of Highly Proliferative and Lentiviral Vector (LV)-Transducible NK Cells Define a Readily Engineered Subset for Adoptive Cellular Therapy. *Front. Immunol.* **2019**, *10*, 2001. [CrossRef]
258. Müller, S.; Bexte, T.; Gebel, V.; Kalensee, F.; Stolzenberg, E.; Hartmann, J.; Koehl, U.; Schambach, A.; Wels, W.S.; Modlich, U.; et al. High Cytotoxic Efficiency of Lentivirally and Alpharetrovirally Engineered CD19-Specific Chimeric Antigen Receptor Natural Killer Cells Against Acute Lymphoblastic Leukemia. *Front. Immunol.* **2020**, *10*, 3123. [CrossRef]

259. Michelet, X.; Dyck, L.; Hogan, A.; Loftus, R.M.; Duquette, D.; Wei, K.; Beyaz, S.; Tavakkoli, A.; Foley, C.; Donnelly, R.; et al. Metabolic reprogramming of natural killer cells in obesity limits antitumor responses. *Nat. Immunol.* **2018**, *19*, 1330–1340. [CrossRef]
260. Pawelec, G.; Verschoor, C.P.; Ostrand-Rosenberg, S. Myeloid-Derived Suppressor Cells: Not Only in Tumor Immunity. *Front. Immunol.* **2019**, *10*, 1099. [CrossRef]
261. Parihar, R.; Rivas, C.; Huynh, M.; Omer, B.; Lapteva, N.; Metelitsa, L.S.; Gottschalk, S.M.; Rooney, C.M. NK Cells Expressing a Chimeric Activating Receptor Eliminate MDSCs and Rescue Impaired CAR-T Cell Activity against Solid Tumors. *Cancer Immunol. Res.* **2019**, *7*, 363–375. [CrossRef]
262. Yang, Y.; Badeti, S.; Tseng, H.-C.; Ma, M.T.; Liu, T.; Jiang, J.-G.; Liu, C.; Liu, D. Superior Expansion and Cytotoxicity of Human Primary NK and CAR-NK Cells from Various Sources via Enriched Metabolic Pathways. *Mol. Ther.-Methods Clin. Dev.* **2020**, *18*, 428–445. [CrossRef]
263. Delconte, R.B.; Guittard, G.; Goh, W.; Hediyeh-Zadeh, S.; Hennessy, R.J.; Rautela, J.; Davis, M.J.; Souza-Fonseca-Guimaraes, F.; Nunès, J.A.; Huntington, N.D. NK Cell Priming From Endogenous Homeostatic Signals Is Modulated by CIS. *Front. Immunol.* **2020**, *11*, 75. [CrossRef] [PubMed]
264. Daher, M.; Basar, R.; Gokdemir, E.; Baran, N.; Uprety, N.; Cortes, A.K.N.; Mendt, M.; Kerbauy, L.N.; Banerjee, P.P.; Shanley, M.; et al. Targeting a cytokine checkpoint enhances the fitness of armored cord blood CAR-NK cells. *Blood* **2021**, *137*, 624–636. [CrossRef] [PubMed]
265. Mhaidly, R.; Verhoeyen, E. The Future: In Vivo CAR T Cell Gene Therapy. *Mol. Ther.* **2019**, *27*, 707–709. [CrossRef] [PubMed]
266. Brendel, C.; Rio, P.; Verhoeyen, E. Humanized mice are precious tools for evaluation of hematopoietic gene therapies and preclinical modeling to move towards a clinical trial. *Biochem. Pharmacol.* **2019**, *174*, 113711. [CrossRef]
267. Eyquem, J.; Mansilla-Soto, J.; Giavridis, T.; van der Stegen, S.J.C.; Hamieh, M.; Cunanan, K.M.; Odak, A.; Gönen, M.; Sadelain, M. Targeting a CAR to the TRAC locus with CRISPR/Cas9 enhances tumour rejection. *Nature* **2017**, *543*, 113–117. [CrossRef]
268. Qasim, W.; Zhan, H.; Samarasinghe, S.; Adams, S.; Amrolia, P.; Stafford, S.; Butler, K.; Rivat, C.; Wright, G.; Somana, K.; et al. Molecular remission of infant B-ALL after infusion of universal TALEN gene-edited CAR T cells. *Sci. Transl. Med.* **2017**, *9*, eaaj2013. [CrossRef]
269. Torikai, H.; Reik, A.; Liu, P.-Q.; Zhou, Y.; Zhang, L.; Maiti, S.; Huls, H.; Miller, J.C.; Kebriaei, P.; Rabinovitch, B.; et al. A foundation for universal T-cell based immunotherapy: T cells engineered to express a CD19-specific chimeric-antigen-receptor and eliminate expression of endogenous TCR. *Blood* **2012**, *119*, 5697–5705. [CrossRef] [PubMed]
270. Morgan, M.A.; Büning, H.; Sauer, M.; Schambach, A. Use of Cell and Genome Modification Technologies to Generate Improved "Off-the-Shelf" CAR T and CAR NK Cells. *Front. Immunol.* **2020**, *11*, 1965. [CrossRef]
271. Mo, F.; Watanabe, N.; McKenna, M.K.; Hicks, M.J.; Srinivasan, M.; Gomes-Silva, D.; Atilla, E.; Smith, T.; Atilla, P.A.; Ma, R.; et al. Engineered off-the-shelf therapeutic T cells resist host immune rejection. *Nat. Biotechnol.* **2020**, *39*, 56–63. [CrossRef]
272. Nezhad, M.S.; Abdollahpour-Alitappeh, M.; Rezaei, B.; Yazdanifar, M.; Seifalian, A.M. Induced Pluripotent Stem Cells (iPSCs) Provide a Potentially Unlimited T Cell Source for CAR-T Cell Development and Off-the-Shelf Products. *Pharm. Res.* **2021**, *38*, 931–945. [CrossRef] [PubMed]
273. Krijgsman, D.; Hokland, M.; Kuppen, P.J.K. The role of natural killer T cells in cancer—A phenotypical and functional approach. *Front. Immunol.* **2018**, *9*, 367. [CrossRef]
274. Heczey, A.; Liu, D.; Tian, G.; Courtney, A.N.; Wei, J.; Marinova, E.; Gao, X.; Guo, L.; Yvon, E.; Hicks, J.; et al. Invariant NKT cells with chimeric antigen receptor provide a novel platform for safe and effective cancer immunotherapy. *Blood* **2014**, *124*, 2824–2833. [CrossRef] [PubMed]
275. Xu, X.; Huang, W.; Heczey, A.; Liu, D.; Guo, L.; Wood, M.; Jin, J.; Courtney, A.N.; Liu, B.; Di Pierro, E.J.; et al. NKT Cells Coexpressing a GD2-Specific Chimeric Antigen Receptor and IL15 Show Enhanced In Vivo Persistence and Antitumor Activity against Neuroblastoma. *Clin. Cancer Res.* **2019**, *25*, 7126–7138. [CrossRef]
276. Cichocki, F.; Valamehr, B.; Bjordahl, R.; Zhang, B.; Rezner, B.; Rogers, P.; Gaidarova, S.; Moreno, S.; Tuininga, K.; Dougherty, P.; et al. GSK3 Inhibition Drives Maturation of NK Cells and Enhances Their Antitumor Activity. *Cancer Res.* **2017**, *77*, 5664–5675. [CrossRef] [PubMed]
277. Mangal, J.L.; Handlos, J.L.; Esrafili, A.; Inamdar, S.; Mcmillian, S.; Wankhede, M.; Gottardi, R.; Acharya, A.P. Engineering Metabolism of Chimeric Antigen Receptor (CAR) Cells for Developing Efficient Immunotherapies. *Cancers* **2021**, *13*, 1123. [CrossRef] [PubMed]
278. Liu, E.; Tong, Y.; Dotti, G.; Shaim, H.; Savoldo, B.; Mukherjee, M.; Orange, J.; Wan, X.; Lu, X.; Reynolds, A.; et al. Cord blood NK cells engineered to express IL-15 and a CD19-targeted CAR show long-term persistence and potent antitumor activity. *Leukemia* **2017**, *32*, 520–531. [CrossRef]

CURRICULUM VITAE

Adriana MARTINEZ TURTOS

9 Avenue Adolphe Isnard, 06000, Nice, France

+ 33 489 06 43 03 +33 766 39 09 96

amartinez@unice.fr

Student ID 21719022| **Sex** Female | **Date of birth** 17.09.1991 | **Nationality** Cuban

CURRENT POSITION PHD STUDENT AT THE UNIVERSITÈ CÔTE D'AZUR. ÉCOLE DOCTORALE SCIENCES DE LA VIE ET DE LA SANTÉ (ED 85)

04.2018-06.2022

PhD program - INTERACTIONS MOLÉCULAIRES ET CELLULAIRE

Mediterranean Center of Molecular Medicine (C3M), INSERM U1065, Nice, France.

The PhD project has received funding from the European Union's Horizon 2020 research and innovation program under the Marie Skłodowska Curie grant agreement No. 766214 (META-CAN) and from la Fondation pour la Recherche Médicale (FRM).

Thesis director: Jean-Ehrland RICCI

Directeur de recherche DR1, C3M, INSERM U1065 ricci@unice.fr (+33) 0489064304

Laboratory: Équipe 3, Métabolism, cancer et réponses immunitaires

C3M, INSERM U1065

Bâtiment Universitaire ARCHIMED 151 route Saint Antoine de Ginestière BP 2 3194, 06204, Nice, France

Thesis title: The anti-tumoral effects of a low protein diet and of the IRE1α signaling

Thesis defense: May 20th, 2022, 14:00

C3M, INSERM U1065, Bâtiment Universitaire ARCHIMED

http://www.unice.fr/c3m/
http://univ-cotedazur.fr/
http://www.metacan.eu
http://www.frm.org

WORK EXPERIENCE

09.2014-04.2015 CONTROL CENTER OF DRUGS, EQUIPMENT AND MEDICAL DEVICES, (CECMED), Havana, Cuba. Quality control assistant.

http://www.cecmed.cu/
Sector Health/quality control

SCIENTIFIC TRAINING

09.2018 FORMATION A SPÉCIALISÉE À L'EXPÉRIMENTATION ANIMALE – INSERM - ADR PACA

03.2013-07.2014 LABORATORY OF STABLE ISOTOPES, AT THE NATIONAL INSTITUTE OF HYGIENE, EPIDEMIOLOGY AND MICROBIOLOGY (INHEM), Havana, Cuba

http://instituciones.sld.cu/inhem/
Sector Health

08.2011-02.2013 CENTER OF PROTEIN STUDIES (CEP) AT THE FACULTY OF BIOLOGY, UNIVERSITY OF HAVANA, Havana, Cuba

http://fbio.uh.cu/cep/es/index.php
Sector Academic

EDUCATION

10.2015-03.2018 MASTER DEGREE IN MOLECULAR MICROBIOLOGY, MICROBIAL ECOLOGY AND IMMUNOBIOLOGY, University of Vienna, Austria

Master thesis: Extracellular vesicles and their impact on the epithelial plasticity of hepatocellular carcinoma cells (unpublished work) at the Institute of Cancer Research, Vienna, Austria

http://www.univie.ac.at/
http:// krebsforschung.meduniwien.ac.at/forschung- research/research-focuses/tumor-progression-and-metastasis/

09.2009-07.2014 DIPLOMA DEGREE IN BIOCHEMISTRY AND MOLECULAR, University of Havana, Cuba.

Bachelor thesis: Chronic inflammation, cardiometabolic risk and antioxidant power associated with overweight in adolescents (unpublished Diploma thesis).

http://fbio.uh.cu/
http://instituciones.sld.cu/inhem/

PUBLICATIONS

11.2021 M. Grima-Reyes*, A. Martinez-Turtos*, I. Abramovich, E. Gottlieb, J. Chiche, and J.-E. Ricci, "Physiological impact of in vivo stable isotope tracing on cancer metabolism," *Mol Metab*, vol. 53, p. 101294, Nov. 2021, doi: 10.1016/j.molmet.2021.101294.
* first co-authors

12.2021 Krug, A*. Martinez-Turtos*, and E. Verhoeyen, "Importance of T, NK, CAR T and CAR NK Cell Metabolic Fitness for Effective Anti-Cancer Therapy: A Continuous Learning Process Allowing the Optimization of T, NK and CAR-Based Anti-Cancer Therapies," *Cancers (Basel)*, vol. 14, no. 1, p. 183, Dec. 2021, doi: 10.3390/cancers14010183.
* first co-authors

Manuscript in preparation IRE1α overexpression in malignant cells is deleterious for tumor progression via the induction of an anti-cancer immune response
Adriana Martinez-Turtos, Rachel Paul, Manuel Grima-Reyes, Hussein Issaoui, Adrien Krug, Rana, Mhaidly, Jozef P. Bossowski, Johanna Chiche, Sandrine Marchetti, Els Verhoeyen, Eric Chevet and Jean-Ehrland Ricci

LANGUAGE

Mother tongue(s) Spanish

Other language(s)

	UNDERSTANDING		SPEAKING		WRITING
	Listening	Reading	Spoken interaction	Spoken production	
English	C2	C2	C1	C1	C2

CONFERENCES AND SEMINARS

04-05.09.2017 Symposium on Extracellular Vesicles. Vienna, Austria

19-20.04.2018 Symposium Inflammation and Disease. C3M, Nice, France

14-18.09.2018 EMBO Workshop on Cellular Signalling and Cancer Therapy. Cavtat, Croatia

23-26.09.2019 Mouse and organomimetic models of cancer and bioinformatics approaches in research. Thermotechnical Institute, Leuven, Belgium